

GENERAL  ELECTRIC

NASA CR- ~~122339~~
122339

GENERAL ELECTRIC COMPANY
CORPORATE RESEARCH AND DEVELOPMENT
Schenectady, N.Y.

CASE FILE COPY

FINAL REPORT ON PHASES 1 AND 2

VHF RANGING AND POSITION FIXING EXPERIMENT USING ATS SATELLITES

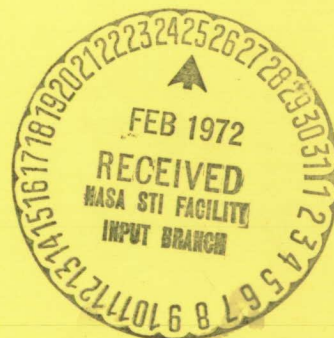
25 November 1968 - 1 May 1971

Contract No.: NAS5-11634

Prepared by
GENERAL ELECTRIC COMPANY
Corporate Research and Development
Schenectady, New York

for

Goddard Space Flight Center
Greenbelt, Maryland



S-71-1109

FINAL REPORT ON PHASES 1 AND 2
VHF RANGING AND POSITION FIXING EXPERIMENT USING ATS SATELLITES

25 November 1968 - 1 May 1971

Contract No.: NAS5-11634

Goddard Space Flight Center

Contracting Officer: C. W. Trotter
Technical Monitor: C. N. Smith

Prepared by

GENERAL ELECTRIC COMPANY
Corporate Research and Development
Schenectady, New York

Project Manager: Roy E. Anderson

for

Goddard Space Flight Center
Greenbelt, Maryland

ACKNOWLEDGEMENT

The National Aeronautics and Space Administration provided support and co-operation that made the experimental program possible. Especially valuable was the program guidance and coordination of the Technical Monitor, Mr. Charles N. Smith, and his colleagues at Goddard Space Flight Center. NASA's ATS Operations and Control made generous allowances of time on the ATS-1 and ATS-3 satellites. They often worked hard to schedule satellite time so that we could take advantage of opportunities that became available within limited time periods.

Many other organizations in the United States and abroad participated voluntarily in the experiments. Every request for cooperation met an enthusiastic and professionally executed response. The following is a listing of the major participants, in addition to NASA and General Electric.

Federal Aviation Administration - Flight testing, often with flights devoted exclusively to the experiments, with DC-6 and C-135 aircraft; radar tracking of aircraft, data collection and analysis.

US Coast Guard - Installation and operation of transponders aboard Coast Guard cutters in port and underway in the Gulf of Mexico and the Pacific Ocean.

Office of Naval Research - Support, under contract N00014-68-C-0467, and co-operation in experiments with the Sea Robin buoy at Bermuda.

Aeronautical Radio, Inc. - Arrangements with foreign governments and airlines for equipment installations and experiments. Communications tests with ARINC Laboratories.

Argentine Air Force - Installation, operation and maintenance of a transponder at Buenos Aires.

Boeing Company - Installation, operation, and maintenance of a transponder at Seattle, Washington.

Canadian Department of Transport - Installation, operation, and maintenance of a transponder at Gander, Newfoundland.

Iceland Civil Aviation Administration - Installation, operation, and maintenance of a transponder at Reykjavik, Iceland.

Irish Department of Posts and Telegraphs - Installation, operation, and maintenance of a transponder at Shannon, Ireland.

COMSAT Corporation - Independent measurements of ranges from satellites to transponders. Computation of range measurement precision for comparison with GE data.

Pan American Airways - Integration and test of tone-code responder with Satcom equipment on 747 aircraft. Communication tests through ATS-3 from 747 aircraft on commercial flights.

Air Force Cambridge Research Laboratories - Cooperative ionospheric propagation measurements, data on ionospheric characteristics.

The General Electric experiment team values the many friendships that were developed with members of each of the participating organizations. It was our privilege to have personal association with many of them. With others, our contacts were by long distance communications, including voice transmissions

through the satellites. Each participant made a valuable contribution to the experiment through the exercise of professional skill and cooperation that was enthusiastic even when it was at personal inconvenience. It is our sincere hope that each participant benefitted from the work, and that the excellent relationships that were developed will continue.

SUMMARY

A two and one-half year testing program with the National Aeronautics and Space Administration's ATS-1 and ATS-3 spacecraft has shown that geostationary satellites can provide superior communications and position surveillance for mobile craft. The tests proved that inexpensive modifications to conventional mobile communications equipment aboard the craft can provide reliable, high quality voice and digital communications with distant ground stations and other vehicles, and automatic surveillance of the positions of all the craft by a ground facility. The tests also demonstrated the location and automatic read-out of remote data collection platforms.

Frequency modulation signals with the narrow audio and radio frequency bandwidths of terrestrial mobile radio communications were relayed through the VHF transponders of the geostationary satellites. The voice and digital communications were far superior in reliability and quality to long-distance mobile communications by other means such as medium or high frequency radio. It was shown that one satellite can provide nearly uniform high quality performance over approximately one-third of the earth's surface.

Position fixes by range measurement from the two satellites were accurate to approximately one nautical mile, one sigma except near the equator and the poles. The ranging signals were narrow bandwidth FM like the voice and digital signals and were highly compatible with the communications. A single interrogation yielded range measurements from two satellites so that a position fix could be determined in about one second of time. The technique can be modified to locate several craft within a second.

Satellite communications with mobile craft and data collection platforms and independent surveillance of their positions is practical at VHF (118-174 MHz). There is no question that a useful system could be implemented with technology that is immediately available and that user equipment would be inexpensive, reliable and convenient.

Figure S-1 compares position fix accuracies achieved with two aircraft during a 5.5 hour flight test under the worst conditions of the experiment, a ship over a two month period under nominal conditions of the experiment, and the specification for an aircraft inertial navigation system after 5 hours of flight time. Reasons for the satellite position fix errors were identified and measured, and practical means to reduce the errors were defined and tested in part.

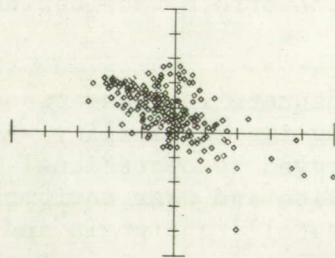
Transmission link reliability was not adequate for operational use under all conditions of the test. Factors affecting its reliability were identified and measured. Link performance could be improved to operational acceptability with modest engineering changes to the satellite and user equipment designs such as the use of circular polarization of satellite signals and more suitable antennas on the mobile craft.

The performance of VHF satellite transmission links is degraded due to ionospheric propagation effects at some times and places, especially in tropical and high latitude regions. The system can be designed to minimize the propagation effects and provide operationally acceptable performance under almost all conditions.

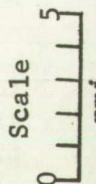
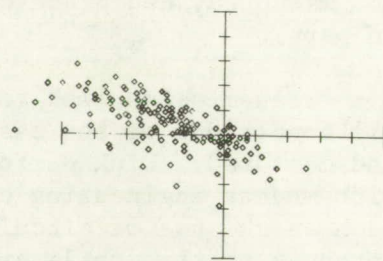
FIGURE S-1

POSITION FIX ACCURACY COMPARISONS

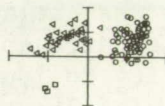
DC-6 FIX ERRORS - 5.5 HOUR FLIGHT - 12/1/70
 "WORST CASE" CONDITIONS" -- (One other fix in
 error by 11 miles - see Figure 29 in the
 Aircraft Tests Section)



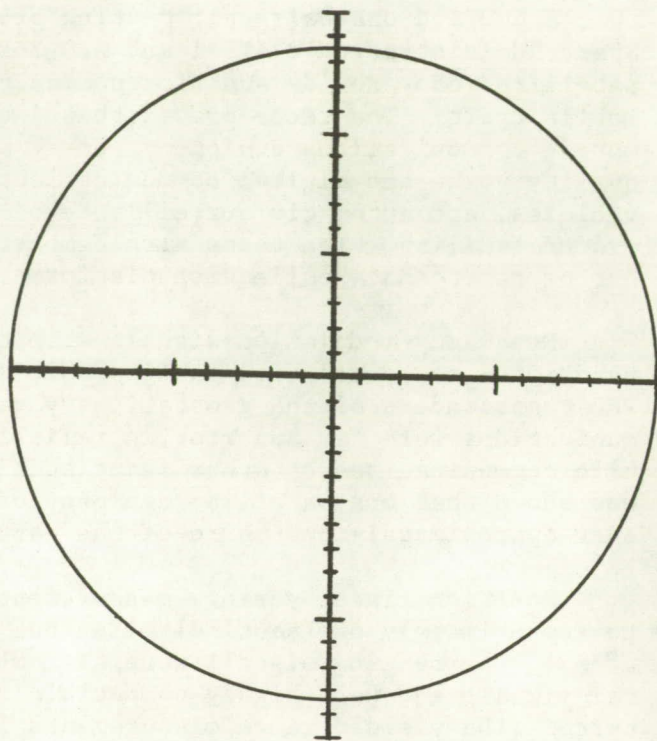
C-135 FIX ERRORS - 5.5 HOUR FLIGHT - 12/1/70
 "WORST CASE" CONDITIONS



FIX ACCURACY - COAST GUARD CUTTER RUSH AT
 SAN FRANCISCO - 5/13/70, 7/10/70, 7/21/70



INERTIAL NAVIGATION SYSTEM - BOEING SPECIFICATION
 95 PERCENT OF FIXES INSIDE THIS CIRCLE AFTER FIVE
 HOUR FLIGHT TIME. (NO MORE THAN 2 nmi. ERROR PER
 FLIGHT HOUR ON 95 PERCENT OF FLIGHTS UP TO TEN
 HOURS DURATION)*



*Edwin L. Hughes. "Inertial Navigation for 747"

The use of VHF for satellite applications is restricted because there is not an adequate number of radio frequency channels to fulfill the anticipated requirements. Data collected during the experiment can be used to estimate the performance that would be achieved with other system parameters and ranging at higher frequencies, such as L-band, where channels can be assigned more easily and where ionospheric propagation disturbances are less than at VHF.

Experiment Procedure

General Electric's Radio-Optical Observatory near Schenectady, New York was the base for the experimental program. Ranging interrogations originated there, ranging time intervals were measured, data recorded, and a computer terminal was used in processing data and computing fixes.

Seven vehicles were used in the tests: a Coast Guard Cutter in the Gulf of Mexico and one in the Pacific Ocean; three aircraft, a DC-6B and a C-135 of the Federal Aviation Administration, and a 747 aircraft of Pan American Airways; a buoy moored in deep water off Bermuda; and a panel truck in up-state New York. In addition, there were fixed ground reference transponders at Shannon, Ireland; Reykjavik, Iceland; Gander, Newfoundland; Seattle, Washington; and Buenos Aires, Argentina. Each vehicle was equipped with a conventional mobile communications transmitter, receiver, and antenna, and had a 6 x 8 x 10 inch, 6 pound experimental tone-code responder unit attached between the receiver and transmitter. The combined receiver, transmitter and responder is termed a transponder.

Each of the ground reference transponders consisted of a mobile radio base station unit, like those used by a taxi cab dispatcher, with a physically small 300 Watt power amplifier and an eight-turn helical antenna. A tone-code responder was connected between the transmitter and receiver of the base station unit. The units are inexpensive, easily installed by a technician, and are fully automatic. They can be turned on by interrogation through the satellite and respond automatically with no person present.

Ground stations as well as the mobile units in the ships and aircraft were useful for voice communications as well as ranging for position fixing. The unit in the buoy responded with an automatic digital read-out of its on-board sensors each time it was interrogated for a ranging measurement.

When a vehicle was to be located, a ground station near Schenectady, New York transmitted a 0.43 second tone-code signal to one of the satellites, the "interrogating satellite", usually ATS-3. The signal consisted of a 2.4414 kHz tone burst followed by the individual user address formed by suppressing an audio cycle for a digital "zero" and transmitting an audio cycle for a digital "one". The tone-code signal was frequency modulated on a 149.22 MHz carrier with a narrow deviation so that the RF bandwidth was within the 15 kHz bandwidth of the mobile receivers.

The satellite repeated the signal on 135.6 MHz. All of the activated vehicle equipments received the signal, and each matched the phase of a locally generated audio tone to the received tone phase. The one vehicle that was addressed responded with a short burst of its properly phased locally generated tone followed by its address code, introducing a very precisely known time delay between reception and retransmission of the code. The vehicle response on

149.22 MHz was through a broad beamwidth antenna. If both satellites were in range of the vehicle, they both repeated it on 135.6 MHz.

The ground station received the returns from the two satellites separately with narrow beamwidth antennas. It measured the time interval from its initial transmission of the signal to the first return from the interrogating satellite and to the two returns from the satellites as they were relayed back from the user. (Figure S-2) From these measurements, the ranges from the two known positions of the satellites to the vehicle were determined. These ranges, together with vehicle altitude and corrections for ionospheric delay, were used to compute the vehicle location. When only one satellite was in range of the vehicle, a line of position was computed and a fix defined as the crossing of the line with latitude or longitude of the vehicle determined by other means.

The time required for the interrogation and response was approximately one second except when a data transmission followed the user's tone-code ranging response. The usual interrogation rate was once every three seconds. A modification to the tone-code signal design is expected to reduce the duration of the signal to 30 milliseconds. In an operational system it would be possible to order the interrogations so that several position fixes could be made within one second.

The 2441 Hz tone frequency and the 15 kHz RF bandwidth were selected to keep within the audio and RF bandwidth limits of conventional mobile communications equipment and channel assignments. Ranging precision achieved within these limits is illustrated in Figure S-3 and Figure S-4. Each dot is an independent range measurement resulting from a single interrogation. Figure S-3 presents range measurements from the Schenectady ground station to ATS-3 and return, and S-4 from Schenectady through the satellite to a ground transponder and return. The largest individual displacement of readings is 1.1 microseconds or approximately 550 feet. The average of a number of readings would yield a precision of approximately ± 0.1 microsecond, or approximately ± 50 feet.

Ranging from Schenectady to ATS-1, less than 2 degrees above the western horizon during sunrise in the ionosphere, yielded standard deviations of 0.3 microsecond on 10/31/70 and 0.43 microsecond on 11/2/70. Each test was of one-half hour duration, making an independent range measurement every three seconds.

The tone-code ranging technique has the following characteristics:

- Useful accuracy can be achieved within the modulation and radio frequency bandwidths of present-day mobile communications.
- The technique can be used with wide bandwidth for high accuracy.
- It requires only one channel for range measurements, receiving and transmitting in the simplex mode if desired without need for an antenna diplexer.
- The time required for the range measurements is a fraction of a second so that the ranging function can time-share a communication channel with little additional time usage of the channel.
- It can be implemented by the addition of an inexpensive, solid-state responder unit attached to a communication receiver-transmitter.
- It can, but need not, employ digital or digitized voice transmissions to provide synchronizing of the user responder, thereby further increasing the efficiency of channel usage.

FIGURE S-2

SYSTEM CONCEPT

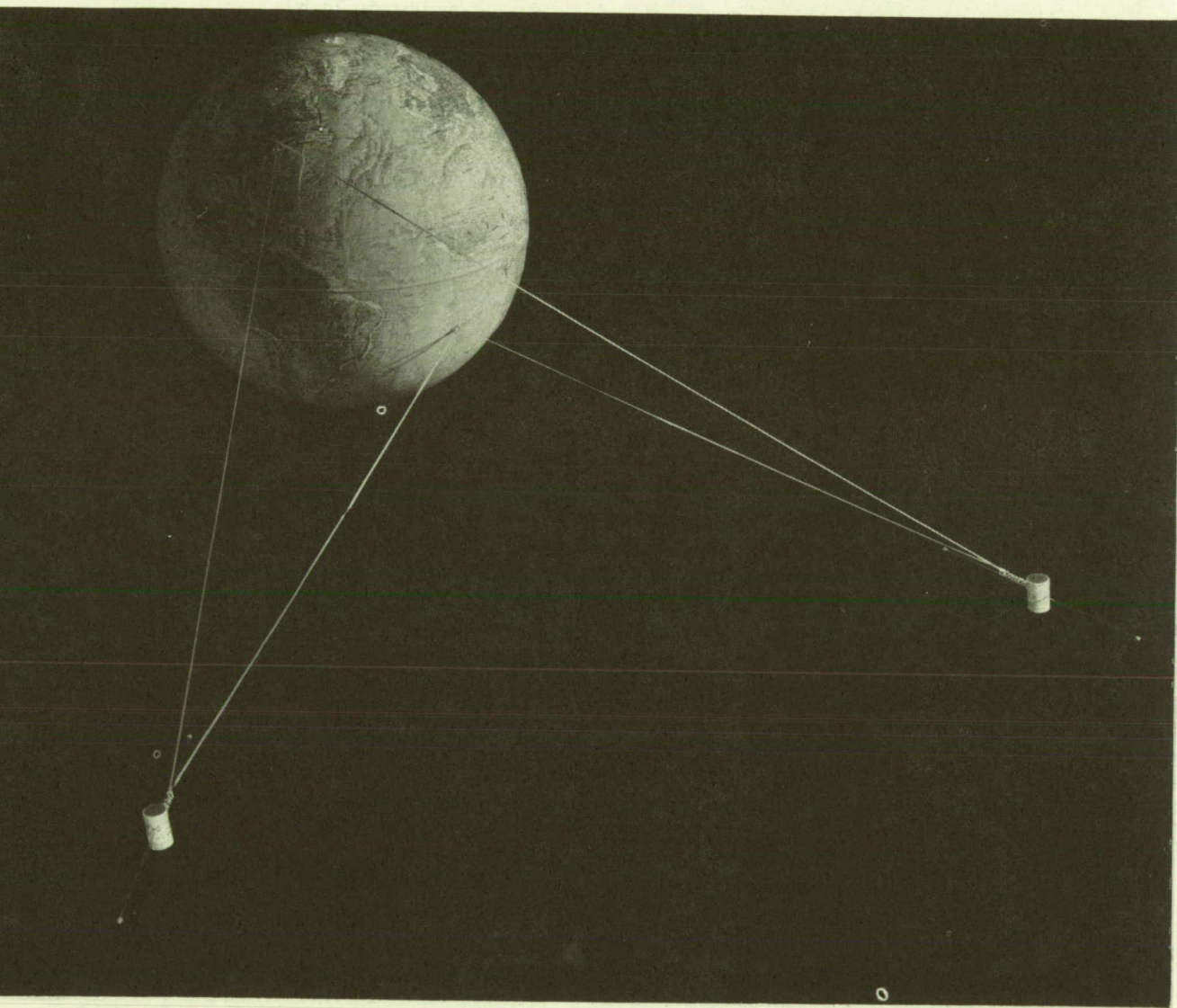


FIGURE S-3

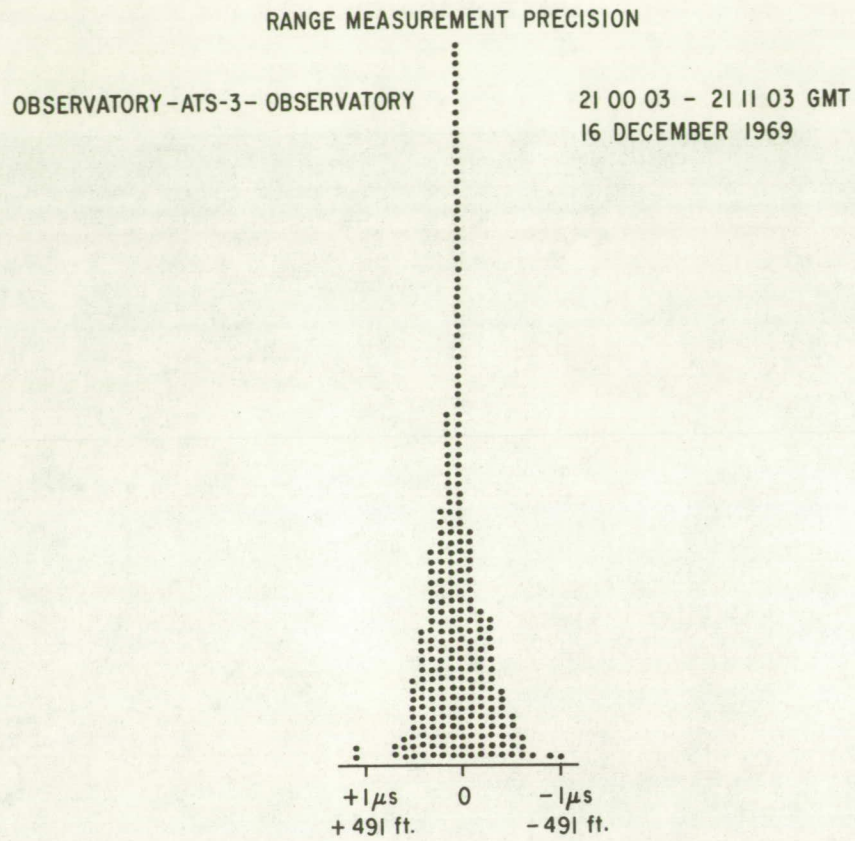
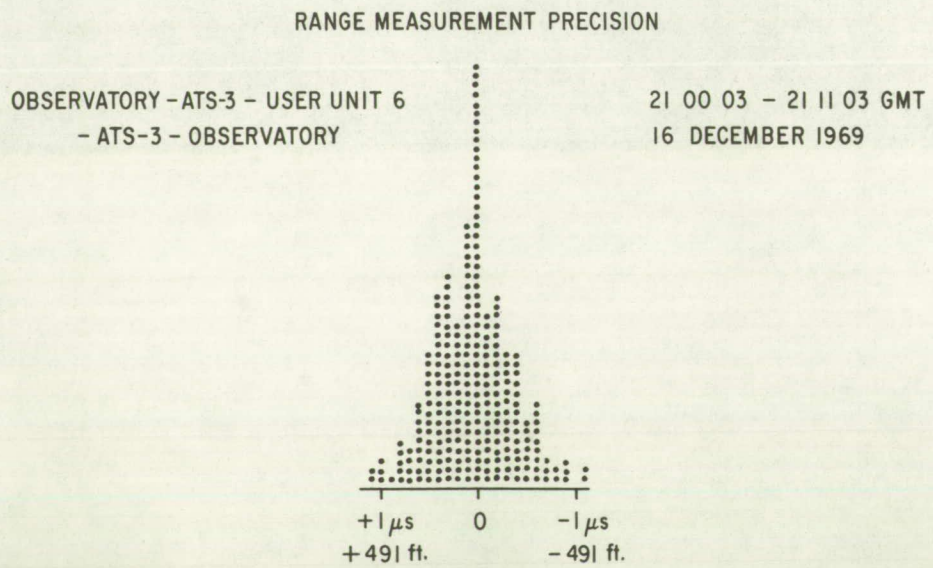


FIGURE S-4



- There are no "lane" ambiguities in the range measurements.
- User identification is simple and is confirmed in the return signal.

Ship Tests

A tone-code transponder, like the one shown in Figure S-5 was installed on the Coast Guard Cutter Rush at San Francisco on May 5, 1970. The transmitting antenna used on the Rush is shown in Figure S-6. The equipment time delay was calibrated after installation by ranging through the satellites while the ship was underway in the Gulf of Farallons near San Francisco on May 5. A refined measurement of the time for the signal to pass through the equipment is necessary after it is installed, since the equipment time delay must be subtracted from the total ranging time measurement in order to yield the propagation time of the radio signal from the satellite to the vehicle and return.

On May 10 the ship was at the dock, shown in the center of the right-hand one mile radius circle in Figure S-7. The ship was interrogated through ATS-3 and its responses were received back through ATS-1 and ATS-3 to yield range measurements from the two satellites so that the position fixes could be computed. Three fixes determined on that date are shown just outside the one nautical mile radius circle on the upper left. The ship then proceeded to its weather station duty half-way between San Francisco and Hawaii where it remained for three weeks. Many position fixes were determined while the ship was enroute and at the weather station. It then continued on to Pearl Harbor, Hawaii, where it was in view of only one satellite, ATS-1. Range measurements from ATS-1 were used to determine the latitude of the ship while it was docked at Pearl Harbor. The latitude determinations bracketed the actual position of the ship within one nautical mile. The ship returned to San Francisco and was again tied up at the dock in the center of the right-hand circle. The position fixes shown near the lower edge of the circle were made by satellite ranging on July 10. All of the fixes can be enclosed in a 5000 foot radius circle. The ship was at the dock in the center of the left hand circle on July 21 and the small ovals are the position fixes determined on that day. Each set of position fixes is biased from the true position. A study of the satellite position predictions as stated by NASA show that the predicted positions for the satellites which are the references for the fix determinations can be in error by amounts that could cause position fix bias errors larger than those plotted in Figure S-7.

No adjustment was made to the equipment while it was installed on the Rush. The only human attention given to it was to turn on the main power in anticipation of the satellite experimental periods and to use the equipment for voice communications through the satellite with the network of ground transponders and with other ships in the Atlantic Ocean. The quality of the voice communications was excellent.

Aircraft Tests

Two transponders were used aboard aircraft of the Federal Aviation Administration. One of the units was a transponder like the one used on the ships. The other consisted of an RTA-41B transceiver with a frequency modulation modem and a 500 Watt power amplifier. A General Electric tone-code responder was connected between the transmitter and receiver of the RTA-41B unit.

FIGURE S-5

GROUND REFERENCE TRANSPONDER

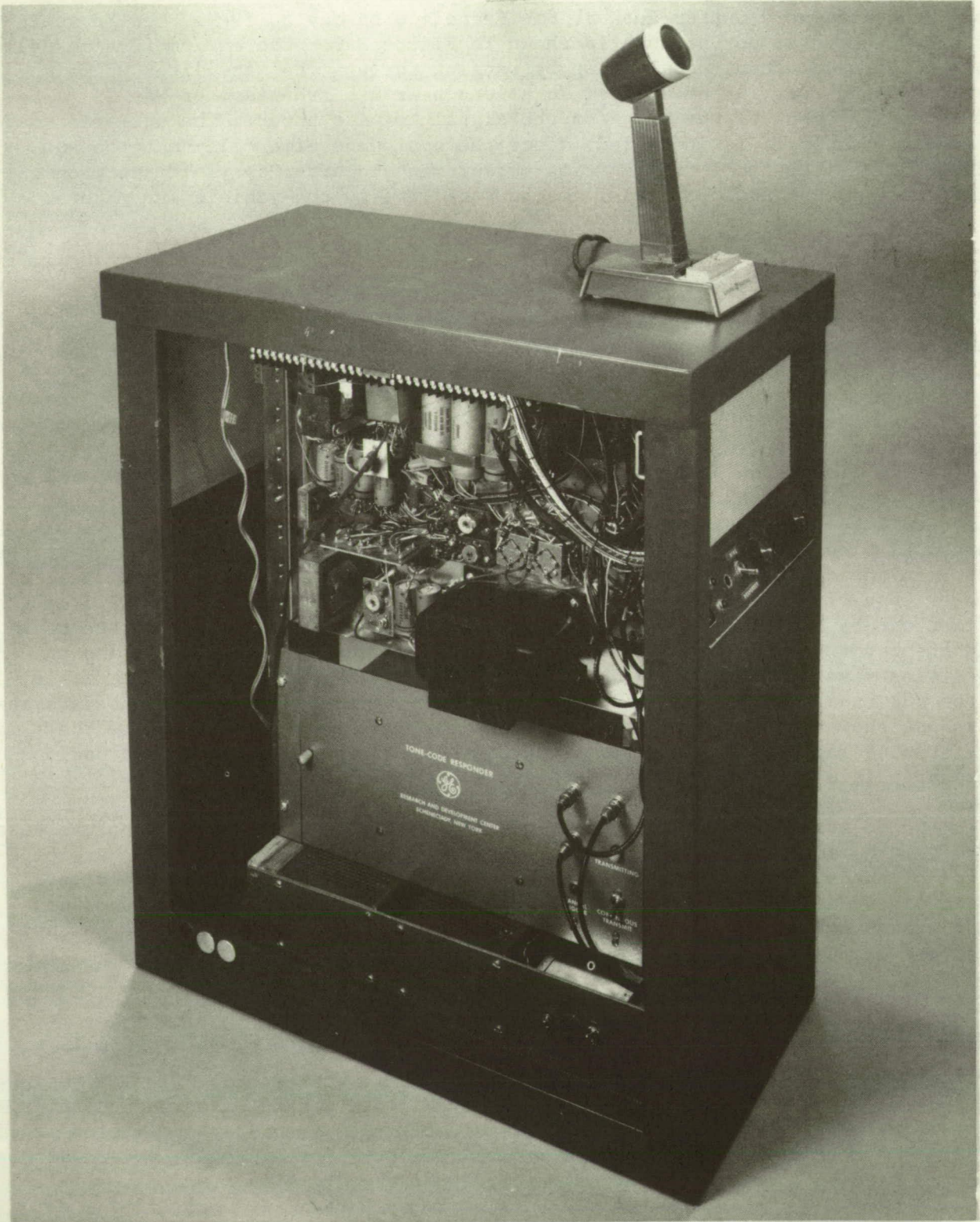


FIGURE S-6

CIRCULARLY POLARIZED TURNSTILE ANTENNA

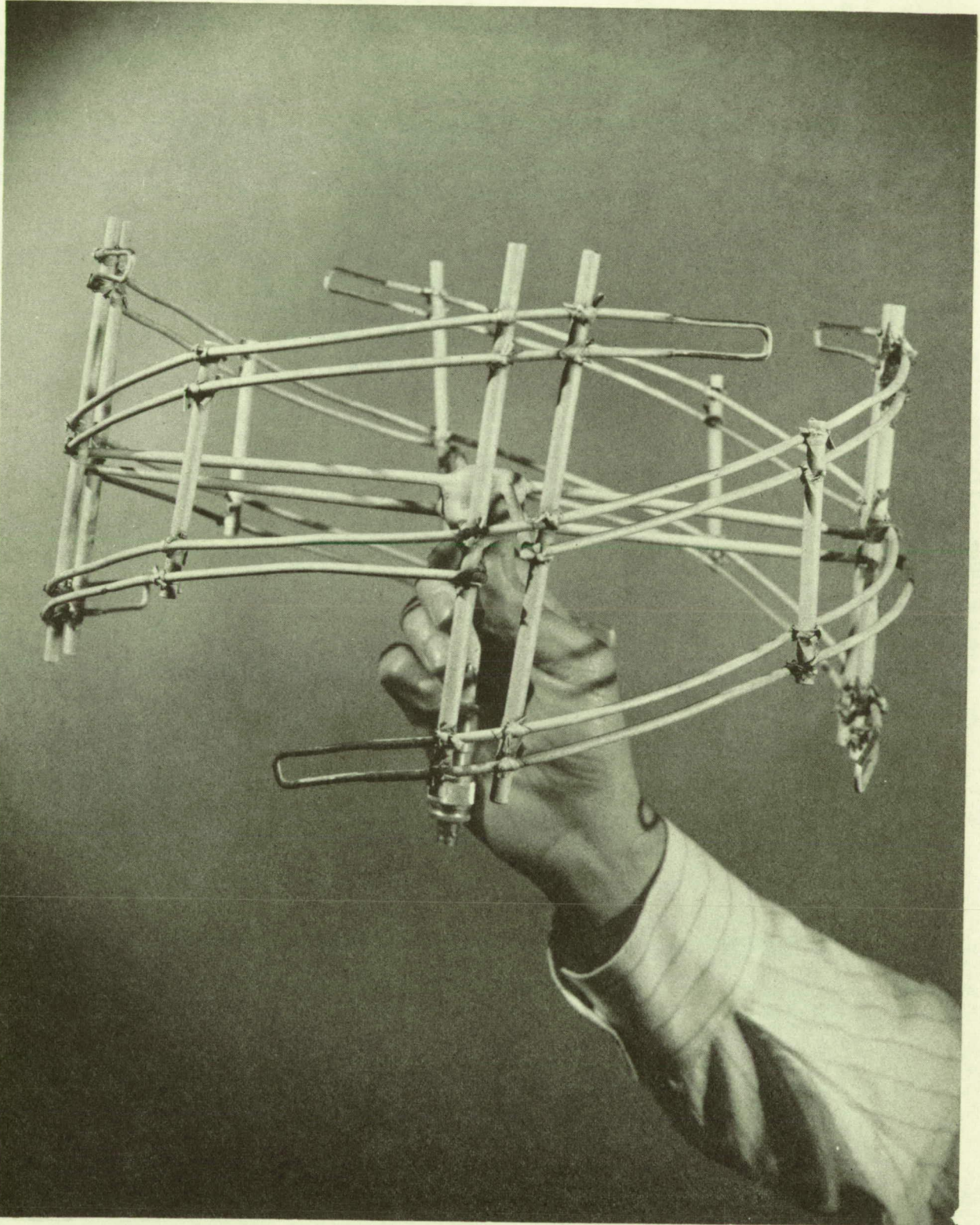
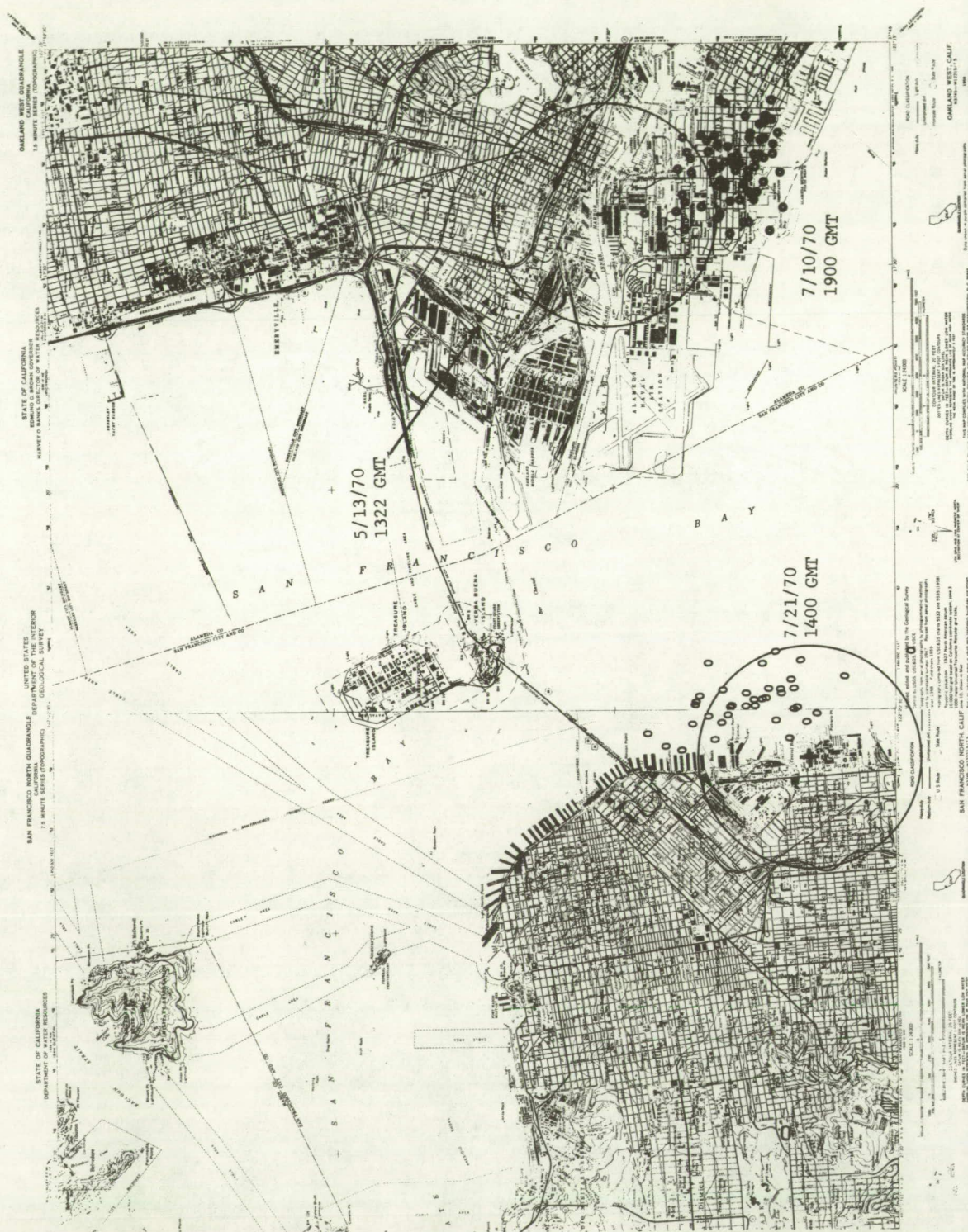


FIGURE S-7

POSITION FIXES, COAST GUARD CUTTER RUSH IN SAN FRANCISCO BAY



Antennas used aboard the aircraft included a conventional VHF blade modified to transmit 500 Watts at the up link frequency of 149.22 MHz and a Dorne and Margolin Satcom antenna. The Satcom antenna is circularly polarized in two modes. The horizon mode is omnidirectional in azimuth and it has a vertical coverage from 10 degrees to 40 degrees elevation. The zenith mode is also circularly polarized and covers a solid angle from approximately 40 degrees elevation upward. Both modes have a maximum gain of approximately 3 dB.

Figure S-8 compares the two-satellite position fixes shown as crosses with precision radar fixes shown as dots as the DC-6 aircraft left the National Aviation Facilities Experimental Center at Atlantic City. The solid lines are one nautical mile on each side of the precision radar track.

When the aircraft arrived at Shannon, Ireland, it was parked on a benchmark. It was in view of only the ATS-3 satellite, being too far east for ATS-1. Range measurements from ATS-3 were used to compute the latitude at which the satellite line of position crossed the known longitude of the benchmark. The average of 14 range measurements was 800 feet north of the benchmark. The largest single errors were 7500 feet north and 6000 feet south of the benchmark. Three range measurements to the ground reference transponders at Shannon were used to derive the ionospheric propagation delay and provide a first order correction for satellite position error, thus testing the concept of using ground reference transponders for real time corrections of the range measurements. Long term stability of the equipment was verified in this test because the equipment time delay calibration for the aircraft was made 9 days different in time when the aircraft was at Atlantic City.

The Federal Aviation Administration provided many hours of flight time for the satellite ranging and communication experiments, with the DC-6 four engine propeller driven aircraft and the C-135 jet aircraft.

One 5.5 hour flight test with both aircraft was made within range of the precision EAIR radar at Atlantic City. Tests were made over water east of the New Jersey Coast and over land northwest of Philadelphia. The aircraft were flown at two altitudes, approximately 20,000 feet and 5,000 feet, and at various headings.

Each satellite fix was plotted relative to the radar fix of the aircraft made at the same second of time. Figure S-9 is a plot of the satellite fixes relative to the radar fixes for the DC-6, the radar fix references being the center of the circle. The divisions are one minute in latitude and longitude. The radius of the circle is 10 nmi., representing the Boeing accuracy specification after 5 hours of flight for the Inertial Navigation Systems used aboard the 747 aircraft. The specification states that the Inertial Navigation System shall accumulate no more than 2 nmi. error per flight hour on 95 percent of flights up to 10 hours duration. (Edwin L. Hughes, "Inertial Navigation for 747 Superjet", Electronics World, 9/70, p. 27.)

One satellite fix with the DC-6 aircraft was in error by 11 miles. It is the worst single fix noted in the entire ranging and position fixing experiment, except for a small number of fixes that were displaced by multiples of 75 miles along a hyperbolic line of position in the aircraft experiments. The large fix errors were caused when the aircraft responder-correlator output occurred a multiple of a bit period early. The bit or tone-code cycle period is 409 microseconds. Errors of that type were rare in the experiment and their occurrence can be reduced to an insignificant probability by improvements in the

FIGURE S-8

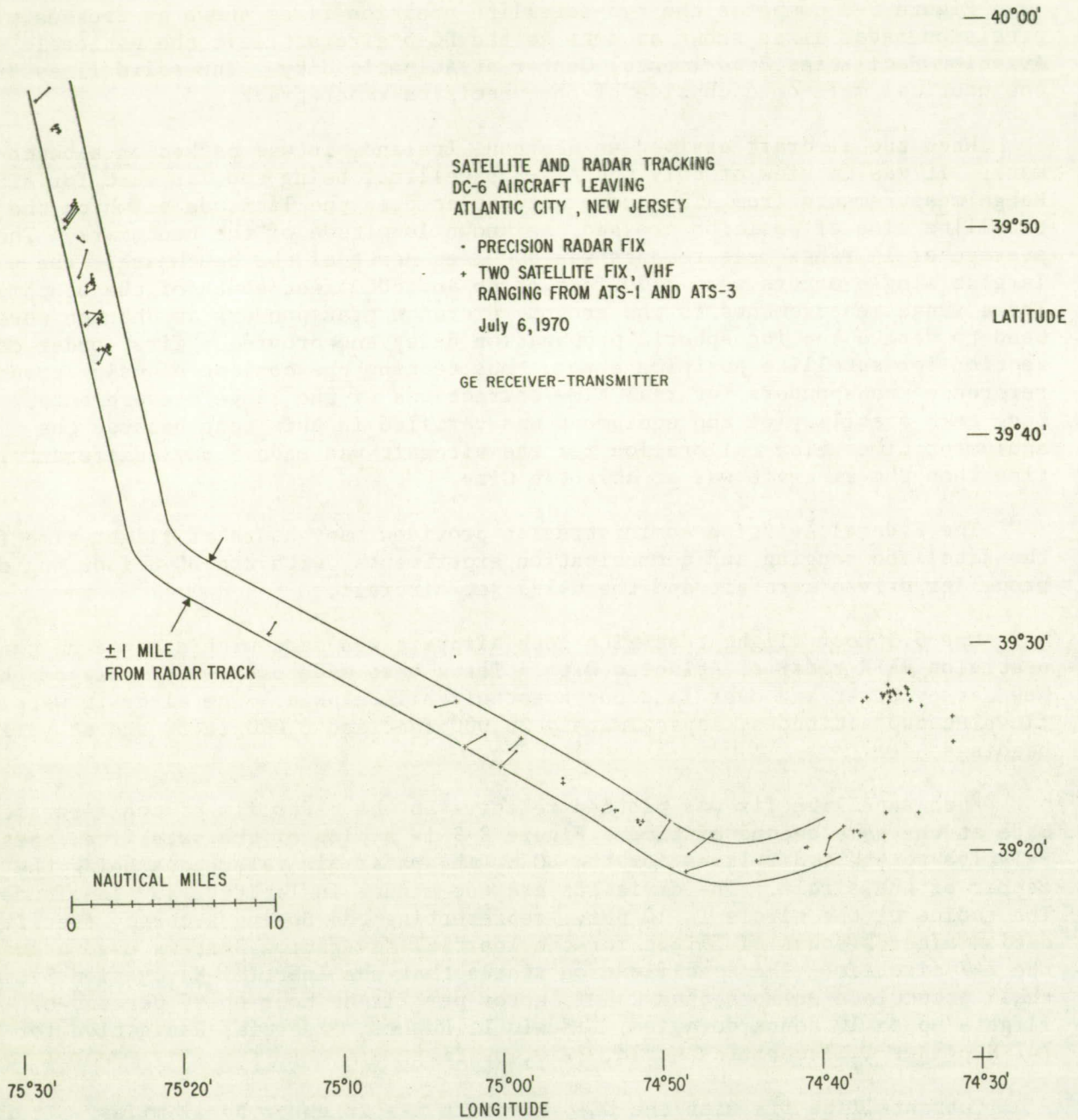
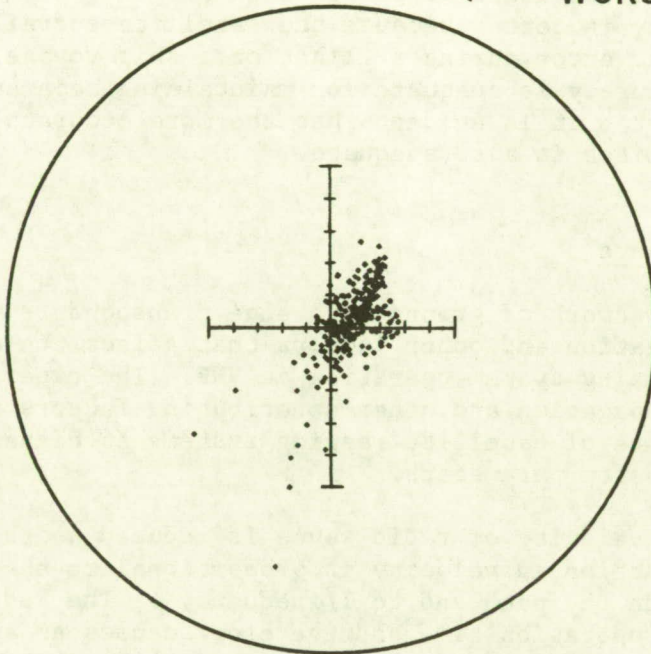


FIGURE S-9

ACCURACY OF AIRCRAFT FIXES
5.5 HOUR FLIGHT
DC-6
'WORST CASE' CONDITIONS

• ← WORST ERROR - 11 nmi.



10 nmi. RADIUS CIRCLE

correlator and code designs. The pattern of position fix errors for the C-135 were similar to the DC-6. There was a larger scatter caused by receiver time delay change with signal amplitude, but no C-135 fixes were outside of the 10 nmi. radius circle, except for a few that were multiples of 75 miles in error.

A study of the aircraft fix errors as a function of time during the 5.5 hour flight reveals the changing bias error due to the diurnally changing satellite prediction errors. The plot of Figure S-9 includes the bias errors due to satellite position fixes. There were no corrections for any of the known causes of error in the plot. It represents a comparison of the worst conditions for the two satellite ranging at VHF with the specified performance for an aircraft inertial navigation system after 5 hours of flight time.

Nominal accuracy, as exemplified by the ship tests, equaled the accuracy specified for the Inertial Navigation System after one hour of flight time. Precision of the satellite fixes is poorer than the Inertial Navigation System, but long-term accuracy is better because the satellite surveillance does not accumulate significant error during a flight or a ship voyage. If Inertial Navigation System accuracy is adequate for maintaining separations of aircraft on transoceanic flights, it is evident that the more accurate tone-code ranging technique with satellites is also adequate.

Propagation Measurements

The widespread network of ground reference transponders was used in tests to measure the propagation and other factors that affect the accuracy of a satellite position fixing system operating at VHF. The experimentally derived information about propagation and other contributing factors can be used to predict the performance of satellite ranging systems at higher radio frequencies and with different system parameters.

The propagation velocity of radio waves is reduced as they pass through the ionosphere. The reduction in velocity is proportional to the integrated electron content along the ray path and to $1/\text{frequency}^2$. The reduced propagation velocity increases propagation time and therefore causes an apparent increase in range measurements. There are two ways to correct for the propagation delay. One way is to estimate the delay by the use of a model of the ionosphere based on the large quantity of data that has been collected over the past several decades. The other way is to measure the propagation delay at a known location and use the measurement to correct range measurements made to other transponders in the geographical region surrounding the known location.

Both ways of correcting for propagation delay were used in the experiments. A simple model provided corrections adequate for position fix accuracy better than 1 nmi., 1 sigma. The other method, using reference transponders at known locations, was also effective and provided the additional benefit of a first order correction for error in satellite position prediction.

A model is useful if there are predictable cyclic changes in the ionosphere. The diurnal cycle is the dominant one. The day-to-day correlation of ionospheric delay is thus important in estimating the value of a model.

The usefulness of reference transponder measurements depends upon the correlation of ionospheric delay at one location with the delay at another. The geographical extent of the correlation is important in evaluating the practical

value of the reference transponders because it determines the number and deployment of the transponders needed to achieve a specified accuracy for the system.

Much of the effort in the experimental program was directed to measuring the time and geographical correlations of ionosphere delay and evaluating the two methods of correcting the range measures. Figure S-10 shows the correlations for Schenectady and Gander, Newfoundland on January 19, 1971. The ionospheres seem to be well correlated at the two locations which were a thousand miles apart. The correlation between Shannon, Ireland and Reykjavik, Iceland was also found to be close enough to provide range corrections within approximately 1500 feet at locations a thousand miles apart on days without unusual ionospheric disturbances.

A few times a year during the peak of the 11 year sunspot cycle solar flares cause ionospheric disturbances that can increase the propagation delay by as much as 50 percent over the average of undisturbed days. These solar disturbances are rare during sunspot minima. There was no opportunity to observe the propagation characteristics resulting from a solar flare.

A solar flare did occur on October 28, 1970 but no ionospheric disturbance resulted from it. During four days after the flare the diurnal variation in the ionosphere was observed for Shannon, Ireland; Gander, Newfoundland; Schenectady, New York; and Seattle, Washington. The day-to-day correlation for Schenectady is plotted in Figure S-11. The four days were found to be correlated within approximately 1 microsecond or 491 feet in two-way ranging. A position fix is degraded by more than the ranging error because of the way the slant range measurement error projects onto the surface of the earth.

The ionosphere sometimes causes a scintillation of the amplitude of the signal received from the satellite. Scintillation is caused by horizontal variations in electron content. As the irregularities in the ionosphere move, the signal level received by an antenna from the satellite changes in signal strength. The signal level can increase above the average value by several dB and may fade below the average level by many dB. The signal fades are usually short. The deep fades are typically less than a second in duration and the fading periods are usually a few seconds to a few tens of seconds.

Scintillation fading is reported to occur frequently in tropical regions and high latitudes. It occurs less frequently at middle latitudes. A few instances of severe scintillation fading were observed at Schenectady during the experiments. The onset of the fading was usually quite sudden and the duration of the fading period would be several minutes to several hours.

The most severe case was observed on October 15, 1970, during a voice communication test with a Pan American 747 aircraft enroute from New York to Paris. Ground terminals participating in the experiment were at Annapolis, Maryland; Miami, Florida; Los Angeles, California; Seattle, Washington; Schenectady, New York. Fades as large as 30 dB were observed on the signals received with the 30 foot diameter antenna at Schenectady. Although the other participating stations reported changing signal levels, the geographical extent of the fading observed at Schenectady is not known. Excellent voice communication tests were maintained throughout the period and there was no noticeable degradation in the quality of the voice communications. It is important to note that speech is highly redundant and that short drop-outs do not have a significant effect on intelligibility. The effect on other forms of communications such as digital

FIGURE S-10

CORRELATION OF DIFFERENCES BETWEEN COMPUTED AND MEASURED SLANT RANGES
Gander, Newfoundland and Schenectady, New York

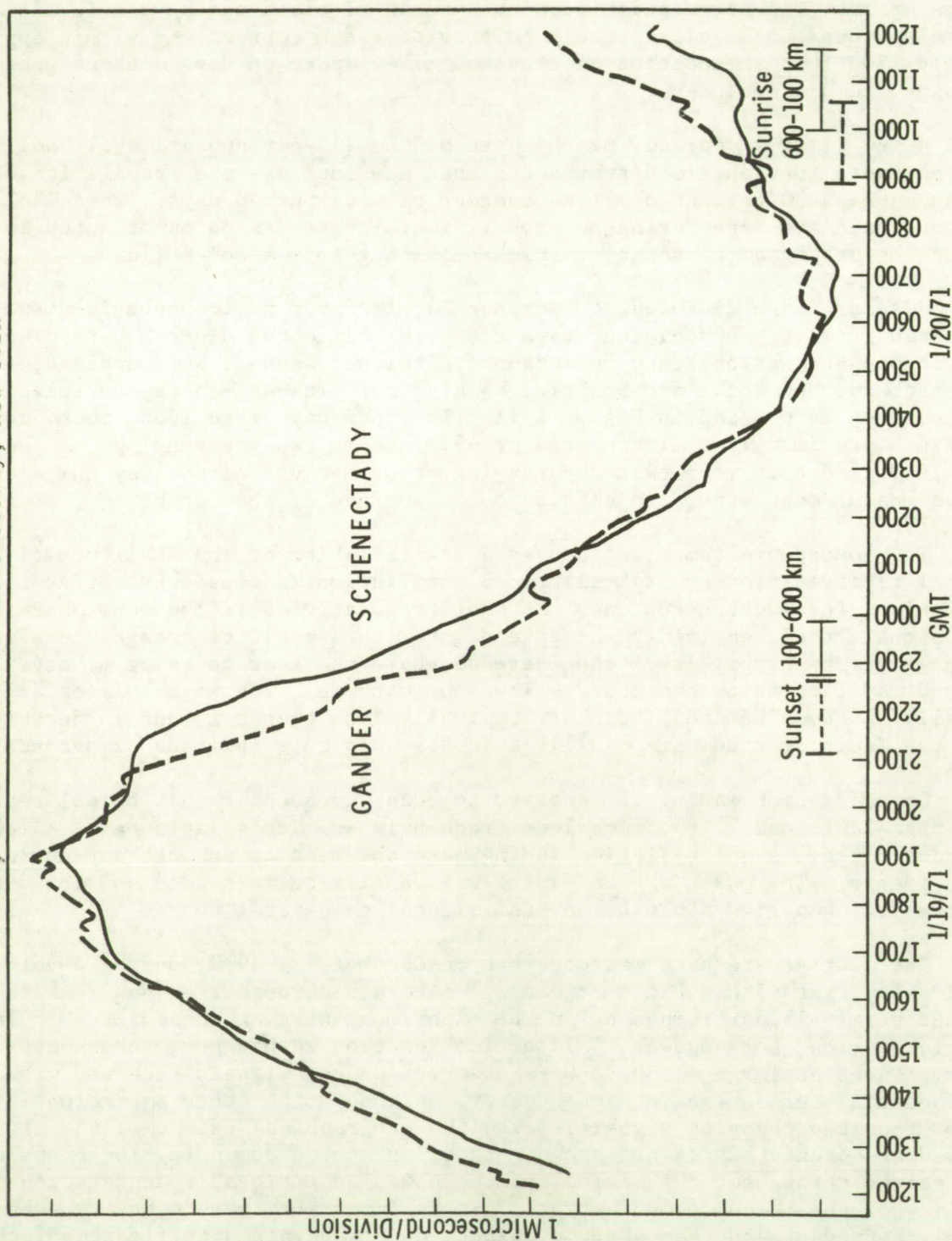
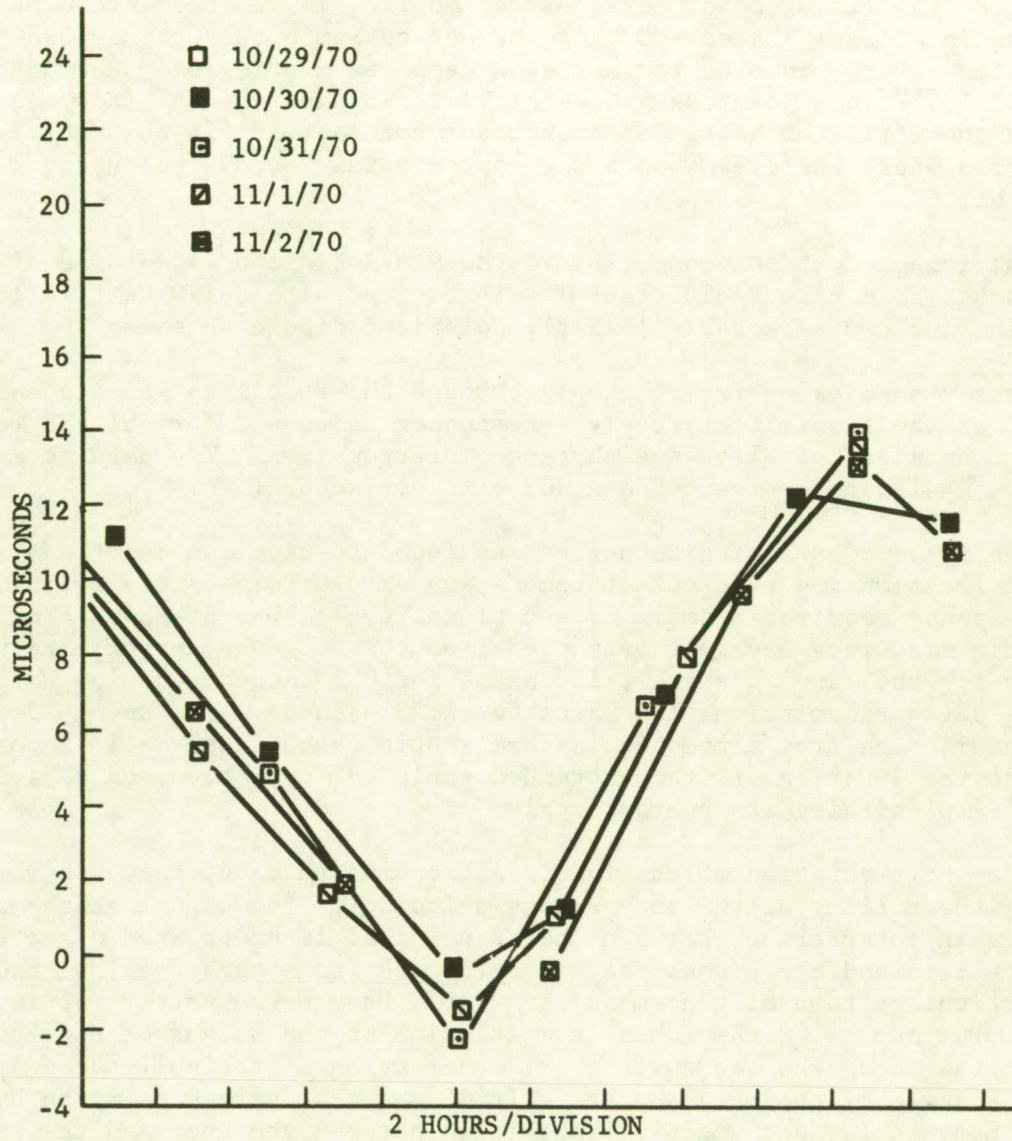


FIGURE S-11

DAY-TO-DAY CORRELATION - SCHENECTADY



which is less redundant would have to be considered in evaluating VHF communication performance when scintillation is present.

Buoy Tests

The first tone-code ranging transponder was installed in the Sea Robin buoy. Sea Robin is a spar buoy approximately 4 feet in diameter and 15 feet long with stabilizing means designed for mooring in the deep ocean or for free floating in all sea states. During the period March through May 1969 the buoy was tested ashore, in a harbor and at a deep sea mooring near Bermuda at $32^{\circ}10'N$ and $64^{\circ}55'30''W$ in a joint Navy-General Electric experiment. (Navy support was through the Office of Naval Research under contract N00014-68-C0467.) The buoy was moored where the ocean depth was approximately 4,000 feet using a 7,000 foot line.

The tone-code transponder aboard the Sea Robin consisted of a 35 Watt solid state FM mobile radio transmitter-receiver with a 120 Watt solid state amplifier and two selectable linearly polarized dipole antennas.

Data transmission from the buoy through the satellite was accomplished by the use of the transmitter-receiver-responder unit used for the VHF ranging. A data transmission followed each range interrogation. Two data rates were tested - 2441 bits per second and 305 bits per second.

The tone-code ranging technique was found to have two important advantages for the location and read-out of remote sensor platforms: transmission of the buoy response required a small amount of energy and was of short time duration. The radio frequency energy transmitted from the buoy was approximately 50 Watt-seconds for the ranging signal, 120 Watts for 0.3 second; and 150 Watt-seconds for the data transmission, 120 Watts for 1.25 seconds. The energy required for the transmission from a remote platform should be kept as small as possible to increase the duration of its unattended period of operation and thus reduce the cost of replenishing its energy supply.

The short duration of the interrogation and read-out sequence was important because the rolling of the buoy causes a fading of the signal at the satellite. There is an interference between the signal that is propagated directly toward the satellite and the signal that is reflected from the surface of the sea. The vertical pattern of transmissions from a buoy has a pattern of lobes and nulls. The number of the lobes is a function of the height of the antenna in wavelengths above the sea surface. The direction of the nulls depends upon the roll angle of the buoy and the tilt of the sea surface near the buoy. As the buoy rolls, the signals transmitted between the buoy and the satellite go through a fading pattern at the roll rate. Under some conditions the signal can be completely cancelled out for a short period during each roll cycle. Tone-code ranging had the advantage that the duration of the interrogation, ranging and data read-out sequence was short compared to the buoy roll cycle so that a complete interrogation and response sequence could be completed between fades. Other techniques that require a lock-up around the complete transmission path from the ground station through the satellite to the buoy and return, or that utilize such low transmission power that the duration of the transmission must be long compared to a roll cycle, present difficulties that must be overcome by expensive and complicated methods such as the use of a narrow beamwidth antenna on a stabilized platform or the use of burst error correction codes in the digital transmissions.

Sea Robin was at its deep sea mooring between April 14 and 25, 1969. It was interrogated from Schenectady each three seconds during three minute interrogation periods spaced throughout each day. While at its mooring the buoy was interrogated a total of 2525 times. It responded to 1711 of the interrogations and a total of 759 latitude determinations were made. Some failures to respond were caused by buoy roll; others were due to causes purposely included in the experiment such as antenna polarization switching to observe Faraday rotation of the linearly polarized signals.

The averages of the median values for each day are plotted as the triangles in Figure S-12. The wind direction and velocity as furnished by the Navy for the area are shown by the vectors near the top of the figure. It is expected that the buoy, which has a small cross section to the wind and much drag at the mooring line, responded slowly to changes in wind. The dashed line suggests the actual position to correlate with the wind directions. If it is assumed that the dashed curve of Figure S-12 represents the true latitude of the buoy, the latitude determinations replotted with respect to the buoy position provide an estimate of the accuracy that was actually achieved as shown in Figure S-13.

Conclusions

The experiments have shown that geostationary satellites can provide high quality, reliable, undelayed communications between distant points on the earth and that they can also be used for surveillance. A combination of undelayed communications and independent surveillance from shore provides the elements necessary for the implementation of effective traffic control for ships and aircraft over oceanic regions. Eventually, the same techniques may be applied to continental air traffic control.

The tests have demonstrated that remote, unmanned platforms can be interrogated, located and their data read out efficiently by satellites. The energy required for the location and data read-out functions is so low that the energy supplied aboard the remote platforms does not have to be replenished at frequent intervals. These tests have provided sufficient information so that it is now possible to proceed confidently with the design of operational systems for air traffic control, marine traffic control, management control of automated shipping and the synoptic location and read-out of a widespread network of remote meteorological and oceanographic sensor platforms.

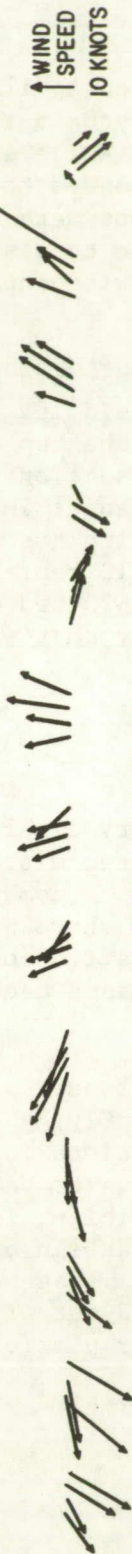
FIGURE S-12

ESTIMATED BUOY POSITION

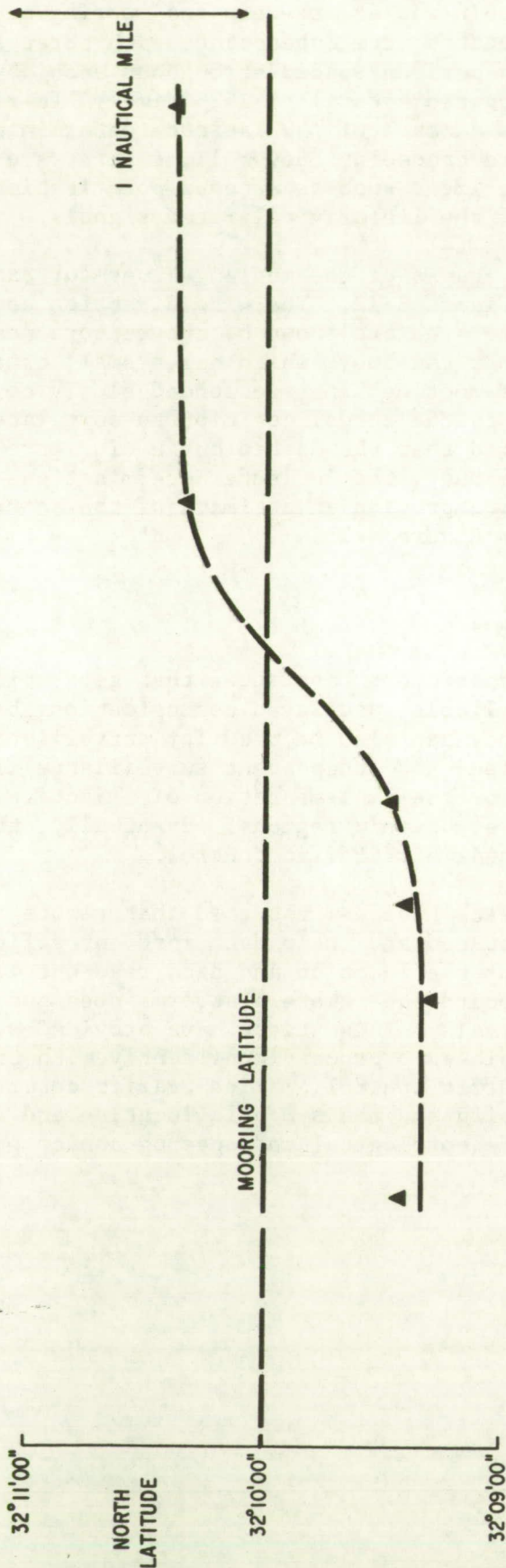
CALENDAR DAY - April 1969

4/13 | 4/14 | 4/15 | 4/16 | 4/17 | 4/18 | 4/19 | 4/20 | 4/21 | 4/22 | 4/23 | 4/24 | 4/25 |

↑ WIND
SPEED
10 KNOTS

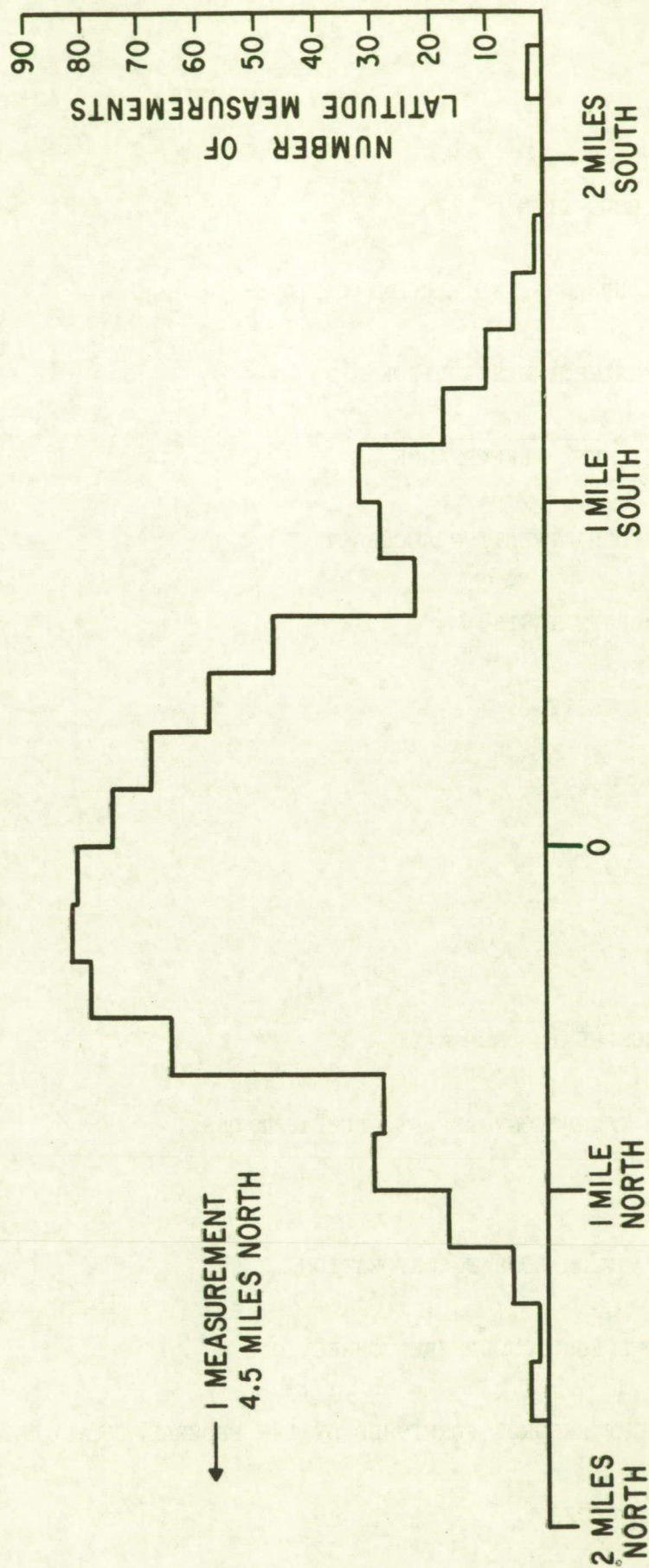


WIND SPEED AND DIRECTION



▲ TRIANGLES ARE AVERAGE OF MEDIAN POSITIONS FOR DAYS INDICATED

FIGURE S-13
DISTANCE FROM ESTIMATED BUOY POSITION (ESTIMATE OF ACCURACY ACHIEVED)



CONTENTS

SUMMARY

1. INTRODUCTION
2. CONCLUSIONS AND RECOMMENDATIONS
3. EXPERIMENT DESCRIPTION
4. EQUIPMENT PERFORMANCE
5. FACTORS AFFECTING ACCURACY
6. AIRCRAFT TESTS
7. SHIP TESTS
8. BUOY TESTS
9. VAN TESTS
10. L.E.S.T. TESTS
11. IONOSPHERIC PROPAGATION
12. NEW TECHNOLOGY REPORT; PUBLICATIONS

APPENDICES

- I. DATA FROM COMSAT CORPORATION
- II. MODEL FOR IONOSPHERE CORRECTIONS
- III. FLIGHT RECORDS FURNISHED BY THE FEDERAL AVIATION ADMINISTRATION
- IV. USER CODES

LIST OF FIGURES

Figure		Page
S-1	Position Fix Accuracy Comparisons	iii
S-2	System Concept	vi
S-3	Range Measurement Precision - Observatory-ATS-3-Observatory	vii
S-4	Range Measurement Precision - Observatory-ATS-3-User Unit 6-ATS-3-Observatory	vii
S-5	Ground Reference Transponder	ix
S-6	Circularly Polarized Turnstile Antenna	x
S-7	Position Fixes, Coast Guard Cutter Rush, San Francisco Bay	xi
S-8	Satellite and Radar Tracking - DC-6 Aircraft Leaving Atlantic City, New Jersey	xiii
S-9	Accuracy of Aircraft Fixes - 5.5 Hour Flight - DC-6 "Worst Case" Conditions	xiv
S-10	Correlation of Differences Between Computed and Measured Slant Ranges - Gander, Newfoundland and Schenectady, New York	xvii
S-11	Day-to-Day Correlation - Schenectady	xviii
S-12	Estimated Buoy Position	xxi
S-13	Distance from Estimated Buoy Position (Estimate of Accuracy Achieved)	xxii
3-1	Radio-Optical Observatory at Schenectady, New York	3-2
3-2	Eight-Turn Helix Antenna	3-4
3-3	Format of Data Recorded on Punched Tape	3-8
3-4	Accuracy of Lines of Position	3-9
3-5	Initial Processing of Ranging Data	3-10
3-6	Tone-Code Ranging Waveform	3-12
3-7	User Equipments	3-13
3-8	Ranging and Position Fixing Experiment Equipment	3-16

Figure		Page
3-9	Five Printed Circuit Boards	3-17
3-10	Assembled Responder Unit	3-18
3-11	Responder Block Diagram	3-19
3-12	Tone-Code Generator and Phase Matcher Correlator	3-21
3-13	Ground Reference Transponder	3-24
3-14	Gonset Amplifier	3-25
3-15	Portion of Log Kept on Transponder Use at Shannon, Ireland	3-27
4-1	Delay versus Signal Strength at Three Frequencies - GE Type ER-52-A Monitor Receiver	4-4
4-2	Delay versus Signal Strength - GE Type ER-41-C Receiver	4-5
4-3	Delay versus Signal Strength - Small Hand Transceiver (GE PR36RDS66)	4-6
4-4	Delay versus Frequency - GE Type ER-52-A Monitor Receiver	4-7
4-5	Delay versus Frequency - GE Type ER-41-C Receiver	4-8
4-6	Performance Curve For a Typical FM Receiver for a Modulation Index of 2	4-10
4-7	Standard Deviation as a Function of Signal-to-Noise Ratio Within a 4 kHz Audio Bandwidth	4-11
4-8	Equipment Performance Test	4-12
4-9	Bit Error Probability as a Function of Signal-to-Noise Ratio Within a 4 kHz Audio Bandwidth	4-15
4-10	Percentage of Correlations as a Function of Signal-to-Noise Ratio Within a 4 kHz Audio Bandwidth	4-16
4-11	Distribution of Time Interval Measurements for Signal-to- Noise Ratio of >20 dB Within a 4 kHz Bandwidth	4-17
4-12	Distribution of Time Interval Measurements for a Signal- to-Noise Ratio of 18 dB Within a 4 kHz Bandwidth	4-18
4-13	Distribution of Time Interval Measurements for a Signal to-Noise Ratio of 14 dB Within a 4 kHz Bandwidth	4-19

Figure		Page
4-14	Distribution of Time Interval Measurements for a Signal-to-Noise Ratio of 10 dB Within a 4 kHz Bandwidth	4-20
4-15	Distribution of Time Interval Measurements for a Signal-to-Noise Ratio of 6 dB Within a 4 kHz Bandwidth	4-21
4-16	Distribution of Time Interval Measurements for a Signal-to-Noise Ratio of 3 dB Within a 4 kHz Bandwidth	4-22
4-17	Distribution of Time Interval Measurements for a Signal-to-Noise Ratio of 0 dB Within a 4 kHz Bandwidth	4-23
4-18	Range Measurement Precision - Observatory-ATS-3-Observatory	4-28
4-19	Range Measurement Precision - Observatory-ATS-3-User Unit 6-ATS-3-Observatory	4-28
4-20	Time Delay Difference Between the Two Receiver Correlators for the Shannon, Gander and Aircraft Returns	4-32
4-21	Comparison of Two Receiver-Correlators - Schenectady-ATS-3-Gander-ATS-3-Schenectady	4-33
4-22	Comparison of Two Receiver-Correlators - Schenectady-ATS-3-Shannon-ATS-3-Schenectady	4-34
4-23	Comparison of Two Receiver-Correlators - Schenectady-ATS-3-Aircraft-ATS-3-Schenectady	4-36
5-1 & 5-2	Line of Position Disagreements Caused by Satellite Position & Prediction Disagreements	5-5
5-3	Line of Position Error Due to Equipment Calibration Error Resulting from Satellite Position Prediction Error	5-7
5-4	Range Measurement Deviations - ATS-3 to C-135	5-10
5-5	Range Error Due to Specular Sea Reflection (One Way)	5-11
5-6	Geometry and Time Delay of Reflected Signal	5-13
5-7	Phasor Relationships with Sea Reflections	5-14
5-8	Effect of Amplitude Change on Phasor Resultant	5-15
5-9	Displacement of Signal Phasor Due to Sea Reflection	5-17

Figure		Page
5-10	Phase Change for 360° (RF) Pathlength Change, Direct and Reflected Signals	5-18
5-11	Range Error Probability Distribution - 25 Microsecond Delay of Reflected Signal - One Way Ranging	5-19
5-12	Range Error Probability Distribution - 25 Microseconds Delay of Reflected Signal - Two Way Ranging	5-21
5-13	Range Measurements from ATS-3 to a DC-6 Aircraft at 21,000 Feet Over Lake Michigan	5-22
5-14	DC-6 Over Lake Michigan	5-23
5-15	Range Measurement Distributions for Two Altitudes Over Ocean	5-24
5-16	Spin Modulation Fading Pattern	5-28
5-17	Geometrical Dilution	5-31
5-18	Position Parallelogram	5-31
6-1	Receiving Antenna Patterns - DC-6, Zenith Mode	6-2
6-2	Receiving Antenna Patterns - DC-6, Horizon Mode	6-3
6-3	DC-6 Antenna Patterns - Transmit	6-4
6-4	Radar Runs - Two Aircraft Flight Test	6-7
6-5	Reference Lines Used in Radar and Satellite Fix Plots	6-8
6-6	Differences, Precision Radar and Satellite Fixes. Radar Fixes as Reference. DC-6 - Run 1	6-9
6-7	" DC-6 - Run 7	6-10
6-8	" DC-6 - Run 8	6-11
6-9	" DC-6 - Run 10	6-12
6-10	" DC-6 - Run 12	6-13
6-11	" DC-6 - Run 13	6-14
6-12	" DC-6 - Run 14	6-15
6-13	" DC-6 - Run 16	6-16

Figure		Page
6-14	Differences, Precision Radar and Satellite Fixes. Radar Fixes as Reference. DC-6 - Run 17	6-17
6-15	" DC-6 - Run 19	6-18
6-16	" C-135 - Run 1	6-19
6-17	" C-135 - Run 2	6-20
6-18	" C-135 - Run 3	6-21
6-19	" C-135 - Run 4	6-22
6-20	" C-135 - Run 13	6-23
6-21	" C-135 - Run 14	6-24
6-22	" C-135 - Run 17	6-25
6-23	" C-135 - Run 18	6-26
6-24	" C-135 - Run 19	6-27
6-25	Radar and Satellite Fixes - DC-6 - Run 19. Direct Plot of Data	6-28
6-26	Radar and Satellite Fixes - DC-6 - Run 19. Plotted with Assumed Correction for Satellite Position Reference Error	6-29
6-27	Radar and Satellite Fixes - C-135 - Run 19. Direct Plot of Data	6-31
6-28	Radar and Satellite Fixes - C-135 - Run 19. Plotted with Correction for Receiver Time Delay	6-32
6-29	"Worst Case" Satellite Fixes Relative to 60 nmi. Track Separation in Transoceanic Air Traffic Control	6-33
6-30	Spin Modulation Fading Pattern	6-36
6-31	Accuracy of Aircraft Fixes - 5.5 Hour Flight - DC-6 "Worst Case" Conditions	6-40
6-32	Comparison of Ionosphere Model and Measured Range Corrections	6-45
6-33	Satellite and Radar Tracking - DC-6 Aircraft Leaving Atlantic City, New Jersey	6-52

Figure		Page
6-34	Satellite and Radar Tracking - DC-6 Aircraft	6-53
6-35	Departure from NAFEC - January 11, 1971	6-57
6-36	Return to NAFEC - January 23, 1971	6-58
6-37	Differences, Precision Radar and Satellite Fixes. Radar Fixes as Reference. DC-6 - January 11, 1971	6-59
6-38 thru 6-43	Differences, Precision Radar and Satellite Fixes. Radar Fixes as Reference. DC-6 - January 23, 1971	6-60 thru 6-65
7-1	Sister Ship of Valiant, Equipment Used in Ship Tests	7-2
7-2	Circularly Polarized Turnstile Antenna	7-4
7-3	Position Fixes, Coast Guard Cutter Rush in San Francisco Bay	7-6
7-4	Position Fixes of Rush While Underway at Sea	7-9
7-5	Satellite Tracking of Rush While Underway at Sea	7-10
7-6	Satellite Fixes of Rush Drifting at Ocean Station November	7-11
7-7	Track of July 1, 1969 Ship Test	7-13
7-8	Coast Guard Cutter Valiant at Sea During Second Turn. ATS-1 Plot	7-14
7-9	Coast Guard Cutter Valiant at Sea During Second Turn. ATS-3 Plot	7-14
7-10 thru 7-15	Fix Error Distribution - US Coast Guard Cutter Valiant	7-10 thru 7-21
8-1	ATS-Buoy Subsystem Block Diagram	8-3
8-2	Polarization Diversity and Antenna Array	8-4
8-3	140 Megacycle $E\theta$ Antenna Pattern	8-5
8-4	140 Megacycle $E\phi$ Antenna Pattern	8-6
8-5	Ranging and Data Readout Signals from Sea Robin Buoy	8-11
8-6	Ranging and Positioning	8-13
8-7	Estimated Buoy Position	8-15
8-8	Diurnal Variation of Latitude Measurement Error	8-16

Figure		Page
8-9	Distance from Estimated Buoy Position	8-18
8-10	Estimate of Residual Errors After Correction for Ionosphere and Satellite Position Uncertainty	8-19
8-11	Response/Pitch and Roll Angles	8-21
8-12	Bit Error Rate Versus Signal-to-Noise Ratio	8-27
8-13	Performance Curve for a Typical FM Receiver for a Modulation Index of 2	8-28
9-1	Ford Econoline Van	9-2
9-2	Range Measurements Through ATS-3 Using Van	9-3
9-3	Route of March 27, 1969 Test	9-4
10-1	L.E.S.T. Experiment System Block Diagram	10-3
10-2	Typical Waveforms - L.E.S.T. Experiment	10-4
10-3	Linear Characteristics of Discriminator	10-5
10-4	L.E.S.T. Circuit Modifications	10-6
11-1	One Way Range Bias Due to Tropospheric and Ionospheric Retardation	11-2
11-2	Electron Content Due to Magnetic Storm	11-5
11-3	Correlation of Differences Between Computed and Measured Slant Ranges - Gander, Newfoundland and Schenectady, New York	11-11
11-4	Correlation of Differences between Computed and Measured Slant Ranges - Reykjavik, Iceland and Shannon, Ireland	11-11
11-5	24 Hour Ranging Test - Gander-ATS-3-Observatory	11-12
11-6	Effect of Scintillation	11-15
11-7 thru 11-11	24 Hour Ranging Test - Gander-ATS-3-Observatory	11-18 thru 11-24
11-12	Curve of Electron Density Computed from Measurements Made by Air Force Cambridge Research Laboratories	11-25
11-13	Uncorrected Latitude Determinations (Gander)	11-26

Figure		Page
11-14	Gander Latitude Determinations Corrected According to AFCRL Data	11-28
11-15	Gander Latitude Determinations Corrected by Schenectady Range Calibration Measurements	11-29
11-16	Gander Latitude Determinations Corrected by Schenectady Range Calibration Measurements Shifted One Hour in Time	11-30
11-17	Difference, Measured and Computed Slant Ranges - Shannon	11-32
11-18	" " " " - Gander	11-32
11-19	" " " " - Schenectady	11-33
11-20	" " " " - Seattle	11-33
11-21	Day-to-Day Correlation - Shannon	11-35
11-22	" " - Gander	11-35
11-23	" " - Schenectady	11-36
11-24	" " - Seattle	11-37
11-25	Correlation of Diurnal Changes for Schenectady and Gander	11-39
11-26	" " " " " "	
	Shifted One Hour in Time	11-40
11-27	Difference, Measured and Computed Slant Ranges—Four Stations	11-41
11-28	Measured Minus Computed Slant Ranges - ATS-3 to Shannon	11-43
11-29	" " " " to Reykjavik	11-44
11-30	" " " " to Gander	11-45
11-31	" " " " to Schenectady	11-46
11-32	" " " " to Buenos Aires	11-47
11-33	" " " " to Thule	11-48
11-34	24 Hour Ranging Test - Gander-ATS-3-Observatory	11-51
11-35	Correlation of Differences Between Computed and Measured Slant Ranges - Gander, Newfoundland and Schenectady, New York	11-52
11-36	F-Layer Critical Frequency - Buenos Aires Monthly Averages	11-54

Figure		Page
11-37	Scintillation Observed at Hamilton, Massachusetts by AFCRL	11-55
11-38	VHF Amplitude Scintillation - ATS-3 to Schenectady, N.Y.	11-57 thru 11-60
II-1	Range Error Due to Ionosphere, Day and Night, Versus Elevation Angle	11-3
II-2	Diurnal Variation in Range Due to Ionosphere (Normalized)	II-4
III-1	Effect of Local Radio Frequency Interference on Tone-Code Ranging Signal Received in DC-6 Aircraft	III-2
III-2	Effects of ATS-3 Spin Modulation on Tone-Code Ranging Signal Received in DC-6 Aircraft	III-3
III-3	Sample of Data Supplied by Federal Aviation Administration	III-4 & III-5

LIST OF TABLES

Table		Page
3-1	Transmitted Powers and Antenna Configurations of Transponders Used in Tests	3-5
4-1	Equipment Performance Test Data	4-14
4-2	Sample Computer Print-out	4-29
4-3	Sample Computer Print-out	4-30
5-1	Effect of Spin Modulation	5-29
6-1	DC-6 Aircraft Data	6-41
6-2	C-135 Aircraft Data	6-42
6-3	FAA DC-6B Enroute from NAFEC, Atlantic City, New Jersey to Griffiss Air Force Base, Rome, New York	6-47 thru 6-50
6-4	FAA DC-6B on Taxiway at Griffiss Air Force Base, Rome, New York	6-51
6-5	DC-6B Aircraft on Bench Mark at Shannon, Ireland Airport	6-54
8-1	ATS Margin - Down Link	8-8
8-2	ATS Margin - Up Link	8-9
8-3	Statistical Data on Buoy Responses	8-24
10-1	L.E.S.T. Word Tests	10-8
11-1	Tropospheric and Ionospheric Propagation Effects	11-3
11-2	Two-way Slant Range Day-Peak-to-Night Minimum Delay Change	11-7
11-3	Two-way Slant Range Day-Peak-to-Night Minimum Delay Change	11-7
11-4	Communication Performance During Scintillation	11-16
11-5	Largest Deviations - 24 Hour Ranging Test - March 1970	11-19
11-6	ATS-3 Position Predictions for November 8	11-34
11-7	Satellite Elevation Angles	11-49

SECTION 1

INTRODUCTION

A growing population and a growing economy in the United States and throughout the world are causing greatly increased travel and shipping for commercial, pleasure and military purposes. Technological developments are increasing the already wide range of speed, size and maneuverability of the ships and airplanes that must share the surface and air space. It is evident that there would be great value in a single world-wide full-time system that combines the functions of accurate frequent position fixing with the current positions simultaneously available ashore and a capability for communication of essential information between traffic advisory and control centers and the craft that are enroute.¹

The Applications Technology Satellites, ATS-1 and ATS-3, of the National Aeronautics and Space Administration were used in a series of tests to determine the usefulness of VHF for locating mobile vehicles by range measurements from satellites. The specific objectives of the experimental program conducted by the General Electric Company for NASA under contract NAS5-11634 were as follows:

1. Demonstrate the feasibility of ranging and position fixing from synchronous satellites to small mobile terminals at VHF radio frequencies. It was expected that the experiment would demonstrate position fixing accuracies adequate for transoceanic air traffic control.
2. Demonstrate the advantages of a tone-code (pulse train) ranging technique that offers promise of the highly efficient use of satellite energy in simple implementation that is compatible with presently used communication equipment. In operation, the system would be easily retrofitted in existing aircraft.
3. Obtain data over a large geographical region at various times of the day to indicate the variations in ranging and position fixing accuracies caused by location and time of day.
4. Demonstrate the General Electric Company's Low Energy Speech Transmission (L.E.S.T.) technique. In an operational system, this technique would be compatible with tone-code ranging in such a way that the pulsed voice transmissions could be used in the range measuring process.

NASA's Applications Technology Satellites have shown the feasibility of voice communications between aircraft and ground terminals. Airlines that fly transoceanic routes desire to replace their inadequate HF voice communication links with the far more reliable satellite links. It is generally agreed that a satellite system should also provide surveillance of aircraft positions for air traffic control over the oceans, so that lateral spacings between the transoceanic routes can be reduced and economy of operations improved. An early implementation of an aeronautical satellite system is technically feasible at VHF. When suitable aircraft antennas and other avionics equipment have been developed the L-band frequencies, 1540 to 1660 MHz, will offer the possibility for improved performance and a sufficient number of communication channels to accommodate many users.

It is widely recognized that the maritime services would benefit from improvements in communications, radio navigation and radio location that could be provided by the use of satellites. Traffic control of ships in confluence areas could reduce the number of ship collisions and improved position fixing could reduce the number of groundings. Weather routing of ships could result in substantial savings. Satellite links can contribute to improved efficiency and productivity of marine operations and aid in ships automation.

Satellites may be useful for data readout and location of remote unmanned sensors such as oceanographic buoys. Buoy location and readout were tested in parallel with the NASA contract under Navy contract N00014-68-CO467. Results of the buoy experiment are included in this report.

One purpose of this report is to present information that will aid in the determination of the feasibility of using satellites in radio navigation and radio location systems and provide the basis for estimating performance and cost of such systems.

Another purpose is to provide experimental results pertaining to all principal factors affecting the use of satellites for position fixing, especially as they influence performance at VHF. The data collected from the experiments can be used to estimate the performance that would be achieved with other system parameters and ranging techniques at higher radio frequencies.

The magnitude of the experimental program and the widespread interest in it is evident in the list of active participants. In addition to NASA and the General Electric Company, they included the Office of Naval Research, the U.S. Coast Guard, the Federal Aviation Administration, Pan American Airways, the Boeing Company, Aeronautical Radio Inc., Comsat Corporation, the Irish Department of Posts and Telegraphs, the Canadian Department of Transportation, the Civil Aviation Administration of Iceland, the Argentine Air Force, and Air Force Cambridge Research Laboratories.

It is hoped that the information this report contains will be useful to the numerous organizations that are studying the application of satellites to navigation and traffic control.

REFERENCE

1. Anderson, Roy E., "Study of Satellites for Navigation"; General Electric Company report for the National Aeronautics and Space Administration on contract NASw-740; February 1964.

SECTION 2

CONCLUSIONS AND RECOMMENDATIONS

Conclusions

- Narrow bandwidth (2.4 kHz tone, 15 kHz RF) ranging signals yielded a ranging precision better than ± 500 feet, 1 sigma, from a ground station through a geostationary satellite to a user craft.
-

The standard deviations of ranging measurements from the ground station to the satellite were approximately 0.3 microsecond (150 feet) under good conditions, and approximately 0.7 microsecond (350 feet) under worst conditions. Standard deviations on the measurements from the ground station through the satellite to a distant transponder and return were approximately 0.5 microsecond (250 feet) under good signal conditions, and 1.4 microseconds (700 feet) under worst signal conditions (Section 4), but not including the effects of sea reflection multipath for aircraft in flight (Section 6).

- A simple model of the ionosphere was adequate to correct position fixes to within approximately one nautical mile, one sigma. (Appendix II).
-

The "Posfix" computer program contained estimates of ionospheric delay as a function of time of day and elevation angle to the satellite. Range measurements were entered into the computer; an initial fix was computed. The initial fix was not printed out, but used to determine the time of day and elevation angles for entry into the sub-routine to compute range corrections. The corrected range measurements were used in a second computation of the fix, which was then printed out. All of the fixes determined in the experiment used this technique. A more refined technique would use real-time ionosphere range measurements based on range measurements to fixed reference transponders.

- Range measurements to fixed ground transponders were useful for correcting range measurements to other transponders 1000 nautical miles distant to within approximately 1500 feet, 1 sigma, at the worst times of "normal" days.
-

Differences between measured and computed slant ranges were determined for fixed transponders at Shannon, Reykjavik, Thule, Gander, Buenos Aires, Schenectady and Seattle. (Section 11). Comparisons of differences, with allowance for difference in sun time, yielded correlations between ionospheric delays at separated locations. Comparisons were made for nearly continuous ranging over twenty-four hour periods, and at intervals during four days following a solar flare, as well as for various times throughout more than a year. The measurements were compared with independent measurements of electron density made by Air Force Cambridge Research Laboratories. All of the measurements would permit ionospheric delay corrections between stations separated by 1000 miles or more to within 1500 feet, but we did not obtain measurements during sunset on a day of a solar disturbance when there would be an abnormally high electron content in the ionosphere. The standard deviation of range measurements did not increase more than approximately 200 feet when severe amplitude scintillation was present.

Amplitude scintillation is caused by moving horizontal gradients in electron density within the ionosphere that focus energy onto or away from a point on or near the earth's surface. There is only a small change, of the order of 2 percent, along the ray path, and hence a small change in propagation delay.

The standard deviation of range measurements made during severe amplitude scintillation was found to increase from the non-scintillating value of approximately 0.5 microsecond to not more than 0.9 microsecond. Most of the increase in standard deviation may have been due to changes in receiver time delay as the signal level changed rather than by the ionosphere. There was no observable change in range measurements associated with the scintillation. (Section 11)

● The largest single source of bias errors in position fixes and lines of position was error in predictions of satellite position.

This is an error that could be reduced by more frequent tracking of the satellite, and perhaps by using longer baselines for the range and range rate measurements than are the usual practices in tracking ATS-1 and ATS-3.

NASA provided satellite position predictions at half hourly intervals with a resolution of 0.001 degree in latitude and longitude and 0.01 nautical mile in earth center-to-satellite distance. The round-off in latitude and longitude limit the resolution of position fixes to 360 feet, and the altitude round-off will add an uncertainty of the same magnitude. (Section 5).

The satellites are not in perfect geostationary orbits, and therefore move north and south of the equatorial plane, tracing a figure "8" pattern and also, changing altitude, with a twenty-four hour period. (Section 5)

Most fix computations were made with a linear interpolation between the half hourly position predictions. The computer program was later modified to make a cubic interpolation, and thus keep the interpolated values to within the 0.001 degree and 0.01 nautical mile altitude limits.

NASA tracked the satellites at intervals of a few weeks and computed the positions for the times in between. A comparison of a predicted position from the previous tracking epoch with the computed position for the same time based on a new tracking epoch showed the predictions could be in error more than 0.02 degree and 0.3 nautical mile in altitude. These can combine to cause position fix errors as large as 3 nmi. (Section 5). A diurnally changing position fix error can result if an erroneous satellite prediction is used in the calibration of the time delay through a transponder. (Section 5).

● A timing error on the received signal at the user transponder causes the position fix to be displaced along a hyperbolic line of position.

A sharp scintillation fade, a signal drop due to spin modulation, or multipath reflection, or noise on the signal received by the user transponder can cause a phase error so that the user's response is displaced in time from its correct value. The returns of the signals relayed by the satellite are displaced equally so that the same error occurs on both range measurements from satellite to user. While the absolute value is wrong, the difference in the two range measurements is not affected, and the position fix is displaced along a hyperbolic

line of position. The largest error due to these causes was eleven miles (Section 6). The magnitude of errors due to these causes can be changed by selection of different signalling parameters.

- An infrequent fix error of integral multiples of approximately 75 miles resulted from improper operation of the address code correlator.

Improper setting of the correlation threshold combined with noise or interference could result in correlation during an incorrect bit interval of the code. The bit interval was 409 microseconds, the period of one tone cycle. Correlation on an early bit period resulted in an error of an integral multiple of 409 microseconds, displacing the fix along a hyperbolic line of position. For the eastern United States, the fix displacement was a multiple of approximately 75 miles. Under good signal conditions and proper setting of the correlators, the effect was virtually non-existent. Under worst conditions, it sometimes occurred on approximately one-tenth to one percent of the range measurements. Better selection of signal parameters and the use of a different modulation for the code, such as PSK instead of suppression of an audio cycle would reduce the occurrence to a low value, perhaps one in 10^{-6} or 10^{-7} .

- If three or more satellites were available, a simple, inexpensive transmitter on a vehicle could be used for surveillance by the hyperbolic location technique.

A coded transmission originating on the craft can provide hyperbolic lines of position by measuring differences in times of arrival at the ground terminal. This was demonstrated in the experiment when poor signal levels, or correlation on an early bit period caused a time displacement of the vehicle response. An equal error was added to range measurements of both satellites, and fixes were displaced along hyperbolic lines of position. (Section 6). A third satellite would have determined two hyperbolic position lines and a fix. A simple tone-code generator attached to a transmitter on the vehicle would suffice for position location.

- Range measurements for position fixing were made in approximately one second.

Ranging interrogations were initiated at a ground station, relayed to all user craft through one satellite; the one user craft that was addressed automatically transmitted a single response that was relayed back to the ground station by two satellites. Propagation time intervals were measured at the ground station, and fixes were computed. The process was accomplished more than one hundred thousand times. (Section 3).

During the experiment, the interrogation and response signals and the built-in user equipment delays were approximately 0.43 second, making a total measurement time of approximately 1.3 seconds to complete the measurements. The signals can be redesigned to complete the process in less than one second.

- Transmission link reliability for mobile craft was not adequate for operational use under most conditions of the experiment.

Poor signal levels, especially on the down link from the satellite to mobile craft, resulted from low vehicle antenna gain combined with irregular patterns, Faraday rotation of the satellite's linearly polarized signals, multipath, and spin modulation of ATS-3. Ionospheric scintillation caused fading of the signals an estimated 5 percent of the time at Schenectady. Interference from routine air traffic control transmissions on channels adjacent to the satellite down link frequency were sometimes experienced during aircraft flight tests in the New York-New Jersey-Pennsylvania area.

- Transmission link reliability with the ground reference transponders was adequate for operational use under all conditions of the test.

The eight-turn helical antennas, with a net gain of 9 dB, combined with 100 to 300 Watts of transmitter power of the transponders provided excellent voice communications and ranging at all times when they were properly adjusted and used.

- Operationally acceptable transmission link reliability could be achieved with the effective radiated power of the ATS VHF transponders, but with circular polarization of the satellite antennas and 0 dB, circularly polarized vehicle antennas.

The estimate is based on an interpolation of the performance achieved with the mobile craft and the ground reference transponders. It is also based on our evaluation of the performance of the VHF transceiver and crossed slot antenna on the Boeing 747 aircraft. The term "operationally acceptable" describes reliability and signal quality that is far superior to long range HF or MF communications for aircraft and ships over coverage areas far exceeding those available from extended range VHF for aircraft. The tests did not yield sufficient data to determine that the reliability would meet the specifications for aircraft satellite communications stated by international committees that have studied the requirements.

- Tone-code ranging at VHF with voice bandwidth signals could be used for surveillance of aircraft in oceanic areas to maintain separation standards.

Under the worst conditions of the test, the accuracy of aircraft position fixes off the east coast of the United States was better than the accuracy specified for the inertial navigation system of the 747 aircraft after five hours of flight time. (Section 6) Nominal accuracy of the system, as exemplified by the ship tests (Section 7) equalled the accuracy specified for the inertial navigation system after one hour of flight. Precision of the satellite fixes is poorer than for the inertial navigation system, but long-term accuracy is better because satellite surveillance does not accumulate significant error during an aircraft flight or a ship voyage. If the inertial navigation system is adequate for maintaining separations of aircraft on transoceanic flights, it is evident that the more accurate tone-code ranging technique with satellites is also adequate.

- A VHF tone-code ranging transponder for satellite communication, position surveillance, and navigation could be installed on a ship for less than \$10,000.

The cost estimate is based on the cost of providing and installing the prototype transponders on the Coast Guard Cutters Valiant and Rush. The unit would be used for long range voice and data communication, and by changing to another channel could also be used for direct harbor and bridge-to-bridge communication. Navigation could be provided by transmitting fix computations from the ground station through the satellite to the ship.

Recommendations

Many of the recommendations that follow refer to tone-code ranging. The reference is to the broad technique of tone-code ranging and is not restricted to the RF frequency bandwidth parameters or modulation technique used in the experimental program. The tone-code ranging technique can be applied at any radio carrier frequency, with any radio frequency and modulation bandwidths and with any type of modulation that is capable of transmitting a signal that has at least one frequency component that has a coherent phase. Tone-code ranging as used in these recommendations refers to the technique of transmitting a repetitive signal such as a sine wave tone or a digital transmission clocked at a fixed rate, in which case the tone may be the highest frequency component of a square wave, and the repetitive signal followed by an identifying code which is transmitted coherently and at the same bit rate as the repetitive signal. At the receiver a locally generated signal at the same repetition rate as the transmitted signal is generated and shifted in phase to match the phase of the received repetitive signal. A correlator adjusted to recognize the individual identification code identifies the source of the received signal and produces a single output timing pulse that is an unambiguous measure of the time of the reception of the tone-code signal.

The broadcast transmission of a tone-code signal to a field of user craft results in the response from the one user craft that is addressed and the measure of the time from the initial transmission to the return provides a range measurement to the craft.

In another application of the technique, a transmission from a user craft is received at two separated locations which have a common timing reference or which relay their signals back to a common point. The difference in arrival time at two known points is measured, and used to compute a hyperbolic line or surface of position for the craft.

In a third application the transmission of tone-code signals is clocked from a universal time reference. User craft that have an on-board time reference in accurately known relationship to the universal time reference can measure the time of arrival of the signals and determine their own range from the transmitting source. Signals received from two sources at known locations are sufficient to determine a fix. Alternatively, reception of the signals transmitted from the universal time source and received at known locations can be used to set clocks at the known locations accurately with respect to the distant universal time source.

In a passive navigation system, tone-code signals may be transmitted in known time relationship from two or more known locations. The differences in arrival times of the signals aboard a craft can be used to determine hyperbolic lines of position.

- Consider tone-code ranging as a candidate for operational surveillance and navigational systems that use satellites.

Tone-code ranging is well adapted to the surveillance of many targets in any desired order. It does not require the simultaneous reception and transmission by the user craft and a simultaneous comparison at the ground station of transmitted and received phases. The transmissions can be short compared to the propagation time through synchronous satellites and therefore it is feasible to interrogate and get responses from several users within the time it takes the signals to propagate from the ground station through the satellites to the users and return. Several position fixes can then be determined within a second. It is also feasible for the user's response to be relayed back to the ground station through more than one satellite so that a position fix can be determined from a single interrogation as was demonstrated thousands of times during the experimental program.

Tone-code ranging results in an unambiguous measurement of range with a single tone frequency. Selective calling of individual craft and identification of the responses is contained in the tone-code signals. No duplexer is required aboard the user craft, thus eliminating a possible source of range measurement error and reducing cost of an installation. Tone-code ranging is compatible with many types of communications. If the communication signals contain coherent frequency components, they can be used for setting the phase of the tone-code responder. The ranging technique then becomes very efficient because a ranging signal then only requires the transmission of a ranging identification code. The technique can be used with or without coherent carrier detection. Tone-code ranging can be as accurate as any technique at any radio frequency because it is not limited in the radio frequency or modulation frequency bandwidth. It can be used with narrow bandwidth or wide bandwidth systems and at any radio frequency.

- Proceed with tone-code ranging tests at L-band.

This report is the final report of the first two phases of contract NAS5-11634. Work has started to add an L-band capability to the Radio-Optical Observatory and a tone-code ranging transponder. Initial experiments will compare L-band and VHF transmissions using NASA's ATS-3 and ATS-5 satellites. The General Electric Company is developing a 300 Watt solid state L-band power amplifier that will be used for the first time in these experiments.

- Test tracking of ships in a confluence area relative to a fixed transponder.

Tests with the Coast Guard Cutter Rush at San Francisco suggest that a ship can be tracked with a precision that may be useful in outer confluence areas and perhaps at closer approaches to harbors, even at VHF and with the narrow bandwidth of voice communications. The tests at San Francisco did not include a fixed reference transponder for real-time correction of the errors due to satellite position prediction and ionosphere. Further tests using equipment that is now on hand would permit a more complete evaluation of this technique. The tests would be conducted by placing a fixed ground reference transponder near a harbor area and tracking a ship by satellite and also by radar and visual sightings. Accuracy of single fixes and the average of several sequential fixes taken by satellite would be compared with the non-satellite position determinations.

- Test tracking of land mobile vehicles.

Several inquiries have revealed that there are applications for tracking land mobile vehicles by satellite. Tests with the van and with the ships have shown that it is feasible to track land mobile vehicles with modest additions to conventional mobile radio communications equipment. Requirements should be defined, suitable antennas selected, and tests conducted using conventional mobile radio transmitters and receivers with tone-code responders attached between them.

- Test satellite surveillance of aircraft in comparison with Inertial Navigation and other on-board systems on commercial flights.

The objective of the tests is to verify the better long-term accuracy indicated for the satellite surveillance system, to test procedures for traffic control using satellite surveillance, and to test the use of the satellite position fixes for updating the on-board navigation equipment.

- Test tone-code ranging signals integrated with several types of communication signals such as digital communications by frequency shift keying, phase shift keying, voice signals by delta modulation, pulse code modulation, and the transmission of signals by spread spectrum techniques.

- Test tone-code ranging at rates of several interrogations per second.

The tone-code ranging transponders used in the L-band experiments will employ transmissions which are approximately 30 milliseconds in duration instead of the 400 milliseconds used in the previous experiments. It is considered feasible to interrogate several transponders in rapid sequence and get their returns without overlap to demonstrate the potential for handling a very large number of user craft on one ranging channel.

- Use the existing widespread network of VHF transponders for ionospheric propagation measurements.

Ionospheric propagation measurements were made at infrequent intervals throughout the experiment. Sufficient data were collected for evaluating the influence of the ionosphere on satellite range measurements at VHF, although data were not collected during times of severe ionospheric disturbance. The widespread network is a unique facility for synoptic measurements of ionospheric propagation. The data taken on the January 19-20, 1971 twenty-four hour test demonstrated the use of the network. The distant transponders are fully automatic and the data that are collected by their use are immediately available at the central location where it is to be collected and processed. The tone-code ranging technique and the network of transponders makes it possible to sample the ionosphere at any desired time and at any desired location where a transponder is in place. The permanent installation of a transponder in the far north, as at Thule, and of transponders in regions such as Buenos Aires, where an intriguing diurnal pattern of electron content variation was noted in the January tests, would be useful in collecting data at lower cost and greater convenience than is available by any other means.

SECTION 3

EXPERIMENT DESCRIPTION

The first satellite ranging measurements of this experimental program were made in the autumn of 1968. Between the time of the first measurements and the preparation of this report, 290 files of data were logged on satellite ranging measurements, totaling 205 hours on ATS-3 and 73 hours on ATS-1. Both satellites were used in two-satellite ranging experiments for a total of 63 hours. Experiments were conducted at all hours of the day and night, in all seasons of the year, and involved geographical locations as widely separated as Thule, Greenland; Buenos Aires, Argentina; Shannon, Ireland; and Hawaii.

In addition to the ranging and position fixing experiments, other experimenters were assisted with their programs involving ships, aircraft and NASA ground stations.

General Electric's Radio-Optical Observatory near Schenectady, New York (Figure 3-1) served as the control station in the experiments. Ranging measurements were made to remote transponders on two aircraft of the Federal Aviation Administration in flight over the continental United States and over the North Atlantic Ocean as far north as Thule, Greenland and as far east as Shannon, Ireland; to ships of the United States Coast Guard in the Gulf of Mexico and in the Pacific Ocean; to a buoy moored in deep water off Bermuda; to a panel truck on roads in upstate New York; and to ground-based transponders at Shannon, Ireland; Reykjavik, Iceland; Gander, Newfoundland; Buenos Aires, Argentina; and Seattle, Washington.

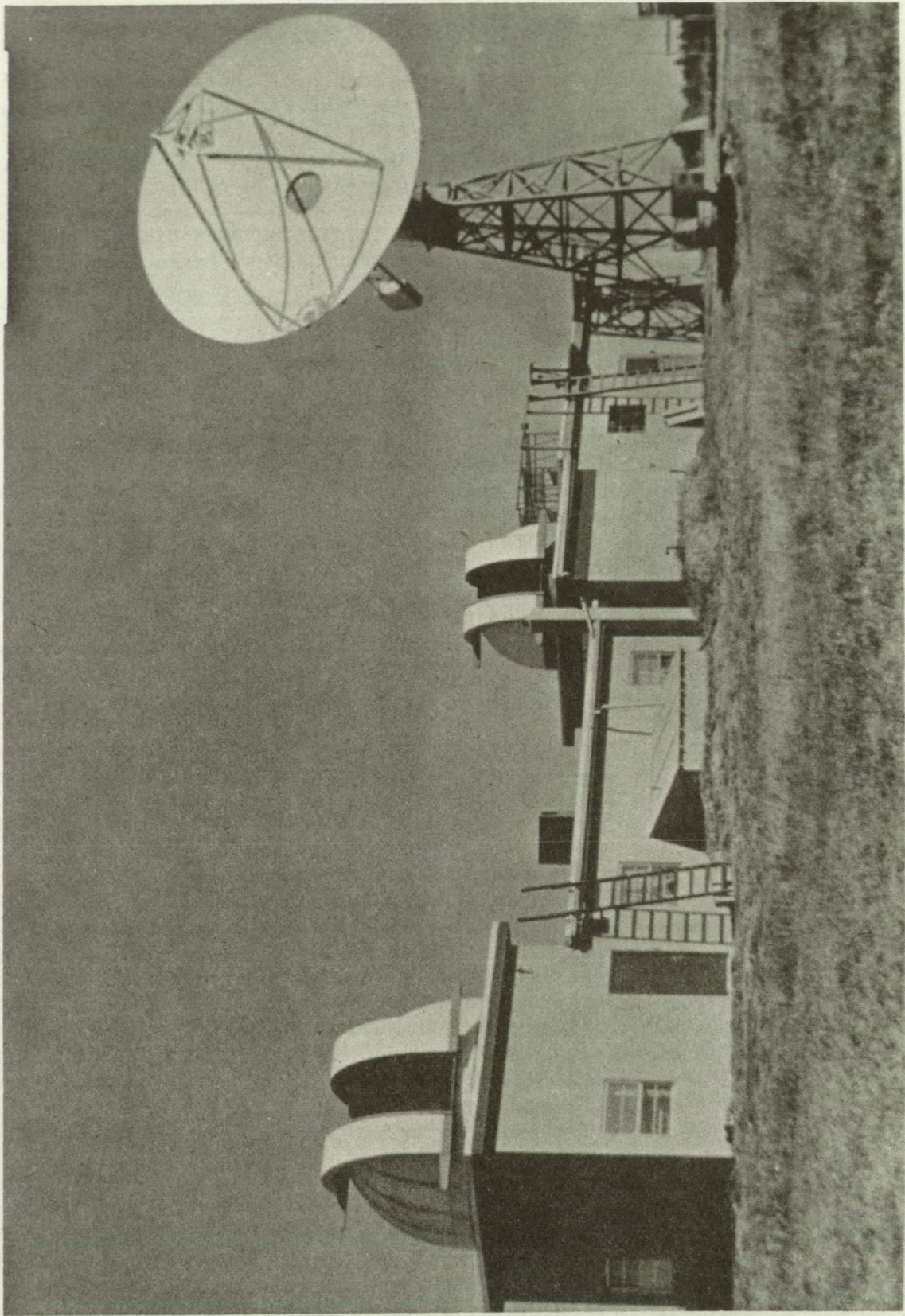
The VHF transponders on NASA's ATS-3 and ATS-1 satellites relayed the signals between the Schenectady control station and the remote transponders. The uplink frequency from the earth to the satellite is centered at 149.22 MHz and the downlink from the satellite to the earth is centered at 135.6 MHz. The bandwidth of the satellite transponders is approximately 100 kHz.

The audio frequency and radio frequency bandwidths for the range measurements were limited to 2.5 kHz audio bandwidth and 15 kHz radio frequency bandwidth in order that the signals be compatible with conventional mobile radio communications equipment and channel assignments. Initial design analyses indicated that these narrow bandwidths would provide adequate ranging resolution to resolve each of the important factors contributing to range error at VHF, and the narrow bandwidth would not limit the accuracy of position fixes. The experiment confirmed the analyses. A one sigma ranging resolution of approximately 200 feet was achieved on single measurements, and a resolution of approximately 50 feet when a number of measurements were averaged.

The experiment demonstrated for the first time that it is practical to locate mobile craft by range measurements from two satellites with a single interrogation from a ground station and a single response from the mobile craft. A short "tone-code" interrogation signal containing a single frequency tone burst followed by a user's address was transmitted from a ground terminal to ATS-1 or ATS-3. The satellite repeated the signal. All of the activated transponders within range of the satellite received the interrogation and each

FIGURE 3-1

RADIO-OPTICAL OBSERVATORY AT SCHENECTADY, NEW YORK



one matched the phase of a locally generated tone to the received tone phase. The unit that was addressed recognized its own code, and transmitted a response through an omnidirectional antenna. Both satellites repeated the response when both were within view of the unit. The ground terminal measured the time from the initial transmission to the return of the interrogating signal from the one satellite, and to the returns from the user as relayed by the two satellites. The time measurements were stored on punched tape and later inserted into a computer. The known equipment delays of the user transponder and the satellites were subtracted from the measurements, and the ranges from the two satellites to the user were determined. An initial fix determination was made, the local time at the initial fix was noted, and corrections for ionospheric delay were obtained from a model of the ionosphere stored in the computer. Range corrections were applied, and the position fix determined by another iteration of the computation.

When a transponder was in view of only one satellite, lines of position were determined from the single range measurements. Computer programs were used to compute the latitude at which the line of position crossed a given longitude, or the longitude at which the line of position crossed a given latitude.

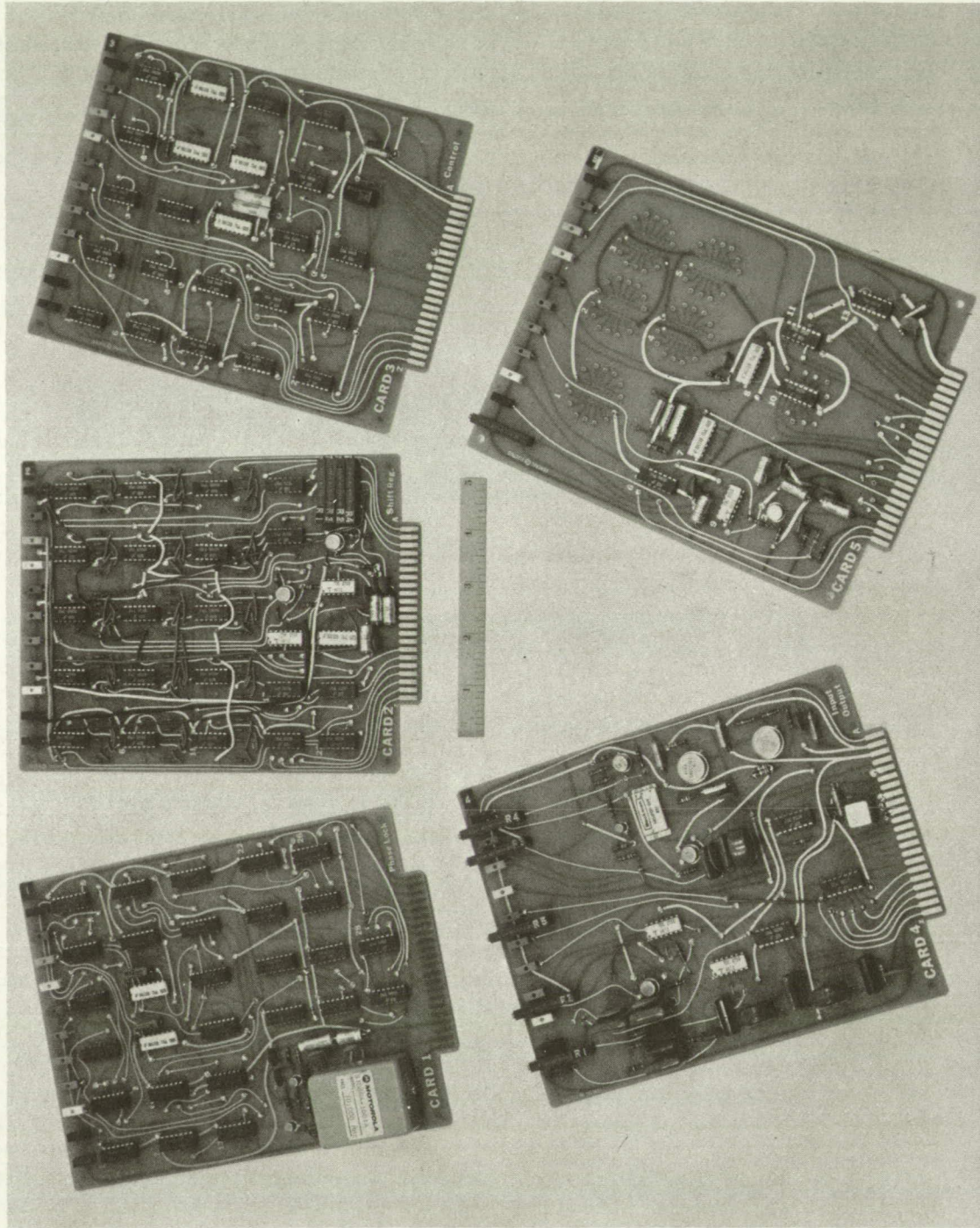
Other data were also collected during the experiment, such as the standard deviations of range measurements between the ground terminal and the satellite, and between the satellite and transponders aboard mobile vehicles or at fixed locations. Ionospheric delays were measured, and observations were made of Faraday rotation, ionospheric scintillation, and sea reflection multipath. Voice and data transmissions were made with the same transmitters and receivers used for ranging.

The fixed transponders at Shannon, Ireland; Reykjavik, Iceland; Gander, Newfoundland; Buenos Aires, Argentina; and Seattle, Washington were used to measure ionospheric propagation characteristics, effects of satellite position prediction inaccuracy, and to test a calibration technique.

The ground control terminal used in the experiment was the Radio-Optical Observatory, located at 42°50'53" North latitude and 74°05'15" West longitude. Interrogations were transmitted to the satellites on 149.195, 149.22 or 149.245 MHz with a transmitter power of 300 Watts. Transmissions were through a 30 foot diameter parabolic antenna having a log periodic feed with selectable linear polarization. The same antenna was used to receive the signals from the interrogating satellite. In the later phases of the experiment a means was provided to switch polarization independently for transmission and reception. Except for brief tests, or when only ATS-1 was in use, the 30 foot antenna was used with ATS-3. When interrogations were made through one satellite and responses received from both satellites, the signals from one satellite were received on the 30 foot antenna, and the signals from the other were received on either a two-bay crossed yagi or a helical antenna. The two-bay crossed yagi antenna had 16 dB of gain and a choice of vertical and horizontal polarizations. The eight turn helical antenna, Figure 3-2, was circularly polarized and had an effective gain of 10 dB when used with the linearly polarized satellite signals.

Signals returned from the satellites were on 135.575, 135.6 or 135.625 MHz. The received signals were applied to pre-amplifiers with a noise figure better than 3 dB, and then detected in FM receivers with IF bandwidths of 15 kHz.

FIGURE 3-2
EIGHT TURN HELIX ANTENNA



Specially designed and constructed circuits detected the timing signals, and electronic counters measured the time intervals. They were then recorded on punched paper tape together with time of day, and information pertaining to digital bit error rates in the received user identification codes. Paper chart recordings were made of signal level and incremental time delay changes. Magnetic tape recordings of digital data returns were made when data were included with the responses.

All of the vehicles and the fixed reference stations used in the test were equipped with FM mobile radio transmitters and receivers with tone-code ranging transponders attached. The transmitted powers and the antenna configurations used on the vehicles are given in Table 3-1.

Table 3-1

TRANSMITTED POWERS AND ANTENNA CONFIGURATIONS OF TRANSPONDERS USED IN TESTS

<u>VEHICLE</u>	<u>POWER</u>	<u>ANTENNA</u>
Buoy	120 W	Selectable linearly polarized dipole.
KC-135	500 W	VHF blade.
DC-6B	500 W	VHF blade and circularly polarized horizon and zenith mode Satcom antenna.
Ship	300 W	Circularly polarized.
Van	80 W	Separate receive and transmit linearly polarized dipoles.
Fixed Reference Stations	300W*	Eight turn helices, circularly polarized, effective 10 dB gain.

*100 W at Shannon, Ireland

The tone-code signal consisted of an audio frequency tone burst followed by a digital address code. The tone burst was 1024 cycles of 2.4414 kHz. The digital address code had 30 bits. A digital "one" was a single cycle of the audio frequency tone and a digital "zero" was a suppressed cycle. The time duration of a complete tone-code signal was approximately 0.43 second. Tone-code ranging is described in detail later in this section.

The tone-code signal modulated the transmitter with a deviation of approximately 5 kHz, resulting in an RF bandwidth for the signal of approximately 15 kHz. The transmitter was a General Electric Mastr Progress Line Desk Mate® station and 4EF5A1 power amplifier. The 300 Watt, 149.22 MHz (or ± 25 kHz) signal was transmitted to the interrogating satellite, usually ATS-3, through the 30 foot antenna.

The satellite received the interrogation signals, converted them to 135.6 MHz (or ± 25 kHz) and retransmitted them with an effective isotropic radiated power (EIRP) of approximately 200 Watts. Bandwidth of the satellite VHF transponders is approximately 100 kHz. The time delay through the transponder was given as 7.3 microseconds, the value assumed in estimates of equipment delay. Uncertainty in satellite time delay was acceptable since total time delay was calibrated for each transponder equipment with the vehicle at a known location.

Each transponder consisted of an antenna, a mobile communications receiver, a tone-code responder unit, and a mobile radio transmitter. In the responder unit, the phase of a locally generated 2.4414 kHz audio tone is compared with and matched to the received tone phase by adding or deleting pulses in the frequency dividing chain. Each pulse added or deleted shifts the output phase by 0.4 microsecond. In this way, the locally generated tone is shifted in steps until it matches the received tone phase within the small quantized interval. The circuit design is such that the phase can be shifted 180 degrees in either direction within 400 cycles of the audio tone. Reception of only 400 cycles out of the 1024 is sufficient to insure phase match. The phase comparison is averaged over approximately 64 cycles to reduce the effects of noise jitter. When the received address code is recognized, the phase shifting and averaging process ends and the locally generated tone remains at the phase established during the comparison with the received tone phase. The accuracy of the oscillator, better than one part in 10^6 , insures that the tone phase as measured by the timing of the zero crossings of the audio tone will not shift by more than 0.25 microsecond in the following 1/2 second.

At the ground terminal the first signal received back from the satellite was the interrogating signal. The propagation time to the geostationary satellite and return was approximately 0.25 second so that the ground station was still transmitting when the first part of the interrogation signal was returning. Consequently, only the last half of the interrogation was received and applied to the phase matcher-correlator, a circuit like that in the mobile responders except that address codes are selectable with a rotary switch. Because the phase matcher can bring the local tone into phase within 400 cycles, or half the tone period, the duration of the received tone was sufficiently long for the phase measurement. Correlation of the address code resolved the tone period ambiguity, and gated out a single clock pulse to mark the end of the time interval for measuring the range from the ground terminal to the satellite, and the start of the time interval for the range from the satellite to the mobile craft. The response from the craft through the interrogating satellite was received and processed by the same equipment and in the same way as the interrogation return. The full duration of the tone was received. The response relayed through the other satellite was received on a different antenna and receiver, and processed in a different phase matcher-correlator.

Three time intervals were measured and recorded. All three time interval measurements started with the transmission of the interrogation signal from the ground station. The actual start time occurred one clock period, 409 microseconds, after the transmission of the last bit in the user address code. The first time interval, approximately 0.25 second in duration, ended with the correlation of the return from the interrogating satellite. The other two intervals, each approximately 0.9 second in duration, ended with correlation of the vehicle responses through two satellites. The intervals were measured with a timing resolution of 0.1 microsecond.

The time from the start of an interrogation to the completion of the range measurements and recording of the data was approximately 1.3 second.

The time intervals were measured using Hewlett-Packard Model 5245L counters with 5262A time interval plug-ins. The time intervals were punched on paper tape along with Greenwich Mean Time, and a number representing the bits

in error in the word synch and address code. The bits in error were directly related to the amplitude of the correlation pulses from the summing circuits which took on discrete values depending on the number of correct bits in the received code. Correlation could be achieved when as many as three bits were in error in the word synch or the individual address code.

The punched tape data recording format is shown in Figure 3-3. The word and address error rate symbols are separate digital voltmeter measurements of the amplitude correlation pulses of the word synch and the user address in the correlator. Numbers of approximately 10065 indicate zero bits error and 10057 would represent one bit error in the 15 bit codes which were at a digital bit rate of 2.4414 kHz.

In addition to the punched tape recording, a four channel paper chart recording was also made. (See Figure 3-4) The chart speed was 2.5 mm per second and each interrogation and response is resolved along the chart. The last three digits of the time interval measurements for the propagation time measurements from the Observatory to ATS-3 and return were converted from digital signals to an analog voltage and recorded in the third track. The time resolution is 1 microsecond per large division. The slope of the average value results from the changing range from the Observatory to the satellite.

When necessary, as in the data readout of Sea Robin, a magnetic tape recording was made of the received audio frequency signals.

The specific uses of the recorded data are described for each transponder in later sections of this report. The usual data processing included the determination of standard deviations for range measurements. Standard deviations for selected portions of the recorded data were computed relative to a "best fit" quadratic curve. A sample of data processed in this way is shown in Figure 3-5. In some cases, the measurements were plotted as a function of time or as histograms to observe distribution patterns influenced by noise, ionosphere propagation effects, or multipath. Lines of position and fixes were computed to determine precision and accuracy for various conditions.

Tone-Code Ranging Technique

The tone-code ranging technique used in the experiment has the following characteristics.

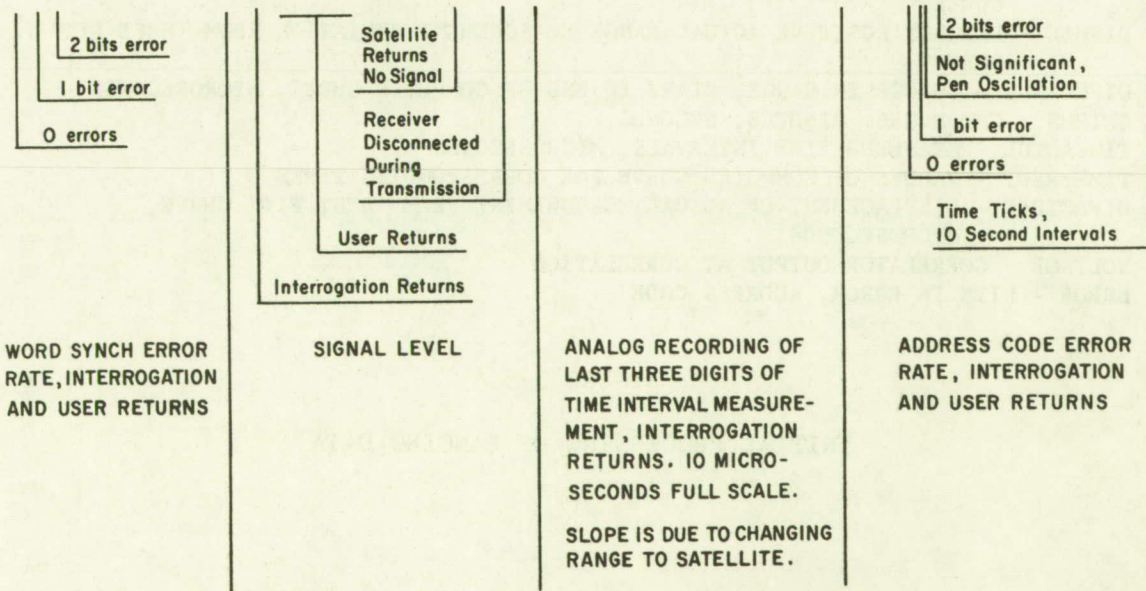
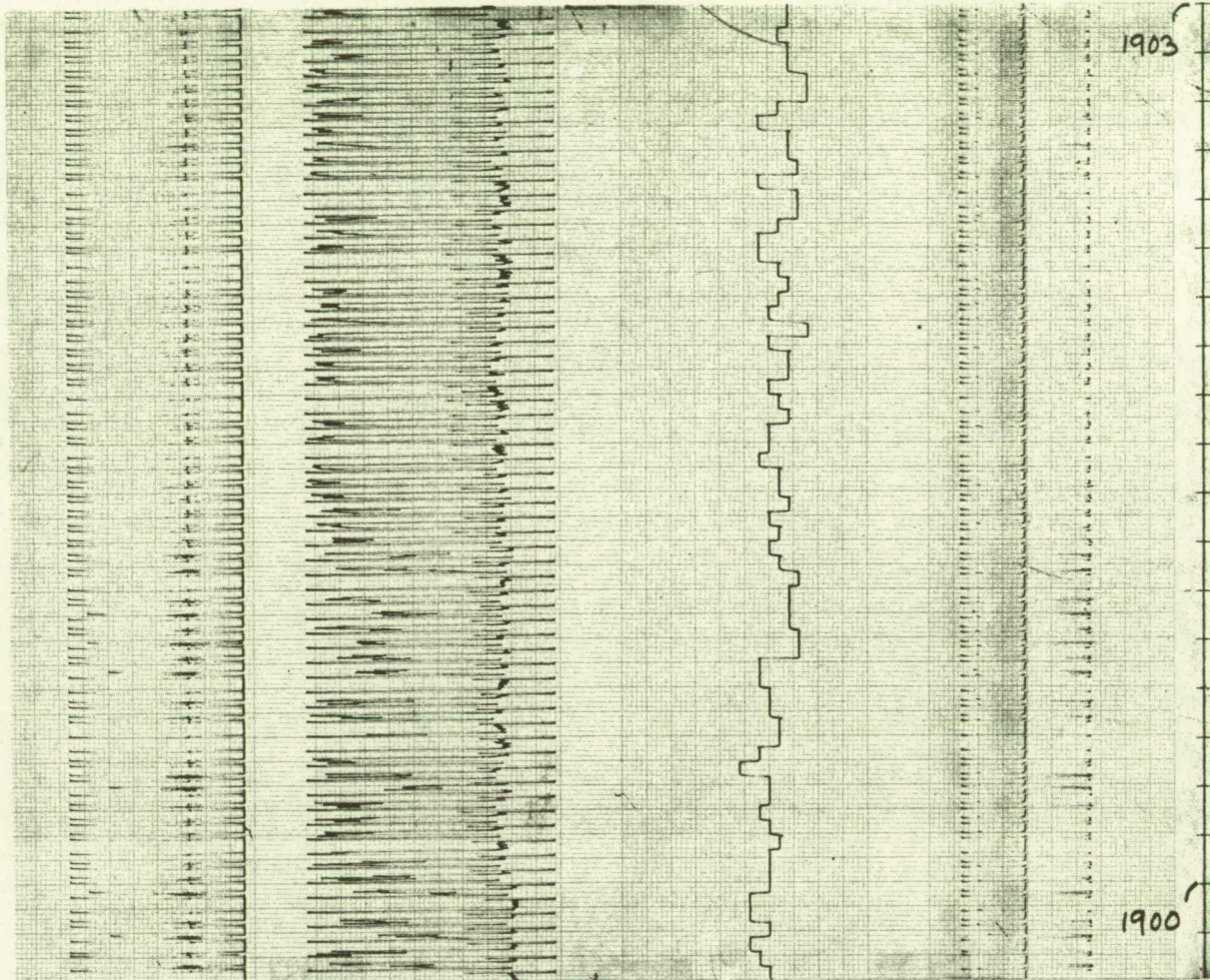
- Useful accuracy can be achieved within the modulation and radio frequency bandwidths of present-day mobile communications.
- The technique can be used with wide bandwidth for high accuracy.
- It requires only one channel for range measurement, receiving and transmitting in the simplex mode if desired without need for an antenna diplexer.
- The time required for a range measurement is a fraction of a second so that it can time-share a communication channel with little additional time usage of the channel.
- It can be implemented by the addition of an inexpensive, solid-state responder unit attached to a communication receiver-transmitter.

FIGURE 3-3
FORMAT OF DATA RECORDED ON PUNCHED TAPE

Time Interval, 0.1 microsecond resolution Observatory-ATS-3-Observatory		User Number	Time, GMT (hours, minutes, seconds)	Time Interval, 0.1 microsecond resolution Observatory-ATS-3-User-ATS-3-Observatory		Time Interval, 0.1 microsecond resolution Observatory-ATS-3-User-ATS-1-Observatory		Word Sync Error Rate	Address Error Rate
02528664	05045356	09304646	09533611	10065423	10066503				
02528659	06045359	09359837	09588263	10065423	10066503				
02528666	05045402	09304640	09533618	10065423	10066503				
02528665	06045405	09359811	09588253	10065423	10066503				
02528668	05045408	09304674	09533628	10065423	10066503				
02528671	06045411	09359833	09588256	10065423	10066503				
02528670	05045414	09304664	09533647	10065423	10066503				
02528681	06045417	09359844	09588282	10065423	10066503				

FIGURE 3-4

ACCURACY OF LINES OF POSITION



FILE 113
 DATE 6/12/69 FAA
 IN FLIGHT END OF RUN
 61240113
 61240113
 61240113
 15255448 63085
 NUMBER OF BAD RECORDS =
 NUMBER OF GOOD RECORDS =

7
 189

IN	NI	TNP	NPU	NPE	GMTLOW	GMTHIG	YMAX	DIFMIN	DIFMAX	SD	ERRORATE
1	1	189	120	123	142010	142958	200.0	-6.02	7.39	2.409E+00	0.
OV	1	189	120	123	142010	142958		-6.02	7.39	2.409E+00	0.

IN	A	B	C
1	-1.52668331E-01	-1.62341159E-01	7.39304170E-06

THATDIINT	THATDIFIN	DIFCHANGE
1360511.3	1360416.3	95.0

K	M	GMT	GMTHMS	TIMEACTUL	TIMEPREDT	DIFACTPRE	VOLTAGE	ERROR
1	12787	142010	1360511.2	1360511.3	-0.1	6.7610	0	
1	12790	142013	1360512.3	1360510.8	1.5	6.7600	0	
1	12793	142016	1360512.2	1360510.3	1.9	6.7610	0	
1	12796	142019	1360508.0	1360509.8	-1.8	6.7590	0	
1	12799	142022	1360508.8	1360509.3	-0.5	6.7600	0	
1	12802	142025	1360506.8	1360508.8	-2.0	6.7610	0	
1	12805	142028	1360511.2	1360508.3	2.9	6.7610	0	
1	12808	142031	1360507.6	1360507.8	-0.2	6.7610	0	
1	12811	142034	1360507.5	1360507.3	0.2	6.7610	0	
1	12814	142037	1360506.8	1360506.8	-0.0	6.7610	0	
1	12817	142040	1360507.9	1360506.3	1.6	6.7610	0	
1	12820	142043	1360509.2	1360505.8	3.4	6.7610	0	
1	12823	142046	1360503.6	1360505.3	-1.7	6.7600	0	
1	12826	142049	1360501.9	1360504.8	-2.9	6.7610	0	
1	12829	142052	1360503.5	1360504.3	-0.8	6.7600	0	

GMT LOW - START TIME OF INTERVAL FOR COMPUTATION OF BEST FIT QUADRATIC
 GMT HIG - END TIME OF INTERVAL FOR COMPUTATION
 YMAX - MAXIMUM DEVIATION IN MICROSECONDS OF A MEASUREMENT THAT WOULD BE
 ACCEPTED IN COMPUTING "BEST FIT" CURVE ($\pm 1/2$ AUDIO CYCLE PERIOD)
 DIFMIN - LARGEST NEGATIVE ACTUAL RANGE MEASUREMENT DEVIATION FROM "BEST FIT"
 CURVE
 DIFMAX - LARGEST POSITIVE ACTUAL RANGE MEASUREMENT DEVIATION FROM "BEST FIT"
 CURVE
 DIFCHANGE - CHANGE IN RANGE, START TO END OF COMPUTED CURVE, MICROSECONDS
 GMTHMS - GMT HOURS, MINUTES, SECONDS
 TIMEACTUL - MEASURED TIME INTERVALS, MICROSECONDS
 TIMEPREDT - VALUES OF COMPUTED CURVE FOR CORRESPONDING TIMES
 DIFACTPRE - DISPLACEMENT OF ACTUAL MEASUREMENT FROM "BEST FIT" CURVE,
 MICROSECONDS
 VOLTAGE - CORRELATOR OUTPUT AT CORRELATION
 ERROR - BITS IN ERROR, ADDRESS CODE

FIGURE 3-5

INITIAL PROCESSING OF RANGING DATA

- It can, but need not, employ digital or digitized voice transmissions to provide synchronizing of the user responder, thereby further increasing the efficiency of channel usage.
- There are no "lane" ambiguities in the range measurements.
- User identification is simple and is confirmed in the return signal.

Range measurements from satellites are made by measuring the propagation time of a radio signal from the satellite to the user and return. The propagation time can then be converted to a range measurement by relating it to the known propagation velocity of the radio signals. The free-space propagation velocity must be corrected for ionospheric and atmospheric propagation effects. Propagation time is measured by placing a time marker in the form of a "tone-code" interrogation (Figure 3-6) on the transmitted signal and observing the time for the tone-code to go to the user and return. As used in the experiment, the interrogation signal is a short audio frequency tone transmission followed by a digital address code in which audio cycles are inhibited for zeros, transmitted for ones. Improved performance would result from the use of phase shift keying. The simpler format was chosen early in the experiment for convenience, and was not changed as its performance fulfilled the test requirements.

Each user transponder is assigned a unique digital address code. When the user's fix is to be determined, the tone burst followed by his address code is transmitted by the Observatory to one of the geostationary satellites, the "interrogating satellite", that repeats it. All of the users receive the satellite transmission, but the transponder that is addressed recognizes the address code automatically, and after a precise delay, retransmits the tone-code. The satellites repeat the signal. The Observatory measures the intervals from the initial transmission to the first repetition by the interrogating satellite and to the times of the user's returns by each of the two satellites. With these measurements, one can compute the ranges from the two known positions of the satellites to the user. The range measurements determine two spheres of position centered at the satellites and having radii equal to the measured ranges. A third sphere of position centered at the earth's center and having a radius equal to the earth's radius plus the user's altitude intersects the other spheres at two points - one in the northern hemisphere and one in the southern hemisphere. By a priori information, the proper point is selected at the user's location.

The tone-code signal is entirely compatible with voice communications and is of such short duration that it can be inserted during pauses in speech. The signals can be relayed by satellites designed for communications with aircraft without requiring any changes to the satellites and without adding a significant load to their communication capacity. The signals are also compatible with data-link digital communications. The phase of the digital clock for communications could also serve as the phase reference for ranging, and then the only signal necessary for ranging is the address code itself.

The user receives the tone cycles from the satellite on its communication receiver, as shown in Figure 3-7. All of the tone cycles received from the satellite, even though they may be interrogations from other craft, are applied to a phase matching circuit. A locally generated tone of the same frequency is also applied to the phase matcher, which adjusts the phase of the locally

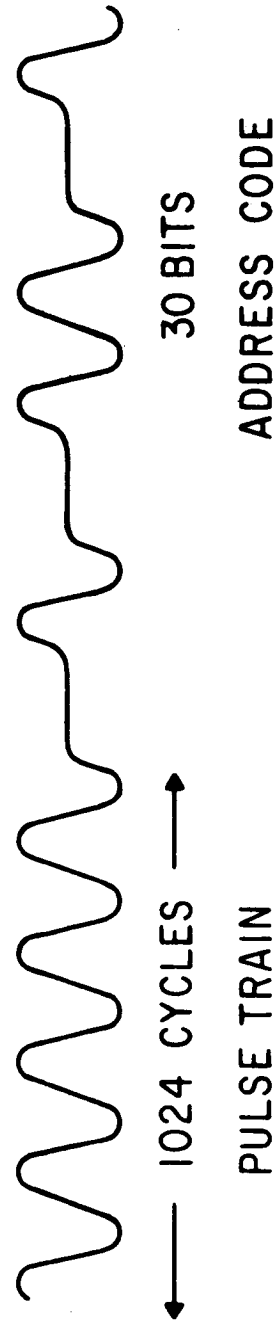


FIGURE 3-6

TONE-CODE RANGING WAVEFORM

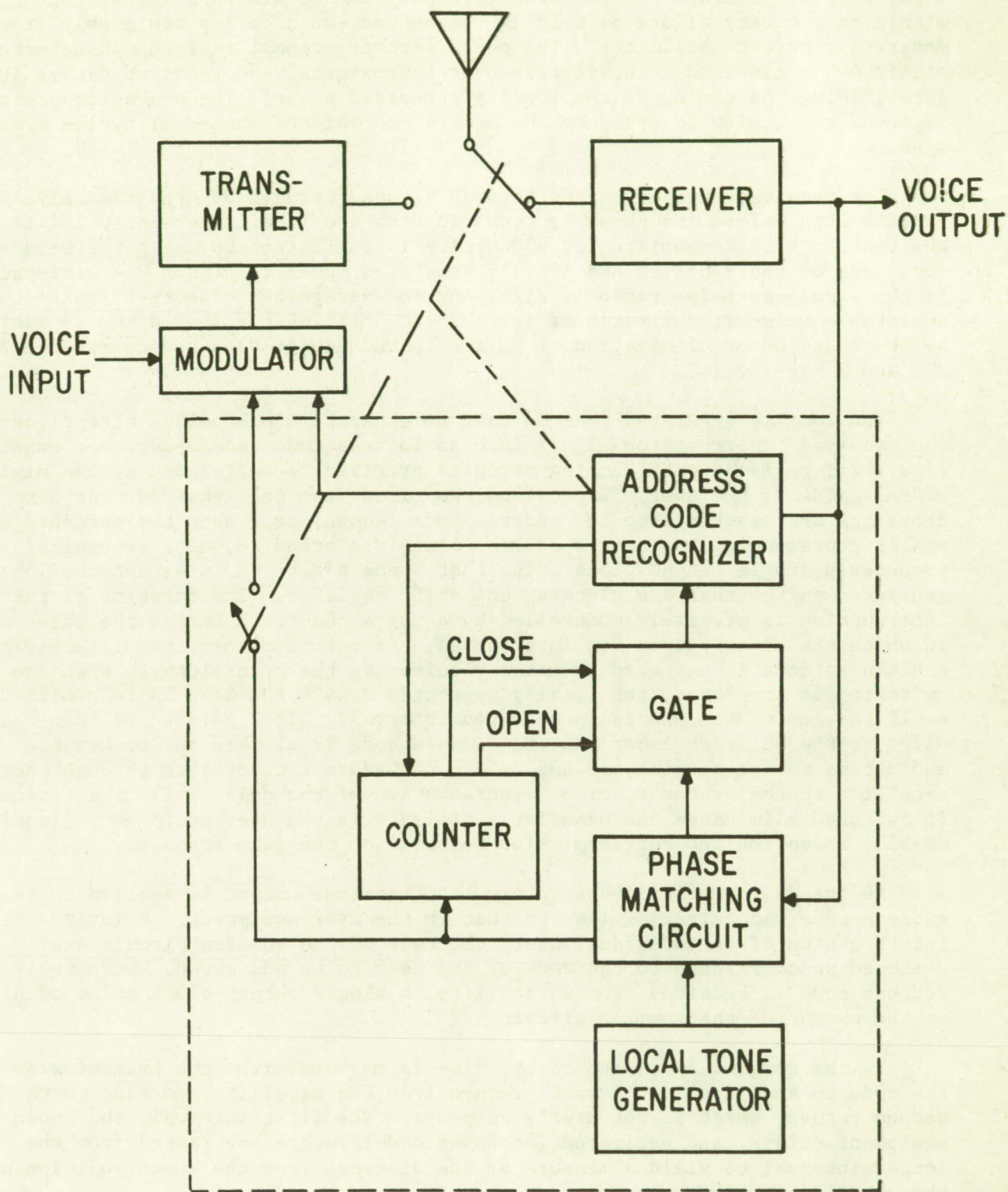


FIGURE 3-7

USER EQUIPMENTS

generated tone so that it corresponds to the phase of the received tone. The local tone is generated at the same frequency as the ground terminal tone within an accuracy of one part in 10^6 or better, an accuracy achievable from a moderately priced oscillator. The phase matcher accomplishes the phase match within 400 cycles and then averages over approximately 64 received cycles in establishing the timing of the locally generated phase. The averaging process improves the timing accuracy by the square root of the number of cycles averaged.

The received tone is passed through a tuned circuit of approximately 120 Hz bandwidth before its phase is compared with the locally generated 2.4414 kHz tone. Phase comparison for 400 cycles is sufficient to match the zero crossings of the received and locally generated tones to within 0.4 microsecond if the signal-to-noise ratio is high, and to average the effects of noise to an acceptable value if the ratio is low. Phase shifting the 2.4414 kHz is achieved by the addition or elimination of pulses in the divide down counter at the 2.5 MHz and 5 MHz levels.

The locally generated tone is used to generate clock pulses that clock the received interrogation signal into an address code recognizer that consists of a shift register with summing circuits prewired to correspond to the digital address code of the user. Digital pulses timed from the received tone zero crossings are clocked into the address code recognizer. When the sequence of pulses representing the user's address code is clocked into the recognizer, it produces a single output clock pulse that opens a gate to interrupt the locally generated pulses that are clocking the shift register. The duration of the interruption is precisely controlled by a pulse counter. During the interval in which the clock pulses are interrupted, the user's transmitter is activated and the antenna is switched from the receiver to the transmitter. When the switching is completed, the locally generated 2.4414 kHz tone is transmitted until the end of the precisely measured interval. Clock pulses are then reapplied to the shift register and the address code is clocked out to key the audio tone to the transmitter and return the address code, back through the satellite to the ground station. Introduction of the delay while the antenna is switched eliminates the need for a diplexer in the user equipment. It also enables reception and retransmission to occur on the same frequency.

At the Radio-Optical Observatory, the receiver output is applied to an address code recognizer similar to that in the user equipment. Prior to the interrogation of an individual user, the taps of the summing circuit are switched to correspond to the code of the user to be addressed. When the address code is received from a satellite, a single output clock pulse occurs at the output of the summing circuit.

In the range measurement tests, time is measured from the transmission of the code to the first or "direct" return from the satellite and also to the second return, which is the user's response. The first interval, the known equipment delays, and estimated ionospheric delays are subtracted from the longer interval to yield a measure of the distance from the known position of the satellite to the user.

Equipment Description

General Electric's Radio-Optical Observatory serves as the ground control terminal for the experiment. Equipment used for the ranging and position

fixing experiment is depicted in Figure 3-8. A tone-code responder unit, shown in the photographs of the five circuit board cards and the assembled unit with its cover removed (Figures 3-9 and 3-10), is used with a mobile receiver and transmitter to form a transponder. The block diagram of a responder is depicted in Figure 3-11.

Each user responder performs the following sequence of functions:

1. Phase alignment of its own 2.4414 kHz clock with the received 2.4414 kHz signal prior to receiving the address code.
2. Recognition of its user address code. Each responder contains a shift register prewired for its own address.
3. Measuring a precise time delay of 1024 tone cycles duration, 419,430.4 microseconds.
4. At the start of the delay, switching transceiver from the receive mode to the transmit mode.
5. Supplying the properly phased tone modulation signal to the transmitter during the precisely known time delay.
6. Transmitting its digital address code starting precisely at the end of the delay.
7. Switching transceiver back to receive mode.

The responder functions on a 30-bit user address code. The code consists of a 15-bit word synch and a 15-bit address. The 15-bit word synch is the same for all users. A unique 15-bit address is assigned to each user. This particular code configuration provides for 128 users with a minimum Hamming distance of 5.

The 15-bit address code shift register is wired specifically for the user's address. When the address is received following the tone, correlation occurs simultaneously in the 15-bit word synch shift register and in the 15-bit address shift register. The outputs of the shift register stages are summed in a current summing network. Centering of the word synch and address code in each of the correlators results in a peak voltage at the correlator output. The voltage peak is threshold detected and used to gate out the next clock pulse for timing purposes since the rise-time of the lead edge of the correlation waveform itself is not sufficiently accurate. The pulse starts a counter that measures a period of 1024 cycles of the locally generated tone. This timing pulse also switches the transponder into the transmit mode, and it then begins to transmit the locally generated, properly phased 2.4414 kHz tone back to the satellite. At the end of the precise time delay, the address code is transmitted. The transponder then returns to the receive mode and awaits further interrogations. During retransmission of the tone and address, the 2.4414 kHz clock has remained in phase with the previously received signal since following correlation no further input is presented to the phase matcher, thereby preventing noise from corrupting the phase alignment.

An additional feature of the responder is a noise inhibit circuit which prevents false correlations on noise during the absence of a received signal.

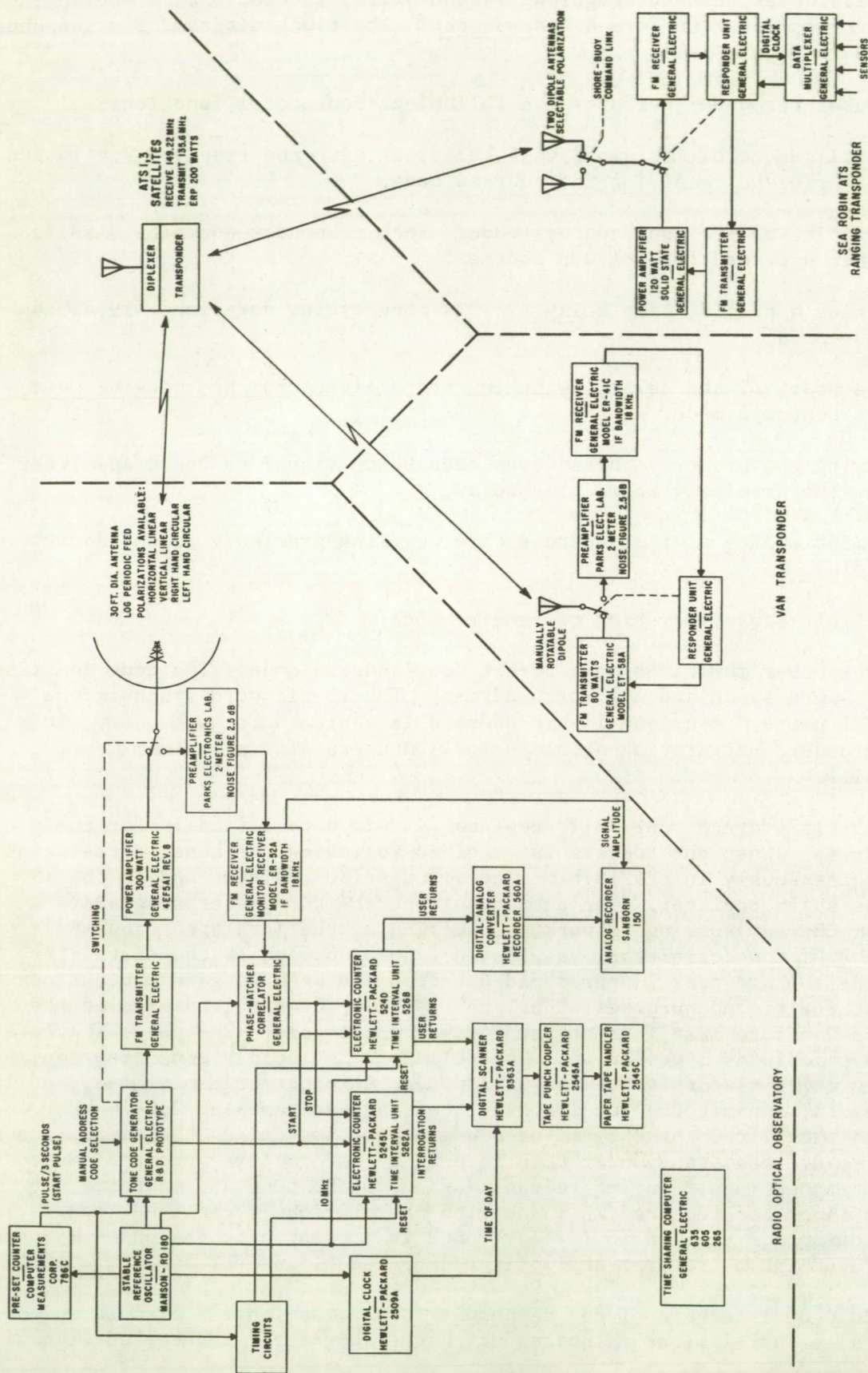


FIGURE 3-8

RANGING AND POSITION FIXING EXPERIMENT EQUIPMENT

FIGURE 3-9

FIVE PRINTED CIRCUIT BOARDS

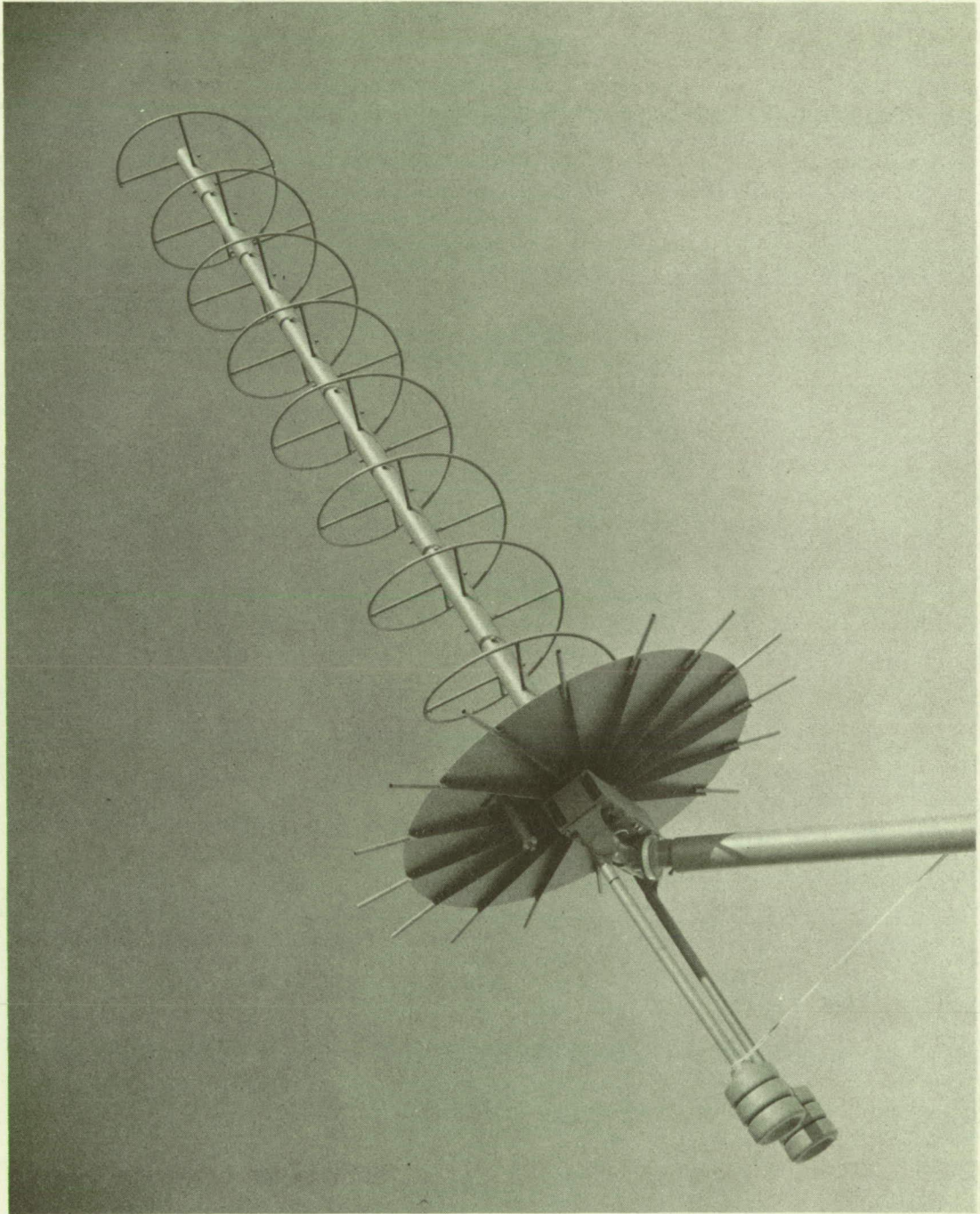
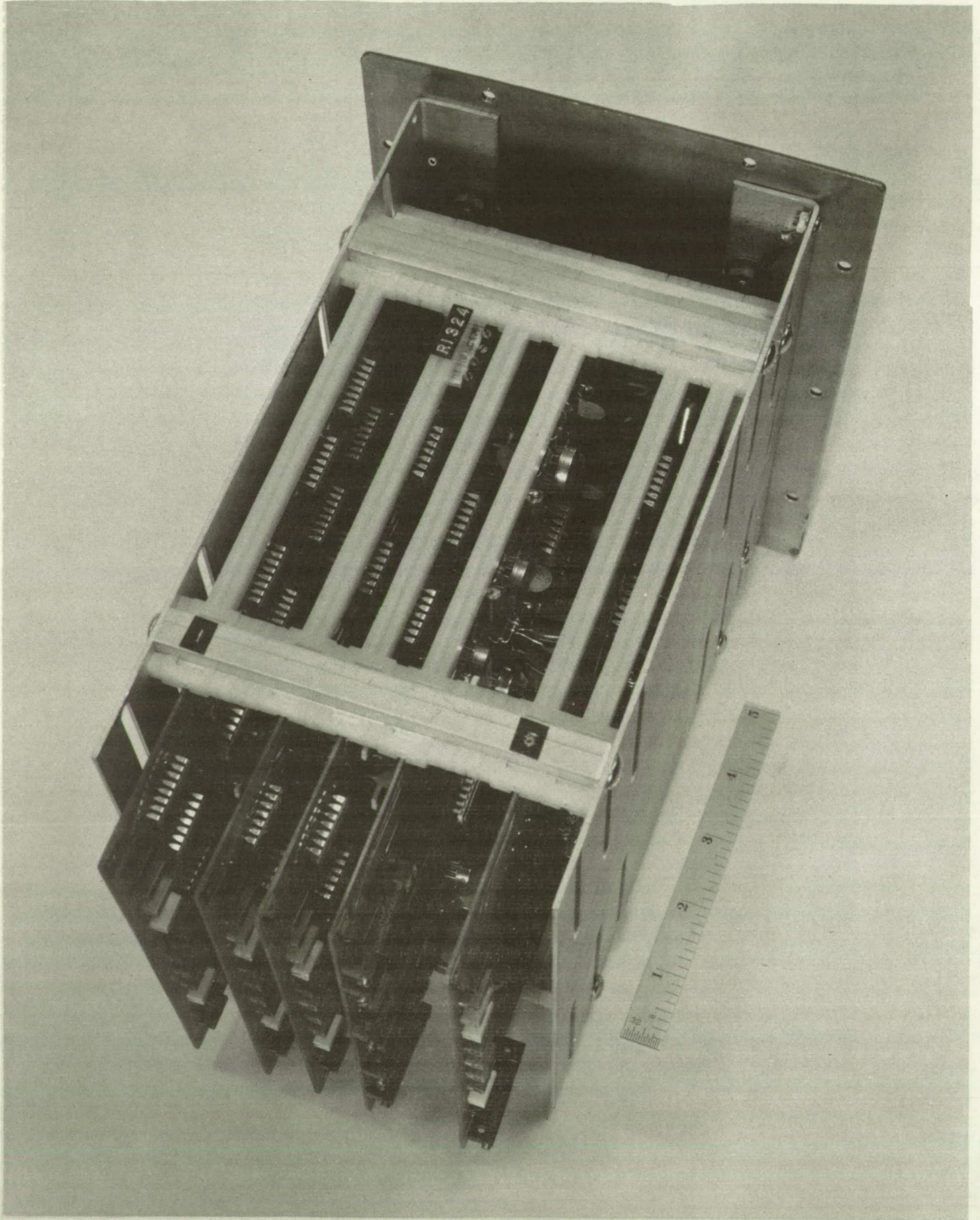


FIGURE 3-10

ASSEMBLED RESPONDER UNIT



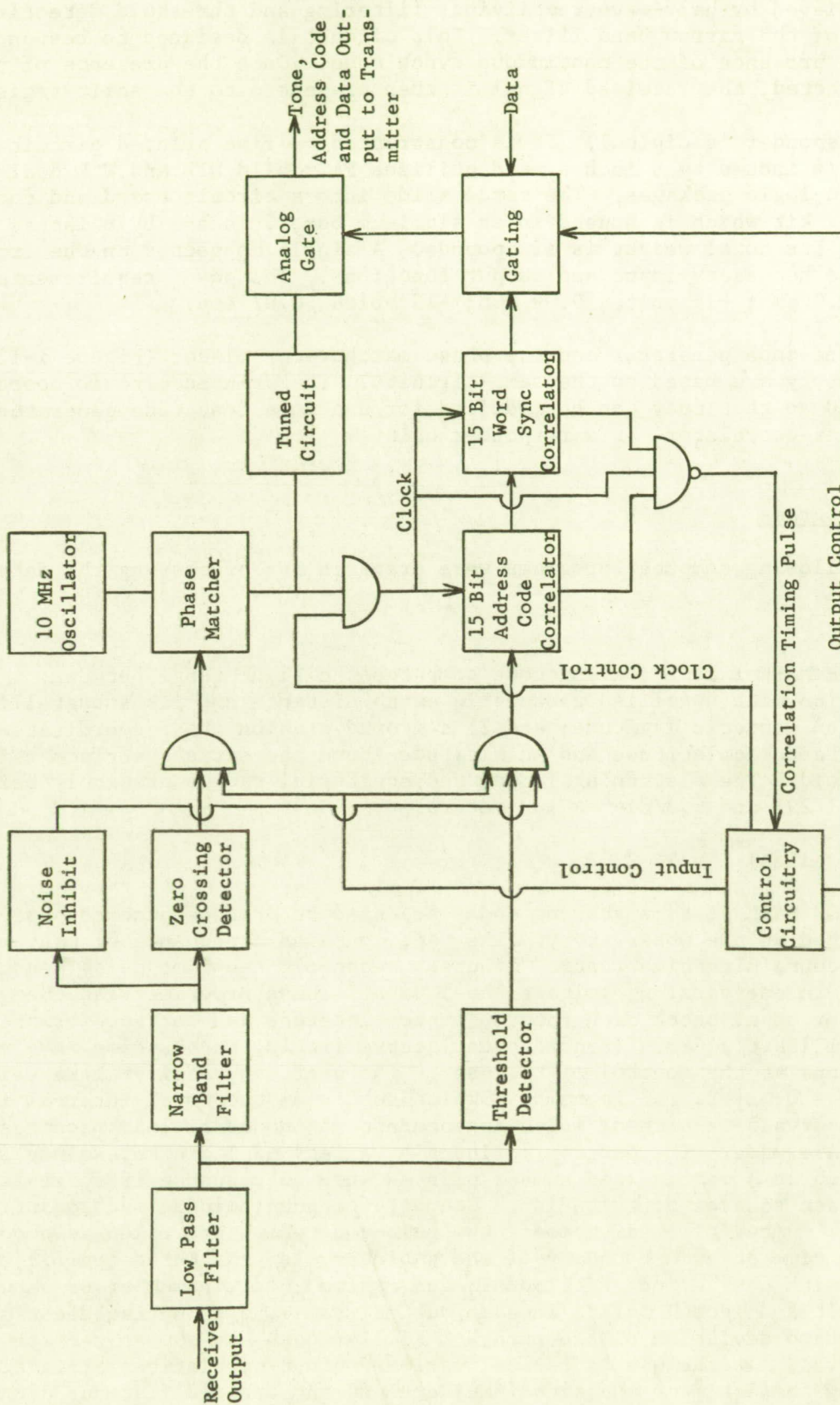


FIGURE 3-11

RESPONDER BLOCK DIAGRAM

This is achieved by half-wave rectifying, filtering and threshold detecting the output of the narrow band filter. This circuit is designed to respond only to the presence of the continuous synch tone. Once the presence of the tone is detected, the received signal is then presented to the shift register.

The responder is digital. It is constructed on five printed circuit boards, 6 1/4 inches by 8 inches, and utilizes Fairchild DTL and T²L dual in-line ceramic logic packages. The cards slide into a circuit board and connector mounting kit which is housed in an aluminum box, 6 inches by 8 inches by 10 inches. Its total weight is six pounds. A single connector on the front provides the necessary input and output functions. The power requirements are: +5 volts, 1.0 amp; +15 volts, 0.09 amp; -15 volts, 0.07 amp.

The tone-code generator and the phase matcher-correlator (Figure 3-12) in the Observatory are based on the same circuits. The printed circuit boards are designed so that they can be modified for use in a tone-code generator, a phase matcher-correlator, or a responder unit.

Computer Programs

The following computer programs were prepared for processing the data.

SLANTM

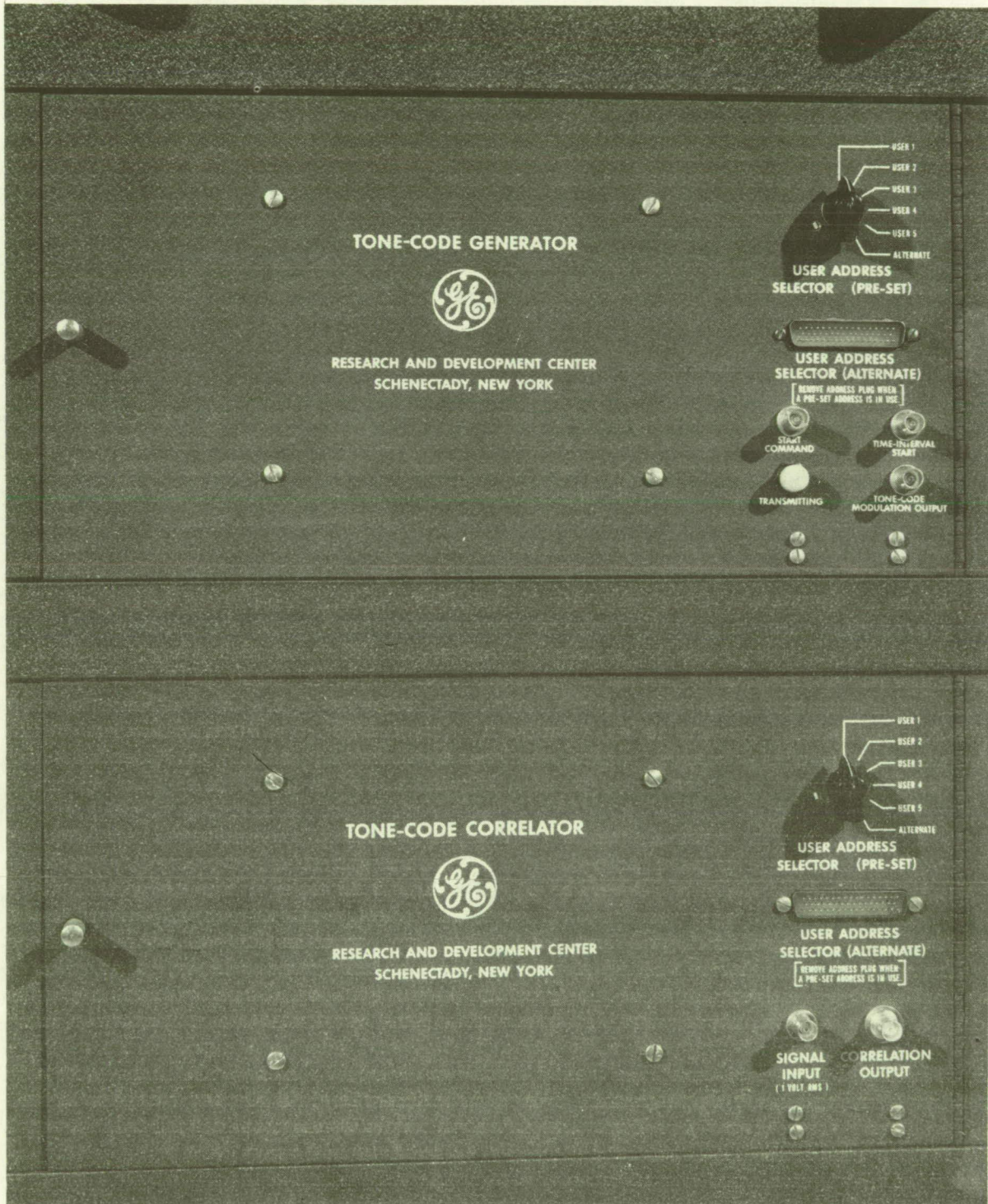
This GE MARK I time sharing code computes the slant range between: 1) a satellite with specified geocentric earth distance and its subsatellite longitude and geodetic latitude; and 2) a ground station whose coordinates are longitude, geodetic latitude and an altitude above the earth's surface reference ellipsoid. The flattening factor and equatorial radius presently being used are: $1/297$ and 6.378166×10^6 meters.

OBSPROC_i (+ files) $i = 1, 2, 3, 4$

These GE MARK II time sharing codes are used to process punched paper tape generated at the Observatory. The tape contains a sequence of many records each containing time (hours, minutes, seconds); two time delay measurements; and, in one version, voltage level data. These programs read the punched paper tape, check each record for completeness and correct format, and then perform least squares (second order) curve fitting versus time in a variety of options at the control of the user. The user can specify "interval markers" ($N = 0, 1, 2, \dots$ in number) which subdivide the total interval into $N + 1$ subintervals in each of which independent second order least squares curve fits are made. The program includes a variety of logic to exclude "wild points", such as a meaningless number printed when no response is received, from the least squares contribution. Standard output includes such quantities as the total number of observations, the number of which are taken as good points; the time at each boundary of the subintervals; the three coefficients associated with the second order model; the maximum and minimum error between the curve fit and "good" points in each subinterval; and an unbiased estimate of the standard deviation of the errors. Similar data are summarized for the whole interval. At the user's choice, various output tabulations are available showing the estimate and actual measurement and their difference along with various other time data.

FIGURE 3-12

TONE-CODE GENERATOR AND PHASE MATCHER CORRELATOR



The four versions are associated with that many different punched paper tape formats. Also, one version operates on the voltage level to give an indicated bit error rate in each subinterval.

LATCOM (+ files)

This code exists in two versions for both GE's MARK I and MARK II time sharing systems. One version is in a "conversational mode" for input, while the other reads files for input. The purpose of LATCOM is to compute a user's geodetic latitude, when given his longitude, altitude above the ellipsoidal first reference and slant range time delay information to one satellite whose ephemeris (geocentric earth distance, longitude and geodetic latitude) are available on a file containing date, time and the preceding quantities. The ellipsoidal earth is presently taken to have a flattening factor of 1/297 and a mean equatorial radius of 6.378166×10^6 meters. At present, the user manually inputs bias terms for equipment delays and corrections for ionosphere delays on propagation path.

POSFIX (+ files)

This GE MARK II time sharing code computes the user's longitude and geodetic latitude, when given his altitude above the ellipsoidal earth reference and slant range time delay information from two satellites whose geocentric earth distances, longitudes and geodetic latitudes are available in an ephemeris file which contains, in addition, date and time. In this code the effects of the ionosphere delays are computed on the basis of an empirical model as a function of the time of day at the intersection of the ray path with an ionosphere layer and the elevation angle associated with the slant range vector from the point on earth to the satellite. Internal to the computer program is a secant solution of two simultaneous nonlinear algebraic equations. This secant subroutine and an associated matrix inversion subroutine are called from the MARK II FSL Library programs.

The Network of Fixed Transponders

The installation of a widespread network of fixed transponders, and the enthusiasm of the personnel and organizations that installed, maintained, and operated them on a cooperative basis made it possible to accomplish a program far beyond the scope of the contractual agreement between the National Aeronautics and Space Administration and the General Electric Company. NASA and its ATS Operations Control (ATSOC) were very generous in the assignment of satellite time to the experiment, often going to great trouble to make satellite time available on short notice, or to re-program to coordinate assigned satellite time with aircraft flights or other events that could not be kept to an inviolate schedule. One of the great satisfactions in conducting the experiment has been the opportunity to work with cooperative, professional colleagues in other lands, in government agencies, airlines, and other commercial and industrial concerns.

The purchase, construction, and shipment of all the units except the one in Iceland was funded by the General Electric Company through its New Businesses Development Operation, Corporate Research and Development. The unit in Iceland was funded by Comsat Corporation.

The installation, operation and maintenance were arranged by the local organizations at each site. It is noteworthy that every request for voluntary participation resulted in an enthusiastic response.

The ground reference transponder used in this network is shown in Figure 3-13. The receiver-transmitter is a General Electric Mastr Progress Line R type DM-76-LAS mobile radio base station unit. The original limiter discriminator of the receiver was bypassed with a unit designed to have a smaller time delay change with signal amplitude than the original limiter discriminator. The receiver was preceded by a Parks model 144-1P preamplifier. A tone-code responder unit is connected between the receiver and transmitter and the transmitter output is amplified by a Gonset model 903 Mark II, 350 Watt power amplifier, shown in Figure 3-14.

The transponder is designed to permit unattended operation. No voltage is applied to the plate circuits in the power amplifier until about 7 seconds after the unit has received an initial interrogation from the ground station. Following this initial interrogation, the transponder is designed to respond through the satellite for a time period which is adjustable up to eight minutes. Each interrogation after the initial activation resets the timer. After the last interrogation, the time delay relay deactivates the power amplifier.

The antenna furnished with the ground reference transponder is an eight-turn helix (shown in Figure 3-2) built by Technical Appliance Corporation. It has 13 dB gain for circularly polarized signals, 10 dB gain for the linearly polarized signals from the ATS satellites.

A detailed description of the transponders is contained in the General Electric report GEK-5821, "Instructions and Operating Characteristics, Tone-Code Transponder System", dated April 1970.

Ground reference transponders were installed at the following locations.

Gander, Newfoundland

Arrangements for the installation of a transponder at Gander were made through Aeronautical Radio, Inc. (Mr. C. Petry) with F. L. Bentley of the Canadian Department of Transport. Mr. Shirley Boothe, also of the Canadian Department of Transport, visited Schenectady on December 17 and 18, 1969 to gain familiarity with the project and evaluate it for his organization. The unit, with user code 6(Appendix IV), was shipped to Gander in January 1970. Mr. James Lewis of General Electric went to Gander on February 17, 1970 to assist in its installation. The Parks preamplifier, base station selector switch and interconnecting cables were damaged in shipment. A minor modification was made to the antenna mount, the unit was trucked seven miles to the installation site, installed, the damage repaired, and the unit placed in operation and tested through the satellite in one eight-hour working day. A concrete pad had been poured in advance for mounting the antenna.

The unit was installed in a building approximately three miles from the Gander airport. Usually unattended, the building also houses aircraft beacon transmitting equipment.

FIGURE 3-13

GROUND REFERENCE TRANSPONDER

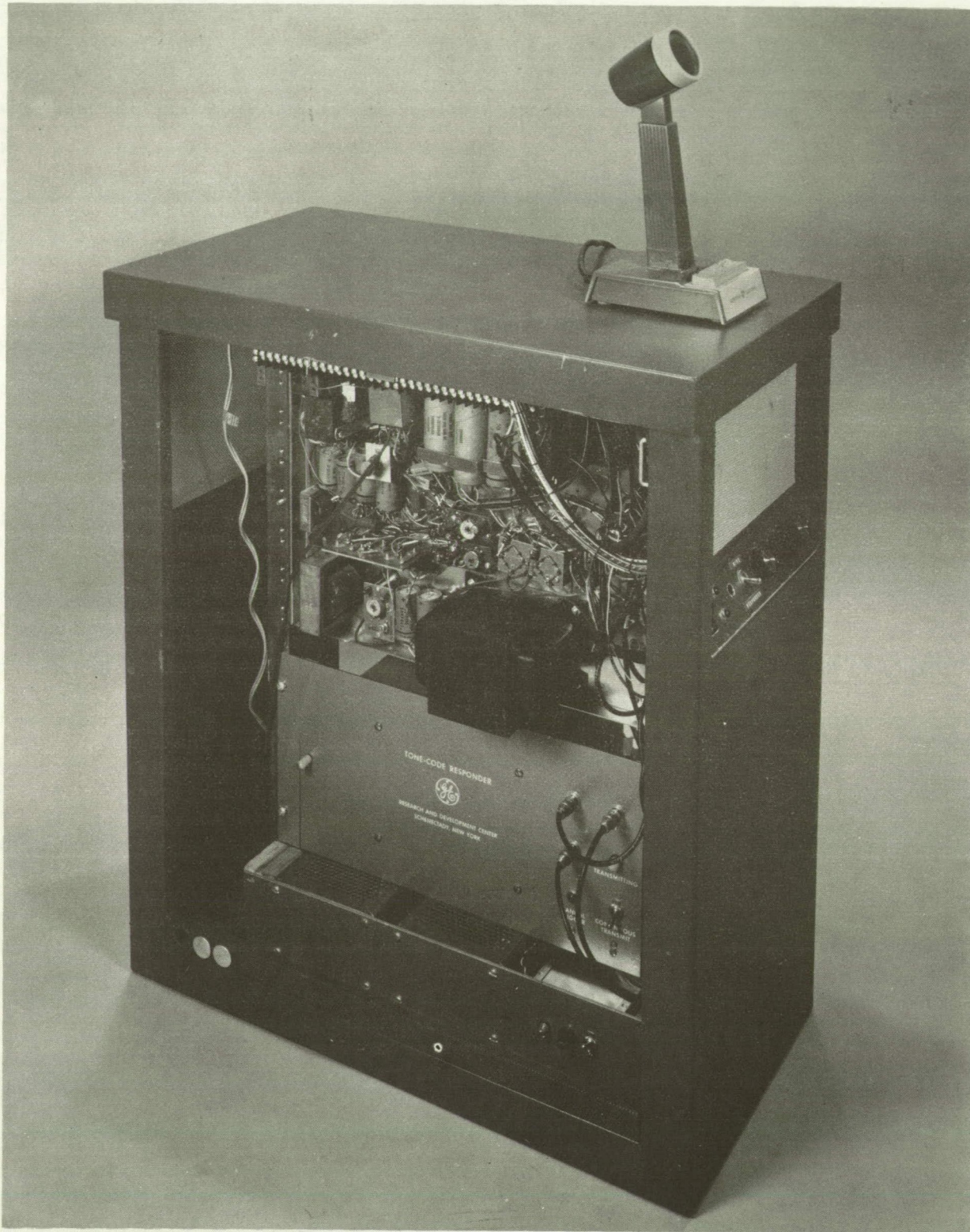


FIGURE 3-14

GONSET AMPLIFIER



Shannon, Ireland

A transponder, with user code 7(Appendix IV), was placed in operation at Shannon, Ireland on April 28, 1970. Arrangements were made with Mr. G. E. Enright, Department of Posts and Telegraphs, Dublin, through Mr. C. Petry of Aeronautical Radio, Inc. The transponder is maintained and operated by the Engineering Branch, Radio Division, Department of Posts and Telegraphs.

The transponder is located in the building that houses the communications operations and facilities for the Shanwick North Atlantic air traffic control sector.

The unit was shipped to Ireland, installed by local personnel using the instructions, GEI-45099, furnished with the unit.

The facilities are located near Shannon airport. A complaint of interference to aircraft communications in the 118-136 MHz band was received, and the transmitter power on the 149 MHz uplink was reduced from 300 Watts to 100 Watts. No further interference was experienced. D. O'Neill kept an excellent written log of the use of the transponder. A portion of the log is reproduced in Figure 3-15. They also furnished a tape recording of the satellite communication signals that is valuable as a record of the experiment as well as useful in evaluating voice communications reliability under the varied conditions of the experiment.

Seattle, Washington

A transponder with user code 10(Appendix IV), was installed by the Boeing Company on July 1, 1970. An initial fault, probably resulting from damage in shipment, was found in the code correlator and corrected so that the unit was operational on July 13, 1970. The transponder was located in a van several miles from the offices of Mr. L. Hutton, who was in charge of its operation and maintenance. A timer was installed in the power line to the unit, so that it was completely inoperative except during preset periods when it was placed in standby condition, ready for interrogations through the satellite. When Boeing personnel were notified in advance of test periods, they set the timer when it was convenient to visit the van, and the tests were conducted later without attendance at the unit.

During much of the experimental program, both satellites were in line-of-sight from Seattle, so that it was necessary to direct the helical antenna to the satellite of interest for each test.

It was often possible to interrogate the Seattle transponder through the satellite that was in the beam of the antenna, and get the response back through both satellites, even though one satellite was receiving its signal from a side lobe or back lobe of the antenna. A position fix computation could then be made from the response.

The ATS-3 satellite was started on its seasonal eastward movement in March 1970. It was stopped at 46° west longitude in December 1970. On November 23, 1970, the satellite was below the horizon for Seattle and could no longer be used for ranging or communications. ATS-1, however, remained useful for a link between Schenectady and Seattle.

The following is copied from the log kept by Mr. D. O'Neill, Engineer-in Charge, Shannon Aeradio, Ballygirreen, Newmarket-on-Fergus, County Clare, Ireland.

SATELLITE RECORDINGS

FROM	TO	SPEED	COUNTER	
<u>8/7/70</u>				
2015			1599 1636	FA114 CLEARING G.E.1 AND VARIOUS ANTENNA TESTS G.E.1 CONFIRMS 9th AND 10th SKEDS WITH EIP
<u>9/7/70</u>				
1550	1 7/8	1638	1722	G.E.1/FAA114 DISCUSS FAULT ON ONE SYSTEM. BOTH SYSTEMS LOUD AND CLEAR HERE. GE1 and FAA114 CONTINUE FAULT TRACING AND TESTING.
<u>10/7/70</u>	1 7/8	0000	0160	FAA114/G.E.1 114 on GROUND AND G.E.1/SNN WILL BE ENGAGED MAINLY WITH FAA 114. THIS SKED A/C WAS SCHEDULED TO BE AT SNN DURING THE 19/21 PERIOD BUT THEY WILL NOT BE THERE TODAY EXCEPT THEY WILL BE THERE ON MONDAY. WILL PASS THE SKEDS FOR MONDAY DURING THE 19/21 PERIOD.
				G.E.1 who is in Command of Aircraft. Are you airborne yet, if not where are you. When do you depart for Shannon FAA114. Mr. John Steinmats is in command of the mission. We are on the ramp at Tooley (Thule). Our ET Shannon unknown. Awaiting some equipment FAA114 depart Thule for SAKALAK will depart. Bound for Shannon <u>sometime</u> Sunday or Monday 12th or 13th respectively. New sked Sunday 12th 1400/1600 if not there Monday 13th.
<u>12/7/70</u>				
1400		0719	1738	G.E.1 tests to FAA114 est EINN 1932. G.E.1 tests EIP and advises remaining skeds for today. 1900/1915 1940/2015 2040/2115. FAA114 to G.E.1 "ETA EINN 1951Z" G.E.1 checking with FAA114. FAA114 "Touching down EINN now" G.E.1/FAA114 Ex. QRKS and remarks G.E.1 to EIP "WE TERMINATE SKED NOW 2015Z. FAA114 not reading me please advise him by phone. No skeds until further notice."

FIGURE 3-15

PORTION OF LOG KEPT ON TRANSPONDER USE AT SHANNON, IRELAND

A test was conducted on March 22, 1971 when the satellite was drifting west and was visible to Seattle. Performance was excellent even though two months had elapsed since the previous test period.

Reykjavik, Iceland

A transponder, with user code 9 (Appendix IV), was installed at Reykjavik on January 6, 1971. Arrangements for its installation were made through Mr. L. Magnusson, Civil Aviation Administration, Iceland. The unit was installed, operated, and maintained by local personnel. No difficulties were experienced in the installation or operation of the unit. It has worked well in the automatic transponding mode, and for voice communication.

Construction and shipment of the unit were financed by the Comsat Corporation.

Buenos Aires, Argentina

The transponder, user code 8 (Appendix IV), that had been used aboard the Coast Guard Cutter Rush was returned to Schenectady for inspection after its nine weeks of use on the ship, then sent on to Buenos Aires, Argentina. No repairs or adjustments were found necessary after its use on the ship.

Arrangements for installation were made through the International General Electric Company, with assistance from Pan American World Airways. The unit was installed and operated by the Argentine Air Force. Installation of the transponder was on the eleventh floor of a building in the city of Buenos Aires, with the helical antenna mounted on the roof of the building.

No difficulties were experienced with the equipment in its installation or operation. This particular unit was used over a period of nine months, was at sea for nine weeks, then transported by truck more than three thousand miles, and by ship five thousand miles, with only minor adjustments and recalibration.

Transponder Calibration Technique

Each user transponder introduces an equipment time delay which is the time required for the ranging signal to pass through the antenna cable, the electronic circuits, and to be processed. User equipment time delay is one of the delays that must be subtracted from the total time of the range measurement to yield the actual range.

Each user equipment delay is unique; therefore, it must be measured, or calibrated, and stored in the computer with the user address and subtracted from each range measurement that is made to that user. This calibration procedure is necessary in all ranging techniques. With tone-code ranging, a single tone technique, only one value need be measured and stored. With some multiple tone ranging implementations, it may be necessary to calibrate and store the delay for each tone.

Each transponder used in the experiment was calibrated initially at the Observatory before it was sent to its user facility. After its installation

aboard the craft or at its ground location, it was recalibrated. The transponder calibrations were rechecked occasionally.

It was found to be simple and practical to measure the equipment delay of a distant transponder, to store the delay calibration with the transponder address in the computer, and to use the calibration measurement in the computation of ranges, lines of position, and position fixes. The technique was used routinely throughout the experiment. In practice, it was convenient to store the sum of the user equipment delay, the satellite equipment delay, and the Observatory equipment delay as a single number.

Procedural steps for calibrating a remote transponder are given below.

- The location of the distant transponder is accurately specified in latitude, longitude, and height above mean sea level. If the transponder is in a mobile craft, it is placed at a benchmark or other accurately known location for calibration.
- A tone-code ranging signal is transmitted from the Observatory to one satellite. The satellite relays the signal to the distant transponder. The transponder responds as it does for any ranging interrogation.
- At the Observatory, a measurement is made and recorded of the Observatory-to-satellite ranging time; that is, the time from the transmission of the ranging interrogation to its return from the satellite.
- At the Observatory, a measurement is made and recorded of the total ranging time; that is, the time from the transmission of the ranging interrogation to the return via the satellite of the response from the distant transponder.
- The Observatory-to-satellite ranging time is subtracted from the total ranging time to yield the satellite-to-transponder ranging time. The satellite-to-transponder ranging time is the sum of the two-way signal propagation time from the satellite to the transponder plus the transponder equipment time delay plus the ionosphere propagation delay.
- Computations are made of the geometrical slant ranges from the satellite to the distant transponder and from the satellite to the Observatory. The ranges are expressed in microseconds two-way propagation time, assuming the propagation velocity is that of light in free space. NASA predictions of satellite position are used.
- An estimate is made of the ionosphere propagation delay. If the distant transponder is within approximately 1000 miles of the Observatory, the Observatory and satellite equipment delays and the Observatory-satellite geometrical slant range are subtracted from the measured range to yield the ionosphere propagation delay. The value is modified to allow for sun time difference and elevation angle difference and used as the estimate of propagation delay for the distant transponder. If the distant transponder is more than approximately 1000 miles from the Observatory, but near another previously calibrated transponder, range measurements to the previously calibrated transponder can be used in the manner described for the Observatory. If no previously calibrated transponder is within approximately 1000 miles of the transponder to be calibrated, an estimate of ionosphere delay is made on the basis of published literature or other data that may be available. In that case it may be

preferable to calibrate during the night when the electron content is low, and an estimate of delay may have a smaller absolute error.

- The computed geometrical slant range plus the estimate of ionosphere propagation delay are subtracted from the satellite to transponder range. The difference is the transponder plus satellite equipment delay.

- As an alternate method, the initial calibration of the equipment, made before it was shipped from the Observatory, is used as a first assumption of equipment delay when the transponder is at its distant calibration site. A range measurement is made in the usual manner, an estimate made of ionosphere delay as described above, and a latitude determination is made from the range measurement using the LATCOM program. The difference between the computed and actual latitudes is noted, and an appropriate correction applied to the equipment delay term in the program; the latitude is determined again. The process is repeated until the computed and actual latitudes coincide. The value of the equipment delay used in the final computation is then accepted as the equipment delay calibration.

Calibration of equipment delay was correct within one microsecond. As an example, range measurements were made to an FAA DC-6 aircraft parked on a benchmark at Shannon, Ireland. Measurements were also made to the ground reference transponder at Shannon. The aircraft then returned to Atlantic City, New Jersey. Nine days after the measurements were made at Shannon, the aircraft equipment delay was calibrated at Atlantic City by the method outlined in the foregoing procedural steps. Latitude determinations for the aircraft at Shannon were made using the Atlantic City equipment delay calibration. The average of the latitude determinations was 800 feet north of the benchmark location of the aircraft (Section 6). Ionosphere propagation delay and satellite prediction error were corrected from the measurements made to the Shannon reference transponder. Equipment delay calibrations of the aircraft transponder, the Shannon reference transponder, and the Observatory equipment all affected the accuracy of the latitude determination. The total of all of these could not have affected the range measurement more than approximately one microsecond. One microsecond represents 491 feet in range. Geometrical dilution would have caused a latitude error of 800 feet for a range error of approximately 500 feet. The satellite was at an azimuth of 240° and elevation of 11° from Shannon at the time of the measurements.

SECTION 4

EQUIPMENT PERFORMANCE

Equipment design, performance, and usage influence the precision and accuracy of ranging measurements. The experiment provided an opportunity to evaluate limitations imposed by the equipment.

Bandwidth of the ranging signal influences the measurement precision. Radio range measurements can only be made by measuring propagation time, and that in turn by measuring the interval between a transmitted and received waveform. Although the modulating wave may take many forms, the highest range resolution that can be achieved is set by the ability to measure the phase of the highest frequency component in the waveform. Phase measurement precision is relatively independent of frequency. A precision of the order of one degree is usually achievable without refined techniques. The higher the frequency, the better the timing resolution.

The designer does not usually have an unrestricted choice of signal bandwidth. In the design of the ranging experiment, the radio frequency and audio frequency bandwidths of aircraft mobile communications were selected as limits. This appears to have been a proper choice, as it permits evaluation of the technique within practical limitations set by existing satellite communications equipment specifications and frequency allocations. The precision achieved within these bandwidth constraints was sufficient to resolve the VHF propagation effects.

Measurement precision is affected by noise, for noise causes a "jitter" of the signal phase. If the noise is random, the error may be reduced by averaging a number of measurements. As the signal-to-noise ratio becomes poorer, the amount of jitter increases, and the measurement precision decreases even if averaging is used. It is important in a ranging measurement that the precision be within acceptable limits at the poorest signal-to-noise ratio that is experienced. In the VHF range experiments this was insured by the use of frequency modulation that yielded better signal-to-noise ratio of the detected signal than that of radio frequency signal, and by post-detection filtering. These techniques insured that an acceptable phase measurement precision was possible whenever the radio frequency signal was strong enough to be detected.

Accuracy is affected by the time delay variations of the equipment. The absolute value of the time delay is not important. If it does not change, it is subtracted from the measured interval in calculating the range. However, if the delay changes in an unknown way, it introduces an error that cannot be compensated. Electronic circuits are subject to changes in delay time, with the delay variations tending to be greater in narrow bandwidth circuits than in wide bandwidth circuits. Delay variations can occur in receivers as a function of signal level. Bandpass filters such as receiver IF stages may have time delay changes if the circuits are slightly detuned. Signals from different users operating in the same channel may experience different time delays if their carrier frequencies are not exactly the same. The effects may be minimized by the use of temperature-stable components and by careful alignment to assure a linear phase characteristic across a bandwidth that includes all significant frequency components of the signals. FM limiters may introduce time delay variations if they do not limit symmetrically about the IF zero crossings and discriminators may introduce changing time delays if they are improperly aligned.

The magnitudes of equipment time delay effects are a function of bandwidth and are independent of radio frequency. Wider bandwidth allocations at L-band than at VHF may be important if full advantage is to be realized from the better propagation characteristics.

All of the factors influencing precision and accuracy, including equipment delay characteristics and signal-to-noise ratio effects, were measured for the various equipments used in the experiment and the results of these measurements are presented in detail in this section.

Equipment Time Delay

Each electronic circuit contributes a time delay to the interval between the initiation of an interrogation and the final readout of the measurement at the ground station. The sum of these delays must be known precisely and subtracted from the total delay to yield the propagation interval. The range uncertainty introduced by uncertainty in equipment delay is the same as that for propagation time uncertainty, or approximately ± 500 feet for 1.0 microsecond. Although the equipment delays may total several hundred microseconds, they must be known to within limits appropriate to the accuracy required of the measurements.

For a statistical estimate of system performance, the delay uncertainties in ground equipment, satellite, and user equipment may be taken as the root-sum-square of their individual uncertainties since they are independent. The contribution of the ground station and satellite equipments can be maintained at a low value because they are in stable environments, and because they are available to the ground terminal for frequent measurement and compensation or calibration.

An operational system would include many user equipments subject to a wide variety of environmental conditions and maintenance skills. It may be impractical to expect that each user equipment be preset and maintained to have a predetermined time delay within the limits assigned for equipment time delay in the error budget of the system. A better procedure, used in the ranging experiments, is to have the ground terminal determine each user's time delay when the user is at a known location. The delay is then be stored with the user's address in the computer memory. Calibration in this manner proved to be simple and it does not tax the computer.

Narrow bandwidth circuits are more apt to contribute time delay uncertainty than wider bandwidth circuits, because a phase error caused by a non-linear phase characteristic in a filter represents a larger time error at a low frequency than the same phase error at a higher frequency. Experience in designing equipment for the experiment indicates that filters employing active components are subject to larger time delay uncertainties than filters employing only passive components. Digital switching and logic circuits can be designed to keep their time delay variations to a negligible value.

Tone-code ranging has a distinct advantage because it does not require an antenna diplexer. In a separate program, a diplexer for reception of 157.86 MHz and transmission of 154.89 MHz was tested in a vehicle on a cold winter day and found to have intolerable time delay variations, depending on its temperature. A diplexer for use with a ranging technique that requires simultaneous reception and transmission by the user equipment would have to be carefully

designed to have a constant time delay over a wide temperature range. A duplexer co-located with an aircraft or ship antenna would be subject to large temperature changes.

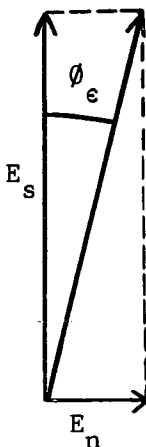
For any active ranging technique, the user receiver must be designed for minimum time delay variations. Receivers designed for communications may have time delay variations with tuning and with signal amplitude. Tuning variations can be minimized by the use of crystal control and proper alignment for a linear phase versus frequency characteristic in the IF and other bandwidth limiting circuits. Carrier phase locking is helpful if the received signal frequency is not accurate.

During the experiment, no significant changes in time delay with tuning were observed with any of the crystal-controlled receivers. Time delay variations with signal amplitude were observed. A General Electric ER-52-A receiver, designed for mobile communications without consideration to time delay variations, was found to have a total variation in time delay of approximately 7 microseconds. A different limiter was substituted for the original and the total variation reduced to less than 1 microsecond, as shown in Figure 4-1.

Figures 4-1 through 4-5 show equipment time delay as a function of signal strength and of tuning for several receivers.

Signal-to-Noise

Noise added to the demodulated tone causes jitter of the zero crossings that are used for the timing measurement. Probable phase error on one cycle may be estimated by a vector addition of the signal and noise phasors. Assuming that the noise has a gaussian distribution, which is the usual case when receiving signals from the satellite, the one sigma probability phase error is the angle in radians between the signal vector and signal-plus-noise resultant when the signal and noise vectors are at right angles, as follows:



where E_n = RMS noise voltage
 E_s = signal voltage
 ϕ_ϵ^s = 1 sigma phase error in radians

Signal-to-noise ratio, dB = $20 \log \frac{E_s}{E_n}$

FIGURE 4-1

DELAY VERSUS SIGNAL STRENGTH AT THREE FREQUENCIES
 GE TYPE ER-52-A MONITOR RECEIVER
 ORIGINAL LIMITER REPLACED BY SPECIAL TUNED LIMITER

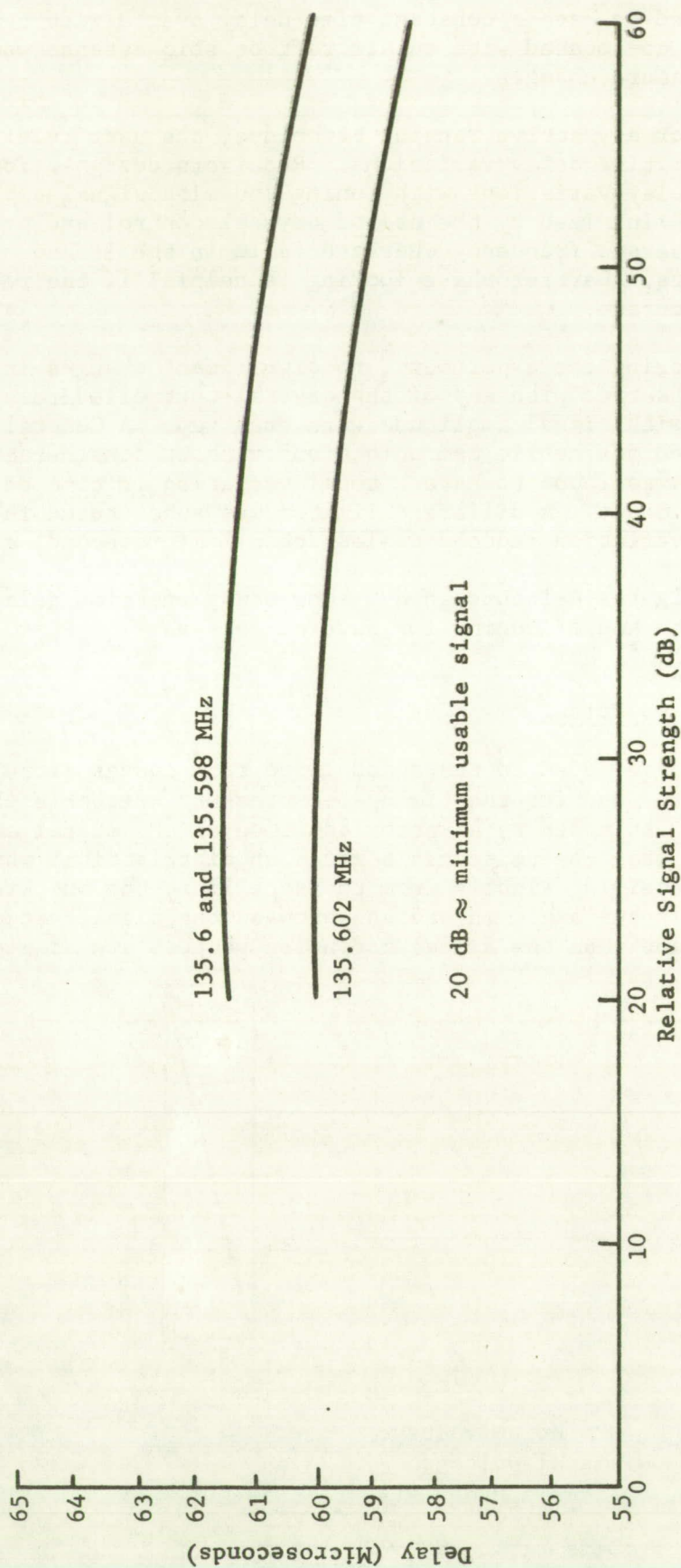


FIGURE 4-2

DELAY VERSUS SIGNAL STRENGTH
GE TYPE ER-41-C RECEIVER, MODEL 4ER41C10-21
ORIGINAL LIMITER REPLACED BY SPECIAL TUNED LIMITER

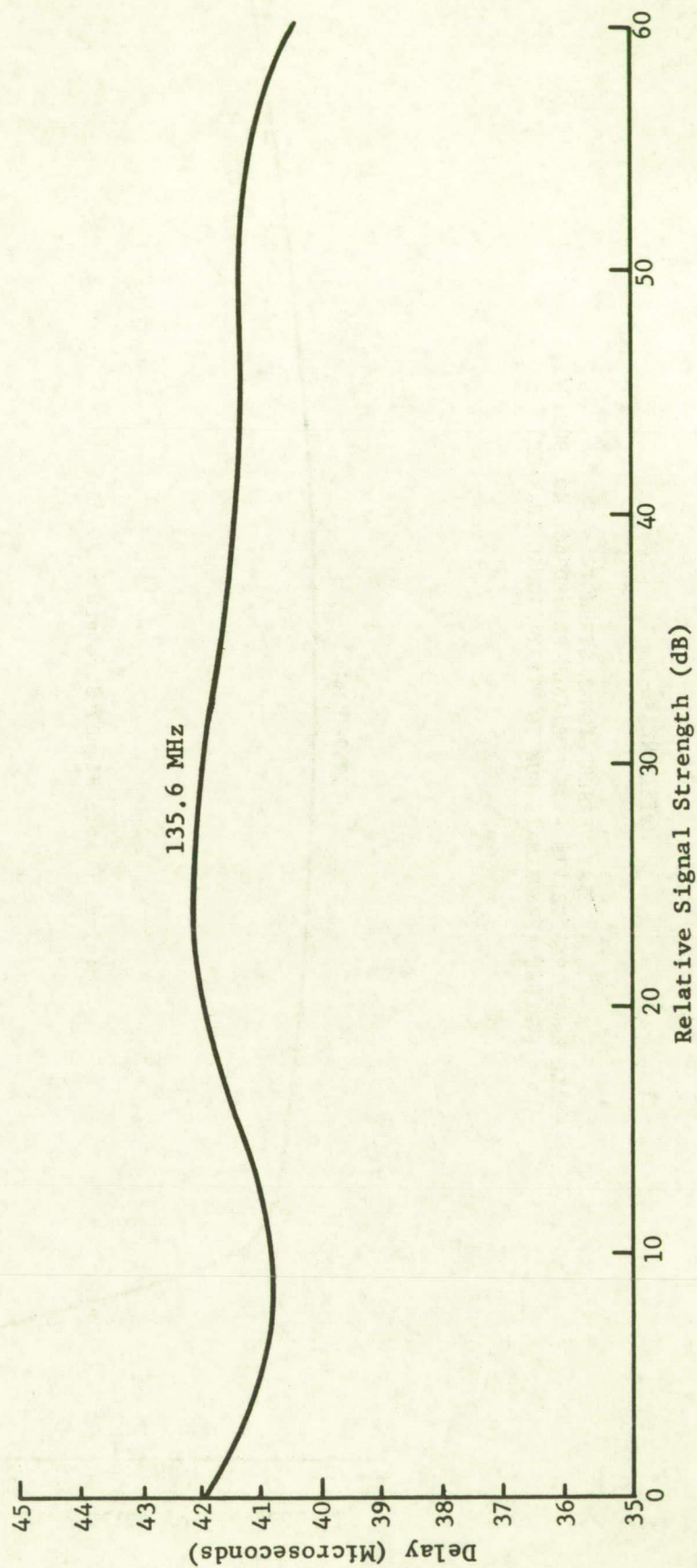


FIGURE 4-3

DELAY VERSUS SIGNAL STRENGTH
SMALL HAND TRANSCEIVER - GE PORTABLE PR36RDS66, NO. 9051072)
(VALUES APPROXIMATE DUE TO STRAY SIGNAL LEAKAGE)

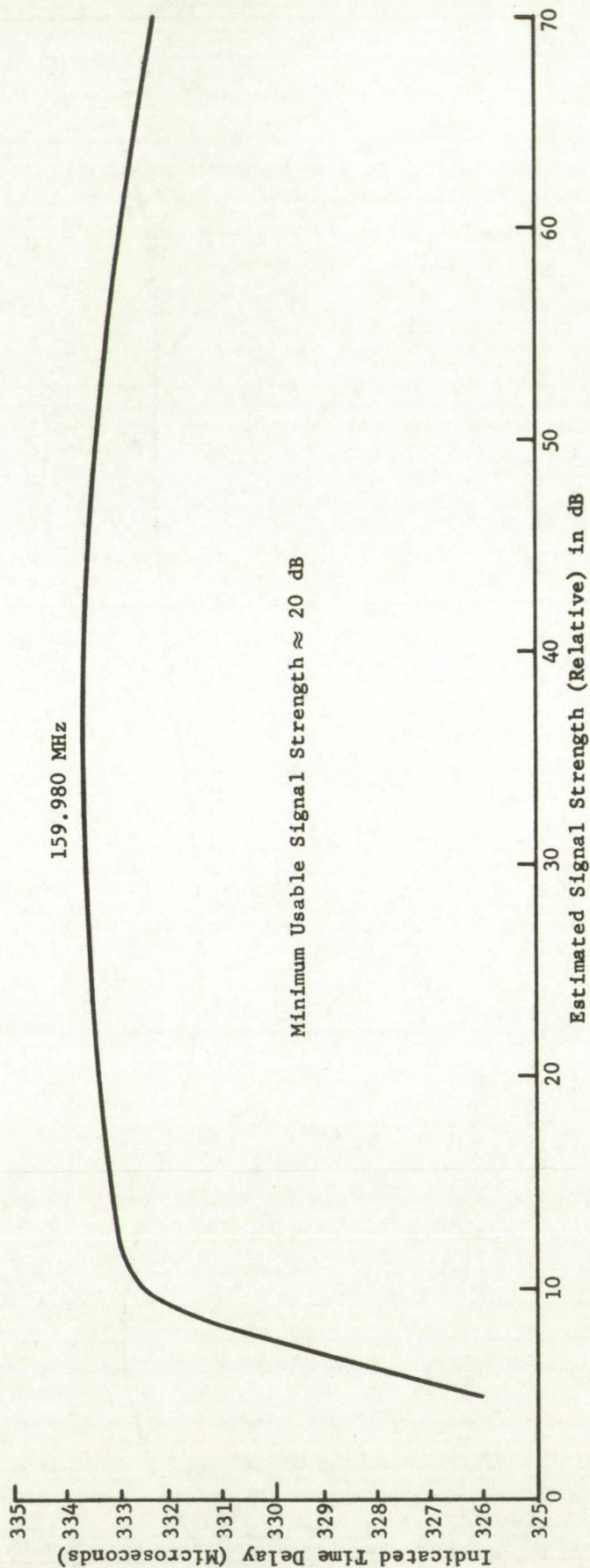


FIGURE 4-4

DELAY VERSUS FREQUENCY
GE TYPE ER-52-A MONITOR RECEIVER

+60 dB Signal Strength (Ref. Figure 4.1)

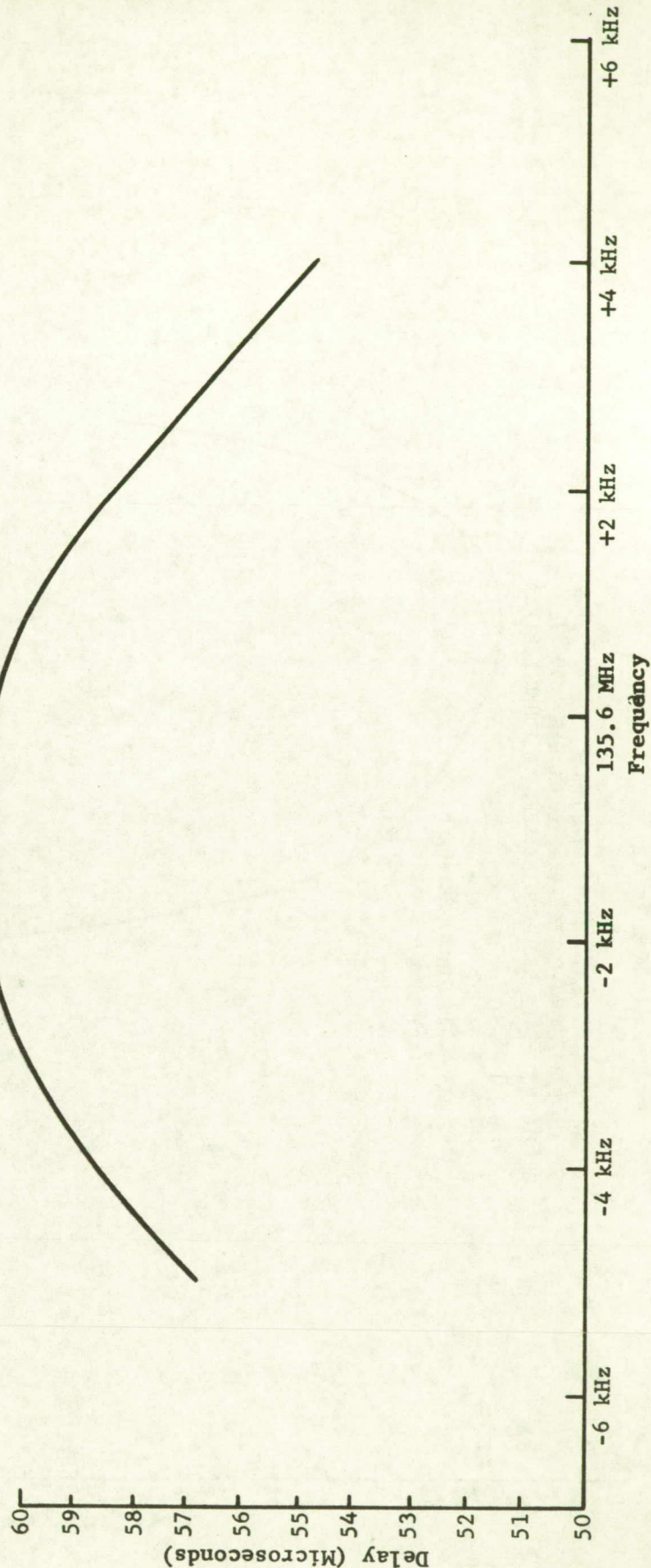
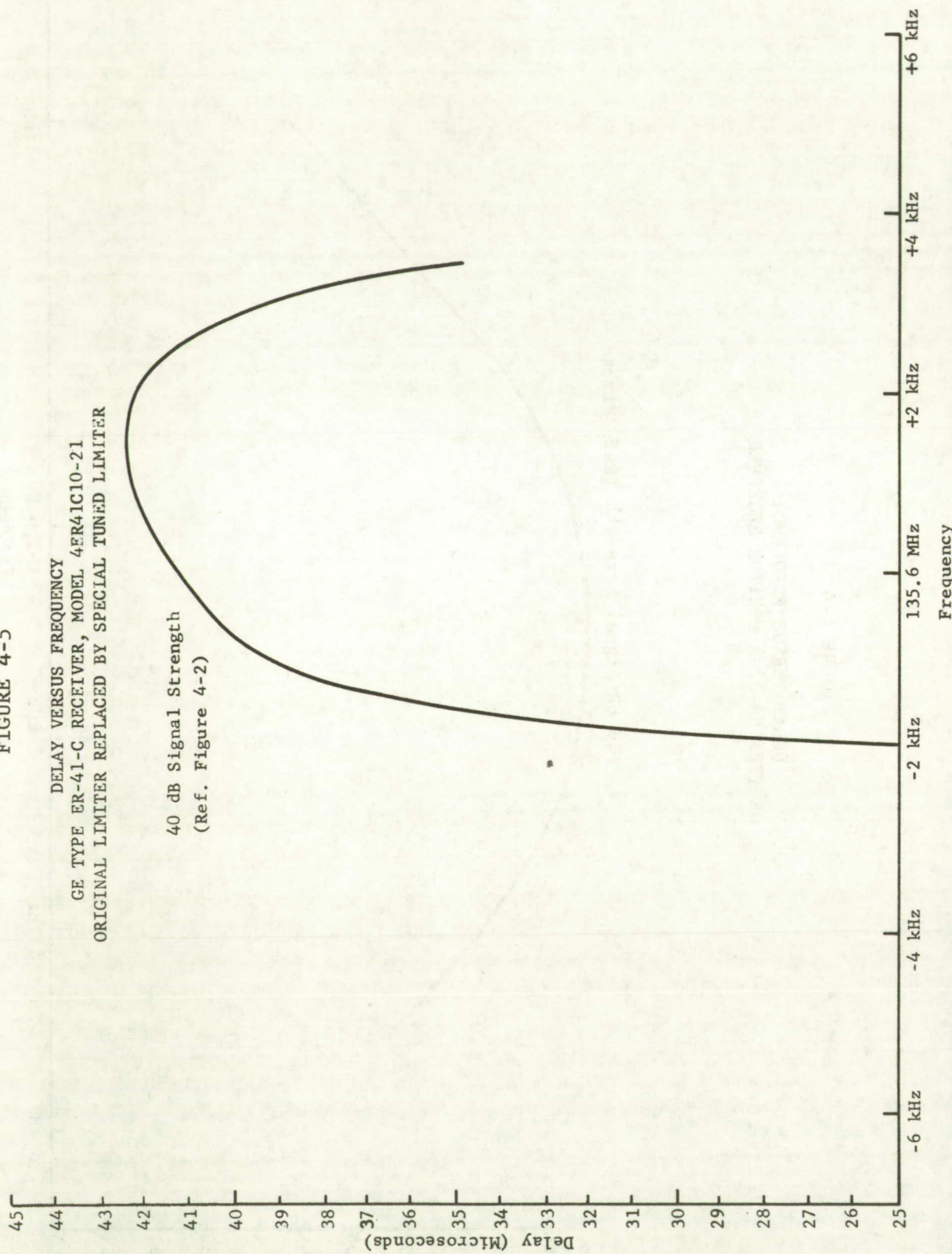


FIGURE 4-5

DELAY VERSUS FREQUENCY
 GE TYPE ER-41-C RECEIVER, MODEL 4ER41C10-21
 ORIGINAL LIMITER REPLACED BY SPECIAL TUNED LIMITER

40 dB Signal Strength
 (Ref. Figure 4-2)



The phase measurement precision is improved by the square root of the number of cycles averaged.

For the narrow bandwidth frequency modulation used in the experiment, the minimum signal-to-noise ratio for detection is 5 dB in the 15 kHz bandwidth of the receiver. The equivalent signal-to-noise ratio out of the 4 kHz bandwidth detector is 10 dB. (Figure 4-6) The detected 2.4414 kHz tone is passed through a 120 Hz bandpass filter before it is applied to the phase detector. Considering fluctuation noise, the signal-to-noise improvement provided by the bandpass filter is 4000/120, or 15 dB. The lowest signal-to-noise ratio into the phase detector is thus ≈ 25 dB. The one sigma phase error on a single cycle is

$$\phi_e = \frac{1}{\sqrt{320}} \times 57.3^\circ \approx 3^\circ$$

The phase measurement is averaged over approximately 64 cycles, to provide an improvement of approximately 8. The one sigma phase error should thus be 0.4 degree. As the period of one audio cycle is 409 microseconds, the timing precision should be

$$0.4 \times \frac{409}{360} \approx 0.45 \text{ microsecond}$$

Measurement of responder performance shows that the theoretical precision was not achieved at the detection threshold. Figure 4-7 relates RF signal-to-noise ratio and one sigma timing precision as determined in laboratory tests. Although the experimental results are worse than the theoretical by a factor of 3:1, the range measurement variation does not exceed practical limits at the lowest received signal levels; i.e. if the signal can be received at all, it is precise enough to be used.

Tests were conducted to determine the performance of the phase matching and correlation process with various signal-to-noise ratios. The tests were performed at baseband (no RF link) by summing the output of the ground terminal tone-code generator with fluctuation noise and feeding the resulting output directly into the ground terminal correlator. The ground terminal correlator uses the same phase matching process as a responder. RMS-signal-to-RMS-noise ratios were measured at the output of the 4 kHz low pass filter used in both the ground terminal correlator and a responder. The signal was held constant at 1 Volt RMS while the noise was adjusted to give the desired signal-to-noise ratio. Each was measured in the absence of the other using a Hewlett-Packard 1400A RMS Voltmeter. A block diagram of the test set-up is shown in Figure -8.

The test consisted of determining the standard deviation and number of bits in error in the 30 bit user code in the absence of additive noise and for signal-to-noise ratios between 20 dB and 0 dB.

Data were collected for ten minutes for each signal-to-noise ratio. The code generator was caused to give an output once per two seconds resulting in 300 correlations for each test condition. The time interval measurements for determining the standard deviation were the intervals from code generation to correlation.

Since each correlation involved the monitoring of a code which is 30 bits in length (15 bits word synch plus 15 bits address), the maximum number of bits monitored during the ten minutes is 9,000. For each missed correlation, the number will be reduced by 30 bits.

FIGURE 4-6

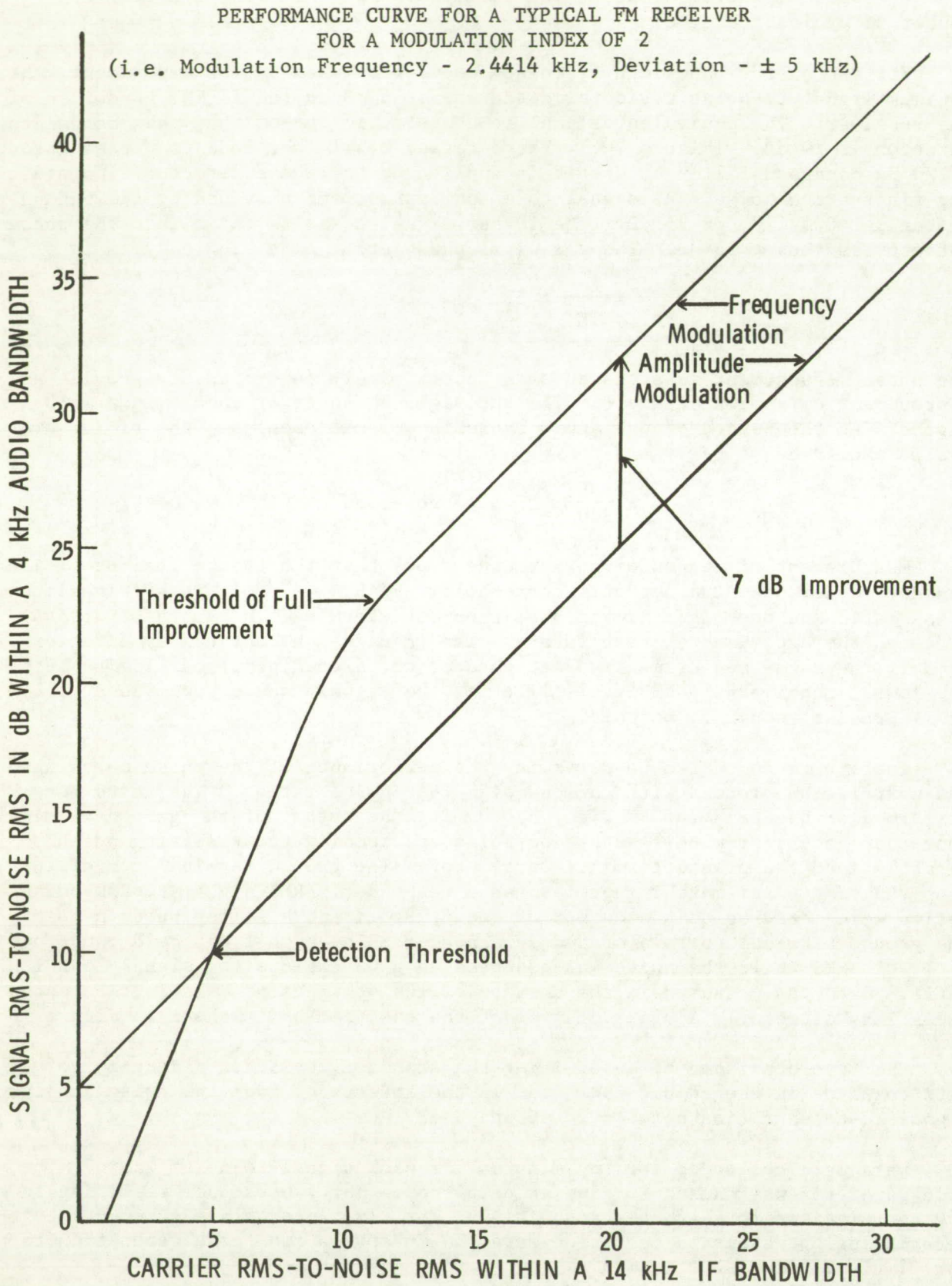


FIGURE 4-7

STANDARD DEVIATION AS A FUNCTION OF
SIGNAL-TO-NOISE RATIO WITHIN A 4 kHz AUDIO BANDWIDTH

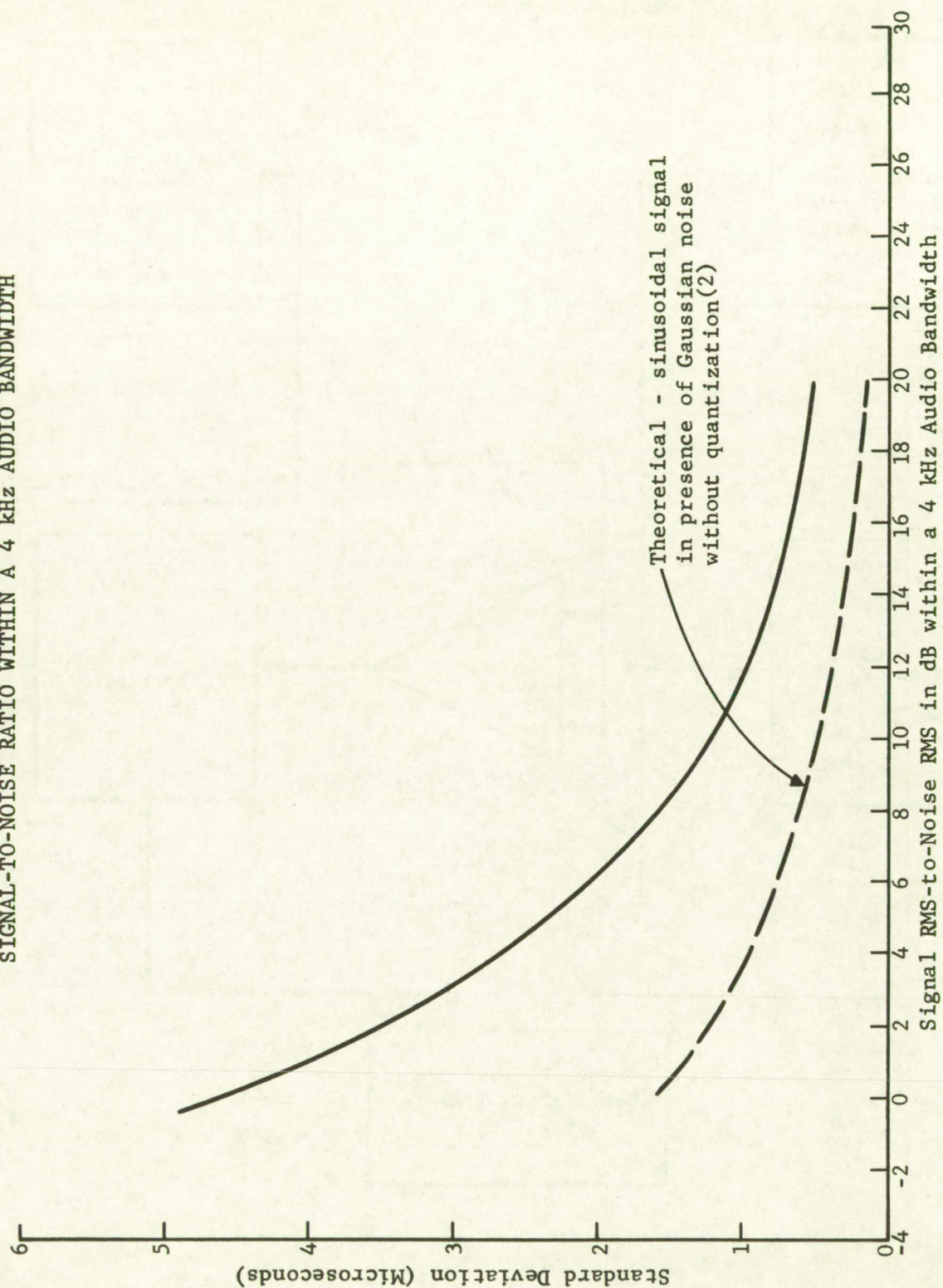
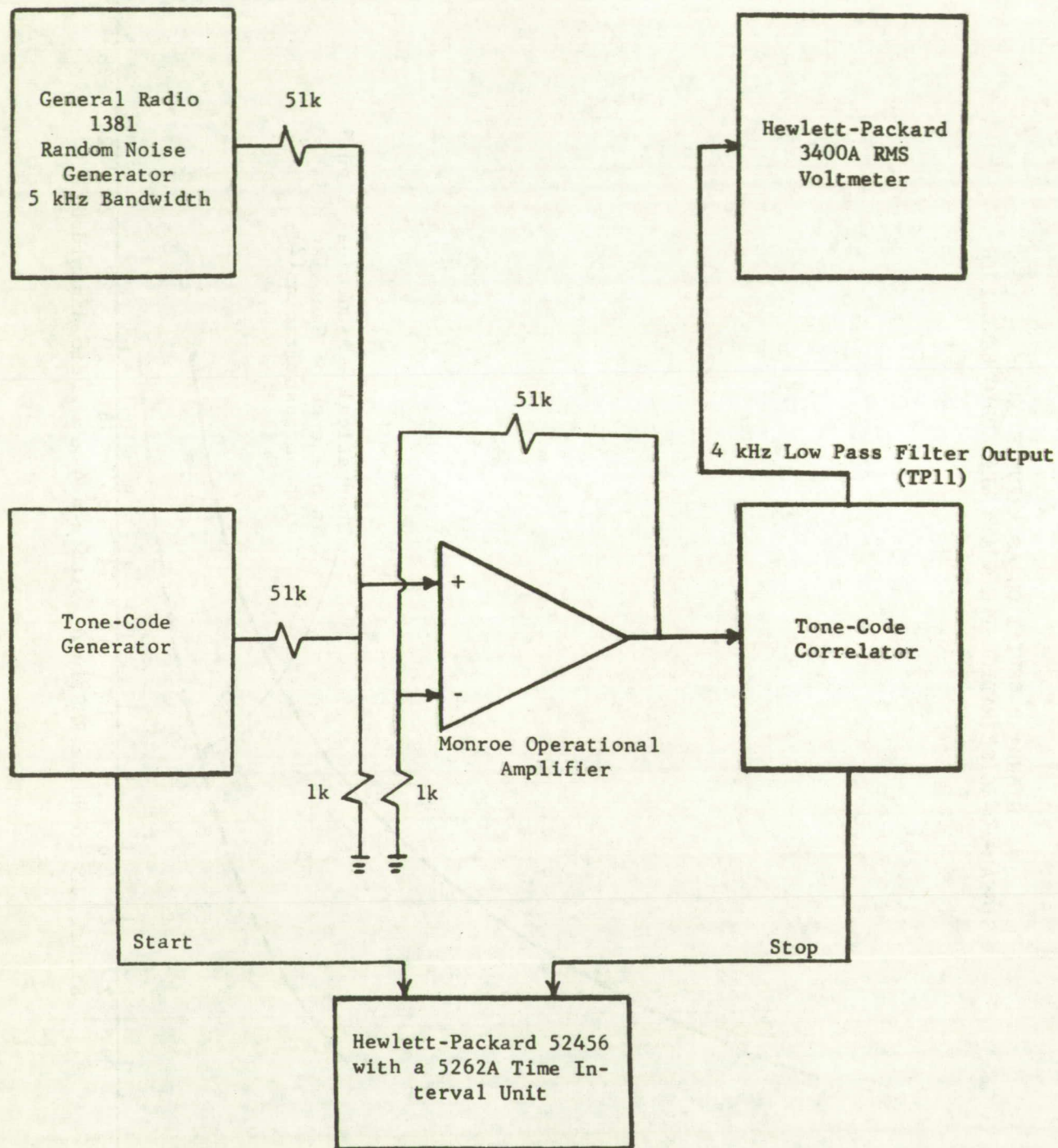


FIGURE 4-8

EQUIPMENT PERFORMANCE TEST



The results of the test are presented in Table 4-1. The bits in error are shown for both the word synch and address since they were monitored independently. The total bits in error is their sum. Also presented are the number of missed correlations and the maximum deviations from the mean in both positive and negative directions. The number of bits monitored is 9,000 minus 30 times the number of missed correlations. P_E is the bit error probability and was calculated by dividing the number of bits in error by the number of bits monitored.

During the test, as during all the experiments, the correlator threshold levels on both word synch and address were set such that correlations will not occur if there are more than 3 bits in error in either word synch or address.

Bit error probability, percent correlations and standard deviation, are each plotted as a function of signal-to-noise ratio in Figures 4-9, 4-10 and 4-7 respectively. The distributions of time interval measurements (histogram) for each signal-to-noise ratio are presented in Figures 4-11 through 4-17.

A measure of system performance in terms of accuracy and reliability is provided by comparison of the solid and dashed theoretical curves shown in Figures 4-7 and 4-9 respectively.

The term reliability is used here in reference to the probability of a successful correlation. This is directly related to the bit error rate. Figure 4-9 presents bit error probability as a function of signal-to-noise ratio within a 4 kHz bandwidth. The dashed curve is theoretical¹ and is representative of that which can be achieved using an optimum filter. Both curves are for on-off modulation. Comparison of these curves indicates that the present system is operating below optimum by a maximum of 3 dB. System reliability can be improved by 3 dB if phase modulation (polar) is used.

A measurement of system accuracy is provided in Figure 4-7. The dashed curve which provides a measure of system performance was derived based on material presented by Mischa Schwartz². In his material, he derives the probability density function for the phase of a sinusoidal signal in the presence of gaussian noise.

The expression for $f(\theta)$ is as follows:

$$f(\theta) = \frac{e^{-S^2}}{2\pi} + \frac{1}{2} \sqrt{\frac{S^2}{\pi}} \cos \theta e^{-S^2 \sin^2 \theta} [1 + \operatorname{erf}(S \cos \theta)]$$

where S = signal-to-noise voltage ratio. For $S^2 = 0$ (no signal) the equation reduces to $f(\theta) = 1/2\pi$, as expected. For signal-to-noise ratios $\gg 1$ and $|\theta| < 5^\circ$, this expression reduces to

$$f(\theta) = \frac{e^{-S^2 \theta^2}}{\sqrt{\pi/S^2}}$$

This represents a gaussian distribution with zero mean and standard deviation

$$\sigma = \frac{1}{S\sqrt{2}} \text{ radians.}$$

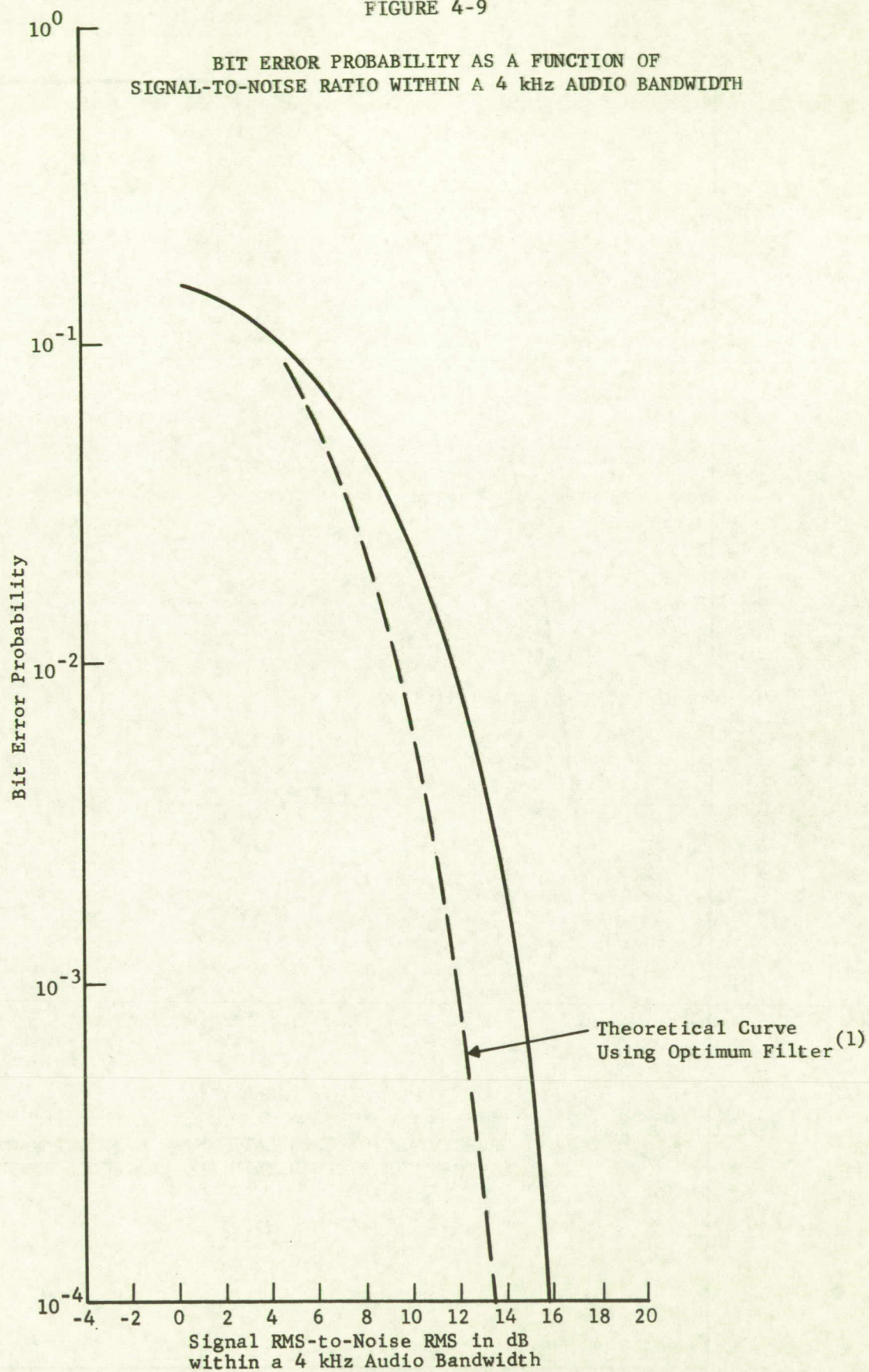
TABLE 4-1
EQUIPMENT PERFORMANCE TEST DATA

S/N RATIO	STANDARD DEVIATION IN μ s	MAXIMUM DEVIATION FROM MEAN IN μ s		NUMBER OF BITS IN ERROR		TOTAL BITS IN ERROR	NO. OF MISSED CORRELATIONS	NO. OF BITS MONITORED	P E
		POSITIVE	NEGATIVE	WORD SYNC	ADDRESS				
>20 dB*	0.4046	1.27	1.54	0	0	0	0	9000	--
20 dB	0.5161	1.99	1.59	0	0	0	0	9000	--
18 dB	0.5663	1.66	1.96	0	0	0	0	9000	--
16 dB	0.6225	2.25	1.79	1	0	1	0	9000	0.00011
14 dB	0.8192	2.18	2.01	11	6	17	0	9000	0.0019
12 dB	0.9368	2.39	2.48	35	25	60	0	9000	0.0067
10 dB	1.283	3.33	3.29	142	116	258	0	9000	0.0287
8 dB	1.619	5.00	4.23	276	244	520	7	8790	0.059
6 dB	2.003	6.25	5.31	394	332	726	30	8100	0.090
3 dB	2.951	7.24	7.29	388	365	753	80	6600	0.114
0 dB	4.566	12.86	12.10	258	238	496	200	3000	0.165

* Noise Generator Off

FIGURE 4-9

BIT ERROR PROBABILITY AS A FUNCTION OF
SIGNAL-TO-NOISE RATIO WITHIN A 4 kHz AUDIO BANDWIDTH



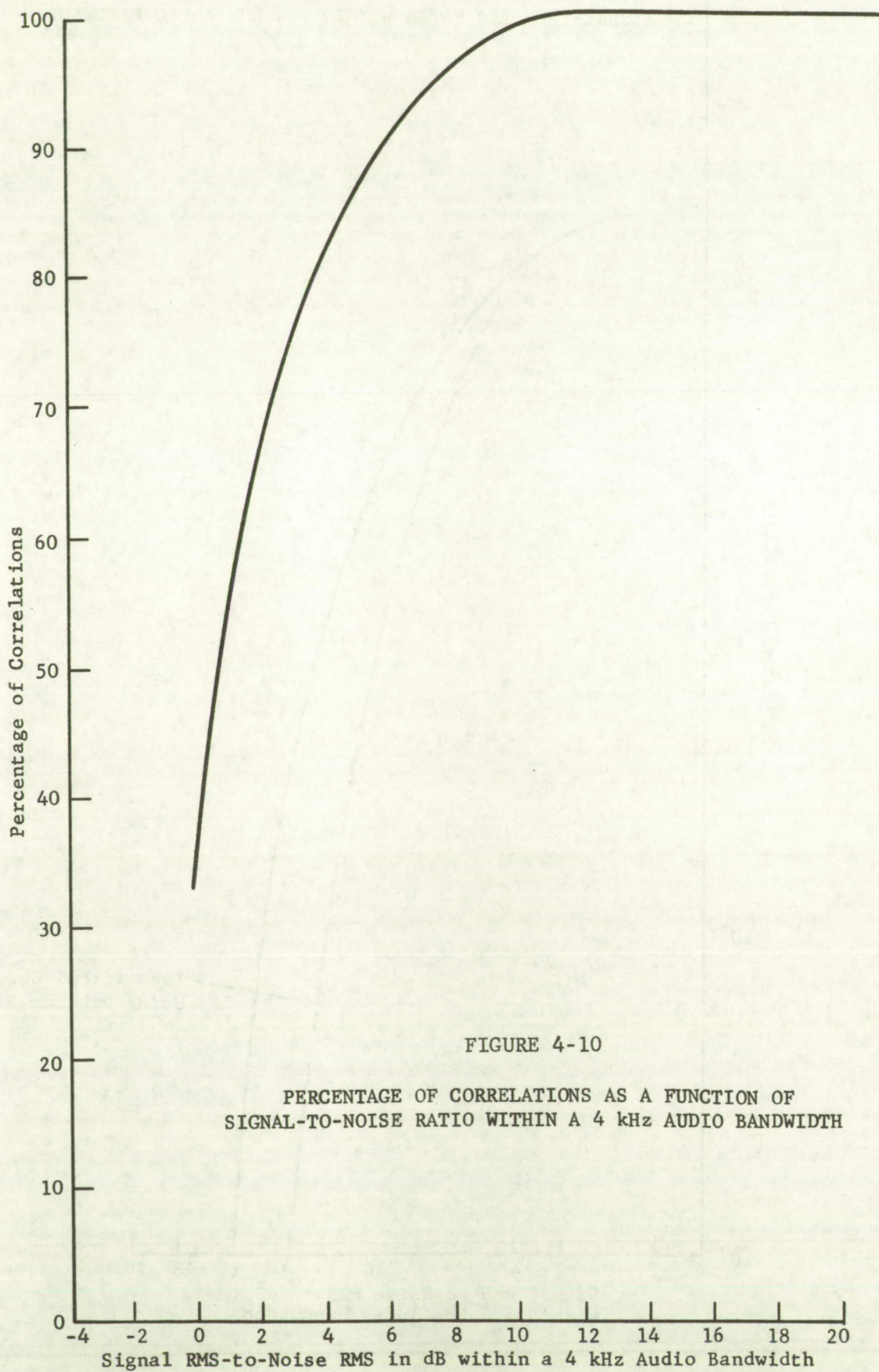
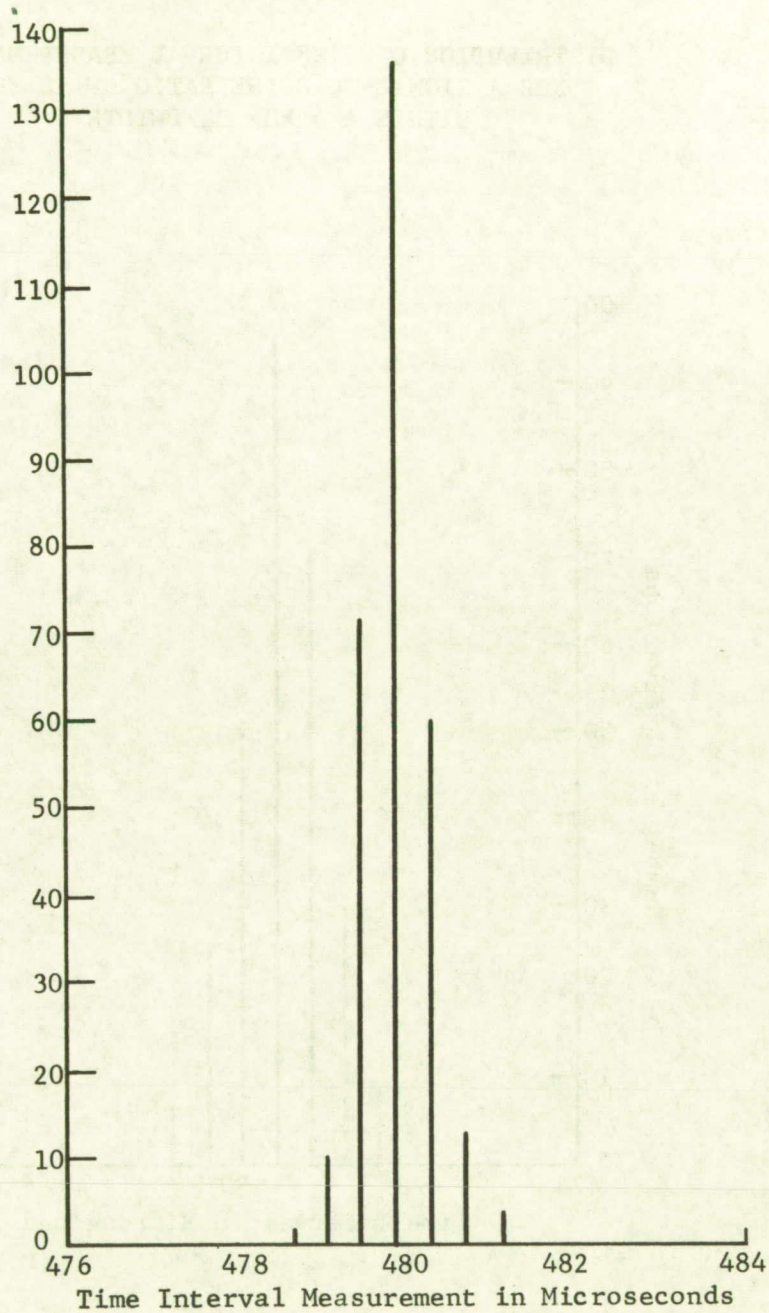


FIGURE 4-10

PERCENTAGE OF CORRELATIONS AS A FUNCTION OF
SIGNAL-TO-NOISE RATIO WITHIN A 4 kHz AUDIO BANDWIDTH

FIGURE 4-11

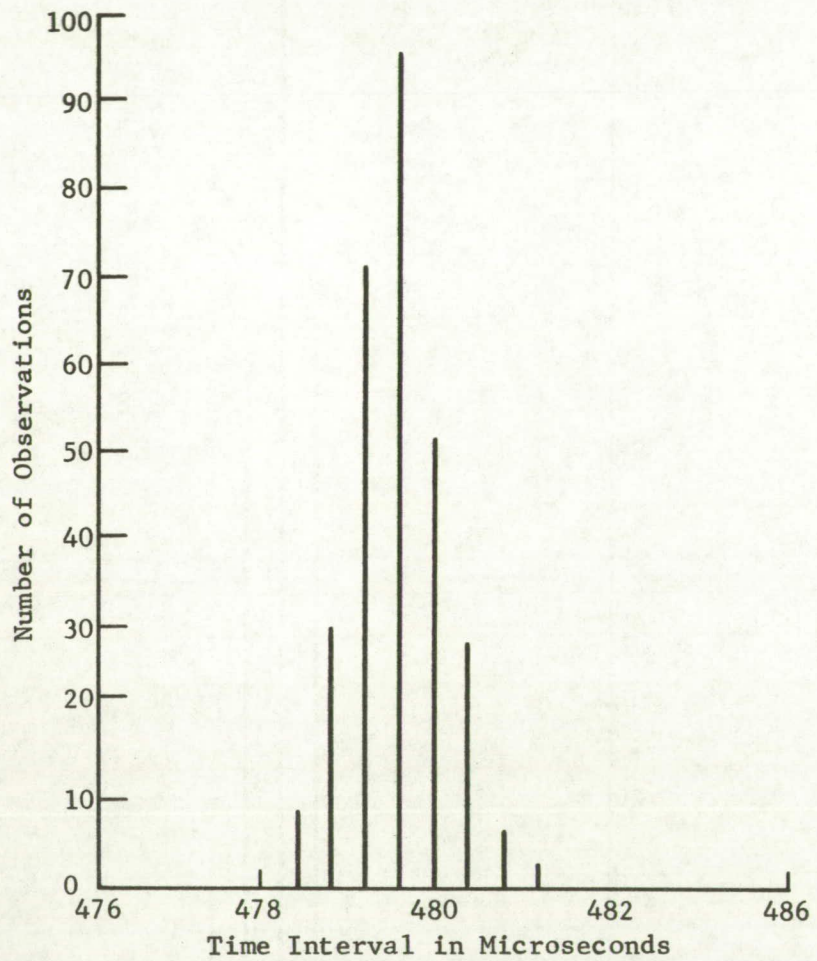
DISTRIBUTION OF TIME INTERVAL MEASUREMENTS FOR
SIGNAL-TO-NOISE RATIO OF >20 dB WITHIN A
4 kHz BANDWIDTH, I.E. NOISE GENERATOR OFF



Standard Deviation 0.4046
100 Percent Correlations

FIGURE 4-12

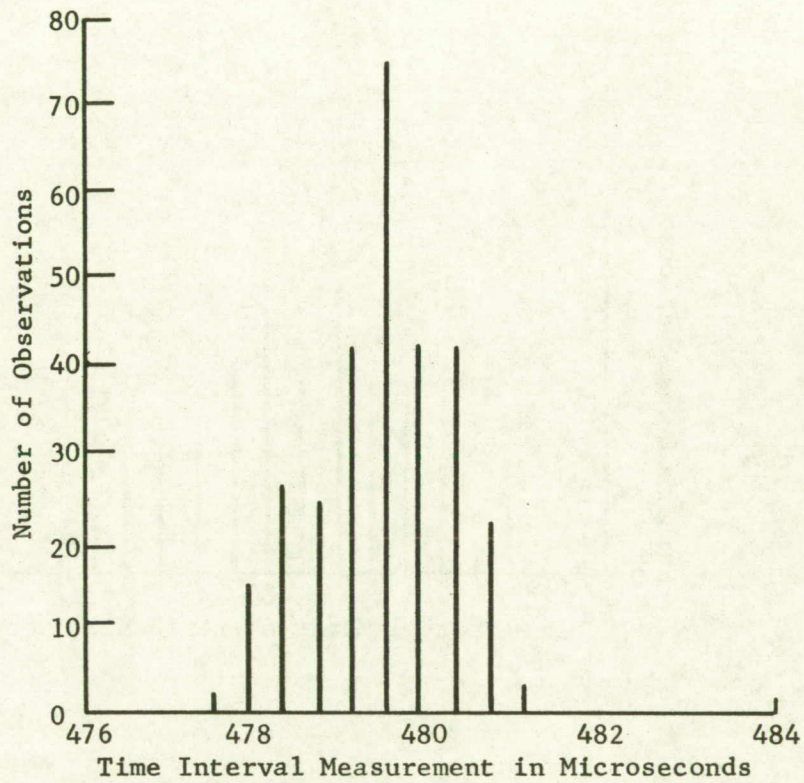
DISTRIBUTION OF TIME INTERVAL MEASUREMENTS
FOR A SIGNAL-TO-NOISE RATIO OF 18 dB
WITHIN A 4 kHz BANDWIDTH



Standard Deviation 0.4046
100 Percent Correlations

FIGURE 4-13

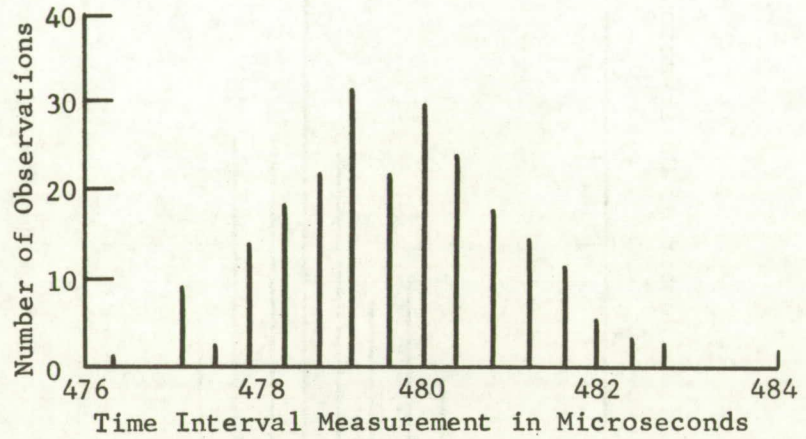
DISTRIBUTION OF TIME INTERVAL MEASUREMENTS
FOR A SIGNAL-TO-NOISE RATIO OF 14 dB
WITHIN A 4 kHz BANDWIDTH



Standard Deviation 0.8192
100 Percent Correlations

FIGURE 4-14

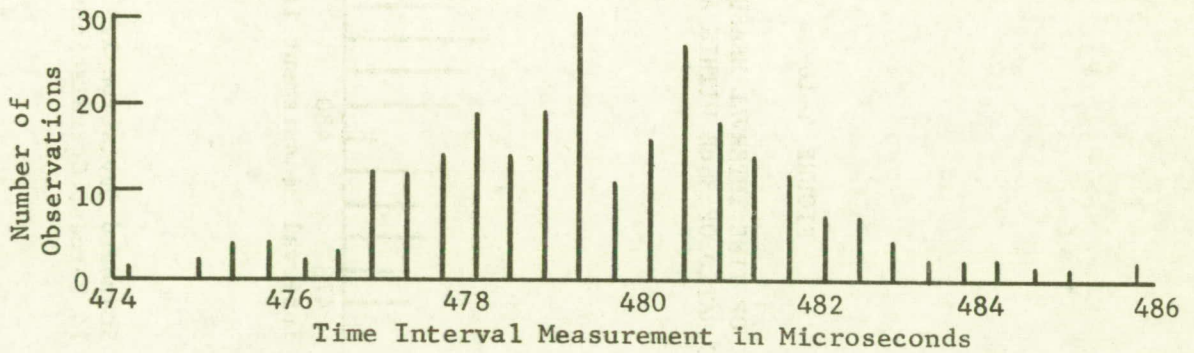
DISTRIBUTION OF TIME INTERVAL MEASUREMENTS
FOR A SIGNAL-TO-NOISE RATIO OF 10 dB
WITHIN A 4 kHz BANDWIDTH



Standard Deviation 1.283
100 Percent Correlations

FIGURE 4-15

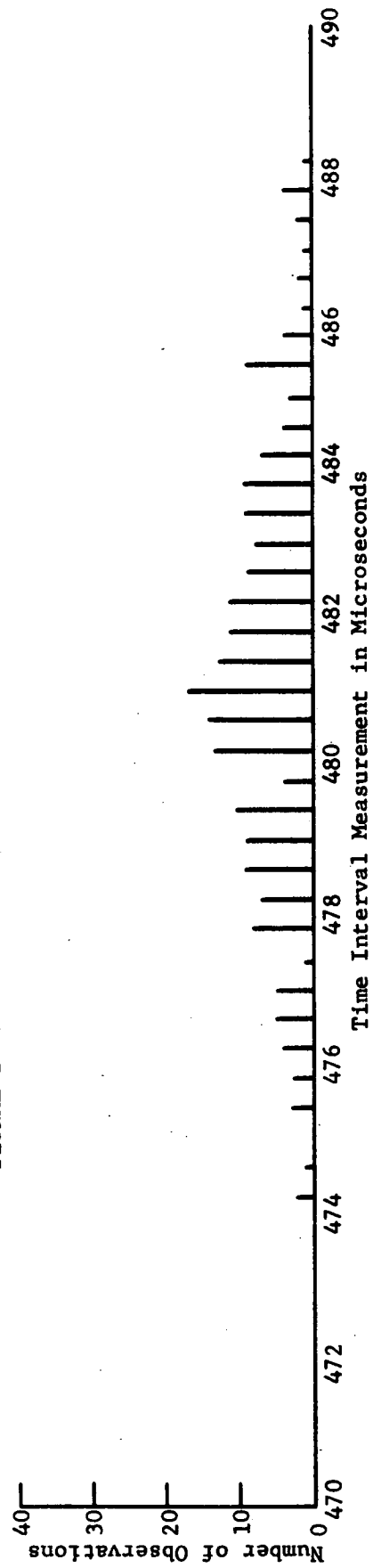
DISTRIBUTION OF TIME INTERVAL MEASUREMENT
FOR A SIGNAL-TO-NOISE RATIO OF 6 dB
WITHIN A 4 kHz BANDWIDTH



Standard Deviation 2.003
90 Percent Correlations

FIGURE 4-16

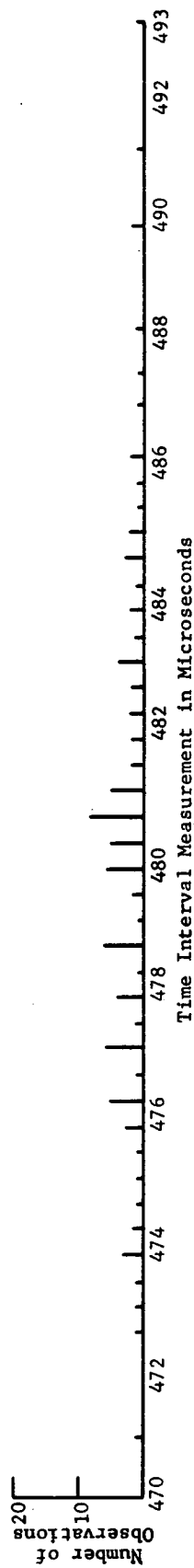
DISTRIBUTION OF TIME INTERVAL MEASUREMENTS FOR A
SIGNAL-TO-NOISE RATIO OF 3 dB WITHIN A 4 kHz BANDWIDTH



Standard Deviation 2.951
74 Percent Correlations

FIGURE 4-17

DISTRIBUTION OF TIME INTERVAL MEASUREMENTS FOR A
SIGNAL-TO-NOISE RATIO OF 0 dB WITHIN A 4 kHz BANDWIDTH



Standard Deviation 4.566
33 Percent Correlations

The digital phase lock loop has a bandwidth of approximately 5 Hz resulting in a 30:1 improvement on the signal-to-noise ratio at the output of the 4 kHz low pass filter. If signal-to-noise ratios of 0 dB and greater within a 4 kHz bandwidth are considered, then the expression

$$\sigma = \frac{1}{s\sqrt{2}}$$

is valid. This is applicable since the equivalent signal-to-noise ratio within the loop bandwidth is ≥ 30 dB (ratio of 30:1) which is much greater than 1. The dashed curve was generated by calculating the standard deviation as a function of signal-to-noise ratio using the expression

$$\sigma = \frac{1}{s\sqrt{2}}$$

radians and converting to microseconds via the relationship

$$1 \text{ rad} = \frac{180}{\pi} \text{ degrees}$$

and one period of a 2.4414 kHz waveform is equal to 409 microseconds. Therefore

$$\sigma = \frac{1}{s\sqrt{2}} \text{ radians} \times \frac{180 \text{ degrees}}{\pi \text{ radians}} \times \frac{409 \text{ microseconds}}{360 \text{ degrees}}$$

or

$$\sigma = \frac{46}{s} \text{ microseconds}$$

A comparison of these curves indicates a possible 3:1 improvement in accuracy.

Interrogation Response Rate

Many thousands of interrogations were made to ranging transponders during the experiment. The usual interrogation rate was once each three seconds although an interrogation rate of once each two seconds was also used successfully. During some interrogation periods, the transponders replied on nearly every interrogation but during some periods the interrogation rate was lower than would be acceptable in an operational system. There were several factors that contributed to lower response rates, some of them deliberately designed into the experiment to study propagation effects, and some factors that suggest precautions that must be taken in the design of a ranging system.

The poorest propagation link was usually the one from the satellite to the transponder. Irregularly shaped antenna patterns, Faraday rotation, and sea reflections sometimes caused the signal level into the vehicle transponder to drop below the detection threshold. Signal amplitude scintillation due to the ionosphere occurred infrequently but was observed. Scintillation causes amplitude fading over a large range at VHF and can cause the signal to fall below the detection threshold.

The Sea Robin buoy was interrogated a total of 2525 times during the periods of April 14 through 25, 1969 and May 9 and 10, 1969. One thousand seven hundred eleven responses were received at the Observatory. Of these, 860 resulted in successful range measurements. The design of the experiment caused a deliberate reduction in the response rate in order to observe the effects of Faraday rotation. Interrogation periods were three minutes long. The best receive polarization for the buoy was selected just prior to the three minute interrogation period and that receive polarization at the buoy was used throughout the entire test period. The responses from the buoy during the first minute and one-half were of the same polarization as the receiver but during the second minute and one-half they were transmitted with the orthogonal polarization. Since the up-link and down-link paths are at different frequencies and Faraday rotation varies as $1/f^2$, the preferred orientation of linearly polarized antennas can be different at the two frequencies. During that period of the experiment the ground terminal antenna had vertical or horizontal polarization but the polarization was the same for both transmission and reception. At a later time the ground terminal was arranged for independent selection on a transmission and reception. The effects of Faraday rotation were evident in these experiments because signal levels were often much better when different polarizations were used for transmission and reception. If the satellite were circularly polarized the response rate would be improved by reducing the effects of Faraday rotation.

Signals reflected from the sea combined with the direct signal from the satellite to enhance or reduce the signal level into the antenna. When the direct and reflected signals arrive in phase, the signal level can be as much as 3 dB stronger than the direct signal alone, but when they arrive out of phase they tend to cancel and the signal level may drop below the detection threshold. For a vehicle with an antenna a few wavelengths above the sea surface, as on a ship or the Sea Robin buoy, the effect is to produce an antenna pattern with lobes representing good signal reception alternating with nulls in the vertical plane. As the sea surface tilts and the antenna moves due to the action of the waves, the lobe pattern moves in elevation angle to cause an alternate enhancement and cancellation of the received signal. In the experiment the transmitted and received wavelengths were different, making the lobe patterns different for reception and transmission. A successful interrogation occurred when the lobe patterns permitted adequate signal strengths on both the up and down links. Tone-code ranging requires a signal duration shorter than the roll period of a buoy or ship and therefore a successful interrogation can be made except when a null in the pattern is directed toward the satellite. Other techniques that require longer signal transmissions for range measurement may suffer greater deterioration due to the rolling of the craft. The effect of sea reflection can be minimized by the use of circular polarization on the satellite and the craft, if the elevation angle to the satellite is above the Brewster angle. Then the rotation sense of the reflected signal is reversed, its amplitude is reduced relative to the direct signal and the depth of the nulls is reduced.

Sea reflections affect received signal amplitude in aircraft much as they do in ships. Because of the higher altitude, the nulls are very closely spaced in elevation and aircraft can fly for several seconds in straight and level flight if the satellite is abeam, but if the aircraft is flying towards or away from the satellite or climbing or descending it passes through the interference pattern quickly and rapid fading of the signal may be experienced. An antenna pattern designed to discriminate against the reflected signal can

reduce or nearly eliminate the effect. The use of circular polarization on the satellite and aircraft would be helpful.

Lower response rates were experienced in aircraft when using the VHF blade antenna than when using the Satcom antenna, due in part to sea reflections, but also to the poor azimuth and elevation pattern characteristics of the VHF blade. During some periods of flight the response rate approached 100 percent for the aircraft when the Satcom antenna was in use. In certain flight directions using the VHF blade antenna, the response rate was as low as 10 or 20 percent, especially when the aircraft was in a noisy environment as when flying in the vicinity of thunder storms.

The mast and other structures of the Valiant and Rush had a large effect on the pattern of the omnidirectional antennas. When the low gain circularly polarized antenna had a clear view in the direction of the satellites, the interrogation response rate was nearly 100 percent. When the mast was between the satellite and the antenna, the response rate dropped to below 50 percent.

Scintillation in the reception of a VHF signal from a satellite results from focusing of the signals due to horizontal gradients of electron density in the ionosphere. The columnar electron content seldom varies more than two percent, so the gradients have very little effect on the propagation delay time and therefore do not significantly affect the accuracy of range measurements. However, the focusing of the energy causes the signal strength to be high at some points on the ground and low at other points. Because the density variations move horizontally, the signal strength observed at a fixed point may vary from a strong enhancement to almost complete cancellation. The fading periods vary from seconds to minutes. The signal level may fall below the detection threshold for periods on the order of a few seconds. The proportion of time that the signal is below the threshold is in part a function of the fading margin designed into the propagation links, but it would not be practical to allow sufficient margin to guarantee 100 percent response at VHF frequencies. The effect is smaller at higher frequencies. Scintillation is experienced at high latitudes more frequently than at mid-latitudes. The effect on a ranging system need not be serious if the ranging techniques require short interrogation periods, although it may require that a user be interrogated more than once during the times when scintillation is present in order to insure that a response is obtained.

The transmission links from ATS to the experimental transponders were considered to be marginal. However, it is concluded from the experiments that modest design changes would insure reliable performance at VHF. These design changes would include the use of circular polarization on the satellite and more suitable design of the antennas on the mobile vehicles. While greater effective radiated power from the satellite would be desirable, it would probably not be necessary.

An occasional false correlation was experienced in the mobile craft, and at the terminal. Under noisy conditions false correlations were observed more than one percent of the time. A one percent false correlation rate would not be acceptable in a system involving a large number of user craft, for there would be frequent transmissions from craft that were not interrogated, thus, tending to increase interference on the transmission links. Several simple

measures are now apparent that would improve the design of the codes and insure an acceptably low rate of false interrogations. These improvements include the use of phase reversal modulation in the codes to improve the signal-to-noise ratio by 3 dB and gating to insure that the correlators search only for the code and are not activated by noise during periods when code transmissions are not being received.

Range Precision on the Satellite Links

Measurements of ranging precision on the satellite transmission links confirmed the laboratory tests of equipment performance. Range measurement precision was determined from the scatter of many independent range measurements made in sequence. The satellite changes in range, so a "best-fit" curve to the data was computed to compensate for the changing range. If the range to the satellite were not changing, the average value of the measurements would be used. The displacement of each independent range measurement from the best fit curve is computed, and also the standard deviation of the measurements from the curve. Figure 4-18 and Figure 4-19 present histograms of the displacements of range measurements from best fit curves. Each dot is an independent range measurement. Figure 4-18 is from the Observatory to ATS-3 and return; Figure 4-19 is from the Observatory through ATS-3 to a transponder and return. The scatter of the range measurements to the transponder is larger than to the satellite because more transmission links and electronic circuits are involved. It is evident that the standard deviations are much less than 1 microsecond. Averaging a number of readings would probably achieve a ranging precision of approximately ± 0.1 microsecond, or 50 feet. The largest individual displacements are 1.1 microsecond. All of the measurements were included in the histograms.

Ranging measurements were made from Schenectady to ATS-1 for half-hour periods, 11:15:00 to 11:45:00 GMT on the mornings of October 31 and November 1, 1970. ATS-1 is less than 2 degrees above the western horizon for the Observatory at Schenectady. The test provided an excellent measure of the ranging precision for the tone-code signal parameters used in the experiment. The standard deviation of the difference between the computed and measured slant ranges for 593 measurements made on October 31 was found to be 0.298 microsecond, and for 596 measurements made on November 2, 0.434 microsecond. Interrogations were made each 3 seconds during the half-hour periods and every interrogation provided a range measurement that was included in the computation of the standard deviation. The standard deviation represents two-way, one sigma ranging resolutions of 150 and 215 feet.

Tables 4-2 and 4-3 show the first few minutes of the computer print-outs for the half-hour interrogation periods. Reading a data line from left to right, the first column, 0, is the user identification for the data print-out; in this case, the Observatory. The second column is the date. The third column is the time in Greenwich Mean Time. The fourth column identifies the satellite. The fifth column is the difference between the measured slant range and the computed slant range from the NASA prediction of the satellite position. The sixth column represents the ground transponder that was interrogated on that interrogation. WASH stands for Washington (Seattle); ICE9 stands for Iceland. None of the data in this particular print-out pertains to those users. The column on the right is the computed slant range from the satellite to the Observatory expressed in the number of microseconds two-way propagation time, assuming the free space velocity of light. The actual range measurement in

FIGURE 4-18

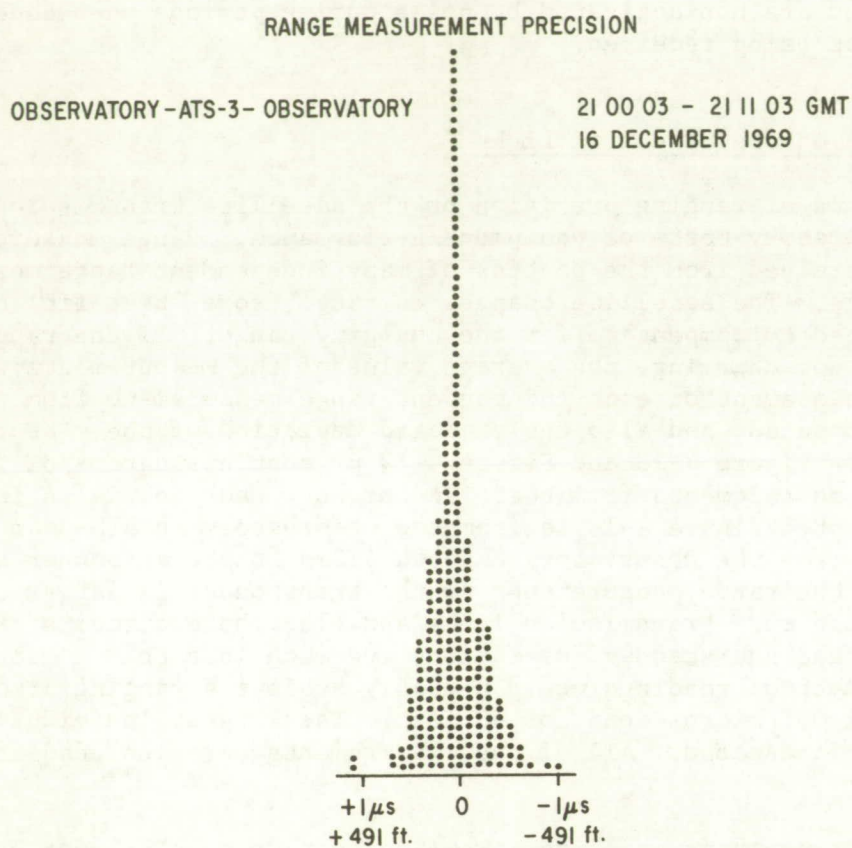


FIGURE 4-19

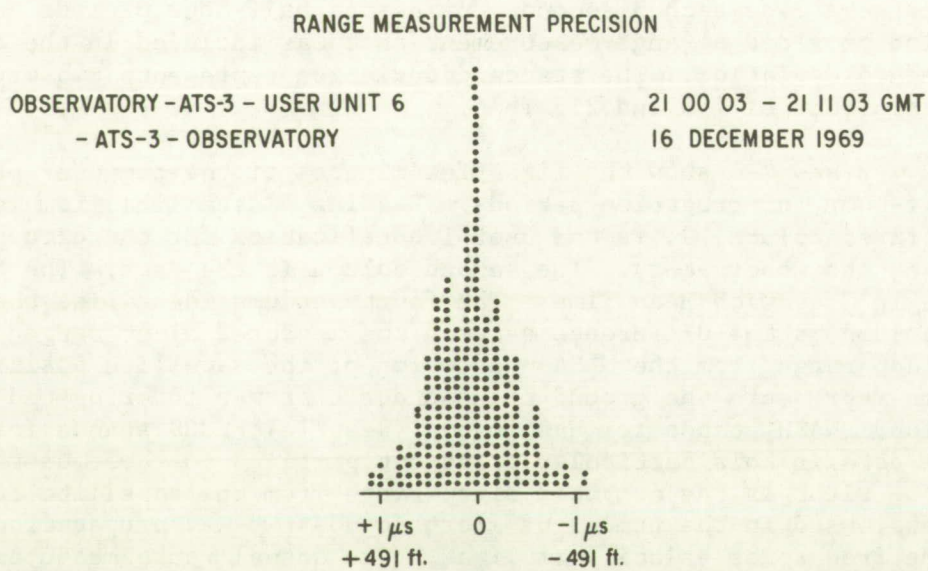


TABLE 4-2

11/23/70 13:08 TABLE DELAYS-3 DATA CF234 10/31/70 50											
D1 FOR ORS= 77.3 HEIGHT = 1325. LAT = 42.8480 LONG = -74.0710											
H	#	CLASS	NAME	JR	D2	D3	CRE	HEIGHT	LAT	LONG	FIXED
U	9	ORS	ICF9	1	431579.1	0.	0.	1325.	42.8481	-74.0708	T
U	10	ORS	WASH	1	431548.2	0.	0.	540.	47.4000	-122.1583	T
FILE 234 10/31/70											
52350	10/31/70	110000	0.	0.	0.	-1.110	-149.087	22759.03			
52360	10/31/70	113000	0.	0.	0.	-0.753	-149.099	22758.90			
0	10/31/70	11:15:04	ATS-1	8.5	WASH	276934.2					
0	10/31/70	11:15:07	ATS-1	9.3	WASH	276933.9					
0	10/31/70	11:15:10	ATS-1	8.8	WASH	276933.6					
0	10/31/70	11:15:13	ATS-1	9.1	WASH	276933.4					
0	10/31/70	11:15:16	ATS-1	9.0	WASH	276933.1					
0	10/31/70	11:15:19	ATS-1	9.0	WASH	276932.8					
0	10/31/70	11:15:22	ATS-1	9.0	WASH	276932.5					
0	10/31/70	11:15:25	ATS-1	8.9	WASH	276932.2					
0	10/31/70	11:15:28	ATS-1	9.3	WASH	276931.9					
0	10/31/70	11:15:31	ATS-1	8.9	WASH	276931.6					
0	10/31/70	11:15:34	ATS-1	8.8	WASH	276931.3					
0	10/31/70	11:15:37	ATS-1	8.0	WASH	276931.0					
0	10/31/70	11:15:40	ATS-1	8.8	WASH	276930.7					
0	10/31/70	11:15:43	ATS-1	9.1	WASH	276930.4					
0	10/31/70	11:15:46	ATS-1	8.7	WASH	276930.1					
0	10/31/70	11:15:49	ATS-1	9.1	WASH	276929.8					
0	10/31/70	11:15:52	ATS-1	8.6	WASH	276929.5					
0	10/31/70	11:15:55	ATS-1	8.6	WASH	276929.2					
0	10/31/70	11:15:58	ATS-1	9.0	WASH	276928.9					
0	10/31/70	11:16:01	ATS-1	8.9	WASH	276928.6					
0	10/31/70	11:16:04	ATS-1	8.9	WASH	276928.3					
0	10/31/70	11:16:07	ATS-1	8.5	WASH	276928.0					
0	10/31/70	11:16:10	ATS-1	8.8	WASH	276927.7					
0	10/31/70	11:16:13	ATS-1	8.7	WASH	276927.5					
0	10/31/70	11:16:16	ATS-1	8.7	WASH	276927.2					
0	10/31/70	11:16:19	ATS-1	8.7	WASH	276926.9					
0	10/31/70	11:16:22	ATS-1	8.6	WASH	276926.6					
0	10/31/70	11:16:25	ATS-1	9.0	WASH	276926.3					
0	10/31/70	11:16:28	ATS-1	8.6	WASH	276926.0					
0	10/31/70	11:16:31	ATS-1	8.9	WASH	276925.7					
0	10/31/70	11:16:34	ATS-1	8.5	WASH	276925.4					
0	10/31/70	11:16:37	ATS-1	8.5	WASH	276925.1					
0	10/31/70	11:16:40	ATS-1	8.9	WASH	276924.8					
0	10/31/70	11:16:43	ATS-1	8.8	WASH	276924.5					
0	10/31/70	11:16:46	ATS-1	8.8	WASH	276924.2					
0	10/31/70	11:16:49	ATS-1	8.8	WASH	276923.9					
0	10/31/70	11:16:52	ATS-1	8.8	WASH	276923.6					
0	10/31/70	11:16:55	ATS-1	8.7	WASH	276923.3					
0	10/31/70	11:16:58	ATS-1	8.7	WASH	276923.0					
0	10/31/70	11:17:01	ATS-1	8.7	WASH	276922.7					
0	10/31/70	11:17:04	ATS-1	9.1	WASH	276922.4					
0	10/31/70	11:17:07	ATS-1	9.1	WASH	276922.1					
0	10/31/70	11:17:10	ATS-1	9.3	WASH	276921.9					
0	10/31/70	11:17:13	ATS-1	8.9	WASH	276921.6					
0	10/31/70	11:17:16	ATS-1	8.5	WASH	276921.3					
0	10/31/70	11:17:19	ATS-1	8.9	WASH	276921.0					
0	10/31/70	11:17:22	ATS-1	8.9	WASH	276920.7					
0	10/31/70	11:17:25	ATS-1	8.8	WASH	276920.4					
0	10/31/70	11:17:28	ATS-1	8.8	WASH	276920.1					
0	10/31/70	11:17:31	ATS-1	8.4	WASH	276919.8					

STANDARD
DEVIATION
0.298 μs
FOR
593 MEASUREMENTS

STANDARD
DEVIATION
0.298 μ s
FOR
593 MEASUREMENTS

TABLE 4-3

11/23/70 13:13 TABLE DELAYS-3 DATA CF248 11/02/70 50
 D1 FOR ORS= 77.3 HEIGHT = 1325. LAT = 42.8480 LONG = -74.0710

H	#	CLAS	NAME	JR	D2	D3	CRE	HEIGHT	LAT	LONG	FIXED
U	9	ORS	ICE9	1	431579.1	0.	0.	1325.	42.8481	-74.0708	T
U	10	ORS	WASH	1	431548.2	0.	0.	540.	47.4000	-122.1583	T
52650	11/02/70	110000	0.	0.	0.	-1.017	-140.104	22758.03			
52660	11/02/70	113000	0.	0.	0.	-0.655	-149.117	22758.71			
0	11/02/70	11:15:02	ATS-1	7.3	ICE9			276893.4			
FILE 248 11/02/70											
0	11/02/70	11:15:05	ATS-1	6.7	ICE9			276893.1			
0	11/02/70	11:15:08	ATS-1	7.3	ICE9			276892.8			
0	11/02/70	11:15:11	ATS-1	7.4	ICE9			276892.5			
0	11/02/70	11:15:14	ATS-1	7.6	ICE9			276892.2			
0	11/02/70	11:15:17	ATS-1	7.8	ICE9			276891.9			
0	11/02/70	11:15:20	ATS-1	7.6	ICE9			276891.6			
0	11/02/70	11:15:23	ATS-1	7.3	ICE9			276891.3			
0	11/02/70	11:15:26	ATS-1	8.3	ICE9			276891.0			
0	11/02/70	11:15:29	ATS-1	7.3	ICE9			276890.7			
0	11/02/70	11:15:32	ATS-1	7.5	ICE9			276890.4			
0	11/02/70	11:15:35	ATS-1	7.6	ICE9			276890.1			
0	11/02/70	11:15:38	ATS-1	7.4	ICE9			276889.8			
0	11/02/70	11:15:41	ATS-1	7.6	ICE9			276889.5			
0	11/02/70	11:15:44	ATS-1	7.0	ICE9			276889.2			
0	11/02/70	11:15:47	ATS-1	7.5	ICE9			276888.9			
0	11/02/70	11:15:50	ATS-1	6.9	ICE9			276888.6			
0	11/02/70	11:15:53	ATS-1	7.9	ICE9			276888.3			
0	11/02/70	11:15:56	ATS-1	7.3	ICE9			276888.0			
0	11/02/70	11:15:59	ATS-1	8.2	ICE9			276887.7			
0	11/02/70	11:16:02	ATS-1	7.2	ICE9			276887.4			
0	11/02/70	11:16:05	ATS-1	7.4	ICE9			276887.1			
0	11/02/70	11:16:08	ATS-1	7.6	WASH			276886.8			
0	11/02/70	11:16:11	ATS-1	7.7	WASH			276886.5			
0	11/02/70	11:16:14	ATS-1	7.9	WASH			276886.2			
0	11/02/70	11:16:17	ATS-1	7.7	WASH			276885.9			
0	11/02/70	11:16:20	ATS-1	7.5	WASH			276885.6			
0	11/02/70	11:16:23	ATS-1	7.6	WASH			276885.3			
0	11/02/70	11:16:26	ATS-1	7.4	WASH			276885.0			
0	11/02/70	11:16:29	ATS-1	7.6	WASH			276884.7			
0	11/02/70	11:16:32	ATS-1	7.4	WASH			276884.4			
0	11/02/70	11:16:35	ATS-1	7.1	ICE9			276884.1			
0	11/02/70	11:16:38	ATS-1	7.7	ICE9			276883.8			
0	11/02/70	11:16:41	ATS-1	7.1	ICE9			276883.5			
0	11/02/70	11:16:44	ATS-1	7.7	ICE9			276883.2			
0	11/02/70	11:16:47	ATS-1	7.4	ICE9			276882.9			
0	11/02/70	11:16:50	ATS-1	8.0	ICE9			276882.6			
0	11/02/70	11:16:53	ATS-1	7.4	ICE9			276882.3			
0	11/02/70	11:16:56	ATS-1	7.2	ICE9			276882.0			
0	11/02/70	11:16:59	ATS-1	6.9	ICE9			276881.7			
0	11/02/70	11:17:02	ATS-1	7.1	ICE9			276881.4			
0	11/02/70	11:17:05	ATS-1	7.3	ICE9			276881.1			
0	11/02/70	11:17:08	ATS-1	7.5	ICE9			276880.8			
0	11/02/70	11:17:11	ATS-1	7.7	ICE9			276880.5			
0	11/02/70	11:17:14	ATS-1	7.0	ICE9			276880.2			
0	11/02/70	11:17:17	ATS-1	7.6	ICE9			276879.9			
0	11/02/70	11:17:20	ATS-1	7.4	ICE9			276879.6			
0	11/02/70	11:17:23	ATS-1	7.6	ICE9			276879.3			
0	11/02/70	11:17:26	ATS-1	7.3	ICE9			276879.0			
0	11/02/70	11:17:29	ATS-1	7.5	ICE9			276878.7			

STANDARD
 DEVIATION
 0.434 μ S
 FOR
 596 MEASUREMENTS

microseconds for any individual interrogation may be determined by adding 77.3 and the value in column 5 to the computed slant range in the right-hand column. The number 77.3 is the total equipment time delay calibration value for the Observatory and the satellite. It is listed at the top of the table as FOR OBS = 77.3. Each value in column 5 therefore represents the difference between the measured range and the sum of the computed slant range and the constant equipment time delay. The standard deviations were determined by computing a "best-fit" quadratic curve to the values in column 5 and then computing the standard deviation of the individual measurements relative to that best-fit quadratic curve.

Each of the tables represents approximately the first 2.5 minutes of the half-hour of ranging data.

Comparison of Two Receiver-Correlators

Two receiver-correlator systems were used in an experiment to compare the differences in range measurements when the same signals are received by similar but different equipments. One receiver-correlator was connected to the 30 foot dish which has 20 dB gain. The other receiver-correlator was attached to a helical antenna with 10 dB gain for the signals received from ATS-3. Range measurements from ATS-3 to Gander, Shannon and to an aircraft in flight over the North Atlantic were received by both correlators and their independently derived measurements were compared. The results provide information on the performance of the narrow bandwidth tone-code ranging equipment for strong signals and for signals that have a poor signal-to-noise ratio. The test was conducted to yield information on the relative scatter due to signal-to-noise ratio and multipath.

There is a bias difference between the two receiver-correlators because of the different time delay through the antenna cables and electronic circuits. Figure 4-20 represents histograms of the time delay difference between the two receiver-correlators for the Shannon, Gander, and aircraft returns while the aircraft was in flight over Ocean Station Alpha at 17,000 feet. There are more data points for the aircraft because the automatically repeated sequence was eight aircraft interrogations, one Gander, and one Shannon interrogation. The interrogation rate was one each three seconds. There were short interruptions for voice exchanges.

The bias difference is estimated to be 15.4 microseconds for the aircraft, 15.8 microseconds for Gander and Shannon. The bias difference is attributed to a difference in time delay with average signal amplitude. Gander and Shannon have consistently strong returns, while the average signal level of the aircraft returns is lower than for ground terminals due to lower antenna gain and occasional signal amplitude reduction due to multipath reflections. The two receiver-correlators receive different signal levels because of their 10 dB difference in antenna gain, hence their delays with average signal level are different when one signal is near the detection threshold, the other is not.

The horizontal dashes in Figures 4-21 and 4-22 are the actual time delays for individual Gander and Shannon returns as received on the receiver-correlator that was connected to the 30 foot parabolic antenna. The tips of the vertical lines are the corresponding measurements for the same individual returns as measured on the other correlator, but displaced by the 15.8

FIGURE 4-20

TIME DELAY DIFFERENCE BETWEEN THE TWO RECEIVER-CORRELATORS FOR THE SHANNON, GANDER, AND AIRCRAFT RETURNS

DISPLACEMENT FROM MEAN TIME DELAY DIFFERENCE OF TWO CORRELATORS, STRONG SIGNALS

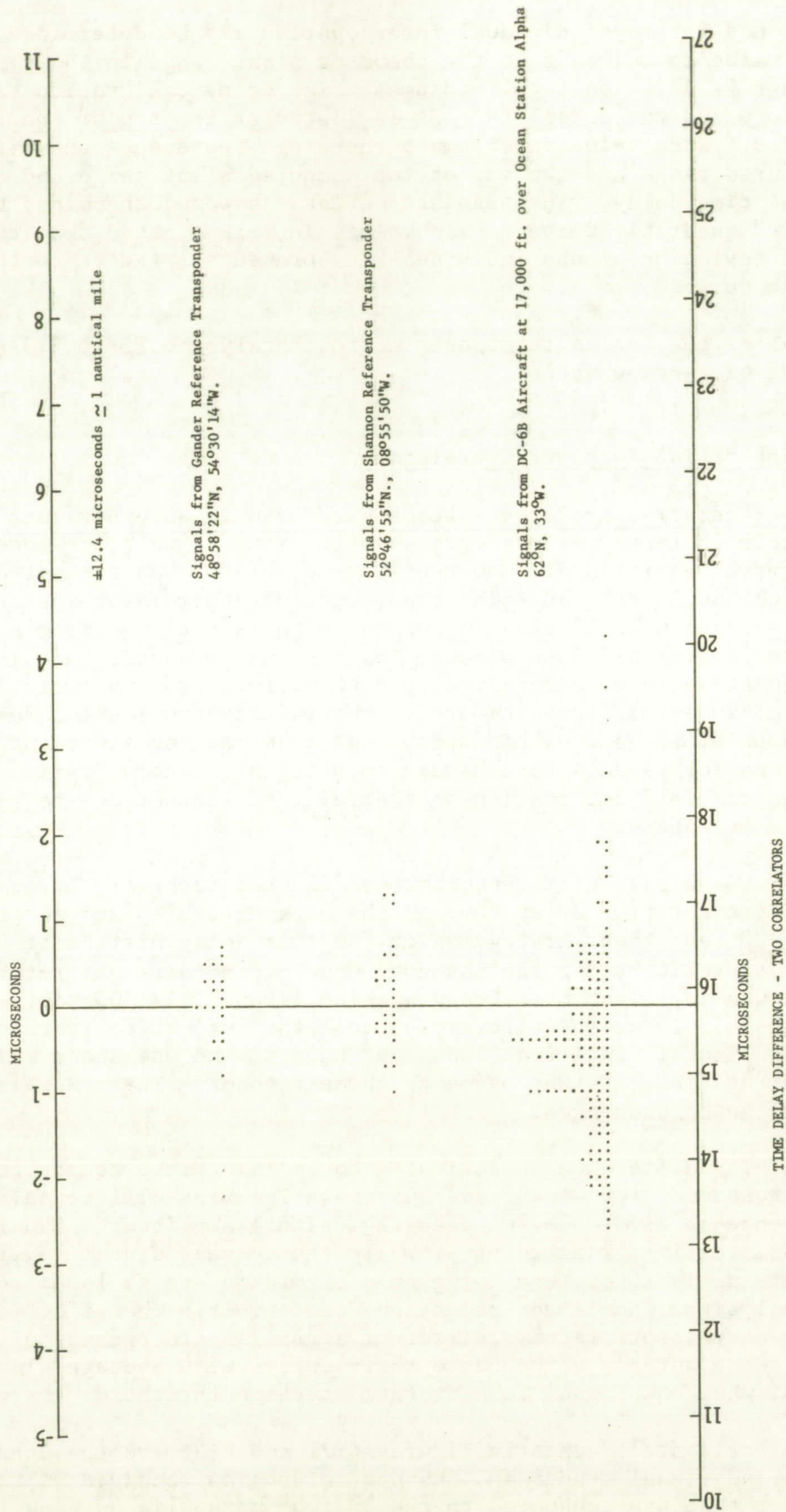


FIGURE 4-21

COMPARISON OF TWO RECEIVER-CORRELATORS
JULY 12, 1970
SIGNAL PATH: SCHENECTADY-ATS-3-GANDER-ATS-3-SCHENECTADY

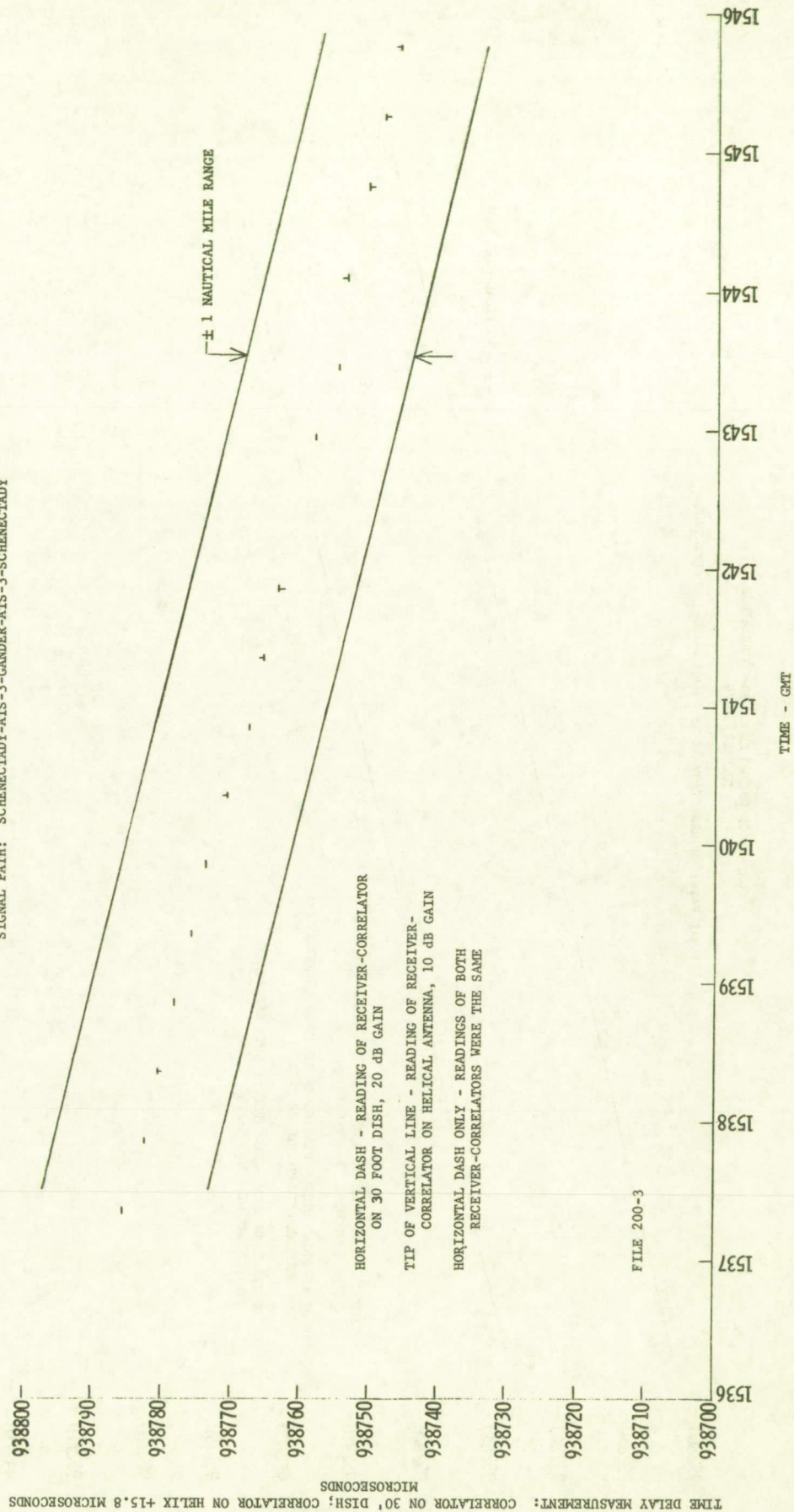
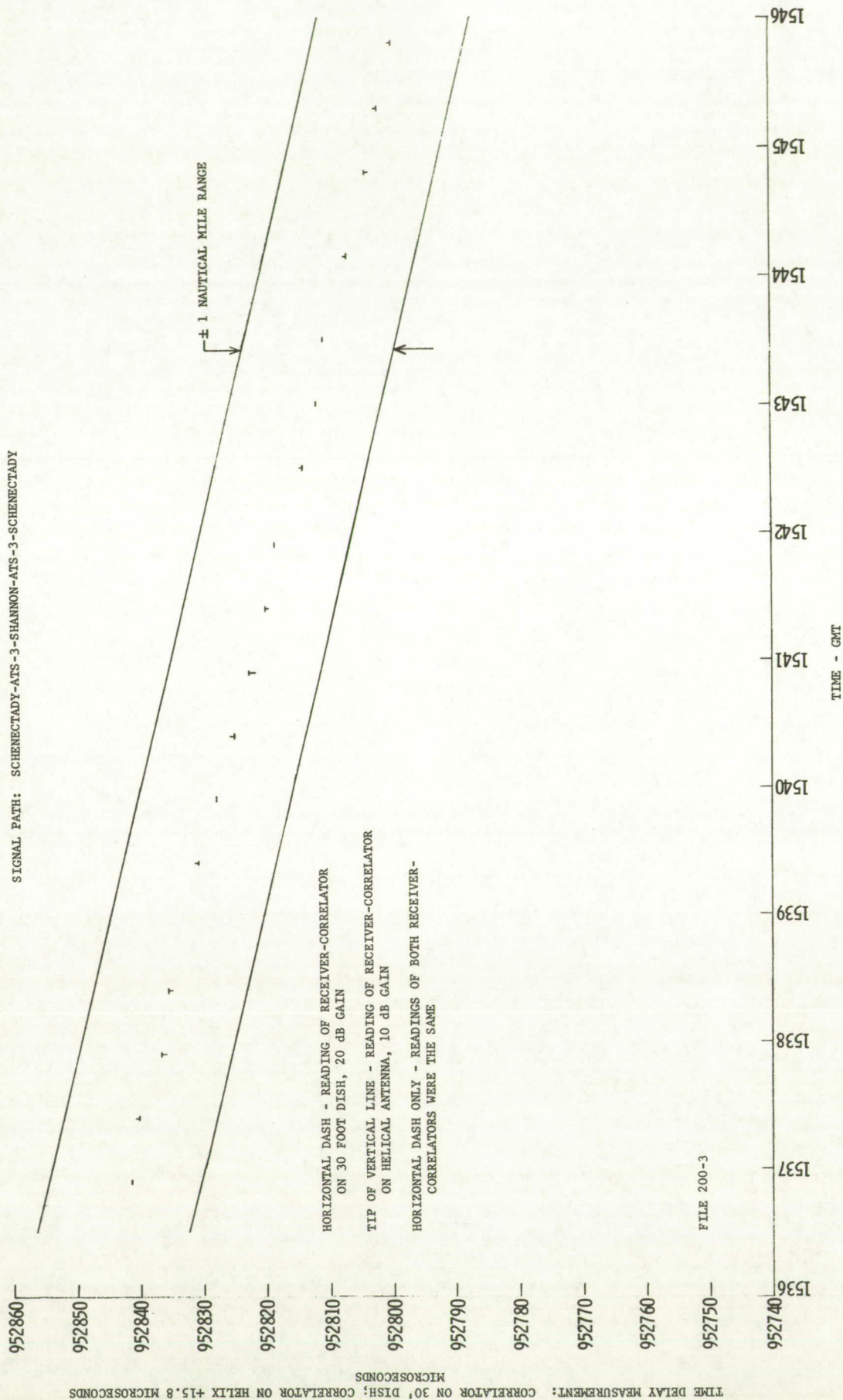


FIGURE 4-22

COMPARISON OF TWO RECEIVER-CORRELATORS
JULY 12, 1970
SIGNAL PATH: SCHENECTADY-ATS-3-SHANNON-ATS-3-SCHENECTADY



microsecond bias difference so that individual returns as measured by the two correlators can be compared directly. Fix computations take into account the actual time delay of each receiver-correlator independently so that they automatically take out the bias difference.

Lines representing ± 1 nautical mile range from a "best fit curve" to the range measurements are drawn relative to each set of ranging measurements. They are included to aid in visualizing the magnitude of the scatter of the readings and the significance of the differences between the correlators. The range change is due to satellite motion. As noted elsewhere, the satellite is in a slightly inclined synchronous orbit, and traces a figure eight relative to the fixed points on the earth's surface.

Figure 4-23 indicates the relative effects of noise on the return path from the aircraft through the satellite, and the effects of multipath on the links to and from the aircraft. The combined effects of phase error and noise on the path to the aircraft, and the effect of phase error on the return path from the aircraft affect both correlators in the same way, causing equal range measurement errors on both correlators. The effect of signal cancellation at the satellite, due to multipath reflection interference on the return path, reduces the signal at the two Observatory receivers, and since their noise components are independent, the part of the range measurement errors that are due to that cause are independent. Except for a few measurements, the range measurement errors for the two receiver-correlators are in close agreement.

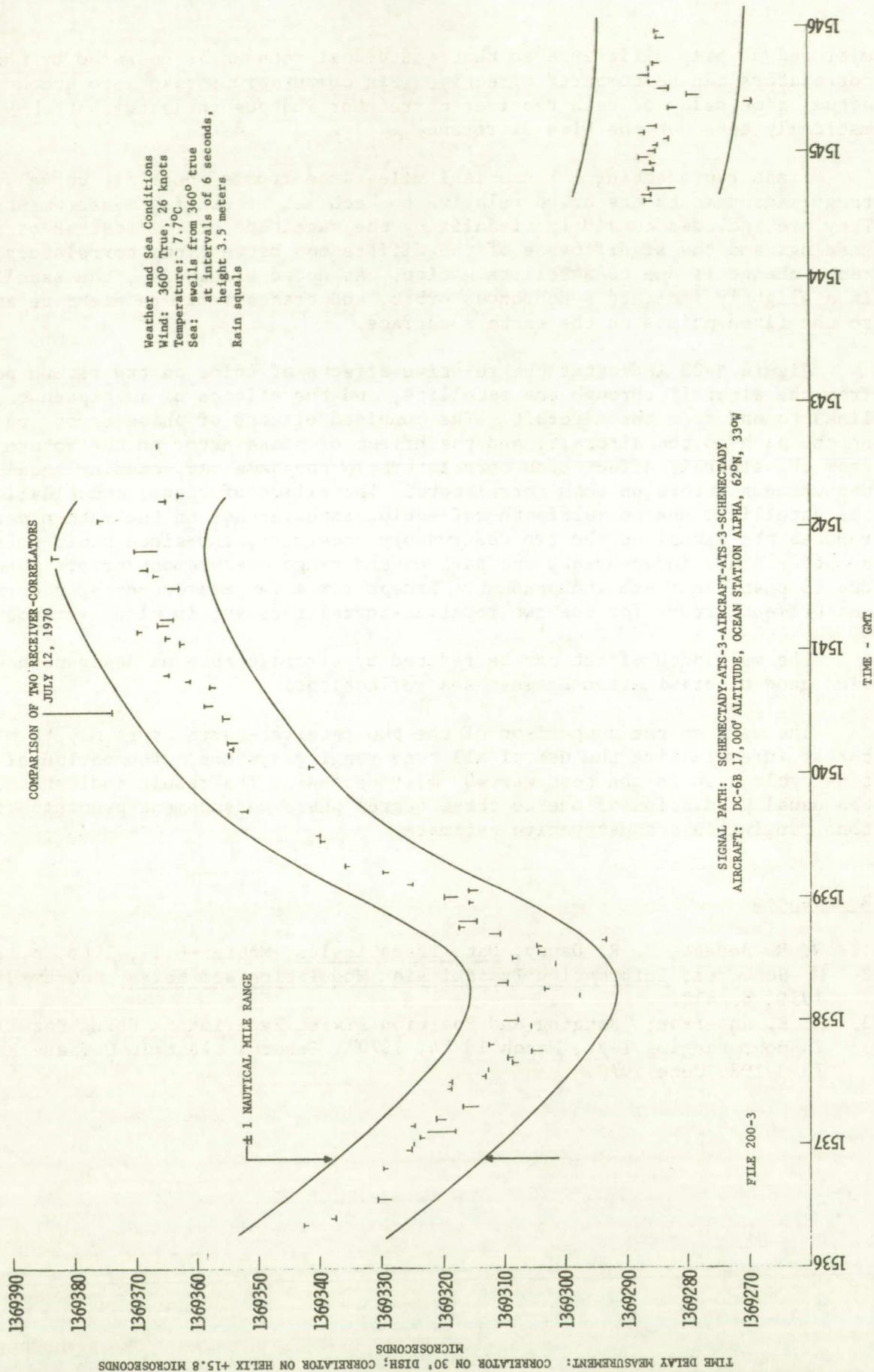
The multipath effect can be reduced by aircraft antenna designs that provide good discrimination against sea reflections.

The data on the comparison of the two receiver-correlators may be of interest in evaluating the use of all tone ranging systems. The period of a tone cycle used in the test was 409 microseconds. The result indicates that the usual prediction of one to three degree phase measurement precision for tone ranging is a conservative estimate.

References

1. W. R. Bennett, J. R. Davey; Data Transmission, McGraw-Hill, 1965, p. 114.
2. M. Schwartz; Information Transmission Modulation and Noise, McGraw-Hill, 1959, p. 412.
3. R. E. Anderson; "Ranging and Position Fixing Experiments Using Satellites: 24-Hour Ranging Test, March 13-14, 1970", General Electric Company Report 70-C-198, June 1970.

FIGURE 4-23



SECTION 5

FACTORS THAT AFFECT ACCURACY

The important factors that contribute to position fix accuracy when ranging from pairs of satellites are the following:

- Ionospheric Propagation Delay
- Satellite Position Uncertainty
- Sea Reflection Multipath
- Equipment Time Delay Uncertainty
- Noise Added to the Ranging Signals
- Fading Due to Factors Such as Ionospheric Scintillation, Spin Modulation, and Faraday Rotation
- Geometrical Dilution of Position

Some of the factors are random; others contain systematic components that can introduce bias errors. The systematic components are in part predictable or measurable and therefore can be reduced by calibration. Their contribution to the error then is the residual uncertainty after the estimated value of the bias component has been removed from the measurement. The individual factors are independent. To the extent that they are random, including the residual uncertainty in the systematic errors, they may be combined as their root-sum-square to estimate their total effect on range measurements.

Although the factors contributing to each range measurement may be random they may not be independent for the two satellites. Some factors may affect the range measurements to the satellites equally and thus introduce a position fix error which is displaced along a hyperbolic line of position (Page 7-15). The geometry of the satellites, the earth and the location of the user craft on the earth may result in the displacement of fixes which are not equally probable in all directions.

Each of the factors is discussed in this section of the report.

Ionospheric Propagation Delay

Measurement and evaluation of this important contribution to position fix error were major objectives of the experimental program. Section 11 of the report is devoted to a discussion of the effect and the results of the ionospheric propagation measurements.

Radio waves pass through the ionosphere more slowly than the free space velocity of light. As a consequence, a radio range measurement, which is always a propagation time measurement, is in error if the free space velocity of light is assumed in converting propagation time to range. The magnitude of the propagation time in the ionosphere is inversely proportional to f^2 . It is therefore an important factor that must be considered in satellite range measurements at VHF. It is of little importance at L-band.

Range measurements from satellites to transponders on or near the earth's surface involve the round trip propagation of the radio signal and therefore two trips through the ionosphere. If the up and down link frequencies are both at VHF, the two-way propagation delay may be as large as 10-15 microseconds

during mid-day at the location where the signal passes through the ionosphere and at night the delay may be approximately 2-4 microseconds. In two-way ranging one microsecond of propagation time represents a range change of 491 feet.

Ionospheric delay has a diurnal variation and also seasonal changes and an 11 year cycle corresponding to the sunspot cycle. The cyclic changes are in part predictable. However, solar flares which are associated with high sunspot activity cause variations which may depart by 2:1 from the average of the cyclic variation.

The earth's magnetic field affects the geographical distribution of the free electron content within the ionosphere and in some regions of the earth, especially in the tropical and high latitude regions, the ionospheric delay is less predictable than at mid latitudes.

An error in the estimate of the ionosphere delay of 1 microsecond will result in a ranging error of 491 feet. The projection of the error on the earth is usually larger than the range measurement error and if similar errors occur on both satellite range measurements, the position fix error may be larger than the line of position error.

There are two ways of correcting for ionospheric propagation error. One is the use of models based on data collected over long periods of time. The usefulness of the model depends upon the day-to-day correlation of the ionosphere. This method was used in most of the position fix determinations in the experimental program and was found to be adequate for the determination of position fixes within 1 nmi., 1 sigma. The other way to correct for ionospheric measurements in real time is by the use of ionospheric sounders or, perhaps better, by the use of fixed ground reference calibration transponders similar to the mobile vehicle transponders. Range measurements to fixed transponders can provide real time measurements of ionospheric delay. The usefulness of the reference transponders depends upon the correlation of the ionosphere delay over a large geographical region. The experimental results indicate the mid-latitude ionosphere corrections derived from ranging measurements to a ground reference transponder will provide range corrections within 3 microseconds for a region of a thousand mile radius around the transponder at the times of day when correlation is the poorest. No measurements were obtained when the ionosphere was severely disturbed by solar flare activity.

Satellite Position Uncertainty

Position location by range measurements from satellites requires that the satellite positions be known because the satellites themselves are the references for the position determination. A transponder on or near the earth's surface is located at the intersection of three spheres. Two of the spheres are centered at the satellite locations and have radii equal to the measured ranges from the satellites to the transponder. The third sphere is centered at the earth's center and has a radius equal to the earth's local radius plus the altitude of the transponder above the earth. There are two intersections for the three spheres. When geostationary satellites are used, one of the intersections is in the northern and one in the southern hemisphere.

A range measurement from one satellite determines a circle of position on the earth. The circle of position is the intersection of two spheres, the earth centered sphere with a radius equal to the earth's radius plus the

altitude of the craft and the sphere centered at the satellite and having a radius equal to the measured range. It may be different from the true circle of position. The true circle is centered about the line that connects the actual position of the satellite and the earth's center. That line passes through the earth's surface at a point defined as the subsatellite point. The subsatellite point is the center of the circle of position that passes through the actual location of the user.

If the position of the satellite is not known accurately and a wrong position is assumed for it, the computed circle of position on the earth will have a displacement in latitude and longitude corresponding to the error in the assumed position of the satellite, and an error in radius that is a function of the error in the assumed altitude, or earth center distance, of the satellite.

Satellite positions used in the position fix determinations throughout the experiment were derived from NASA acquisition tables. The tables state the satellite's position in latitude, longitude and earth center distance. Values are given at each half hour. The positions are predictions based on tracking data taken on specific epoch dates. The epoch date is the day on which range and range rate tracking measurements were made at C-band, which is not significantly affected by the ionosphere, from ground stations at Rosman, N. C. and Mojave, California. The epoch dates are separated at intervals of approximately two weeks. The positions given in the acquisition table for any day are predictions based on the most recent tracking epoch date.

The computation of a line of position or a position fix based on range measurements from satellites requires the positions of the satellites at the time when the range measurements were made. The LATCOM and POSFIX programs included a third order interpolation for satellite positions based on four sequential half-hourly predictions from the NASA acquisition tables. The resolution of the interpolation was sufficient to determine a satellite position to 0.001 degree in latitude and longitude and 0.01 of a nautical mile in earth center distance, which is the precision of the acquisition table data.

The error in the satellite position is the difference between the actual position of the satellite and the latitude, longitude and earth center distance values used in the position determination. An error in latitude and longitude for the satellite position in its orbit sphere produces an equal shift in the latitude and longitude of the subsatellite point on the earth's surface and a corresponding shift in the circle of position on the earth.

An arc distance displacement on the orbit sphere of the satellite will produce approximately one-seventh that arc distance displacement on the earth's surface. The angular displacements are equal and the arc distance displacements are in the ratio of the earth's radius to the orbit radius.

An error in the earth's center distance to the satellite results in a change in the radius of the circle of position on the earth.

A small segment of the circle of the position in the vicinity of the transponder is called a line of position and may be approximated by a straight line which is perpendicular to the azimuth direction from the transponder to the subsatellite point.

At locations on the earth which are not in the immediate vicinity of the subsatellite point, an error in the earth center distance of the satellite will

produce an error in the line of position which is the error in earth center distance multiplied by the secant of the elevation angle from the transponder to the satellite. If the assumed position of the satellite has an earth center distance which is greater than the actual earth center distance of the satellite, the displacement of the line of position will be towards the subsatellite point. If the assumed earth center distance to the satellite is less than the actual earth center distance, the line of position will be displaced away from the subsatellite point.

NASA acquisition table predictions based on two different tracking epoch dates may be compared to illustrate the errors in position determination that can result from the use of available satellite position predictions.

The ATS-1 and ATS-3 satellites are not in perfect geostationary orbits. The slight inclination of the orbits cause them to move north and south of the equator so that their subsatellite points trace narrow "figure eights" on the earth's surface. The period to trace a figure eight is twenty-four hours, the orbit period. The satellite may move more than one degree north and south of the equator over the twenty-four hour period. The orbits also have some eccentricity so that the earth center distance changes with a twenty-four hour period. The ATS-3 satellite was sometimes moved in longitude so that there was a drift of a fraction of a degree in longitude each day while the satellite was moved between approximately 45 and 80 degrees west longitude.

The result of all these motions can be range changes on the order of 100 miles in 12 hours, relative to a point on the earth. The position fixing experiments are affected by errors of a few hundred feet. Since NASA's primary concern with the satellite tracking was for acquisition of the satellites, it is not surprising that there were sometimes errors in the NASA predictions that were significantly large for the ranging and position fixing experiments.

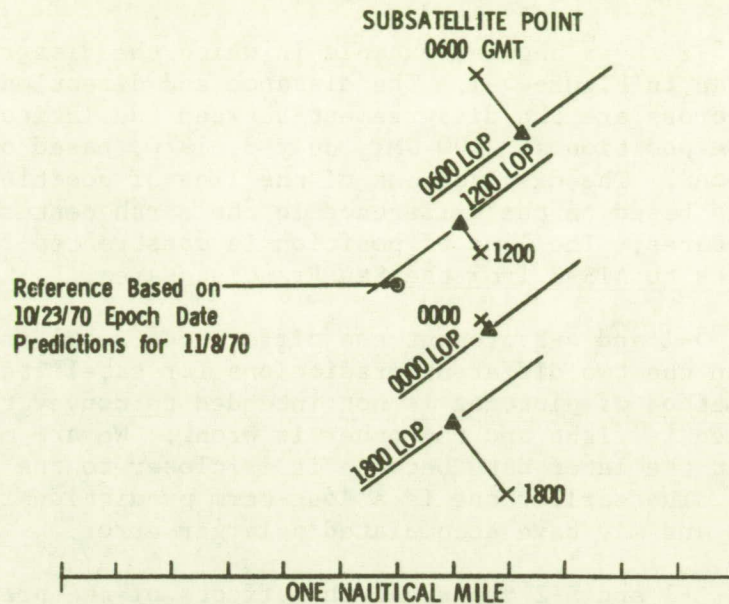
The magnitude of the position fix errors that could be caused by errors in the satellite position predictions can be illustrated by comparisons based on acquisition table predictions for a single time but based on two different tracking epoch dates. Examples of the effects are presented in Figures 5-1 and 5-2.

An encircled dot is a reference based on the earlier of two epoch date predictions for a single time. A cross is the displacement in latitude and longitude of the subsatellite point based on the later tracking epoch date prediction. The dot in the triangle represents the displacement of the line of position from the subsatellite point because of the difference in the earth center distance based on the later tracking epoch date as compared with the earlier epoch date. The displacement of the subsatellite point is true for all of the circles of position, but the displacement of the triangle and the line of position represents a specific example because the direction and displacement of the line of position depends upon the azimuth and elevation angles to the satellite from the transponder that is to be located.

The effect of the diurnal change in the disagreement between the two tracking epoch dates is apparent in Figure 5-1. The predictions are from the acquisition table predictions for ATS-3. The difference in distance and direction between the encircled dot and the cross for 0000 GMT is the difference in latitude and longitude of the satellite predictions for 0000 GMT on November 8 based on the two tracking epoch dates, October 23, 1970 and November 8, 1970. Similarly, the distance and direction between the encircled dot and the cross

FIGURE 5-1

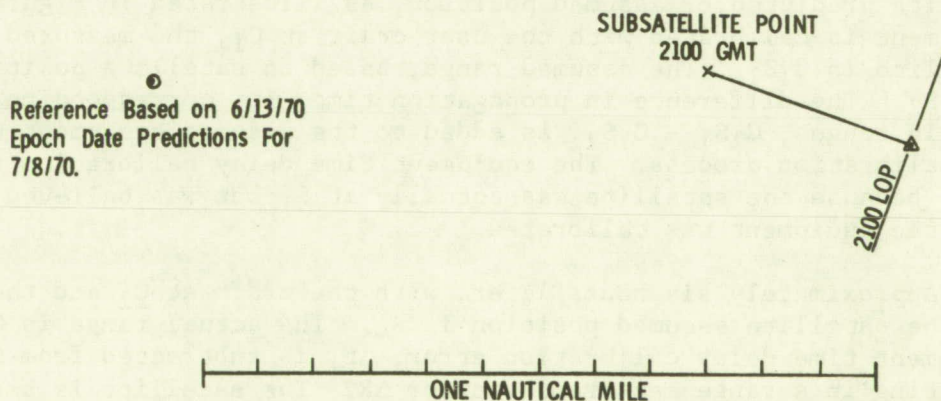
LINE OF POSITION DISAGREEMENTS
CAUSED BY SATELLITE POSITION
PREDICTION DISAGREEMENTS



SUBSATELLITE POINTS AND LINES OF POSITION ARE SHIFTED FROM REFERENCE DUE TO DIFFERENCES BETWEEN 10/23 PREDICTION FOR 11/8 AND 11/8 COMPUTATION FOR 11/8.
ATS-3 SATELLITE
TRANSPONDER ON NEW JERSEY COAST

FIGURE 5-2

LINE OF POSITION DISAGREEMENTS
CAUSED BY SATELLITE POSITION
PREDICTION DISAGREEMENTS



SUBSATELLITE POINT AND LINE OF POSITION ARE SHIFTED FROM REFERENCE DUE TO DIFFERENCES BETWEEN 6/13 PREDICTION FOR 7/8 AND 7/8 COMPUTATION FOR 7/8.
ATS-3 SATELLITE
TRANSPONDER AT SAN FRANCISCO

representing the 0600 GMT subsatellite point is the difference in latitude and longitude of the two-satellite predictions for November 8, 1970 at 0600 GMT based on the October 23 and November 8 epoch dates. The displacements of the lines of position are computed for a 35 degree elevation angle to the satellite and an azimuth angle of 145 degrees.

Figure 5-2 shows another example in which the disagreement was of larger magnitude than in Figure 5-1. The distance and direction between the encircled dot and the cross are the disagreement between the latitudes and longitudes for the satellite position at 2100 GMT, July 8, 1970, based on June 13 and July 8 tracking epochs. The displacement of the line of position from the subsatellite point is based on the difference in the earth center distance predictions for the two dates. The line of position is constructed for the elevation and azimuth angles to ATS-3 from the San Francisco area.

Figures 5-1 and 5-2 present the differences resulting from the disagreements between the two different predictions for satellite position at the same time. The method of plotting is not intended to convey the impression that one prediction is right and the other is wrong. We are more confident of the prediction at the later date because it is closer to the time of the tracking measurement. The earlier one is a long-term prediction from the tracking measurements and may have accumulated a larger error.

Figures 5-1 and 5-2 represent the effects of the prediction error for one satellite. Similar prediction errors may exist for the other satellite resulting in displacements of its lines of position. Position fix errors may be larger than the displacement of the line of position for either satellite, although at some locations on the earth, the errors may tend to cancel.

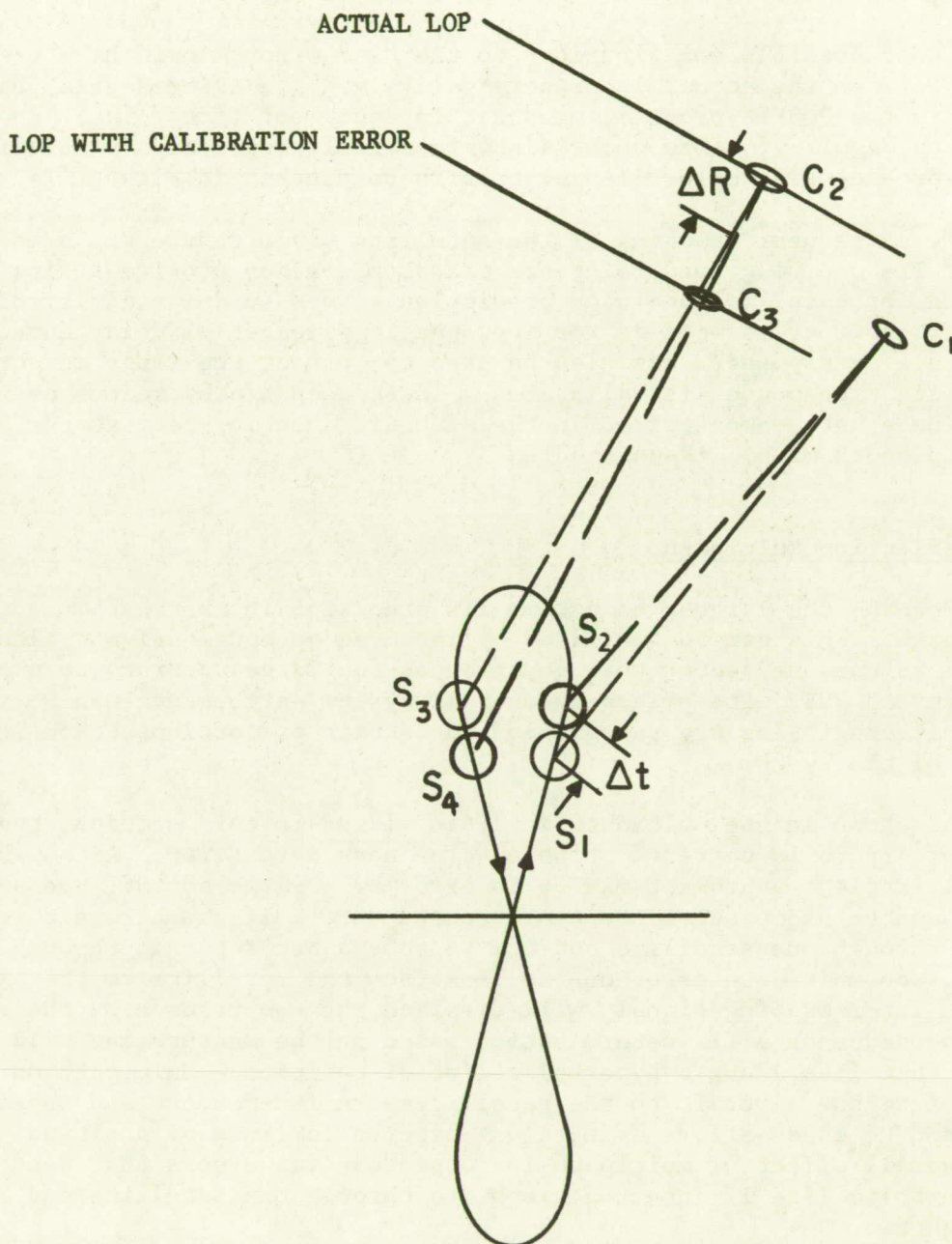
The satellite position predictions for ATS-1 and ATS-3 that were available during the ranging and position fixing experiment were sometimes in error by an amount that would result in position fix errors exceeding one nautical mile.

The fix error due to satellite position error is aggravated if the user equipment is calibrated when the actual position of the satellite is different than its predicted or assumed position, as illustrated in Figure 5-3. If the equipment is calibrated with the user craft at C_1 , the measured range to the satellite is C_1S_1 . The assumed range, based on satellite position prediction, is C_1S_2 . The difference in propagation time, Δt , corresponding to the difference in ranges, $C_1S_1 - C_1S_2$, is added to the assumed equipment time delay in the calibration process. The equipment time delay calibration is then in error at Δt because the satellite was actually at S_1 but was believed to be at S_2 when the equipment was calibrated.

Approximately six hours later, with the craft at C_2 and the satellite at S_3 , the satellite assumed position is S_4 . The actual range is C_2S_3 . The equipment time delay calibration error, Δt , is subtracted from the measurement, resulting in a range measurement error ΔR . The satellite is assumed to be at S_4 , and the range measurement ($C_2S_3 - \Delta R$) is used to plot the line-of-position of the craft with reference to the assumed position S_4 . The computed position of the ship is determined to be on a line-of-position through C_3 instead of its actual line-of-position, through C_2 .

If the craft remained at C_1 , the lines of position would go through a diurnal change reflecting the diurnal change in satellite position error relative to C_1 .

FIGURE 5-3
 LINE OF POSITION ERROR DUE TO EQUIPMENT CALIBRATION ERROR
 RESULTING FROM SATELLITE POSITION PREDICTION ERROR
 (Not to Scale)



Twenty-four hours after the calibration, with the satellite back at S_1 and assumed to be at S_2 , lines of position for the craft would be correct again if the craft were near position C_1 .

Bias errors in position fixes of the Coast Guard Cutter Rush may have resulted in part from an error in the prediction of satellite position when the transponder was calibrated on May 5. Figure 7-3, Section 7 shows bias errors of about one nautical mile for groups of fixes taken at 13:22 GMT on May 13, 19:00 GMT on July 10, and 14:00 GMT on July 21.

Other possible contributions to the bias errors could have been differences between the actual ionosphere delay, and the assumed delay based on the model in the POSFIX program, or drift in equipment time delay. However, as noted on Page 5-6, the uncertainty in satellite position prediction alone could produce bias errors larger than those plotted in Figure 7-3.

More frequent tracking of the satellite would reduce the prediction errors. The use of ground reference transponders can provide a first order correction for satellite position prediction errors in the vicinity of the reference transponder as well as for ionospheric propagation delay uncertainty. The reference transponders can also be used to correct the range measurements when a vehicle transponder is calibrated. These uses of the reference transponder techniques were demonstrated in the aircraft location test at the Shannon, Ireland bench mark. (Page 6-53)

Sea Reflection Multipath

Perhaps the largest effect on fix precision in the test was sea reflection multipath. This can be minimized by improved antenna designs, although it may remain as the one factor that contributes the largest errors to position fix accuracy at VHF. Its effect on overall system performance can be minimized if its characteristics are recognized and certain precautions taken in the operation of the system.

As shown in the multipath analysis, later in this section, the distribution of errors is centered about a value near zero error. Although an occasional single measurement may be in error by a large amount, the average error for a number of measurements tends toward zero. If the aircraft is interrogated through one satellite and the responses are returned through two satellites, the multipath error on the link from the satellite to the aircraft, that is the interrogating signal, will displace the two returns by the same amount. As a consequence a fix determination based on the measurement will have a fix error that lies along a hyperbolic line of position. Multipath on the return links from the aircraft to the satellites are independent and therefore will not tend to cause errors lying along hyperbolic lines of position. However, the overall effect of multipath is to produce fix errors that tend to lie along a hyperbolic line if interrogations are through one satellite and responses through two.

The accuracy of the VHF system can be improved by taking more than the minimum number of position fixes that are required and by relating these position fixes to each other so that the track of the craft can be monitored and those occasional fixes that show a large deviation from the expected track can be regarded with less credence than the others. If fixes are required on a craft at infrequent intervals it would be advantageous to take three or more

fixes and compare them to arrive at the accepted value of the position fix. Since the largest uncontrollable factor appears to be the sea reflection multipath, surface craft will be less subject to occasional fix errors of large magnitude.

The June 12 flight from Joliet to Omaha via Minneapolis was a test of two satellite position fixing performance over land. It was the first test made with an aircraft in flight where the elevation angles from both satellites to the aircraft were high enough to correspond with the minimum elevation angles that would be used in an operational system, although the path from ATS-1 to the Observatory which influences the accuracy of the system was much below the elevation angle expected for an operational system. The signal-to-noise ratio at the aircraft receiver was poor because the aircraft was flying in the vicinity of thunder storms. As a result, the link performance was worse than that of the following day when the aircraft was in the same geographical area. All three antenna modes were tested: the horizon and zenith modes of the Satcom antenna, and the VHF blade. Interrogations were made through ATS-1 as well as through ATS-3. Although the link performance was marginal throughout most of the tests, the accuracy of the position fix measurements made were not significantly different from the results obtained under good signal conditions the following day.

The June 20 flight test was made to evaluate the precision of ranging measurements through ATS-3 to a high performance jet aircraft on the North Atlantic principal routes. The KC-135 aircraft flew at 39,000 feet. The blade antenna was used throughout the test so that the effects of multipath combined with ranging fluctuations due to low signal-to-noise and receiver delay characteristics to produce scatter in the readings. Standard deviation of the measurements varied from approximately 8 microseconds to 11 microseconds. A histogram of all the range measurements is plotted in Figure 5-4. The envelope of the histogram suggests the shape of range error probability distribution that could be obtained by convolving a curve like one of the dashed line curves in Figure 5-11 of the multipath analysis that follows later in this section. The limits of the convolved curve would be double the limits of a one-way ranging curve as shown in Figure 5-5. The histogram shows a maximum deviation range measurement in the long direction which is approximately twice that of the largest deviation in the short direction. The lower scale shows the approximately cross-track error if the range measurements are projected on the earth for a satellite having an elevation angle of 25 degrees. It indicates the precision of cross-track monitoring that would be achieved for a satellite at mid-ocean longitude while monitoring cross-track positions of aircraft flying at maximum altitudes on North Atlantic routes with signal conditions like those of the experiment. It is expected that an operational system would have stronger signals, antennas with better discrimination against multipath than the VHF blade, and better ground station receiver characteristics than were used in the experiment. Nevertheless, the experimental result, as it stands appears to have sufficient precision for useful cross-track surveillance.

Range error due to sea reflection multipath is a function of the relative amplitudes of the reflected and direct signals, the delay of the reflected signal behind the direct signal, and the radio frequency phase difference between the direct and reflected signals. As an aircraft flies through a distance such that the radio frequency path length difference of the direct and reflected signals changes by one wavelength at the radio frequency, the one-way range error due to specular sea reflection will vary in a manner typified

FIGURE 5-4

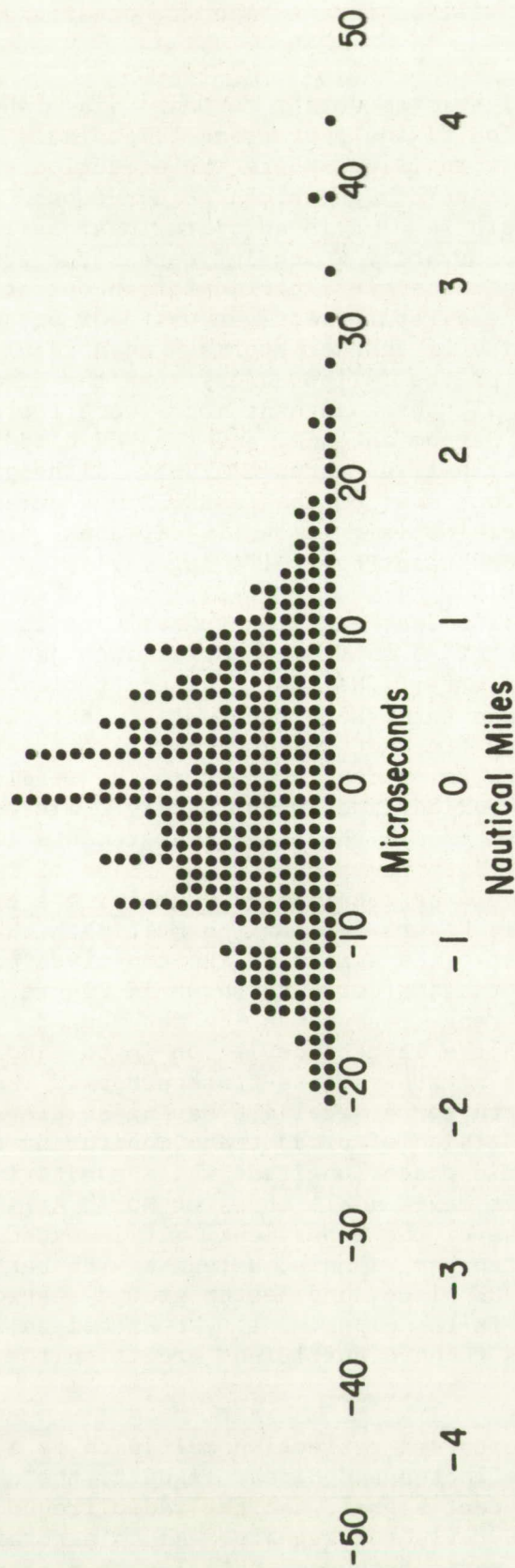
RANGE MEASUREMENT DEVIATIONS

ATS-3 to KC-135 Aircraft

Blade Antenna

56°N, 55°W to 63°N, 30°W

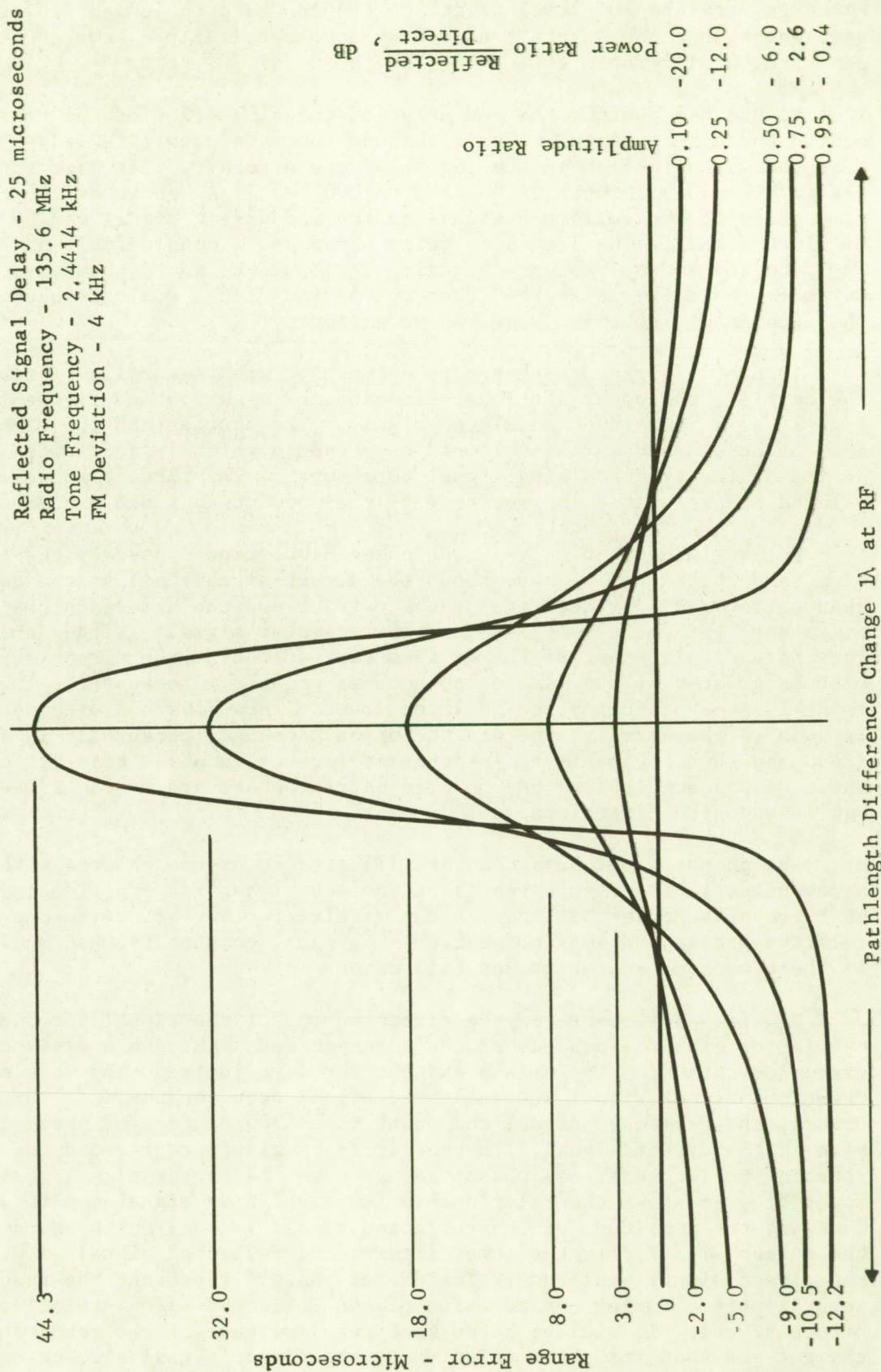
Altitude 39,000 feet



Approximate Cross-Track Error, North Atlantic Routes

FIGURE 5-5

RANGE ERROR DUE TO SPECULAR SEA REFLECTION (ONE-WAY)



by one of the curves in Figure 5-5. The aircraft may fly a considerable distance in straight and level flight to change the path length difference by one wavelength, but the aircraft need only move vertically a few feet to change the path length difference by one wavelength at VHF.

Figure 5-6 depicts the geometry and the time delay of the reflected signal behind the direct signal. It is assumed that the satellite is very distant and that the earth is flat in the region of the aircraft. Jet aircraft commonly fly at altitudes between 29,000 and 41,000 feet. As shown by the curve, the time delay of the reflected signal behind the direct signal can be several tens of microseconds. The long time delay can cause a considerable phase error in the detected audio frequency signal. It should be noted, however, that the maximum time delay is shorter than the period of the audio frequency used in the experiment, so that there was no ambiguity.

Figure 5-7 presents phasor relationships with sea reflection present for the carrier, the upper and lower sidebands of a narrowband frequency modulated signal, or an amplitude modulated signal. The carrier and the sidebands may each be considered as a single radio frequency which is continuous for the period of the synchronizing signal tone burst. The three signals are coherently related and separated in frequency by the modulating audio frequency.

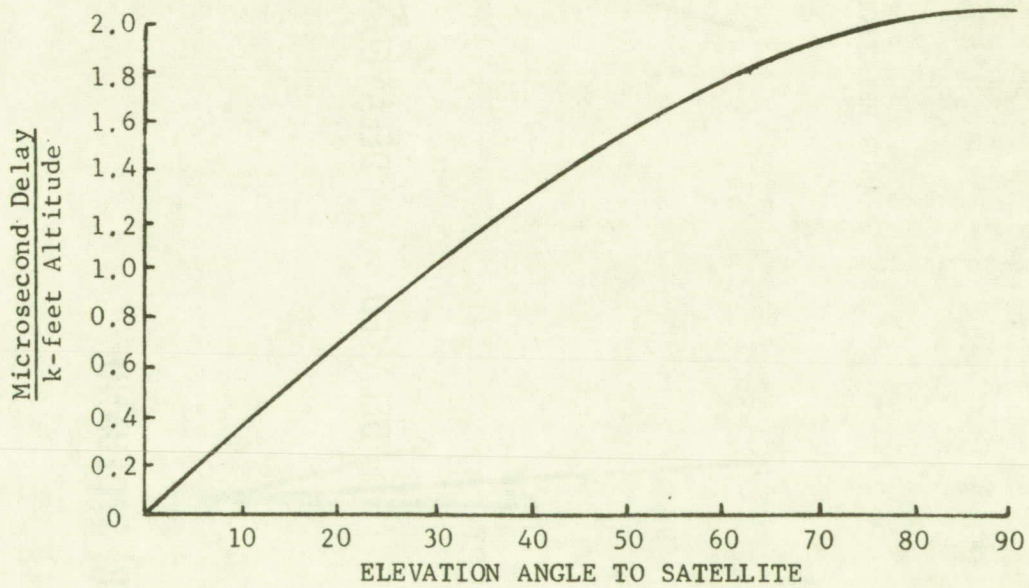
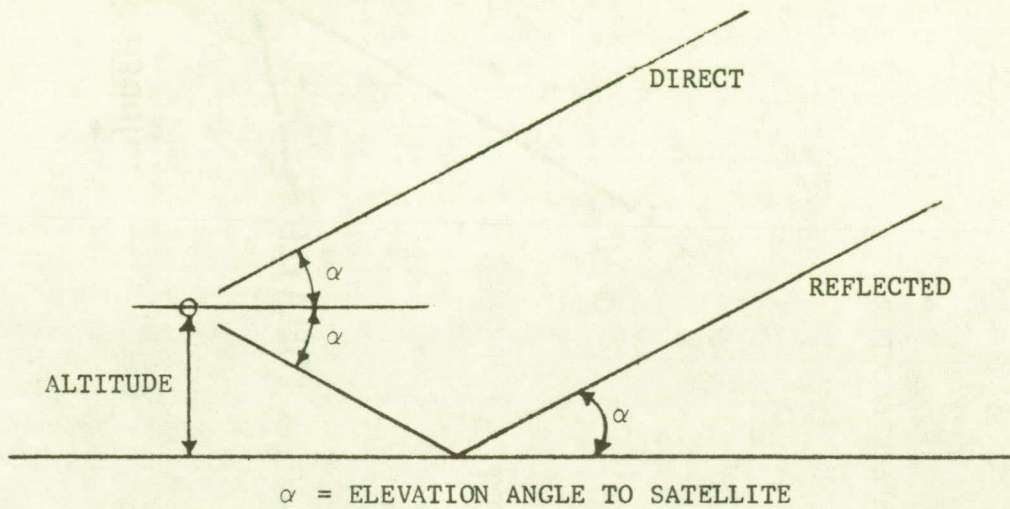
We are interested only in the phase distortion caused by the sea reflection; and therefore, we have shown the direct signals all at the same reference phase. The radio frequencies of the carrier and the sidebands are slightly different, but the time delay for the reflected signals is the same for all. The phase displacement of the delayed carrier behind the direct carrier signal becomes greater as the time delay becomes greater. Because the lower sideband is at a lower frequency, the delayed lower sideband is not displaced in phase as much as the carrier; whereas the upper sideband, because it is at a higher frequency than the carrier, is advanced farther in phase than the carrier. Their displacements from the delayed carrier phase are of the same magnitude, but in opposite directions.

The phasor resultants that are illustrated by the phasors with large arrow-heads in the figure represent the actual carrier and sideband components that are present at the input to the receiver. They are different in their relative phases and amplitudes from the signal components that would be present if there were no sea or ground reflection.

Figure 5-8 illustrates the effect on one of the signal components, the carrier or either sideband, as the aircraft moves through a distance and direction such that there is a change of one radio frequency wavelength between the direct signal and reflected signal path lengths. As this change occurs, the reflected signal component makes 360 degrees of phase change relative to the direct signal. In the figure, a circle represents the tip of the rotating reflected signal phasor relative to the direct signal phasor. The upper diagram shows the relationship for a relative signal amplitude of 0.25; that is, the amplitude of the reflected signal is one-fourth the amplitude of the direct signal. In the lower figure, the reflected signal is 0.75 times the direct signal amplitude. The dashed phasors represent the resultants for several points during the rotation of the reflected signal relative to the direct signal. It will be noted that the amplitude of the resultant phasor changes and that its phase relative to the direct signal also changes. The larger the ratio of the reflected to direct signal, the larger is the relative

FIGURE 5-6.

GEOMETRY AND TIME DELAY OF REFLECTED SIGNAL



Multiply ordinate value by aircraft altitude in thousands of feet to determine reflected signal delay in microseconds.

FIGURE 5-7
PHASOR RELATIONSHIPS WITH SEA REFLECTIONS

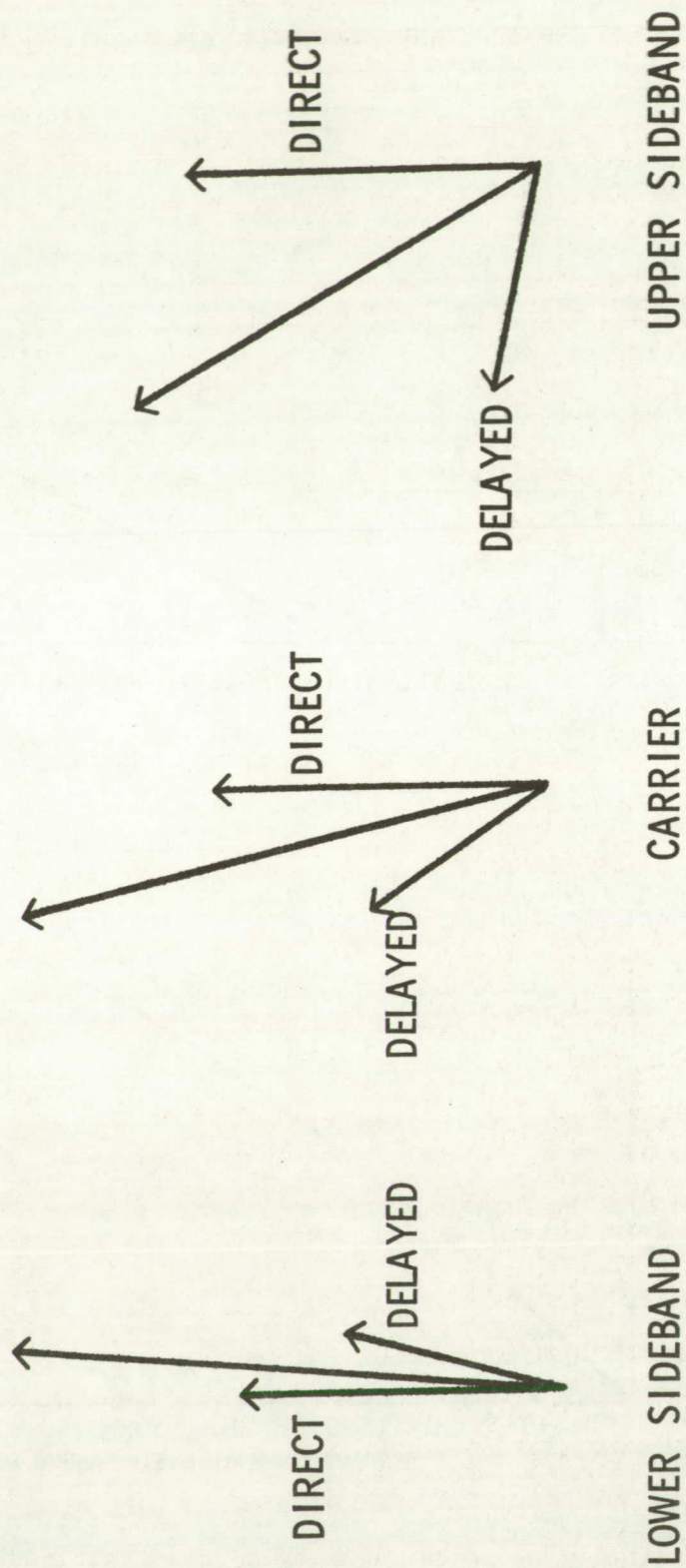
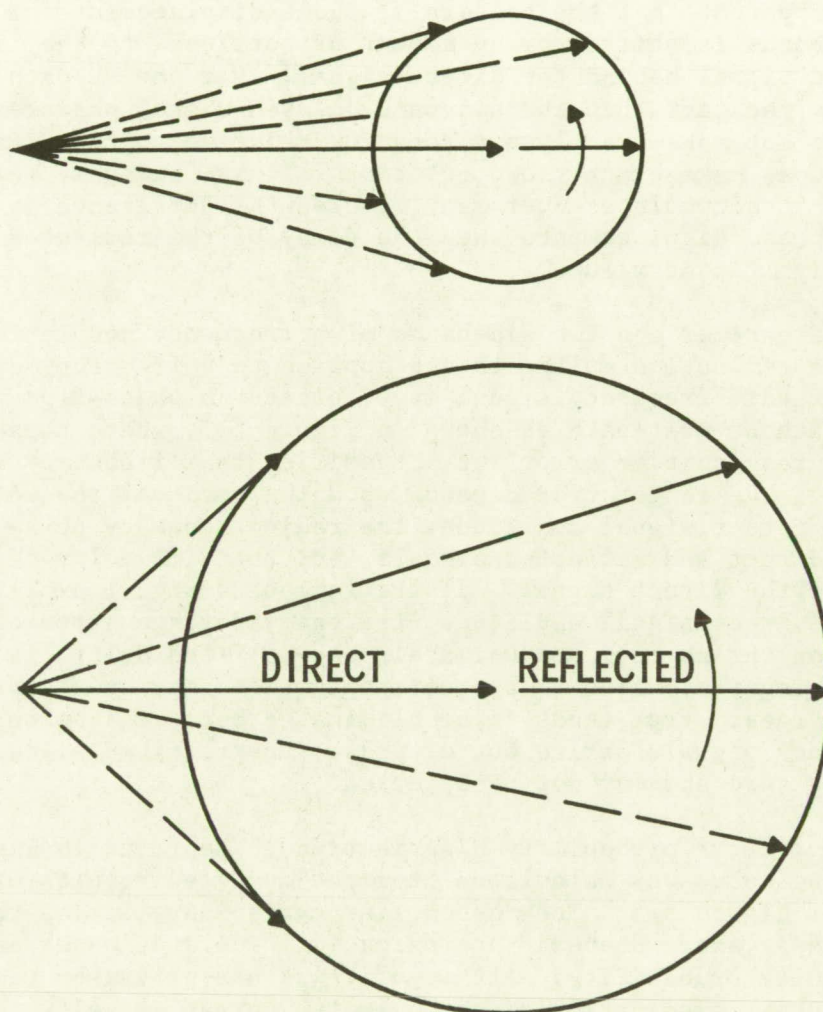


FIGURE 5-8
EFFECT OF AMPLITUDE CHANGE ON PHASOR RESULTANT



phase change. It is also important to note that the phase change of the resultant relative to the direct signal is not sinusoidal, but changes rather slowly when the reflected and direct signals are in phase, and changes very rapidly when they are out of phase.

Figure 5-9 presents the phase displacement of the phasor resultant relative to the direct signal phase for four different amplitude ratios as the relative path lengths change by one wavelength.

Figure 5-10 compares the phase changes of the carrier and the two sidebands as the difference in path length changes by one wavelength at the radio frequency. Referring to Figure 5-7, the Phasor Relationships with Sea Reflection, it is apparent that the pattern of phase displacement for the carrier and the sidebands is shifted by an amount proportional to the time delay of the reflected signal behind the direct signal. For one RF path length change, we may ignore the fact that the sideband delayed signal phasors as depicted in Figure 5-8 do not make exactly one rotation relative to the direct signals if the carrier does make exactly one rotation. It is, however, this very small difference that accumulates over many wavelengths difference in path length to produce the phase displacements when the delay of the reflected signal increases to significant values.

When the carrier and two sidebands of a frequency modulation signal distorted by sea reflection multipath are applied to a frequency discriminator, the detected audio frequency signal is displaced in phase from the phase it would have without multipath as shown in Figure 5-5, where phase error is plotted as a ranging time error for a specified tone frequency and reflected signal delay. The range error depends upon the ratio of the reflected signal amplitude to direct signal amplitude, the radio frequency phase difference between the direct and reflected signals, and the time delay of the reflected signal behind the direct signal. If the reflected signal amplitude is nearly equal to the direct signal amplitude, the one-way range error due to specular sea reflection varies from approximately one-half the delay time less than the true ranging time value to approximately two times greater than the delay time. The largest error tends to be eliminated because it occurs when the radio frequency signals arrive out of phase, the received signal strength tends towards zero and may not be detected.

The range error probability distribution is depicted in Figure 5-11. The solid line curve was calculated from the computed results of the 0.1 amplitude curve of Figure 5-5. The dashed line curves have limits that were computed, but their exact shape is approximated. The area under each curve represents unity probability. Although it was not proven by rigorous mathematical analysis, examination of the computed curves suggests that the probability of a range error being longer than the true value is equal to the probability that it is shorter than the true value. The magnitudes of the errors in the long direction can be larger than the magnitudes of the errors in the short direction, but their probability of occurrence is lower. The average error for a large number of range measurements tends towards zero error in the presence of specular sea reflection.

The down-link and up-link frequencies for the ATS ranging and position fixing experiment were different, being 135.6 MHz on the down-link and 149.22 MHz on the up-link. Sea reflection multipath can affect both links. Because of the very large number of RF wavelengths between the satellite and the aircraft, the radio frequency phase differences on the two paths are independent

FIGURE 5-9

DISPLACEMENT OF SIGNAL PHASOR DUE TO SEA REFLECTION

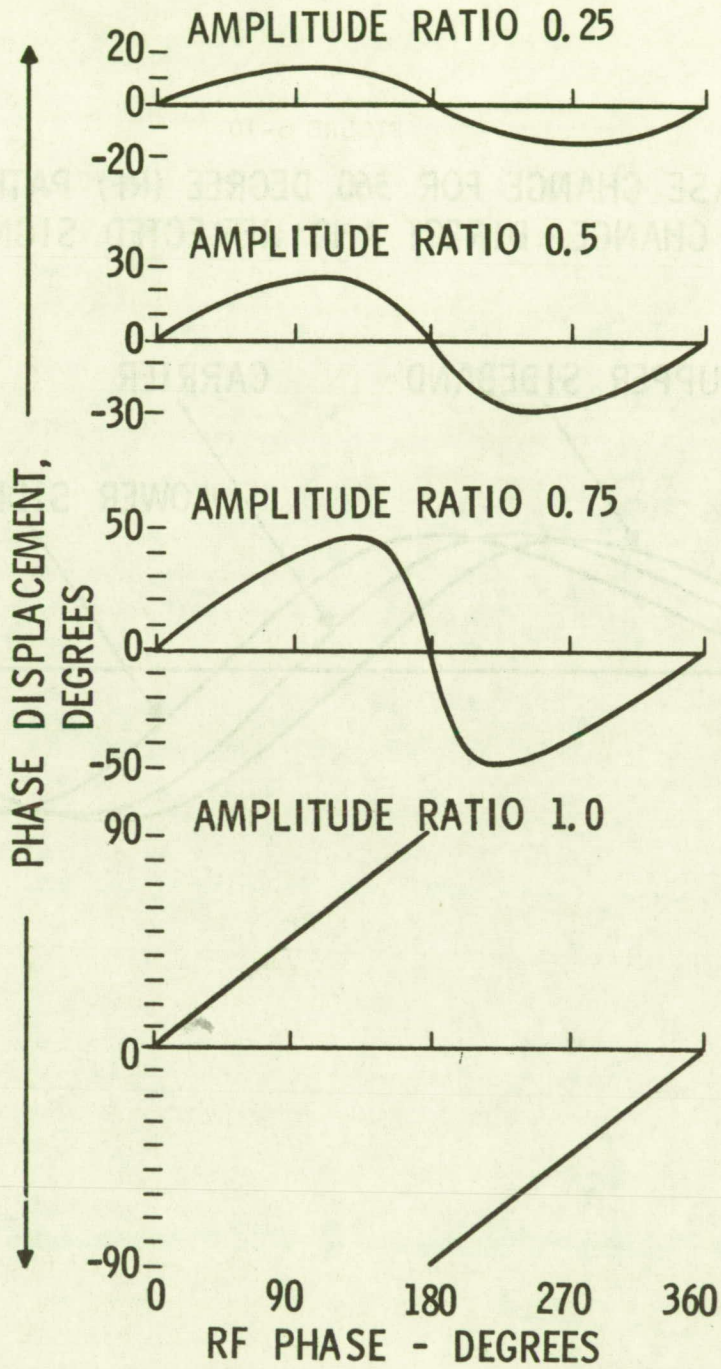


FIGURE 5-10

PHASE CHANGE FOR 360 DEGREE (RF) PATHLENGTH
CHANGE, DIRECT AND REFLECTED SIGNALS

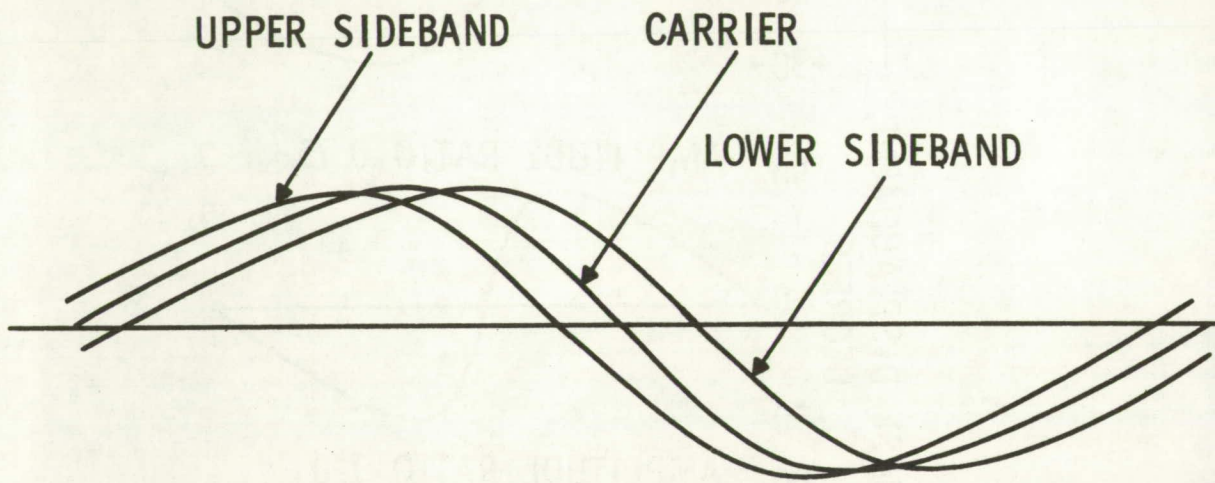
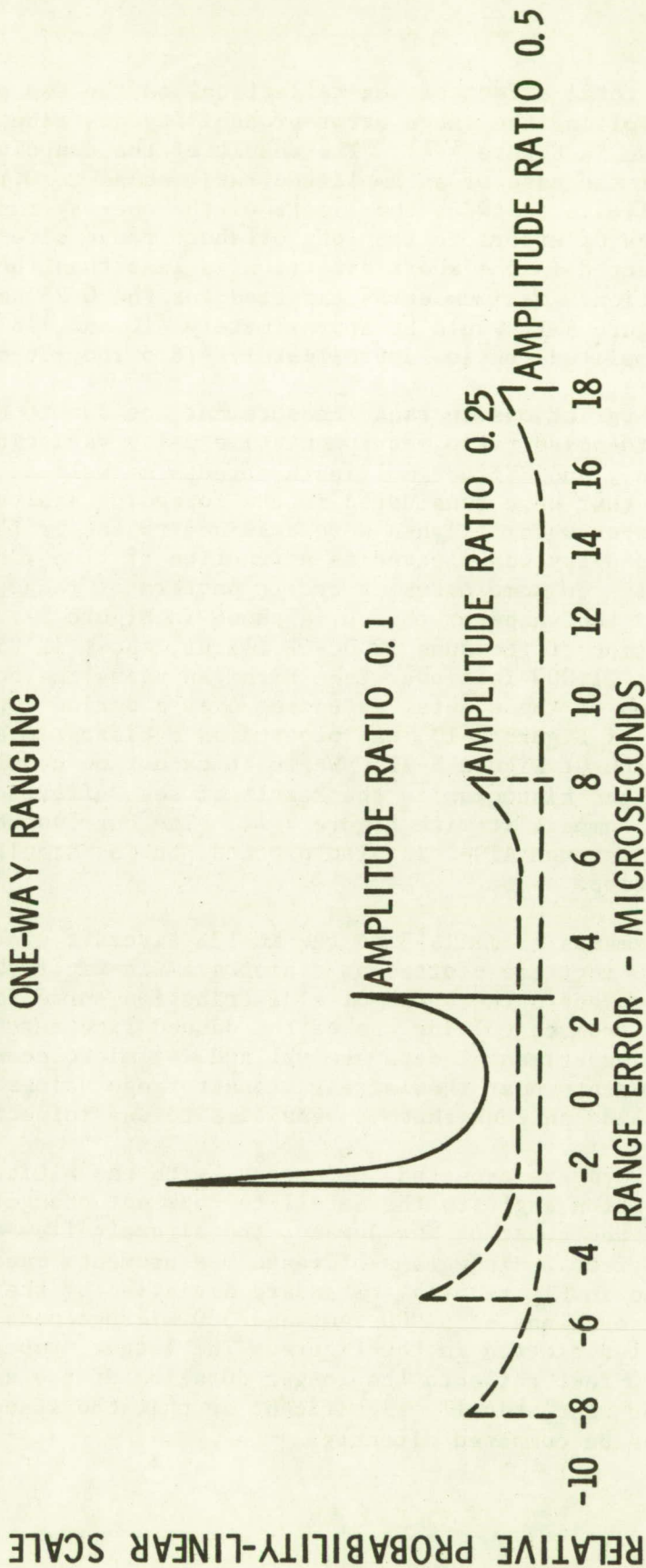


FIGURE 5-11

RANGE ERROR PROBABILITY DISTRIBUTION
25 MICROSECONDS DELAY OF REFLECTED SIGNAL
ONE-WAY RANGING



and therefore the total effect of sea reflections on the two paths must be determined by convolving the range error probability distribution for the one-way path, shown in Figure 5-11. The result of the convolution is depicted in Figure 5-12 for the case of an amplitude ratio equal to 0.1. The convolution extends the limits to twice the limits of the one-way ranging curves with equal probabilities of errors in the long or short range directions. The maximum error expected in the short direction is less than the maximum error in the long direction. Maximum errors expected for the 0.25 amplitude ratio dashed line of Figure 5-11 would be approximately -10 and +16 microseconds, and for the 0.5 amplitude ratio, approximately -16.5 and +36 microseconds.

Experimental variations in range measurement are due to many factors, including signal-to-noise ratio, equipment time delay variations as a function of signal amplitude, and diffuse multipath effects as well as the specular multipath effects that were considered in the foregoing analysis. Some of the data obtained on over-water flights were examined to see if the effects could be observed. Time delay was plotted as a function of time for some of the over-water flights. In some cases, a cyclic pattern of range variation about the mean suggested the shape of the curve shown in Figure 5-5. An example is the plot of a portion of the June 13 DC-6B flight, shown in Figure 5-13. The DC-6B craft was at 21,000 feet over Lake Michigan using the horizon mode antenna. A portion of these data, extending over a period longer than the 2.5 minute period of Figure 5-13, was plotted as a histogram and is presented in the lower portion of Figure 5-12. While it cannot be concluded that the envelope shape of the histogram is the result of sea reflection multipath, it is interesting to compare it with Figure 5-12. The corresponding histogram for the responses through ATS-1 is also plotted, but no significance is attached to its envelope shape.

Range measurements from ATS-3 to the KC-135 aircraft over the North Atlantic at 39,000 feet are plotted as a histogram in Figure 5-4. The envelope of the histogram suggests the shape of a distribution curve for two-way ranging that would result from convolving one of the dashed line curves of Figure 5-11. The limits of the experimental data are -21 and +44 microseconds, with comparatively few measurements near the largest, longer range values. The aircraft was using a VHF blade antenna that is sensitive to sea reflections.

Multipath errors are expected to increase with the altitude of the aircraft if the elevation angle to the satellite does not change. During the June 6 flight off the coast of New Jersey, the aircraft flew at 20,000 feet and also at 5,000 feet. Histograms of range measurements made at each altitude are presented in Figure 5-15. Standard deviation of the range measurements was 2.1 microseconds at 5,000 feet and 3.0 microseconds at 20,000 feet for the data samples plotted in the figure. The larger number of points plotted for 20,000 feet reflects the longer duration of the data sample. Both are believed to be statistically significant so that the standard deviations and histograms can be compared directly.

FIGURE 5-12

RANGE ERROR PROBABILITY DISTRIBUTION
25 MICROSECONDS DELAY OF REFLECTED SIGNAL
AMPLITUDE RATIO - 0.1
TWO-WAY RANGING

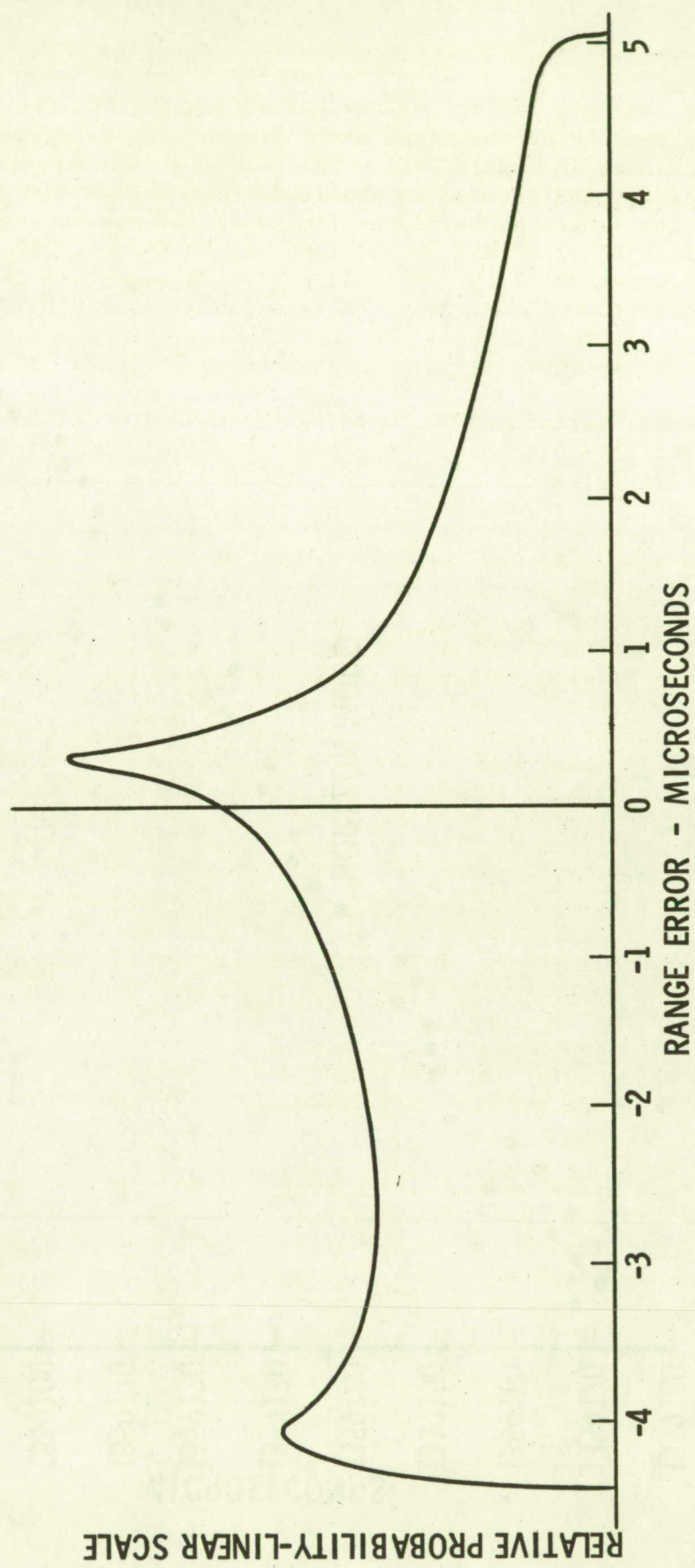


FIGURE 5-13

RANGE MEASUREMENTS FROM ATS-3
TO A DC-6 AIRCRAFT AT 21,000 FEET
OVER LAKE MICHIGAN
(6/13/69)

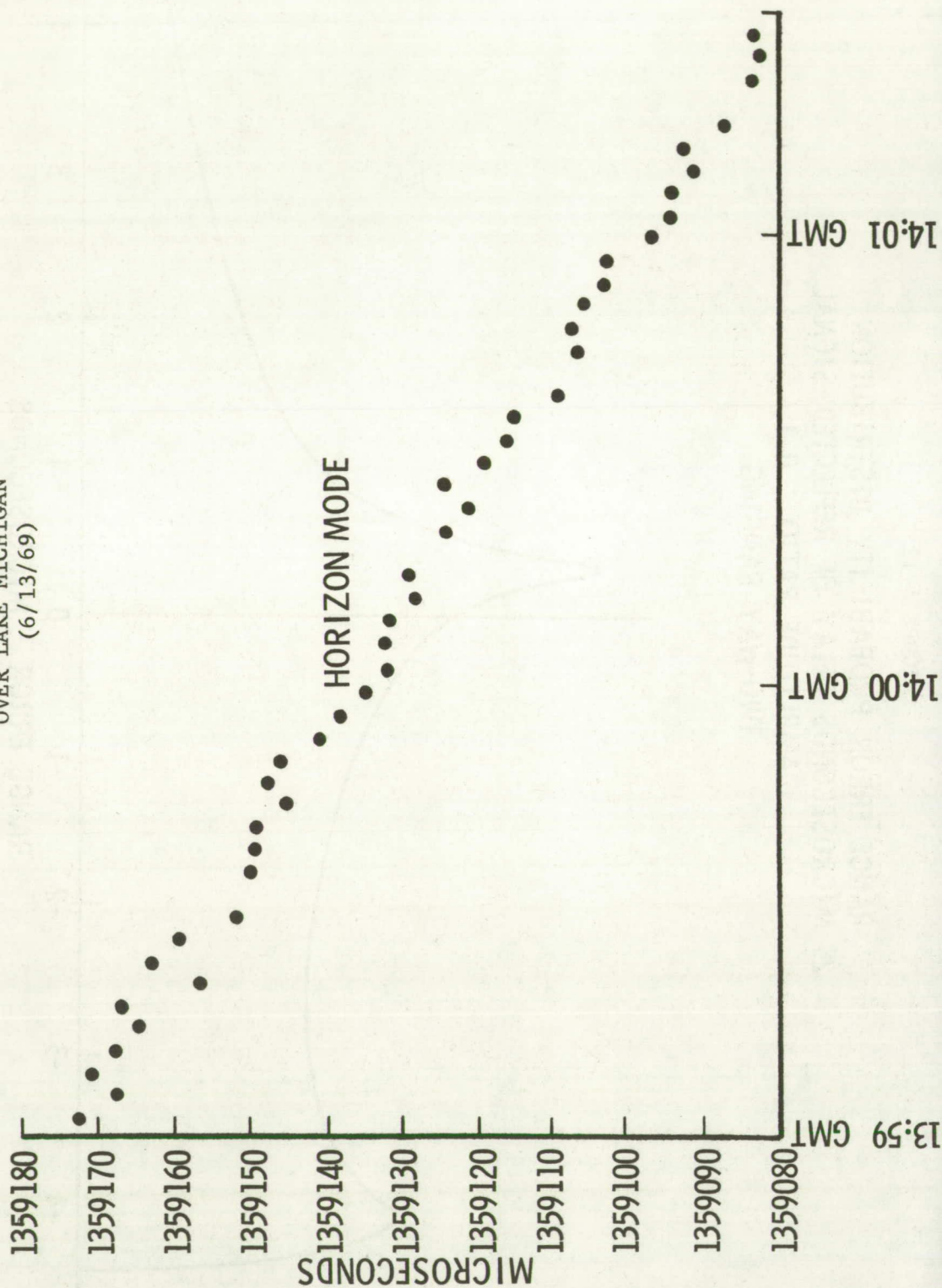
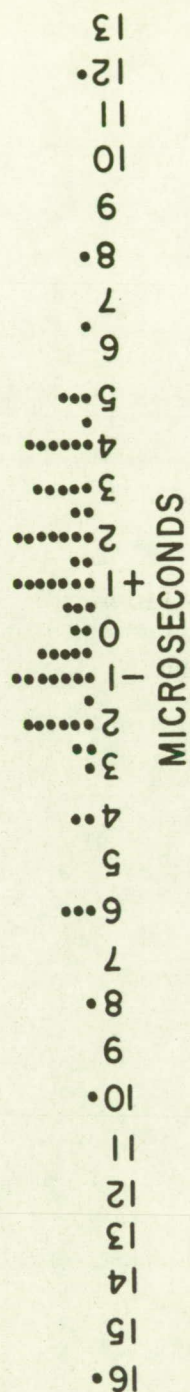


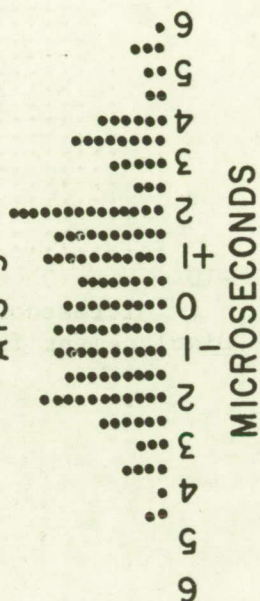
FIGURE 5-14

DC-6 OVER LAKE MICHIGAN

ATS-1



ATS-3



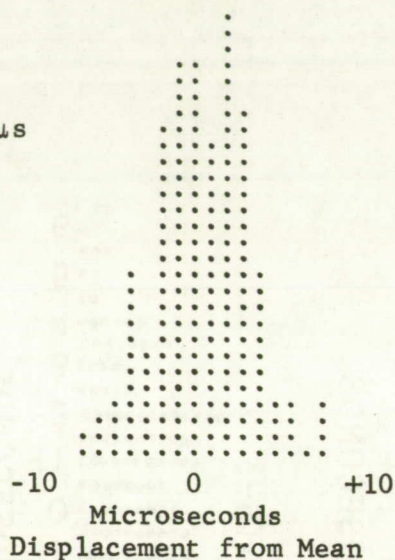
(HORIZON MODE)

FIGURE 5-15

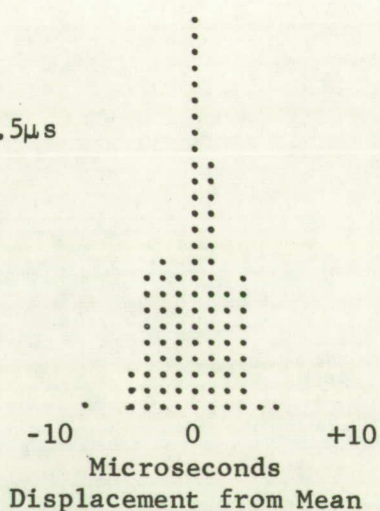
RANGE MEASUREMENT DISTRIBUTIONS
FOR TWO ALTITUDES OVER OCEAN

June 6, 1969

Altitude: 20,000 feet
Heading: South
Time: 1345 - 1355 GMT
Reflected Signal Delay: $26\mu\text{s}$
Standard Deviation: $3\mu\text{s}$



Altitude: 5,000 feet
Heading: NNE
Time: 1308 - 1313 GMT
Reflected Signal Delay: $6.5\mu\text{s}$
Standard Deviation: $2.1\mu\text{s}$



Aircraft: DC-6B
Location: Off New Jersey Coast

Satellite: ATS-3, Elevation $\approx 40^\circ$
Antenna: Satcom, Zenith Mode

Equipment Time Delay Uncertainty

The range measurement from a satellite to a transponder on or near the surface of the earth is based upon the time of the radio signal propagation between the satellite and the transponder. The actual measurement includes the sum of the propagation time and the time for the signal to propagate through the electronic circuits in the satellite, the transponder to be located, and the measuring apparatus at the ground station. The equipment time delays must be subtracted from the total time interval measurement in order to yield the propagation time and therefore the range.

If the range measurement depends upon the two-way propagation time of the signal, a 1 microsecond error in equipment time delay represents an error in the range measurement of 491 feet. If one-way range measurements are used, the error due to equipment time delay is 982 feet per microsecond. It is therefore necessary that the equipment time delay be known to an accuracy commensurate with the required ranging resolution.

It is necessary to calibrate the delay of the user transponder after its installation on its platform or mobile craft which is to be located. The equipment time delay is different for each user equipment unless means are taken to adjust them all to the same delay. It was found practical in the experimental program, and we recommend for any operational system that user time delay be calibrated with the user equipment at a known location and the delays stored with the user address for computing fixes. This proved to be simple and practical.

User equipment time delay depends upon the bandwidth, the number of circuits and the method of processing the ranging signals within the user transponder. Time delays through a radio receiver and transmitter depend upon the bandwidth and number of stages through which the signal must propagate. VHF receivers with voice bandwidth circuits may have total propagation time delays of several hundred microseconds. The amount of delay may vary with signal amplitude and with receiver tuning. It may also change with temperature. These factors are discussed in Section 4.

Tone-code ranging involves the matching of the phase of a locally generated tone to the phase of a received tone. It is essential that the local tone retain its phase coherently within the precision required of the system throughout the time that the transponder is transmitting its response to the interrogation. In the experiment the response was 0.43 second long for all transponders except the one that employed the RTA-41B transceiver. That one required a response with a duration of 0.86 second. If the oscillator in the transponder is accurate to one part in 10^6 , it will not accumulate more than 0.5 microsecond error in the time of its zero crossings in one second of time. Long term stability of the oscillator is not required. An inexpensive temperature-compensated crystal oscillator was sufficiently stable and accurate so that oscillator error was not a significant factor in the experiments.

Noise Added to Ranging Signals

Random noise like that generated in the input stage of a radio receiver causes a random "jitter" or time fluctuation of the modulated baseband signal. Random or white noise is usually the most frequently encountered type of noise in VHF ranging signals from satellites. However, interfering signals or radio

frequency interference as from electrical machinery can introduce noise components that are not random and may have systematic effects. Although interfering signals of this type were occasionally encountered in the experimental program, their overall effect was random because they did not often have significant components of the tone frequency. The subject of the effects of noise is treated in Section 4.

Fading Due to Factors such as Ionospheric Scintillation, Spin Modulation and Faraday Rotation

Amplitude fading of the signals can produce ranging errors if they affect the time delay of the signal through the receiver. The effect can be significant with receivers that are not designed to have small time delay changes with signal amplitude, but the effects can be minimized by the substitution of a balanced limiter when frequency modulation is used to transmit the tones or by reduction in time delay as a function of signal amplitude for the type of modulation used in a system.

Fading of the signals tends to reduce the reliability of the transmission links and may result in lost interrogations for the ranging system or increased bit error rates especially through introduction of burst errors in digital communications.

Fading can be due to many causes - Faraday rotation, if linearly polarized antennas are used on the satellite; multipath by reflection from the sea or ground; ionospheric scintillation fading (Section 11); loss of signal due to nulls in the antenna pattern at certain headings of the vehicle; or by spin modulation of the satellite.

ATS-1 and ATS-3 transmitted linearly polarized signals. As linearly polarized signals pass through the ionosphere the plane of polarization is rotated by an amount that depends upon the electron content along the ray path and the direction of propagation relative to the earth's magnetic field.

Faraday rotation is inversely proportional to the square of the frequency. At the VHF frequencies used in the experiment the plane of polarization may rotate several times as the signal propagates through the ionosphere.

When the signal is received on a linearly polarized antenna the signal strength depends upon the orientation of the receiving antenna relative to the plane of polarization. If the electric field of the wave is aligned with the antenna the signal is received with full strength but no signal is received if the field is oriented at right angles to the antenna. Circularly polarized antennas will receive a linearly polarized signal at all polarization angles but the signal strength is 3 dB below its full amplitude.

The diurnally changing electron content causes the plane of polarization to change through the day. At the VHF frequencies used in the experiment a linearly polarized antenna of fixed orientation experiences fades at rates as high as approximately once per five minutes after sunrise and during sunset in the ionosphere along the ray path and fades at rates of approximately one-half to one hour during mid-day and mid-night. Faraday rotation was observed to be significantly different on the up link frequency of 149.22 and the down link frequency of 135.6 MHz.

Loss of signals due to ionospheric scintillation is discussed in Section 11, due to multipath in Sect. 6 and pg. 5-8, and due to antenna patterns in Section 6.

ATS-1 and ATS-3 both exhibited detectable fading due to spin modulation throughout the period of the experiment. It was not severe enough to degrade ranging or communication performance through ATS-1. Most of the time it was not significant on the signals from ATS-3. After February 1970 it became so pronounced on the ATS-3 signals that it did affect performance.

Figure 5-16 is a chart recording of received signal amplitude from ATS-3 on 1/14/71. The fade rate corresponds to the spin rate of the satellite, 100 fades per minute. The period between fades is 0.6 second.

The depth of the fade depended on the strength of the up link signal to the satellite. When the NASA-Rosman station transmitted with 2 kW through a 14 dB antenna, the transponder of the satellite was saturated, and fading depth was 2-4 dB. When one of the General Electric reference transponders transmitted with 300 Watts, and an effective antenna gain of 9 dB, the satellite transponder was not saturated during the fade, and the depth of fade as received from the satellite was approximately 8 dB. Mobile units, such as the aircraft, with lower gain antennas, did not saturate the satellite during any part of the spin, and the signal sometimes dropped below the Observatory FM receiver detection threshold during the fade.

The cause of the spin modulation was not clearly explained. The satellite is cylindrical in shape. It is spin stabilized to maintain the axis of the cylinder parallel with the earth's axis. The VHF antenna array comprises light monopole elements projecting from one end of the cylinder with the monopoles parallel to the axis of the satellite. The eight monopole elements are phased to form a beam directed toward the earth. The width of the beam in the earth's equatorial plane is approximately the angle subtended by the earth as seen from the satellite. The beam in the orthogonal plane is essentially that of a dipole, so that the nominal gain of the antenna is 8 dB.

Each of the monopoles is driven by a 5 Watt transistor power amplifier, for a total of approximately 40 Watts RF radiated power. With the 8 dB gain of the antenna array the effective isotropic radiated power toward the earth is approximately 200 Watts.

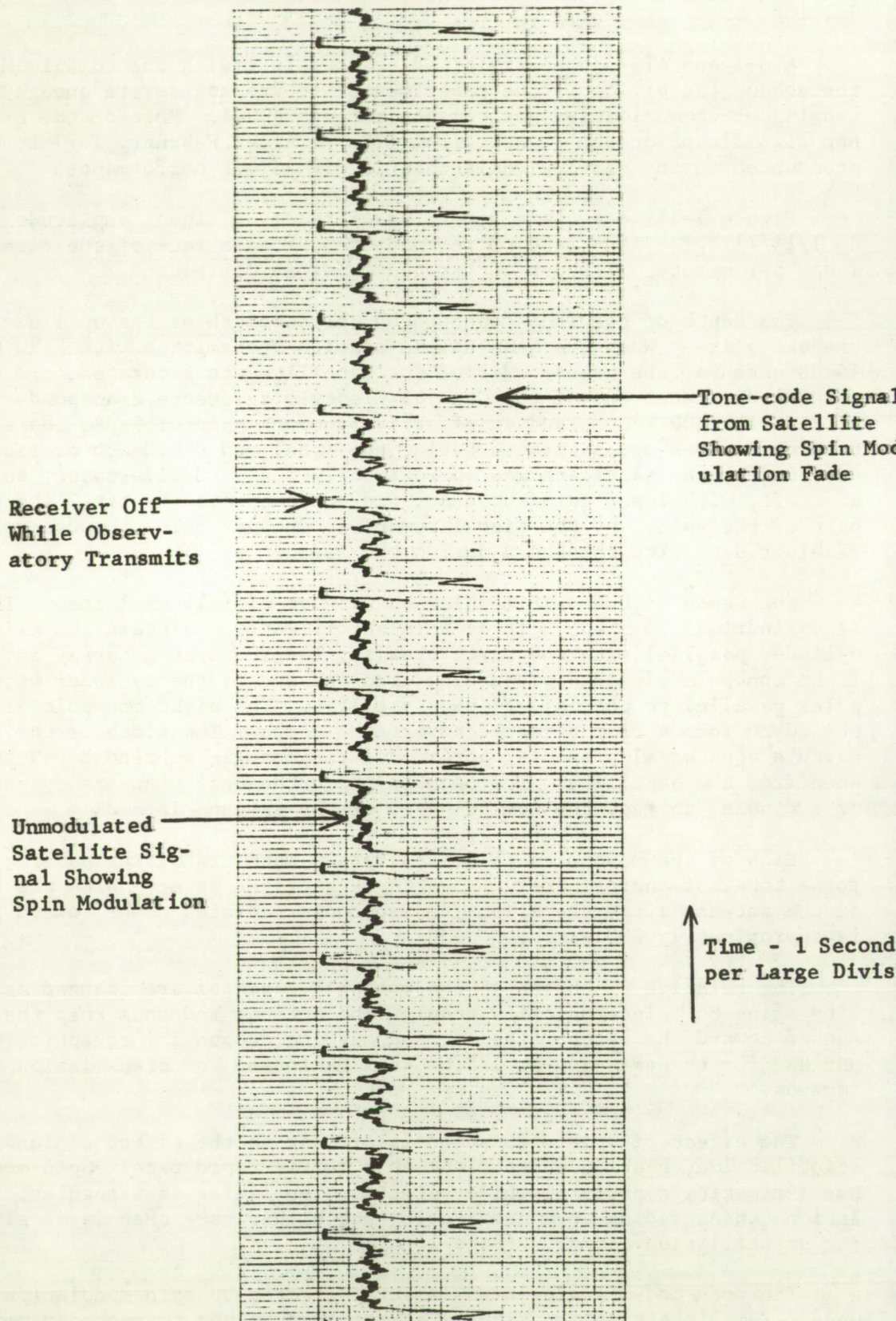
The relative RF phases at the monopole elements are changed as the satellite spins to "electronically despin" the antenna and thus keep the beam directed toward the earth. The antenna must be despun for reception at 149.22 MHz and for transmission at 135.6 MHz. Reception and transmission are simultaneous.

The effect of spin modulation is similar to the effect of ionospheric scintillation, causing short fades at a fairly rapid rate. Spin modulation has a repetitive pattern, while scintillation fading is irregular. Spin modulation causes fading at a comparable, but higher rate than is usually observed for scintillation fading. (Page 11-52)

The tone-code ranging signals were affected by spin modulation in several ways. Some interrogation signals as received by the transponder were broken up by the fades. When the first portion of the tone was cut off by a fade, the activation of the address code recognizer was delayed so that part or all

FIGURE 5-16

SPIN MODULATION FADING PATTERN



of the code was missed. In that case, the transponder did not respond. Similarly, it would fail to respond if the fade destroyed the code. If the later portion of the tone were cut off, noise could reduce the accuracy of the fading, and if the code were received, the transponder would respond but with a less accurate phase measurement than if the tone were not affected by the fade. Transponder returns received at the Observatory were affected by spin modulation in ways similar to the transponders.

The effects of spin modulation were reduced in some of the later tests by timing the interrogations so that the spin modulation fades were avoided on the interrogation relay by the satellite and also avoided on the response from the transponder as relayed by the satellite. An interrogation was transmitted every 2.4 seconds, timed to be relayed by the satellite between spin fades. The propagation time to the transponder and return occupied the period of the fade, so that the transponder's return was also relayed by the satellite, essentially between fades.

The effect of spin modulation was measured for a variety of situations, as shown in Table 5-1. The interrogation rate was a constant (once every fourth cycle of spin, approximately 2.4 seconds). The timing phase of the transmissions was shifted to determine the results of best and worst case conditions. Under a particularly adverse situation, it is possible to have the received code occur primarily within the fade window and result in no correlations at all. This was demonstrated during the test, but is not indicated in Table 5-1, since no range measurements resulted.

The Observatory used a net gain 9 dB helix for transmitting and receiving part of the time, and a net 19 dB parabolic antenna the remainder of the time. Output power was approximately 300 Watts into the antenna. The Gander station used an identical helix and power amplifier.

The phase of the transponding station (Gander) was a fixed built-in delay and was determined solely by the timing (phase) of the Observatory transmissions.

TABLE 5-1

EFFECT OF SPIN MODULATION

Condition	<u>Standard Deviation (Microseconds)</u>	
	<u>Observatory</u>	<u>Gander, Newfoundland</u>
Poor Phase for Observatory Transmission, Fair Phase Gander Return -- Helical Antenna	2.39	2.38
Poor Phase for Observatory Transmission, Fair Phase Gander Return -- Parabolic Antenna	0.61	0.76
Good Phase for Observatory Transmission, Poor Phase Gander Return -- Helical Antenna	0.49	2.27
Good Phase for Observatory Transmission, Poor Phase Gander Return -- Parabolic Antenna	0.35	2.08
Best Compromise for Both Observatory Trans- mission, Gander Return -- Helical Antenna	0.52	0.73
Best Compromise for Both Observatory Trans- mission, Gander Return -- Parabolic Antenna	0.37	0.70

Geometrical Dilution

An uncertainty in the range measurement projects onto the earth an uncertainty in the line of position greater than the uncertainty in the measurement. The magnitude of this "broadening" of the line of position is a function of the elevation angle to the satellite.

Figure 5-17 shows these projections for range measurement uncertainty and the projection for altitude uncertainty.

At the subsatellite point, where the elevation angle is 90° , the projection for either the range or elevation uncertainty may be approximated by

$$\delta_m = E_r \cos^{-1} \frac{E_r - \Delta_m}{E_r}$$

where δ_m = line of position uncertainty for either range or altitude uncertainty

E_r = earth's radius

Δ_m = measurement uncertainty, radius or altitude

There is further geometrical dilution in calculating a fix from two lines of position. The broadened lines of position intersect at an angle to produce a parallelogram of position, as shown in Figure 5-18:

One-half the longest diagonal of the parallelogram may be taken as the probable error of the fix.

$$\Delta P = \frac{1}{2} \left[A^2 + B^2 + 2 AB \cos \alpha \right]^{1/2}$$

where $A = \delta_{m_1} \sec \alpha$

$B = \delta_{m_2} \sec \alpha$

and α is the angle of intersection of the lines of position, or the difference in azimuth angles to the two satellites from the user's location.

Satellite altitude uncertainty will produce errors very close in value to range errors of the same value.

For calculating position error at the subsatellite point, errors in range measurement, user altitude, and satellite altitude should be added directly to determine the total Δ_m before applying them to the above equation. The error is the projection of their sum rather than the sum of their projections.

The assumptions in this section are made to simplify the presentation. They are valid because: 1) the altitude of the satellite is large compared to the earth's radius; 2) the angle subtended by the earth at the satellite is not large; and 3) all of the measurement uncertainties are very small compared to the earth's radius.

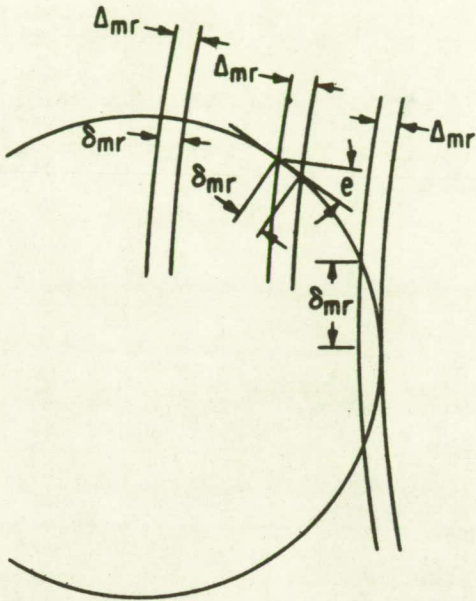
FIGURE 5-17

GEOMETRICAL DILUTION

$$\delta_{mr} = \Delta_{mr} \sec e$$

EXCEPT FOR $e = 90^\circ$

$$\text{THEN } \delta_{mr} = E_r \cos^{-1} \frac{E_r - \Delta_{mr}}{E_r}$$



$$\delta_{ma} = \Delta_{ma} \tan e$$

EXCEPT FOR $e = 90^\circ$

$$\text{THEN } \delta_{mr} = E_r \cos^{-1} \frac{E_r - \Delta_{ma}}{E_r}$$

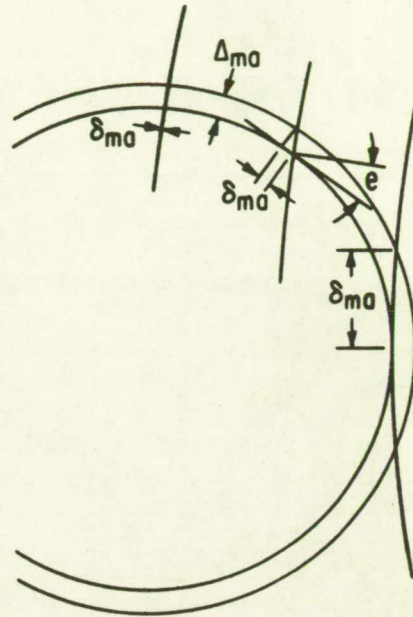
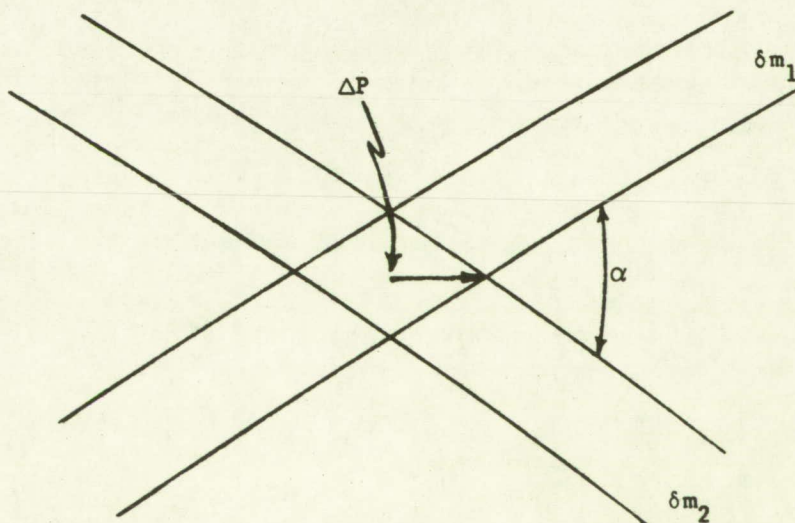


FIGURE 5-18

POSITION PARALLELOGRAM



SECTION 6

AIRCRAFT TESTS

The Federal Aviation Administration furnished the use of two aircraft, a DC-6B and a C-135. The DC-6B is a four engine propeller driven aircraft and the C-135 is a four engine jet aircraft.

A tone-code responder was also installed on a Pan American 747 aircraft.

The DC-6B aircraft was equipped with two antennas. The Dorne and Margolin DMC33-1 was mounted topside at station 590 on the aircraft. The antenna is similar in appearance to a VHF blade antenna except that it has a horizontal disc on top. Elements in the vertical and horizontal portions of the antenna are combined to provide two circularly polarized operational modes. One mode, variously called the horizon, azimuth, or horizontal mode, is nominally omnidirectional in azimuth and has a vertical coverage pattern from an elevation angle of ten degrees to forty degrees. The other mode of the antenna, called the zenith mode, covers the solid angle above forty degrees of elevation. Maximum gain in each mode is nominally 3 dB above isotropic. The antenna has sufficient bandwidth to cover the ATS up link frequencies, 149.22 MHz, and the down link frequency, 135.6 MHz. The Federal Aviation Administration furnished the measured receiving antenna patterns for the two modes of the antenna as mounted on the DC-6, shown in Figures 6-1 and 6-2. The patterns were made where the elevation angle to the satellite was near the upper elevation limit for the horizontal mode and the lower limit for the zenith mode.

The other antenna available on the DC-6B aircraft and the only antenna available on the C-135 were VHF blade antennas similar to the conventional blade used for air-to-ground communications except that their upper frequency limit was extended to 150 MHz and their transmitter power up to 500 Watts. The VHF blade antennas have a vertical linear polarization.

Transmit antenna patterns for the blade antenna on the DC-6B aircraft and for the Dorne and Margolin zenith and horizon mode antennas are shown in Figure 6-3. The patterns were made by transmitting from the aircraft while it was on the ground at the National Aviation Facilities Experimental Center, Atlantic City, New Jersey, to the ATS-3 satellite. The changes in received signal at Schenectady were recorded as the aircraft was rotated to scan all azimuth angles. Transmit antenna patterns were made with the satellite at an elevation angle from the aircraft of approximately 41 degrees.

It is apparent from the antenna pattern recordings that the gain patterns are highly dependent upon the heading of the aircraft and that the gain variations are large. Only relative gains are shown in Figure 6-3. There were no accurate means to measure the gain relative to an isotropic antenna, but the values shown are probably not much different than the values that would be recorded relative to a 0 dB isotropic antenna.

The signal links to and from the aircraft are affected not only by the irregular antenna patterns, but also by Faraday rotation that can cause a complete signal loss in the blade antenna or partial signal loss due to ellipticity of the polarization of the Dorne and Margolin antenna. The signal can be further degraded by sea reflection multipath. Many of the tests with the aircraft were made in areas where the elevation angle to ATS-1 was very near

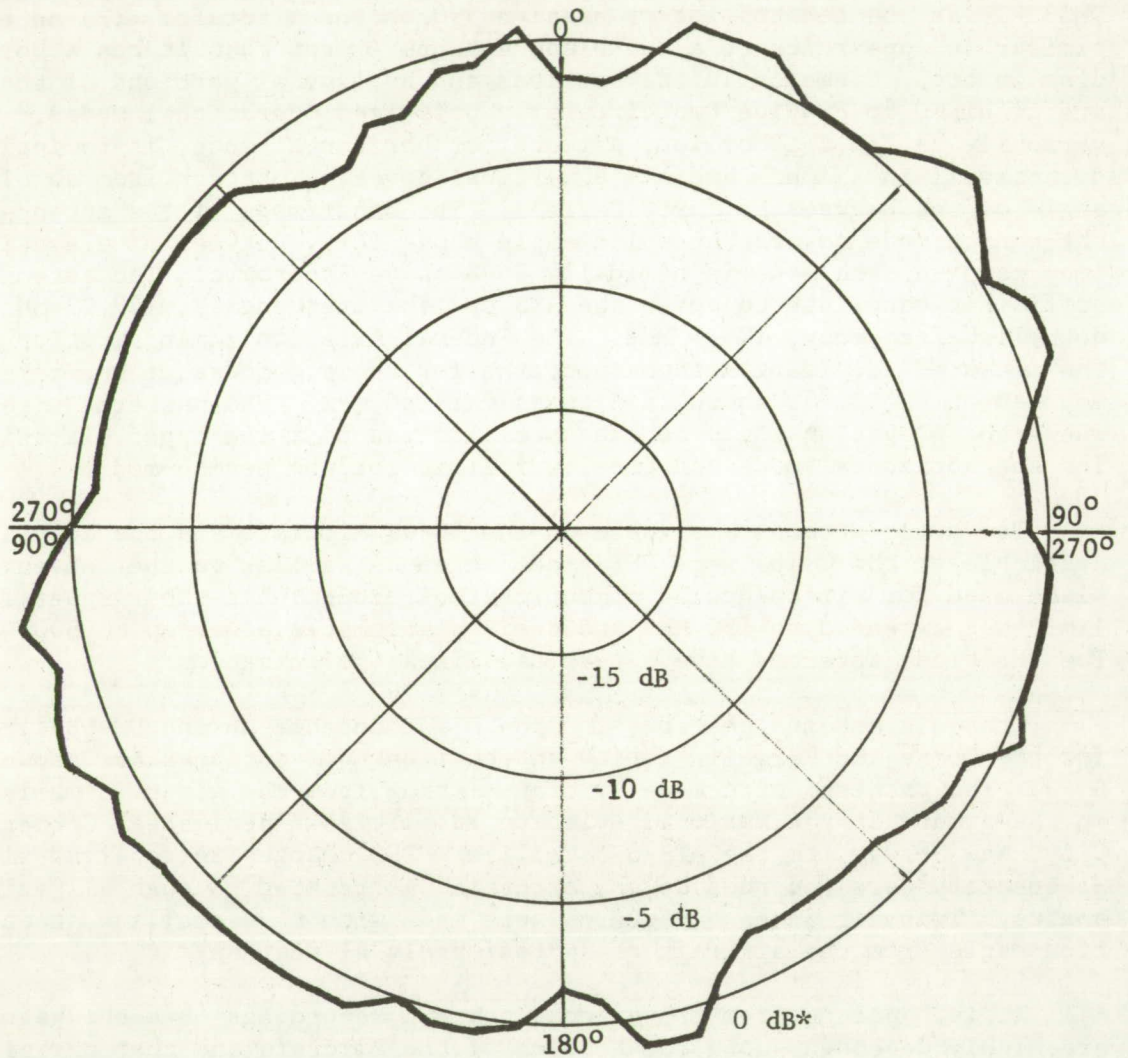
FIGURE 6-1

RECEIVING ANTENNA PATTERNS - DC-6 - ZENITH MODE

Receiving Antenna Pattern, 7/21/70, 19:34:11.1-19:36:24.4
Dorne and Margolin Antenna in Zenith Mode

Antenna Located Topside at Station 590 on DC-6B Aircraft

Test Frequency - 135.575 MHz; Elevation Angle to ATS-3 - 44°

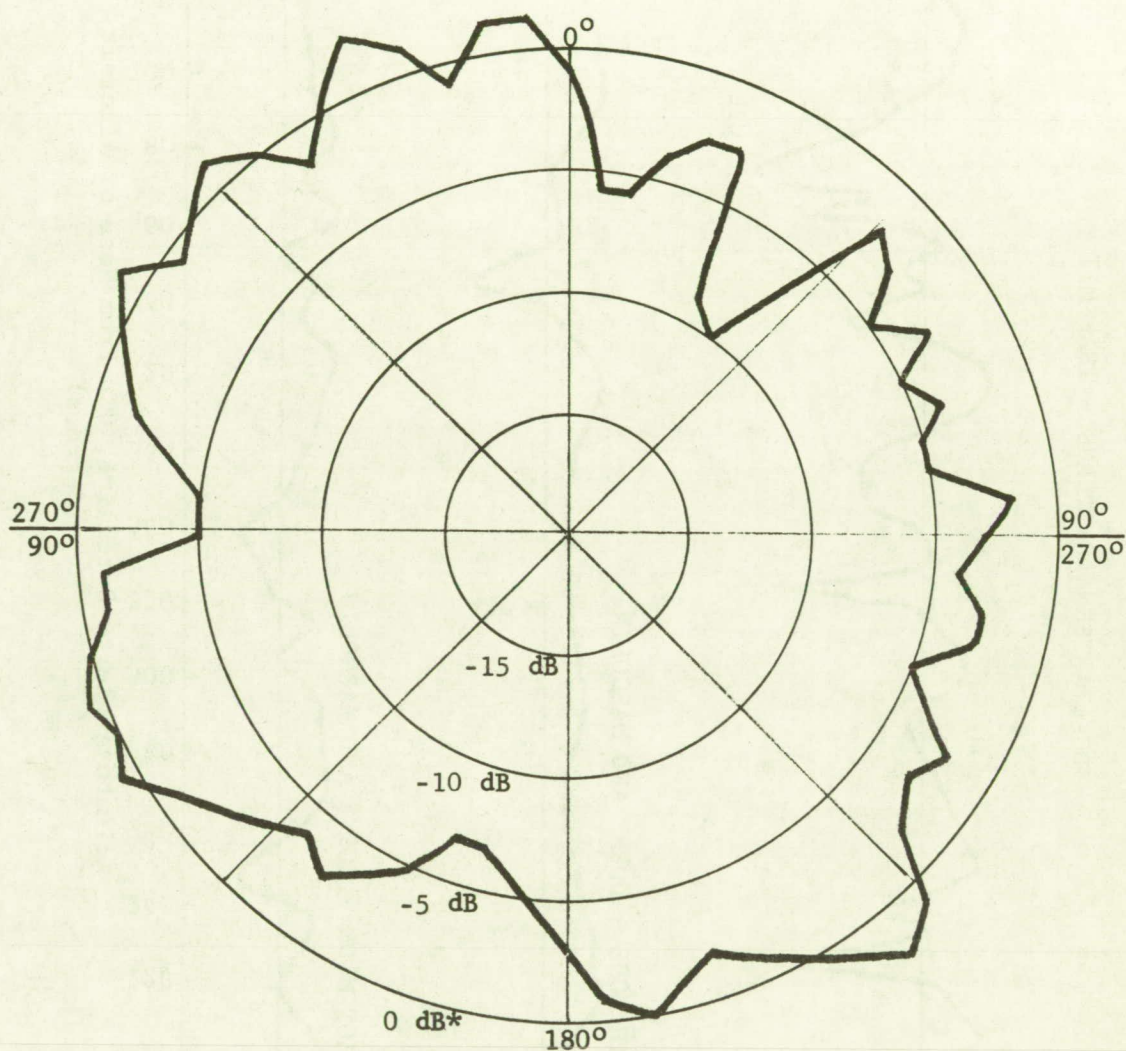


*reference only

FIGURE 6-2

RECEIVING ANTENNA PATTERNS - DC-6 - HORIZON MODE

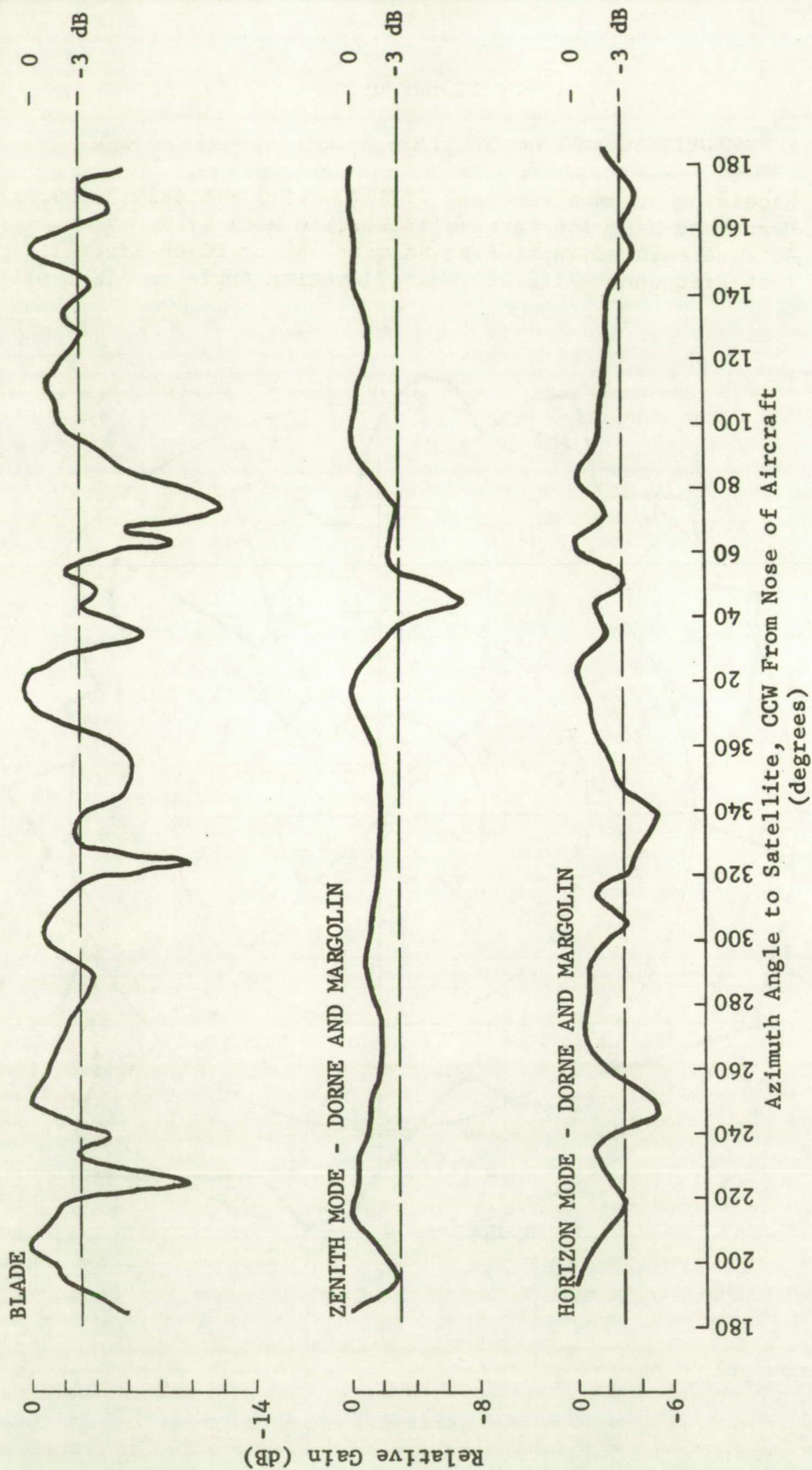
Receiving Antenna Pattern, 7/21/70, 19:32:16.4-19:34:09.2
Dorne and Margolin Antenna in Horizon Mode
Antenna Located Topside at Station 590 on DC-6B Aircraft
Test Frequency - 135.575 MHz; Elevation Angle to ATS-3 - 44°



*reference only

FIGURE 6-3

DC-6 ANTENNA PATTERNS - TRANSMIT



0 degrees, placing the satellite outside of the nominal pattern of the Dorne and Margolin antenna, although that antenna was sometimes used when responses were expected through ATS-1.

For flights near the east coast of the United States, ATS-3 was between approximately 40 and 32 degrees elevation angle, depending on the seasonally changed longitude of the satellite; and ATS-1 was approximately 0 degrees elevation angle, so that the interrogation signals through one satellite would be received strongly in the aircraft and a good return through that satellite received but a very poor return or none at all through the other satellite. The aircraft antenna mode and the satellite for the interrogation were sometimes selected to get the most consistent returns through both satellites. Under these conditions, the interrogating signal into the aircraft was frequently poorer than it would have been with another antenna mode, so that the signal level into the aircraft receiver was poor resulting in time delay variations that displaced fixes along hyperbolic lines of position.

Two transponder equipments were used with the aircraft. They were interchanged between the aircraft for specific test flights and on some test flights both transponders were carried on a single aircraft and used alternately. As used in this report, the term "transponder" refers to a complete unit including a receiver-transmitter with a tone-code responder attached between the receiver and transmitter.

One transponder employed a Bendix type RTA-41B transceiver with an MDA-41 modem for frequency modulation and a PAA-41A 500 Watt power amplifier. A type LNA-41 low noise preamplifier was used ahead of the receiver. A General Electric tone-code responder was connected between the transmitter and receiver. This unit is identified elsewhere in the report as the Bendix or RTA-41B transponder.

The other transponder employed the General Electric Mastr Progress Line[®] type DM-76-LAS mobile radio base station unit, with the tone-code responder connected between the transmitter and receiver. The original limiter-discriminator of the receiver was by-passed with a unit designed to have a smaller time delay change with signal amplitude than the original limiter-discriminator. The receiver was preceded by a 144-1P Parks preamplifier and the transmitted output amplified by a Gonset model 903 Mark II 350 Watt power amplifier. The unit is identical to the ground reference transponders, and is referred to in this report as the GE transponder.

A third aircraft installation was made in a Pan American 747 aircraft. A tone-code responder was repackaged to fit in a three-quarter ATR box and connected between the receiver and transmitter of one of the two operational air-to-ground communication transceivers. All type 747 aircraft built by the Boeing Company are equipped with a crossed slot antenna designed for VHF satellite communications. Their VHF communications equipment is built in accordance with ARINC characteristics 566. At least two of the aircraft have flown with a full complement of equipment for VHF satellite communications. The General Electric tone-code transponder was carried on one of these aircraft, but operating and maintenance schedules for the aircraft frustrated every schedule for in-flight testing of the unit. One successful two-satellite ranging test was made to the aircraft while it was on the ground at Kennedy Airport. The test and the several voice communication tests with Pan American and other ground terminals suggest that the performance with the 747 aircraft would have been much superior to the performance achieved with the FAA aircraft because of the better antenna characteristics of the Boeing slot dipole antenna.

Relative Position Accuracy for Two Aircraft in Flight

The Federal Aviation Administration flew two aircraft with measured and controlled separations for the purpose of measuring relative position accuracy of the satellite position fixes with the aircraft over land and over water. The flight test was made on December 1, 1970 with a DC-6 four engine propeller-driven aircraft and a C-135 jet aircraft. Each aircraft was equipped with a tone-code ranging transponder. The DC-6 used the GE transponder and was equipped with a Dorne and Margolin Satcom antenna and a blade antenna. The C-135 aircraft was equipped with the RTA-41 transponder and a blade antenna. Both aircraft were located by range measurements from the two satellites and also by the EAIR Precision Radar at the FAA National Aviation Flight Experimental Center (NAFEC).

The radar tracks of the flight paths for the aircraft are shown in Figure 6-4. On each leg, the aircraft started with the C-135 approximately one mile ahead and 500 feet higher than the DC-6. As the aircraft proceeded, the C-135 pulled ahead so that at the end of fifteen minutes flight time it was approximately 8 miles ahead of the DC-6.

Flights were made over land and water and at altitudes of approximately 20,000 and 5,000 feet. The test occupied approximately 5.5 hours of flight time.

Satellite ranging data were recorded at the General Electric Observatory at Schenectady, New York on punched paper tape in the usual manner. The EAIR Precision Radar data were processed at NAFEC and furnished for comparison with the two satellite ranging fixes. The aircraft were tracked on alternate minutes by the radar because the radar could lock onto only one aircraft at a time. Aircraft positions were interpolated for each aircraft during the times when the radar was tracking the other craft. The interpolations are accurate because the aircraft were flying straight and level flights during the legs on which the measurements were made for separation comparison.

Results of the flight test are presented as follows:

Figure 6-5 shows the directions to the satellites, their elevation angles, the directions of the lines of position through the radar reference locations for each satellite, and the direction of the hyperbolic line of position representing the plot of constant range differences to the satellites. The directions are correct within the plot precision for all radar and satellite positions because the flight test was confined to a region small compared to the size of the earth and the orbit geometry.

Figures 6-6 through 6-24 are plots of the difference between satellite fixes and radar fixes with radar fixes as reference. A separate plot is presented for each radar run for each aircraft.

Figure 6-25 is a plot in latitude and longitude of satellite and corresponding radar fixes for a portion of one radar run for the DC-6 aircraft. The plot was made near the end of the test flight, and it is believed that the satellite fixes have a bias error due to satellite position prediction error.

Figure 6-26 is the same data as Figure 6-25 but with the satellite fixes shifted by the amount believed necessary to correct for the satellite reference position bias error.

FIGURE 6-4

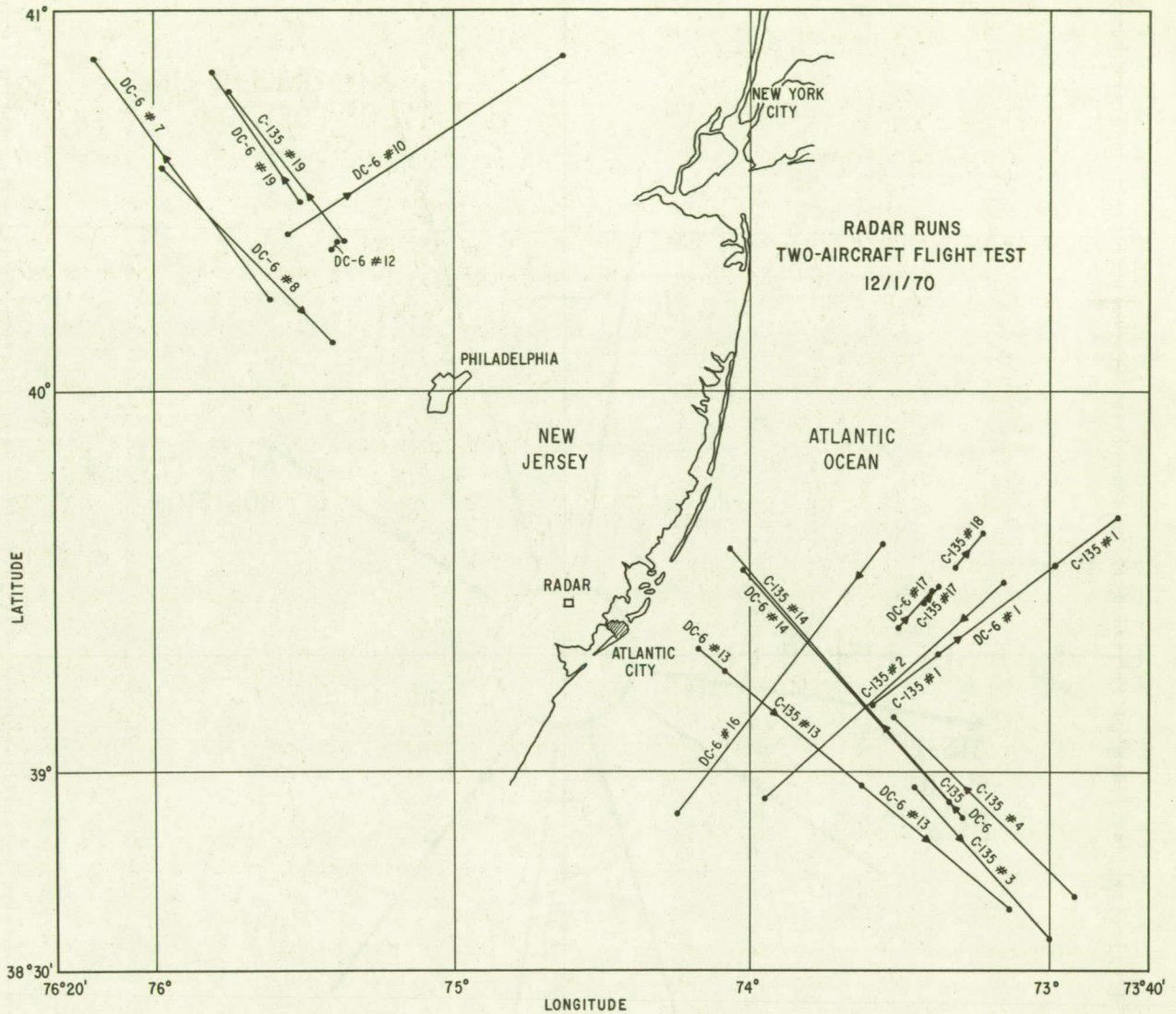


FIGURE 6-5

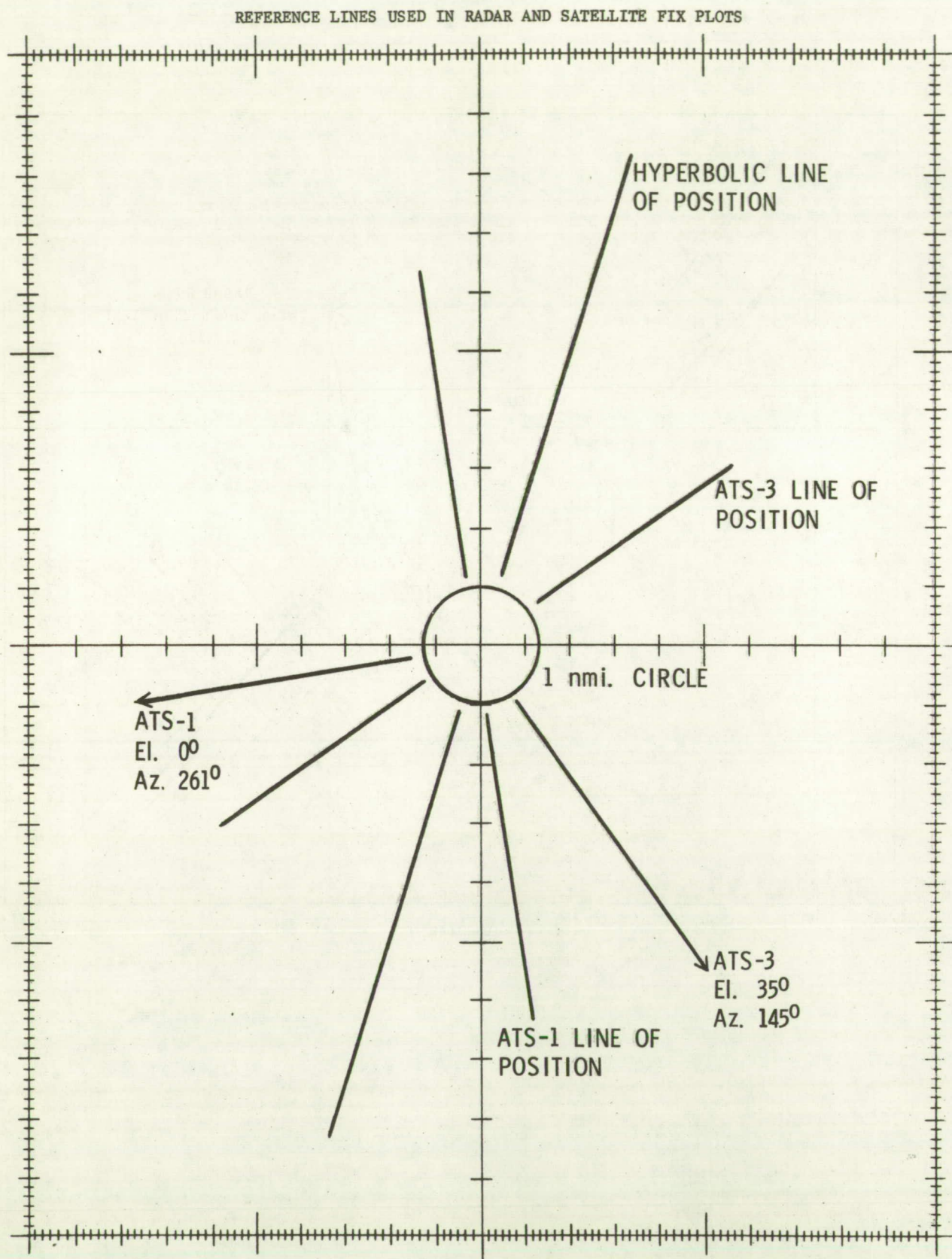


FIGURE 6-6

DIFFERENCES, PRECISION RADAR AND SATELLITE FIXES. RADAR FIXES AS REFERENCE.

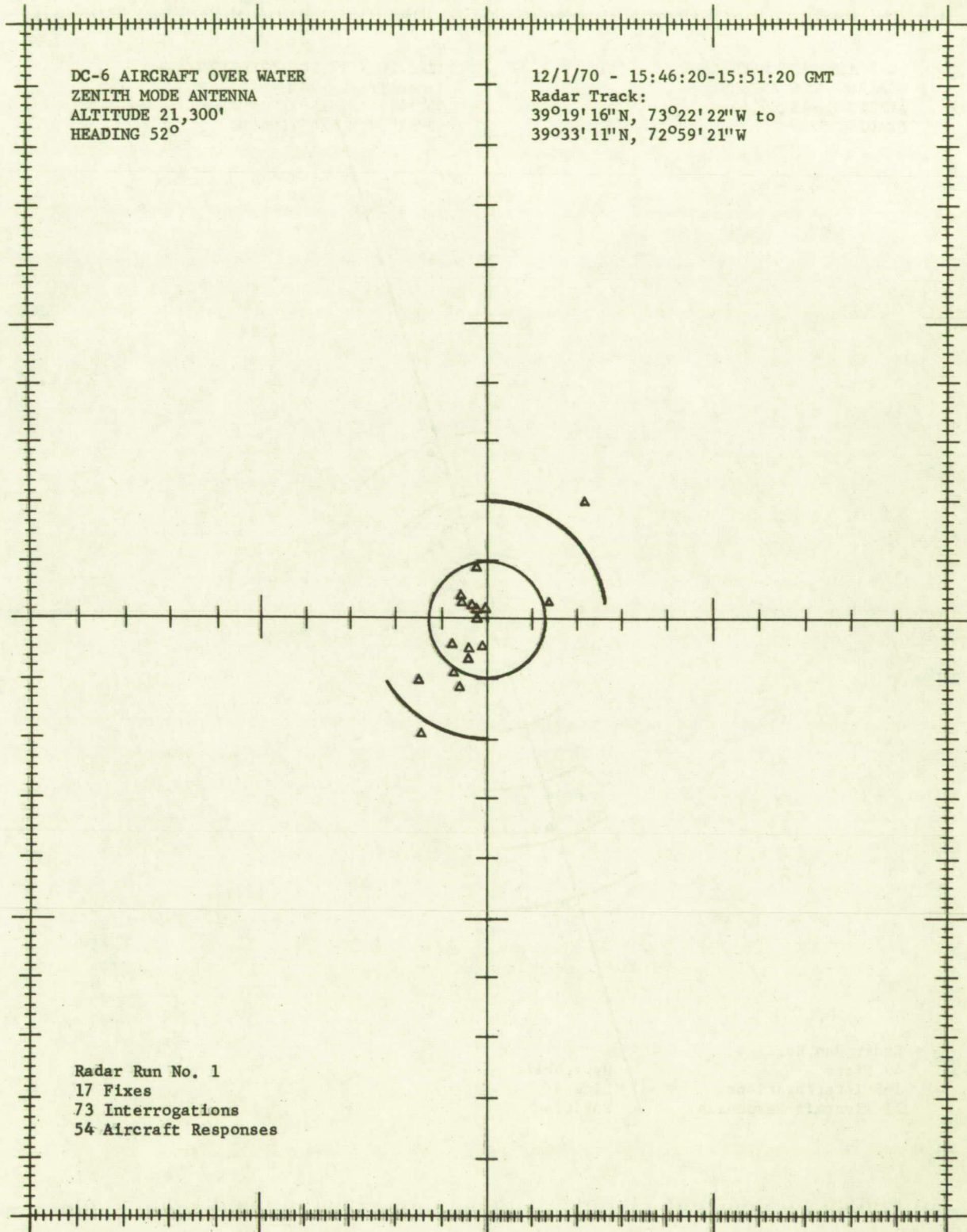


FIGURE 6-7

DIFFERENCES, PRECISION RADAR AND SATELLITE FIXES. RADAR FIXES AS REFERENCE.

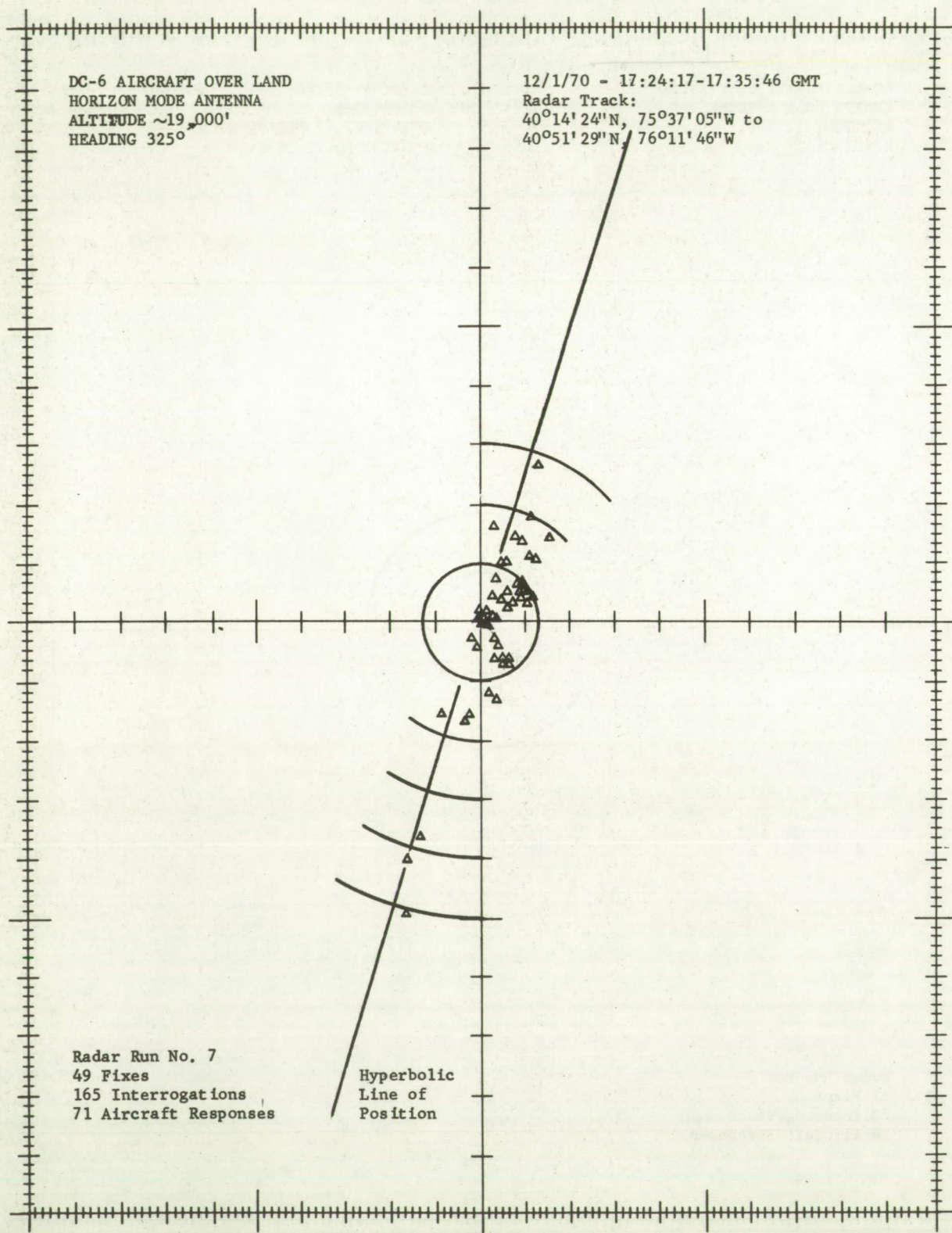


FIGURE 6-8

DIFFERENCES, PRECISION RADAR AND SATELLITE FIXES. RADAR FIXES AS REFERENCE.

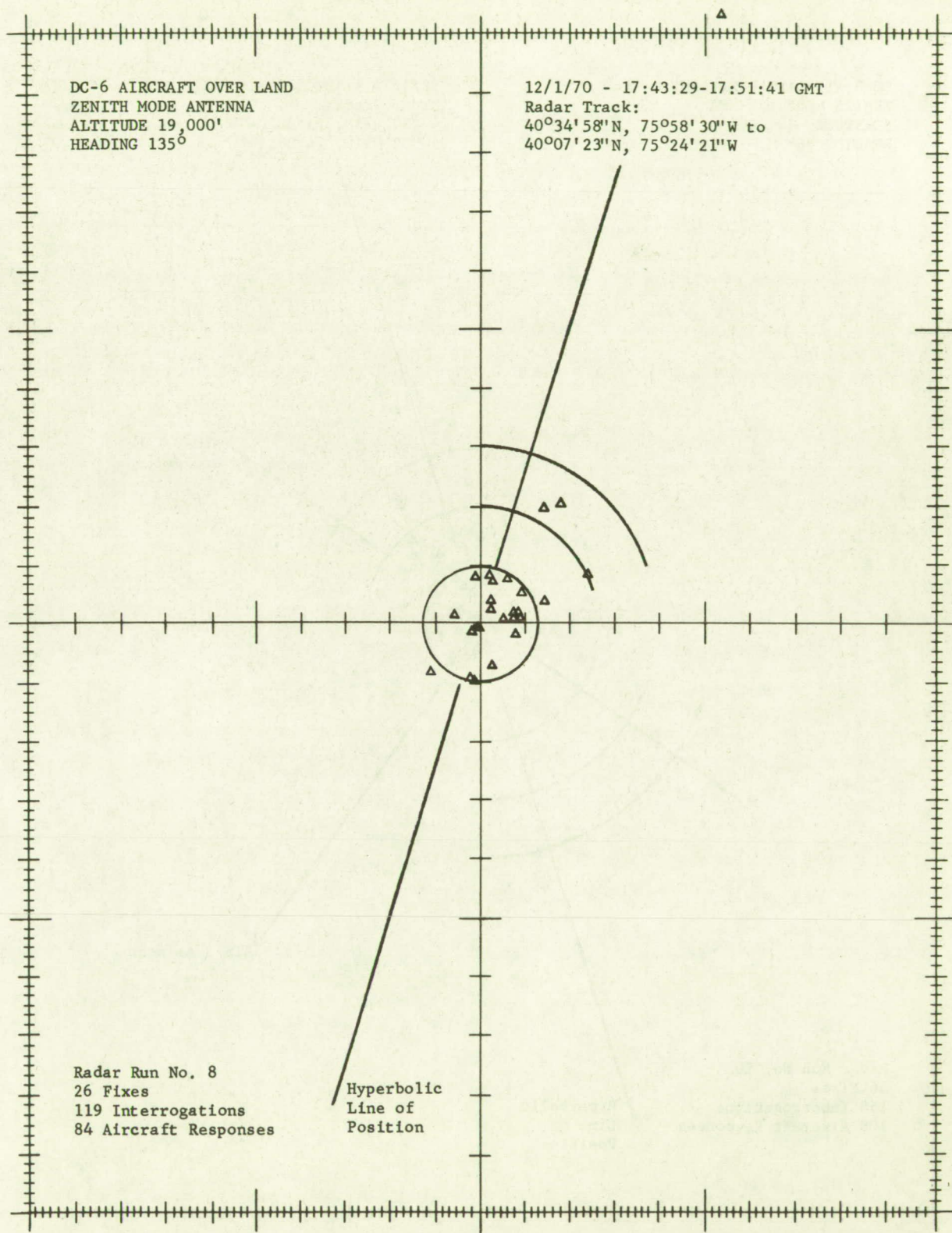


FIGURE 6-9

DIFFERENCES, PRECISION RADAR AND SATELLITE FIXES. RADAR FIXES AS REFERENCE.

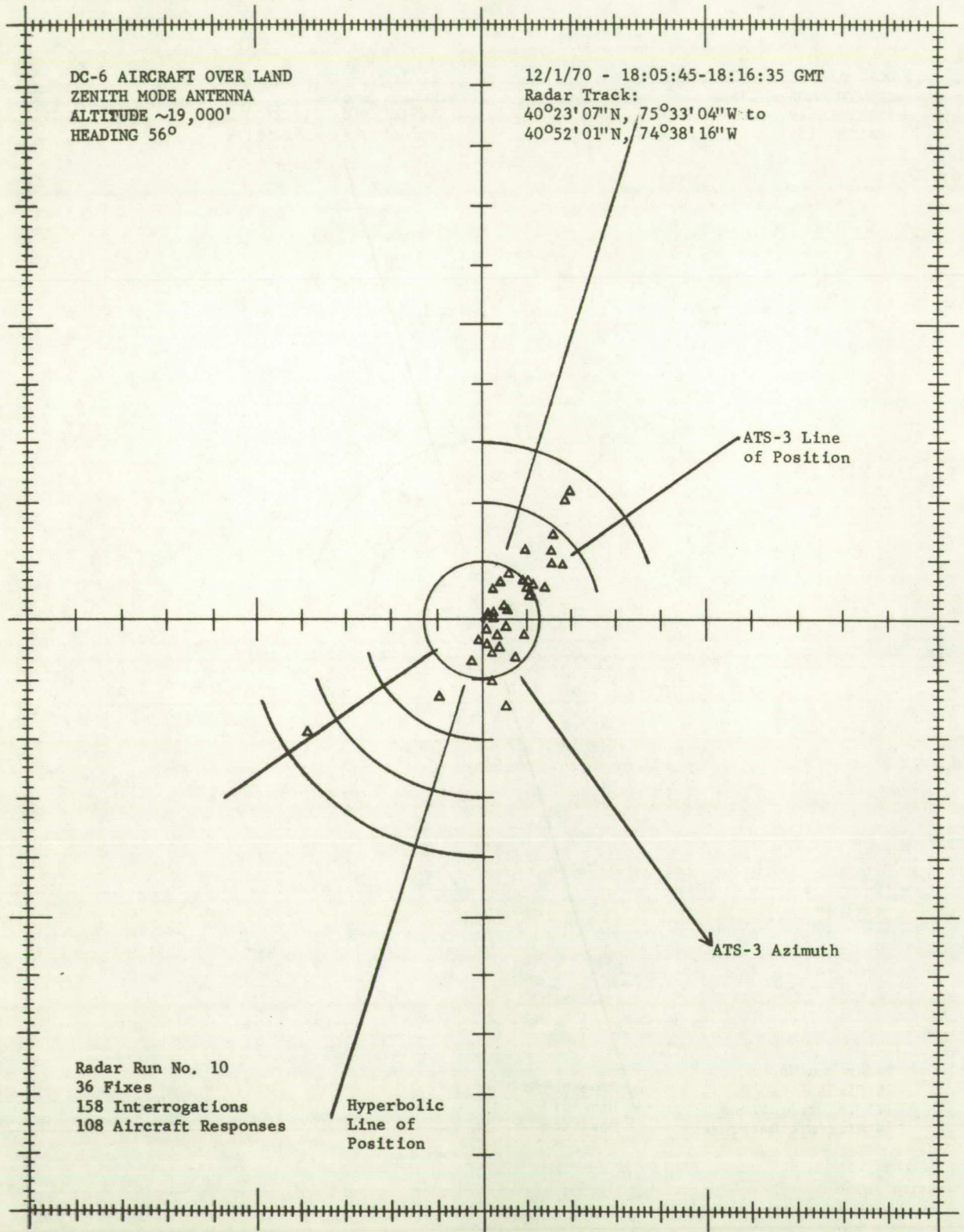


FIGURE 6-10

DIFFERENCES, PRECISION RADAR AND SATELLITE FIXES. RADAR FIXES AS REFERENCE.

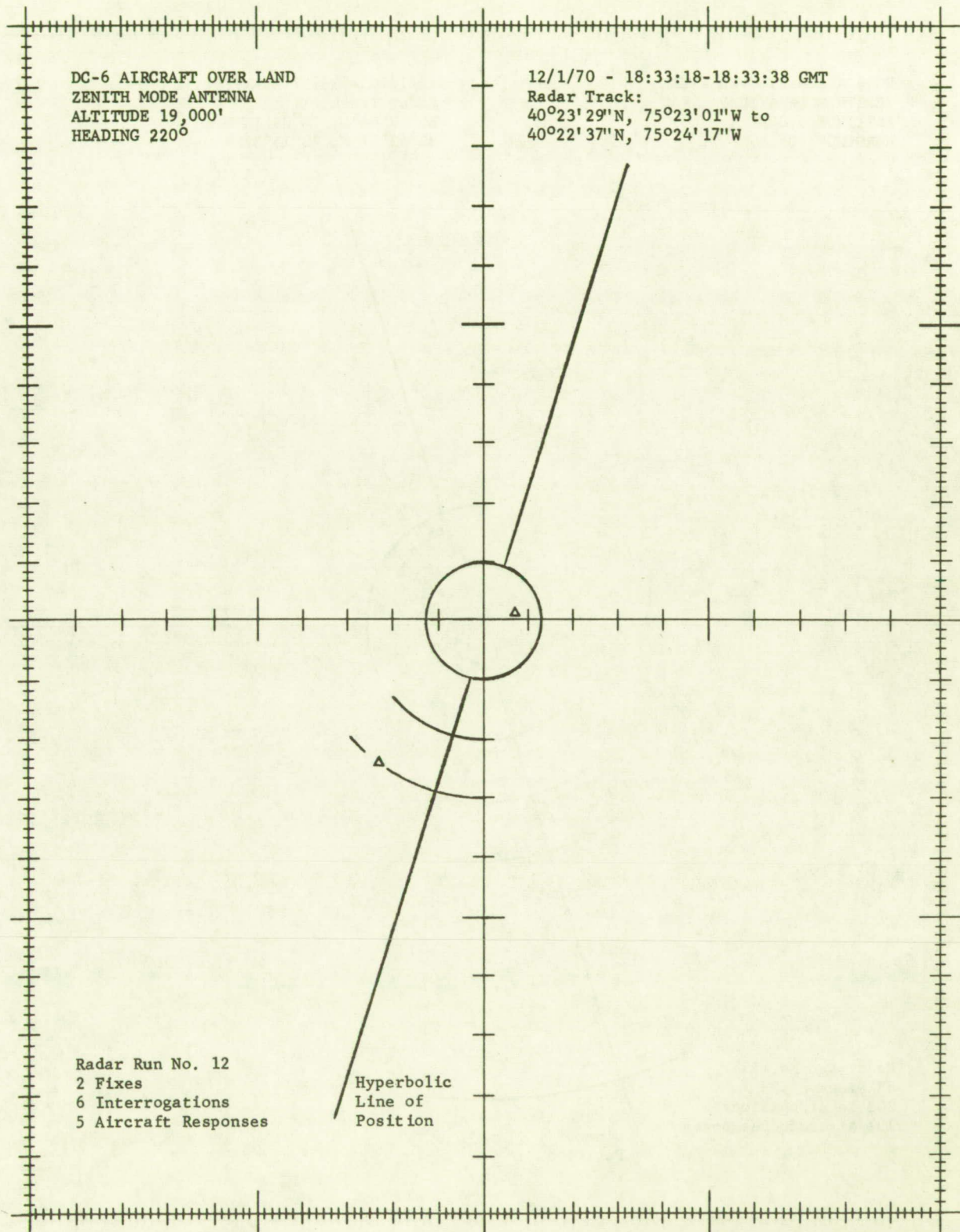


FIGURE 6-11

DIFFERENCES, PRECISION RADAR AND SATELLITE FIXES. RADAR FIXES AS REFERENCE.

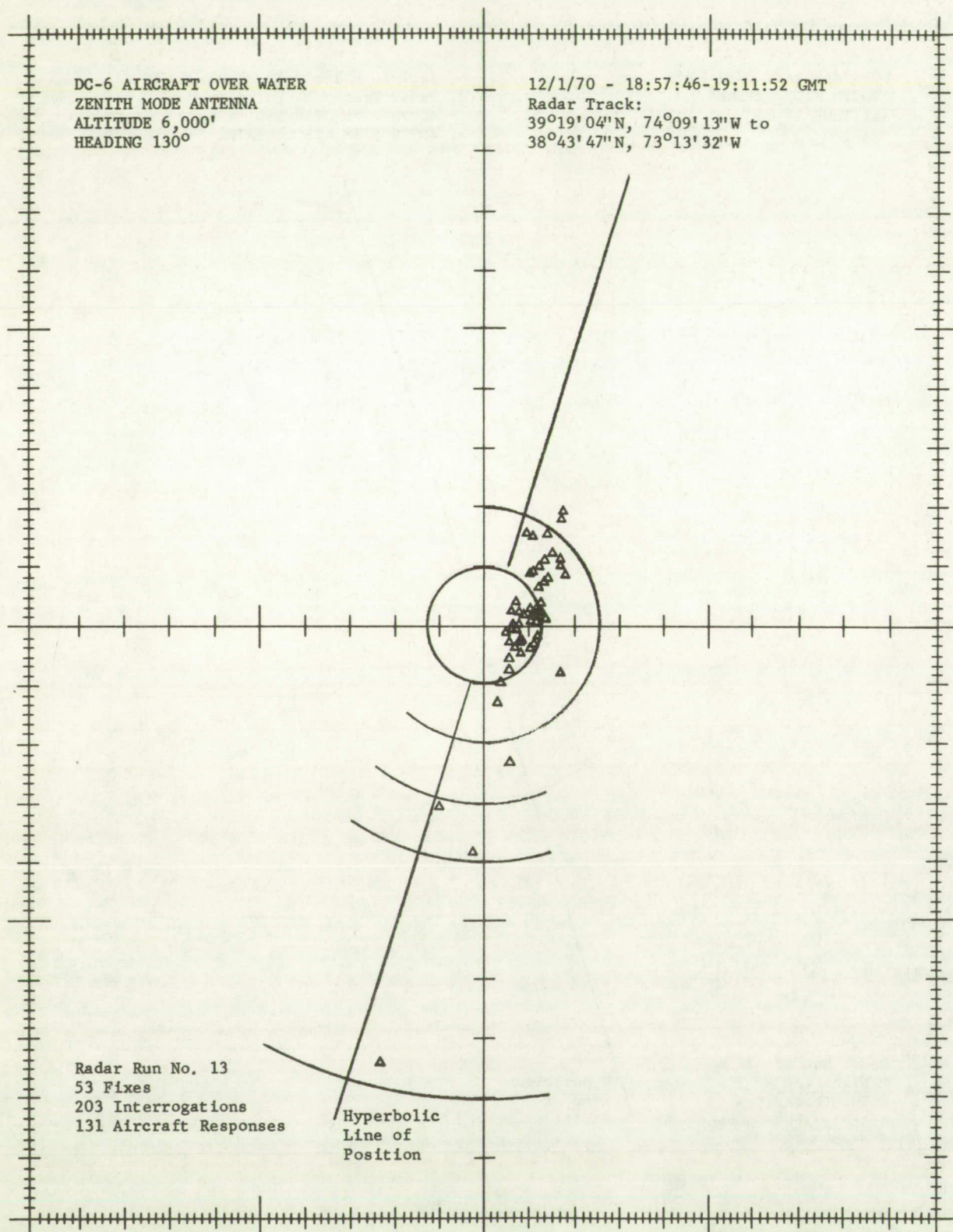


FIGURE 6-12

DIFFERENCES, PRECISION RADAR AND SATELLITE FIXES. RADAR FIXES AS REFERENCE.

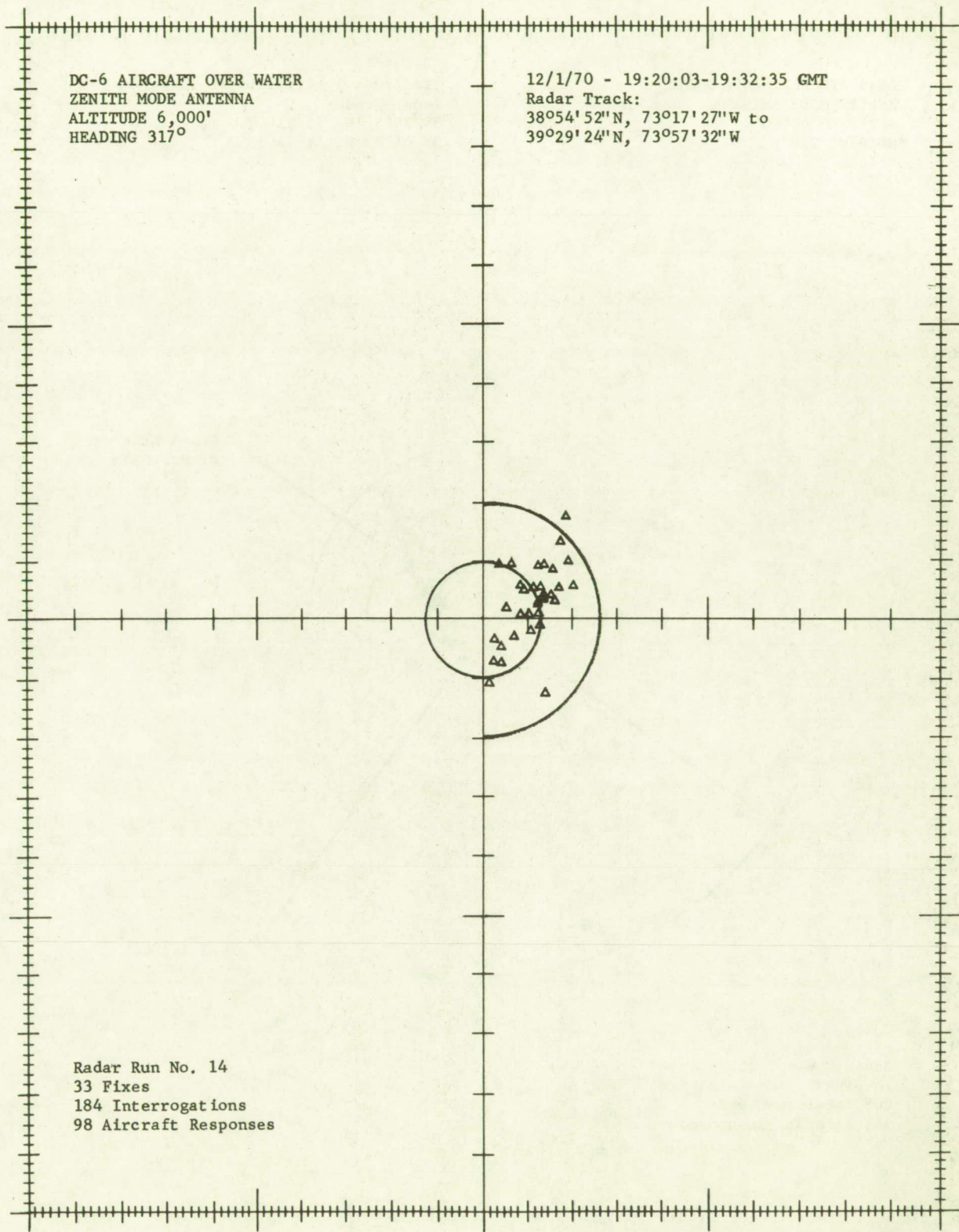


FIGURE 6-13

DIFFERENCES, PRECISION RADAR AND SATELLITE FIXES. RADAR FIXES AS REFERENCE.

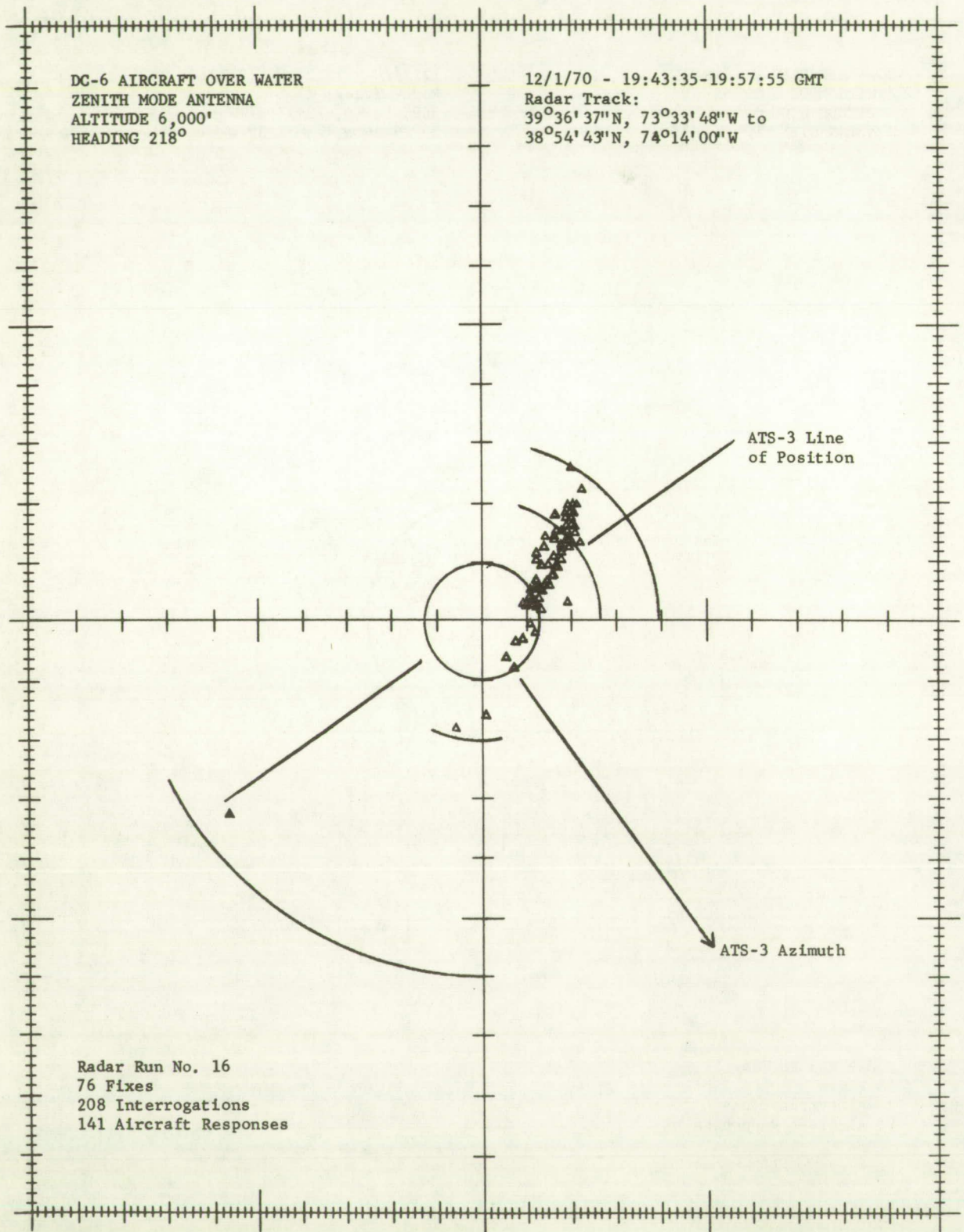


FIGURE 6-14

DIFFERENCES, PRECISION RADAR AND SATELLITE FIXES. RADAR FIXES AS REFERENCE.

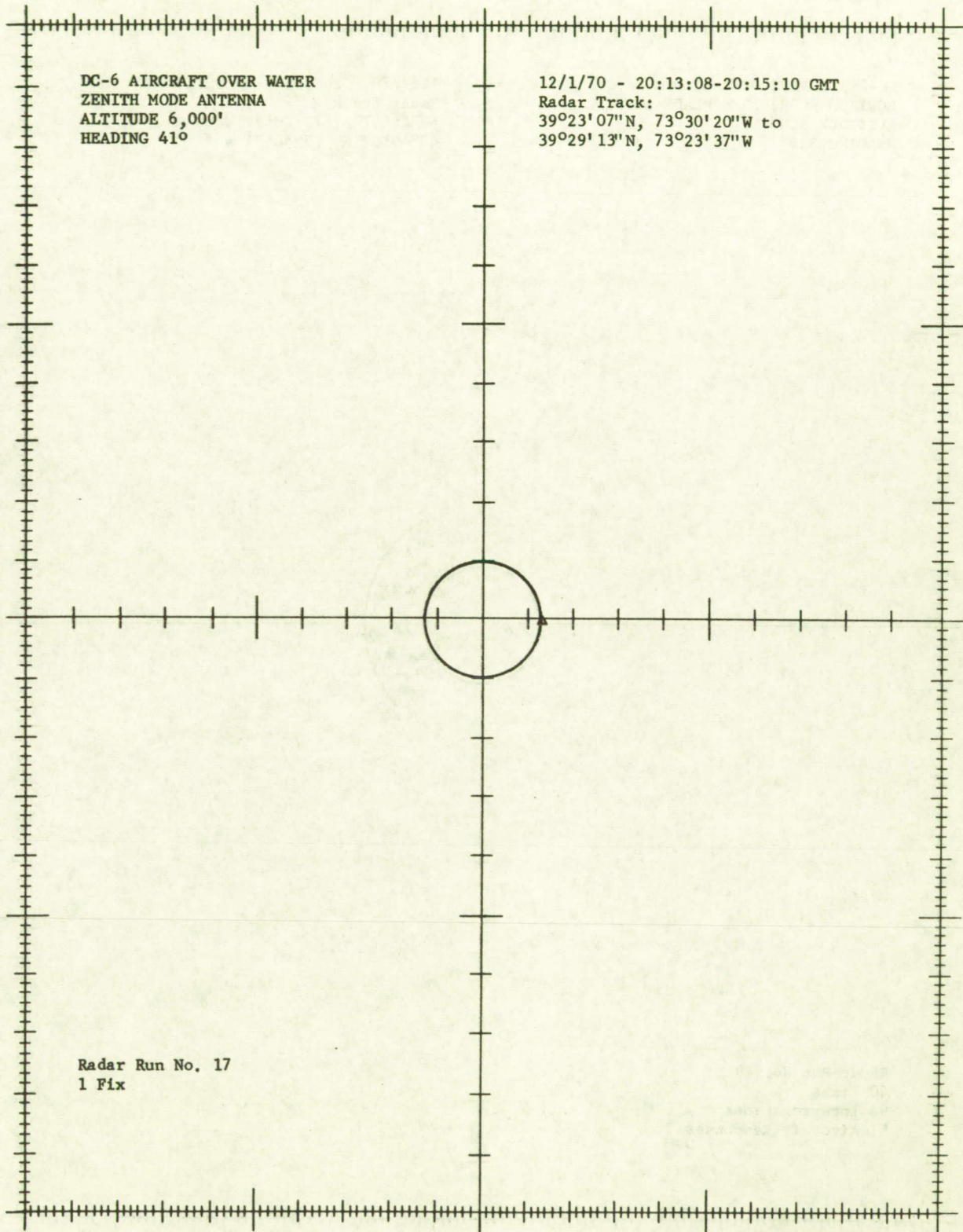


FIGURE 6-15

DIFFERENCES, PRECISION RADAR AND SATELLITE FIXES. RADAR FIXES AS REFERENCE.

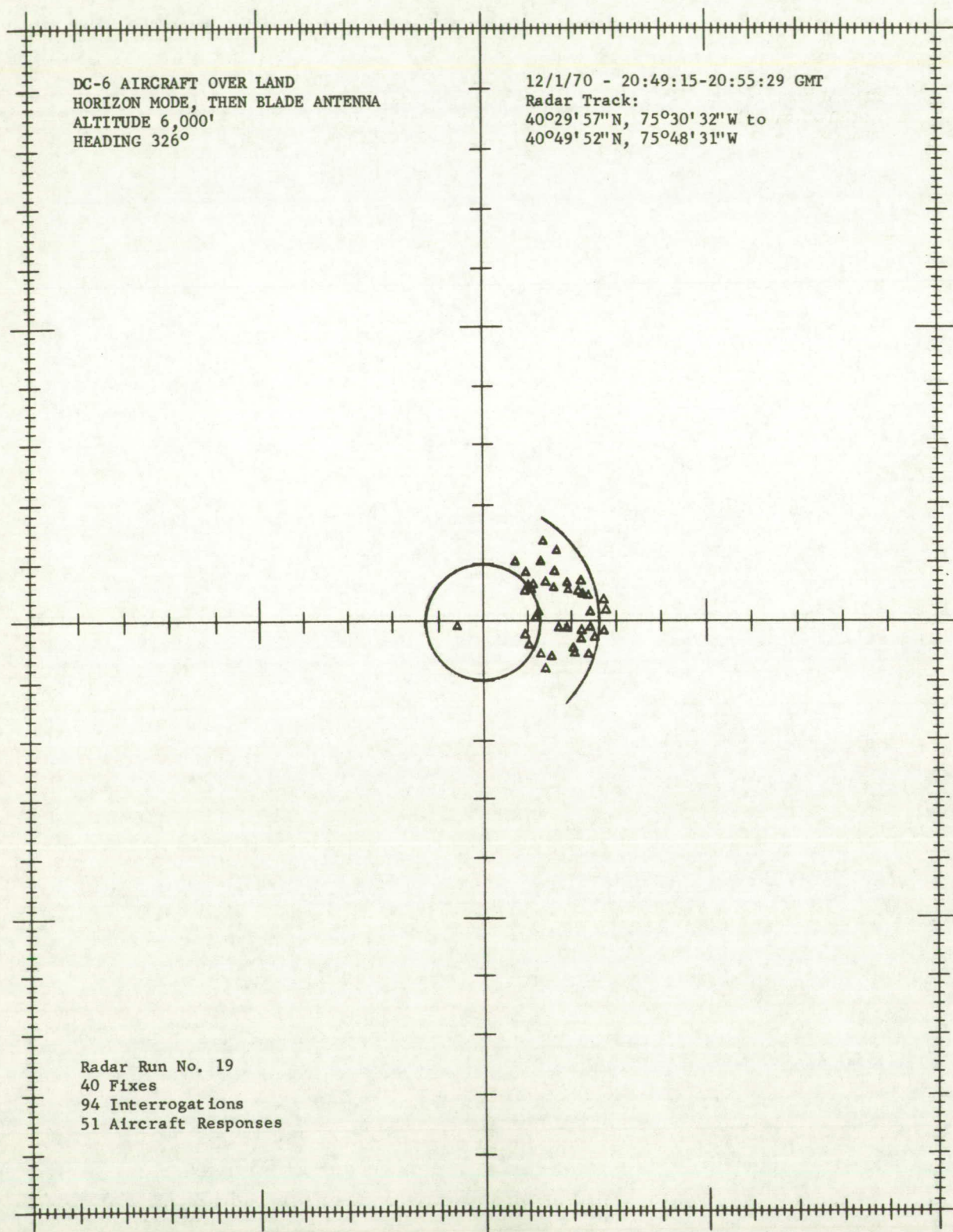


FIGURE 6-16

DIFFERENCES, PRECISION RADAR AND SATELLITE FIXES. RADAR FIXES AS REFERENCE.

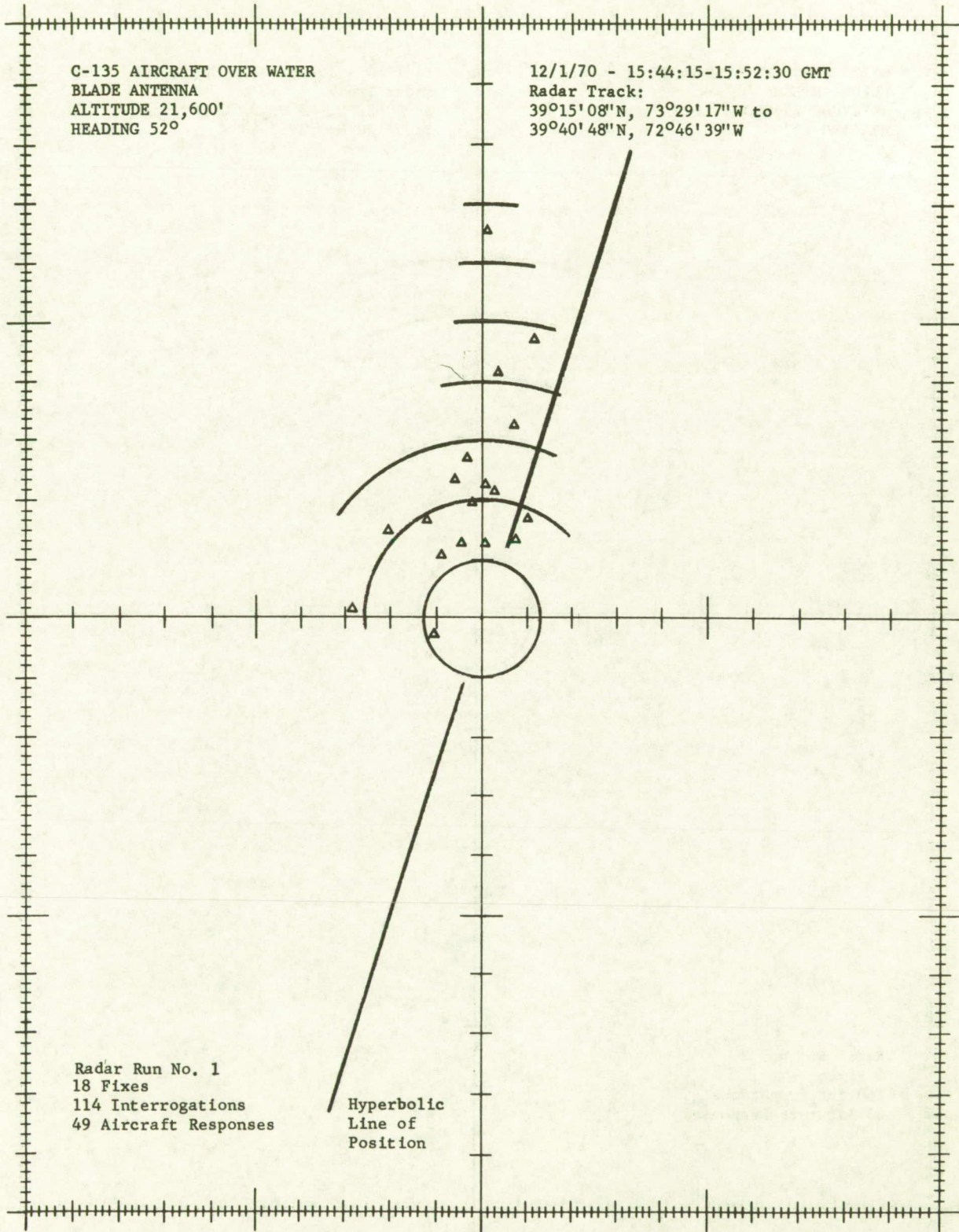


FIGURE 6-17

DIFFERENCES, PRECISION RADAR AND SATELLITE FIXES. RADAR FIXES AS REFERENCE.

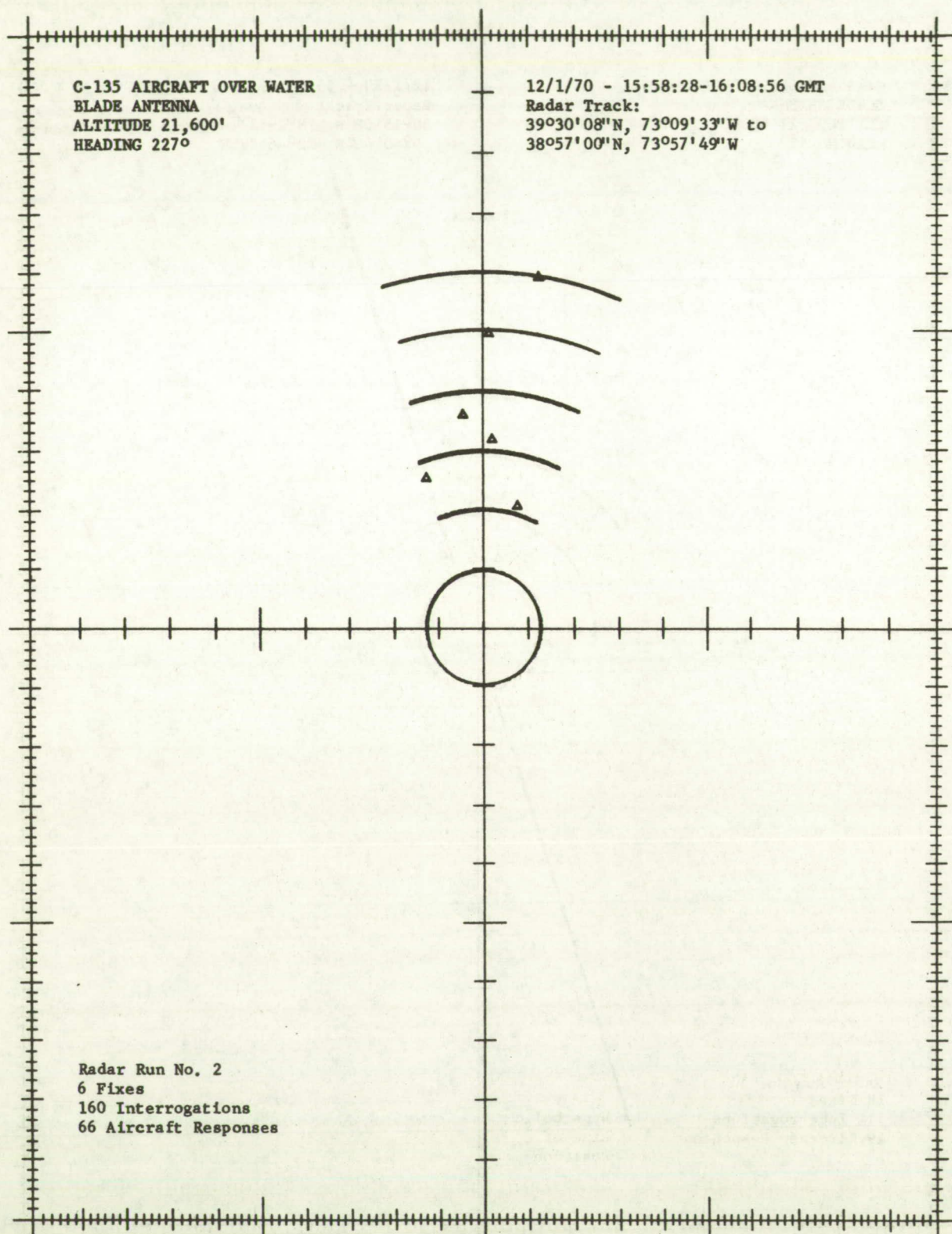


FIGURE 6-18

DIFFERENCES, PRECISION RADAR AND SATELLITE FIXES. RADAR FIXES AS REFERENCE.

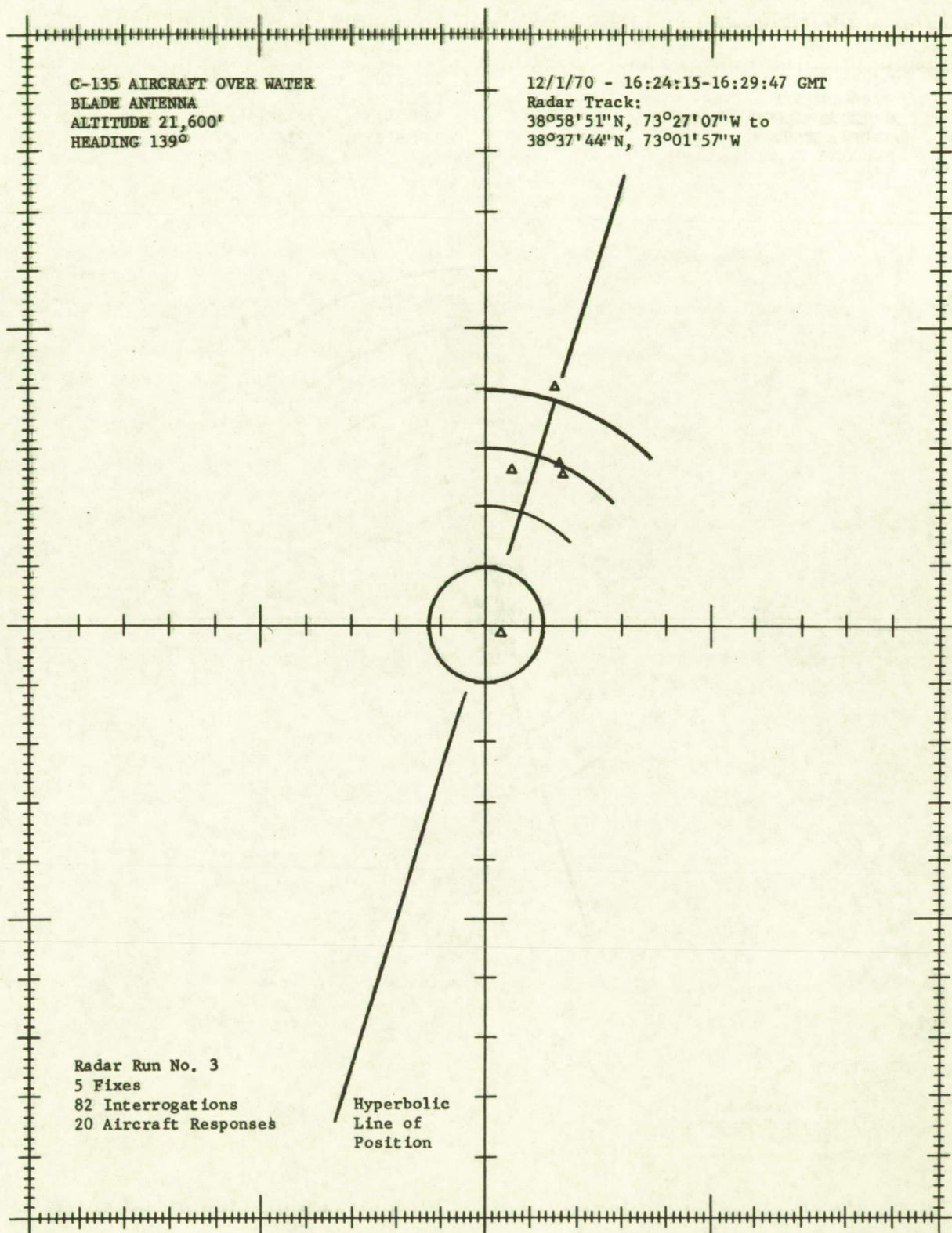


FIGURE 6-19

DIFFERENCES, PRECISION RADAR AND SATELLITE FIXES. RADAR FIXES AS REFERENCE.

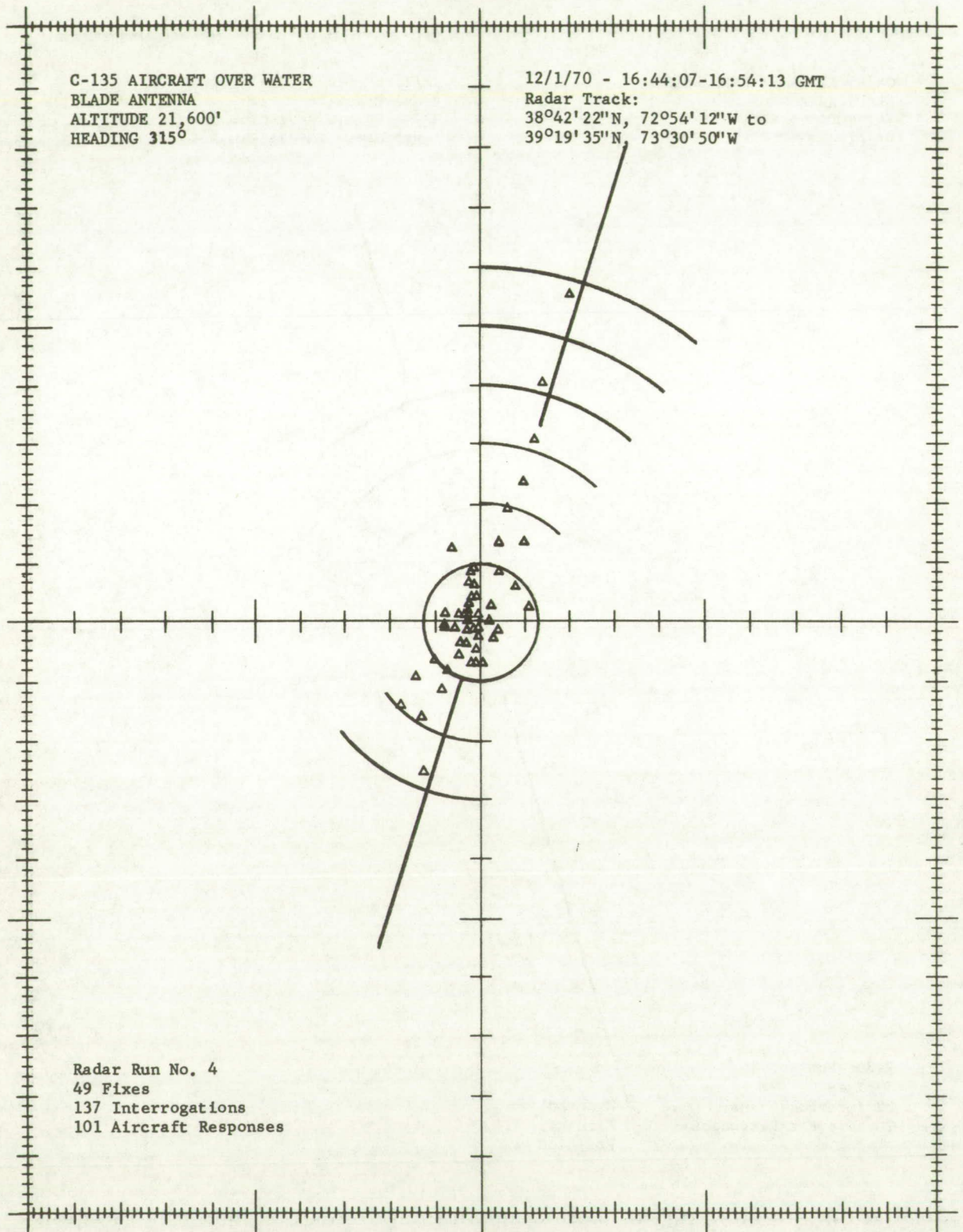


FIGURE 6-20

DIFFERENCES, PRECISION RADAR AND SATELLITE FIXES. RADAR FIXES AS REFERENCE.

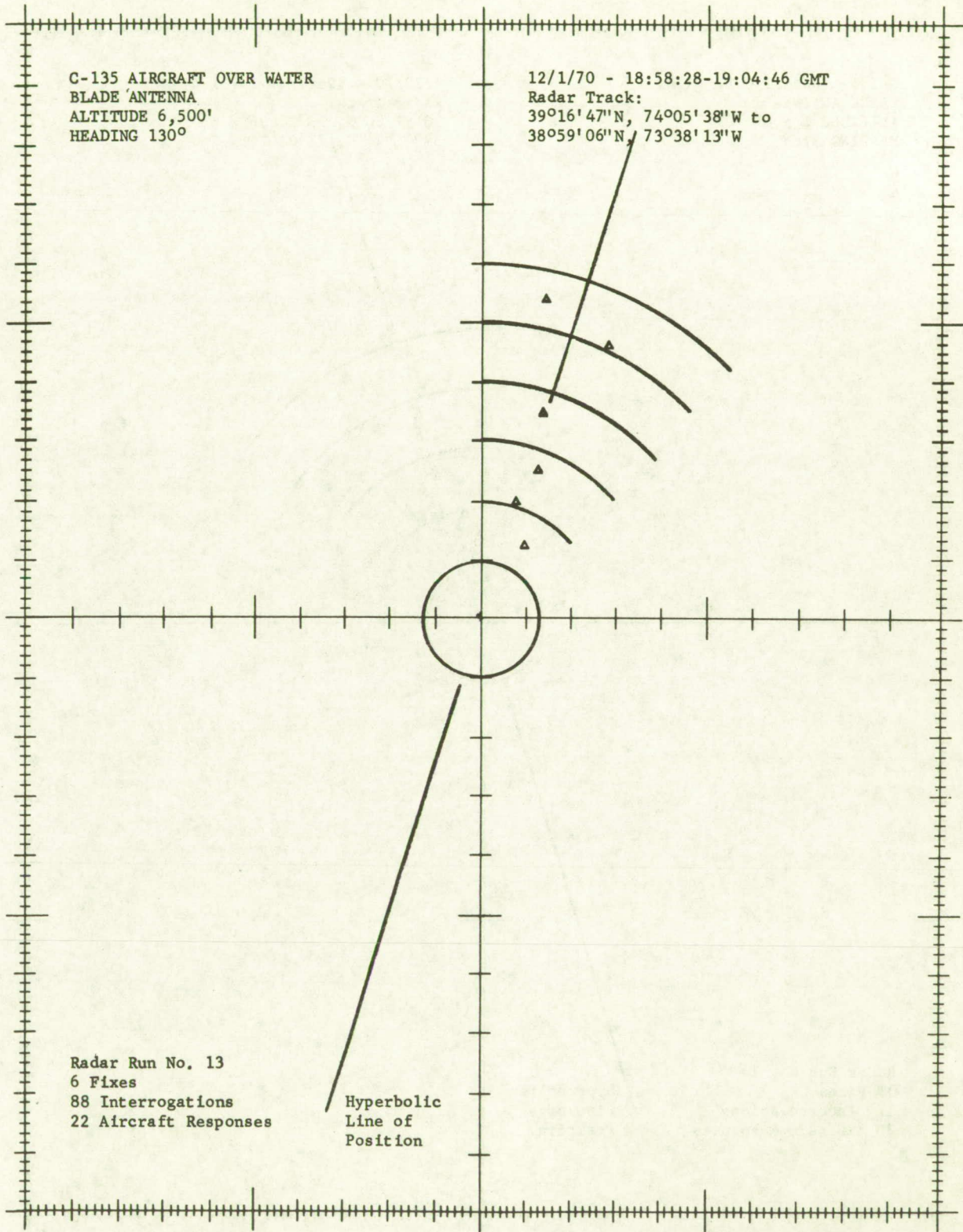


FIGURE 6-21

DIFFERENCES, PRECISION RADAR AND SATELLITE FIXES. RADAR FIXES AS REFERENCE.

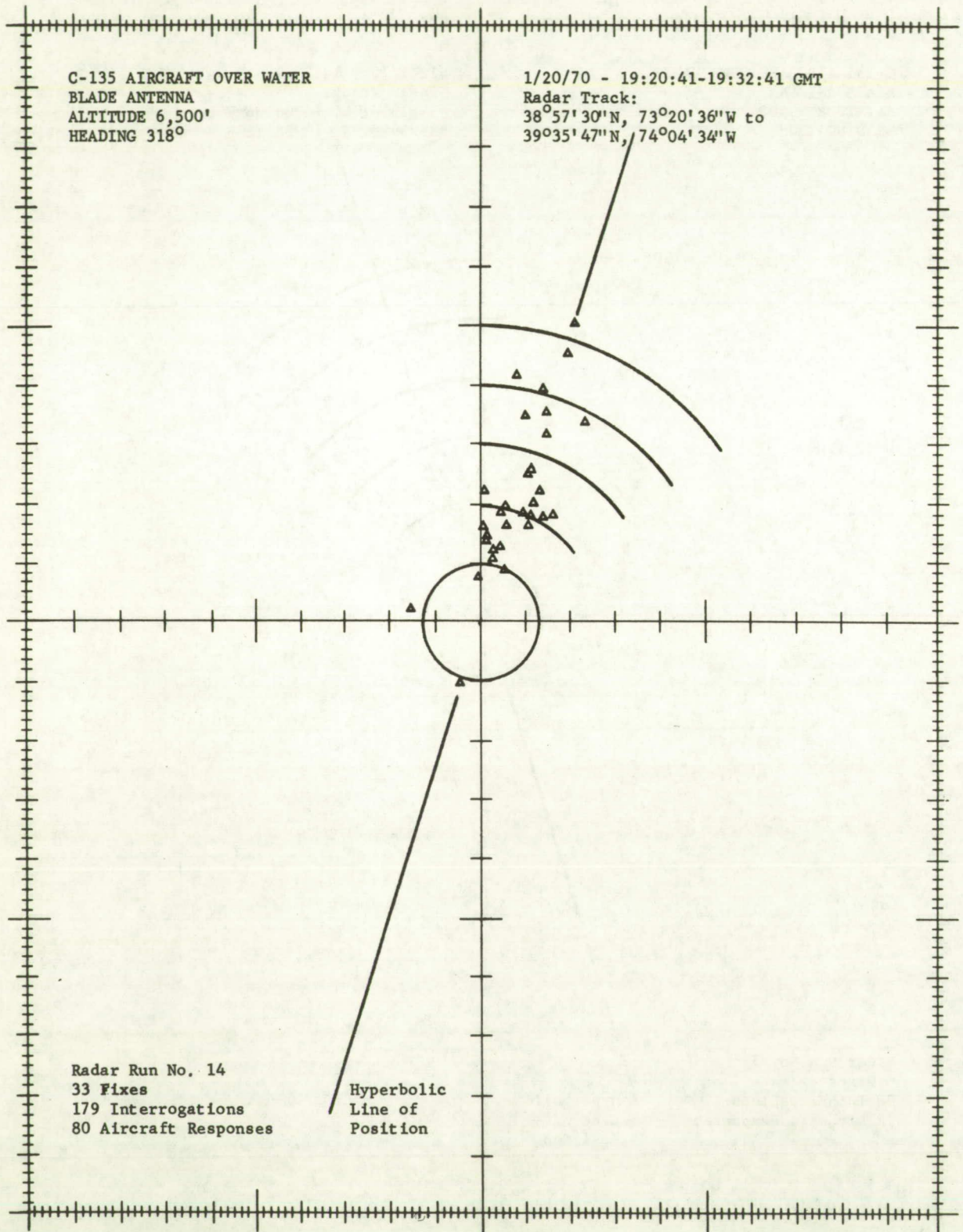


FIGURE 6-22

DIFFERENCES, PRECISION RADAR AND SATELLITE FIXES. RADAR FIXES AS REFERENCE.

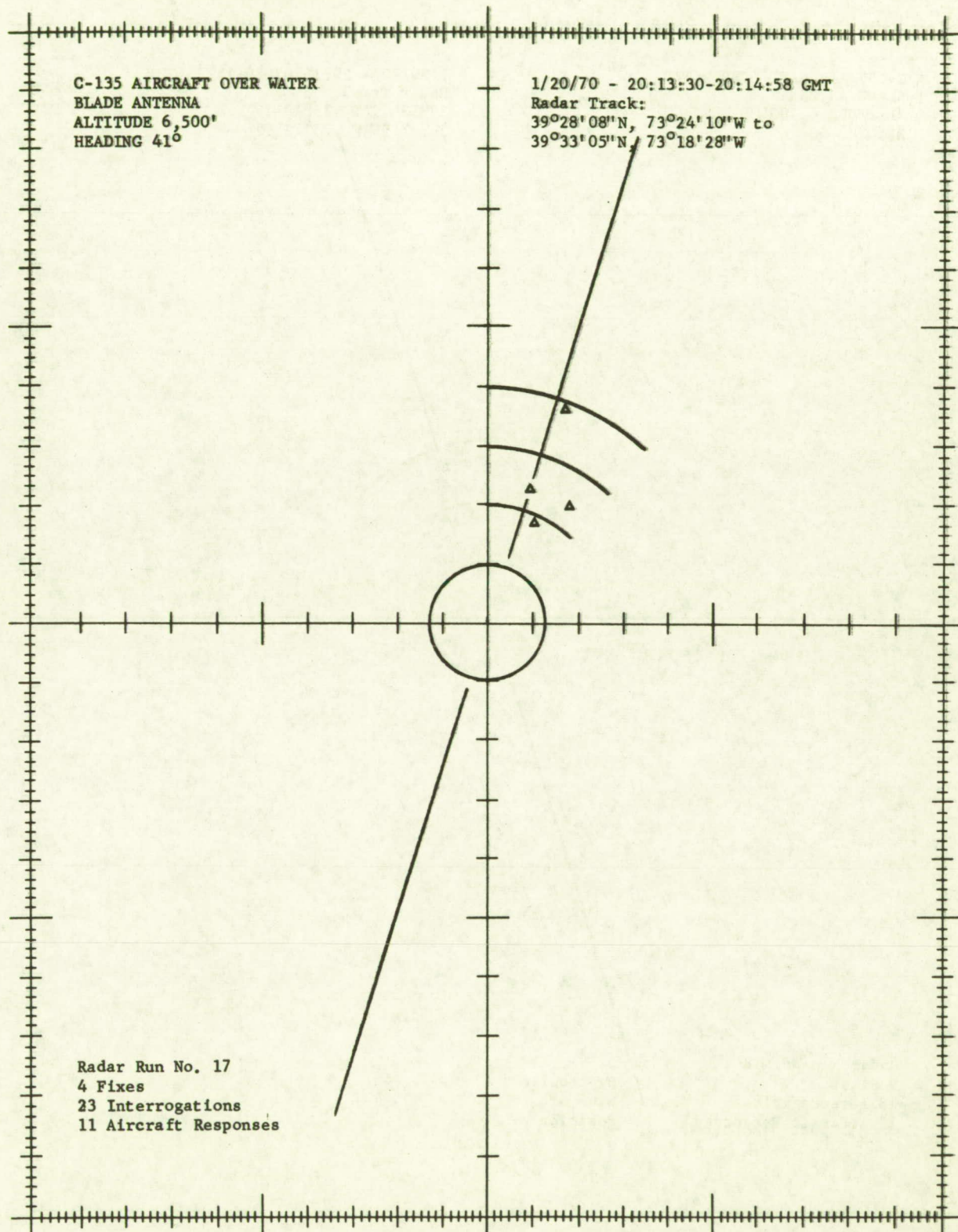


FIGURE 6-23

DIFFERENCES, PRECISION RADAR AND SATELLITE FIXES. RADAR FIXES AS REFERENCE.

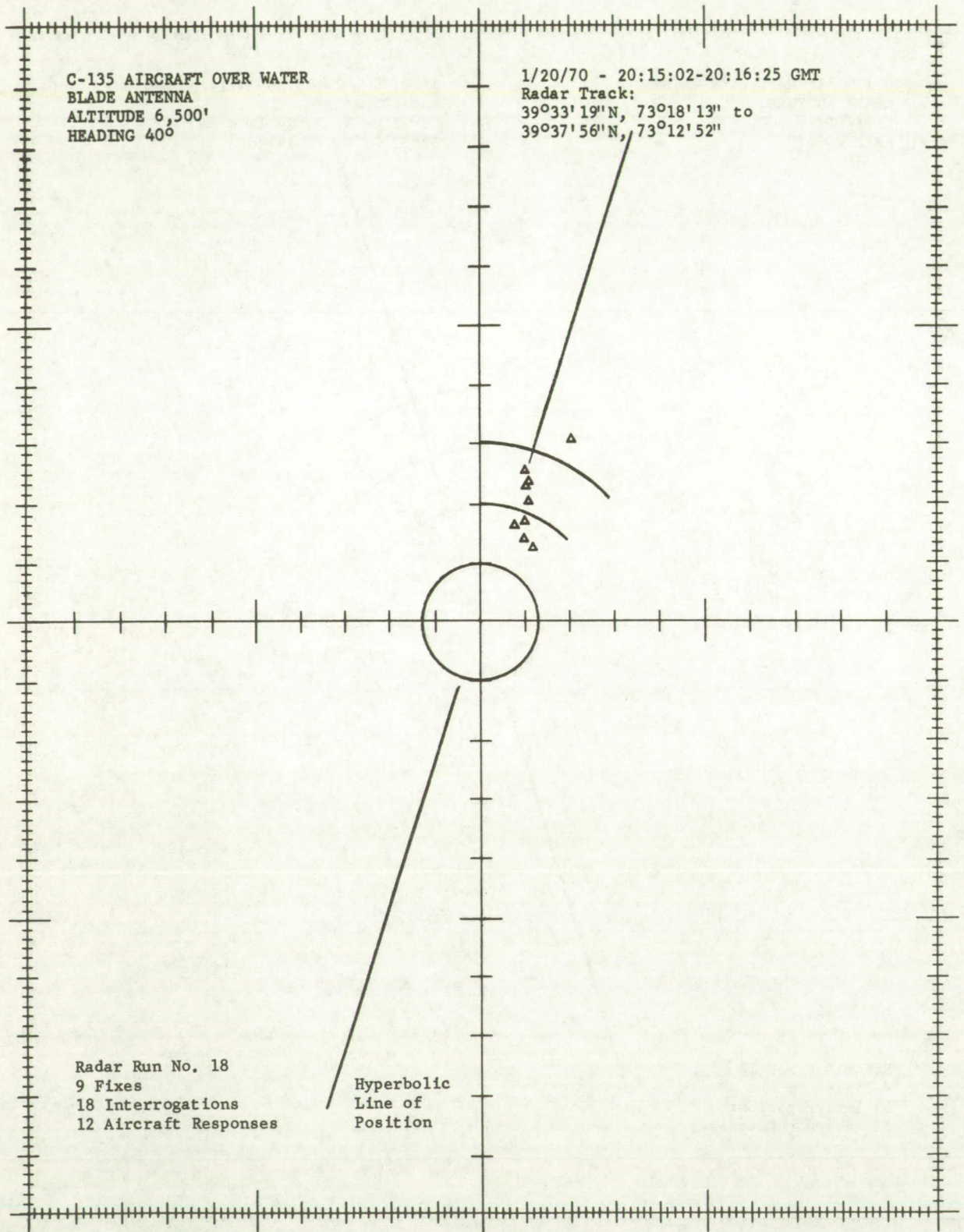


FIGURE 6-24

DIFFERENCES, PRECISION RADAR AND SATELLITE FIXES. RADAR FIXES AS REFERENCE.

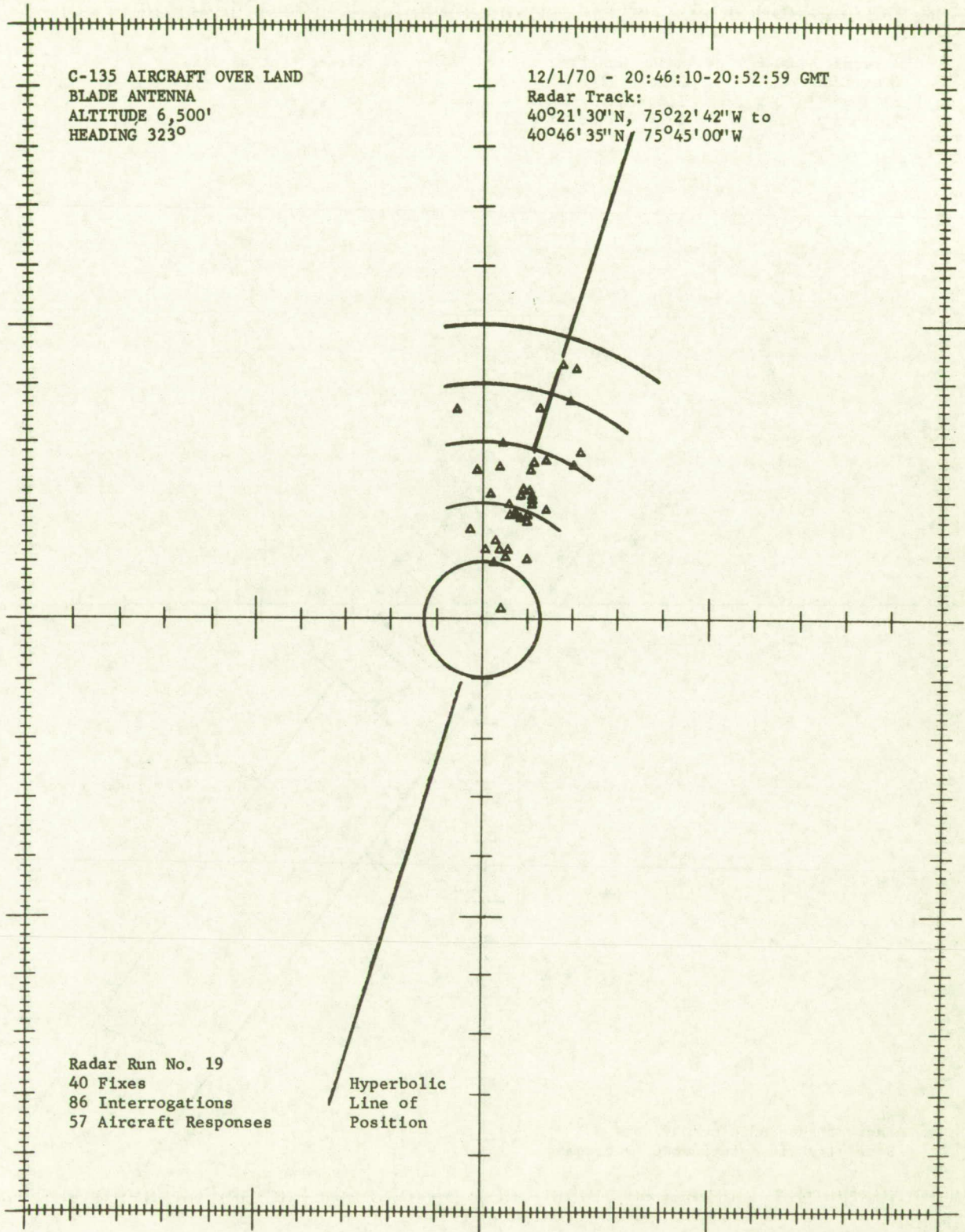


FIGURE 6-25

RADAR AND SATELLITE FIXES

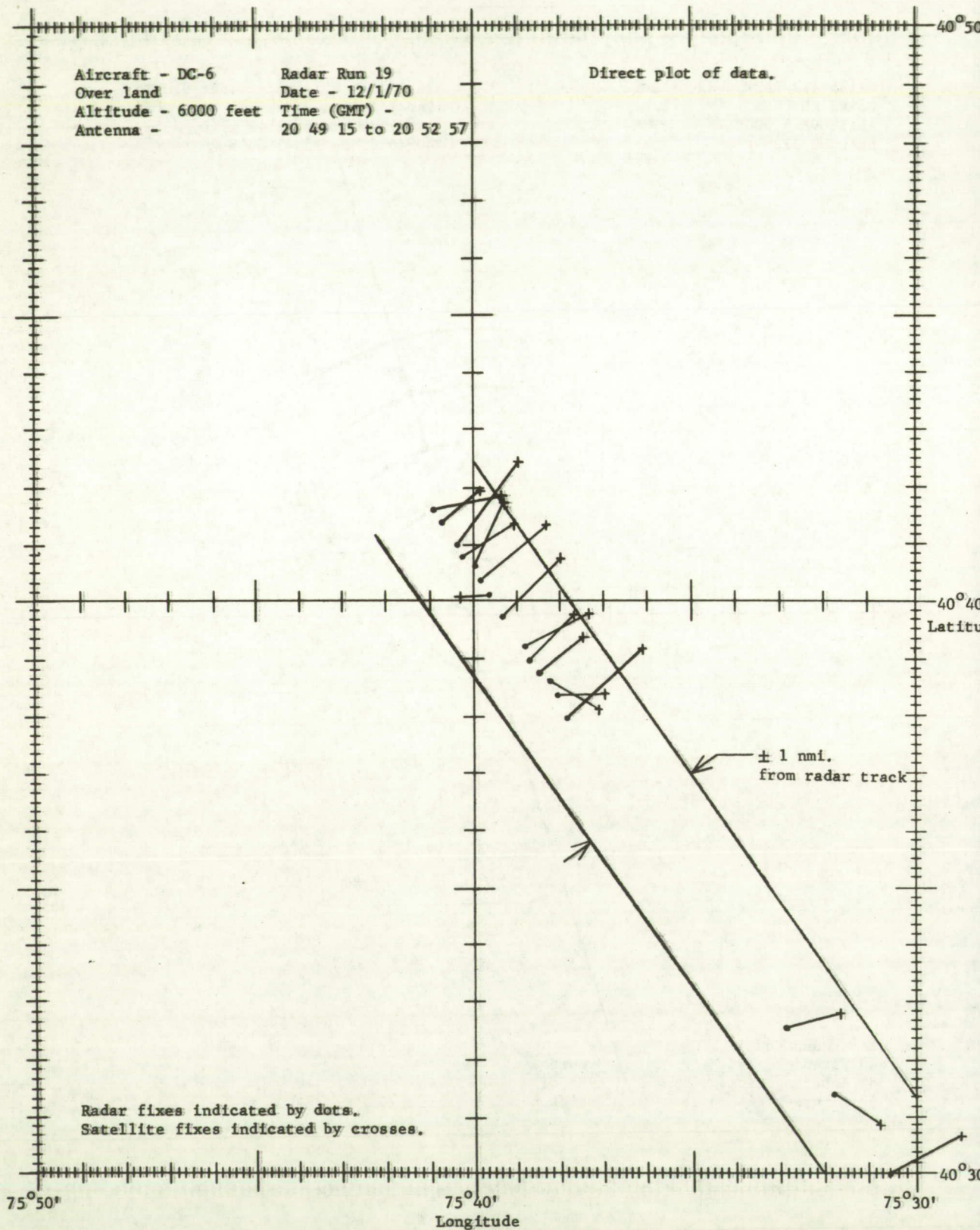


FIGURE 6-26

RADAR AND SATELLITE FIXES

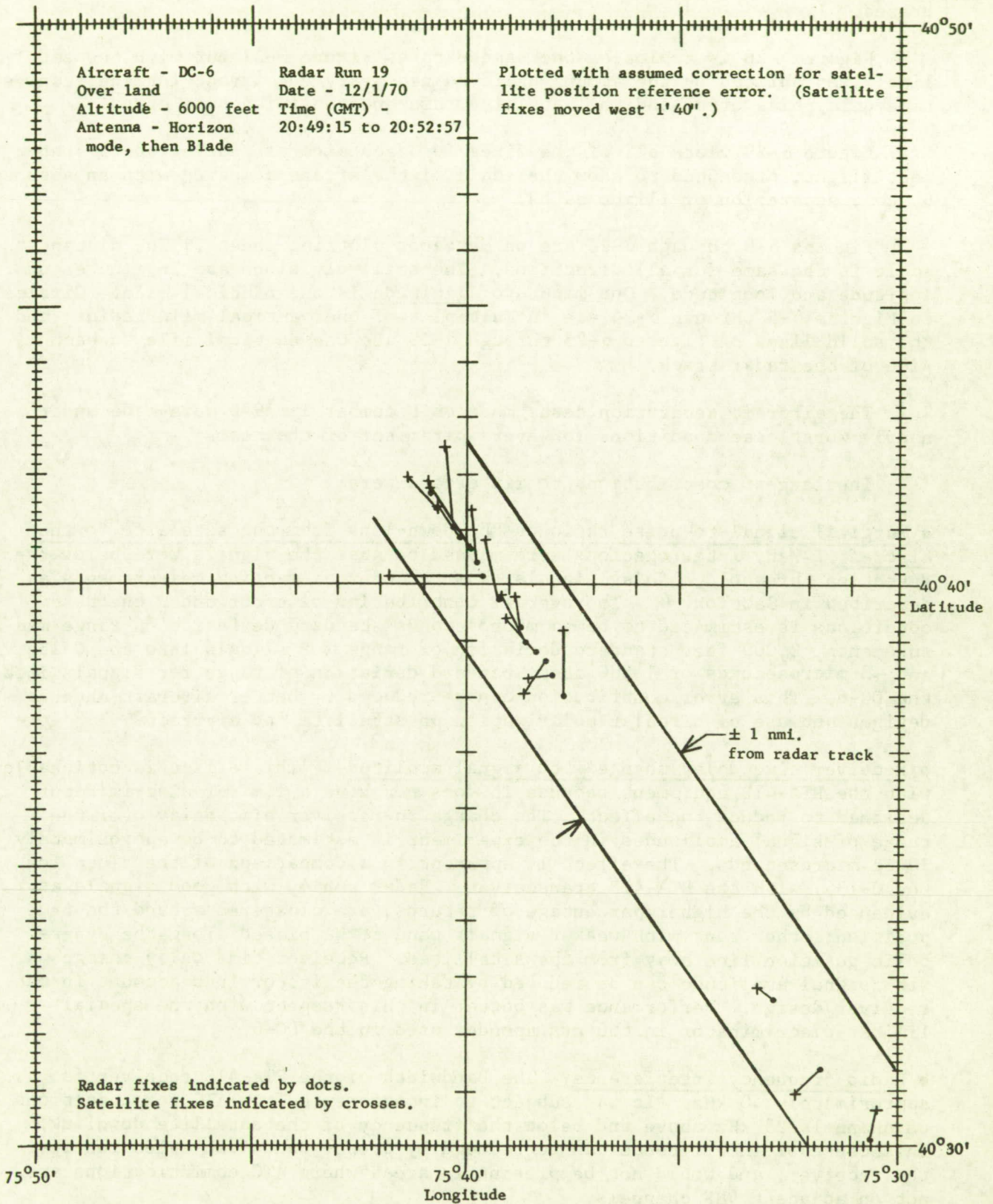


Figure 6-27 is a plot in latitude and longitude of satellite and radar fixes for a portion of one radar run for the C-135 aircraft. It is believed that the fixes are displaced along a hyperbolic line of position resulting from low received signal level in the aircraft with its corresponding receiver time delay change from the signal level when the transponder delay was calibrated.

Figure 6-28 is a plot of the same data as Figure 6-27 but with the satellite fixes shifted by the amount believed necessary to correct for the receiver time delay bias error and the satellite reference position bias error.

Figure 6-29 plots all of the fixes for each aircraft during the 5.5 hour test flight, presented to show the scale of the errors compared with an assumed 60 nmi. separation of flight paths.

Figures 6-5 through 6-28 are on Mercator plotting sheets. The distance scale is the same for all directions. The small divisions are in minutes of latitude and longitude. One minute of latitude is one nautical mile. Circles on Figures 6-5 through 6-24 are in multiples of one nautical mile radius, and the solid lines on Figures 6-25 through 6-28 are one nautical mile on each side of the radar track.

The aircraft separation tests made on December 1, 1970 were made under nearly worst case conditions for every parameter of the test.

The largest contributions to fix errors were:

- Marginal signal-to-noise ratio on the down-link from the satellite to the aircraft. Many interrogations were missed because the signals were below the detection threshold. Noisy signals cause scatter of ranging measurements as described in Section 4. The overall contribution of error under the test conditions is estimated to be ~4 microseconds standard deviation on range measurements, 2,000 feet standard deviation of range for signals into the C-135, and ~3 microseconds or 1,500 feet standard deviation of range for signals into the DC-6. This error contribution can be reduced by better aircraft antenna designs and use of circular polarization on satellite and aircraft.
- Receiver time delay change with signal amplitude. This effect is noticeable with the RTA-41B equipment because it does not have a limiter-discriminator designed to reduce the effect. The change in receiver time delay over the range of signal amplitudes in the experiment is estimated to be approximately 10-12 microseconds. The effect is apparent in a comparison of the plots for the C-135, with the RTA-41B transceiver. Radar run 4, with good signals as evidenced by the higher percentage of returns, are clustered around the true position; other runs with weaker signals tend to be biased along the hyperbolic position line away from the satellites. Receiver time delay change with signal amplitude can be reduced by taking the factor into account in the receiver design. Performance was better in this respect with the special limiter-discriminator in the transponder used in the DC-6.
- Radio frequency interference. The bandwidth of the RTA-41B receiver is approximately 40 kHz. It was subject to interference from ATC communications on channels 25 kHz above and below the frequency of the satellite downlink. This cause of interference can be reduced by proper bandwidth selection for the receiver, and would not be present in areas where ATC communications are not on adjacent VHF channels.

FIGURE 6-27

RADAR AND SATELLITE FIXES

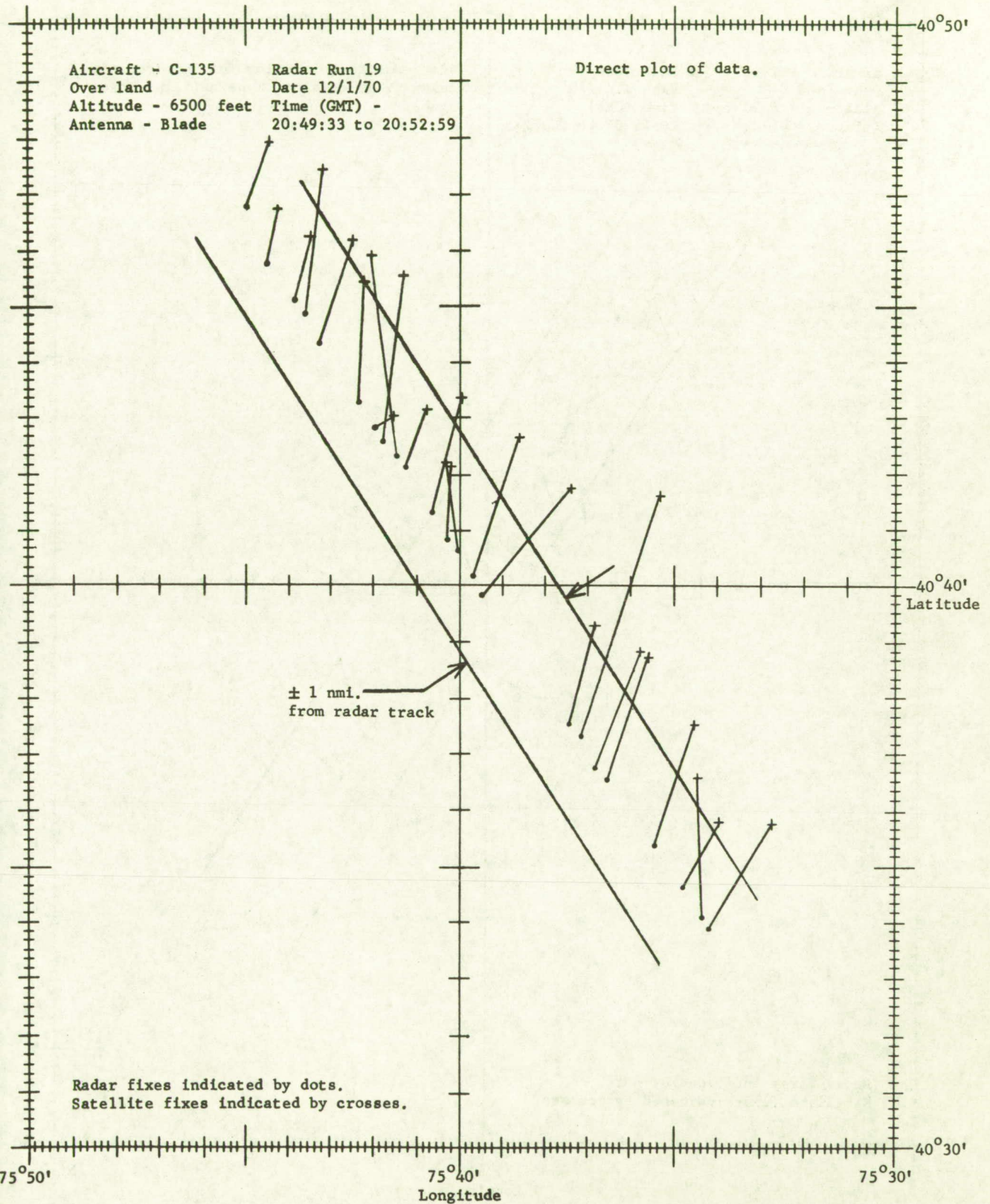


FIGURE 6-28

RADAR AND SATELLITE FIXES

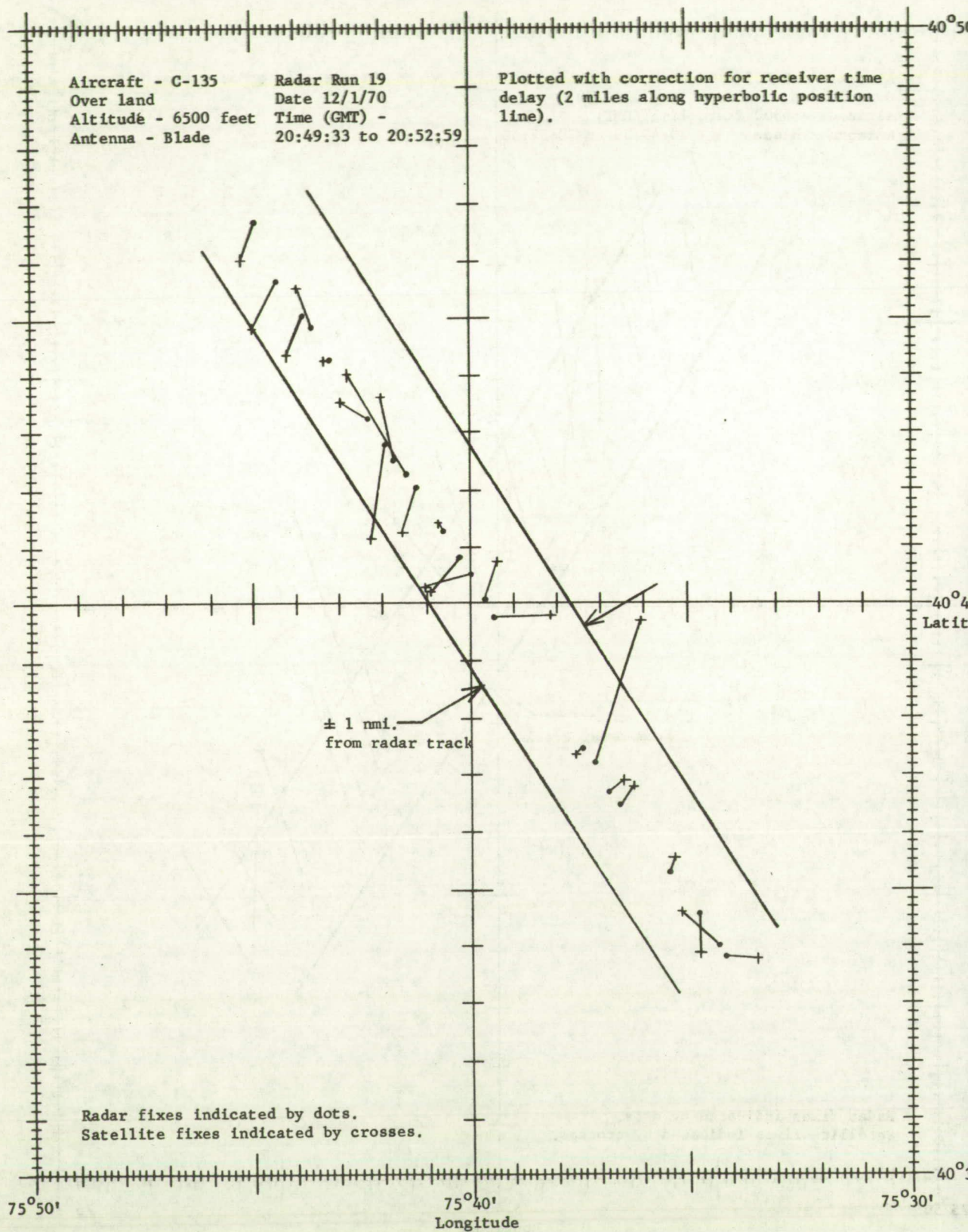
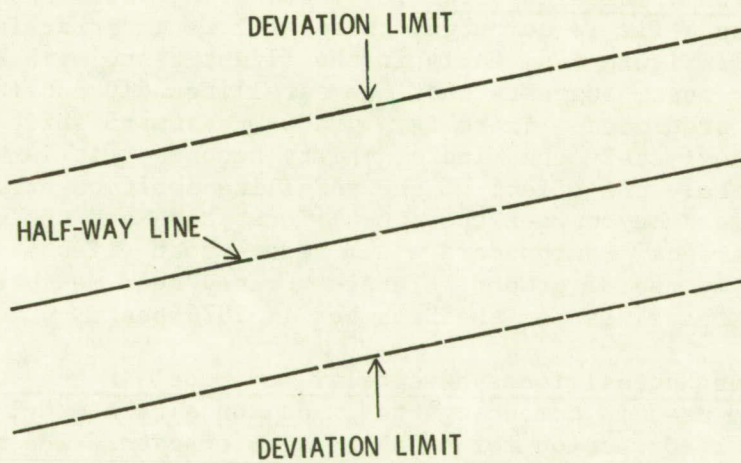
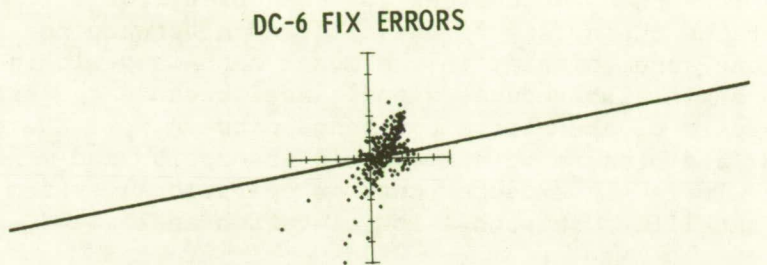


FIGURE 6-29

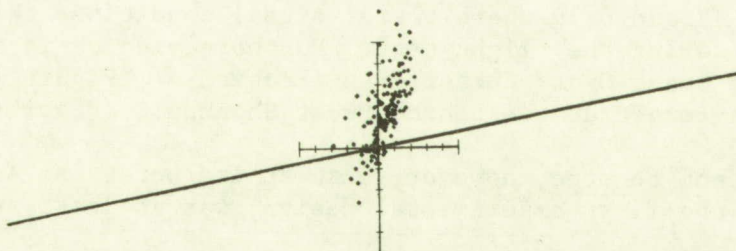
"WORST CASE" SATELLITE FIXES RELATIVE TO 60 nmi.
TRACK SEPARATION IN TRANSOCEANIC AIR TRAFFIC CONTROL

(Reference - National Academy of Sciences Summer Study
on the Useful Applications of Earth-Oriented Satellites - 1967/68)

* — Worst Error - 11 nmi.



C-135 FIX ERRORS



- Spin modulation of ATS-3. The effect is similar to ionosphere amplitude scintillation, except that it occurs at a higher average rate. During the test, it resulted in loss of interrogations, increased scatter of readings due to changing signal amplitudes, and may have been a contributing factor to the correlations on wrong bit periods. The spin modulation is an intermittent defect in the performance of the satellite. It is not expected in an operational satellite.

- Low elevation angle of ATS-1. ATS-1 was at zero degrees elevation angle for the aircraft, and less than two degrees for the Observatory. The low elevation angle exaggerates the effect of the difference between the actual ionosphere delay and the assumed delay in the model contained within the POSFIX program. The low angle also reduces signal level because the satellite is in an unfavorable part of the aircraft antenna pattern, off the peak of the satellite pattern, and because of atmospheric absorption and maximum range to the satellite. It is not expected that an operational system would routinely employ satellites at such a low elevation angle.

- Sea reflection multipath. Other contributions to error tend to obscure the multipath effects. Multipath contributes to the scatter of the fixes. Multipath can contribute larger errors than in the test, because jet aircraft fly at higher altitudes. Figure 6-29 includes low altitudes and over-land flights so that the plots do not represent a "worst case" for multipath. Multipath effects can be reduced by aircraft antenna designs and the use of circular polarization.

- Satellite position prediction errors. If the wrong positions are used for the satellites when a fix is computed, there will be an error in the position fix. Comparison of Figure 6-6, early in the flight test, with Figure 6-15, late in the flight test, suggests that the satellites did not follow their orbits exactly as predicted. There is a gradual eastward shift in the fix error bias of approximately one minute, thirty seconds. It is not possible to separate accurately the effect of the satellite position errors from the effect of the difference between the actual ionosphere and the model. The use of ground reference transponders would reduce both effects. The technique of correction by use of ground reference transponder measurements was not used in computing the fixes for the December 1, 1970 test.

- Difference between actual ionosphere delay and model in the POSFIX program. The POSFIX program used in computing the fixes contains a model for the ionosphere that gives a correction for each propagation path. The model and its use are described in Appendix II. The model may not describe the actual ionosphere delays at the time of the measurements, so that a ranging error results. The model may not describe the actual ionosphere delays at the time of the measurements, so that a ranging error results. The error can be reduced by the use of ground reference transponders.

Precision and accuracy can be much improved at VHF with the narrow bandwidth signal parameters used in the test. Evidence of this is contained in Figures 6-13, 6-15 and 6-19 where better signal conditions than the average were experienced during the flight test. Further evidence is the accuracy achieved with the Coast Guard Cutter Rush (Section 7, Figure 7-3), and the location of the aircraft at the benchmark at Shannon. (Page 6-53)

It is important to note, however, that at its worst the satellite ranging technique, using the first experimental design, was at least as accurate as

other non-satellite electronic or radio navigation aids now in use over the oceans, and the means to improve its precision and accuracy are clearly evident.

An examination of plots for individual radar runs and comparisons of plots for various radar runs reveal the magnitudes of specific contributions to position fix error. Identification of the causes of error and the magnitudes of their contributions defines the engineering changes that can be made to minimize the effects.

Severe spin modulation was experienced with ATS-3 throughout the flight test. The signal level dropped by 8 dB during a portion of each rotation of the satellite so that there was a signal drop-out on the signals into the aircraft occurring once each 0.6 second. The spin modulation fading pattern is shown in Figure 6-30. The interrogation rate was once each three seconds. It was not synchronized with the satellite spin modulation. As a result many interrogations were lost entirely because the address code was not received in the aircraft.

A portion of the tone was lost on some of the interrogations, so that the aircraft responder did not match its phase as accurately to the received tone phase as it would have without the spin modulation. The result of the incorrect phasing is that the aircraft response is a few microseconds early or late. It adds or subtracts a constant value to the range measurement from each of the two satellites. The difference in their values remains correct so that position fixes made under these circumstances are displaced along a hyperbolic line of position corresponding to the line of position measured by a range difference technique, similar to LORAN. The result is clearly evident in Figures 6-7 and 6-19. The hyperbolic position lines were constructed by connecting points that have a constant difference in range as the range measurements are projected onto the earth in the region of the user craft.

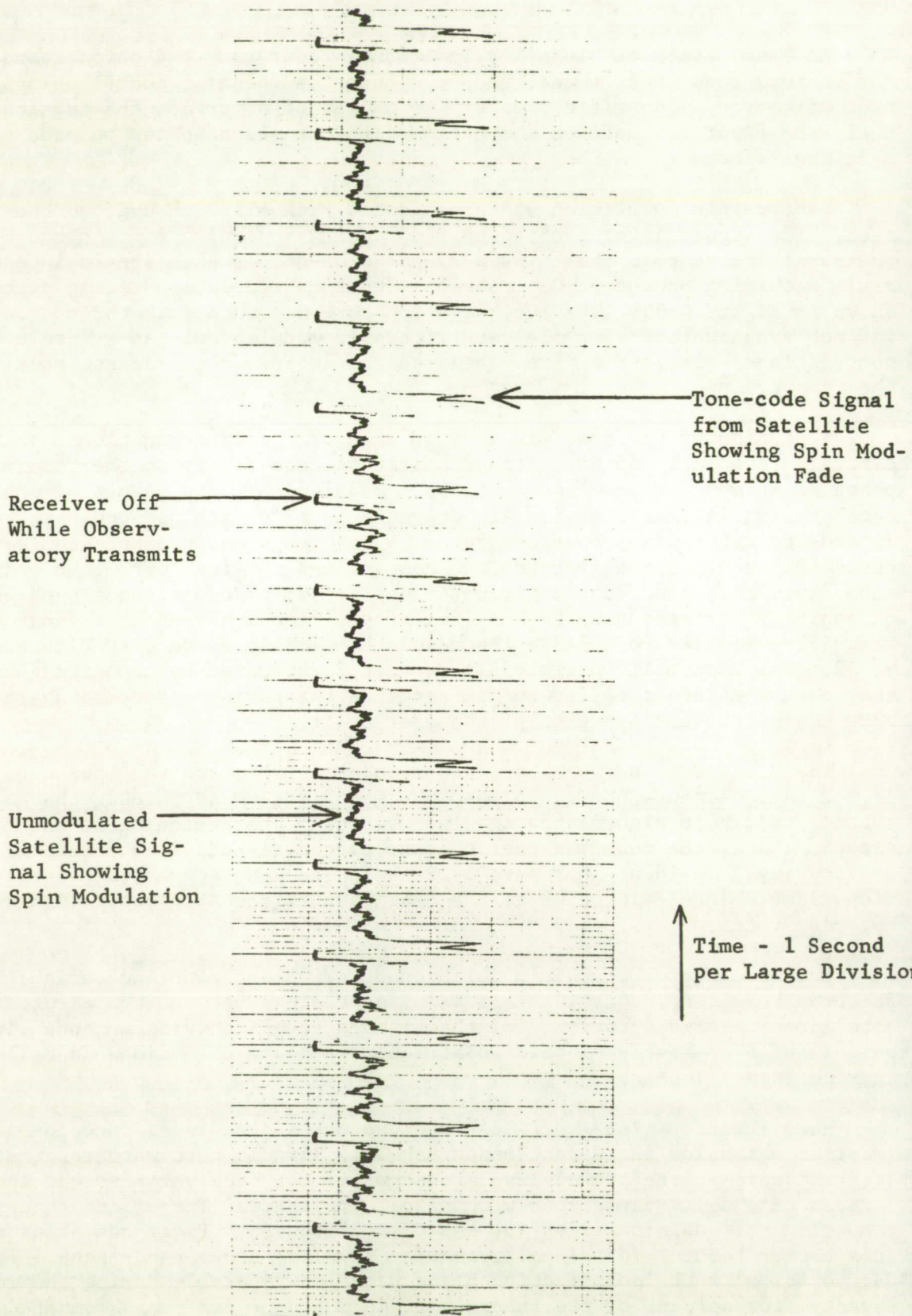
The difference between the spin modulation rate and the tone code interrogation rate caused a "beat" so that the spin fade moved through the tone-code signal. Early in Figure 6-30 the fade was near the beginning of the tone-code signal. Later the fade was near the end of the signal. The effect of "beat" on accuracy is evident in Figure 6-28 where the accuracy of the satellite position fixes changes with time at the beat rate of the spin modulation and interrogation rates.

The combination of spin modulation on ATS-3 and poor and variable antenna patterns resulted in unreliable transmission links between the aircraft and the satellites. Faraday rotation of the signals, combined with antenna linear polarization or highly elliptic polarization at some directions contributed further to signal losses.

Many interrogations were lost because the signal level into the aircraft receiver was below the detection threshold. Signals that were received in the aircraft were in the signal level range where the receivers exhibit their largest time delay variations with signal amplitude. The effect is evident by comparing the position fixes for the C-135 aircraft. Radar run 4 was evidently in a better heading for signal reception than the other radar runs. The Faraday rotation of the polarization plane was also favorable during the run. Seventy-four percent of the interrogations during radar run 4, compared with an overall average of forty-seven percent, resulted in two-satellite fixes,

FIGURE 6-30

SPIN MODULATION FADING PATTERN



suggesting a stronger average received signal level in the aircraft. The satellite fixes of radar run 4 are centered more closely with the radar fixes than in the other runs, although there are individual fixes displaced along the hyperbolic line of position. The displacements are probably due to the spin modulation. The fixes taken during the other runs are biased away from the radar fixes along the hyperbolic line of position in a direction suggesting that the weak signals experience a longer time delay through the RTA-41B receiver than the stronger signals. The displacement of the fixes indicates that the delay is increased by about 12 microseconds, a reasonable value for the RTA-41B receiver.

The time delay effect with signal amplitude change is less evident in the position fixes with the General Electric receiver-transmitter in the DC-6 because that receiver has a special limiter-discriminator designed to reduce the signal delay change with signal amplitude. (Page 4-3)

There is evidence of probable error in satellite position predictions in the plots of satellite positions referenced to the radar positions. The duration of the test was approximately 5.5 hours. An examination of the plots in Figures 6 through 15 shows a gradual eastward shift of the satellite position fixes relative to the radar fixes as time goes by. For example, the earliest plots of the DC-6 aircraft are centered about the radar positions but the last one, radar run 19, shows the satellite position fixes clustered about a point which is approximately one minute, thirty seconds east of the radar positions. This was the justification for replotting the data of Figure 6-25 into Figure 6-26.

The effects of multipath on position fix accuracy are not clearly separable from the other factors that cause scatter of the position fixes. Multipath effects are expected to be larger over sea than over land, and to be larger at high altitude rather than low altitude. (Section 5) It was for these reasons that the test was designed to include flights over water and over land, and at two altitudes. The effect of multipath on range measurements is expected to be about equal in magnitude on the link from the satellite to the aircraft and on the return links from the aircraft to the two satellites. Each of the contributions is independent of the others. The multipath contribution on the downlink from the satellite to the aircraft will affect the phasing of the transponder and contribute equally to the two return paths so that the contribution of multipath should tend to displace the fix along the hyperbolic line of position. However, the return paths from the aircraft to the satellite will be independent and displace the position lines for each of the two satellites in a random fashion. The presence of multipath should increase the scatter of the readings with some preference in the scatter along the line of position, but with a larger displacement of the scatter of the readings in directions which are independent of the azimuth angles to the satellite or to the hyperbolic position line. The amount of the scatter should be larger at high altitudes and larger over water than over land. A comparison of the plots for radar run 19 over land at ~6,000 feet, runs 13 through 18 over water at ~6,000 feet, runs 7 through 12 over land at 19,000 feet, and runs 1 through 4 over water at ~21,000 feet may reveal some evidence of the multipath effects but they cannot be quantified in the presence of the other effects that cause the scatter of the fixes. An upper bound on multipath effects can certainly be defined. It is obviously smaller than the sum of all the effects that cause scatter of position fixes.

It is possible to relate some individual position fix errors to the transmission link in which they occurred. For the DC-6 aircraft, radar runs 7 and 16 and for the C-135 aircraft, radar runs 4, 13 and 14 show a definite pattern of displacement of fixes along the hyperbolic line of position. These indicate that the signal path from the satellite to the aircraft was affected by spin modulation or other cause of low signal-to-noise ratio so that the transponder returned its signal a little early or a little late. The links through the two satellites to the Observatory were usually good during these runs so that the phase matcher-correlators at the Observatory performed with good precision. As a result, the same error was added to each of the range measurements and the position fix displaced on the hyperbolic line. For the DC-6 aircraft, radar run 10, there is a position fix approximately 3.5 miles displaced from the radar fix along the ATS-3 line of position. Its proximity to the ATS-3 line of position indicates that the aircraft responded properly, that the signal path back through ATS-3 was good, but that there was some error in the measurement of the phase at the Observatory on the return from ATS-1. There is a similarly displaced fix in radar run 16 of the DC-6.

There were 29 fixes with very large errors that are not plotted in Figures 6-6 through 6-24. The fixes were displaced along the hyperbolic line of position toward the satellites. Four were approximately 75 miles displaced, four approximately 150 miles displaced, three approximately 225 miles displaced, three approximately 300 miles displaced, and the remainder were displaced many hundreds or thousands of miles from the true position of the aircraft. Twenty-six of these fixes occurred with the equipment in the C-135 and three occurred with the equipment in the DC-6. The large errors occurred because the correlator correlated on the code early by a multiple of the bit periods in the code. One bit period, a period of the 2.4414 kHz cycle, is 409 microseconds. All of the improper correlations occurred before the time of the correct correlation, none later - so that all of the fix errors due to this cause are displaced along the hyperbolic line toward the satellite, none farther from the satellites than the true position.

The early correlations occurred because the detection threshold in the correlator was set too low. (Section 4) The adjustment was set too low to increase the number of responses to interrogations in spite of the poor signal-to-noise ratio due to the low antenna gain and the spin modulation fading. As a consequence, a noise pulse added to one of the side lobes of the correlator output would bring the correlator output above the decision threshold during a bit period prior to the one in which the correlation actually occurred. This is correctable by the design and adjustment of the equipments. Overall in the ranging and position fixing experiment, it was a rare occurrence. In a properly designed operational system with better signal-to-noise ratio and improved coding design, its occurrence would be negligible - a reasonable design expectation being once in 10^6 or 10^7 interrogations.

The use of a satellite surveillance system for traffic control is described in the National Academy of Sciences Summer Study Report, "Useful Applications of Earth Oriented Satellites", 1967-1968. Aircraft are assigned flight paths over the ocean, with the flight paths separated laterally by an assigned distance. Each aircraft flies according to its flight plane with its on-board navigation. Its position is monitored by the traffic control agency using the surveillance system. When an aircraft is observed to depart from its assigned flight path out to a deviation limit, the control agency instructs the aircraft to change its course so that it returns to its intended flight path. The

probability that an aircraft is displaced more than half-way to the next track is the product of two probabilities, that the aircraft deviated to the half-way line because of its faulty navigation and that the surveillance system failed to detect it.

Results of the five and one-half hour relative position experiment on December 1, 1970 are plotted in Figure 6-29 to suggest the ability of the experimental equipment to provide surveillance for maintaining a separation of sixty miles. The plots in Figure 6-29 are the superposition of Figures 6-6 through 6-24 for each of the two aircraft. All of the fixes are included, except those that are multiples of approximately seventy-five miles in error, resulting from correlation during wrong bit periods. The errors in the plots are caused by the "worst case" conditions described for Figures 6-6 through 6-24. The fix errors can be reduced to a fraction of their values by modest improvements in the satellite-to-aircraft link, in the aircraft equipment, and in the tracking of the satellites.

Although the position fix errors are larger than they would be in an operating system, even a narrow bandwidth VHF system, they appear to be adequate for maintaining aircraft separations much smaller than the present track assignments over the North Atlantic.

The accuracy of the position fixes in Figure 6-29 is at least equal to the accuracy specified by Boeing for an inertial navigation system at the end of a 5.5 hour flight. The Boeing specification states that the inertial navigation system shall not accumulate more than 2 nmi. error per flight hour on 95 percent of flights up to ten hours duration.

Figure 6-31 compares the accuracy of the DC-6 fixes with the Boeing specification for a 5 hour flight. The satellite fixes in Figure 6-31 include all "worst case" errors including satellite position bias errors. One DC-6 fix was 11 miles in error. A check of signal chart recordings in the aircraft and at the Observatory for that individual fix showed that it was affected by ATC interference in the aircraft, and by spin modulation of the satellite. It is the worst fix identified in the entire two and one-half year experiment, except for those that are caused by correlations early by an integral number of bit periods. Other fixes several miles in error are also found to be caused by factors that can be reduced by better signal levels on the down link or other engineering design changes.

The precision of the satellite fixes is poorer than the INS fixes, but the long term accuracy is better.

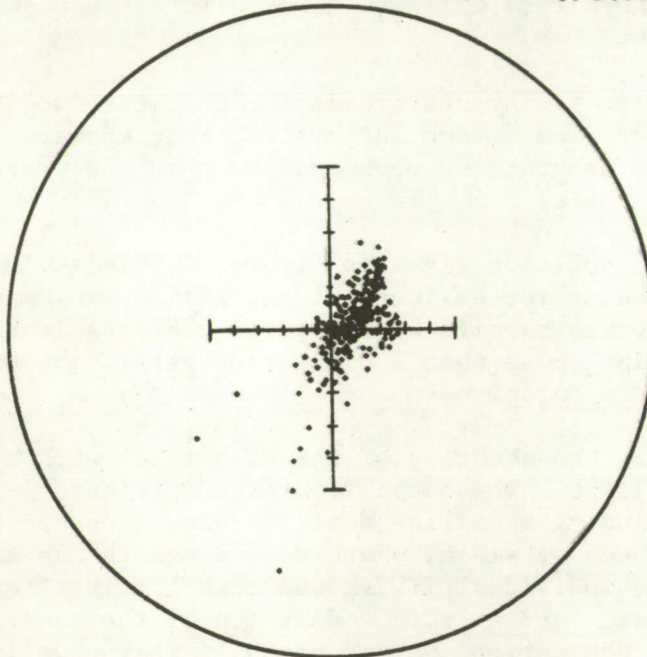
The results of the flight test are summarized in Tables 6-1 and 6-2. Information in the tables can be compared in various ways to reveal the effects of individual contributions to position fix error and other factors affecting the overall performance.

The transmission links to and from the aircraft were not sufficiently reliable for an operational system. The downlink from the ATS-3 interrogating satellite to the aircraft resulted in only 62 percent responses to interrogations by the DC-6 aircraft and 47 percent for the C-135. The downlink is the weakest transmission link and it was affected by the variability of the antenna patterns (Figures 6-1 and 6-2), by Faraday rotation because of the linear polarization of the satellite, by multipath reflections and by interfering signals

FIGURE 6-31

ACCURACY OF AIRCRAFT FIXES
5.5 HOUR FLIGHT
DC-6
'WORST CASE' CONDITIONS

• ← WORST ERROR - 11 nmi.



10 nmi. RADIUS CIRCLE

DC-6 AIRCRAFT

Radar Run Number	Number of Interrogations	Number of Aircraft Responses	Percent Aircraft Responses to Interrogations	Percent Interrogations Yielding Fixes	Number of Two Satellite Fixes	Number of Fixes Within 1 nmi.	Percent Fixes Within 1 nmi.	Number of Fixes Within 1 nmi. With Correction*	Percent Fixes Within 1 nmi. With Correction*	Antenna	Over (Land/Water)	Altitude (feet)
------------------	--------------------------	------------------------------	----------------------------------------------	---------------------------------------	-------------------------------	-------------------------------	-----------------------------	------------------------------------------------	----------------------------------------------	---------	-------------------	-----------------

1	73	54	74	23	17	11	65	12	71	Zenith	Water	21,300
2												
3												
4												
7	165	71	43	30	49	31	63	33	68	Horizon	Land	19,000
8	119	84	71	22	26	20	77	19	73	Zenith	Land	19,000
10	158	108	68	23	36	22	61	24	67	Zenith	Land	19,000
12	6	5			2	1		1			Land	19,000
13	203	131	65	26	53	29	55	39	74	Zenith	Water	6,000
14	184	98	53	18	33	15	45	27	82	Zenith	Water	6,000
16	208	141	68	37	76	14	17	38	50	Zenith	Water	6,000
17					1	1		1			Water	6,000
18												
19	94	51	54	43	40	7	18	37	92	Horizon, Blade	Land	6,000

Total	1210	743	62	27	333	151	46	231	70			
Overall												

*Correction for sum of uncertainties in ionosphere delay and satellite position. Between 15:45:00 and 21:00:00 GMT the assumed error changes linearly with time, one minute, thirty seconds along 70 degree track.

TABLE 6-2

C-135 AIRCRAFT

Radar Run Number	Number of Interrogations	Number of Aircraft Responses	Percent Aircraft Responses to Interrogations	Percent Interrogations Yielding Fixes	Number of Two Satellite Fixes	Number of Fixes Within 1 nmi.	Percent Fixes Within 1 nmi.	Number of Fixes Within 1 nmi. With Correction*	Percent Fixes Within 1 nmi. With Correction*	Antenna	Over (Land/Water)	Altitude (feet)
1	114	49	43	16	18	1	5	7	39	Blade	Water	21,600
2	160	66	41	4	6	0	0	0	0	Blade	Water	21,600
3	82	20	24	6	5	1	20	0	0	Blade	Water	21,600
4	137	101	74	36	49	36	72	34	70	Blade	Water	21,600
7												
8												
10												
12												
13	88	22	25	7	6	0	0	2	33	Blade	Water	6,500
14	179	80	45	19	33	2	6	22	66	Blade	Water	6,500
16												
17	23	11	48	17	4	0	0	3	75	Blade	Water	6,500
18	18	12	66	50	9	0	0	8	89	Blade	Water	6,500
19	86	57	66	46	40	2	5	31	77	Blade	Land	6,500
Total	887	418	47	19	170	42	25	107	63			
Overall												

*Correction for receiver time delay error, 12 microseconds or 2 nautical mile fix displacement along the hyperbolic line of position (except for radar run 4, no delay correction) plus correction for sum of uncertainties in ionosphere delay and satellite position. Between 15:45:00 and 21:00:00 GMT the assumed error changes linearly with time, one minute, thirty seconds along 70 degree track.

within the passband of the aircraft receivers, especially the C-135 aircraft receiver which had a 40 kHz bandwidth making it subject to interference from air traffic control communications on channels adjacent to the satellite downlink. Throughout the test the satellite signals received by the aircraft varied above and below the FM detection threshold, and were never strong.

The data reflects the expected characteristics of the Dorne and Margolin and blade antennas. The zenith mode of the Dorne and Margolin antenna provided the best downlink performance from the ATS-3 interrogating satellite which was at an elevation angle of 32° . When the azimuth mode was used, the aircraft responded to approximately 70 percent of the interrogations; with the horizon mode the response rate was approximately 50 percent; and for the blade antenna on the C-135, it was 47 percent. The zenith mode did not transmit well to ATS-1 which was at 0° elevation so that when the zenith mode was used about one-fourth of the interrogations were successfully relayed through both satellites and received at the Observatory to provide a two-satellite position fix. Although the horizon mode antenna did not respond as reliably to the interrogations from ATS-3, more than 30 percent of the interrogations were relayed back through both satellites to yield two-satellite position fixes, a higher percentage yield than the zenith antenna. The blade antenna on the C-135 aircraft yielded two-satellite fixes on 19 percent of the interrogations.

An examination of Figures 6-6 through 6-24 shows an eastward shift of the position fixes as a function of time during the 5.5 hour flight test. It is clearly evident in the columns headed "Percent Fixes Within 1 nmi." in Tables 6-1 and 6-2 that the percentage drops noticeably for radar runs 13 and 14 and takes a very sharp drop for radar runs 16 and 19.

A close examination of the runs for the DC-6, Figures 6-6 through 6-15, suggested that the fixes shifted along a track at 70 degrees and by a distance equal to one minute, thirty seconds during the 5.5 hour period. The shift was assumed to be linear with time. The position fixes for each plot were shifted approximately for the time of the plot and the number of fixes within a one nautical mile radius circle were determined for each radar run, and the percentage of the fixes was recomputed. As shown in the columns "Percent Fixes Within 1 nmi. With Correction" there was no significant change in the percentage when the correction had been made. With these corrections, 70 percent of the DC-6 fixes were within one nautical mile.

An additional correction was assumed for the C-135 fixes. A comparison of radar run 4 with the other radar runs for the C-135 shows that run 4 fixes are clustered about the radar reference position, whereas the fixes for all of the other runs appear to be displaced along the hyperbolic line of position in a direction away from the satellites. An examination of the link performance for run 4 compared with the others showed that the signal levels into the aircraft were stronger, on the average, for that run. Seventy-four percent of the interrogations resulted in aircraft responses whereas the response rate was much lower for most of the other runs. A probable explanation is higher gain for the aircraft antenna in the direction of the satellite during that run, combined with more favorable Faraday rotation angle. The RTA-41B receiver used in the C-135 aircraft is subject to receiver time delay change with signal amplitude and is especially sensitive in this respect when operating with weak signals. A typical value for receivers of this type is 10-15 microseconds change in receiver time delay between a signal at the detection threshold and one that is five or 10 dB above the detection threshold. This characteristic

has been measured in General Electric receivers before the installation of the special limiter discriminator as was used in the DC-6 aircraft.

The fixes for the C-135 were re-evaluated with two corrections for the reference position. One correction applied to all of the radar runs was the same as the one applied to the DC-6 aircraft. In addition for all runs except run 4, the position reference was shifted two miles along the hyperbolic line of position. Two miles is the distance that would result in this geometry for a 12 microsecond change in receiver time delay.

A shift in the position reference must have a justification beyond fitting the data. It is shown in Section 5, Figures 5-1 and 5-2, that satellite prediction errors can produce line of position errors and fix errors larger than a nautical mile. It is also shown that these errors have a diurnal variation. The magnitude of the error is further increased if the equipment time delay calibration was made when the satellite position prediction was in error. (Page 5-6)

A further contribution to the shift in the position fixes during the period would be a change in ionosphere propagation delay that is different than the predicted change in propagation delay.

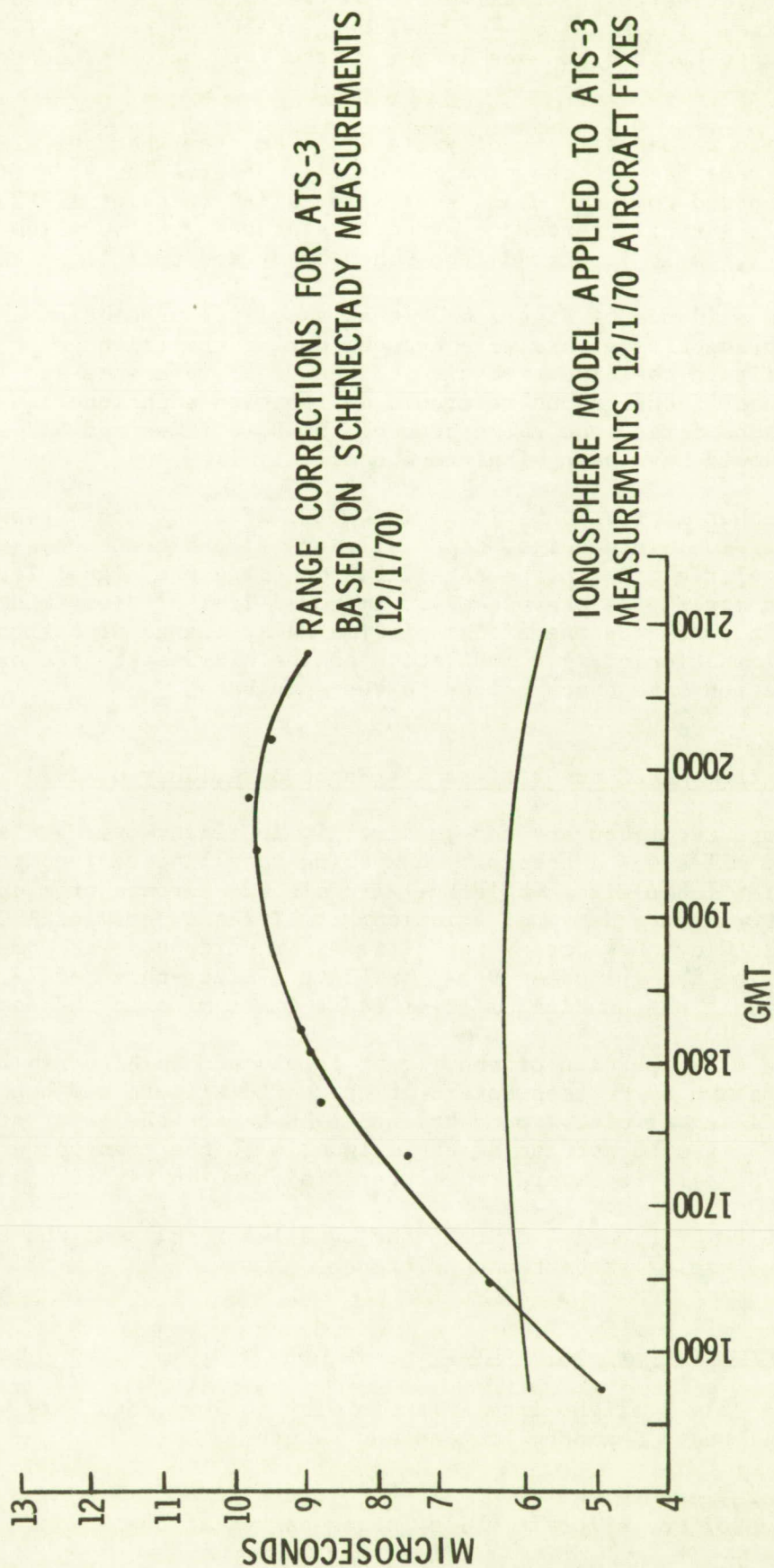
Although it can be shown that satellite prediction errors and an incorrect estimate of the ionosphere propagation delay could shift the fixes by the magnitude observed in the test, it is further necessary to show that these conditions may have existed during the test. Figure 6-32 is a plot of the difference between the measured and computed slant ranges from ATS-3 to Schenectady during the test. Schenectady is close enough to the flight test area so that corrections for the satellite position error and the ionosphere as measured at Schenectady would be valid for the test area.

The difference between the measured and computed slant ranges represents the sum of the effects of satellite position error and ionosphere propagation delay on the range measurement from ATS-3 to Schenectady and to the aircraft. Also shown in Figure 6-32 is the correction for the ionosphere propagation delay that was actually applied to the position fixes. It is derived from the model which is a part of the POSFIX computer program. The differences between the measured and computed slant ranges is the correction that should be applied and would be applied if Schenectady were used as the ground reference calibration for the fix measurements. The measurement was not applied in the program because it was not written to accommodate that type of correction and because there was no similar correction available for ATS-1.

The difference between the two curves represents the residual error in the range measurement resulting from the error in satellite position and the error in estimating ionosphere delay. The model and the measured correction agree near the beginning of the flight test where the position fixes also agree with the radar position fixes. As time advanced through the test, the difference between the proper correction curve and the one actually used in the POSFIX program increased until they differed by approximately 4 microseconds. The correction derived from the Schenectady measurements is larger than the correction applied in the POSFIX program. If the Schenectady measurement had been used as a correction, the range from the assumed position of the satellite would have been reduced by approximately 4 microseconds causing the position fixes to be moved towards the satellite ATS-3 by about 2500 feet. This is in

FIGURE 6-32

COMPARISON OF IONOSPHERE MODEL AND MEASURED RANGE CORRECTIONS



the proper direction and about the right magnitude to correct for the observed shift relative to the radar position reference in the direction of the ATS-3 satellite. The magnitude of the change relative to the ATS-1 azimuth direction suggests that an even larger correction would be necessary for the ATS-1 satellite.

While no data are readily available to show what the ATS-1 correction should have been at the time, we usually observe larger differences between measured and computed slant ranges for ATS-1 than for ATS-3. We attribute these larger differences to effects related to the very low elevation angle of ATS-1, as it is viewed from Schenectady and the flight test area.

The evidence of Figure 6-32 that satellite prediction and/or ionosphere delay prediction errors were present during the flight test appears to justify the shift in the fixes relative to the radar reference and lead to the conclusion that if the ground reference calibration technique had been used in computing the fixes that 70 percent of the DC-6 fixes and 63 percent of the C-135 fixes would have been within one nautical mile.

Further improvements in position fix accuracy would result from better transmission link design, especially the aircraft antennas and the use of circular polarization on the satellites to bring the signal levels above the detection threshold, the use of an improved limiter-discriminator in the C-135 aircraft to reduce the effect of time delay change with signal amplitude and the elimination of spin modulation on the ATS-3 satellite or the use of interrogation rate synchronized to the spin rate.

Flight from NAFEC to Griffiss Air Force Base, July 6, 1970

Short-term accuracy for an aircraft in flight over a distance of a few hundred miles was assessed by comparing satellite derived position fixes with precision radar fixes while the aircraft was enroute from the Federal Aviation Administration's National Aviation Facilities Experimental Center (NAFEC) at Atlantic City, New Jersey to Griffiss Air Force Base at Rome, New York, and then on to the ground at Rome, New York. Sixty-three of 79 satellite fixes were within one nautical mile of radar fixes made at the same time.

The first portion of the flight is plotted in Figure 6-32. The satellite fixes, shown by crosses, start at the NAFEC airport and continue as the aircraft took off and circled around to the right before the radar started tracking the plane. A second portion of the flight, with the transponder employing the Bendix RTA-41B receiver-transmitter, is shown in Figure 6-33.

Tables 6-3 and 6-4 contain the detailed results of the test and the notes with the tables state the conditions.

Long-Term Trans-Ocean Accuracy

The July 6 flight from Atlantic City to Rome, New York was the first leg of a flight to Shannon, Ireland and return.

Range measurements from ATS-3 to the aircraft were used to determine the latitude of the aircraft while it was parked at the Shannon airport. A time

TABLE 6-3

FAA DC-6B ENROUTE FROM NAFEC, ATLANTIC CITY, NEW JERSEY
TO GRIFFISS AIR FORCE BASE, ROME, NEW YORK

<u>TIME-GMT</u>	<u>POSITION FIX, RANGING FROM ATS-3 AND ATS-1 **</u>	<u>POSITION FIX BY EAIR PRECISION RADAR, NAFEC</u>	<u>POSITION FIX ERROR NAUTICAL MILES</u>
14 13 12	39°21'12" 74 38 48	39°20'43" 74 39 21	0.6
14 13 15	39 19 55 74 39 48	39 20 40 74 39 30	0.8
14 13 45	39 20 12 74 40 59	39 20 10 74 41 4	0.1
14 14 18	39 19 36 74 44 6	39 19 44 74 42 51	0.9
14 15 24	39 19 7 74 48 48	39 19 37 74 46 30	1.7
14 16 00	39 20 53 74 46 54	39 19 56 74 48 25	1.5
14 16 36	39 20 33 74 49 29	39 20 44 74 50 8	0.5
14 17 03	39 21 38 74 51 43	39 21 21 74 51 25	0.3
14 17 09	39 21 32 74 51 10	39 21 29 74 51 42	0.4
14 17 36	39 22 6 74 52 58	39 22 6 74 52 56	0 (See Note 4)
14 17 42	39 22 4 74 53 45	39 22 14 74 53 13	0.4
14 18 48	39 23 27 74 56 14	39 23 41 74 56 19	0.2
14 19 48	39 24 13 75 0 3	39 24 59 74 59 10	1.0
14 19 54	39 25 39 74 58 46	39 25 7 74 59 28	0.9
14 20 27	39 25 11 75 2 23	39 25 49 75 1 4	1.1
14 21 30	39 27 27 75 2 54	39 27 11 75 4 11	0.8
14 24 45	39 30 37 75 14 32	39 31 19 75 14 3	0.8
14 30 30	39 44 40 75 24 48	39 44 27 75 24 21	0.4
14 30 33	39 44 46 75 24 23	39 44 35 75 24 23	0.2

(See Note 2)

**See Note 1

TABLE 6-3 continued

<u>TIME-GMT</u>	<u>POSITION FIX, RANGING FROM ATS-3 AND ATS-1 **</u>	<u>POSITION FIX BY EAIR PRECISION RADAR, NAFEC</u>	<u>POSITION FIX ERRO NAUTICAL MILES</u>
14 30 36	39°44' 39" 75 25 2	39°44' 43" 75 24 25	0.4
14 30 39	39 43 58 75 25 8	39 44 52 75 24 27	1.0
14 31 03	39 46 9 75 25 0	39 46 2 75 24 47	0.2
14 31 06	39 45 56 75 24 59	39 46 11 75 24 49	0.3
14 31 09	39 46 29 75 25 45	39 46 20 75 24 52	0.7
14 31 12	39 45 53 75 25 51	39 46 29 75 24 54	0.9
14 31 36	39 47 29 75 25 41	39 47 44 75 25 16	0.4
14 31 39	39 47 43 75 25 44	39 47 54 75 25 17	0.4
14 31 42	39 47 46 75 25 10	39 48 4 75 25 19	0.2
14 31 45	39 47 53 75 25 18	39 48 13 75 25 22	0.5
14 32 09	39 48 10 75 26 15	39 49 32 75 25 44	1.4
14 32 15	39 50 6 75 26 14	39 49 53 75 25 49	0.3
14 32 42	39 50 32 75 27 3	39 51 25 75 26 13	1.0
14 32 45	39 50 51 75 26 55	39 51 35 75 26 16	0.9
14 32 48	39 50 56 75 27 3	39 51 45 75 26 20	1.0
14 32 51	39 51 38 75 26 36	39 51 54 75 26 23	0.8
14 33 48	39 55 10 75 27 19	39 55 9 75 27 18	0
14 33 51	39 55 18 75 27 41	39 55 19 75 27 21	0.2
14 33 54	39 55 26 75 27 30	39 55 29 75 27 25	0.1
14 34 24	39 56 39 75 28 41	39 57 15 75 27 50	0.8
14 38 19	40 10 35 75 34 37	40 10 34 75 32 34	1.2

(See Note 2)

**See Note 1

TABLE 6-3 continued

<u>TIME-GMT</u>	<u>POSITION FIX, RANGING FROM ATS-3 AND ATS-1 **</u>	<u>POSITION FIX BY EAIR PRECISION RADAR, NAFEC</u>	<u>POSITION FIX ERROR NAUTICAL MILES</u>
14 38 31	40°10' 48" 75 33 2	40°11' 14" 75 32 54	0.4
14 38 40	40 11 53 75 33 27	40 11 43 75 33 7	0.3
14 39 22	40 14 27 75 34 15	40 13 58 75 34 15	0.4
14 39 25	40 14 45 75 35 57	40 14 9 75 34 18	1.3
14 39 58	40 17 53 75 33 45	40 15 55 75 35 11	2.3
14 40 01	40 19 57 75 38 49	40 16 6 75 35 14	4.8
14 40 04	40 17 22 75 34 12	40 16 16 75 35 17	1.4
14 40 07	40 15 34 75 34 51	40 16 24 75 35 24	0.9
14 40 13	40 17 2 75 34 17	40 16 44 75 35 32	1.0
14 40 16	40 17 19 75 37 31	40 16 55 75 35 36	1.4
14 40 22	40 17 12 75 35 13	40 17 14 75 35 45	0.4
14 40 28	40 16 38 75 35 13	40 17 31 75 35 57	1.0
14 40 34	40 17 17 75 38 58	40 17 51 75 36 6	2.1
14 41 22	40 20 14 75 35 38	40 20 29 75 37 11	1.2
14 41 25	40 20 7 75 36 42	40 20 40 75 37 14	0.7
14 41 34	40 21 25 75 36 35	40 21 10 75 37 26	0.6
14 41 40	40 21 41 75 36 43	40 21 30 75 37 33	0.6
14 41 43	40 21 59 75 36 37	40 21 40 75 37 36	0.8
14 41 55	40 22 15 75 38 0	40 22 19 75 37 52	0.1
14 42 04	40 21 53 75 38 28	40 22 49 75 38 3	1.0
14 42 10	40 22 46 75 38 54	40 23 9 75 38 10	0.7

(See Note 3)

**See Note 1

TABLE 6-3 continued

TIME-GMT	POSITION FIX, RANGING FROM ATS-3 AND ATS-1 **	POSITION FIX BY EAIR PRECISION RADAR, NAFEC	POSITION FIX ERROR NAUTICAL MILES
14 42 19	40°23'26" 75 37 52	40°23'37" 75 38 23	0.4
14 42 52	40 25 13 75 38 59	40 25 26 75 39 7	0.2
14 43 04	40 25 54 75 38 56	40 26 6 75 39 21	0.4
14 43 40	40 28 19 75 40 19	40 28 3 75 40 8	0.3
14 43 43	40 27 50 75 39 14	40 28 13 75 40 12	0.8
14 43 46	40 28 16 75 40 55	40 28 22 75 40 18	0.5
14 43 49	40 28 21 75 40 49	40 28 32 75 40 19	0.4
14 43 52	40 28 42 75 40 3	40 28 41 75 40 25	0.3
14 43 58	40 28 22 75 40 14	40 29 2 75 40 31	0.6
14 44 10	40 30 1 75 41 4	40 29 40 75 40 47	0.3
14 44 25	40 30 30 75 41 53	40 30 30 75 41 7	0.5
14 44 37	40 30 13 75 42 53	40 31 10 75 41 22	1.5
14 48 33	40 44 41 75 42 39	40 44 27 75 43 56	0.9
14 59 10	41 19 53 75 39 18	41 19 44 75 38 51	0.4
14 59 13	41 21 5 75 38 55	41 19 57 75 38 36	1.2
14 59 46	41 22 42 75 39 7	41 21 54 75 38 6	1.0
14 59 52	41 22 58 75 39 19	41 22 15 75 38 7	1.1
15 01 22	41 28 35 75 40 8	41 27 17 75 39 4	1.5

**See Note 1

Note 1. ATS-1 was below 2° elevation to the aircraft and Observatory.

Note 2. Transponder with GE receiver-transmitter with special limiter discriminator

Note 3. Transponder with RTA-41B receiver-transmitter

Note 4. GE receiver-transmitter time delay calibration according to this radar fix.

Note 5. RTA-41B receiver-transmitter time delays calibrated according to these radar fixes.

TABLE 6-4

FAA DC-6B ON TAXIWAY AT GRIFFISS AIR FORCE BASE, ROME, NEW YORK
July 6, 1970

<u>TIME-GMT</u>	<u>POSITION FIX, RANGING FROM ATS-3 AND ATS-1</u> (See Note 1)	<u>LOCATION OF TOWER AT GRIFFISS AIR FORCE BASE</u> (See Note 2)	<u>DISTANCE FROM TOWER</u> (Feet)
15 55 56	43°13'26" 75 23 28	43°13'37"N 75 24 24 W	4000 ESE
15 56 10	43 13 20 75 24 01	(See Note 3)	2400 SE
15 56 28	43 12 42 75 24 04		5400 SSE
15 56 46	43 13 21 75 24 02		2400 SE
15 56 55	43 12 50 75 24 15		4900 SSE

Note 1. GE transmitter-receiver used. Receiver-transmitter time delay calibration made near NAFEC referenced to a radar fix. See Note 2, Table 6-3.

Note 2. Information furnished by Griffiss Air Force Base.

Note 3. Aircraft was on taxiway approximately 3500 feet southeast of tower.

FIGURE 6-33

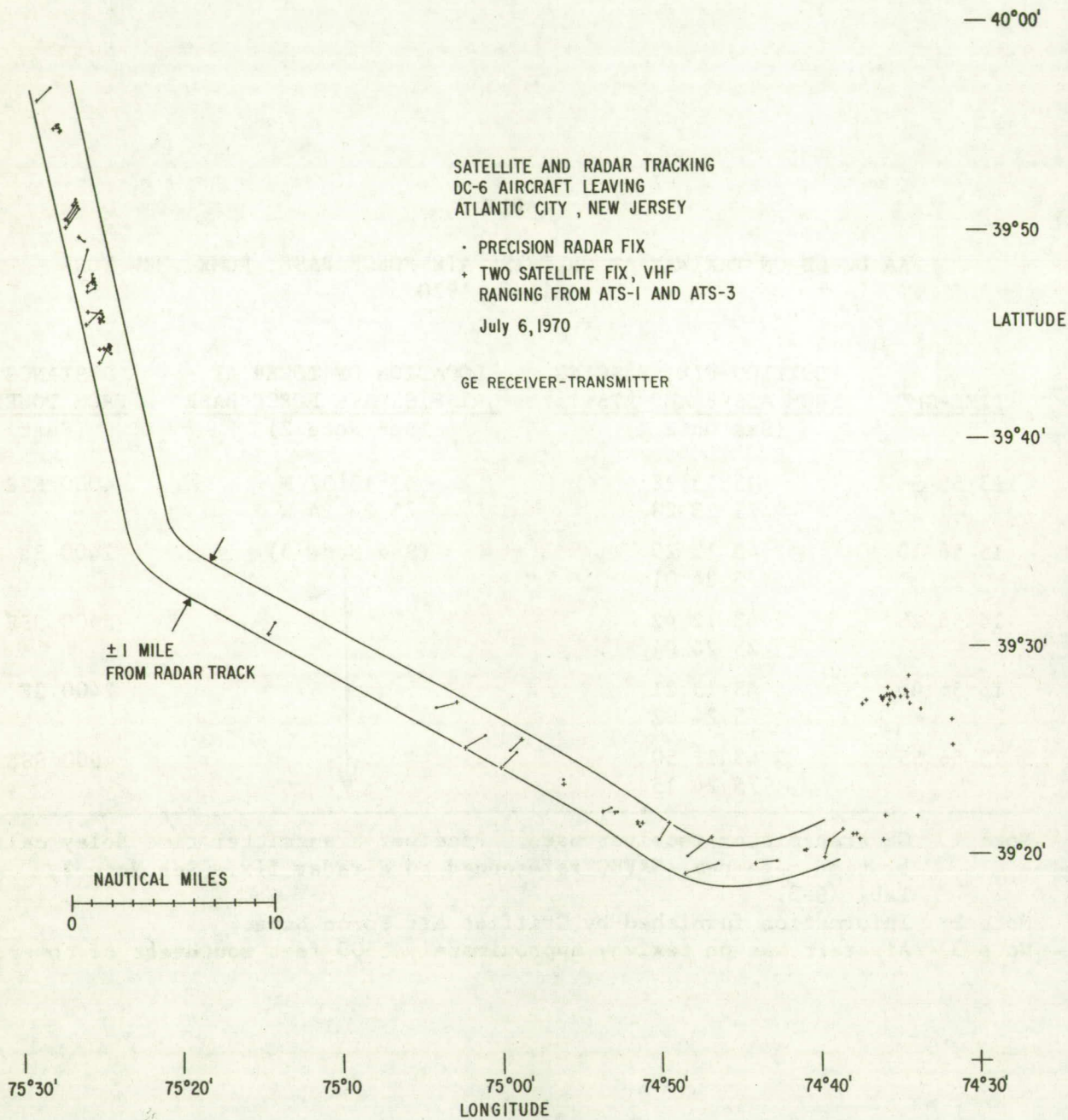
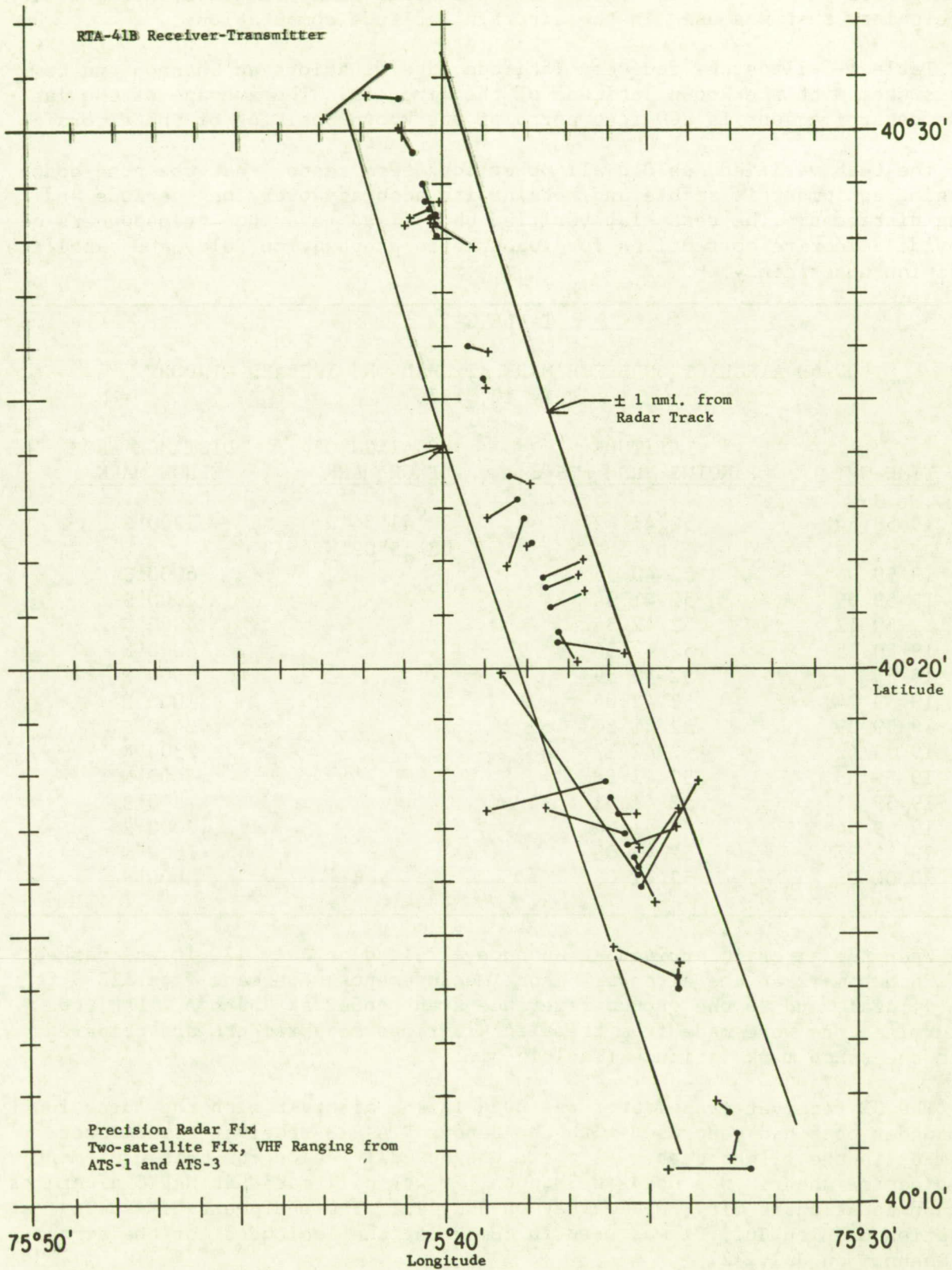


FIGURE 6-34

SATELLITE AND RADAR TRACKING DC-6 AIRCRAFT

7/6/70



delay calibration made at Atlantic City nine days different in time was used in computing the latitude determinations so that they truly represented the long-term stability of the aircraft equipment. Range measurements from ATS-3 to the ground reference transponder at Shannon were made in the same time period as the range measurements to the aircraft. The measurements to the reference transponder yielded a correction for ionospheric delay and satellite position uncertainty that was used in the aircraft latitude computations.

Table 6-5 lists the fourteen latitude determinations at Shannon and compares them with the known latitude of the aircraft. The average of the latitude determinations is 800 feet north of the known position of the aircraft.

The test verified, as did all other long term tests, that the tone-code ranging equipment is stable and retains its accuracy over long periods and long distances. The test also verified that fixed reference transponders can provide effective corrections for ionospheric propagation delay and satellite position uncertainty.

TABLE 6-5

DC-6B AIRCRAFT ON BENCH MARK AT SHANNON, IRELAND AIRPORT
July 12, 1970

<u>TIME-GMT</u>	<u>LATITUDE RANGING FROM ATS-3</u>	<u>LOCATION OF BENCH MARK</u>	<u>DISTANCE FROM BENCH MARK</u>
19 58 54	52°41'42"	52°41'54"N 08°55'02"W	1200'S
19 59 06	52 40 55		6000'S
19 59 09	52 41 34		2000'S
19 59 12	52 42 34		4000'N
19 59 15	52 42 34		4000'N
19 59 21	52 42 59		6600'N
19 59 24	52 42 04		1000'N
19 59 39	52 41 30		2400'S
19 59 42	52 42 17		2300'N
19 59 45	52 42 38		4400'N
19 59 51	52 41 51		300'S
19 59 54	52 41 34		2000'S
19 59 57	52 43 08		7500'N
20 00 06	52 41 08		4600'S

When the aircraft arrived at Shannon, Ireland on July 12, it was parked at a bench mark at the airport. Range measurements were made from ATS-3 to the aircraft and to the ground reference transponder at Shannon. Latitude determinations were made from the aircraft range measurements and compared with the bench mark latitude (Table 6-5).

The GE receiver-transmitter was used in the aircraft with the "user four" responder that had been used with the Bendix RTA-41B receiver-transmitter earlier in the flight test. As there was no calibration for that equipment combination when it was used at Shannon, it was calibrated at NAFEC after its return to Atlantic City, New Jersey on July 21. The equipment time delay calibration made on July 21 was used in computing the latitudes for the aircraft at Shannon on July 12.

The equipment calibration was made with the aircraft at the bench mark at NAFEC by the following procedure:

1. Range measurements were made between ATS-3 and the aircraft, and between the satellite and the Radio-Optical Observatory at Schenectady.
2. The computed slant range to Schenectady was subtracted from the measured slant range to yield a correction for ionospheric delay and satellite prediction uncertainty. For that test, the correction was 4.3 microseconds.
3. The 4.3 microseconds were subtracted from the range measurements between the satellite and the aircraft.
4. The LATCOM program was used to compute the latitude of the aircraft at NAFEC with the corrected range measurement.
5. The term in the LATCOM program that represents the aircraft transponder equipment time delay was adjusted so that the computed latitude agreed with the known latitude of the aircraft at the bench mark. The adjusted value was then the correct value for the transponder equipment time delay, and is the value used in all computations of aircraft latitudes when the GE receiver-transmitter was used with the "user four" responder at Shannon.

Latitude determinations were processed for the July 12 range measurements to the aircraft at the Shannon bench mark. The following procedure was used:

1. Three range measurements from ATS-3 to the Shannon ground reference transponder were averaged. The measurements were made within one minute of the aircraft range measurements. The computed slant range from the satellite was subtracted from the average of the measured slant ranges to yield a 7.2 microsecond correction for the ionosphere and satellite prediction error.
2. The 7.2 microsecond correction was subtracted from each of the fourteen range measurements from ATS-3 to the aircraft, and the LATCOM program used to compute the latitude of the aircraft at Shannon.

This procedure resulted in latitude determinations using an equipment time delay calibration made on the other side of the ocean and nine days difference in time, and using corrections for the ionosphere delay and satellite prediction error made close to the aircraft and at the same time as the aircraft range measurements.

The latitudes determined from the LATCOM program are the crossing of lines of position with the known longitude of the craft. Look angles to the satellite from Shannon were approximately 243° azimuth and 09° elevation. There is a considerable geometrical dilution in the latitude determinations.

Long Term Accuracy - January 11-23, 1971

The DC-6 aircraft of the Federal Aviation Administration left the National Aviation Facilities Experimental Center (NAFEC) on January 11, 1971, enroute to Thule, Greenland for the twenty-four hour synoptic test described in Section 11. The aircraft returned to NAFEC on January 23, 1971. Comparison of the satellite and radar fixes for those two days provides information on the long term accuracy of the transponder that employed the transceiver.

The aircraft was tracked by the EAIR Precision Radar on its departure and on its return. The radar tracks and altitudes of the aircraft are shown in Figures 6-34 and 6-35. The aircraft was also tracked by two-satellite ranging using the RTA-41B transponder. After its return it was parked on the bench mark at NAFEC and the equipment time delay calibrated. The same equipment time delay calibration was used for computing the fixes made while the aircraft departed from NAFEC on January 11, 1971 and when it returned to NAFEC on January 23, 1971. Figures 6-36 through 6-42 show the differences between the radar fixes and the satellite fixes while the aircraft was departing from NAFEC and for various portions of the flight path as the aircraft descended and landed at NAFEC when it returned.

The differences between the precision radar and the satellite fixes as the aircraft departed are plotted in Figure 6-36. Signal levels from the satellite to the aircraft were poor, contributing to the large scatter of the position fixes. The IF bandwidth of the RTA-41B receiver is approximately 40 kHz. During the test periods the downlink frequency was 135.575 kHz. The bandwidth of the receiver is such that it received almost continuous interference from air-to-ground communications on ATC channels centered 25 kHz above and 25 kHz below the satellite downlink frequency. These interfering signals can contribute to phasing errors and thus a degradation in the accuracy of position fixes when that transceiver is used.

Figures 6-37 through 6-42 trace the accuracy of the position fixes as the aircraft returned on January 23, 1971, descended and landed at NAFEC. The scatter of the satellite fixes and their displacement to the northward of the radar fixes and their tendency to be displaced in a direction away from the satellites along the hyperbolic line of position are similar in characteristic to the performance of the same equipment during the 5.5 hour flight test when the relative positions of the DC-6 and C-135 were measured on December 1, 1970.

During December 1 tests the RTA-41B equipment was carried in the C-135 aircraft and used with the blade antenna. On January 11 and 23 it was in the DC-6 aircraft and the blade antenna and Dorne & Margolin antenna were both available for its use.

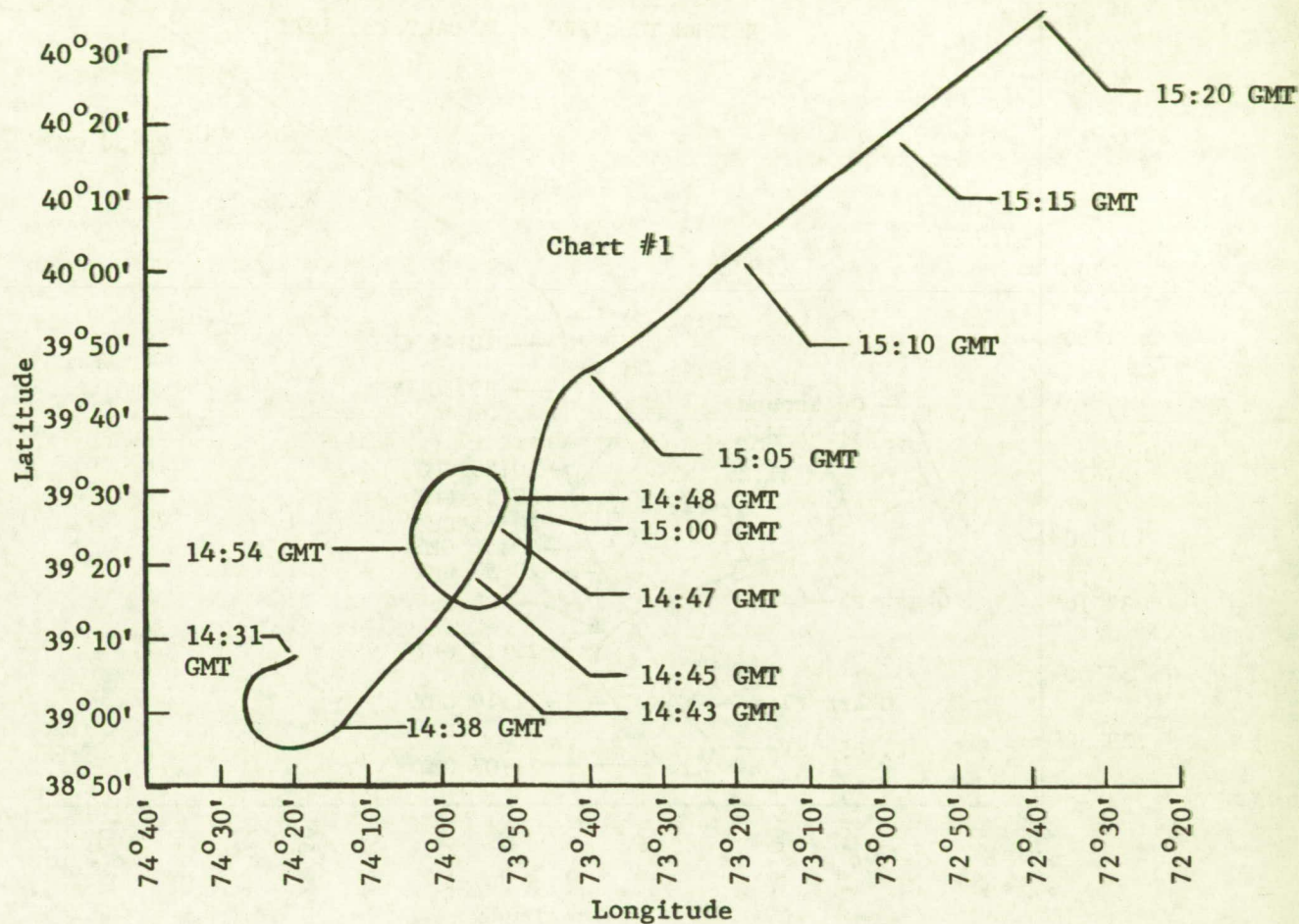
The largest contribution to the northward displacement and the scatter of the fixes is believed due to the low average signal level into the aircraft which places the signal level in that portion of the receiver amplitude characteristic where the receiver time delay is greater than at larger signal amplitudes. Multipath and interfering signals from other aircraft and ground stations may also be contributing factors.

An important difference between the January 11 and 23 tests as compared with the December 1 tests is that the interrogation rate in the January tests was synchronized with the spin rate of the ATS-3 satellite so that spin modulation effects were not significant. The phasing of the interrogations was adjusted so that the signals to the aircraft and from the aircraft were relayed through the satellite between the spin modulation fades.

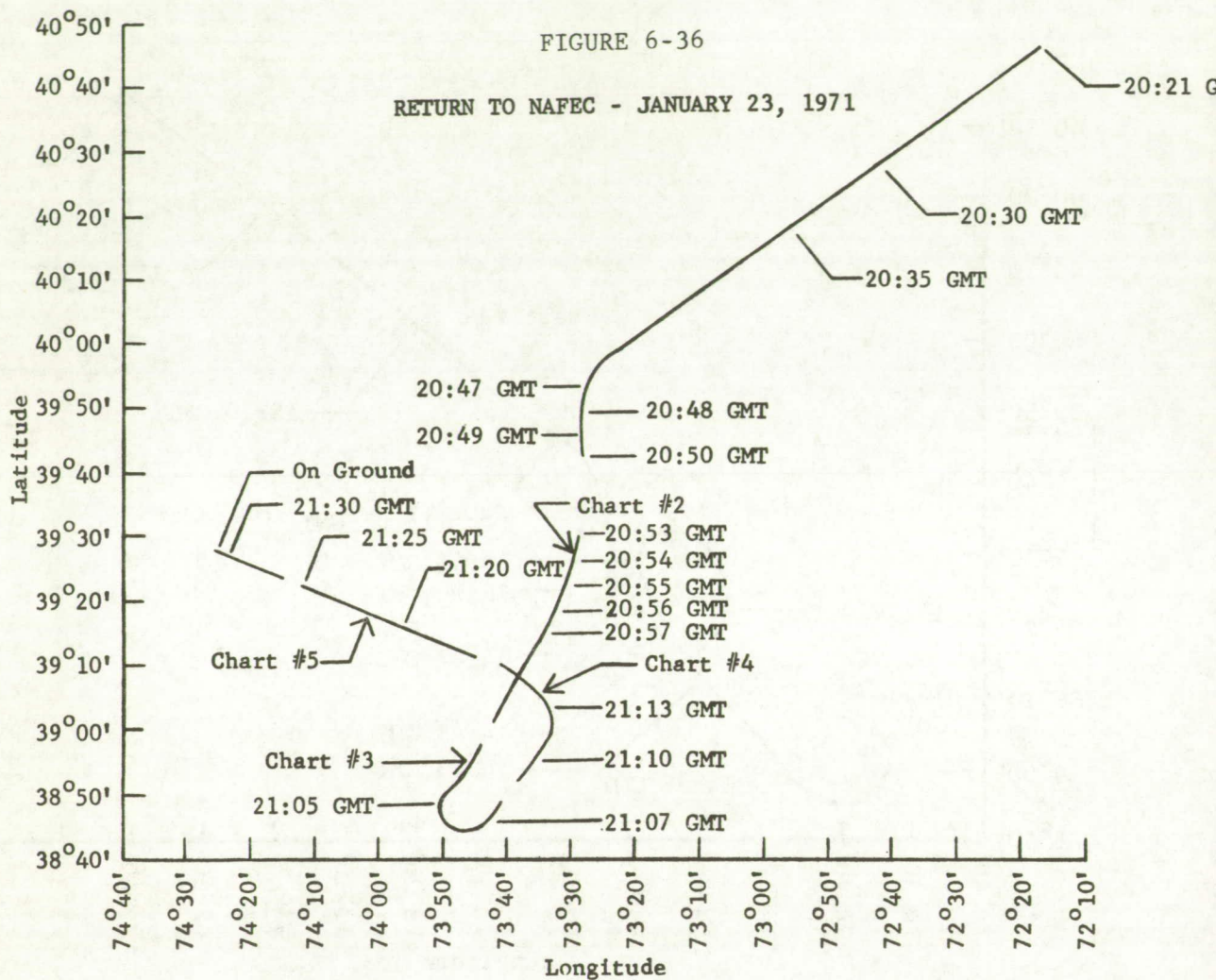
Figure 6-42 shows the satellite positions when the aircraft was parked on the bench mark for calibration of the equipment time delay. The aircraft was oriented favorably with respect to its antenna patterns so that the signals into the aircraft and from the aircraft were above the detection threshold. The range measurements used to compute these fixes were also used to calibrate

FIGURE 6-35

DEPARTURE FROM NAFEC - JANUARY 11, 1971



<u>Time</u> (GMT)	<u>Altitude</u> (Feet)	<u>Time</u> (GMT)	<u>Altitude</u> (Feet)
14:31	12,700	14:42	18,000
14:32	13,200	14:43	18,500
14:33	13,800	14:44	19,000
14:34	14,300	14:45	19,200
14:35	14,800	15:05	19,400
14:35	15,300	15:10	19,800
14:38	16,000	15:12	20,000
14:39	16,500	15:16	20,500
14:40	17,000	15:19	21,000
14:41	17,500		



Time (GMT)	Altitude (Feet)	Time (GMT)	Altitude (Feet)
20:21	22,000	21:01	9,000
20:28	21,500	21:01:30	8,000
20:34	21,000	21:02	7,800
20:42	20,500	21:02:30	7,000
20:49	20,000	21:03	6,500
20:50	19,500	21:03:30	6,000
20:51	18,700	21:04	5,500
20:52	17,800	21:21	5,000
20:53	17,200	21:22	4,500
20:54	16,200	21:22:30	4,000
20:54:30	15,400	21:23	3,400
20:55	14,800	21:23:30	2,800
20:56	14,000	21:24	2,100
20:57	13,200	21:25	1,500
20:58	12,200	21:27	1,000
20:59	11,500	21:29	500
21:00	10,500	21:30	100
21:00:30	9,500		

FIGURE 6-37

DIFFERENCES, PRECISION RADAR AND SATELLITE FIXES. RADAR FIXES AS REFERENCE.

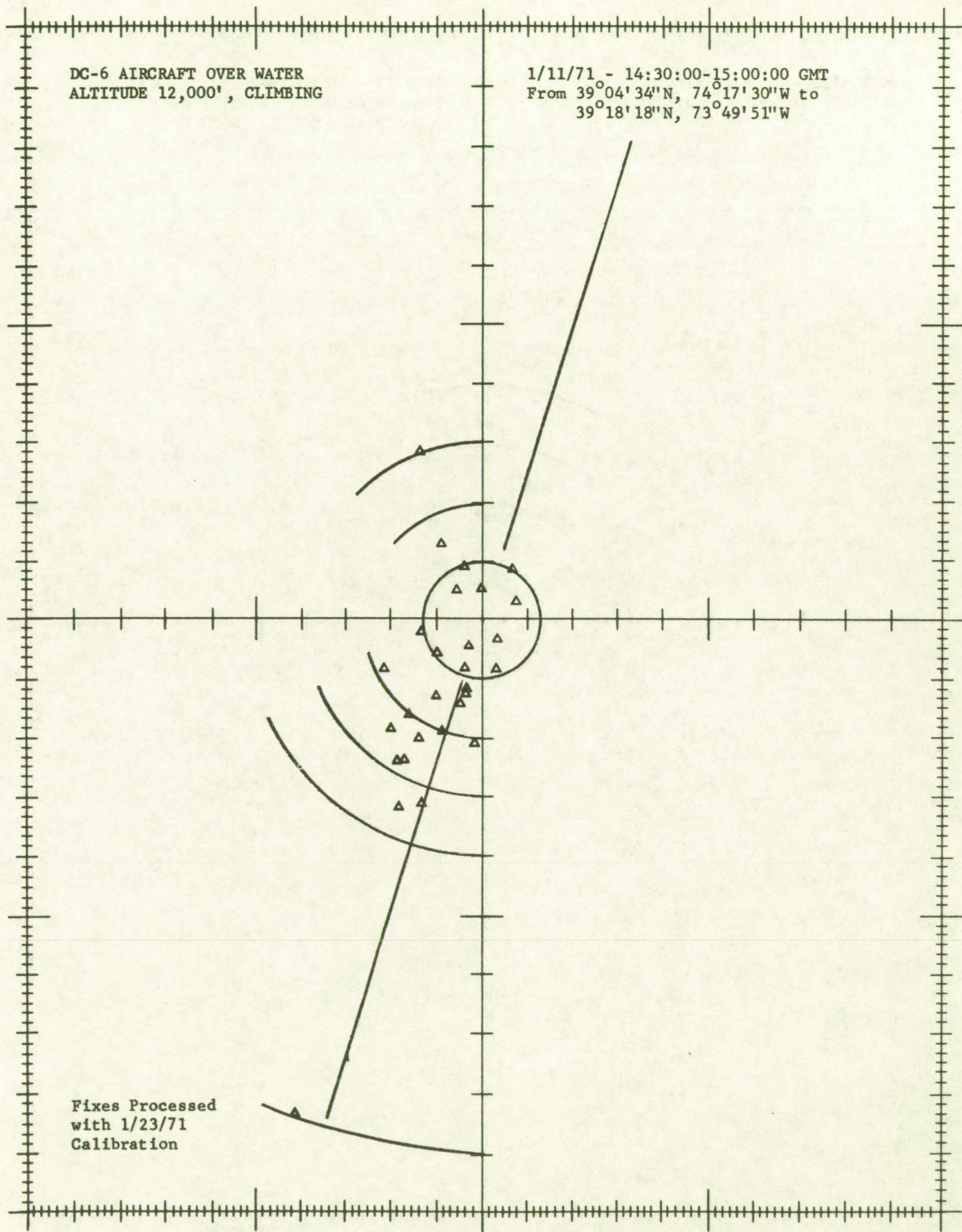


FIGURE 6-38

DIFFERENCES, PRECISION RADAR AND SATELLITE FIXES. RADAR FIXES AS REFERENCE.

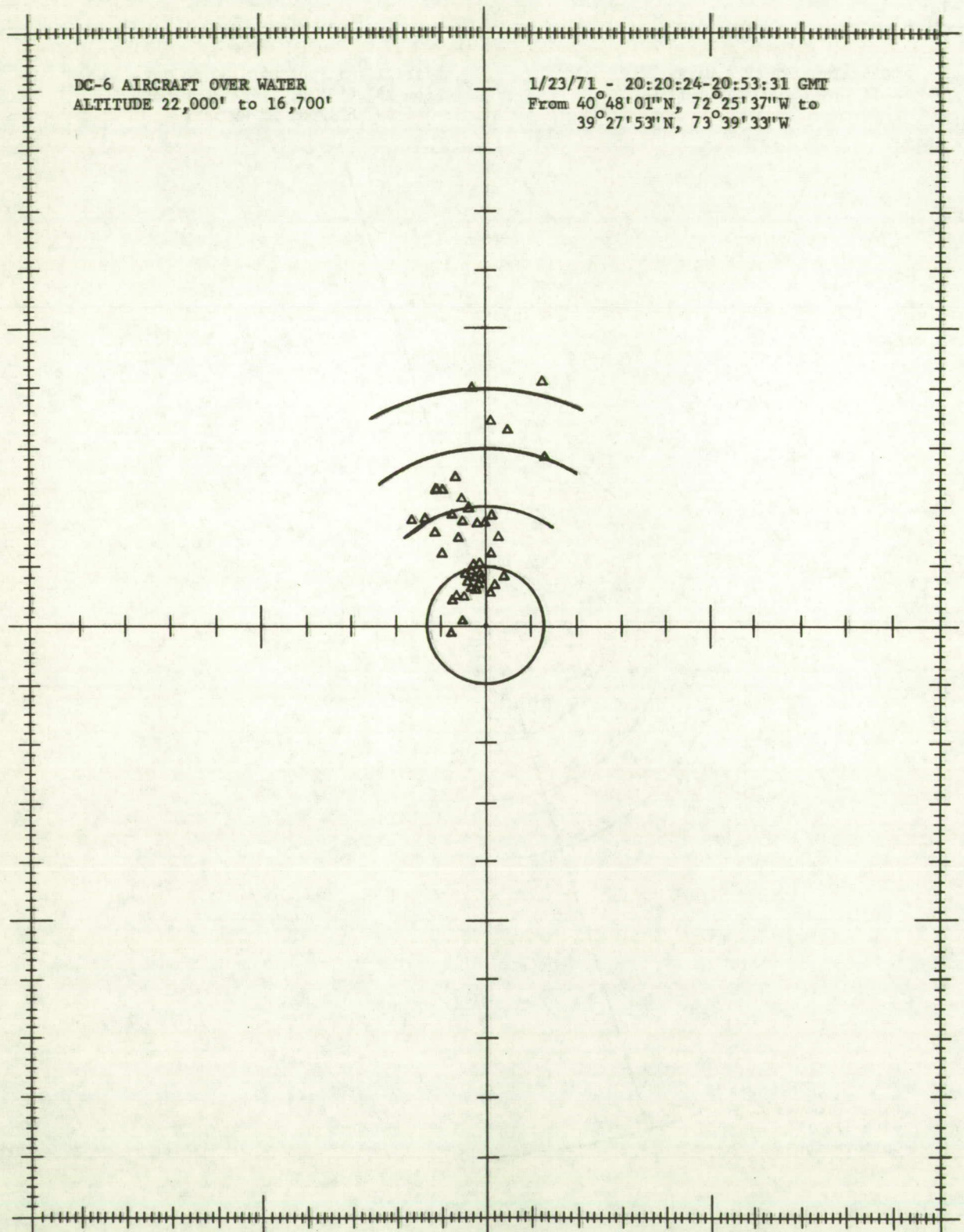


FIGURE 6-39

DIFFERENCES, PRECISION RADAR AND SATELLITE FIXES. RADAR FIXES AS REFERENCE.

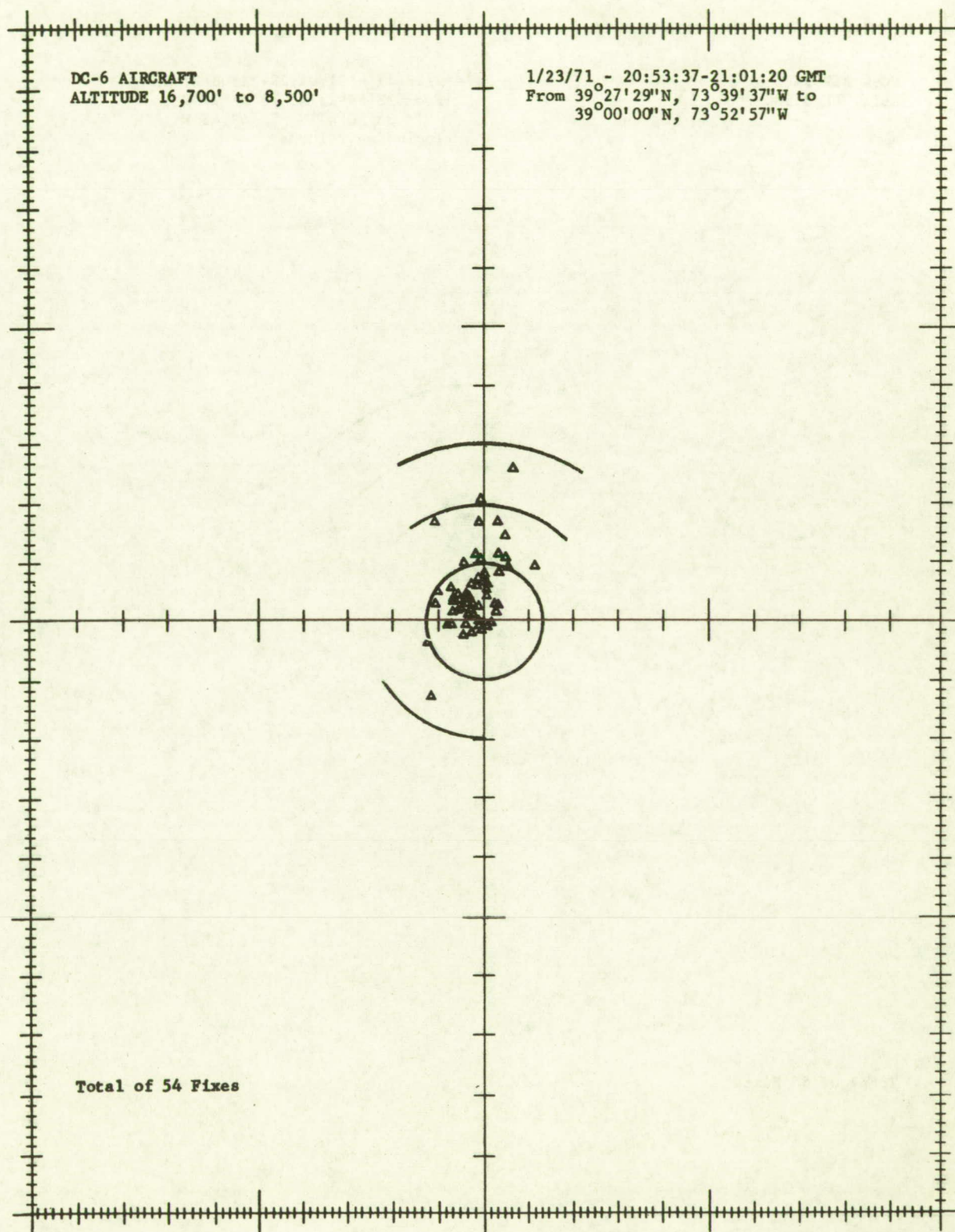


FIGURE 6-40

DIFFERENCES, PRECISION RADAR AND SATELLITE FIXES. RADAR FIXES AS REFERENCE.

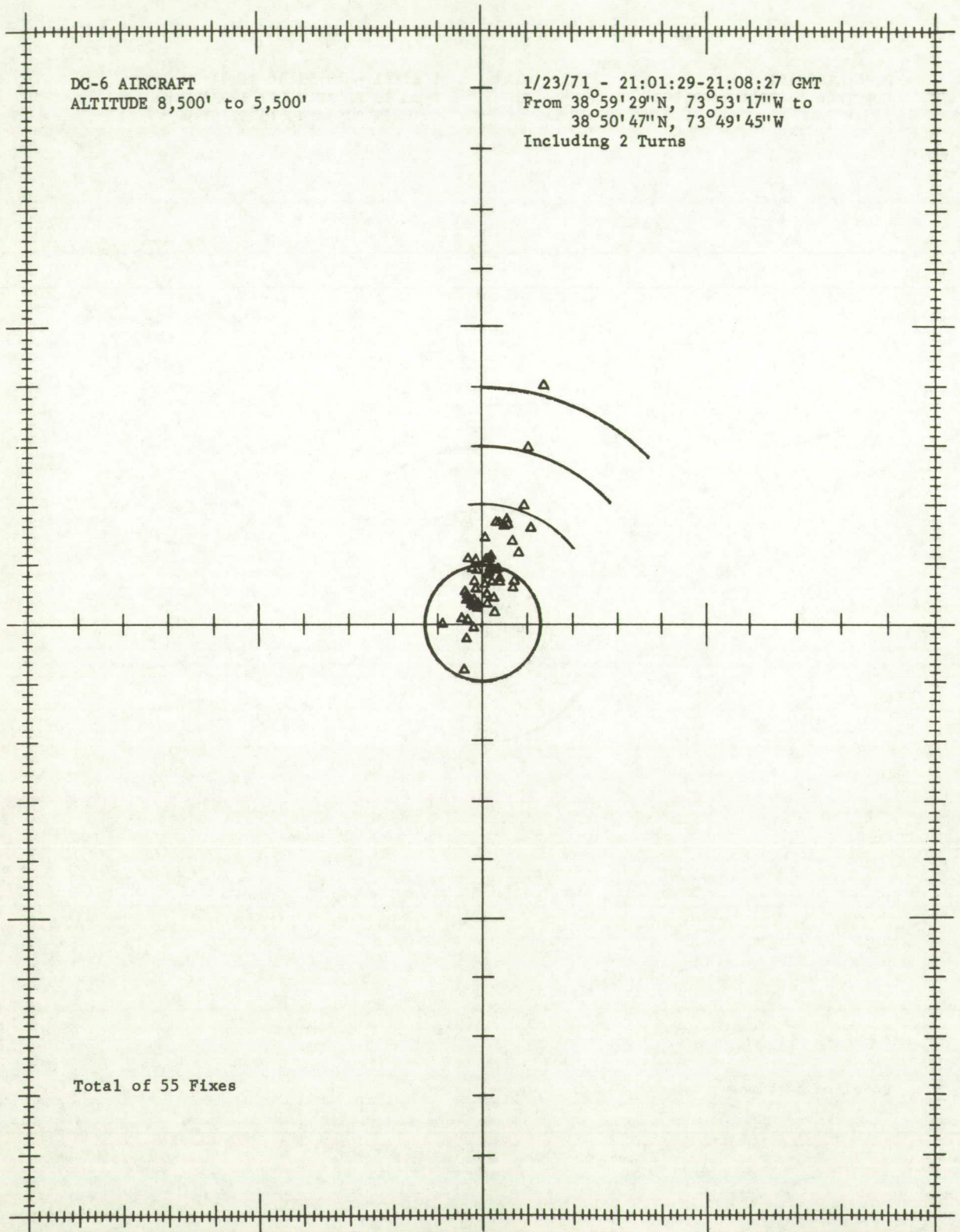


FIGURE 6-41

DIFFERENCES, PRECISION RADAR AND SATELLITE FIXES. RADAR FIXES AS REFERENCE.

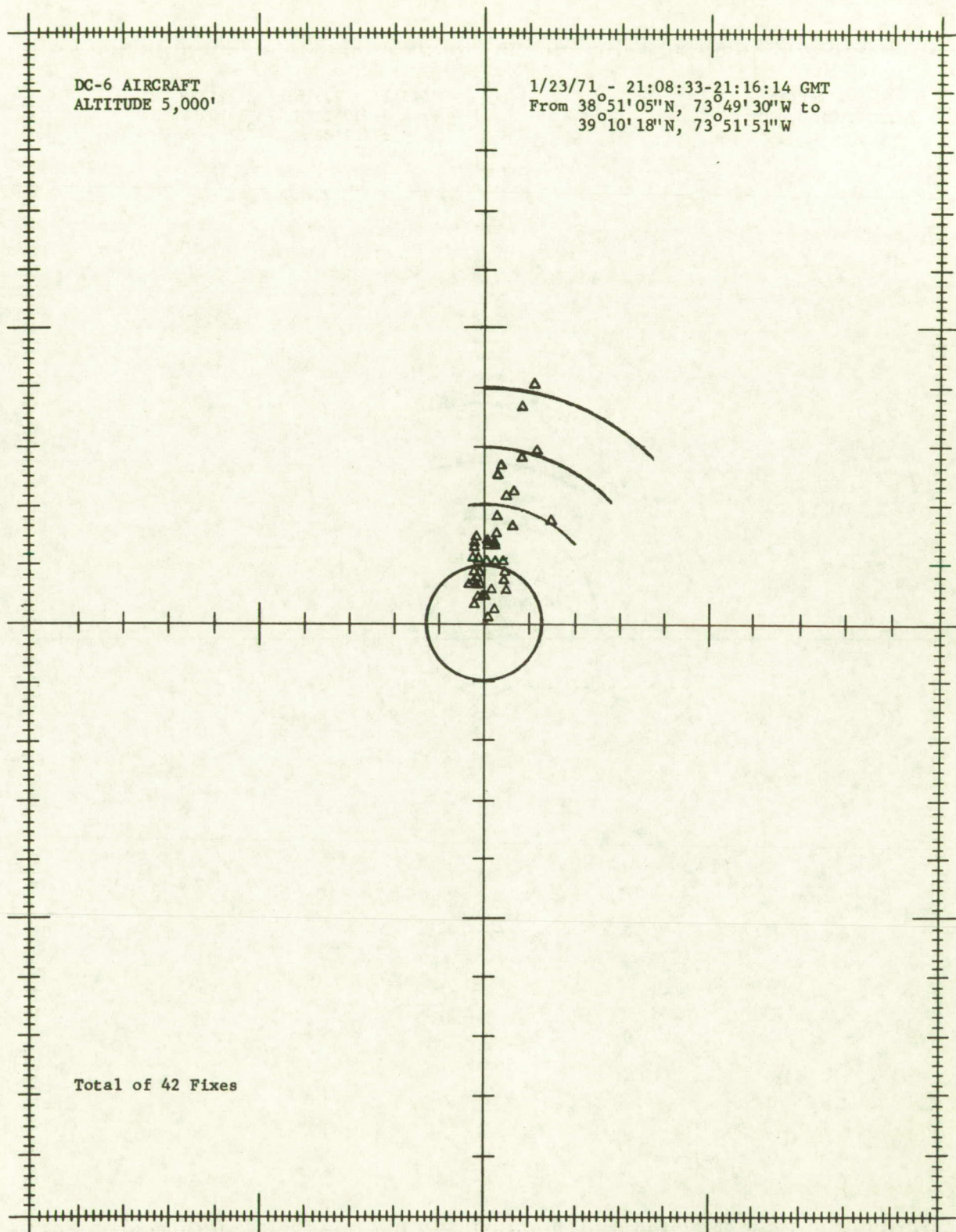


FIGURE 6-42

DIFFERENCES, PRECISION RADAR AND SATELLITE FIXES. RADAR FIXES AS REFERENCE.

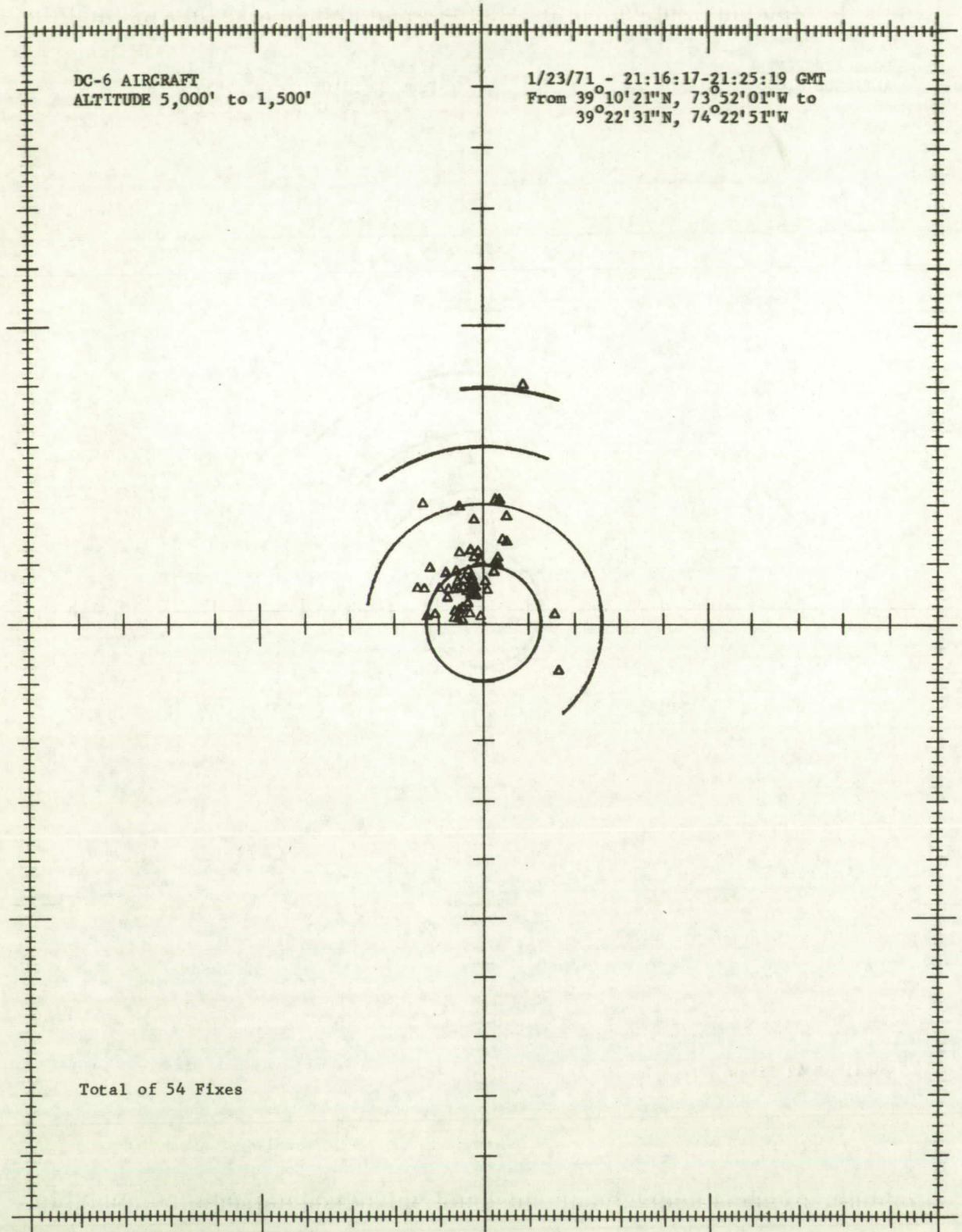
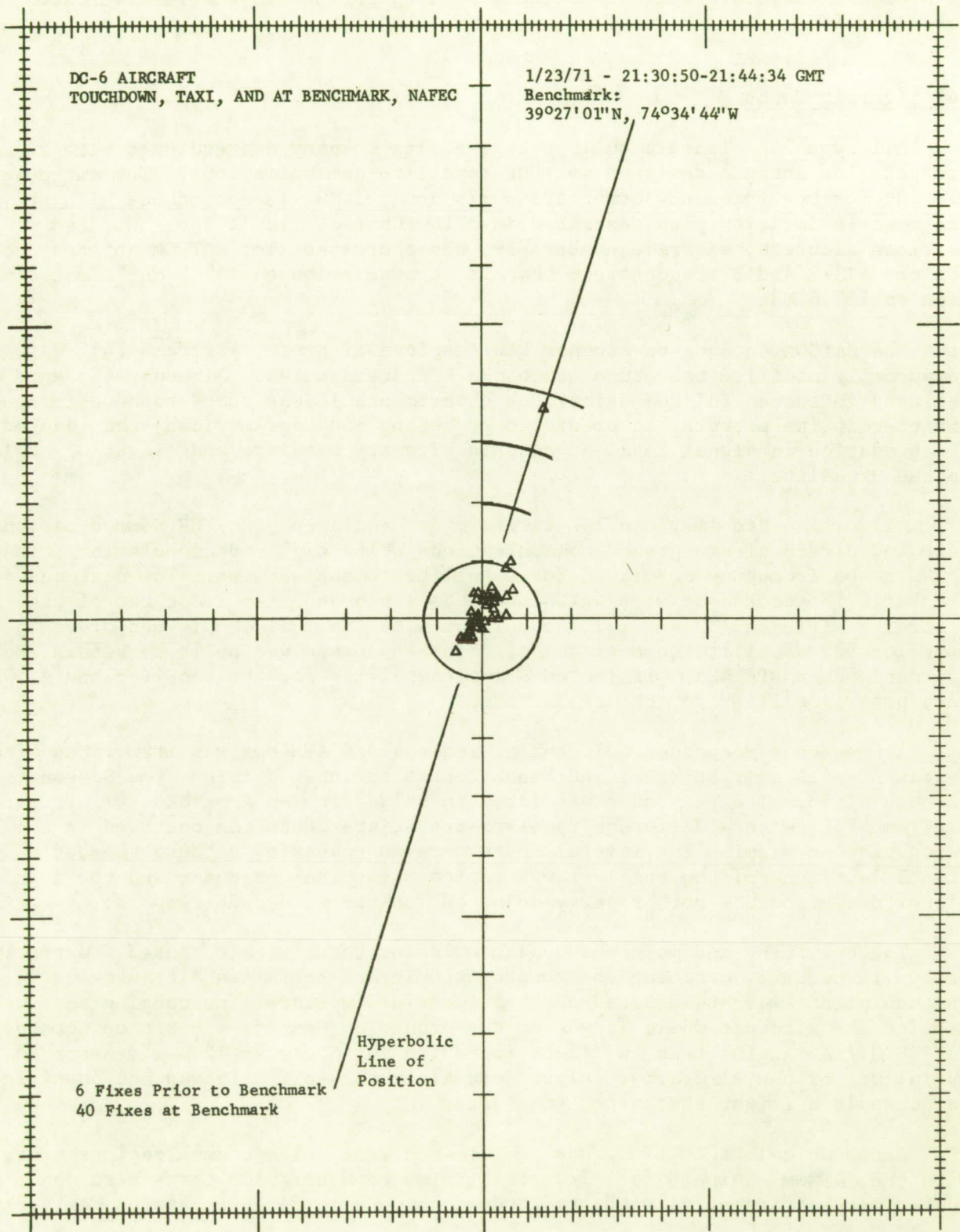


FIGURE 6-43

DIFFERENCES, PRECISION RADAR AND SATELLITE FIXES. RADAR FIXES AS REFERENCE.



the equipment time delay that was used in the computation of all the fixes made on January 11 and 23 with that equipment. The precision of the fixes used for calibrating the equipment delay is considered to be good. All but two of the 46 fixes plotted in Figure 6-42 are within one nautical mile radius and one of those two is just beyond one nautical mile. One single fix is displaced along the hyperbolic position line approximately 3.8 miles. It is probable that that fix was affected by interference in the receiver aboard the aircraft.

747 Aircraft Tests

All type 747 aircraft built by the Boeing Company are equipped with a crossed-slot antenna designed for VHF satellite communications. The antennas are cut for the frequency combination 125 and 131 MHz in accordance with the frequency allocation plan described in ARINC Characteristic 566. One Pan American aircraft, airframe number 739, has a crossed slot SATCOM antenna cut for the ATS-1 and 3 frequencies; that is, transmission on 149.2 MHz and reception on 135.6 MHz.

The SATCOM antenna on another Pan American aircraft, airframe 741, was temporarily modified to retune it to the ATS frequencies. Although the antenna was used in successful communications experiments it was found to have irregularities in its pattern, as predicted by Boeing and Pan American, that caused a degradation in signal level at certain aircraft headings and elevation angles to the satellite.

All of the Pan American 747 aircraft are equipped with VHF communications gear for direct air-to-ground communications using amplitude modulation. They can also be frequency modulated for satellite communications. The equipments are built in accordance with ARINC Characteristic 566. At least two of the aircraft, airframe 739 and 741, have flown with the full complement of equipment for VHF satellite communications. The equipment was built by Bendix and was designated RTA-42A. It includes a preamplifier for the receiver and a 500 watt power amplifier for the transmitter.

A tone-code responder unit built within a 3/4 ATR box was integrated with Bendix RTA-42A gear at Miami and bench tested by interrogation from Schenectady through ATS-3. The responder was later installed in Pan American 747 aircraft, airframe 739, with a different receiver-transmitter than the one used in the bench test at Miami. The initial tests were unsuccessful because the audio signal level out of the receiver was improper for the responder and the transmitter deviation was not properly adjusted for the tone-code response.

The operating and maintenance schedule for the aircraft caused frustrating delays in properly matching the responder unit and the RTA-42A transceiver. The equipments were readjusted and a successful two-satellite ranging test was made to the aircraft while it was on the ground at Kennedy airport on October 16, 1970. A ranging test in flight scheduled for November 12 was frustrated by failure of the aircraft receiver just after take-off. It was not possible to schedule a flight test after that date.

Aeronautical Radio, Inc. has coordinated many voice communications tests with the SATCOM equipped 747 aircraft. Voice communication tests were conducted with airframe 741 with its retuned antenna on flights between New York

and Paris on October 15, 1970 and again between New York and San Juan on October 22, 1970. The tone-code ranging responder was not installed in the 741 airframe and therefore it was not possible to make ranging experiments in addition to the voice communication tests. The scintillation effects observed during the October 15 flight are described in another section of the report.

No propagation disturbances were experienced during October 22 flights from New York to San Juan and return. Voice communications were excellent except during sharply defined time periods when the signal levels into the aircraft dropped below the level necessary to operate the squelch control of the receiver. During those periods the aircraft did not receive signals from the ground terminals. Boeing and Pan American attribute the signal drop-outs to irregularities in the pattern of the retuned antenna.

The intelligibility and quality of the voice signals as received from the aircraft are comparable to face-to-face communications. During the October 15 flight the Captain of the aircraft expressed his opinion that the voice signals received from the satellite were as clear as the "side-tone", directly wired, communications between crew members in the aircraft.

SECTION 7

SHIP TESTS

Tests with Coast Guard ships were conducted during two periods: June of 1969 with the Coast Guard Cutter Valiant, WMEC-621, in the Gulf of Mexico; and May through July 1970 with the Coast Guard Cutter Rush, WHEC-723, in the Pacific Ocean. The tests with the Valiant yielded information on the precision of the fixes, the quality of the voice communications, and the effects of ship structures on signal reliability. Fix accuracy could not be checked with the Valiant because the ATS-3 satellite was not accurately tracked during the period of the tests due to a malfunction in a mechanically despun tracking antenna on the satellite.

Tests with the Rush yielded information on the accuracy of the position fixes over a long period of time and at widely separated locations: San Francisco, Ocean Station November at 140°W and 30°N, and Hawaii. The position fixes include the effects of satellite position errors and of the differences between the actual ionosphere and the ionosphere model used in the POSFIX program. The equipment time delay calibration did not change significantly in the 2.5 month period of the tests. Signal reliability and quality of voice communications were good. The transponder functioned well without attention and demonstrated the operational convenience of the tone-code ranging equipment.

The Coast Guard Cutter Valiant, based at Galveston, Texas, is a 210 foot ship like the one shown in Figure 7-1. It was equipped with a ranging transponder, also shown in Figure 7-1. The lower unit is a General Electric type DM76LAS mobile radio base station with tone-code responder. The 5 Watt exciter output of the radio transmitter was applied to a Gonset Model 903 Mark II 300 Watt power amplifier, shown above the base station unit. The oscilloscope was used for display of the signal and is not a part of the transponder. The equipment was mounted on the bridge of the ship.

The antenna shown in Figure 7-1 was mounted on the flying bridge. Originally designed for the NASA OPLE project, the antenna consists of a pair of crossed dipoles connected for circular polarization. Its gain is 3 dB toward the zenith. It has 0 dB for circular polarization at 45 degrees elevation. Variation in azimuth gain is approximately 2 dB. When used with the linearly polarized antenna on the satellite, the antenna gain is effectively reduced by 3 dB so that its zenith gain is approximately 0 dB; its gain at 45 degrees is -3 dB. It is even lower at the elevation angles to the satellites, which were 29 degrees for ATS-3 and 17 degrees for ATS-1. Figure 7-1 shows the location of the antenna on the flying bridge relative to other structures of the ship. For certain headings of the ship, the mast shielded the antenna from one satellite or the other.

The equipment was shipped from Schenectady, New York to Galveston, Texas by air on June 20, 1969. It was installed on the ship and operated without adjustment.

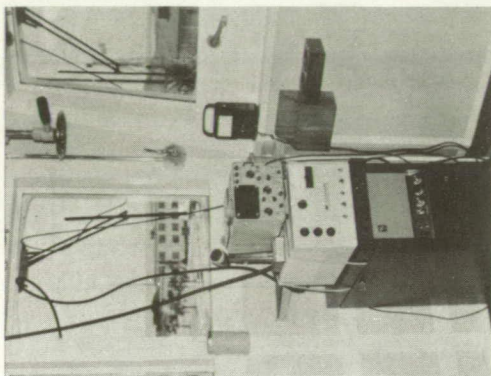
At the completion of the tests with the Valiant, the equipment was returned to Schenectady and later shipped by air to San Francisco where it was installed on the Rush on May 5, 1970. The transponder unit was strapped to a

FIGURE 7-1

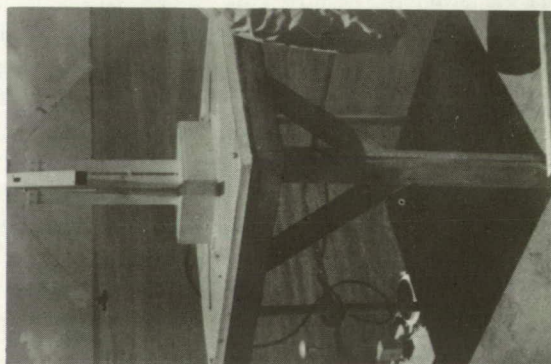
SISTER SHIP OF VALIANT, EQUIPMENT USED IN TESTS



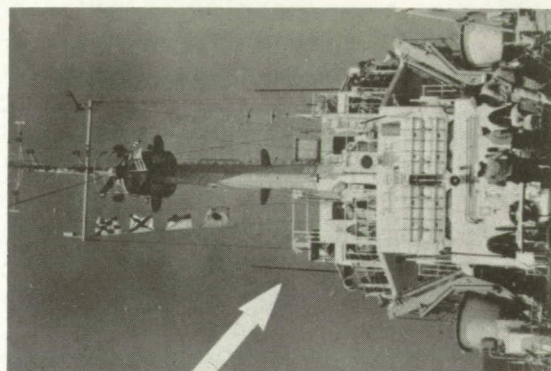
210' COAST GUARD CUTTER SISTER SHIP OF VALIANT



RANGING TRANSPONDER ON
BRIDGE OF VALIANT



ANTENNA USED FOR
SATELLITE RANGING
AND COMMUNICATIONS



ANTENNA LOCATION
ON FLYING BRIDGE
OF VALIANT

bulkhead in the CIC (Combat Information Center), one deck below the antenna location on the ship. Cable runs approximately 35 feet long connected the transponder to the antenna. The antennas were located on the bridge deck (03 level) directly above the CIC. There was an HF fan antenna mounted above the satellite antennas. Three satellite communication antennas were available for use on the Rush. One was the NASA OPLE antenna, previously used on the Valiant; another was a circularly polarized turnstile antenna, consisting of four folded dipole elements bent to conform to the surface of a cylinder. It is pictured in Figure 7-2. Originally designed by Hughes Aircraft Company, it was built by the Coast Guard and designated the "Coast Guard antenna". The OPLE antenna has a bandwidth sufficient to receive on 135 MHz and transmit on 149 MHz, but the Coast Guard antenna bandwidth is not sufficient to cover both the transmit and receive frequencies. The Coast Guard antenna was tuned to the transmit frequency, 149 MHz. It is circularly polarized, omnidirectional in the horizontal plane, and has essentially a dipole pattern in the vertical plane. Throughout the experimental program the OPLE antenna was used to receive signals from the satellites and the Coast Guard antenna transmitted from the ship to the satellites. The OPLE antenna has rather poor coverage to the horizon, while the Coast Guard antenna has rather poor coverage at high elevation angles. Estimates of the gain of the OPLE antenna and the Coast Guard antenna as used in the areas of the Rush operations ranged from about -6 to 0 dB. A third antenna, a three-element yagi that could be manually pointed to provide a higher gain than either of the other antennas was available on the ship but only used infrequently to receive signals from a satellite.

Transmission links to and from the ship were reliable except at headings of the ship where the antennas were shielded from one or the other of the satellites. Voice communications with the ship were reliable and of high quality. While the ship was at a San Francisco dock, it communicated with Shannon, Ireland through ATS-3. The ship transmitted through the Coast Guard antenna with only 60 Watts of RF output power. Shannon reported that the communications were "5 x 5" - that is, strong and perfectly readable. At other times, the ship communicated from Ocean Station November through ATS-3 to Shannon, Ireland and to other ships in the Atlantic Ocean and the Coast Guard Laboratories, as well as to the Radio-Optical Observatory.

Mr. James R. Lewis of General Electric supervised the installation of the equipment on each of the two ships. He was aboard the Valiant while the tests described later in this report were conducted, and he was present on the Rush while the equipment was tested and calibrated in the vicinity of San Francisco. No General Electric person was present on the Rush when it left San Francisco for Ocean Station November and Hawaii or after its return to San Francisco. The equipment was operated by the crew throughout the voyage. It did not require any maintenance or adjustments.

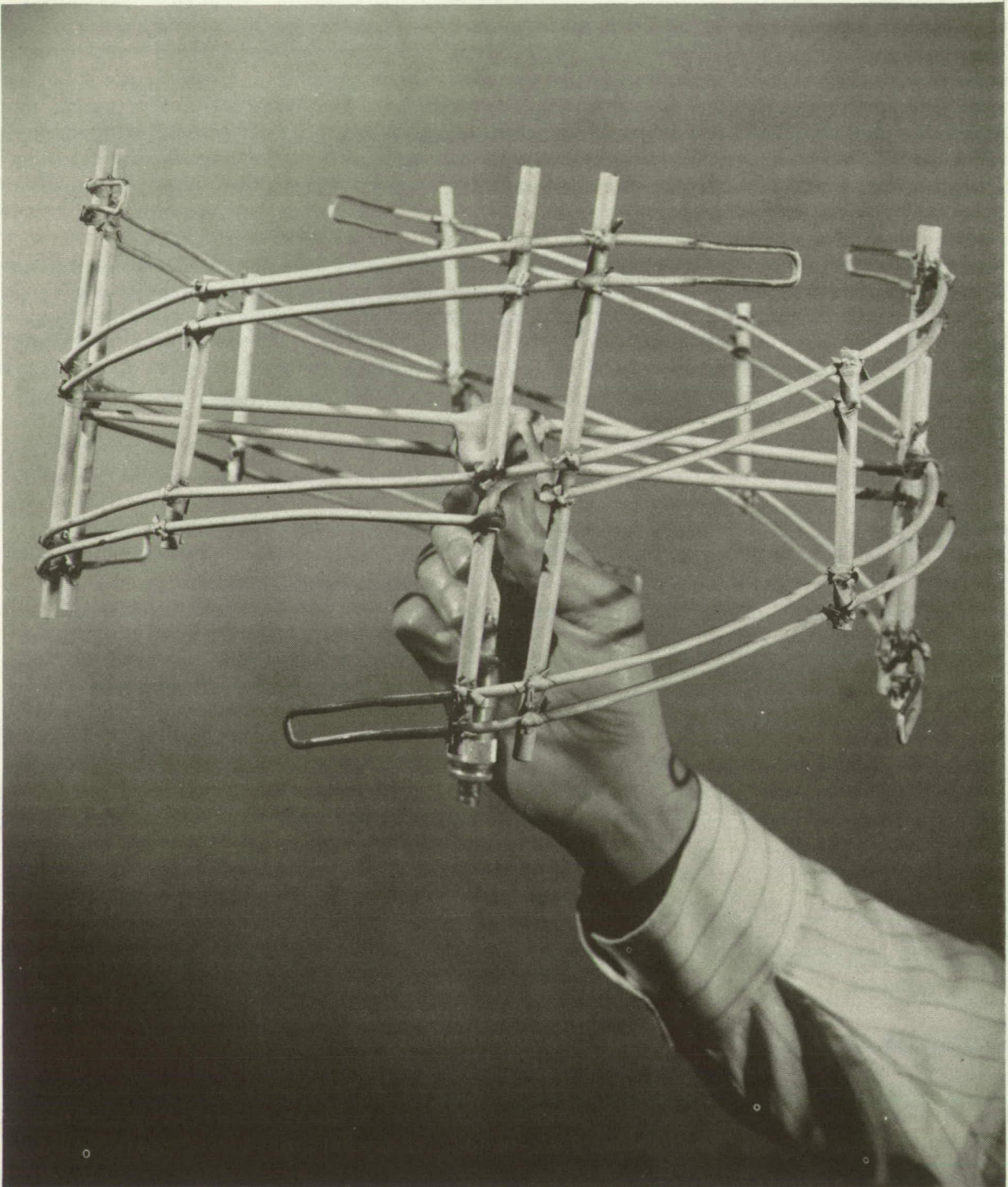
Tests with the Coast Guard Cutter Rush

Tests with the Coast Guard Cutter Rush provided information on the long-term stability of the system and on factors that affect accuracy. The results indicate that:

- There was no long-term drift of equipment calibration that contributed bias errors as large as those that could have been caused by satellite position prediction errors and the use of a crude ionospheric model.

FIGURE 7-2

CIRCULARLY POLARIZED TURNSTILE ANTENNA



- The commercial grade equipment used in the transponder together with the laboratory built responder and simple antennas performed reliably and without attention for more than two months at sea.

The tone-code ranging transponder was installed on the Rush at San Francisco. The time delay of the equipment after its installation was calibrated at 23:55 GMT on May 5 while the ship was under way in the Gulf of Farallons near San Francisco at 37°52'53" N and 122°09'02" W. On May 13 the ship was at the Alameda Administration Center dock in the Oakland Inner Harbor at the position marked in Figure 7-3 by the cross in the center of the right hand circle. The three triangles near the upper edge of the one nautical mile radius circle were fixes determined by ranging from the two satellites at 13:22 GMT on May 13. The ship left San Francisco, spent three weeks at Ocean Station November, 140° W and 30° N, approximately half-way between San Francisco and Hawaii. It then proceeded to Hawaii where its latitude was determined while it was docked at 20°21' N and 157°57' W on June 26. Range measurements were made from ATS-1 and the latitude at which the lines of position crossed the longitude of the ship were computed and found to be:

<u>Time-GMT</u>	<u>Position Fix, Ranging from ATS-1</u>	<u>Position Stated By Coast Guard</u>	<u>Position Error - nmi</u>
20:31:31	21°21'32" N	21°21' N	Latitude determinations bracket the stated latitude within ± 1 nmi.
20:31:37	21°20'44" N	157°57' W	
	21°20'42" N		
	21°21'07" N		

Ionospheric correction was not used in the latitude determinations. Its inclusion would have moved the lines of position south a few thousand feet.

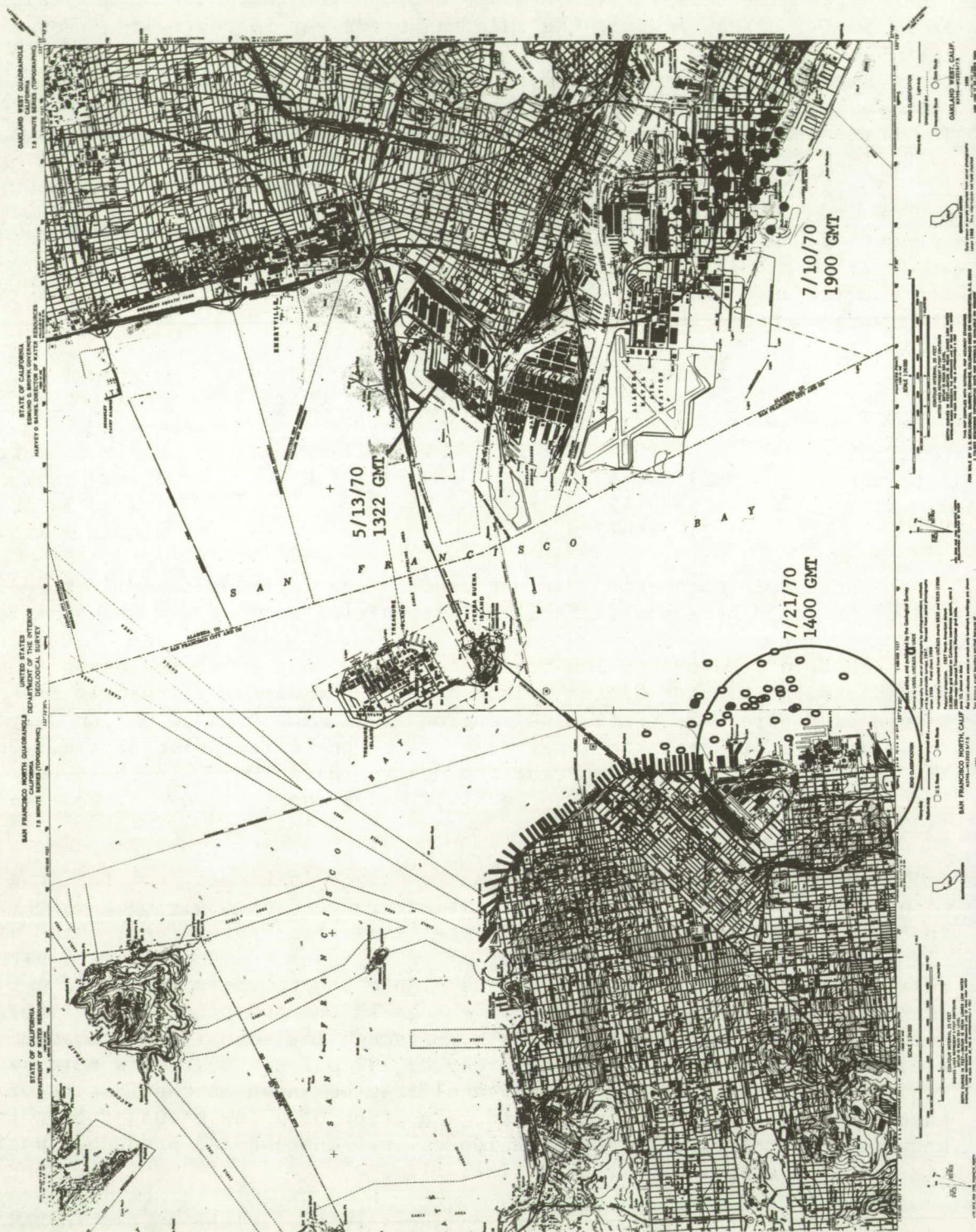
The ship returned to San Francisco and on July 10 it was again at the Alameda Administration Center dock, shown in the center of the right-hand circle of Figure 7-3. Satellite ranging fixes made at 1900 GMT on July 10 are shown as the dots near the lower edge of the one mile radius circle. On July 21, the ship was at the San Francisco Central Basin Dock, in the center of the left-hand circle in Figure 3. The fixes, shown as small ovals, were made at 1400 GMT.

Each of the sets of fixes at San Francisco is biased from the true position. There is evidence that the bias errors were probably caused by errors in the predictions of the satellite positions. The satellites, which are inclined slightly from a true equatorial orbit, each trace a Figure 8 pattern relative to the earth's surface. The Figure 8 pattern is traced in a 24-hour interval so that there is a diurnal change in the position of the satellite relative to any point on the earth's surface. The actual range change during the one day period may be on the order of 100 miles. Every fix computation requires that the position of the satellites be known at the instant of time that the position fix is determined. An error of a few thousand feet in the knowledge of the satellite's position at that instant can produce a position fix error of approximately a nautical mile.

The position fixes were based on satellite positions stated in NASA's ATS-1 and ATS-3 acquisition tables. With NASA's cooperation, a check was made of NASA acquisition table accuracy as a function of time from their tracking epoch to see if prediction of the satellite positions could account for the fix errors.

FIGURE 7-3

POSITION FIXES, COAST GUARD CUTTER RUSH IN SAN FRANCISCO BAY



The check with NASA confirmed that satellite predictions can account for fix errors of the magnitude observed. For example, the predicted positions of ATS-3 based on two epoch dates were as follows:

<u>Epoch Date</u>	<u>Position Date</u>	<u>Position</u>		<u>Longitude</u>	<u>Earth Center</u>
		<u>Time GMT</u>	<u>Latitude</u>		<u>Distance</u>
6/13/70	7/8/70	2100	0.894° N	65.320° W	22742.04
7/8/70	7/8/70	2100	0.894° N	65.299° W	22742.36

If the predictions are in error, there will be a diurnal change in position fix errors. Ground reference transponders can provide a first order correction, but none was used for the Rush fixes.

A further contribution to fix error will result from the difference between the actual ionosphere propagation delays at the time of the fix and the assumed propagation delays from the ionosphere model used in the POSFIX program.

The biases in the position fixes are well within the limits of error that could be introduced by the combined effects of satellite position error and ionospheric propagation delay uncertainty, and there is no evidence of a significant long-term drift in the equipment calibration.

There was no fixed reference transponder in the western United States at the time the tests were made with the Rush. A fixed reference transponder would have enabled us to obtain a first order correction for satellite position error and ionospheric propagation delay. One can conjecture on the basis of other evidence such as our measurements to the aircraft at Shannon, Ireland, where a reference transponder was used (Page 6-45), that the position fixes of the Rush would have been clustered about points much closer to the true positions of the ship if a ground reference transponder had been used.

The bias errors are correctable by better tracking of the satellites and better estimates of the ionosphere. Both of these can be accomplished without the use of fixed reference transponders in the area to be served, but the use of the fixed transponders has been shown to be a convenient way of determining the corrections. The accuracy achieved, the certainty that bias errors can be corrected, and the precision of the measurements demonstrate that the accuracy of a narrow bandwidth VHF system for ships can be well within one nautical mile for operating periods longer than two months without adjustments or other attention to the ship-board equipment.

Precision of the measurements is well within the limits expected for the experiments. While the three fixes on May 13 are clustered close together they are not sufficient in number to indicate precision. Sixty-eight fixes made on July 10 are all within a circle of 5,000 foot radius. Fifty-three are within a circle 0.5 nautical mile in radius. All but one of the thirty-nine fixes on July 21 were within one nautical mile radius. The essentially omnidirectional antennas were poorly located on the ship, the transmitter power was 300 watts, and the antennas were located where they are subject to urban radio frequency noise environment and to multipath reflections from structures in the vicinity of the ship so that signal and environmental conditions were less favorable than expected at sea.

Each of the position fix measurements was determined from a single interrogation from Schenectady and a single response from the ship relayed through the two satellites. The averaging time of the phase measurements is approximately 64 cycles of the 2.4414 kHz signal. (See Section 4). A longer averaging time on each interrogation or averaging the fixes for a number of interrogations would improve the precision of the position delays by the square root of the ratio of averaging time or the number of fixes averaged. The averaging time of each phase measurement is approximately 26 milliseconds. An averaging time of approximately 1/4 second or averaging ten of the position fixes would reduce the scatter of the fixes by a factor of three, so that the fixes would then be within approximately a 2,000 foot radius circle.

The Rush left San Francisco on May 13, 1970, arrived at Ocean Station November on May 16, 1970, left Ocean Station November for Hawaii on May 29, 1970; and was enroute back to San Francisco from Hawaii between July 4 and 8, 1970. While the ship was at sea there were fifty-two periods of operation with the Radio-Optical Observatory through one or both satellites, totaling forty-five hours of operation, including ranging for position fixing and voice communications with the Observatory, with the Coast Guard Laboratories at Falls Church, Virginia and with other ships including another Coast Guard ship and the New Amsterdam in the Atlantic Ocean, as well as with other ground transponders in the General Electric network including Shannon, Ireland and Gander, Newfoundland. The ship was in line-of-sight of ATS-1 during the entire cruise and was in line-of-sight of ATS-3 at Ocean Station November and beyond until it approached Hawaii.

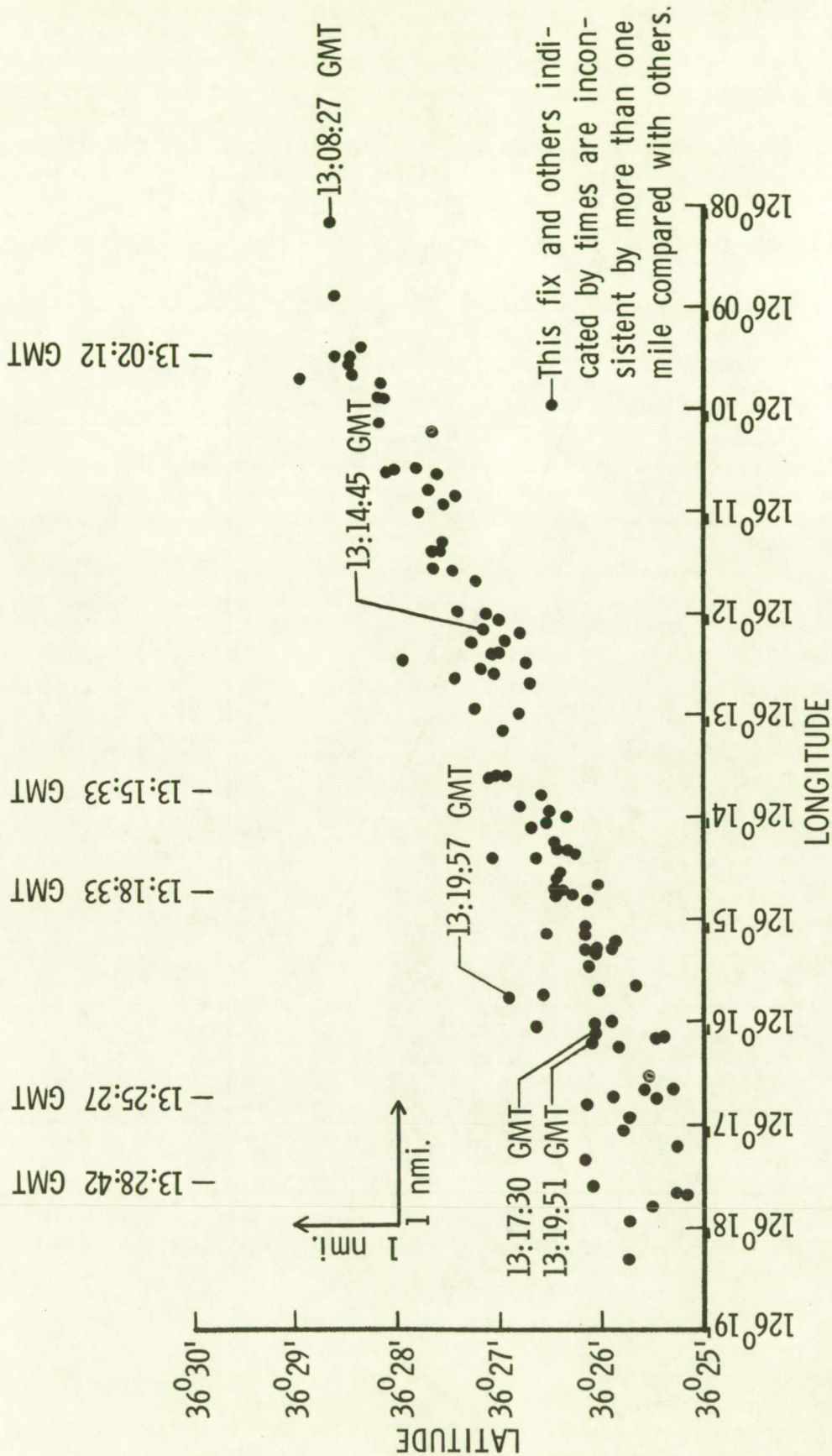
More than 4,500 ranging responses were received through both satellites and recorded, and are available for determining position fixes for the ship.

Figure 7-4 shows a sequence of position fixes taken while the ship was enroute from San Francisco to Ocean Station November. Individual position fixes which appear to be in disagreement by more than a mile with a smooth track through the data points are marked with the time at which they were taken so that they can be distinguished from the other fixes.

Three fixes were selected at random, one near the beginning of the period, one near the middle and one near the end. The only criterion for selection was that they be one of a sequence of fixes while the ship was responding consistently to all of its interrogations. The three fixes were plotted in Figure 7-5 and found to fall on a straight line. The direction and length of the line were measured and show the ship to be on a course of 246 degrees at a speed of 17.5 knots. The Rush reported its heading as 247° and its speed at 18 knots. The position stated by the Rush at 13:25 GMT with a resolution of one minute, or approximately one nautical mile, agrees with the satellite position fix within about 1.5 nautical miles. The position is plotted as the encircled dot in Figure 7-5.

Many two-satellite ranging measurements were made to the ship while it was at Ocean Station November. The accuracy of the position fixes cannot be verified because there is no accurate reference by which to compare them. The ship was equipped for LORAN A and OMEGA. Star fixes and sun lines were also used to determine ship's position. Ocean Station November is not in a favorable part of the coverage area for either OMEGA or LORAN.

One group of satellite fixes for the ship is plotted in Figure 7-6. During a half hour period from 11:30 to 12:00 GMT on May 25, approximately 250



5/14/70 POSITION FIXES OF RUSH WHILE UNDERWAY AT SEA

FIGURE 7-5
SATELLITE TRACKING OF RUSH UNDERWAY AT SEA

5/14/70

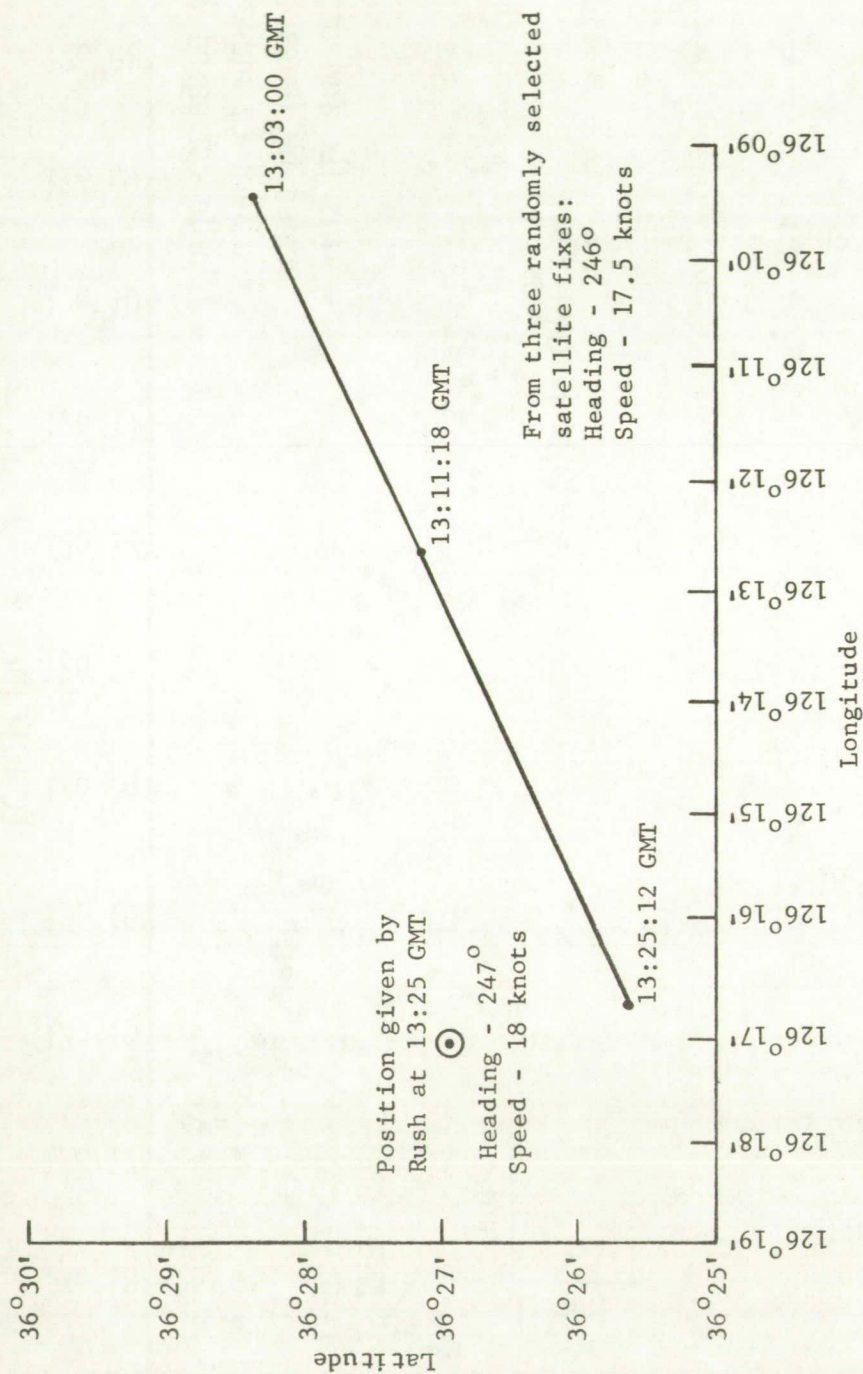
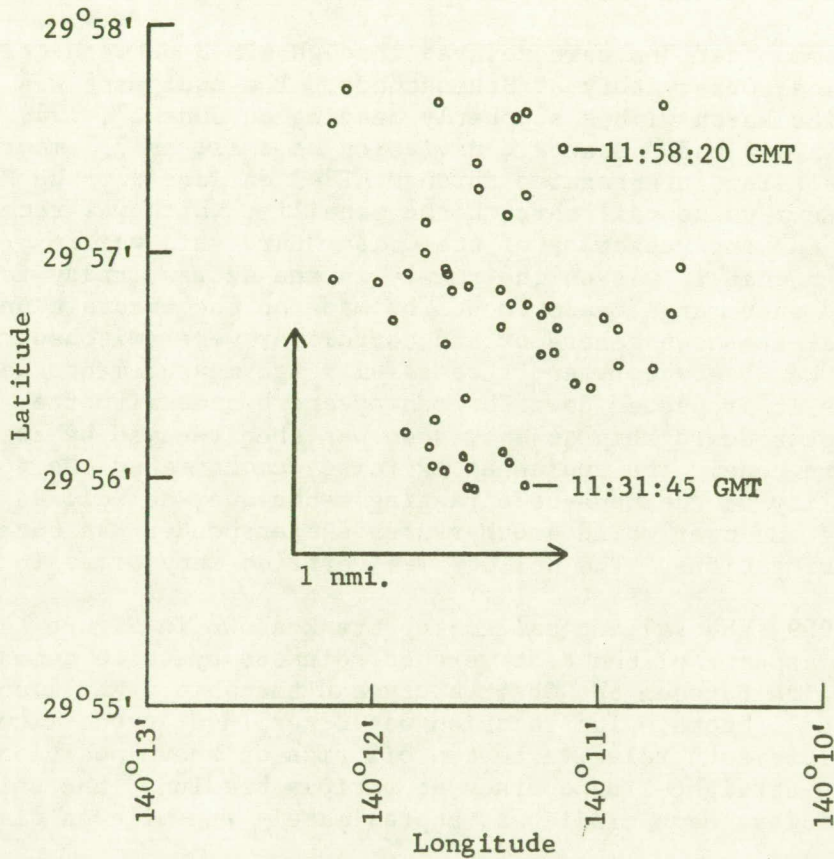


FIGURE 7-6

SATELLITE FIXES OF RUSH DRIFTING AT OCEAN STATION NOVEMBER

5/25/70



Approximately 50 fixes computed from approximately 250 satellite returns (every fifth one). Time sequence of fixes indicates 1.5 minute northward drift in 27 minutes.

interrogations provided range measurements from the two satellites from which position fixes could be computed. The computer was instructed to determine a fix position from every fifth pair of range measurements, and these are plotted in Figure 7-6. The position fixes are scattered approximately ± 0.5 mile in an east and west direction and the time sequence of the fixes indicates that the ship drifted northward about 1.5 minutes, that is about 1.5 nautical miles, during the 27 minute period between the first and last fixes.

Tests with the Coast Guard Cutter Valiant

Tests with the Valiant were conducted in June and July of 1969. The transponder was shipped to Galveston, Texas on June 20, 1969. It was installed on the ship and operated without adjustment.

Good voice communications were relayed through ATS-3 between the Valiant and the Radio-Optical Observatory at Schenectady. The equipment was tested with the ship at its berth with a southerly heading on June 27, 1969. Interrogations through ATS-3 had a standard deviation as small as 0.7 microsecond. While the ship was being interrogated through ATS-3 on June 27, the FAA C-135 aircraft, N96, made a voice call through the satellite which was received at Schenectady while the interrogation of the Coast Guard ship was in progress. The aircraft stated that it was on the runway in the Azores, ready for take-off, and requested that range measurements be made on the aircraft until it was airborne. The tone-code generator and correlator were switched to the aircraft code at the Observatory and successful range measurements were made to the aircraft as it proceeded down the runway and became airborne. Interrogation of the Coast Guard ship at Galveston was then resumed by switching back to its address code. The unplanned exercise demonstrated the voice and ranging compatibility of the tone-code ranging technique, as well as the ability to interrogate one user while another user's transponder was turned on and receptive to interrogations. The ability was verified many times in later tests.

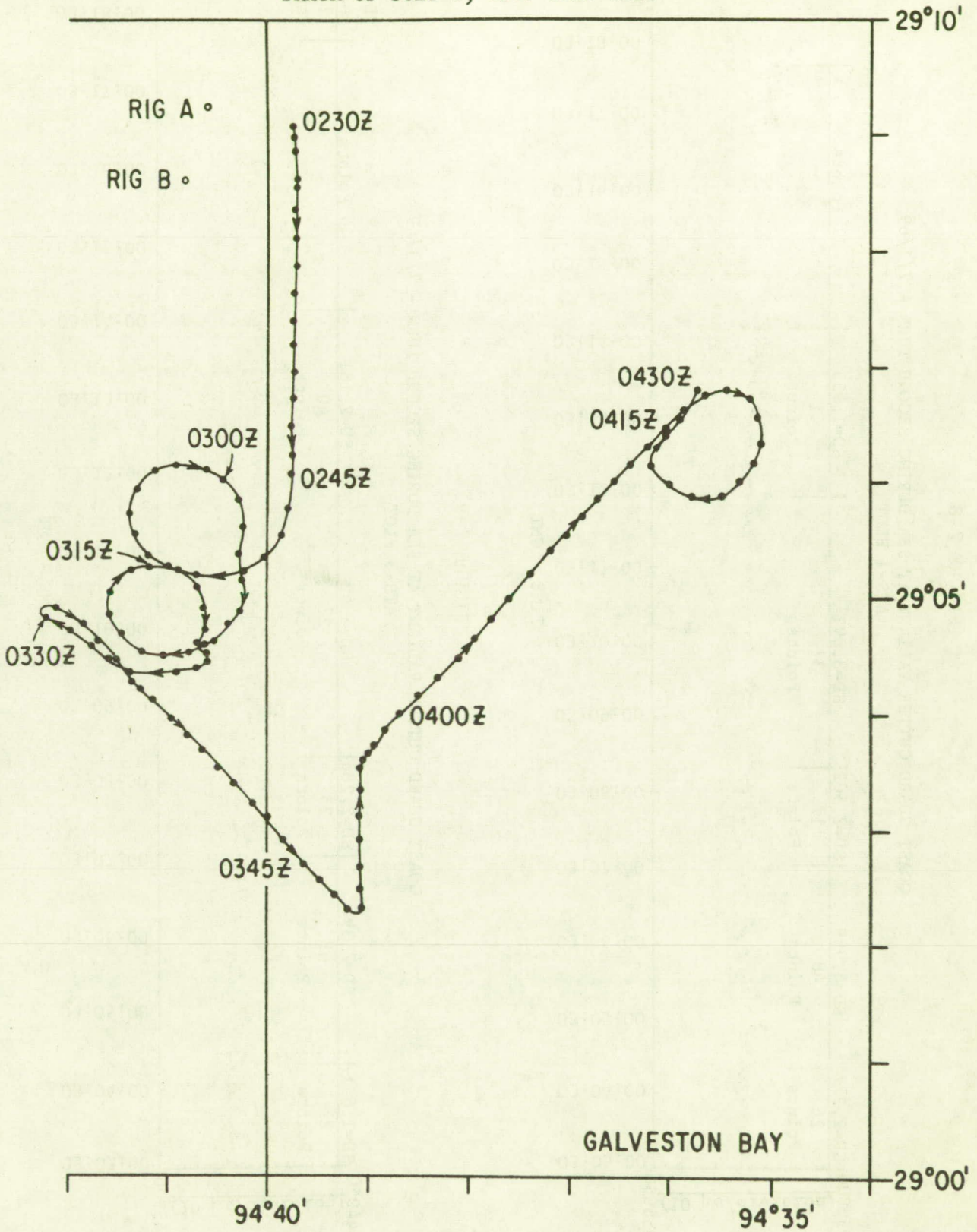
On July 1, 1969, the Valiant sailed the track shown in Figure 7-7. Course changes and other aspects of the test were coordinated by voice communication through the satellite between the Observatory and the ship. While underway, the ship sailed at 15 knots. Its location was determined at one-minute intervals by radar measurements relative to two oil rigs at known positions A and B. In addition to straight-line courses at various headings, the ship sailed three complete circles; each circle was approximately one mile in diameter.

Except during short periods of voice communication, the ship was interrogated through one of the satellites at three-second intervals. Responses from the ship were relayed back through both satellites to the Observatory. Most of the interrogations were made through ATS-3. It was also successfully interrogated through ATS-1, although the percentage of responses was lower for ATS-1 interrogations because of the relatively poorer down-link from ATS-1 to the ship.

Figures 7-8 and 7-9 show the ranging time intervals for the satellites ATS-1 and ATS-3 as the ship sailed the circle shown in Figure 7-7 between the times 03:03:00 and 03:18:00 GMT. The number of returns as well as the magnitude of the variations of the time intervals clearly shows the effect of the mast and perhaps other ship structures on the antenna pattern. The performance changed with ship heading so the data were examined separately for short time intervals during the circle.

FIGURE 7-7

TRACK OF JULY 1, 1969 SHIP TEST



COAST GUARD CUTTER VALIANT AT SEA DURING SECOND TURN - 7/1/69

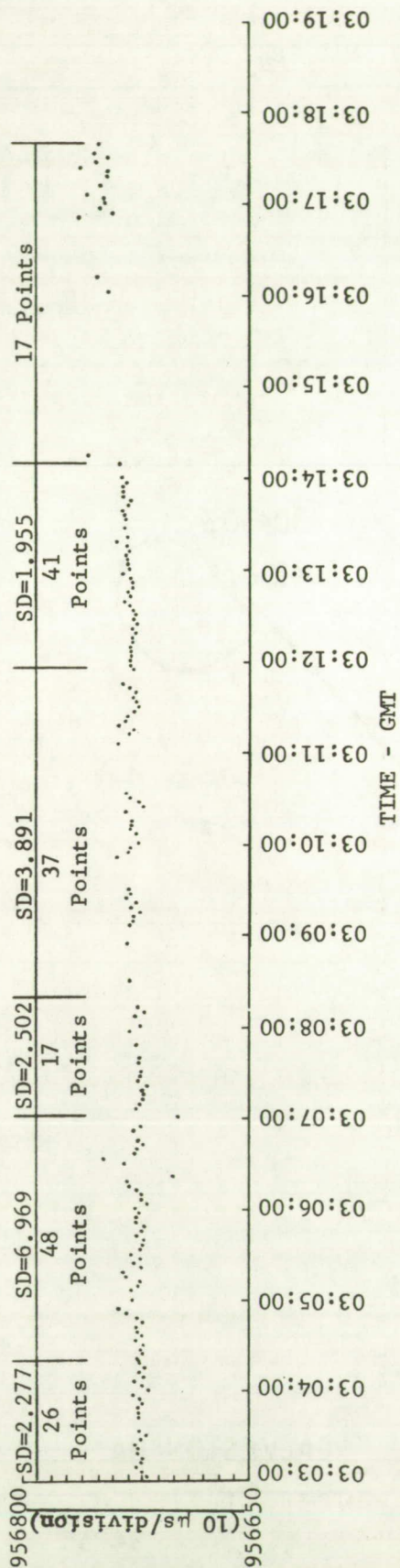
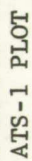
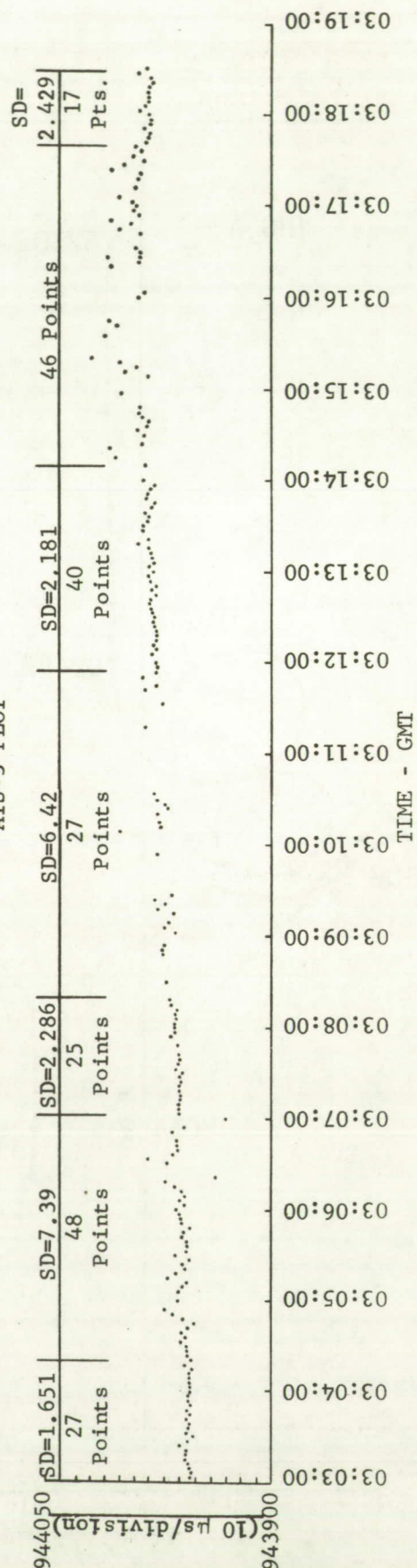
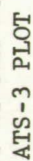
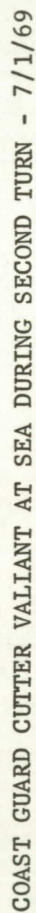


FIGURE 7-9



A plot of fix precision was made for each time interval. These are shown in Figures 7-10 through 7-15. The fix precision plots were constructed by first computing a best fit curve to the plots of Figures 7-8 and 7-9. Lines of position for ATS-1 and ATS-3 were then plotted for the two returns from each individual interrogation. The intersection of the two lines of position is shown as a small circle. Each line of position was constructed at right angles to the azimuth toward the satellite with the line of position advanced or retarded by an amount proportional to the displacement of the range measurement from the best fit curve. The scale factors were calculated to take into account the projection on the earth of the range measurement for the elevation angle to the satellite. Each small circle is a measure of fix precision including the effects of instrument measurement resolution, time delay variations in the instrumentation with signal amplitude or detuning, the effects of noise on the signal and geometrical dilution of position. It does not include bias errors due to the ionosphere, error in the estimates of the satellites' positions or in the estimate of equipment time delay.

During the first period from 03:03:00 to 03:14:18 GMT, the signal paths were relatively good. Only one of the twenty-six fix estimates falls outside of a one nautical mile radius circle. The period from 03:04:20 to 03:07:00 GMT had generally good signal levels but there are several points which are displaced farther from the best fit curve than is typical of the previous or following time periods. The reason has not been definitely assigned but it is most probable that it represents a known characteristic of the receiving equipment. The receivers exhibited a change in time delay of 5 to 7 microseconds with changes in received signal level. A comparison of the range measurements for ATS-1 and ATS-3 as shown in Figures 7-8 and 7-9 reveals that the displacement of the range measurements is highly correlated in the returns from the two satellites, indicating that the variance in time delay occurred in the receiver on the ship as it received the interrogation signal from ATS-3. Because the error causes an advance or delay in the transmission of the response from the ship, it adds or subtracts an equal delay to the returns from the two satellites. The range difference of the measurements remains unchanged and therefore the fix errors tend to lie along a hyperbolic line of position. The effect is clearly evident in Figure 7-11 where the position fixes are concentrated along a generally north-south line.

The period from 03:07:03 to 03:08:18 GMT was characterized by good signal levels, small standard deviation of the measurements, and fixes lying within a 1 nautical mile radius. Between 03:08:30 and 03:11:54 GMT the ship was at a heading such that the antenna was partially shielded from ATS-3 by the ship's mast. The standard deviation of the measurements was relatively high. Again, the position fixes are concentrated along the hyperbolic lines of position. The antenna was again in view of both satellites between 03:11:57 and 03:14:09 GMT. Standard deviations were low and the fix precision was good. From 03:14:15 to 03:17:39 GMT the antenna was shielded by the mast from ATS-1. The loss in signals to ATS-1 is evident in Figure 7-8. The interrogation signal from ATS-3 was not received well and the scatter of the range measurements are biased in one direction relative to the data received at good signal levels, suggesting that the signal levels as received during the period were in part of the receiver's dynamic range to cause a change in time delay through the receiver. The cause of the changing time delay through the receiver was traced to the limiter.

FIGURE 7-10

FIX ERROR DISTRIBUTION
USCGC VALIANT (WMEC-621)
1 July 1969, 03 03 00 - 03 04 18 GMT

Ship Heading: S
27 Interrogations
26 Dual Responses

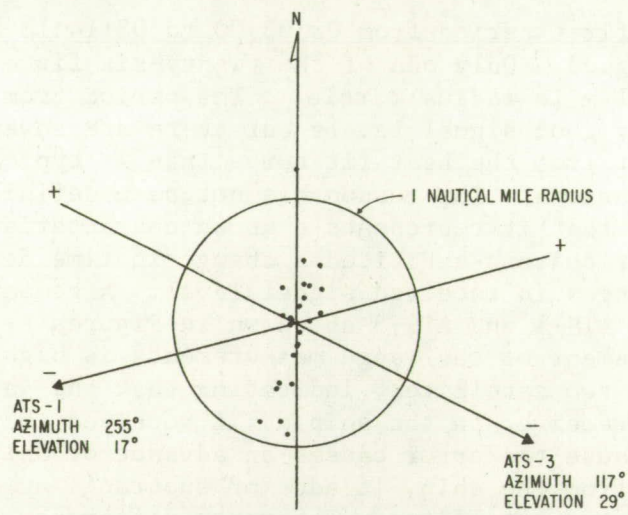


FIGURE 7-11

FIX ERROR DISTRIBUTION
USCGC VALIANT (WMEC-621)
1 July 1969, 03 04 20 - 03 07 00 GMT

Ship Heading: S to SW
54 Interrogations
48 Dual Responses

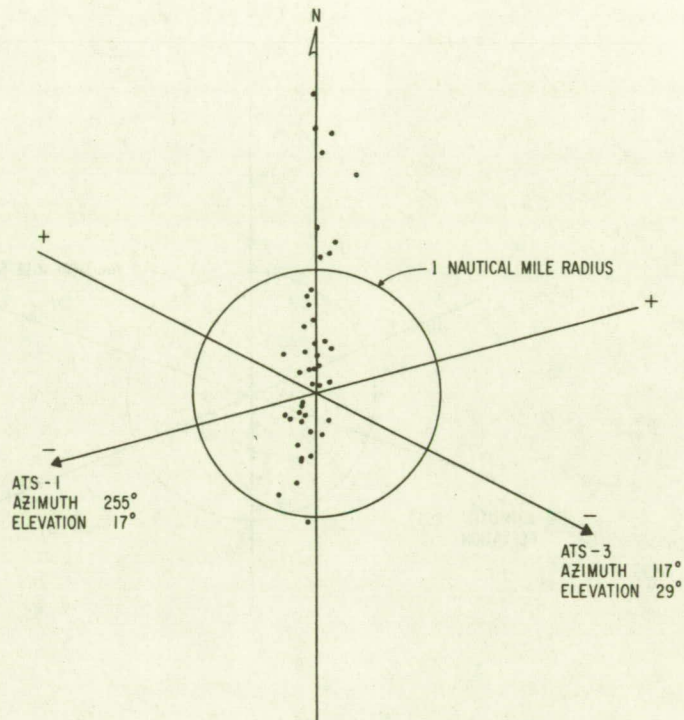


FIGURE 7-12

FIX ERROR DISTRIBUTION
USCGC VALIANT (WMEC-621)
1 July 1969, 03 07 03 - 03 08 18 GMT

Ship Heading: W
26 Interrogations
17 Dual Responses

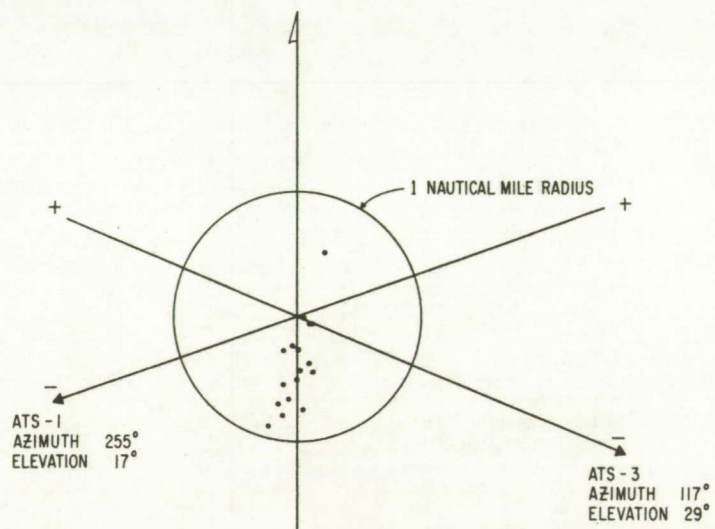


FIGURE 7-13

FIX ERROR DISTRIBUTION
USCGC VALIANT (WMEC-621)
1 July 1969, 03 08 30 - 03 11 54 GMT

Ship Heading: W to NW
Antenna Shielded From ATS-3
71 Interrogations
37 ATS-1 Responses
27 ATS-3 Responses
22 Dual Responses

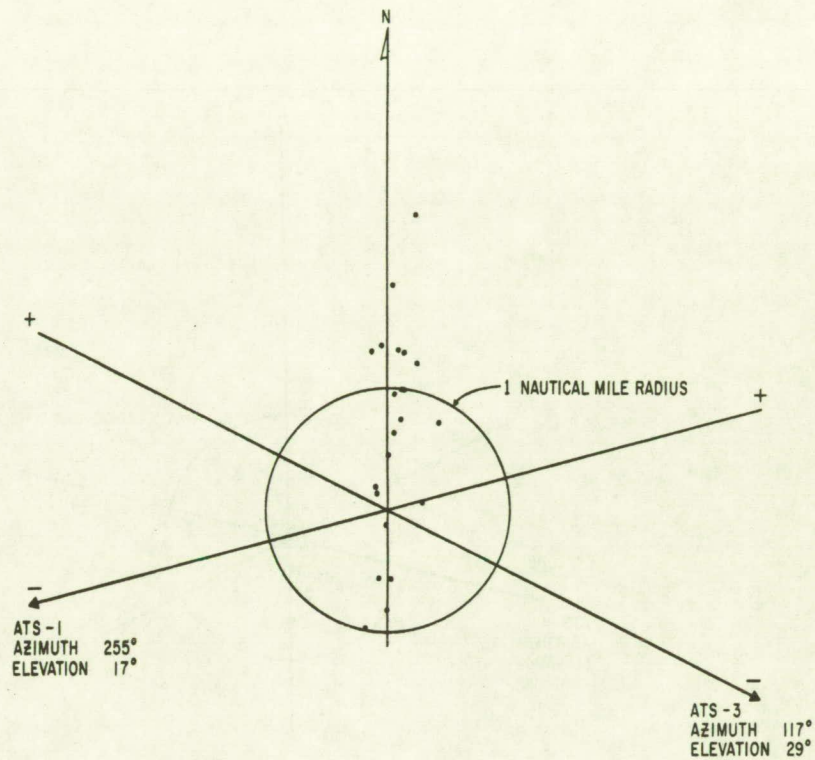


FIGURE 7-14

FIX ERROR DISTRIBUTION
USCGC VALIANT (WMEC-621)
1 July 1969, 03 11 57 - 03 14 09 GMT

Ship Heading: NNE
44 Interrogations
40 Dual Responses

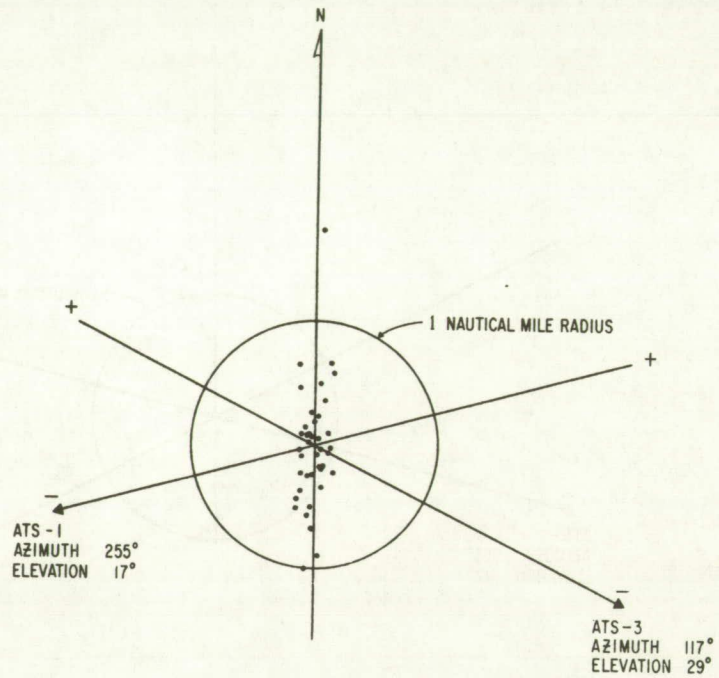
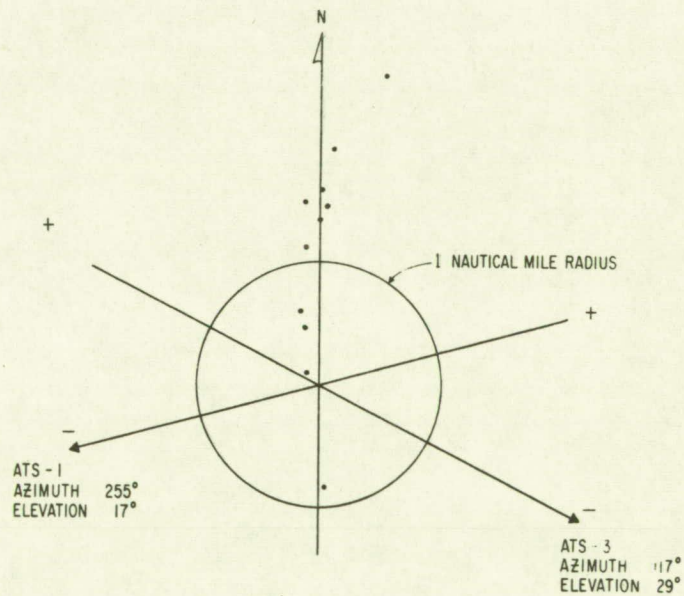


FIGURE 7-15

FIX ERROR DISTRIBUTION
USCGC VALIANT (WMEC-621)
1 July 1969, 03 14 15 - 03 17 39 GMT

Ship Heading: NE-E-SE
Antenna Shielded From ATS-1
70 Interrogations
46 Responses from ATS-3
17 Responses from ATS-1
15 Dual Responses



SECTION 8

BUOY TESTS

The first tone-code ranging transponder that was placed at a remote location and interrogated through a satellite was on a deep moored buoy anchored off Bermuda with checkout and harbor test in February/March and deep moored test in April/May of 1969. The experiments were supported by the Office of Naval Research under contract N00014-68-CO467 and by the General Electric Company's Ocean Systems Programs. The General Electric experimental buoy, Sea Robin, was modified to serve as a support test platform for the comprehensive experiment. Three basic communications experiments were conducted in this program. Each experiment was supplied by a different organization and integrated into the buoy and its support subsystems by General Electric Ocean Systems. NASA's Goddard Space Flight Center provided the OPLE (Omega Position Location Experiment) Platform Electronics Package. The OPLE Control Center in Greenbelt, Maryland periodically interrogated the package through the ATS-3 satellite and read out the OPLE data.¹ A Company-sponsored direct link experiment transmitted data on four HF links from the buoy to a receiving station at General Electric's Electronics Laboratory in Syracuse, New York. Field support was provided by the U.S. Navy Underwater Sound Laboratory at TUDOR HILL, Bermuda and by the U.S. Naval Station, Bermuda. Ship services were furnished by the Geophysical Field Station of Columbia University at St. Davids, Bermuda.

Tone-Code Ranging and Data Readout

During the period February through May of 1969 the buoy was tested ashore, in the harbor, and at a deep sea mooring near Bermuda, at 32°10'00" N, 64°55'30" W. Tone-code interrogating signals addressed to the buoy were transmitted from General Electric's Radio-Optical Observatory near Schenectady, New York to NASA's Applications Technology Satellite, ATS-3. The satellite repeated the interrogation. The buoy received the signals, recognized its own address, and responded with a tone-code signal followed by a data transmission. The satellite received and retransmitted the buoy's response, which was received at the Observatory. Propagation time measurements were made to determine the range from the satellite to the buoy, and the sensor data readouts were recorded on magnetic tape. The complete interrogation and response, including the ranging time measurement and data recording, were completed in little more than one second. Many independent measurements and data recordings were obtained by interrogating the buoy each three seconds.

Equipment on the buoy consisted of a small mobile radio-receiver of the type used in police cars and taxi-cabs, a solid-state RF power amplifier of 120 Watts output, a solid-state "tone-code" ranging responder 6 inches by 8 inches by 10 inches in size, means to couple the responder to the digital sensors, and dipole antennas. As the buoy was in view of only one satellite, the range measurements provided only lines of position. The accuracies of the lines of position were determined by computing the latitude at which they crossed the known longitude of the buoy, and comparing the results with the known latitude.

All objectives of the experiment to read data and locate the buoy by satellite were fulfilled, and the following results were obtained:

- The buoy was interrogated with its individual address through the satellite and it responded with a verification of its address, a signal from which its location could be determined, and a readout of its sensor data in digital form.
- Data readout of more than one complete frame of bits at 305 bits per second, or more than eight complete frames of bits at 2.4414 kilobits per second was accomplished in 1.25 seconds with an RF transmission energy of 200 Watt-seconds.
- Under best signal conditions of the experiment, the digital error rate was 3.3×10^{-2} at 2.4414 kilobits per second. The number of bits available for analysis at 305 bits per second was not sufficient for a statistical evaluation; a burst error caused the loss of two bits in the 4496 analyzed. Extrapolation from the 2.4414 kilobits per second rate based on laboratory tests with random noise interference, suggests bit error rates at 305 bits per second will be as low as 10^{-8} at the best signal-to-random-noise conditions of the test.
- Line-of-position measurements within ± 1 nautical mile, 1 sigma of the latitude of the buoy mooring were accomplished with an RF transmission energy of less than 50 Watt-seconds per measurement. Largest deviations of any of the 759 determinations were 3.25 nautical miles north and 2.75 nautical miles south of the mooring latitude. Winds and currents moved the buoy from south to north of the mooring, and the measured positions follow the motion expected from the wind. Diurnal variations in measurements suggest that better knowledge of the ionosphere and the satellite position would improve line-of-position accuracy to approximately ± 0.5 nautical mile, 1 sigma.

Ranging and data readout performance were observed under varying signal and environmental conditions. Information obtained during the experiment provided engineering data for systems that would accomplish rapid, reliable data readout and location of each buoy in a large number of buoys deployed over entire oceans. The small size and low energy requirements of the tone-code technique make it attractive for air-droppable buoys with long unattended life. The use of solid-state conventional components and circuits minimize cost and contribute to reliable performance.

A block diagram of the buoy subsystem is shown in Figure 8-1. The buoy VHF antenna (Figure 8-2) design provides for a beamwidth of 100 degrees with a nominal gain of +3 dB 50° off the horizontal. Polarization diversity is desired on the buoy to assist in evaluating VHF propagation as affected by multipath (as a result of sea state/buoy motion), and Faraday rotation of the transmitted polarization. The antenna consists of four sets of "V" shaped dipole elements located 90° apart with opposite elements used as a pair for a given polarization. The desired pattern shape is controlled by varying the distance between the elements and a five foot ground plane, and the elements' inclination angle from the local vertical. Antenna patterns are shown in Figures 8-3 and 8-4.

The antenna pair to be used at any time is controlled by the VHF antenna coupling network. It consists simply of an interconnection of RF switching and control relays. The network provides complete flexibility to select transmission and reception on either polarization, or reception on one and transmission on the other.

FIGURE 8-1

ATS BUOY SUBSYSTEM BLOCK DIAGRAM

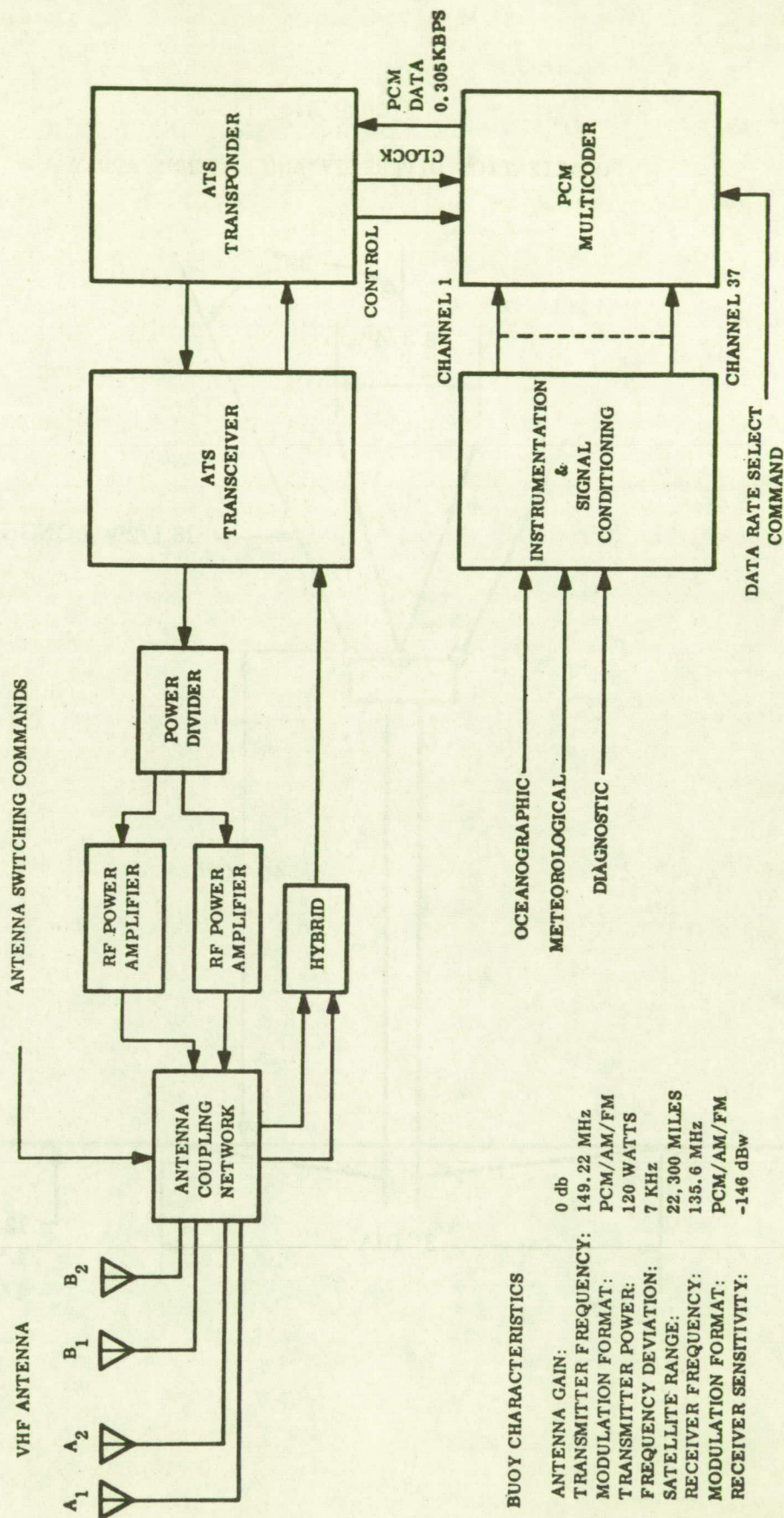
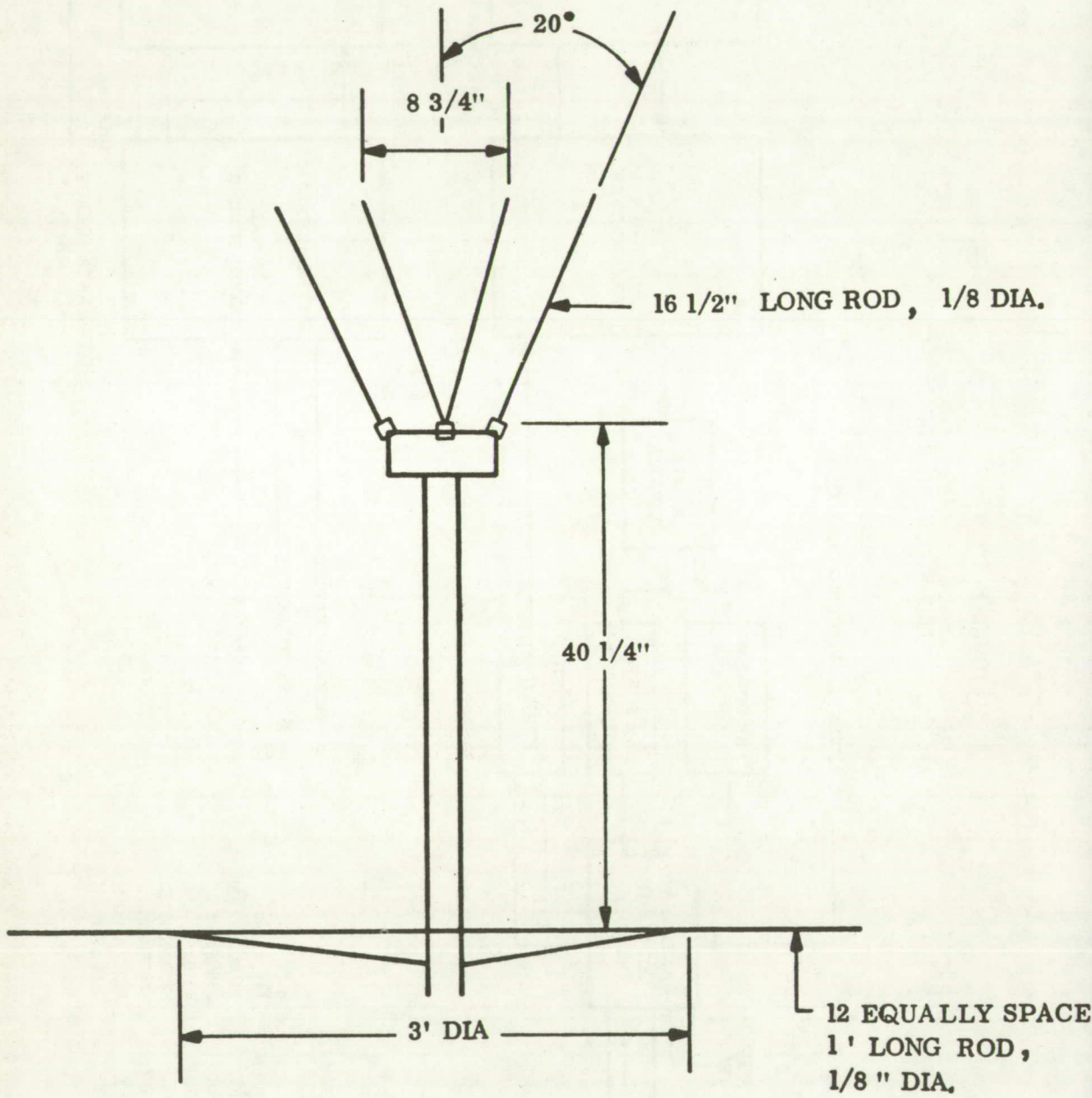
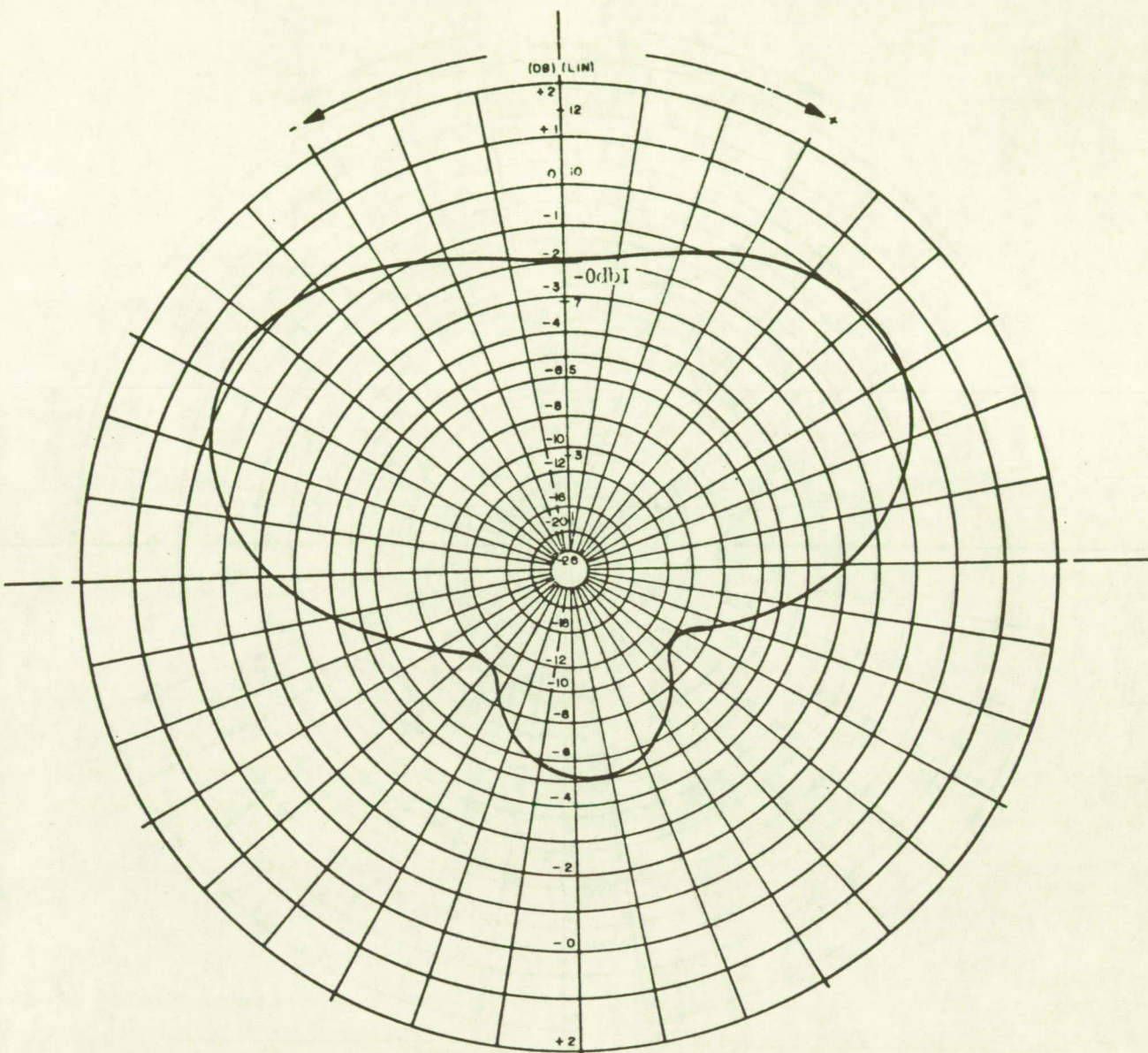


FIGURE 8-2

POLARIZATION DIVERSITY AND ANTENNA ARRAY



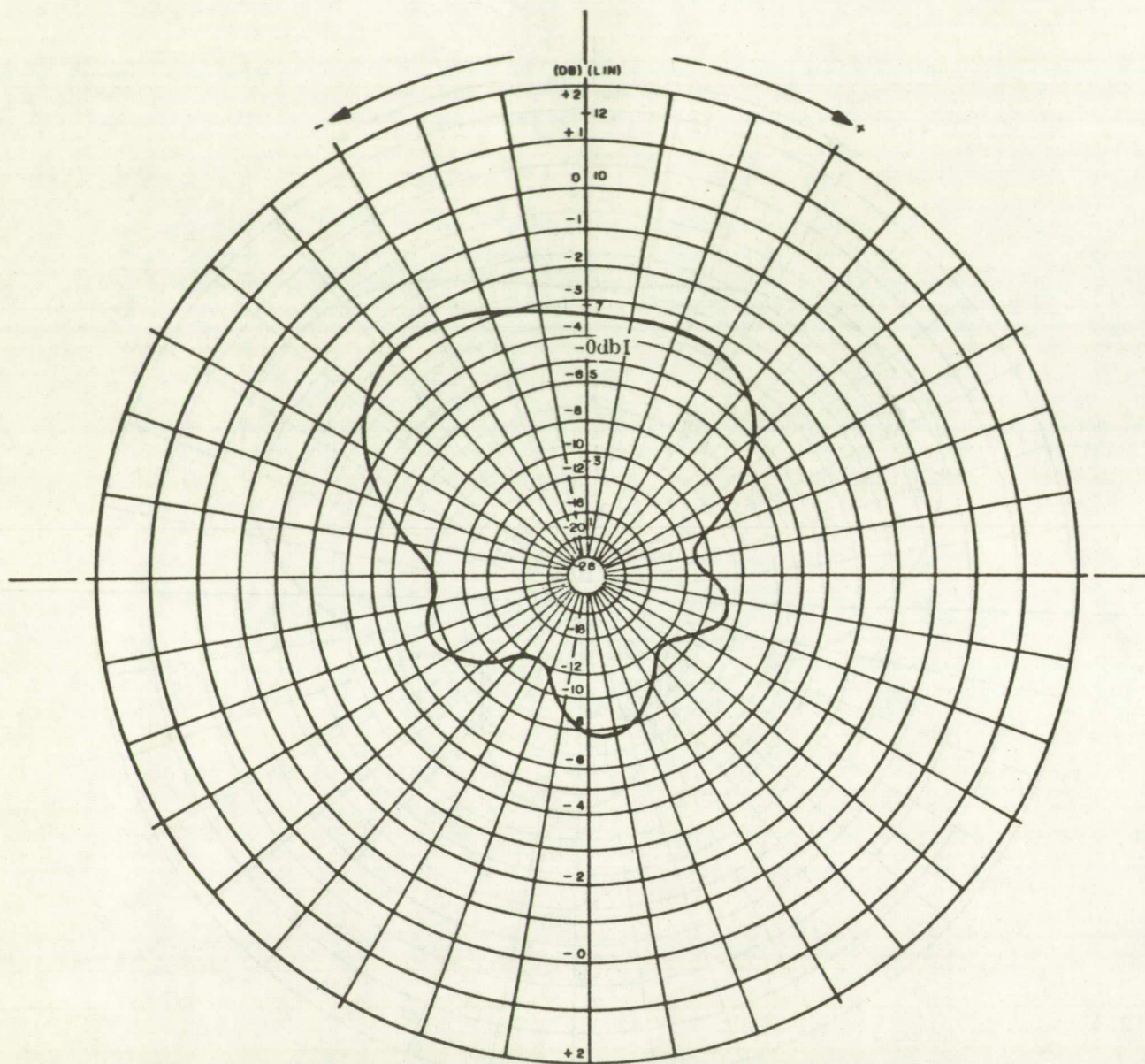


FREQ. - 140 mc	VAR. ANGLE - θ
POLARZ - E ϕ	PATTERN NO. - 2
DATE - 10/18/68	OBSERVER
VOLTAGE (✓)	POWER () LOG ()

NOTES -
OUT OF PHASE
Gnd PLANE 40" BEHIND FEED
20 db ATT.

FIGURE 8-3

140 MEGACYCLE E ϕ ANTENNA PATTERN



FREQ. - 140 mc	VAR. ANGLE - θ
POLARZ - $E\theta$	PATTERN NO. - 3
DATE - 10/16/68	OBSERVER
VOLTAGE (✓)	POWER () LOG ()

NOTES -
180 OUT OF PHASE
15 db ATT.
Gnd PLANE 40 1/4"

FIGURE 8-4

140 MEGACYCLE $E\theta$ ANTENNA PATTERN

The outputs of the coupling network are combined in a hybrid before they are presented to the buoy ATS FM receiver. The solid-state receiver used in the experiment is a modified receiver half of a standard General Electric mobile radio transceiver. Modifications included the removal of the receiver's de-emphasis and output filter networks and the addition of an AGC circuit and associated telemetry monitoring point. The detected output in the form of the gated 2.4414 kHz sine wave is presented to the ATS transponder.

The ATS transponder consists of an address decoder, phase matcher, stable oscillator, divider, and gating circuit. Within the transponder the phase of the incoming synchronizing tone burst is compared to the phase of a locally generated 2.4414 kHz signal derived from a highly stable source. The phase matcher adjusts the phase of the local signal to agree with the received signal. This phase matcher adjusts the phase of the local signal to agree with the received signal. This phase-matched local signal provides the necessary modulating, synchronizing, and gating signals for the complete buoy subsystem response. Once phase match has occurred, the transponder is conditioned for receipt and detection of the 30 bit digital address. This is accomplished in the address decoder which consists of a shift register and summing circuit prewired for the particular address.

Upon address recognition, a precise time delay is introduced for the purpose of switching from the receive to transmit mode of operation. At the completion of this switching operation, the phase-matched, locally generated 2.4414 kHz signal is outputted to the transmitter. This is followed by the 30 bit reconstructed address code. The modulation format takes the same form as that used for the interrogation signal.

At completion of the reading out of the address code, the subsystem is prepared for the transmission of one frame of PCM telemetry data. At this time, clock and control signals are forwarded to the multicoder for the purpose of resetting and synchronization of the multicoder. Upon receipt of these signals, the multicoder switches from internal clock to the transponder clock and resets itself to the beginning of the frame. The data frame is forwarded to the transponder in an NRZ format in 1.1 seconds. In the transponder, the data, at a bit rate of 1/8 the address code rate, modulates the 2.4414 kHz signal in the same manner as the address code. This modulated signal is forwarded to the transmitter. At the completion of one frame of data, the multicoder generates an end of frame pulse that initiates the sequence of events that terminates the buoy transmission. Upon receipt of the end of frame pulse, the clock and control signals to the multicoder are removed and the data input line disconnected. The multicoder reverts to internal clock. The transponder completes the buoy response by resetting the subsystem back to a receive mode of operation to await the next interrogation signal from the satellite.

The solid-state oscillator-driver that forms the basis for the RF transmitter for the experiment is the transmitter section of the mobile transceiver. The FM modulated 35 Watt RF power output of the transceiver is split in a power divider and its outputs used to drive two 55 Watt solid-state power amplifiers. These outputs are combined in the VHF antenna coupler to drive the selected pair of antenna elements in such a manner as to provide an effective radiated output power of 110 Watts.

Communications margins for the buoy-satellite link were computed in the early design phase of the experiment. For the assumed parameters, these calculations indicated a 6.8 dB margin for the satellite-buoy link and a 2 dB margin for the buoy-satellite link. These calculations are tabulated in Tables 8-1 and 8-2.

TABLE 8-1

ATS MARGIN - DOWN LINK

$$\begin{aligned}
 \text{MS56 Receiver Sensitivity} &= 0.25 \mu \text{ volts ElA } 12 \text{ dB} \\
 &= 1.24 \times 10^{-15} \text{ watts} \\
 &= -150 + 1.0 \text{ dB} \\
 &= -149.0 \text{ dBw}
 \end{aligned}$$

$$\text{Path loss @ 136 MHz and 22,500 miles} = 166.7 \text{ dB}$$

System Losses

$$\begin{aligned}
 \text{Path Loss} &= 166.7 \text{ dB} \\
 \text{Satellite Losses} &= 1.5 \text{ dB} \\
 \text{Buoy Losses} &= 1.5 \text{ dB}
 \end{aligned}$$

$$\text{Total Losses} = 169.7 \text{ dB}$$

System Gains

$$\begin{aligned}
 \text{Transmitted Power} &= 16.0 \text{ dBw} \\
 \text{Satellite Antenna Gain} &= 8.5 \text{ dB} \\
 \text{Buoy Antenna Gain} &= 3.0 \text{ dB}
 \end{aligned}$$

$$\text{Total Gains} = 27.5 \text{ dBw}$$

$$\begin{aligned}
 \text{Received Signal Power} &= -169.7 \text{ dB} + 27.5 \text{ dBw} \\
 &= -142.2 \text{ dBw}
 \end{aligned}$$

$$\begin{aligned}
 \text{System Margin} &= -142.2 \text{ dBw} - (-149.0 \text{ dBw}) \\
 &= 6.8 \text{ dB}
 \end{aligned}$$

$$\text{ATS Down Link Margin} = 6.8 \text{ dB}$$

TABLE 8-2

ATS MARGIN - UP LINK

System Gains

Radiated Power	= P_t dBw
Buoy Antenna Gain	= 3 dB
Satellite Antenna Gain	= 8.5 dB
<hr/>	
Total Gains	= $11.5 + P_t$ dBw

Satellite Receiver NF = 3.5 dB

Path Loss = 167.5 dB @ 149.2 MHz and 22,500 miles

Satellite Receiver NBW = -154 dBw (100 KHz)

System Losses

Path Loss	= 167.5 dB
Satellite Losses	= 1.5 dB
Buoy Losses	= 1.5 dB
<hr/>	
Total Losses	= 170.5 dB

For a 10 dB SNR in the 100-KC Satellite Receiver IF

$$P_t + 11.5 \text{ dB} - 170.5 \text{ dB} = -154 \text{ dBw} + 3.5 \text{ dB} + 10 \text{ dB}$$

$$P_t = -140.5 \text{ dBw} + 159 \text{ dB} = 18.5 \text{ dBw}$$

or

$$P_t = 71 \text{ watts for a 0 dB margin}$$

Actual transmitter power is 110 watts which corresponds to a 2.0-dB margin.

ATS Up Link Margin = 2.0 dB

Buoy Interrogation and Data Readout

For the data transmission, the buoy sensed nineteen housekeeping, weather and oceanographic conditions. Each data transmission totaled 336 bits. Data were transmitted directly by telemetry to a van on shore at Bermuda which also commanded functions aboard the buoy and monitored its position by radar and telescope.

Data transmission through the satellite was accomplished by the use of the transmitter-receiver-responder unit used for the VHF ranging experiment. A data transmission followed each range interrogation as shown in Figure 8-5. Two data rates were tested, 2.4414 bits per second and 305 bits per second. At the higher rate, a "one" bit was formed by transmitting an audio cycle, a "zero" by suppressing a cycle. At the lower rate, eight audio cycles were transmitted for a "one", and eight suppressed for a zero. A complete response from the buoy consisted of the transmission of 1024 cycles at 2.4414 kHz followed by the address code, consisting of 30 bits at the 2.4414 rate, and the address code followed by a 1.25 second data transmission to accommodate slightly more than one complete data frame at the low rate. The radio frequency energy transmitted from the buoy was approximately 50 Watt-seconds for the ranging signal (120 Watts for 0.43 second) and 150 Watt-seconds (120 Watts for 1.25 seconds) for the data transmission.

The transponder aboard the Sea Robin consisted of a 35 Watt, solid-state FM mobile radio transmitter-receiver with a 120 Watt solid-state amplifier, and the first experimental responder unit for phase matching, address correlating, clocking for the digital data readout, and switching of the receiver and transmitter. Despite the early state of the responder development, it performed reliably throughout the test at the mooring. The tests confirmed the advantages of the tone-code ranging technique.

The satellite antenna is linearly polarized. Horizontal and vertical linear, and circular polarization were available at the Radio-Optical Observatory. Sea Robin had two linearly polarized antennas mounted at right angles with a switching arrangement to permit transmission and reception on either, or reception on one and transmission on the other. These antenna arrangements were designed so that information could be obtained about the difference in Faraday rotation between the up-link frequency of 149.22 MHz and the down-link frequency of 135.6 MHz. Separate receive and transmit polarization angles were not available at the Observatory during the test period. The capability was added later. A difference of approximately 90 degrees in the Faraday rotation of polarization at the two frequencies was observed frequently, making it desirable to receive on one linear polarization and transmit on the other. A switching sequence was deliberately introduced at the buoy to observe the effect, resulting in an anticipated failure to respond to some interrogations.

When the buoy was on station, it was determined that the means for measuring received signal amplitude was not sensitive enough for a positive selection of the best receive polarization. As a result, the test was less effective than planned, although useful. One receive polarization was used nearly all of the time, resulting in a smaller ratio of responses to interrogations than would have been obtained had the best receive polarizations been selected for all test periods.

Ranging interrogation periods for Sea Robin totaled 222 minutes between February 13 and May 22, 1969. Full-scale operation testing began on April 13

FIGURE 8-5

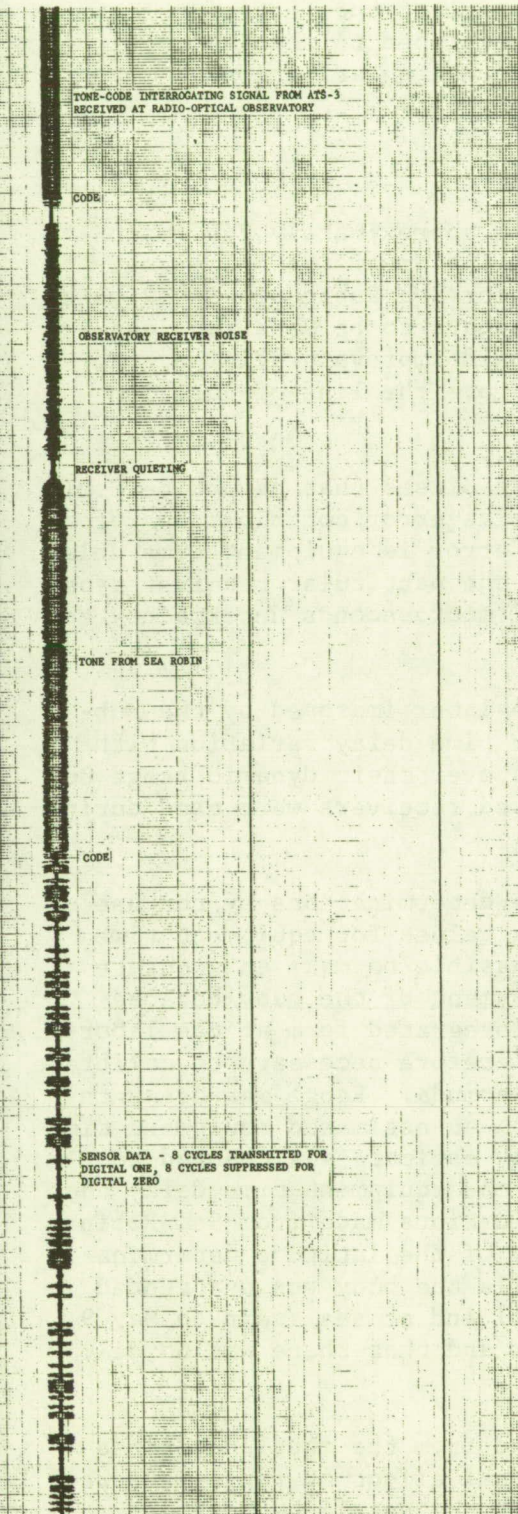
RANGING AND DATA READOUT SIGNALS FROM SEA ROBIN

The compatibility of tone-code ranging with digital communications was demonstrated by transmitting sensor data from the buoy in digital form using the clock of the tone-code responder. A sample read-out is recorded at left.

At the top of the page is the last half of the tone-code interrogation as it was received at the Radio-Optical Observatory. During this time it was also being received by Sea Robin and the tone was used to phase the local tones in the buoy and the Observatory. The code at the end of the tone is evident in the recording as a pattern of 2.4414 kHz transmitted and suppressed cycles. Correlation of the code identifies Sea Robin and provides a timing pulse for the start of the ranging time interval. Receiver noise is evident for the time interval representing the built-in time delay in Sea Robin. The Sea Robin return signal quiets the receiver and the tone reception follows. After the tone, the address code is received and correlated. The time between correlations of the address code at the Observatory is the ranging time interval. Following the code from Sea Robin is a portion of the data read-out at

$$\frac{2.4414}{8} \approx 305 \text{ bits per second}$$

with eight transmitted cycles representing a digital one and eight suppressed cycles representing a digital zero. Sensor data were also successfully transmitted at the 2.4414 kHz rate by transmitting a single audio cycle for a one and suppressing a cycle for a zero, as in the address code transmission.



when the buoy was anchored 6.5 miles south of Bermuda in 4272 feet of water. Operation of the system continued periodically until May 30, 1969 when testing was terminated and the buoy and complete mooring were recovered. While at the deep sea mooring, an interrogation period was three minutes long with an interrogation to the buoy each three seconds. Each interrogation period was preceded by a 30 second tone transmission from the ground station through the satellite. The signal was received in the control van at Bermuda, where the best of two linear polarization angles was determined. The Sea Robin VHF antenna was then switched by command from the van to select the best of the two polarization choices for reception. The buoy was equipped to receive on either polarization and transmit on the same or the orthogonal polarization.

Ranging and Positioning

Range measurements had a standard deviation of approximately 2.0 microseconds, as shown in Figure 8-6 representing a ranging precision of approximately 1000 feet and a line-of-position precision for Sea Robin of approximately 1400 feet. Distribution of the measurements appears to be Gaussian, suggesting that averaging a number of measurements would improve precision. For example, the average of ten measurements would improve the line-of-position measurement precision to approximately 500 feet.

Accuracy is affected by residual variations in biases that cannot be estimated for a particular measurement. The largest bias error contribution for Sea Robin is the ionosphere. Another significant error is equipment time delay change with signal amplitude. The ionosphere and the particular receiver type used in the experiment can each contribute several microseconds uncertainty to a range measurement.

Receivers at the Schenectady Observatory were later improved by the substitution of different limiters that reduced their time delay variation with signal amplitude from approximately 7 microseconds over their dynamic range to less than one microsecond. The original, unimproved receivers were used during the Sea Robin tests.

Range measurements were converted to latitude determinations by the use of the LATCOM computer program. The program requires values for equipment time delays and ionospheric corrections. It was not feasible to make an accurate calibration of equipment time delay prior to deployment of the buoy because all components were not available in their final integrated form at the laboratory in Schenectady prior to shipment. It was therefore necessary to calibrate equipment time delay with the buoy on station at Bermuda. Range measurements made during one interrogation period were used with an estimated equipment time delay to determine the latitude, and the time delay estimate was changed to correct the result. It is important to note that the equipment time delay thus determined was used for all other latitude determinations made from Sea Robin range measurements. The correctness and constancy of the latitude determinations over the period from April 14 through 25 while the buoy was unattended at sea, while it was in the harbor earlier in April and at sea again on May 9 and 10, indicates that the calibration was correct and that there was no detectable change in calibration over the period.

Corrections for the ionosphere were determined from the model described in Appendix II. There is evidence of another diurnal effect on range measurement due to a small uncertainty in the knowledge of the satellite position.

FIGURE 8-6

RANGING AND POSITIONING

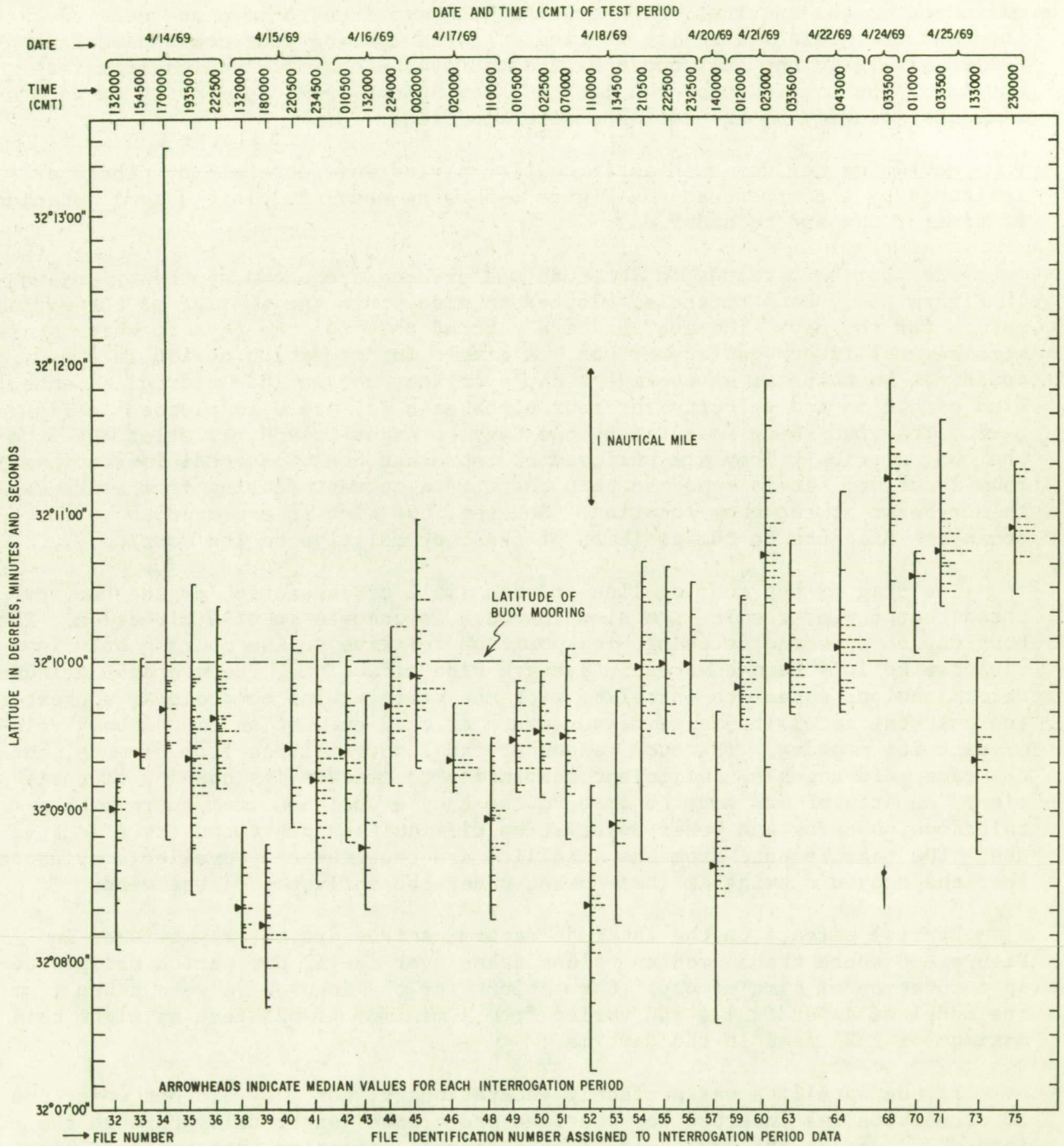


Figure 8-6 is a plot of all the 759 latitude determinations made during the period from April 14 through 25. They are plotted as histograms, one for each of the 33 three-minute interrogation periods. Calendar day and time of day are indicated for each period. The standard deviation of the latitude determinations referenced to the mooring latitude is approximately ± 1 nmi, 1 sigma. The largest displacement of any measurement is approximately 3.5 nmi. north and 2.8 nmi south of the mooring. Only one measurement was more than 2 nmi north or the mooring. However, the buoy was free to move at least several thousand feet relative to its mooring. If the mooring line could have been pulled straight, the buoy could have moved over a one mile radius from its mooring. The magnitude of the latitude deviations from the mooring do not define the accuracy of the latitude determinations.

Median values for each interrogation period were determined. These are indicated by the arrowheads on Figure 8-6 where they are plotted as a function of time of day and calendar day.

The long term trends in latitude measurement are shown by the triangles in Figure 8-7. Each triangle, plotted at midday, is the average of the median values for the day. The averages are plotted only for the days on which there were several interrogation periods. A single interrogation period in a day could not be taken as an average because it does not include diurnal effects. Wind direction and velocity for four times each day are also plotted on Figure 8-7. The winds were measured by the Navy at Argus Island, 15 miles WSW from the buoy mooring. They are believed to represent the wind conditions at the buoy location. It is reported that there is a current flowing from southwest to northeast at the buoy location. However, the wind is expected to be the dominant influence on the position of the buoy relative to its mooring.

The drag of the mooring line and the small cross section of the buoy exposed to the wind result in a slow response to changes in wind direction. The buoy can be expected to change its position relative to the mooring only in response to long-term changes in average wind direction. The average latitude determinations appear to correlate with the average wind conditions, suggesting that the satellite range measurements tracked the motion of the buoy relative to its mooring. The buoy was under radar surveillance from Bermuda, but the radar did not have sufficient resolution to measure its changes of position. An attempt was made to observe the buoy's position from shore with a telescope, but fog and other observation difficulties prevented its effective use. The measurements from the satellite are thus the only available evidence that the buoy did swing at its mooring under the influence of the wind.

Diurnal effects on the latitude determinations are clearly evident in Figure 8-8 where the 33 median values taken over the 12 day period are plotted as a function of time of day. Corrections for the ionosphere were taken from the model of Appendix II, and varied from a minimum of 625 feet at night to a maximum of 2325 feet in the daytime.

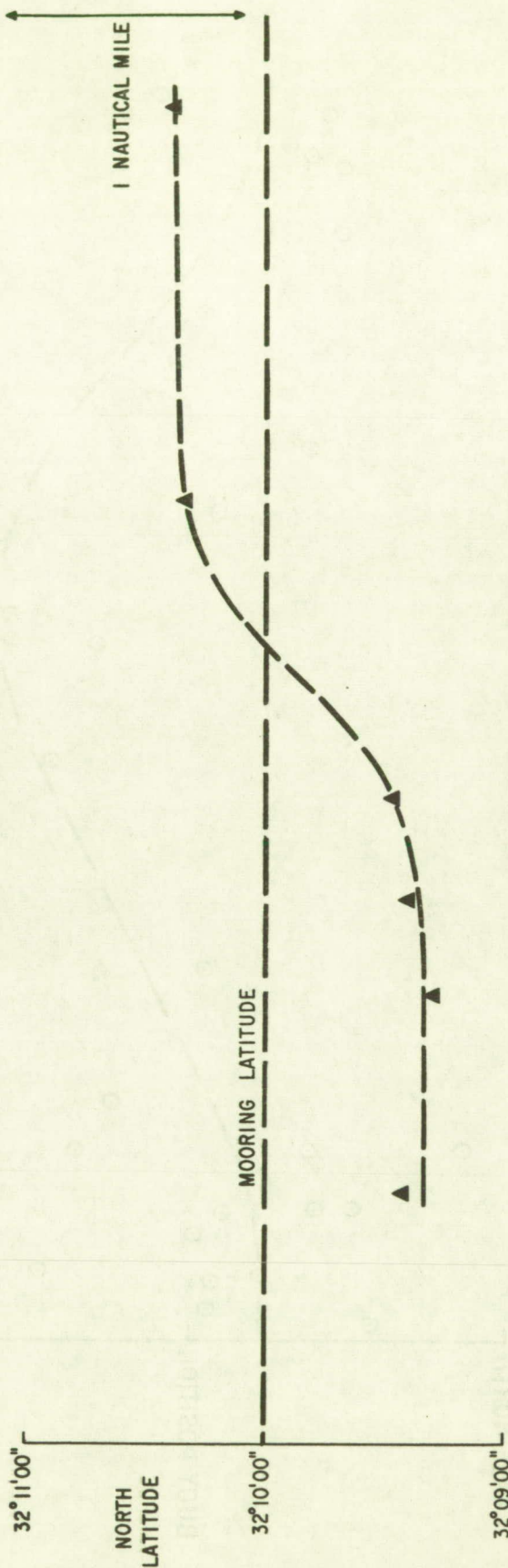
If the satellite was perfectly geostationary, the buoy did not move, and no correction was inserted for the ionosphere, the longer delay through the ionosphere during the day would cause a diurnal variation that would displace the measured latitude toward the north in the daytime. The ionosphere model in the computer program is intended to correct for the diurnal change in radio propagation path delay and result in improved accuracy through the day.

FIGURE 8-7

ESTIMATED BUOY POSITION

CALENDAR DAY - April 1969

| 4/13 | 4/14 | 4/15 | 4/16 | 4/17 | 4/18 | 4/19 | 4/20 | 4/21 | 4/22 | 4/23 | 4/24 | 4/25 |



▲ TRIANGLES ARE AVERAGE OF MEDIAN POSITIONS FOR DAYS INDICATED

FIGURE 8-8

DIURNAL VARIATION OF LATITUDE MEASUREMENT ERROR

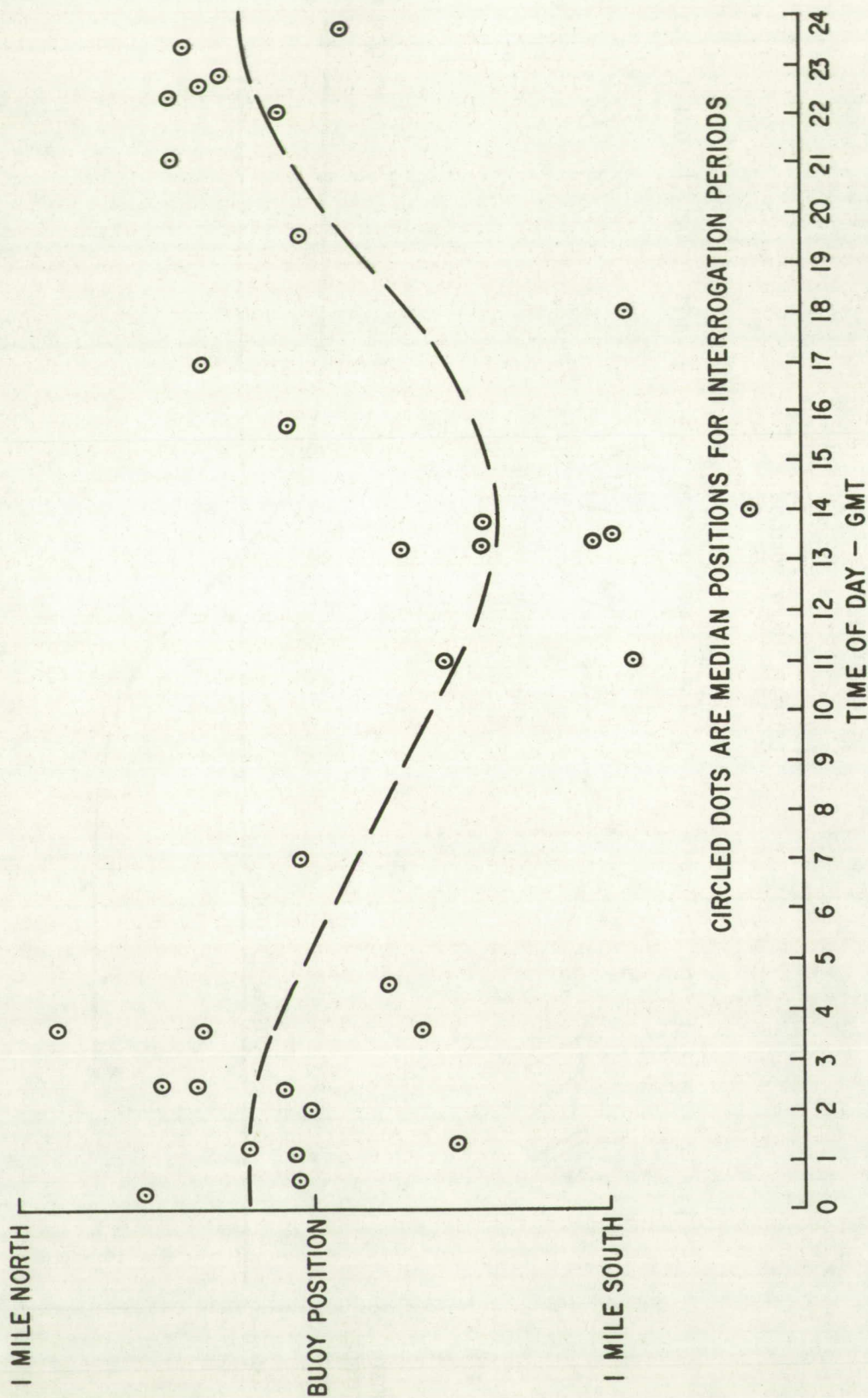


Figure 8-7 shows that the latitude determinations in the daytime hours are south of the nighttime determinations, as would be the case if the ionosphere model estimated a diurnal change in path delay that is larger than the actual change. However, an examination of the magnitude of the change shows it to be larger than the total ionosphere correction inserted by the model. Some other diurnal effect must have affected the latitude determinations.

The satellite position is the only other factor with a diurnal variation that we can identify. The satellite orbit is slightly inclined to the earth's equatorial plane so that the sub-satellite point traces a figure-eight pattern on the earth, moving north and south of the equator, with a 24-hour period. On April 14 the maximum northward excursion of the satellite was 0.313 degree at approximately 14:30 GMT, and the maximum southward excursion was also 0.313 degree at approximately 02:30 GMT. By April 25 the motion had changed slightly to maximum north and south excursions of 0.286 degree at 14:00 GMT and 02:00 GMT respectively. It is interesting to note that the extremes of the latitude displacements occur at corresponding times, although the times at which the satellite had its greatest and least earth center distances do not correspond to these times. Uncertainty in earth center distance could also affect the latitude determinations. On April 14, the earth center distance varied from a maximum of 22,756.4 nmi at 05:30 GMT to a maximum of 22,749.2 at 17:30 GMT, and on April 25 from 22,756.8 nmi at 05:30 GMT to 22,750.2 nmi at 17:00 GMT.

If the ionospheric correction was of the right magnitude, there is a residual diurnal variation of approximately $\pm 3,000$ feet, representing an imprecision of approximately ± 0.01 degree at the extremes of the satellite positions. The imprecision could be due to computer round-off in our linear interpolation between the half-hourly satellite position predictions of NASA, to inaccuracy in the predictions, or to a combination of such factors.

Figure 8-6 plots the latitude determinations as actually measured. It does not indicate the accuracy of measurements because the buoy was free to move relative to its mooring. If the average change in the latitude measurements, shown in Figure 8-7, represent the actual motion of the buoy, accuracy of the latitude determinations can be estimated by comparing the latitude determinations with the buoy latitudes as shown by the dashed line in Figure 8-7. A histogram of the latitude determinations plotted relative to the estimated positions of the buoy is presented in Figure 8-9. The accuracy indicated by the plot is approximately ± 0.7 nautical mile, 1 sigma.

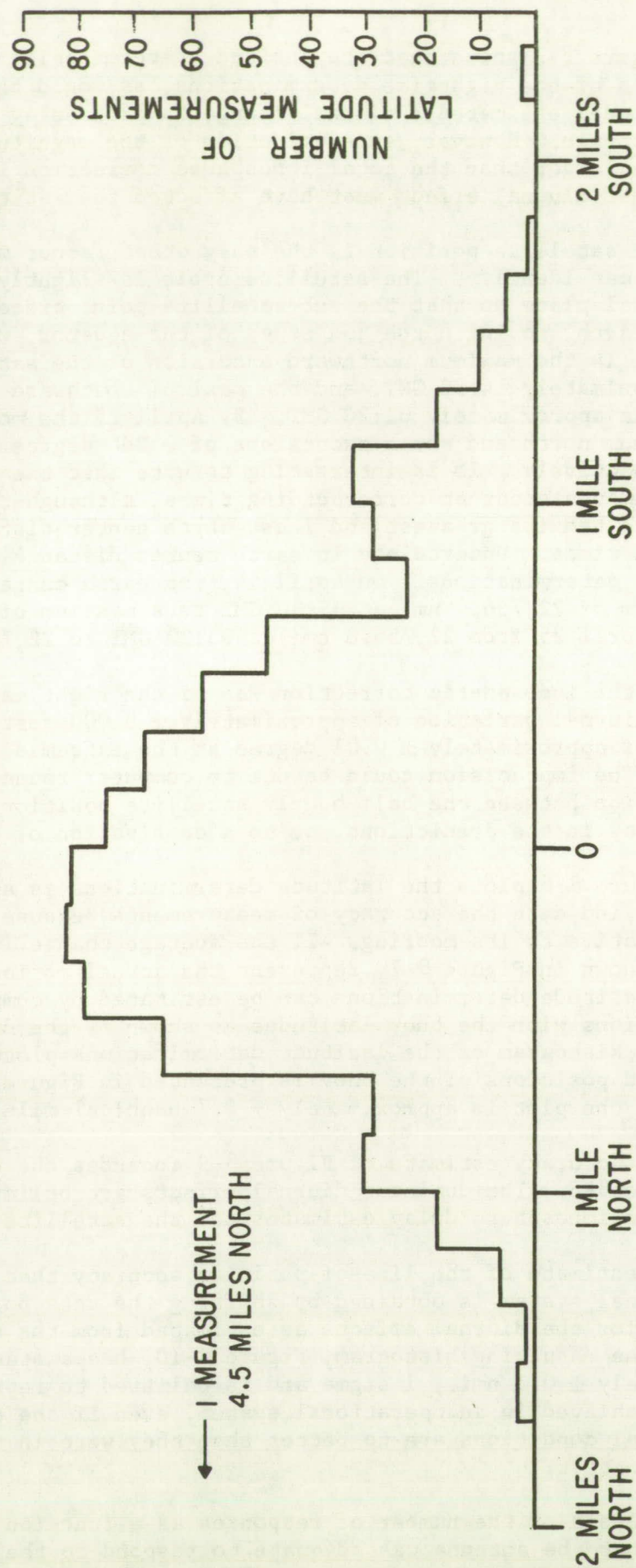
The accuracy estimate of Figure 8-9 includes the diurnal effects shown in Figure 8-8. The dominant diurnal effects are believed to be due to imprecision in ionosphere delay estimates and the satellite reference positions.

An estimate of the line-of-position accuracy that would be achieved in an operational system is obtained by shifting the data points of Figure 8-10 to correct for the diurnal effects as estimated from the dashed curve of Figure 8-8. The resulting histogram, Figure 8-10, has a standard deviation of approximately ± 0.5 nmi., 1 sigma and is believed to represent the accuracy that can be achieved in an operational system, even if the equipment, techniques, and signal conditions are no better than they were in the April 14 through 25 Sea Robin test.

Analysis of the number of responses as a function of buoy attitude revealed that the antenna was adequate to respond to the satellite interrogations

FIGURE 8-9

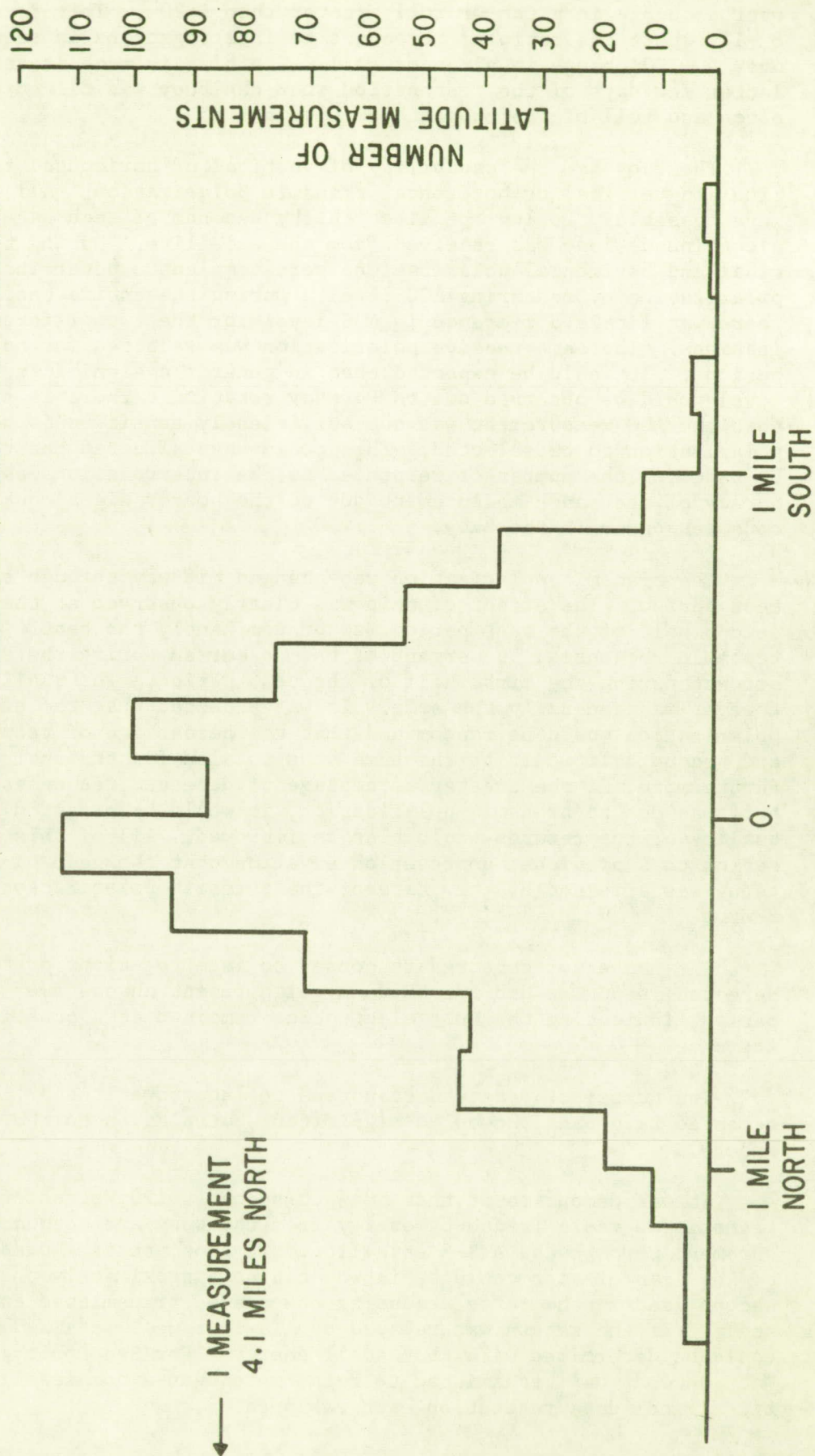
DISTANCE FROM ESTIMATED BUOY POSITION (ESTIMATE OF ACCURACY ACHIEVED)



1 MEASUREMENT
4.5 MILES NORTH

FIGURE 8-10

ESTIMATE OF RESIDUAL ERRORS AFTER CORRECTION FOR IONOSPHERE AND
SATELLITE POSITION UNCERTAINTY (ESTIMATED ACCURACY IF CALIBRATION
STATION HAD BEEN USED)



over a change in pitch or roll greater than $\pm 20^\circ$. This is shown in Figure 8 -11, where the ratio of responses to interrogations is seen to be constant over a $\pm 20^\circ$ change in pitch or roll. The bias in each is attributed to the latter few days of the test period when the buoy was tilted slightly. Normal pitch and roll of the buoy stayed within $\pm 15^\circ$.

The buoy had the capability of vertical or horizontal receive polarization and vertical or horizontal transmit polarization. All four combinations were possible. During the first thirty seconds of each satellite test period a continuous tone was received from the satellite. During the tone both vertical and horizontal polarizations were sampled to determine the best receive polarization by measuring AGC level. During the entire test of the buoy, there was little difference in AGC level for the two different receive polarizations. The same receive polarization was selected for most of the test periods. It would be expected that in general a significant difference in AGC level would be observed due to Faraday rotation. There is some indication that the AGC measurement was not sufficiently sensitive to permit the optimum polarization to be selected. This could have affected the results considerably by reducing the number of responses to the interrogations as well as the accuracy of the range measurement due to the poorer signal quality into the tone code responder in the buoy.

The transmit polarization was changed mid-way through each three minute test period. The effect of this was clearly observed at the Observatory. The second half of the test period was predominantly the best. Of the total detectable responses, 55 percent of them occurred during the second half and 45 percent during the first half of the test period. The quality of the returns however was generally the same. It was expected that the effects of transmit polarization would be random and that the percentage of returns for the first and second half would be the same when totaled for the entire test period. Furthermore, if the greater percentage of detected responses in the second half was due to transmit polarization, it would be expected that the overall quality of the returns would also be improved. All of this gives some verification to a previous, unproven observation that the gain of the receiving antenna was affected by the state of the transmit polarization switching arrangement.

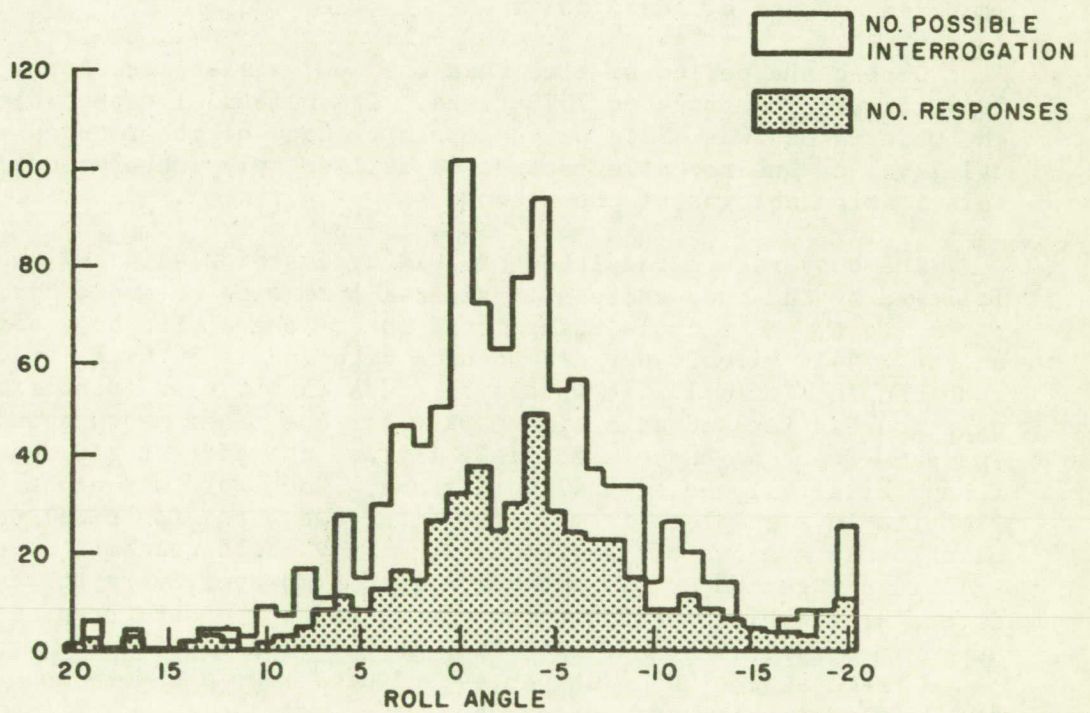
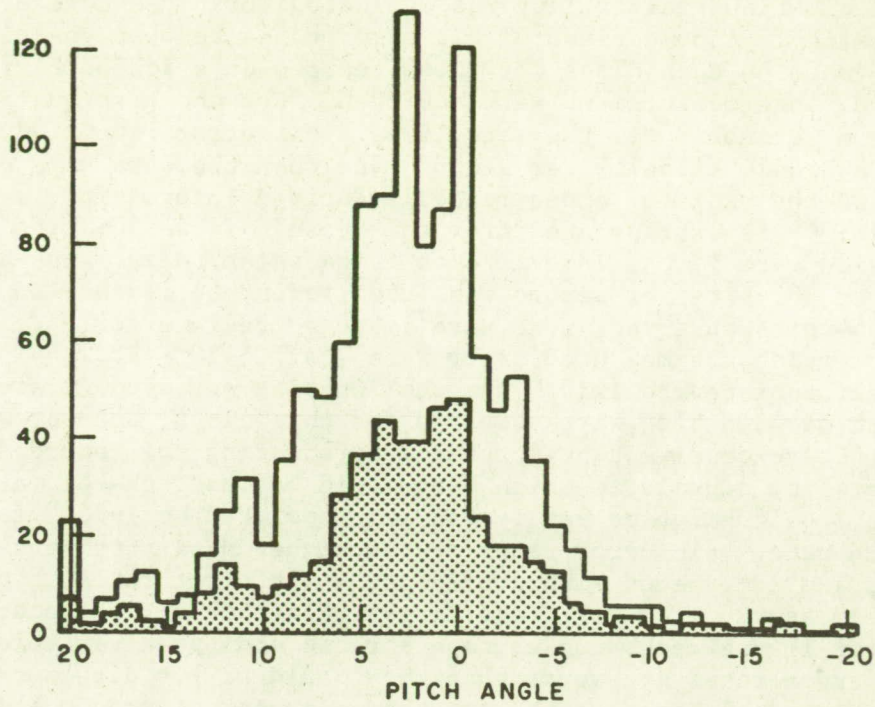
The number of detected responses to interrogations or the quality of the detected responses did not show any significant change over the entire test period, indicating the buoy electronics remained at a constant level of performance.

The number of detected responses to interrogations or the quality of the detected responses showed no significant correlation to the state of the ionosphere.

It was demonstrated that 50 Watt-seconds (120 Watts for 0.43 second) of transmitted radio frequency energy from the buoy are adequate for a range measurement through the ATS-3 satellite. In fact, tests showed that the duration of the transmission could be introduced to approximately one-half the 0.43 second used in the tests, reducing the needed transmitted energy proportionately. If the return was relayed by ATS-1 as well as ATS-3, a position fix could be determined with that small energy. For Sea Robin, an additional 150 Watt-seconds was transmitted to relay more than a complete frame of the 320 bit digital data readout on each response.

FIGURE 8-11

RESPONSE/PITCH AND ROLL ANGLES



Communication Reliability

Communications reliability was evaluated for three categories of received signal quality. A comparison of bit error rates between the high and low data rates was made on each class for those returns on which both frame sync recognition and range measurement were achieved. For the best quality signals received from Sea Robin via the satellite, a bit error rate of 3.3×10^{-2} was measured at a 2.4414 kilobits per second rate when the data were processed as received. On the basis of experimentally derived information, a bit error rate of only 1×10^{-8} is extrapolated from this result for a 305 bits per second transmission rate if the interference is gaussian noise. The amount of data recorded at 305 bits per second was insufficient to measure an error rate. Out of 4064 bits observed, none were found to be in error. For the medium quality signals, the measured error rate was 7.5×10^{-2} at 2.4414 kilobits per second, extrapolated to 1×10^{-6} for the 305 bits per second rate. Five bit errors out of 4368 bits were observed for this class, but three of these are attributed to excessive tape stretch in processing the recorded data. For the poorest quality signals at which data could be read, the bit error rate was 1×10^{-1} at 2.4414 kilobits per second, extrapolated to 1×10^{-4} for the 305 bit per second rate. Bit error rates at the higher data rate were recorded as received, and are viewed with confidence. Bit error rates at the lower data rate were measured from tape recordings. Playback of the recordings introduced noise-like effects due to tape stretch and speed variations so that the observed error rates are worse than they would be for direct readout. The extrapolations are based on the repeated playback of good quality signals with measured amounts of added noise.

During the period of time that the buoy was at sea, April 14 through 25, 1969, it was interrogated 2525 times. The number of detectable responses at the Observatory was 1711, or 68 percent. Many of the returns were of low signal level or undetectable because of deliberately introduced factors, such as polarization changes of the antenna.

The buoy return consisted of 1024 cycles of 2.4414 kHz tone immediately followed by the buoy address in digital form with an audio cycle suppressed for a "zero" and a cycle transmitted for a "one". The buoy address is also at the 2.4414 kilobit per second data rate and is 30 bits long. The address code consists of a 15 bit word sync and a 15 bit user identification. The user address is used as a time marker for the range measurement determination. The data from the buoy immediately follows the address and consists of eight random bits followed by a 40 word frame. Each word was eight bits long with 320 bits in a complete frame. The first two words (16 bits) were frame synchronization of a known bit sequence. The buoy could transmit at either 2.4414 kilobits per second or 305 bits per second. However, very few data returns were at the 2.4414 kilobits per second data rate. The data transmission was for approximately 1.2 seconds resulting in the transmission of more than one complete frame at the 305 bits per second data rate and more than nine frames at the 2.4414 kilobits per second data rate.

Statistical information derived from the data processing includes the number of range measurements, the bit error rates at the 2.4414 kilobits per second and 305 bits per second data rates, and relates them to signal-to-noise condition of the returns. The number of range measurements was available on punched paper tape or in hard copy form. Bit errors in the 30 bit buoy address code at the 2.4414 kilobits per second data rate were recorded on punched paper tape as the signals were received from the satellite. This was accomplished

at the time of address code recognition by measuring the voltage level at the outputs of each 15 bit correlator, one for the word sync and one for the user identification portions of the address code. This voltage level is proportional to the number of correct bits. A threshold level was set on each correlator such that if more than three bits were in error in either the 15 bit word sync or 15 bit user identification, address code recognition would not occur and no range measurement would be made.

The bit error rates at the 305 bits per second data rate were determined from the magnetic tape data recordings made at the Observatory. Recordings of the transmissions from the buoy were also made at the control van in Bermuda and were intended as an accurate reference for comparison with the magnetic tape recordings of the satellite signals made at the Observatory. Interference on the magnetic tape recordings made at Bermuda placed their accuracy in doubt, so that it was decided to measure the bit error rates in the known 16 bit frame sync word at the start of each data frame. A demodulator and a 16 bit frame sync correlator were developed for measuring the number of bits in error in each frame sync at the 305 bits per second data rate.

Bit errors were detected by measuring the voltage level at the output of the 16 bit correlator. The threshold level was set so that if there were more than 3 bits in error, frame sync recognition would not occur.

The buoy experiment was designed so that the signal conditions varied over a wide range, thus an overall bit error rate would not be significant. The buoy returns varied in signal-to-noise ratio within a 4 kHz bandwidth from less than 0 dB to greater than 15 dB. This wide range in signal level was due to scheduled changes in transmit polarization from the buoy, changes in the degree of polarization match between the satellite and both the buoy and Observatory antenna due to Faraday rotation, and changes in the attitude and orientation of the buoy antenna due to wave action.

Signal-to-noise ratio measurements were not made on each return from the buoy while the tests were conducted. Instead, the returns were visually classified into three categories of signal quality, A, B, or C, by observing playback of their tape recordings on an oscilloscope. The classification was based upon the data portion of the return only and did not include the 1024 cycles of 2.4414 kHz tone or the 30 bit address code. The "A" class represented returns for which it would appear no errors should exist, the "B" class represented returns where most of the data should be recoverable, and the "C" class represented returns where it appeared little of the data could be recovered.

Of the 1711 detected returns, 22 percent were of "A" quality, 30 percent "B" quality, and 47 percent "C" quality. For each category of returns, a determination was made of the number of range measurements, the bit error rates at the 2.4414 kilobit per second and 305 bit per second data rate, and the average signal-to-noise ratio. A summary of the statistics is presented in Table 8-3.

The statistics obtained for this table do not include all the test periods that were conducted while the buoy was at sea. A few test periods were excluded because a mis-adjustment in a detector threshold setting changed the conditions so that the responses could not be compared statistically with the greater portion of the data. However, the remaining sample size is sufficient

TABLE 8-3
STATISTICAL DATA ON BUOY RESPONSES (NUMBER OF INTERROGATIONS IS 1958)

Statistics on Returns for which Frame Sync was Achieved but a Range Measurement was Not Achieved								Statistics on Returns for which Both Frame Sync and Range Measurements were Achieved							
Data Rate				305 Bit/Sec			305 Bit/Sec			2.4414 Kilobits/Sec			Approximate S/N Ratio		
Sea Robin Data Return Classification	Number of Responses	Number of Range Measurements	Number of Frame Sync Recognitions	Number of Bits Monitored	Number of Bits in Error	Bit Error Rate	Number of Bits Monitored	Number of Bits in Error	Measured Bit Error Rate	Extrapolated Bit Error Rate Based on Bit Error Rate Measured for the 2.4414 Bit/Sec Data Rate	Number of Bits Monitored	Number of Bits in Error	Measured Bit Error Rate	15 kHz I. F.	4 kHz Audio
A	297	254	281	432	2	--	4064	3*	--	1.0×10^{-6}	7620	250	3.3×10^{-2}	5db	9db
B	415	273	366	1488	19	1.3×10^{-2}	4368	5**	4.6×10^{-4}	1.0×10^{-6}	8190	614	7.5×10^{-2}	4db	6.5db
C	633	110	350	3840	181	4.7×10^{-2}	1760	22	1.25×10^{-2}	2.0×10^{-4}	3300	339	1.0×10^{-1}	3db	5db

*These errors attributed to excessive tape stretch or variation in tape speed

**Three of these errors attribute to excessive tape stretch or variation in tape speed

and is representation of the total. The number of interrogations used is 1958 and the total responses 1355. Thus, buoy responses were detected on 69 percent of the interrogations selected for analysis, which agrees closely with the overall response rate of 68 percent. The percentage of responses in the classes A, B, and C are the same as the overall response rate: 22, 31 and 47 percent respectively. The number of range measurements achieved in each class is shown in Table 8-3. The range measurements as a percentage of the number of responses in the classes A, B, and C are 82 percent, 66 percent and 17 percent respectively. The number of frame sync recognitions at the 305 bits per second data rate as a percentage of the number of responses in the classes A, B, and C are 92, 88 and 55 percent respectively. However, not all the responses were properly timed. Some responses were early or late because the buoy produced a correlator output at some time other than when the address code was centered in the correlator. An occasional correlator output occurs early or late by a multiple of a bit period due to noise. This effect results in a loss of a range measurement, but would not necessarily result in a failure to read data. The effect can be eliminated by more sophisticated address code design. In the data analysis, frame sync could not occur on early or late responses because it is not timed properly with respect to the correlator clock, and thus the data was not read out. The percentage of range measurements and frame sync recognitions would be slightly higher if only the properly timed responses were considered.

In determining bit errors the responses in each of the classes, A, B and C, were separated into two sets. One set included those responses on which frame sync recognition was achieved. This was done to permit a comparison between performances at the two data rates which are possible on the set in which both frame sync recognition and range measurement were accomplished.

There were a total of five bits in error in the A class at the 305 bits per second data rate. Two bit errors occurred in one frame sync on a return for which a range measurement was achieved. Each return was displayed on an analog paper chart recording to see the nature of the errors. The return with two bits in error had been affected by a reduction in signal-to-noise for a period of 0.2 second and which included frame sync. The return with three bits in error was of excellent quality, fully recoverable from the tape recording, and the errors are attributed to a large shift on the frame sync position due to excessive tape stretch or a large variation in tape speed at the moment the three passed through the tape recorder. In either set, A or B, the number of bits in error at the 305 bits per second data rate are too small to make an estimate of bit error rates that is statistically significant. However, this can be compensated by the known relationship between the two data rates and a high confidence level on the bit error rates determined for the 2.4414 kilobits per second data rate where the number of accumulated error in all three classes is large.

In the B class there were only five bits in error in the set of returns for which both frame sync recognition and range measurement were achieved. A review of the data revealed that three of these errors occurred in one frame sync which was of good quality. These three errors are also attributed to excessive tape stretch or a large variation in tape speed. As with the A class, the ratio of the number of bits in error to the total number averaged is too small for a reliable statistical estimate of bit error rate. Once again the bit error rate determined for the 2.4414 kilobits per second data rate provides an improved estimate.

In the "C" class, there were 22 bits in error at the 305 bits per second data rate in the set for which both frame sync and range measurement were achieved. Although this is a reasonable sample size for a reliable statistical estimate, it is expected that it has also been affected by tape stretch and variations in tape speed. However, it is difficult to determine this on the "C" type returns due to the poor signal-to-noise ratio preventing any visible estimate on the quality of the frame sync.

The bit error rates shown in Table 8-3 in the set for which both frame sync recognition and range measurement were achieved are plotted in Figure 8-12. Figure 8-12 is a plot of two calibration curves which present bit error rate as a function of the rms signal-to-rms noise within a 4 kHz audio bandwidth. Both curves were produced under controlled conditions using a random noise generator as the noise source. The 2.4414 kilobits per second curve was generated by adding noise to the outputs of the tone-code generator and then feeding the resulting signal directly into the tone-code correlator. The 305 bits per second curve was generated by forming a loop of magnetic tape which contained three "A" type responses and playing it continuously while adding noise from the same random noise generator. The resulting signal was fed into the demodulator and frame sync correlator.

The improvement of the 305 bits per second data rate over that of the 2.4414 kilobits per second data rate can be observed to be approximately 10 dB at signal-to-noise ratios above 0 dB. This agrees with the bandwidth improvement of from 4 kHz to approximately 400 Hz or 10:1.

The bit error rates for the three classes of returns from the buoy are plotted on these two curves.

It would be expected that in each class the bit error rates at the two data rates would align one above the other along a common signal-to-noise ratio. The fact that this does not occur in the "B" and "C" class is a result of the small number of errors not providing a reliable statistic compounded by the effects of the tape recorder which act as additional noise to the system.

There is a higher confidence in the bit error rates for the 2.4414 kilobits per second data rate because they were measured as the signals were received from the satellite and not from the magnetic tape recordings. If the bit error rates at the 2.4414 kilobits per second data rate are projected down to intersect the 305 bits per second data rate calibration curve, the bit error rates at the 305 bits per second data rates for the classes A, B and C are 1×10^{-8} , 1×10^{-6} and 1×10^{-4} respectively. These predictions are based on gaussian noise and ignore the effects of burst errors caused by impulsive noise for which no data is available.

The average signal-to-noise ratio for the three classes is shown in Table 8-3 for the set of returns on which both frame sync and range measurement were achieved. The signal-to-noise in the 4 kHz bandwidth was obtained from Figure 8-3 by observing the signal-to-noise ratio corresponding to the bit error rates determined for the 2.4414 kilobits per second data rate. The signal-to-noise in the I.F. bandwidth was determined from Figure 8-13 which shows the relationship between the audio and I.F. bandwidths for the parameter of the FM system used in the tests.

FIGURE 8-12

BIT ERROR RATE VERSUS SIGNAL-TO-NOISE RATIO

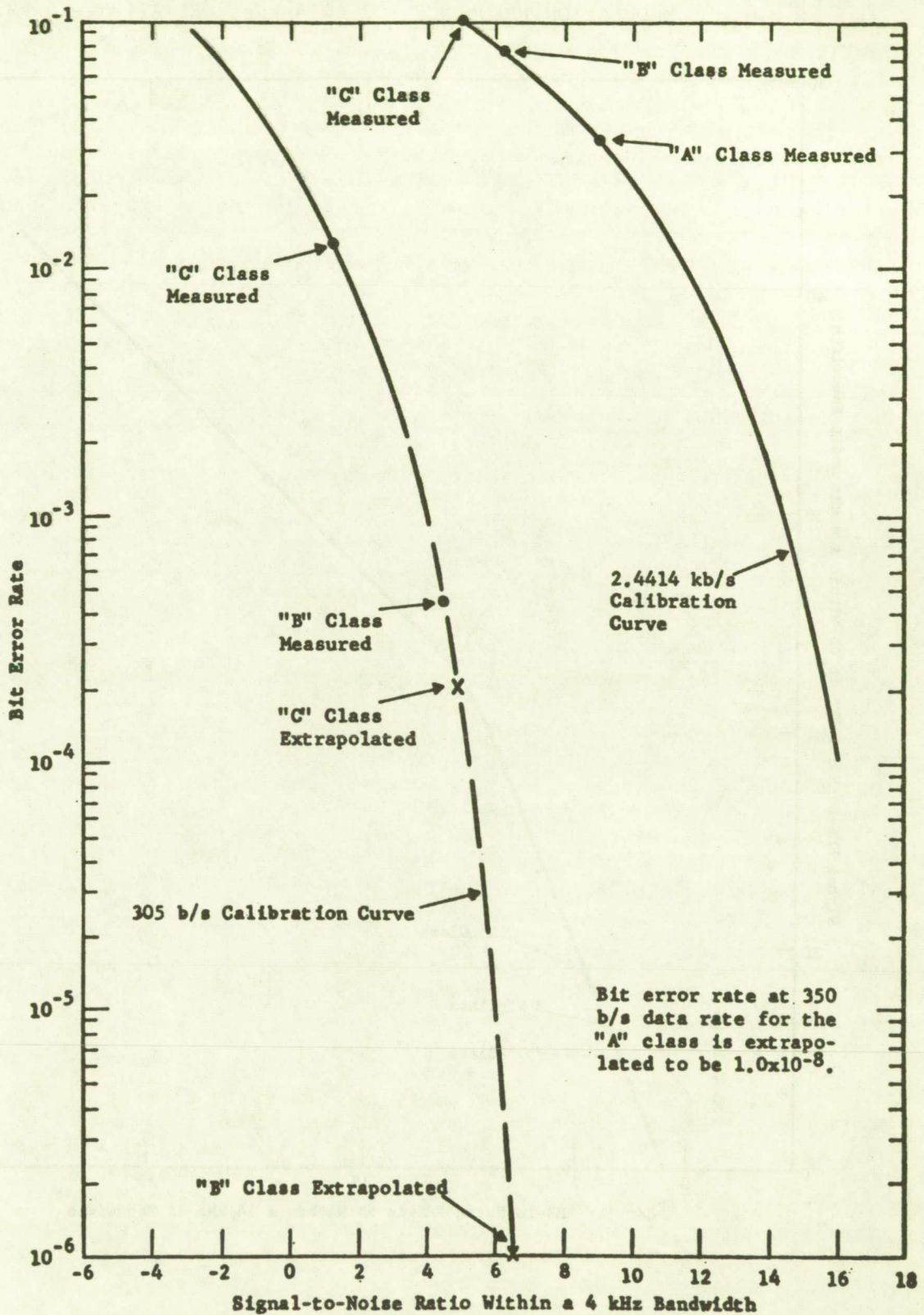
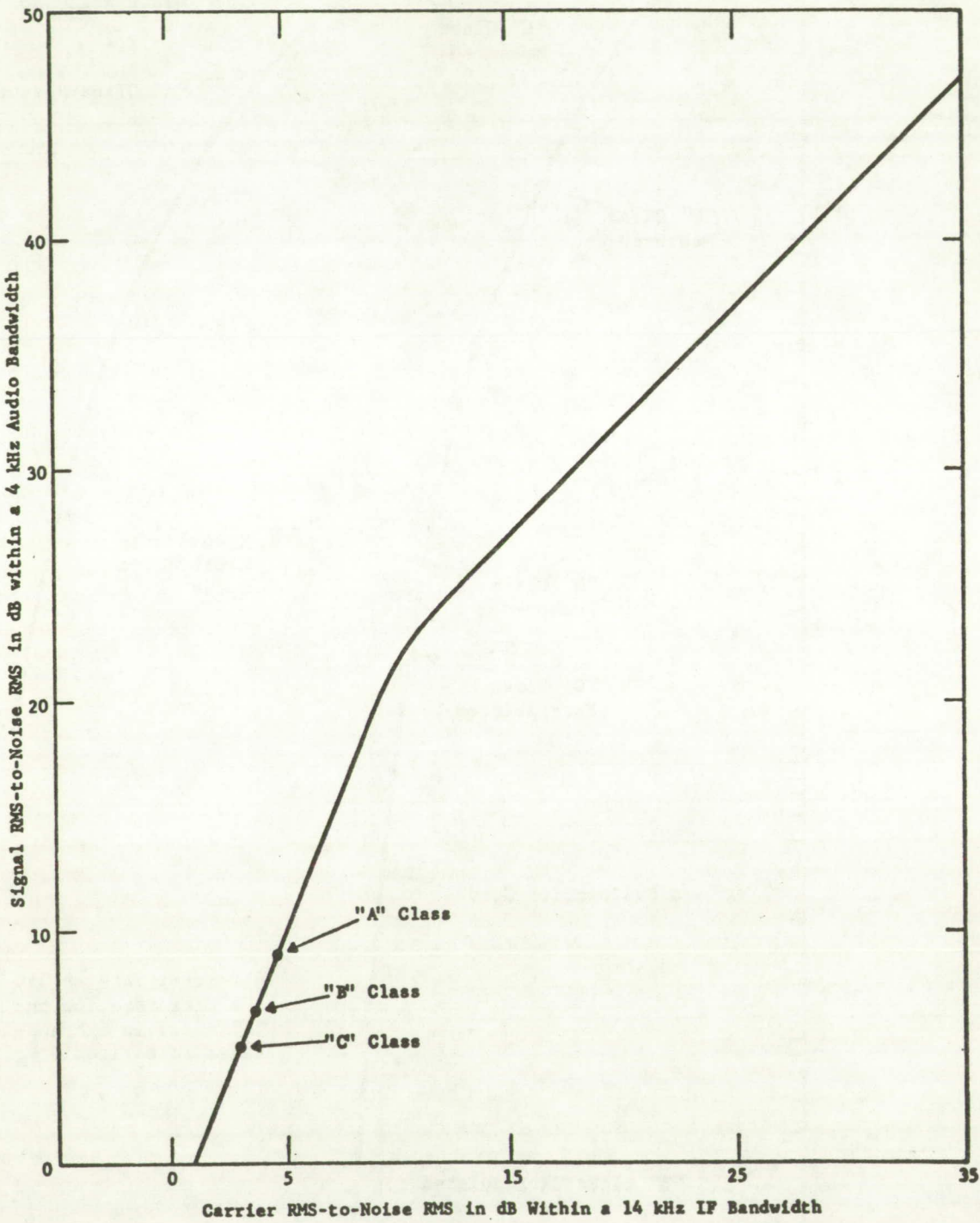


FIGURE 8-13

PERFORMANCE CURVE FOR A TYPICAL FM RECEIVER FOR A MODULATION INDEX OF 2;
i.e., MODULATION FREQUENCY - 2.4414 kHz, DEVIATION - 5 kHz



SECTION 9

VAN TESTS

A Ford Econoline van, Figure 9-1, was equipped with a General Electric mobile radio, as used in taxi cabs and police cars. A responder unit was connected between the receiver and the transmitter. A Parks Electronics Laboratories preamplifier model 144-1P preceded the receiver. The transmitter output power was 80 Watts. Separate dipole antennas were provided for the receiver and transmitter. They are visible as the horizontal elements near the front of the vehicle, as shown in Figure 9-1.

On March 27, 1969, the van was driven from the village of Manny Corners, New York, northward through the village of Hagaman, New York, to Route 29, then eastward on Route 29.

Range measurements were made through ATS-3 during the one-hour test period. The dipole antennas were separately oriented for best signals.

In previous mobile radio ranging tests not using satellites, it was observed that reflected signals can arrive at the receiving station antenna in any phase relative to the direct signal, and severely affect the received signal level. A vehicle position change of only a few feet can result in a large change in signal amplitude at the receiver.

During the first portion of the March 27 satellite ranging experiment, the van was moved in small increments; one foot, then two feet, then four feet, etc., to determine if a similar effect occurred between the vehicle and the satellite. The amplitude change was observed. No effects on range measurements were observed that could not be attributed to the change in receiver time delay with signal amplitude as described in Section 4). The receiver was an unmodified production unit with a time delay change of approximately 7 microseconds with signal amplitude change.

Figure 9-2 is a plot showing every range measurement made during the March 27 test. Note that the ordinate scale is marked in 10 microsecond steps rather than 1 microsecond steps, as on some other data plots. The shape of the data curve matches the changing range from the satellite to the vehicle. Events during the test are marked on the plot. There is a change in measured range noticeable during the first part of the test greater than the movement of the vehicle. The change in range is due to satellite motion, an effect clearly noticeable in similar plots in Section 11). Gaps in the data occurred because the range measurements were stopped when voice communications were used to coordinate the experiment. Scatter of the data points includes the variations in the time delays through the van and Observatory receivers.

Some of the range measurements were used to compute the intersection of the line of position with the road. The computation included an estimate of the equipment and ionospheric time delays. A first estimate for the delays resulted in a bias error to the south of approximately one and one-half miles. A new estimate was made to place the first location at Manny Corners, then the same equipment and ionospheric time delays were used for all the rest of the computations. Figure 9-3 shows the route which was traced from a topographic map. The actual positions of the vehicle are plotted as dots and the positions as determined from the satellite range measurements are plotted as short horizontal line segments. The satellite was nearly due south of the area at the time.

FIGURE 9-1
FORD ECONOLINE VAN

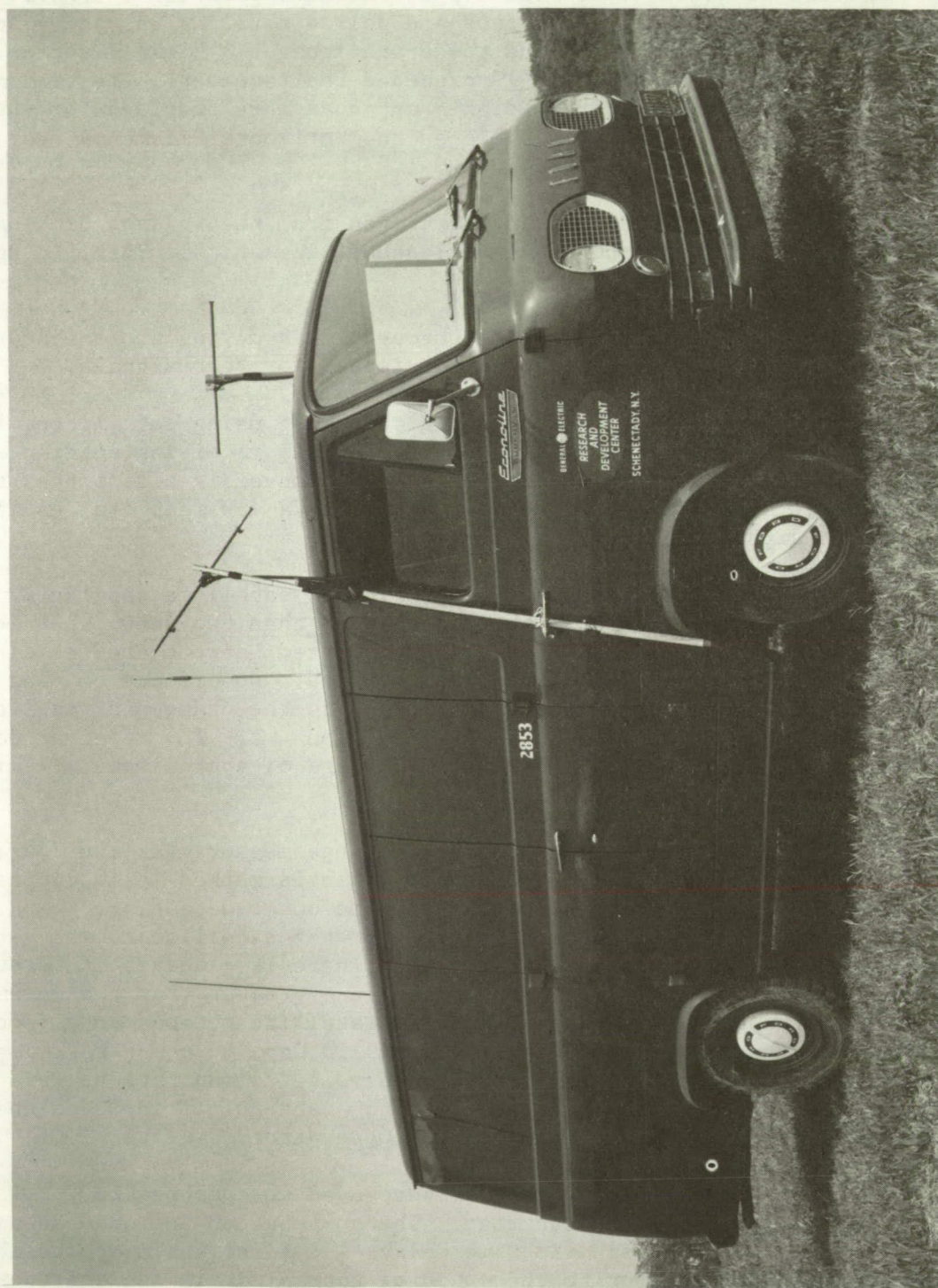
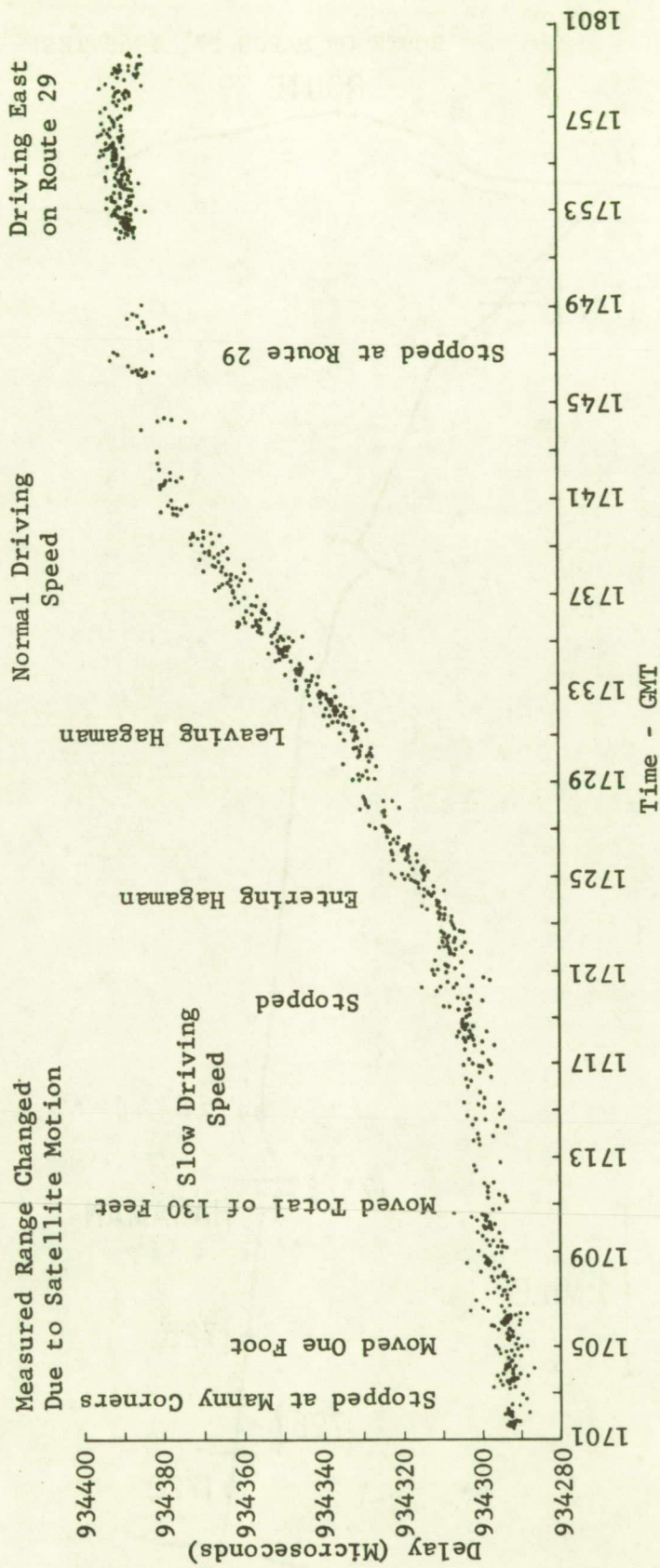


FIGURE 9-2
 RANGE MEASUREMENTS THROUGH ATS-3 USING VAN



ROUTE OF MARCH 27, 1969 TEST
ROUTE 29



SECTION 10

L.E.S.T. TESTS

L.E.S.T. is an abbreviation for Low Energy Speech Transmission, a technique for processing and transmitting speech at a saving in power over more frequently employed techniques. The technique, developed in the General Electric Research and Development Center, is based on the work of Licklider and Pollack¹ who showed that speech, clipped nearly at the zero crossings, i.e. "infinitely" clipped speech, is highly intelligible. In L.E.S.T., the input waveform is first pre-emphasized by differentiation, then infinitely clipped and finally a short pulse is generated at each zero crossing of the infinitely clipped waveform.

The maximum rate of zero crossing pulses is limited by the audio passband, but since the average rate is far below the maximum, the duty cycle of the transmission is very low, approximately 5 percent during speech, resulting in a significant energy savings. At the receiving end, the pulses are applied to a bistable multivibrator to regain the infinitely clipped waveform of the original speech signal.

The full energy saving is accomplished by generating a pulse of RF energy at each zero crossing pulse. The transmitter is turned completely off between pulses. In the ATS-1 test, the waveform was simulated by frequency deviation rather than keying the satellite transmitter. As a result, the energy saving could not be directly demonstrated, but could be inferred from the duty cycle. Duty cycle estimates were based on laboratory measurements. The ATS-1 tests revealed that L.E.S.T. waveforms can be transmitted without distortion over satellite links.

L.E.S.T. equipment developed and constructed on a previous program was used in the experiments. Since this L.E.S.T. equipment was primarily intended for use in AM transmission systems, some modifications were necessary to adapt it to FM. Dual-polarity pulses were used to modulate the carrier frequency in an FSK (frequency shift key) mode where the carrier is on continuously but is shifted by the L.E.S.T. pulses. In the experiment, the carrier also acted to suppress noise during pauses in the L.E.S.T. speech. The low energy features of the L.E.S.T. system were simulated by considering the time during which the carrier is keyed by the L.E.S.T. pulses compared with the total time of speech transmission. Speech intelligibility was evaluated by use of spondaic word lists. These tests are described in more detail later.

Under the conditions of these experiments, one can estimate the L.E.S.T. savings in power to be between 24:1 and 48:1 compared with an FM system with continuous carrier. However, the equipment used in the experiments was not well suited for transmitting narrow L.E.S.T. pulses (low duty cycle). Therefore, the power estimates given are a limit of the experiment only and further savings should be expected in an optimum L.E.S.T. system.

Results of intelligibility tests on transmitted L.E.S.T. speech using spondaic word lists were very encouraging. Scores for two groups of listeners averaged 93.3 percent for in-house tests without the satellite link using a transponder and dummy load in the system. The scores for the fully implemented experiment using the link to ATS-1 were 96.6 percent for a word list that was familiar to the listeners and 91.5 percent for an unfamiliar list. These tests

indicate that L.E.S.T. can be used for voice communications through satellites and that insignificant loss in intelligibility results from the transmission.

The L.E.S.T. equipment used in this experiment was loaned by the Company's Space Systems Operation in Philadelphia. The L.E.S.T. encoder unit is a bread-board unit while the decoder is a prototype designated #E-012. The L.E.S.T. pulses modulated the RF carrier by an amount of ± 7.5 kHz about the center frequency. Only the duty cycle of the L.E.S.T. pulses was considered when estimating the low energy properties of the system.

Figures 10-1 and 10-2 show the system block diagram and the typical waveforms respectively for the L.E.S.T. experiment. Speech input to the L.E.S.T. encoder was from a microphone or a tape player which contained recordings of spondaic word lists. The waveform at (A) shows the typical clipped speech after pre-emphasis and clipping. There is a voltage transition for each point of zero crossing in the original speech waveform.

Pulses are produced at each transition of the clipped speech waveform - a positive pulse for a positive transition and a negative pulse for a negative transition, as shown in (B). These pulses are 70 microseconds wide and are used to modulate the 149.22 MHz carrier of the transmitter. Thus, the frequency out of the transmitter would have approximately the same waveform as shown in (C) where frequency deviation would be plotted along the ordinate.

The returned transmission at 135.6 MHz is received with the typical waveform out of the FM receiver shown in (D). The discriminator output has a waveform similar to (B) and (C) because of the linear characteristics of the discriminator as shown in Figure 10-3.

Because of response limitations in the receiver and/or transmitter, the width of the pulses out of the receiver are longer than the L.E.S.T. pulses to the transmitter. The pulse width at (D) was found to be 140 microseconds, indicating some bandwidth limitation in the system. However, the highest frequency in the speech is only 2500 Hz; thus, no serious degradation in performance would be expected from these bandwidth limitations in this FM system.

Waveform (E) shows the receiver output after rectification (to make it compatible with the input requirements of the L.E.S.T. decoder). The decoder contains a flip-flop circuit which returns the waveform as shown in (F) to the same form as the clipped L.E.S.T. speech (A). Some additional high frequency filtering is done in the decoder before the output is recorded.

Figure 10-4 shows the modifications made to the L.E.S.T. equipment to make it compatible with the FM experiment. These modifications consist of a dual pulse forming circuit for the output of the encoder and an amplifier and rectifier circuit for the input to the decoder section of the L.E.S.T. equipment.

It was noted during earlier experiments that the output of the receiver could be understood by a listener even though the signal at that point had not passed through the L.E.S.T. decoder. For this reason the output of the receiver was recorded on a second channel at the same time the L.E.S.T. output was recorded to allow for separate tests of intelligibility on the two outputs. The results, to be described later, show that the level of intelligibility was significantly higher out of the L.E.S.T. decoder than out of the receiver even though the receiver output was clear enough for most speech to be understood.

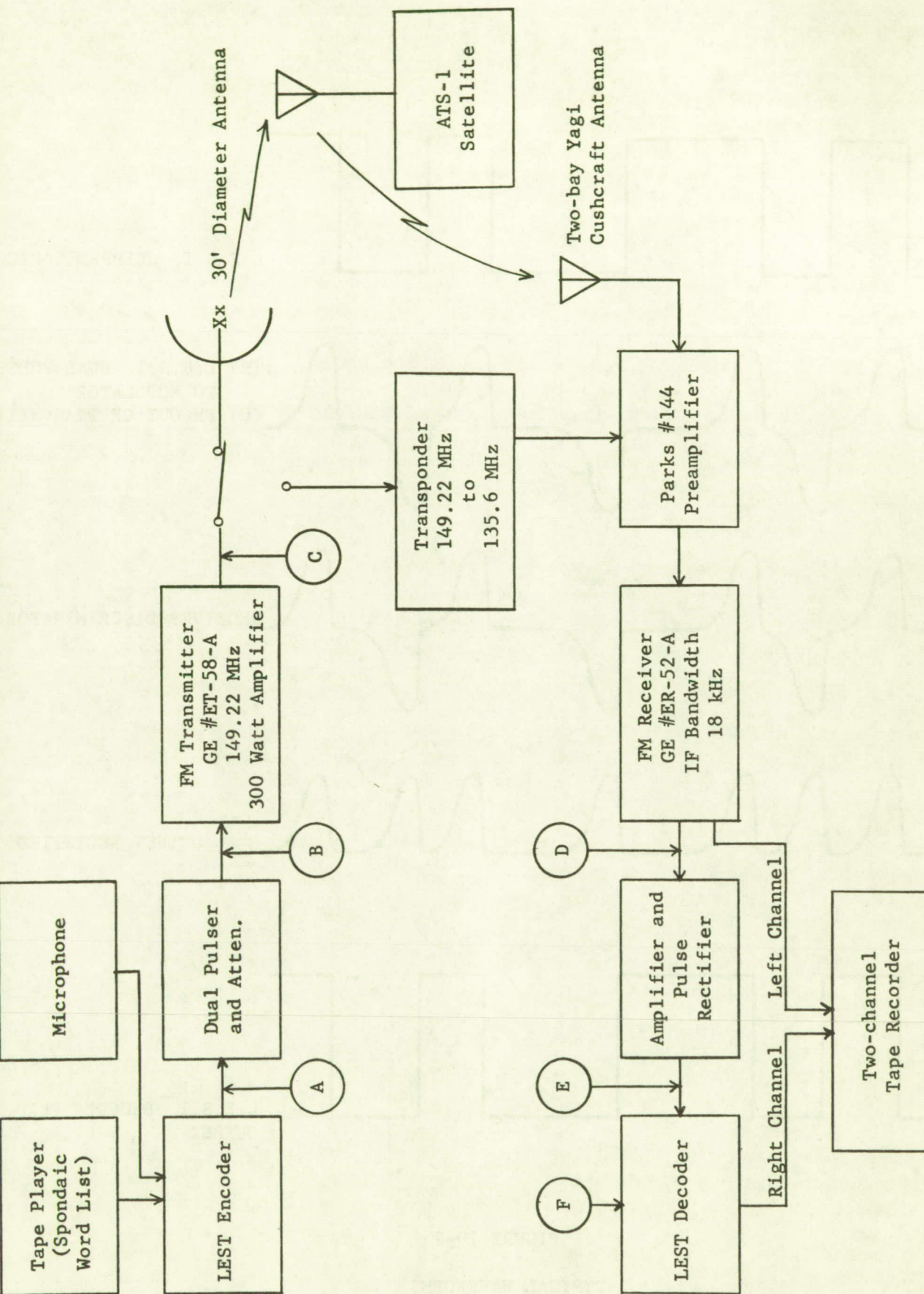


FIGURE 10-1. L.E.S.T. EXPERIMENT SYSTEM BLOCK DIAGRAM

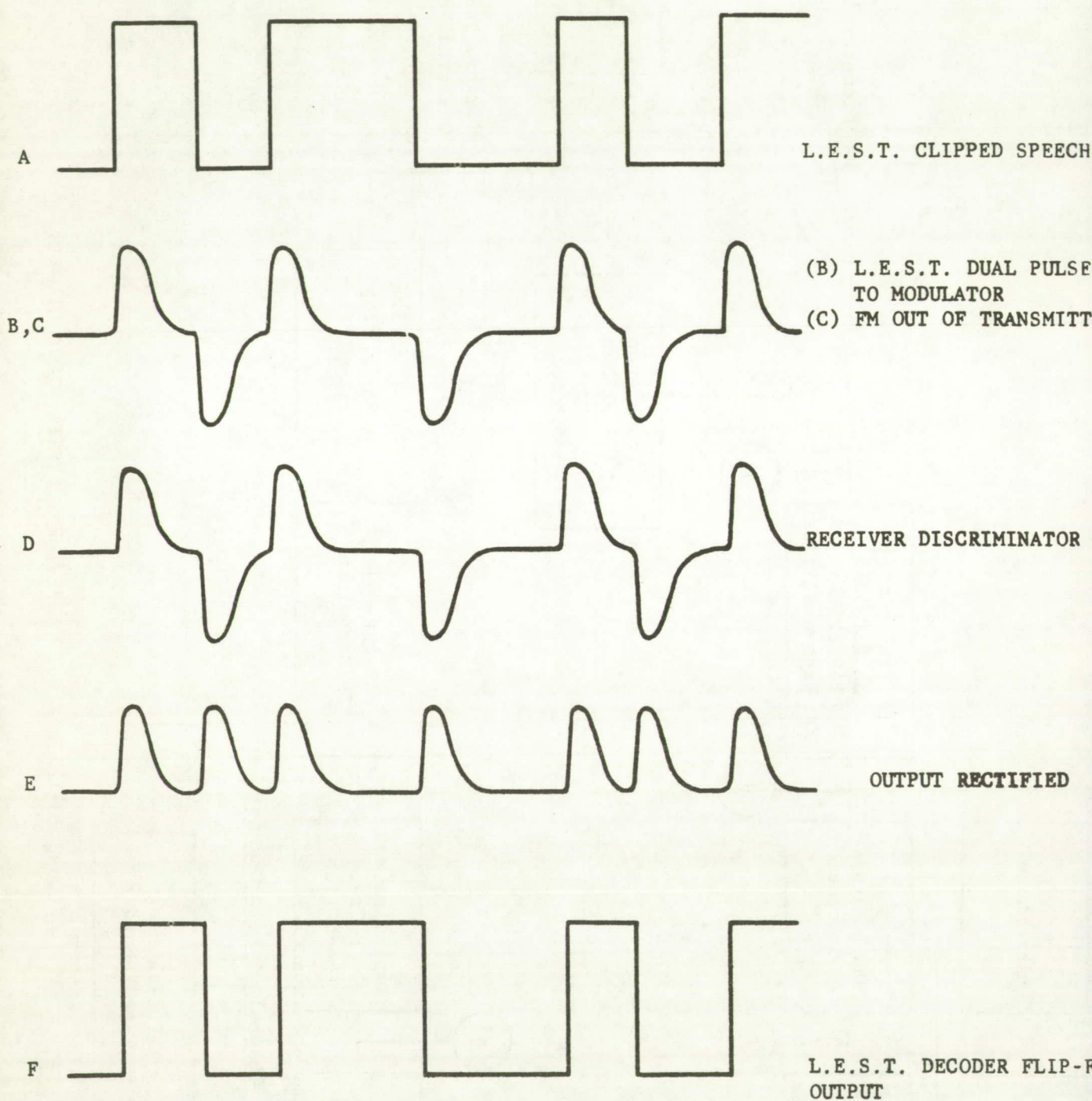


FIGURE 10-2

TYPICAL WAVEFORMS
L.F.S.T. EXPERIMENT

FIGURE 10-3

LINEAR CHARACTERISTICS OF DISCRIMINATOR

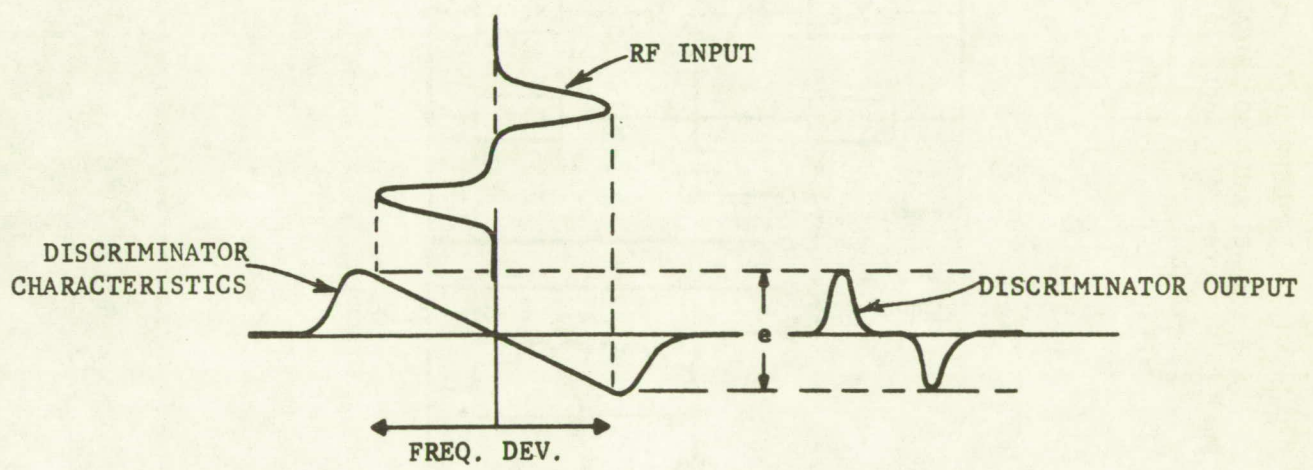
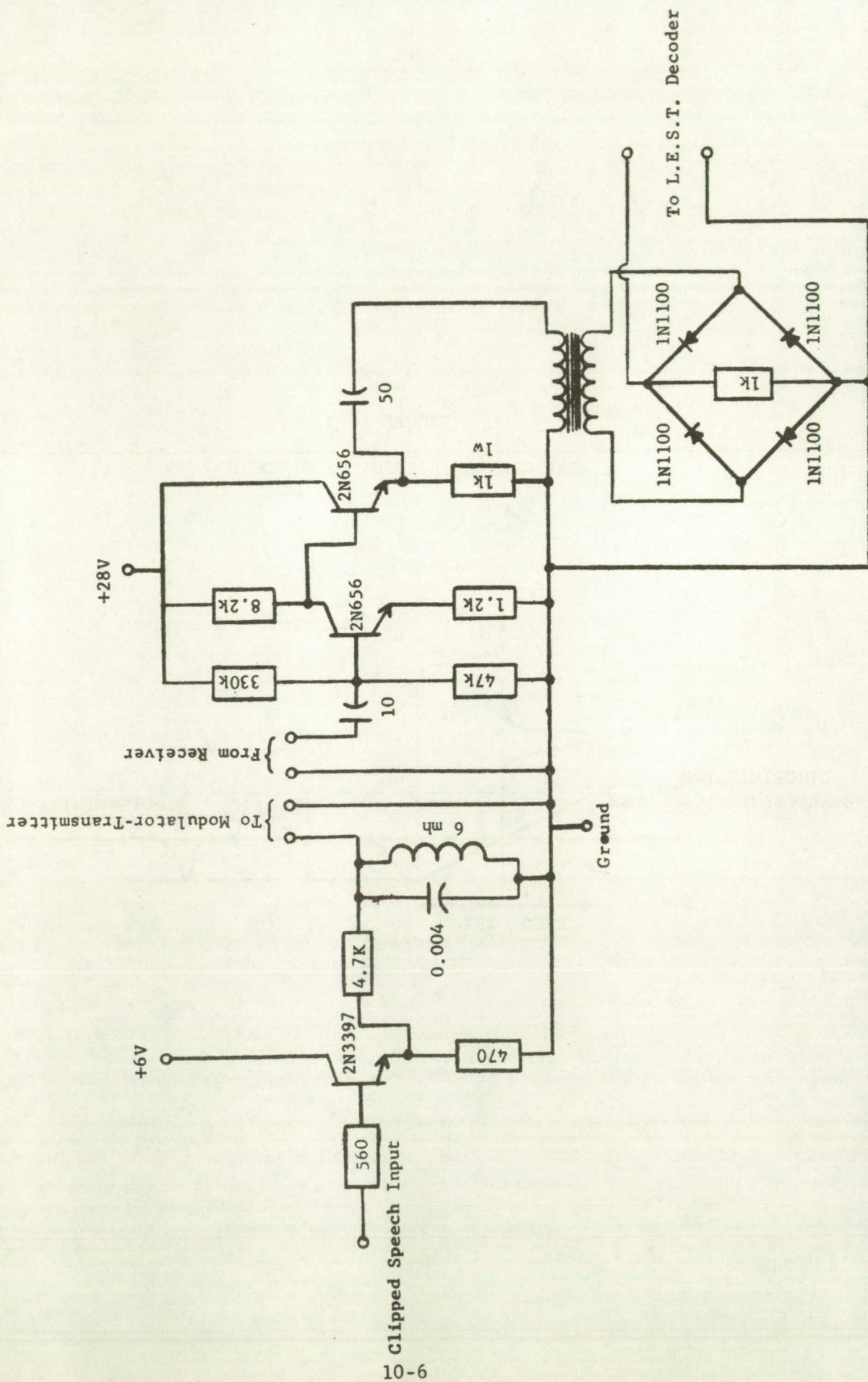


FIGURE 10-4
L.E.S.T. CIRCUIT MODIFICATIONS
Dual Pulse Former and Rectifier Circuits



The system was operated during tests in one of two modes. The first for in-house testing did not use the satellite link. During these tests the transmitter was connected to a dummy load instead of the 30 foot dish antenna and an in-house transponder was used to convert from the transmit to the receive frequency. Tests through the satellite were conducted using the 300 watt transmitter connected to the 30 foot diameter antenna to transmit to ATS-1 at 149.22 MHz. A transponder in ATS-1 converts the frequency and transmits at 135.6 MHz. This returned signal was received back at the Radio-Optical Observatory using two bays of a yagi antenna.

Lists of spondaic words were used in the experiment to aid in the determination of the intelligibility level for L.E.S.T. speech. Spondaic words have two syllables of approximately equal emphasis on each syllable. Tape recordings of the L.E.S.T. spondaic words were played before two groups of untrained listeners, five persons per group. These intelligibility tests were performed in an anechoic chamber to reduce the level of background noise, echoes, and general distractions. The test is more severe than normal speech patterns in that consecutive words are unrelated. The listener either understands the complete word or misunderstands it and both syllables must be correct. As the test was conducted, the listeners wrote the words on a prepared form.

The tests were divided into fifty-word lists. The first fifty-word test resulted from an in-house test using the local transponder and no link to the satellite. This test served to familiarize the listeners for the first time with the sound of L.E.S.T. and to calibrate the performance of the L.E.S.T. equipment against similar tests conducted on earlier programs. After a break, the listeners heard a one hundred-word list resulting from the complete test using the link to ATS-1. The first fifty words of the one hundred-word list were the same as in the first test, while the second fifty words were heard for the first time. For this reason, the two groups of fifty words were scored separately.

During the tests with ATS-1 on September 23, 1969, some difficulty was experienced in transmission due to ionospheric effects resulting in amplitude scintillation. This caused some words to be lost during transmission of the one hundred-word list. Three words in the first fifty and one word in the second fifty were completely lost and were discounted from the test. All other words including some which had amplitude fading and noise difficulties were counted in the test.

Table 10-1 shows the results of the intelligibility tests. The numbers are for the percentage of correct word answers in each test. Ten of the one hundred words used in the tests are: necktie, woodwork, greyhound, bobsled, catcall, browbeat, playmate, doormat, courtship, and hardware.

The following conclusions can be drawn from the results of these tests:

1. The scores in the calibration tests number 1 and 3 compare favorably with previous tests for L.E.S.T. speech having scores of 90 percent or better.
2. Only a slight loss in intelligibility resulted in transmission to ATS-1 compared with the laboratory test. The measured intelligibility for the ATS-1 test was 91.5 compared to 94.5 for the laboratory test.

TABLE 10-1

L.E.S.T. WORD TESTS

GROUP 1

<u>Listener</u>	<u>Test No. 1</u> <u>First 50 Words</u>	<u>Test No. 2</u> <u>First 50 Words</u>	<u>Test No. 2</u> <u>Second 50 Words</u>
1	98 percent	98 percent	86 percent
2	92 percent	96 percent	90 percent
3	100 percent	98 percent	96 percent
4	98 percent	98 percent	96 percent
5	<u>84 percent</u>	<u>94 percent</u>	<u>90 percent</u>
	94.5 percent	96.6 percent	91.5 percent

GROUP 2

<u>Listener</u>	<u>Test No. 3</u> <u>First 50 Words</u>	<u>Test No. 4</u> <u>First 50 Words</u>	<u>Test No. 4</u> <u>Second 50 Words</u>
6	86 percent	79 percent	82 percent
7	92 percent	94 percent	76 percent
8	98 percent	96 percent	84 percent
9	90 percent	88 percent	74 percent
10	<u>94 percent</u>	<u>85 percent</u>	<u>71 percent</u>
	92 percent	88.5 percent	77.5 percent

Test No. 1 and Test No. 3: In-house test recorded at L.E.S.T. decoder output.
 Test No. 2: ATS-1 test recorded at L.E.S.T. decoder output.
 Test No. 4: ATS-1 test recorded at receiver output (not decoded).

3. Although L.E.S.T. speech is understandable directly out of the receiver, the level of intelligibility is significantly lower than the decoded speech out of the L.E.S.T. equipment. Test number 4 compared with test number 2.
4. In both test number 2 and test number 4 the scores were considerably higher for the first fifty words which were by that time familiar to the listeners.

The low energy characteristics of the L.E.S.T. experiments can be evaluated by considering the time during which the FM carrier is keyed by the L.E.S.T. pulses compared with the total time of speech transmission.

Pulse width of L.E.S.T. input to transmitter (modulator) is equal to 70 microseconds. Pulse width of returned L.E.S.T. out of the receiver (discriminator) is equal to 140 microseconds.

Average frequency in normal speech is equal to 600 Hz, as measured in previous studies of L.E.S.T. speech.

There are two zero crossings per pulse, or an average of 1200 pulses per second during spoken words. Short gaps in forming words and sentences total approximately half the time while speaking, and longer pauses occupy about one-half the total time during normal speech so that the average pulse rate during conversation is typically 300 pulses per second. The pulse duration in the satellite tests was 140 microseconds. The duty cycle is thus

$$\frac{300 \times 140}{10^6} = 0.042$$

It is probable that the L.E.S.T. pulses could have been detected with approximately the same signal-to-noise ratio if they had been transmitted by AM rather than the narrow bandwidth FM. The FM noise improvement with the small deviation ratio results in a detector output signal-to-noise which is approximately the same as the input signal-to-noise, and thus the FM is approximately equivalent to AM, suggesting that the same result could have been attained with a satellite having a peak effective radiated power of 200 Watts, but an average e.r.p. of only ten Watts.

REFERENCE

1. J. C. R. Licklider and I. Pollack, "Effects of Differentiation, Integration and Infinite Peak Clipping Upon the Intelligibility of Speech," Journal of the Acoustical Society of America, Volume 20, Number 1, January 1948.

SECTION 11

IONOSPHERIC PROPAGATION

A major objective of the experiment was to obtain data on the effect of the ionosphere on the ranging and position fixing accuracy of range measurements from satellites at VHF. The up and down link frequencies of the ATS satellites are near the lower limit that may be considered for useful range measurements.

The largest effect of the ionosphere is propagation time delay because the index of refraction of the ionosphere is different than that of free space. In addition to the time delay, the refractive effect causes bending of the ray so that the ray path length between the satellite and the earth's surface is increased.

The presence of the earth's magnetic field in the ionosphere causes a rotation of the plane of polarization of a radio signal, called Faraday rotation, that can influence the strength of a received radio signal unless circular polarization is employed.

There is a propagation delay or radio wave retardation in the troposphere as well as in the ionosphere. Tropospheric retardation is independent of frequency. At sea level, 100 percent humidity, and zero elevation, it is 116 meters¹. It decreases with increasing elevation angle from the observer to the satellite and his altitude.

A summary of atmospheric propagation effects is presented in Table 11-1.

Ionospheric Bias Error

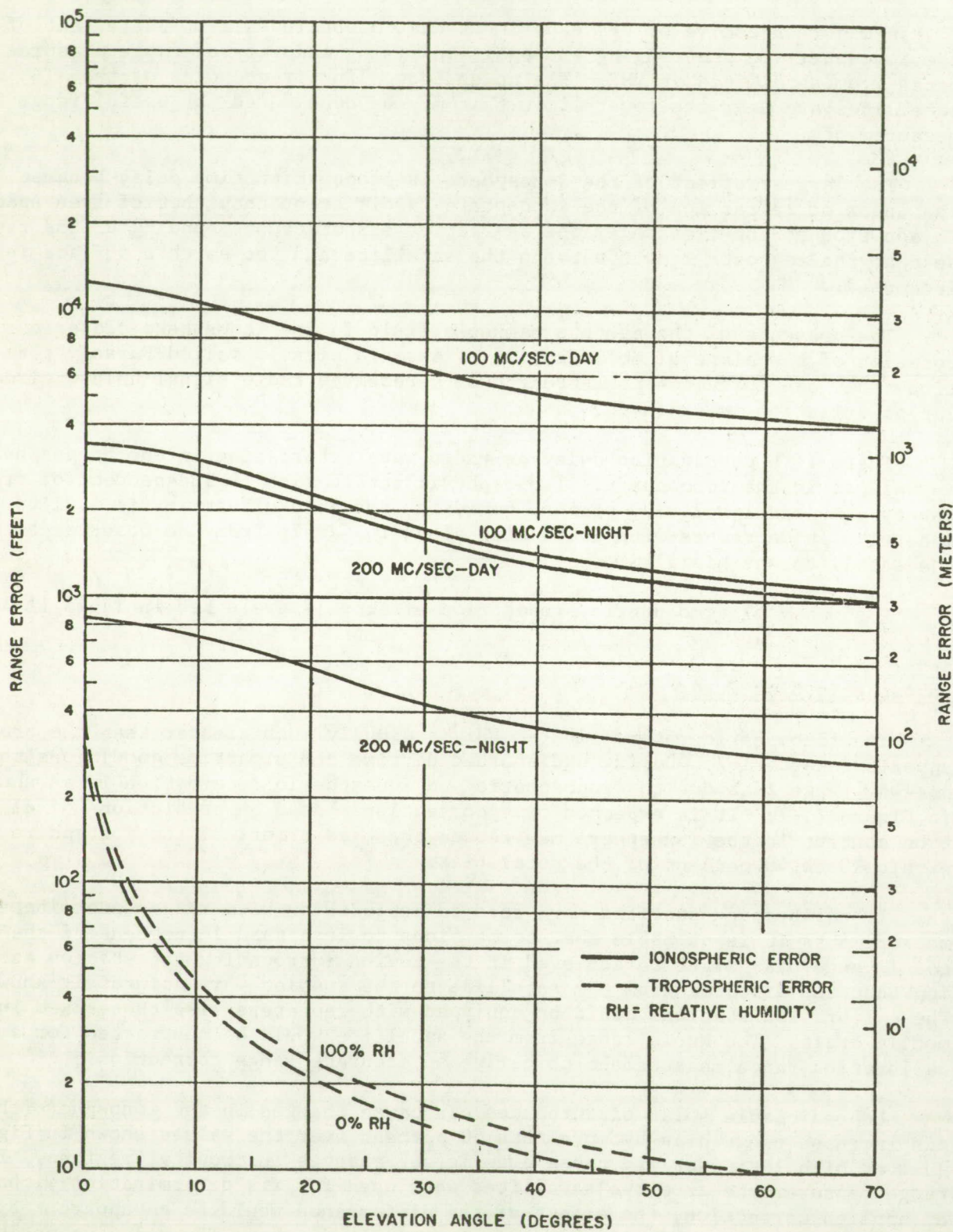
The ionospheric retardation at VHF is usually much greater than the tropospheric retardation. During undisturbed daytime and nighttime conditions the one-way range bias due to tropospheric and ionospheric retardation is as shown in Figure 11-1. It is expected that corrections based on predictions of electron content in the ionosphere may reduce the bias errors of the ionosphere to within 20 to 40 percent of the total bias.

If calibration stations were used in conjunction with range determination measurements it is probable that corrections to less than 10 percent of the total range bias might be achieved in the region surrounding the station assuming that the distance from the satellite to the station were accurately known. The calibration stations could be equipped with repeaters like those used in mobile craft. The known range from the satellite would be subtracted for a calibration range measurement to derive an accurate range correction.

Unpredictable solar disturbances can cause changes in the ionosphere that can increase range bias by more than 50 percent over the values shown in Figure 11-1 at high latitudes and cause even larger changes in tropical regions. If range measurements from two satellites were used for fix determination without an applied correction, the effect of the disturbance would be an apparent systematic displacement of all the craft in a limited area. The relative position determinations of these craft would not be significantly affected.

FIGURE 11-1

ONE-WAY RANGE BIAS DUE TO TROPOSPHERIC AND IONOSPHERIC RETARDATION



EFFECTS	MATHEMATICAL DESCRIPTIONS	DEFINITION OF TERMS & COMMENTS
Tropospheric Refraction	$(n - 1) \times 10^6 = \frac{a}{T} \left(p + \frac{b\epsilon}{T} \right)$	n = refractive index T = air temperature (°K) p = total pressure (millibars) ε = partial pressure of water vapor (millibars) Note: Refraction is frequency independent
Ionospheric Refraction	$n = 1 - \left[\frac{4\pi N_e e^2}{n\omega^2} \right]^{1/2}$	n = refractive index N _e = number of electrons/cm ³ e = electron charge (4.8 × 10 ⁻¹⁰ esu) m = electron mass (9.1 × 10 ⁻²⁸ gm) ω = angular frequency of incident waves (radians/second)
Ionospheric Attenuation	$A = \frac{1.17 \times 10^{-2}}{f^2} \int_0^S N_e \nu ds$	f = frequency (cps) N _e = electrons/cm ³ ds = path differential (cm) ν = electron collision frequency (collisions/sec.)
Ionospheric Polarization Rotation	$\varphi = \frac{2.362 \times 10^4}{f^2} \int_0^h f(h) H \cos \theta N_e dh$	φ = angular rotation H = magnetic field intensity (gauss) f(h) = secant of angle between ray path and zenith dh = height differential (cm) θ = angle between magnetic lines and propagation path
Ionospheric Dispersion	$\Delta\varphi = \frac{40 \times 10^6}{c f^2} \int_0^S N_e ds$	Δφ = differential phase shifts (in cycles) for CW transmissions of frequency separation f _s f = average of the two transmitted frequencies (cps) The integral is the integrated electron density along the path (electrons/cm ²).
Angle of Arrival Scintillation	$\overline{\theta^2} = \frac{2 \times 10^{-12} \sqrt{\pi} L \overline{AN^2}}{l_o}$ Angle of Arrival for a Turbulent Troposphere	$\overline{\theta^2}$ = mean squared angle of arrival L = path length through turbulence l _o = scale length of the turbulence eddy ΔN ² = mean square fluctuations in the refractivity, N
Tropospheric Phase Scintillation	$\overline{\Delta\varphi^2} = \frac{8 \times 10^{12} \pi^2 l_o L \overline{AN^2}}{\lambda^2}$	Δφ ² = mean square phase fluctuations Note: Typical values for 100 Kilometer path length • 1000 MHz: $(\overline{\varphi^2})^{1/2} \approx 2^\circ$ • 100 MHz: $(\overline{\varphi^2})^{1/2} \approx 0.2^\circ$
Ionospheric Phase Scintillation	$\overline{\Delta\varphi^2} = \frac{l_o L \omega^4}{4 c^2 \omega^2} \left(\frac{\overline{\Delta N_e}}{N_e} \right)^2$	ω _N = angular plasma frequency C = speed of light $\left(\frac{\overline{\Delta N_e}}{N_e} \right)^2$ = mean square fractional deviation of electron density Note: Typical values for 100 Kilometer path length at 100 MHz is 1.9°
Amplitude Scintillation	$\left(\frac{\Delta A}{A} \right)^2 = \frac{\pi^2 z^2 L \omega^4}{l_o^3 \omega^4} \left(\frac{\overline{\Delta N_e}}{N_e} \right)^2$ or $\left(\frac{\Delta A}{A} \right)^2 = \left(\frac{2\pi cz}{l_o^2 \omega} \right)^2 \overline{\Delta\varphi^2}$	$\left(\frac{\Delta A}{A} \right)^2$ = mean square fractional deviation of amplitude of signal from infinite distance where ΔA and A are the amplitude deviation and mean amplitude of the resultant signal. Z = distance of ionospheric scatters from the ground
Tropospheric Time Delay		Independent of frequency. Maximum range error of 380 feet at sea level. Effect negligible at jet aircraft altitude.
Ionospheric Time Delay	$\Delta R_g = \frac{40 \times 10^6}{f^2} \int_0^S N_e ds$	ΔR _g = one way range increase (cm)
Tropospheric Doppler Shift Error	$\Delta f_d = -\frac{f}{c} \Delta E_T V \sin \psi$ where $\Delta E_T = \cos^{-1} \left[\frac{r_o}{r_o + h} \cos (E - \Delta E) \right]$ $-\cos^{-1} \left[\frac{n_G r_o}{n_T (r_o + h)} \cos E \right]$	Δf _d = additional doppler shift over free-space doppler caused by troposphere V = velocity of moving object c = free-space velocity of propagation ΔE _T = angle defined by second equation (radians) n _G = refractive index at the ground n _T = refractive index at the space vehicle r _o = earth radius ΔE = refraction angle error at elevation angle, E, and height, h
Ionospheric Doppler Frequency Error	$\Delta f_d = -\frac{40 \times 10^6}{cf} \frac{d}{dt} \int_0^S N_e ds$	Δf _d = additional doppler shift over free-space doppler caused by the ionosphere

More data are needed on the size of the area in which the information from a calibration station can be used, and therefore the number required in the area served. However, an estimate can be made on the basis of an extreme case reported by Mendillo, et al², Figure 11-2. In that instance, sunset occurred at the peak of the disturbance, and the total electron content dropped by a factor of ten in one hour. It would have caused a change in total range bias from approximately 2700 to 270 meters for an elevation of 20 degrees. Assuming that the principal cause of the decay is related to sunset, the east-west gradient of electron density and hence range bias would have been over a distance approximating the distance the terminator moved over the earth in one hour, or approximately 1000 kilometers. Calibration stations at 1000 kilometer intervals would probably have been sufficient to determine the range bias correction during that event.

Ionospheric time delay is reduced a $1/f^2$ so that it would be negligible at L-band, 1540-1660 MHz. As stated in a previous study³, 400 to 700 MHz is the technically optimum frequency band for most applications of range measurements from satellites.

The time delay in the ionosphere is important at 135 to 150 MHz because the exact delay at any time or place cannot be predicted accurately. An ionospheric model adapted from Lawrence, et al⁴ and Millman¹ was used in the computer program for determining fixes. (Appendix II) The procedure for including the bias in the fix determination was to compute the fix on the basis of the measurements without correction to find the approximate location of the user equipment, then to determine the time of day at the user's location. An ionospheric correction for each satellite-to-user ray path was determined from the ionospheric model. The range measurements were then corrected in accordance with the estimates derived from the model, the fix was immediately recomputed and then printed out.

As noted in Table 11-1, ionospheric range error is related to free electron content along the ray path by the expression:

$$\Delta R_g = \frac{40 \times 10^6}{f^2} \int_0^s N_e ds \quad (11-1)$$

where ΔR_g = range increase (cm)

N_e = electrons per square cm column

It is convenient to express ΔR_g in the number of microseconds added to the propagation time in the range measurements, and electron content is often given in electrons per square meter. Equation (11-1) then becomes:

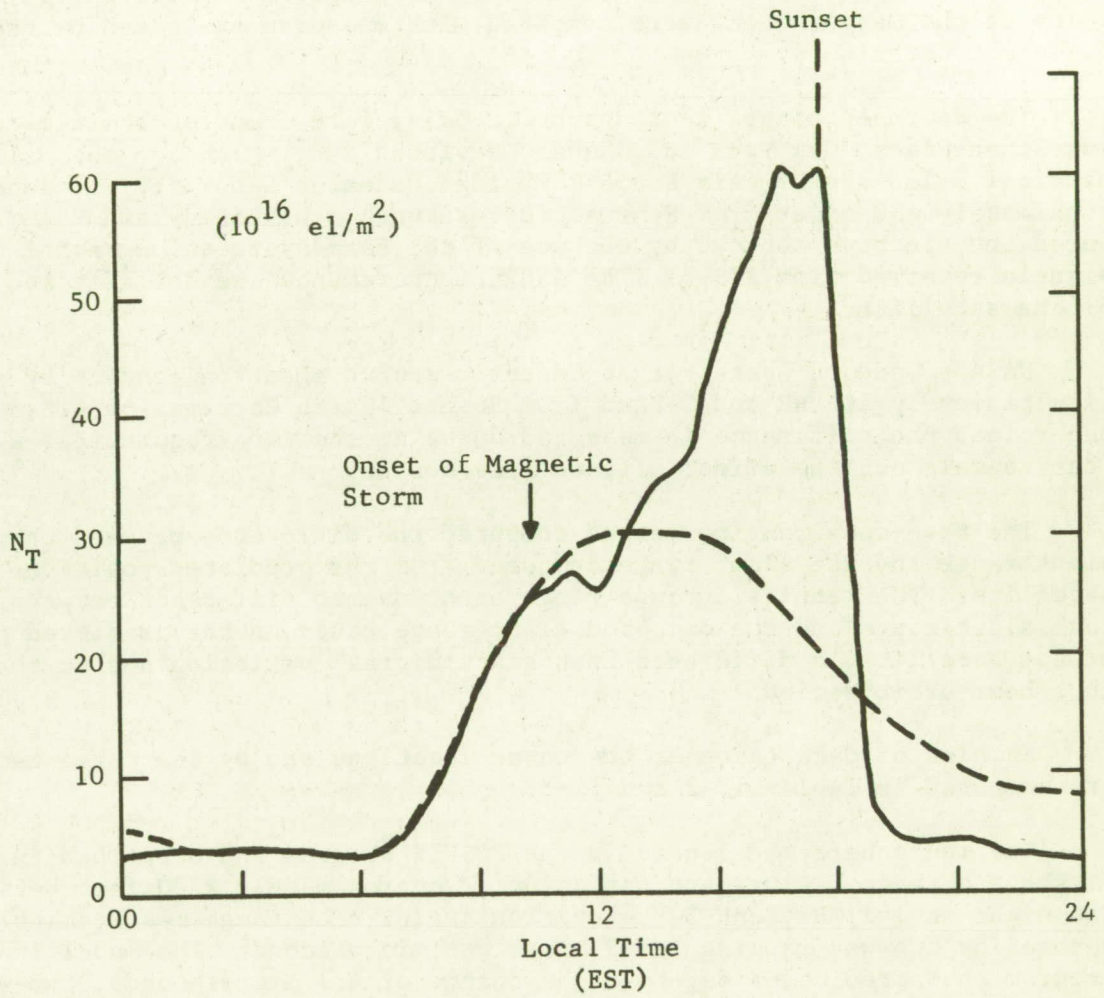
$$\Delta t = \frac{40 \times 10^8}{Cf^2} \int N_e ds$$

where C = free space velocity of light (3×10^8 m/sec)

N_e = electrons per square meter column

FIGURE 11-2

ELECTRON CONTENT DUE TO MAGNETIC STORM²



February 2, 1969

Using an up link frequency of 149 MHz and a down link frequency of 135.6 MHz, time delay is related to the total electron content by the following equation (John A. Klobuchar, Air Force Cambridge Research Laboratories, private correspondence):

$$T = 1.32 \times 10^{-17} \times \text{TEC (microseconds - round trip)}$$

TEC is expressed in el/M^2 .

Several tests were conducted to measure the day-to-night change in electron content, the correlation between the diurnal changes in content at separated locations, and the day-to-day correlation of electron content variations. Results of the measurements were compared with measurements taken by others using different techniques.

The diurnal changes in ionospheric delay were found to be well correlated for Schenectady, New York and Gander, Newfoundland, which are approximately 900 nautical miles apart. Air Force Cambridge Research Laboratories, located approximately 150 miles from Schenectady, between Schenectady and Gander, measured the electron content by the use of the Faraday rotation technique on VHF signals received from ATS-3. The AFCRL measurements are not affected by motion of the satellite.

NASA's Goddard Space Flight Center measured electron content by ranging simultaneously at VHF and C-band from Rosman, North Carolina to ATS-3. They determined the difference in measured delay at the two frequencies, a method that cancels out the effect of satellite motion.

The tone-code ranging method computed the difference between the measured slant range and the slant range computed from the predicted positions of the satellite. The results include range error due to difference between the actual slant range and the computed slant range based on the predicted positions of the satellite, a difference that has a diurnal variation due to the twenty-four hour orbit period.

Samples of data taken at the three locations and by the three techniques are compared in Tables 11-2 and 11-3.

The ionosphere model used in the POSFIX program and described in Appendix II shows a range measurement variation of approximately 2300 feet between day and night at 142 MHz, and 30° elevation angle. The range measurement time delay change for two-way ranging is 491 feet per microsecond. The model in the POSFIX program thus predicts a day-to-night change of 4.7 microseconds, two-way ranging delay.

Geography and Time Correlations of Ionospheric Propagation Delay

The propagation velocity of radio waves is reduced as they pass through the ionosphere. The reduction in velocity is proportional to the integrated electron content along the ray path and inversely proportional to frequency squared. (Eq. 11-1) Ionization in the upper atmosphere is caused by radiation from the sun, and its distribution over the earth is affected by the earth's magnetic field.

TABLE 11-2

TWO-WAY SLANT RANGE DAY-PEAK-TO-NIGHT MINIMUM DELAY CHANGE

<u>Date</u>	<u>AFCRL-Hamilton - ATS-3</u>	<u>GE-Schenectady - ATS-3</u>
10/28/70	6.9 μ s change	
10/29/70	7.9 μ s change	
10/30/70	7.9 μ s change	12.3 μ s change
10/31/70	8.8 μ s change	16.0 μ s change
11/01/70	7.6 μ s change	13.5 μ s change
11/02/70	8.4 μ s change	15.0 μ s change
1/19-20/71 (1200 - 1200)	7.6 μ s change	15.8 μ s change
3/13-14/70 (1000 - 1000)	6.3 μ s change	13.3 μ s change

TABLE 11-3

TWO-WAY SLANT RANGE DAY-PEAK-TO-NIGHT MINIMUM DELAY CHANGE

<u>Date</u>	<u>Time</u>	<u>Rosman, N.C. Delay Change</u>	<u>Electron Content</u>	
			<u>Minimum</u>	<u>Maximum</u>
/31/71	1100 - 2400 GMT	9 microseconds	9.8×10^{17}	16.6×10^{17}
/01/71	1100 - 2400 GMT	9 microseconds	9.3×10^{17}	16.2×10^{17}

The reduced propagation velocity increases propagation time, and therefore causes an apparent increase in range measurements. The day-to-night change in two-way propagation time due to the ionosphere is usually between 10 and 15 microseconds at the radio frequencies used in the experiments. Solar disturbances may sometimes increase the propagation delay by more than 50 percent.

One microsecond, in two-way ranging, represents 491 feet, or approximately 12 microseconds per nautical mile. It is evident that if no correction is made for ionospheric propagation delay, the ionosphere can cause position fix errors of several miles.

There are two methods to correct for the propagation delay. One method is to estimate the delay by the use of a model of the ionosphere based on the large quantity of data that has been collected over the past several decades. (Appendix II). The other method is to measure the propagation delay at a known location, and use the measurement to correct range measurements made to other transponders in the geographical region surrounding the known location.

Both methods of correcting for propagation delay were used in the experiments. A simple model provided corrections adequate for position fix accuracy better than one nautical mile, one sigma. The other method, using reference transponders at known locations, was also effective and provided the additional benefit of a first order correction for error in satellite position prediction.

To be useful, a model requires that there be predictable, cyclic changes in the ionosphere. The diurnal cycle is a dominant one. The day-to-day correlation of ionospheric delay is thus important in estimating the value of a model.

The usefulness of the reference transponder measurements depends upon the correlation of ionospheric delay at one location with the delay at another. The geographical extent of the correlation is important in evaluating the practical value of the reference transponders because it determines the number and deployment of the transponders needed to achieve a specified accuracy for a system.

The ultimate limitation on accuracy of a VHF satellite ranging system is imposed by the residual error after the ranging measurements have been corrected for ionospheric delay. Much of the effort in the experimental program was directed to measuring the time and geographic correlations of ionosphere delay, and evaluating two methods of correcting the range measurements.

Reference transponders were deployed across the North Atlantic and the continental United States, at Thule, Greenland, and at Buenos Aires, Argentina. The transponders were supplied by the General Electric Company. Construction of the unit located at Reykjavik, Iceland was funded by the Comsat Corporation. The units were installed, maintained, and operated by local personnel:

Shannon, Ireland
Gander, Newfoundland
Seattle, Washington
Buenos Aires, Argentina
Reykjavik, Iceland

Irish Department of Posts & Telegraphs
Canadian Department of Transport
The Boeing Company
Argentine Air Force
General Civil Aviation, Iceland

The Federal Aviation Administration installed and operated two transponders on their own craft, and flew the aircraft with FAA engineers on all of the FAA

Flight tests. (Section 6). One transponder was removed from the aircraft, placed in the hanger at Thule, Greenland, a helical antenna installed, and the unit operated for the twenty-four hour synoptic ranging test, described later in this section.

Ionospheric propagation delay was measured by subtracting the computed slant range from the measured slant range, both expressed in microseconds propagation time. The computed slant range propagation time assumes the propagation velocity is the speed of light in a vacuum. NASA predictions of satellite position were used in computing the slant range from a satellite to a fixed transponder.

Ranging interrogations were transmitted from the Observatory at rates appropriate to the experiment, usually one each three seconds, unless several transponders were in the sequence; then the interrogation rate was usually one every two seconds. When spin modulation of ATS-3 became of such magnitude that it could affect the measurements, the interrogation rate was matched to the spin rate. (Page 5-27)

The sequence of interrogating the transponders was set up and operated automatically.

Range measurements were recorded on punched paper tape together with other pertinent data. (Section 3).

Data were transferred from the punched tape to a GE-600 computer. NASA position predictions for the satellite state the latitude, longitude, and height. Precision of the tone-code ranging measurements proved to be so good that the linear interpolation between the half-hourly position fixes furnished by NASA could sometimes introduce errors larger than the precision of measurement. The computer program was rewritten to provide a cubic interpolation so that the estimated positions of satellite between the half-hourly stated points were precise within the 0.001 degree of latitude and longitude, and the 0.01 nautical mile earth center distance precision of the NASA predictions. The program interpolated the position of the satellite at the time of each range measurement, then computed the slant range, and subtracted the computed from the measured range for both the Observatory and the distant transponder.

An additional program computed a "best fit" quadratic curve to the differences, and the standard deviation of the actual difference measurements from the computed curve. The value of the "best fit" curve at a specific time provides a better estimate of the correct value of our measured ionospheric propagation delay than a single, randomly chosen measurement. The standard deviation is an estimate of the ranging precision and hence the confidence that can be placed in an individual measurement.

The cyclic variations in electron content were observed from observations taken continuously over twenty-four hour periods, and at many different times of day on many days during more than a year, and for widely separated locations, and at elevation angles near zero to higher than 40 degrees.

Spatial correlation of electron density was observed by comparing the measurements at various geographical separations.

Air Force Cambridge Research Laboratories provided their independent measurements of electron content for comparison with the tone-code ranging

measurements. It was especially interesting to compare the AFCRL measurements with the Schenectady and Gander measurements, because the AFCRL observations were made at Hamilton, Massachusetts, between Schenectady and Gander.

The data show evidence of errors in predicting the positions of the satellites on some occasions. Satellite prediction errors cause a diurnal variation in range measurement, the same as the period of the ionospheric variations. It is not possible to make an exact separation of the two causes of diurnal range variation, although the AFCRL data are helpful. Widely separated locations for the transponders are also helpful in identifying errors in satellite position predictions because the phase of the range error caused by satellite prediction error is different at each of the separated locations.

Data collected with the Shannon, Reykjavik, Gander and Schenectady transponders is believed sufficient to show that ground reference transponders spaced approximately one thousand miles apart are useful for correcting range measurements at VHF for aircraft and ships along the principal North Atlantic routes. Under all conditions of the tests the correlations of the measurements appear adequate to provide range correction sufficient for one nautical mile, one sigma position fix accuracy. The differences between the computed and measured slant ranges from a ground reference calibration transponder to the satellites can be applied as useful corrections to the range measurements from a mobile craft to the satellites. The calibration measurements will provide corrections for satellite position prediction error as well as for ionosphere propagation delay.

If the mobile craft is within approximately one thousand miles of the reference transponder, the range corrections will be accurate within approximately three microseconds at the times of day when the electron content in the ionosphere is changing most rapidly. Three microseconds represents approximately 1500 feet in two-way ranging. When errors of this magnitude occur in each range measurement, geometrical dilution of position, noise and other factors will result in position fix errors approaching one mile.

The three microsecond estimate applies to the ionosphere as observed under the conditions of the test, including diurnal and seasonal changes, but not including conditions associated with severe magnetic storms. The estimate is derived from the correlations of differences between computed and measured slant ranges in Figures 11-3, 11-4, and 11-5. If the satellite positions had been known more accurately, the observed diurnal changes would have been smaller in most cases, and the corrections would have been better. Three microseconds is considered to be a conservative estimate for the observed conditions.

Errors in satellite predictions are apparent in the differences between computed and measured slant ranges. It is therefore evident that the network of ground reference calibration transponders could be used to track the satellites. The widely spaced deployment of the transponders, their low cost, and automatic operation would appear attractive for the purpose. A few minutes of tracking at intervals spaced through each day would provide a nearly continuous update of satellite positions, and provide accurate position determinations at all times and at low cost. If the transponders operated at L-band or C-band, the effects of the ionosphere would be negligible and high accuracy would be achieved.

FIGURE 11-3

CORRELATION OF DIFFERENCES BETWEEN COMPUTED AND MEASURED SLANT RANGES
GANDER, NEWFOUNDLAND - SCHENECTADY, NEW YORK

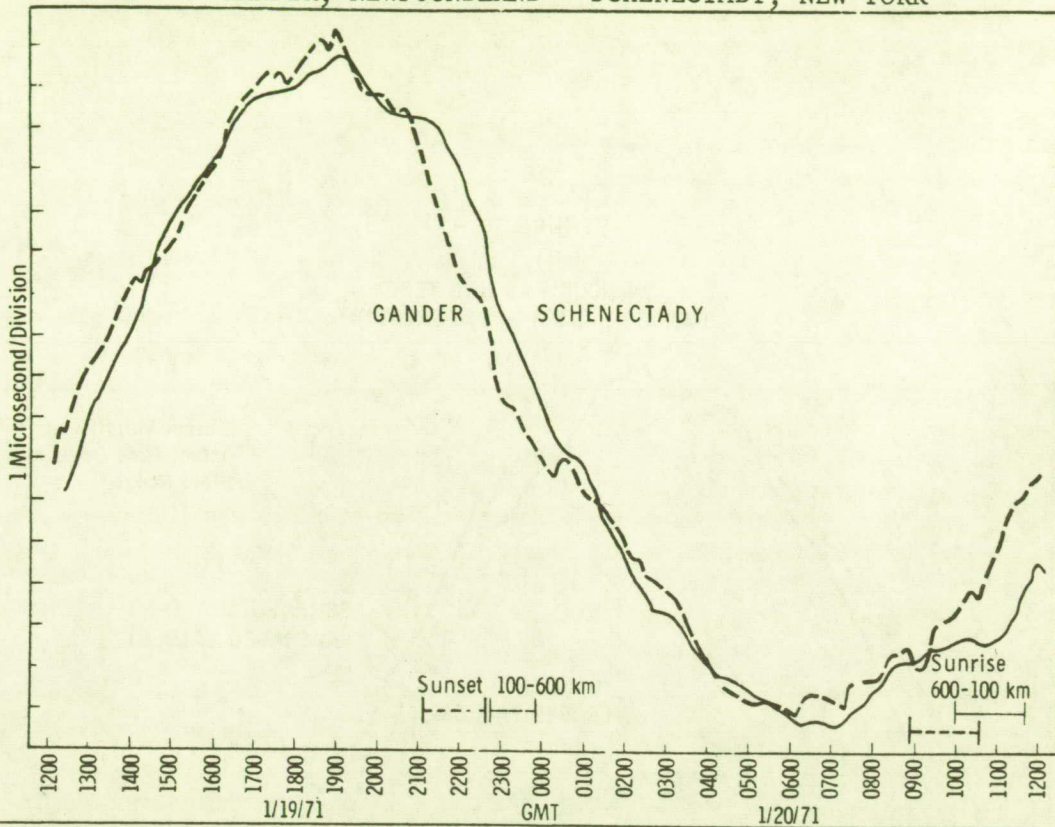


FIGURE 11-4

CORRELATION OF DIFFERENCES BETWEEN COMPUTED AND MEASURED SLANT RANGES
REYKJAVIK, ICELAND - SHANNON, IRELAND

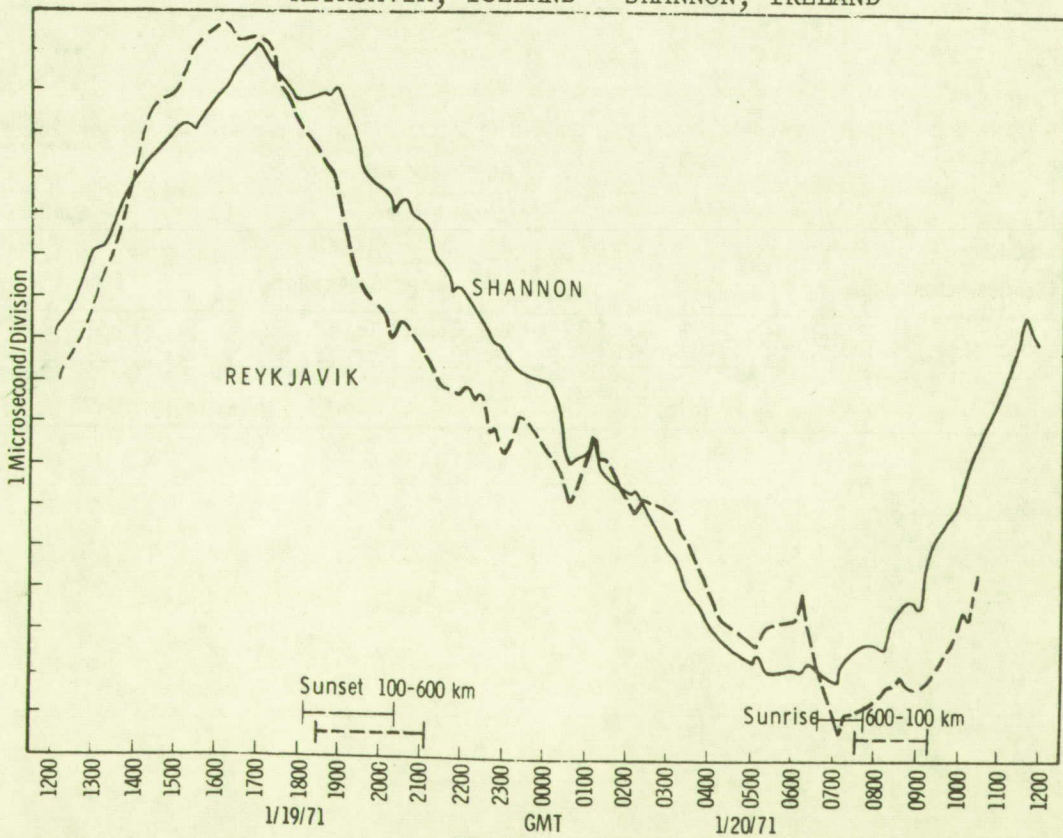
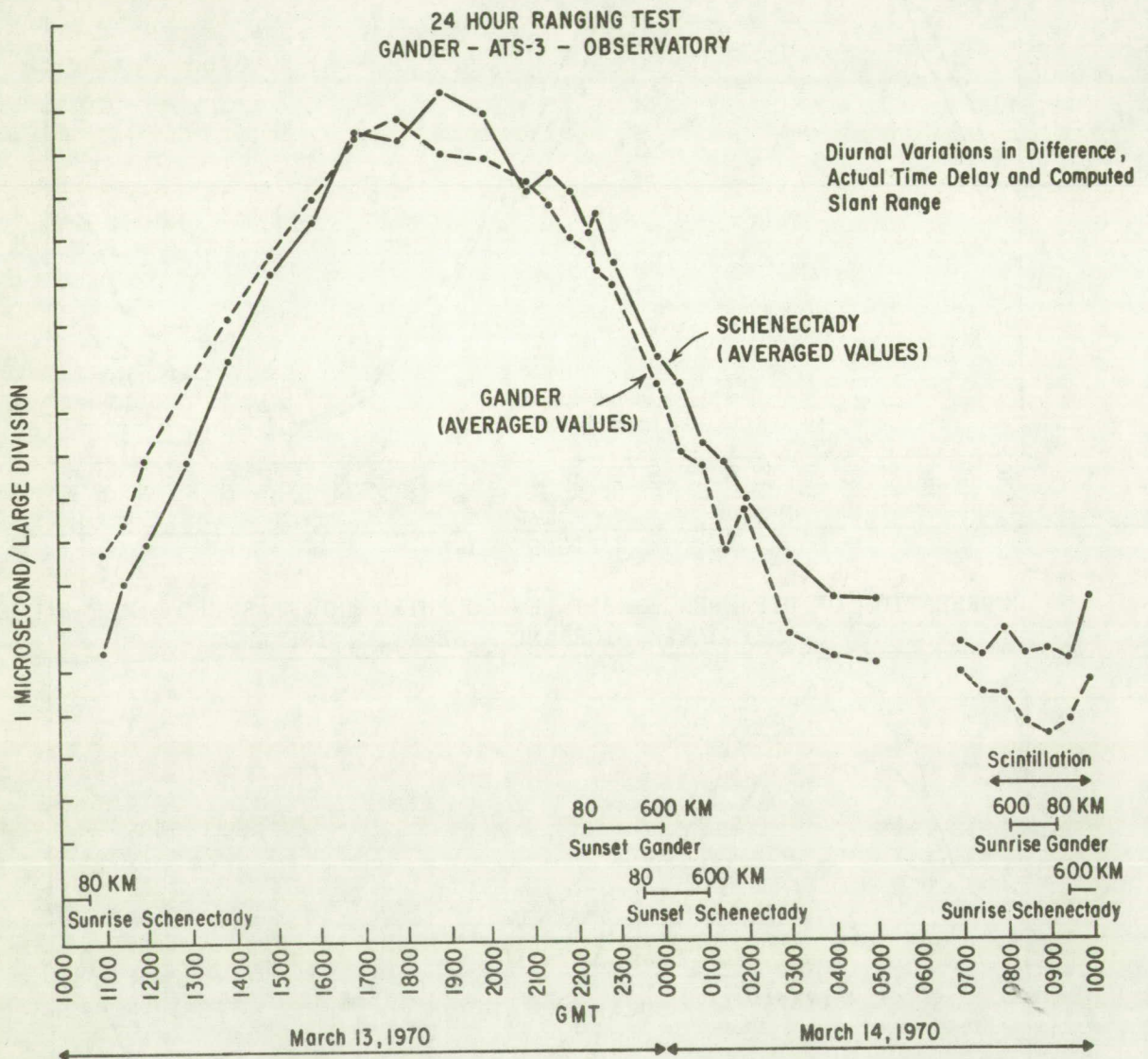


FIGURE 11-5



Twenty-four Hour Test, Gander and Schenectady, March 1970

The National Aeronautics and Space Administration's ATS-3 satellite was used in a ranging and propagation experiment for a twenty-four hour period on March 13 and 14, 1970. (This experiment was performed under General Electric Company funding.) Starting at 1000 GMT on March 13, and continuing until 1000 GMT on March 14, except for the satellite eclipse period from 0430 to 0700, General Electric's Radio-Optical Observatory transmitted tone-code ranging interrogation signals through the satellite to a fixed ground reference transponder at Gander, Newfoundland. Interrogation signals returned from the satellite and responses from the transponder relayed back through the satellite were studied to determine diurnal variations in range measurements. A two-hour period of severe scintillation due to the ionosphere was experienced, and the effects on ranging accuracy and signal reliability were measured for that condition.

Voice communications between an aircraft in flight and several ground terminals were relayed through the satellite on another channel simultaneously with ranging tests. Voice was transmitted from Gander, Newfoundland through the satellite while the General Electric Observatory at Schenectady ranged on the satellite on the same channel.

Ranging interrogations were made at a rate of once per three seconds during the periods from 1000 to 1135 GMT on March 13, from 2130 on March 13 to 0207 on March 14, and from 0700 to 1007 on March 14, to insure the collection of high resolution data on ionospheric changes during sunrise and sunset periods. Interrogations were made once each three seconds for five minutes each half hour, and once each thirty seconds throughout the rest of the experiment.

Ranging data on Gander were not collected during the first thirty-eight minutes of the experiment because the fuse in the power supply of the transmitter was loose in its socket. After the fuse was tightened, the unit responded immediately to interrogations and continued to operate perfectly throughout the test.

Responses to the interrogations provided time interval measurements from the Observatory to the satellite and return, and from the Observatory through the satellite to Gander and return. Measurements from each interrogation were completely independent of the others.

Standard deviations of the range measurements were computed for the five minute higher-rate interrogation periods each half hour. Standard deviations during the five minute periods for the Schenectady-Satellite-Schenectady path were from 0.3 to 0.83 microsecond, with an average value of 0.48 microsecond. Standard deviations on the returns from Gander were from 0.49 to 1.2 microseconds with an average of 0.75 microsecond. The largest observed standard deviation for Gander during a five minute period was 1.12 microseconds, and the smallest was 0.5 microsecond. For Schenectady, the maximum was 0.83 microsecond and the minimum was 0.33 microsecond.

During a two-hour period from 0736 to 1007 GMT on March 14, scintillation occurred with signal levels ranging from several dB above the average of -98 dBm to short dropouts below -121 dBm. The sun was rising in the ionosphere for portions of the ray paths to both ground stations at that time. We do not ascribe the scintillation to the effect of sunrise, as we have observed scintillation at other times when the sun was not rising on the ray path.

The diurnal variation in range measurements due to the ionosphere, satellite position uncertainty, and any other bias changes, was determined by computing the radio propagation time for the geometrical slant ranges from the satellite to Gander and Schenectady at the time of each analyzed data point. The differences between the computed and measured time delays are the sum of a constant component of equipment delay, plus all variables including ionosphere, satellite position uncertainty, and changes in equipment time delay.

The Pan American 747 aircraft enroute from Kennedy airport to Puerto Rico communicated by voice to the Observatory, to Aeronautical Radio at Annapolis, Maryland, and to NASA-Goddard mobile units at Miami and Los Angeles.

Transmission between the ground terminals and the aircraft was on a nominal up link frequency of 149.245 MHz, and a down link frequency of 135.625 MHz. The aircraft transmission frequency was 5 kHz above the nominal. The nominal frequency is 50 kHz above the frequencies used between the Observatory and Gander. The bandwidth of the satellite is 100 kHz.

No voice communications were conducted during the five minute periods each half-hour while the higher-rate range measurements were taken. Range measurements were made every thirty seconds during the voice communications. Standard deviation of the range measurements on Gander was $\approx 0.9 \mu s$ (≈ 450 feet) during aircraft voice transmissions, compared with an average of $\approx 0.75 \mu s$ (≈ 390 feet) when the satellite was not relaying both signals.

Voice transmissions were made on the 149.195 up link frequency from Gander and relayed on the 135.575 down link frequency, using the transponder equipment. Simultaneously, ranging measurements were made from the Observatory to the satellite on the same frequencies. Standard deviations of the Schenectady-satellite signals averaged 0.65 microsecond during the Gander voice transmissions, compared with 0.37 microsecond average for a five-minute period immediately following when the satellite was not relaying two signals simultaneously. The voice and ranging signals were both received simultaneously at the Observatory, and the receiver-correlator was able to separate the ranging returns from the strong voice signals, which had modulation components at the tone frequency. When one signal was stronger than the other, the FM capture effect tended to suppress the weaker signal.

Signal strength between Gander and Schenectady was good except for short, sometimes deep fades during the two hour period of scintillation. It was occasionally necessary to change the transmit and receive polarizations at the Observatory to correct for Faraday rotation. Because the up and down link frequencies were different, the transmit and receive polarizations were sometimes orthogonal.

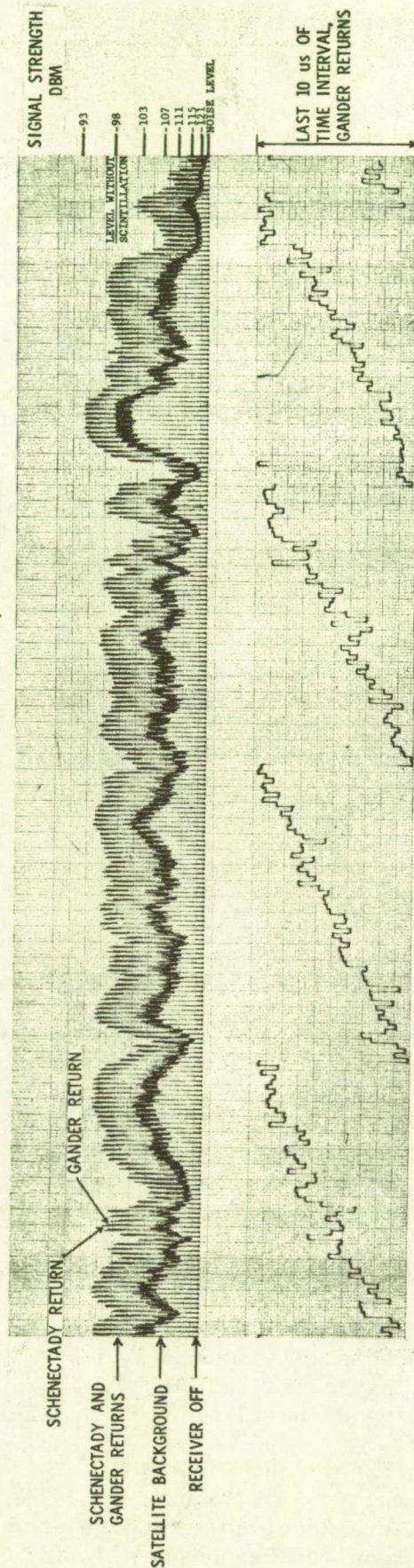
Figure 11-6 is a chart recording of a twelve minute segment of the period of scintillation. It is not sufficient merely to state the magnitude of signal fading due to scintillation because the effect of the scintillation on communications or ranging is determined by the time pattern of fading. The Figure chart recording shows vertical lines at three second intervals. A close examination shows that each vertical line is really a pair, the first being the amplitude of our own return from the satellite, and the second being the return from Gander. The dark irregular band through the middle of the recording represents the background signal received from the satellite when there is no signal input to the satellite. The baseline of the amplitude recording is the receiver out

FIGURE 11-6

EFFECT OF SCINTILLATION

March 14, 1970

09 09 30 to 09 22 00 GMT (12 minutes, 30 seconds)



NUMBER OF INTERROGATIONS: 250

MISSED CORRELATIONS: 0 ON GANDER RETURNS
1 ON SCHENECTADY RETURNS

TOTAL NUMBER OF BITS: 14,970

BIT ERRORS: 1 ON GANDER RETURNS
7 ON SCHENECTADY RETURNS

STANDARD DEVIATIONS: GANDER - 0.77 microseconds
SCHENECTADY - 0.66 microseconds

level when the receiver is switched off during our transmission to the satellite. The amplitude scale is not linear.

The highest signal amplitudes, the tips of the vertical lines, are at 93 dBm signal level into the receiver using our 30 foot antenna. The lowest signal value recorded by the receiver is -121 dBm. The amplitude scale is logarithmic. While the signal level did not actually drop to -121 dBm during the twelve minute, 30 second period depicted, there were brief times when it did drop below that level during the two hour scintillation period. The signal level changes shown here are typical of the entire period.

The scintillation that we measured during this period was on the path from the satellite to Schenectady. We do not have an independent measure of the scintillation at Gander. Because of its northern location, it is expected that it was comparable with fading at Schenectady. Its fading pattern is not observable in the returns as recorded at Schenectady because the Gander returns are correlated in amplitude with the Observatory returns. This is believed to have occurred because the Gander transmissions were strong enough to approach saturation of the satellite during all but the deepest fades.

Communications reliability was good in spite of the severe scintillation. However, it is necessary to consider that the gain of the antenna at Gander is approximately 10 dB and the gain at Schenectady approximately 20 dB. The scintillation would have caused a greater degradation of communications reliability to a mobile terminal with a smaller antenna and therefore a smaller fading margin. One may judge the amount of time that communications dropout would have been experienced by a mobile terminal by drawing a line along the recording below the -98 dBm line, displaced by the number of dB representing the fading margin of the mobile link. The -98 dBm level should be used, as that is the normal signal level without scintillation and therefore the reference for the link margin.

The scintillation fading experienced on March 14 was unusually severe. Scintillation fading is not uncommon. A general impression is that scintillation occurs less than 5 percent of the time at Schenectady with an amplitude that is usually only a few dB, peak to minimum.

Communications performance during the period of scintillation is summarized in Table 11-4.

TABLE 11-4

COMMUNICATION PERFORMANCE DURING SCINTILLATION

March 14, 1970, 08:16:15-10:07:00 GMT

Average Signal Level (no scintillation)	-98 dBm
Maximum Signal Level During Scintillation	~-93 dBm
Minimum Signal Level During Scintillation	Less than -121 dBm
Number of Interrogations	2215
Responses Received (Observatory and Gander)	4342
Missed Responses: Observatory - 39; Gander - 49	88
98 percent of Responses Were Received and Correlated	
Total Number of Bits in Received Responses	130,260
Bit Errors: Observatory - 82; Gander - 79	161

The digital coding used was relatively crude. A 3 dB improvement could be obtained using bi-phase modulation rather than the technique of suppressing cycles for zeros. Error rates during the experiment were higher than might be experienced on the same links with better coding. A missed interrogation does not necessarily mean the signal was not received. If more than 3 bits in the word sync or user address part of the code are in error, the ranging correlator rejects the response.

The lower chart recording of Figure 6 shows the ranging time intervals for Gander. It is an analog chart recording of a digitized time interval showing the change in measured interval for each interrogation. One large division on the chart is one microsecond, and the full scale is ten microseconds. The slope on the line is due to the changing range to the satellite. As shown in Figures 6 and 7, scintillation had no serious effect on range measurements. The number of interrogations, missed correlations, bits and bit errors for the twelve minute period are also shown in Figure 6, as are the standard deviations of the range measurements.

Ranging performance and line-of-position accuracy were determined by using satellite position predictions furnished by NASA. The determinations were made for most of the five minute periods each half hour throughout the twenty-four hour test period. Tone-code range measurements were compared with computed slant ranges to Schenectady and Gander. The differences between the measured and computed slant ranges were plotted to show the total diurnal bias change due to ionosphere and other factors such as possible error in predicted position of the satellite. The measured slant ranges and the NASA satellite predictions were used to compute the latitude at which the line-of-position crossed the longitude of Gander. The first computations did not include any corrections except for equipment time delay. The latitude determinations were then corrected by the use of an independent measure of the ionosphere made at Hamilton, Massachusetts by Air Force Cambridge Research Laboratories. The original latitude determinations were then corrected by taking the differences between measured and computed slant range measurements at Schenectady, and using the differences to correct the Gander range measurements.

Range measurements taken at 3 second intervals during five minute periods were analyzed for standard deviation. A "best-fit" quadratic curve was fitted to the approximately 100 range measurements. The standard deviations of the measurements were computed, and the largest single deviations from the best fit curves were printed out by the computer program. Standard deviations are plotted in Figure 11-7, and the largest single deviations are listed in Table 11-5. Sunrise and sunset at 80 kilometer and 600 kilometer heights along the ray paths from Schenectady and Gander to the satellite are shown in Figure -7, and a period of severe amplitude scintillation is identified during the last hours of the test.

NASA position predictions show that the ATS-3 satellite is not in a perfect geostationary orbit. A slight inclination causes it to move slightly north and south of the equator, tracing a figure eight in a twenty-four hour period. Its orbit has a slight eccentricity so that its altitude changes through a twenty-four hour cycle and during the period of the experiment the satellite was drifting eastward. Figure 11-8 is a plot of each of these motion components as derived from NASA predictions.

FIGURE 11-7

24 HOUR RANGING TEST
GANDER - ATS-3 - OBSERVATORY

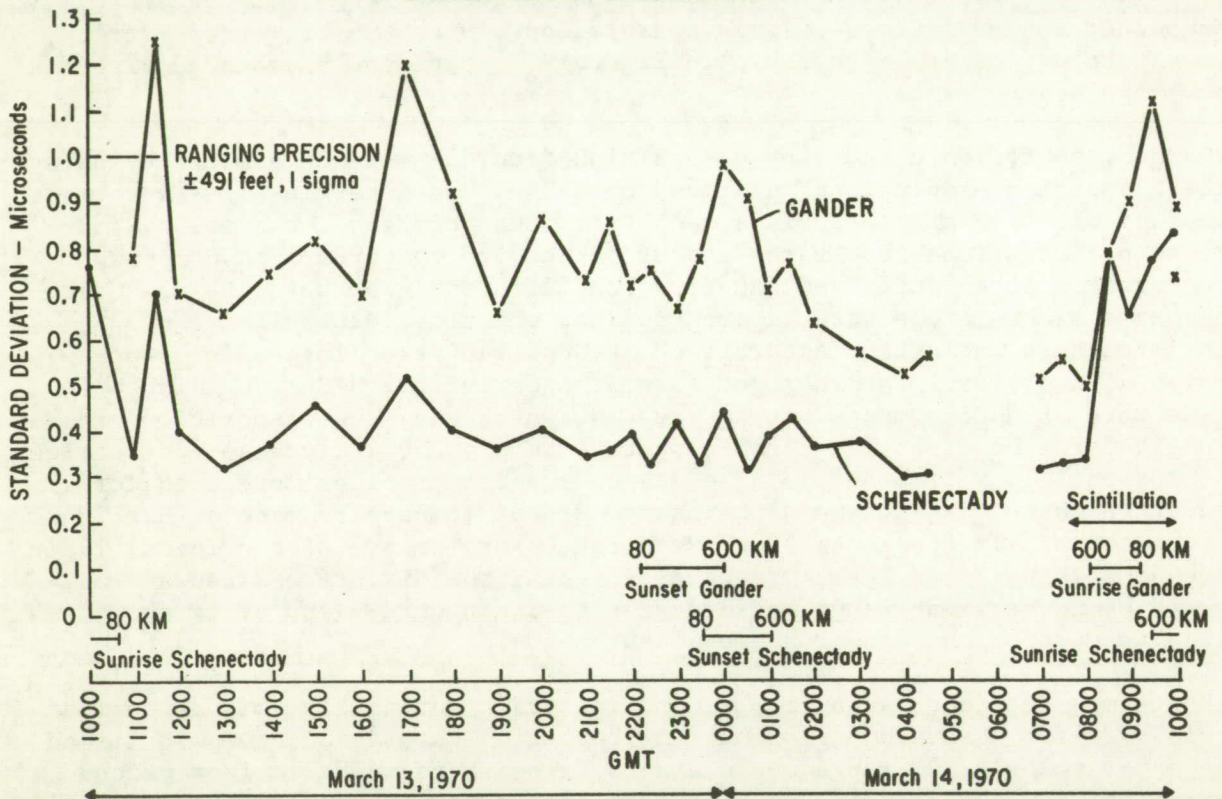


TABLE 11-5

LARGEST DEVIATIONS - 24 HOUR RANGING TEST

GANDER - ATS-3 - OBSERVATORY

March 13, 1970 (1000 - 2400 GMT)

March 14, 1970 (0000 - 1000 GMT)

<u>Number of Measurements</u>	<u>Observatory</u>		<u>Gander</u>		<u>Time</u>
	<u>Minimum</u>	<u>Maximum</u>	<u>Minimum</u>	<u>Maximum</u>	
101	-1.66	+1.81	-----	-----	1000
101	-1.06	+0.87	-----	-----	1030
101	-0.80	+0.79	-3.55	+1.66	1100
101	-4.25	+1.92	-2.00	+6.22	1130
87	-1.03	+0.85	-2.15	+1.59	1200
95	-1.02	+0.74	-1.58	+1.85	1300
61	-0.80	+0.93	-2.88	+1.53	1400
101	-1.79	+1.47	-1.71	+3.57	1500
101	-1.19	+0.95	-2.08	+1.94	1600
102	-1.55	+2.22	-3.37	+7.50	1700
100	-1.35	+0.82	-4.00	+2.72	1800
95	-0.94	+0.98	-1.58	+1.57	1900
101	-1.59	+1.41	-5.08	+2.78	2000
101	-1.17	+0.78	-3.33	+1.92	2100
101	-1.12	+0.94	-4.53	+1.63	2130
101	-1.68	+0.76	-2.32	+2.78	2200
101	-1.04	+0.77	-2.05	+2.68	2230
87	-1.40	+0.78	-2.10	+1.50	2300
93	-0.82	+0.75	-1.97	+2.23	2330
101	-1.86	+2.11	-3.87	+2.21	0000
101	-0.90	+0.70	-3.89	+1.74	0030
101	-1.18	+0.83	-2.48	+1.52	0100
77	-0.99	+1.43	-1.63	+1.85	0130
101	-1.31	+0.68	-2.34	+1.48	0200
98	-1.29	+0.89	-1.79	+1.78	0300
101	-0.84	+0.56	-1.61	+1.40	0400
101	-0.69	+0.84	-1.52	+1.19	0430
113	-0.73	+0.89	-1.36	+1.48	0700
101	-0.75	+0.88	-1.14	+1.32	0730
101	-0.81	+0.83	-1.34	+2.10	0800
99	-1.10	+3.31	-1.96	+2.55	0830
101	-0.89	+2.86	-2.16	+3.92	0900
101	-1.68	+4.06	-2.32	+4.72	0930
*81	-4.08	+2.35	-2.18	+3.88	1000
**140	-1.29	+1.80	-2.28	+1.96	1000

* Reading taken just prior to 1000 GMT

**Reading taken just after 1000 GMT

FIGURE 11-8

24 HOUR RANGING TEST
GANDER - ATS-3 - OBSERVATORY

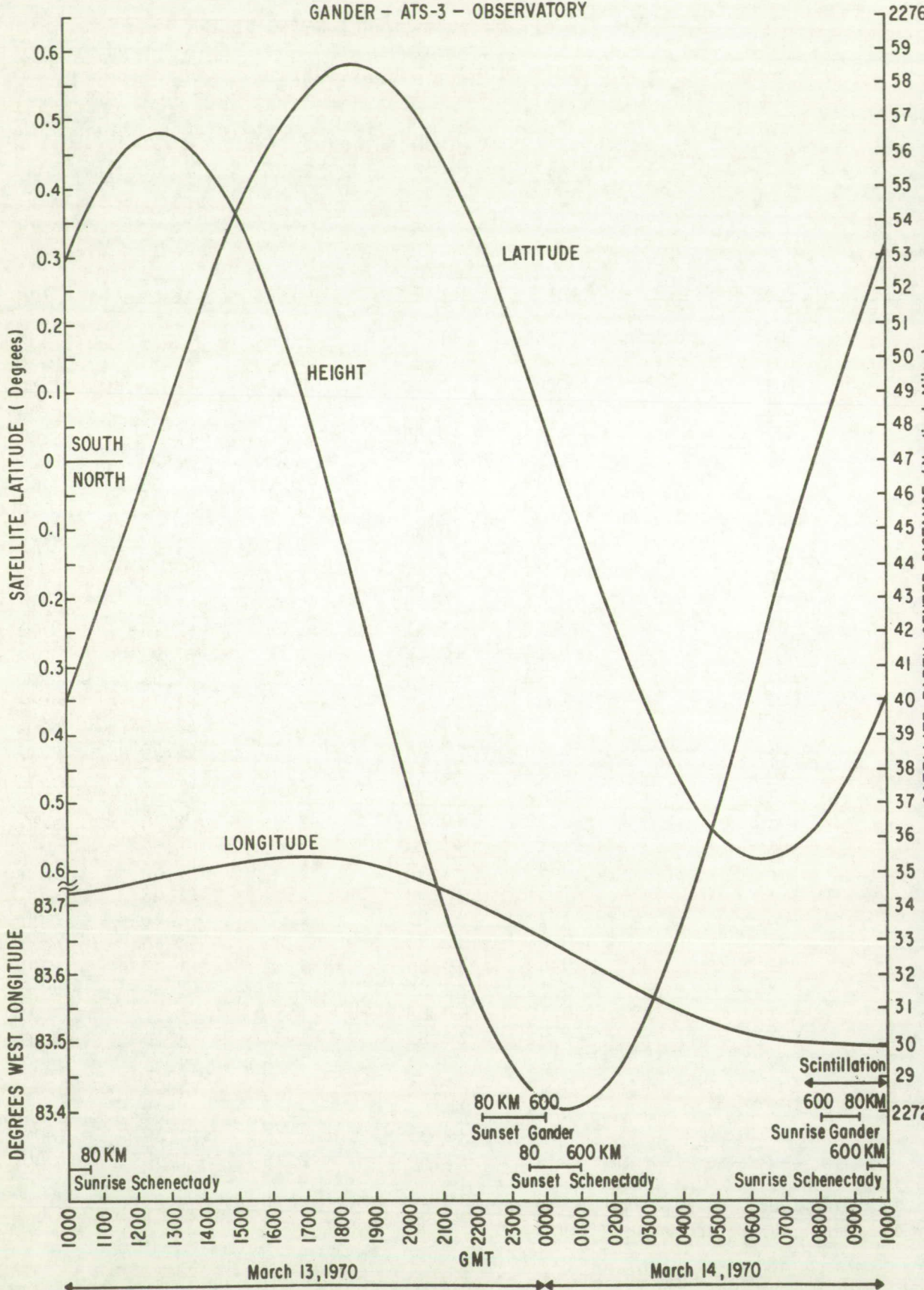


Figure 11-9, based on the NASA predictions, shows the computed slant range from the satellite to the Observatory as the solid line curve. The actual range measurements are shown as X's. The curves have a greater difference during the daylight hours when the VHF range measurements are affected by increased delays through the ionosphere. The differences are the total bias changes in the range measurements. The accuracy of a line-of-position depends upon the exactness of the correction for the bias changes.

Figure 11-10 shows the measured ranging time to Gander through the satellite. The amplitude of the curve is larger because satellite motion affects the range measurements on both paths and the sum of the effects appeared in the range time to Gander.

Figure 11-11 gives the difference in measured time delay and the computed time delays for the geometrical slant ranges between the satellite and Schenectady and Gander. It is plotted from specific data points that fall on or very close to the best fit curve through each five minutes of data. These averaged values thus remove individual fluctuations in the measurement and provide a plot of the diurnal variations in range measurements due to the ionosphere and satellite position uncertainty.

The total diurnal bias change was approximately 13 microseconds, and was the same, within approximately one microsecond for Gander and Schenectady. Approximate values are stated here to indicate magnitudes. Individual data points, as plotted, are precise to tenths of a microsecond.

Gander is approximately 850 nautical miles east and 360 nautical miles north of Schenectady. The curves of bias change for the two locations are correlated, with the Gander curve shifted earlier in time, as expected, because of its eastward location.

Air Force Cambridge Research Laboratories furnished a curve of electron density for the period of the experiment. The curve, Figure -12, is computed from differential Faraday rotation of the beacon signals of ATS-3 as measured at Sagamore Hill, Hamilton, Massachusetts. The electron density curve correlates with the range bias curves. The total change in vertical electron content was 33×10^{16} electrons per square meter. Based on the AFCRL data, the total change in range measurement bias due to the ionosphere would be $\sim 7.0 \mu\text{s}$. As the observed change was $13 \mu\text{s}$, some other diurnal effect must have contributed to the bias. The computed change in range time to the satellite was $\sim 780 \mu\text{s}$ with the maximum range occurring at approximately 1630 GMT, whereas the peak in electron density occurs at 1800 or 1900 GMT, so that the maximum range due to satellite motion occurs near the time of maximum range delay due to the ionosphere. The diurnal changes due to the ionosphere and the satellite range change are in phase so that the effects add. It seems reasonable to assign the $6 \mu\text{s}$ difference between the computed ionosphere bias change and the measured bias change to uncertainty in satellite position. A bias change of that magnitude would result if the satellite moved 1500 feet closer to the ground terminals than predicted by NASA at the northern limit of its motion, and 1500 feet farther away at its southern limit. The total range change was ~ 63 nautical miles. Ranging time delays as stated in this report are for the two-way radio signal travel time.

Figure 11-13 plots the latitude determinations using the range measurements to Gander uncorrected for any diurnal variations. The latitudes were computed

FIGURE 11-9

24 HOUR RANGING TEST
GANDER - ATS-3 - OBSERVATORY

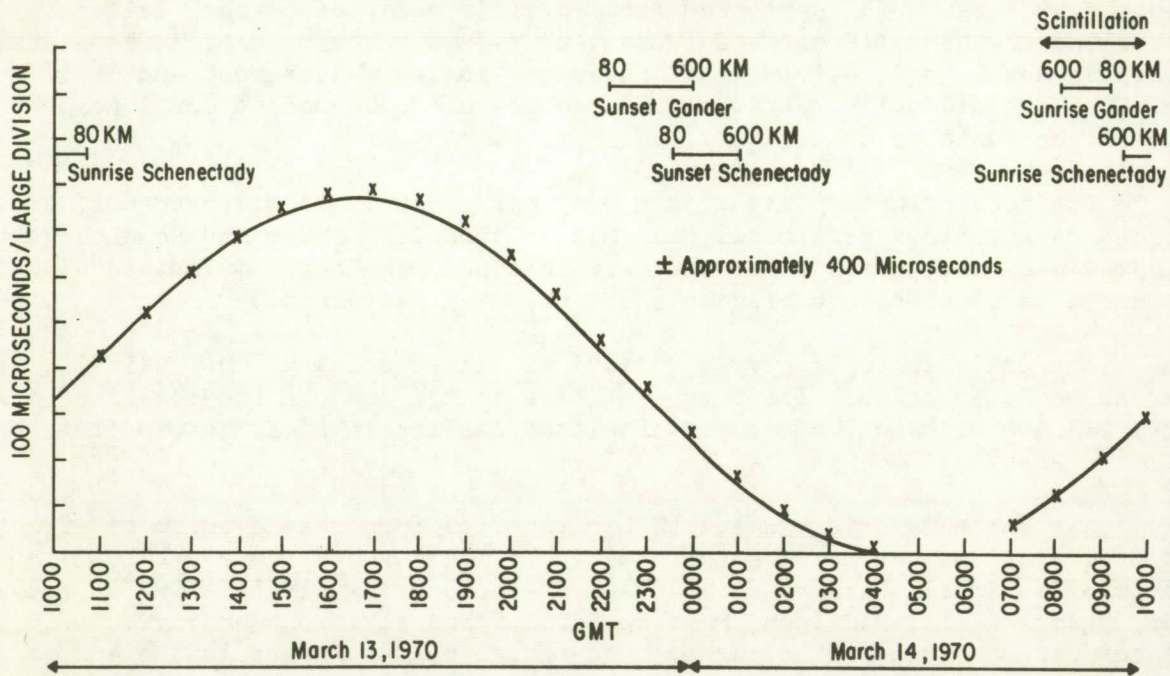


FIGURE 11-10

24 HOUR RANGING TEST
GANDER - ATS-3 - OBSERVATORY

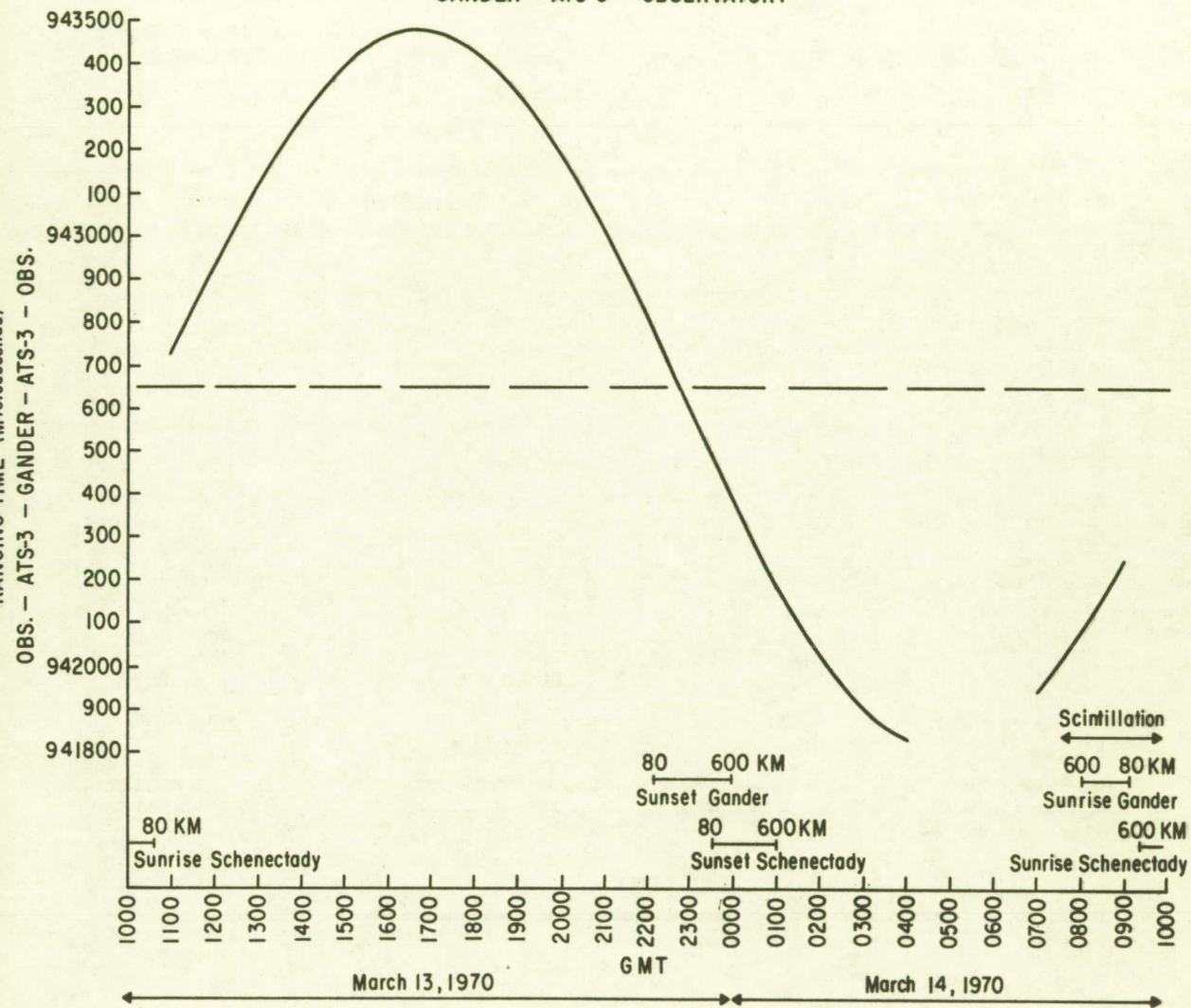
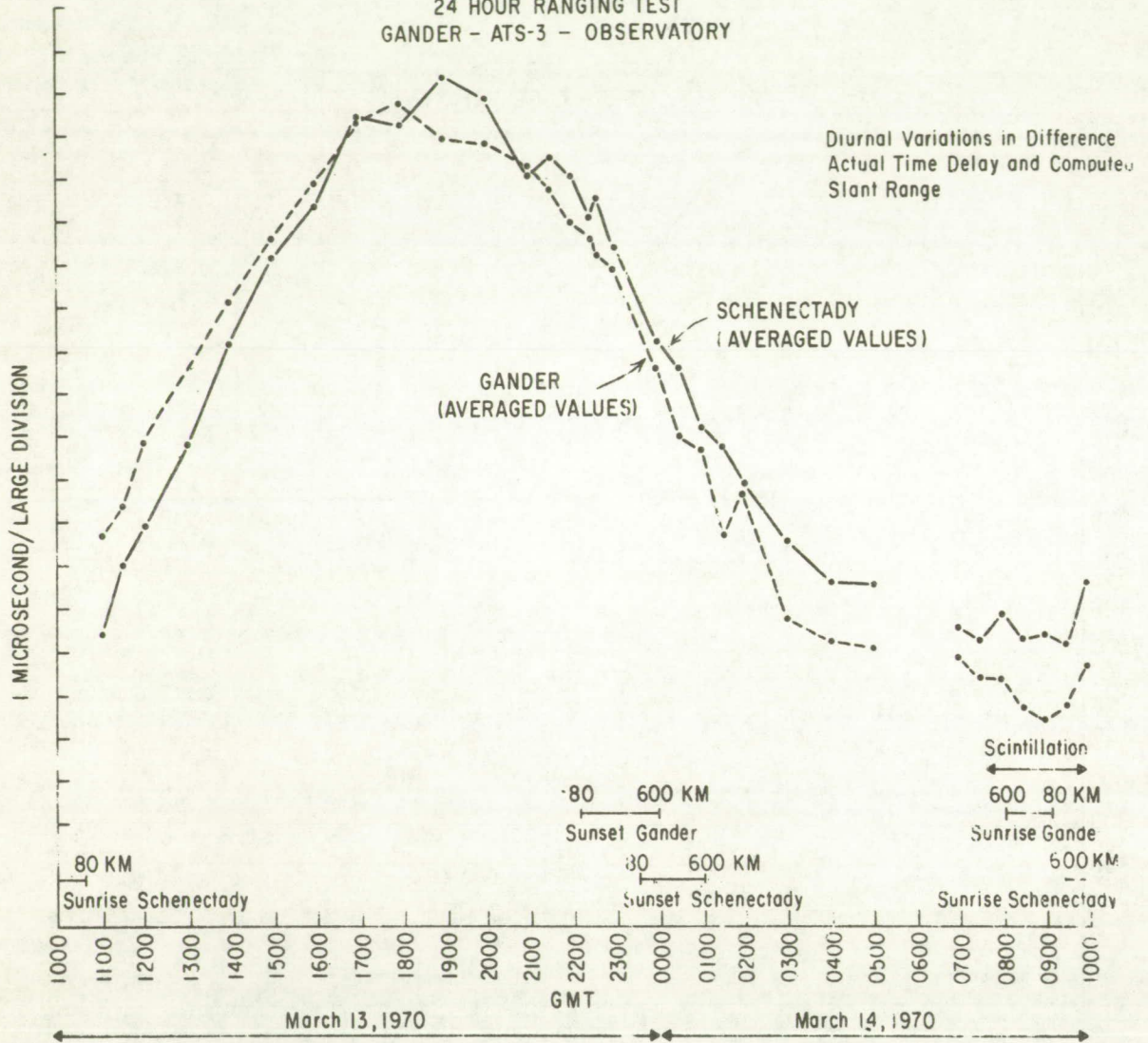


FIGURE 11-11

24 HOUR RANGING TEST
GANDER - ATS-3 - OBSERVATORY



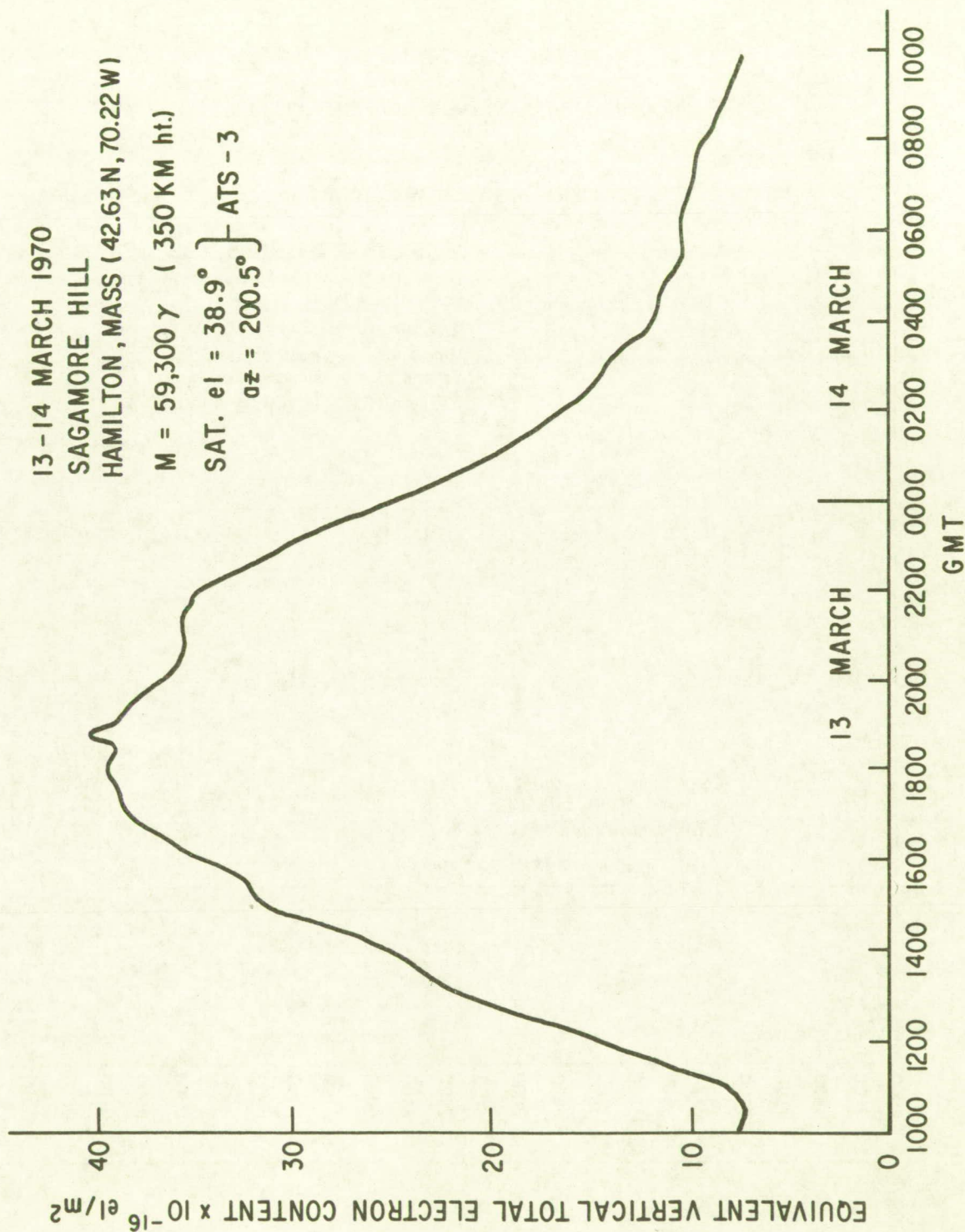
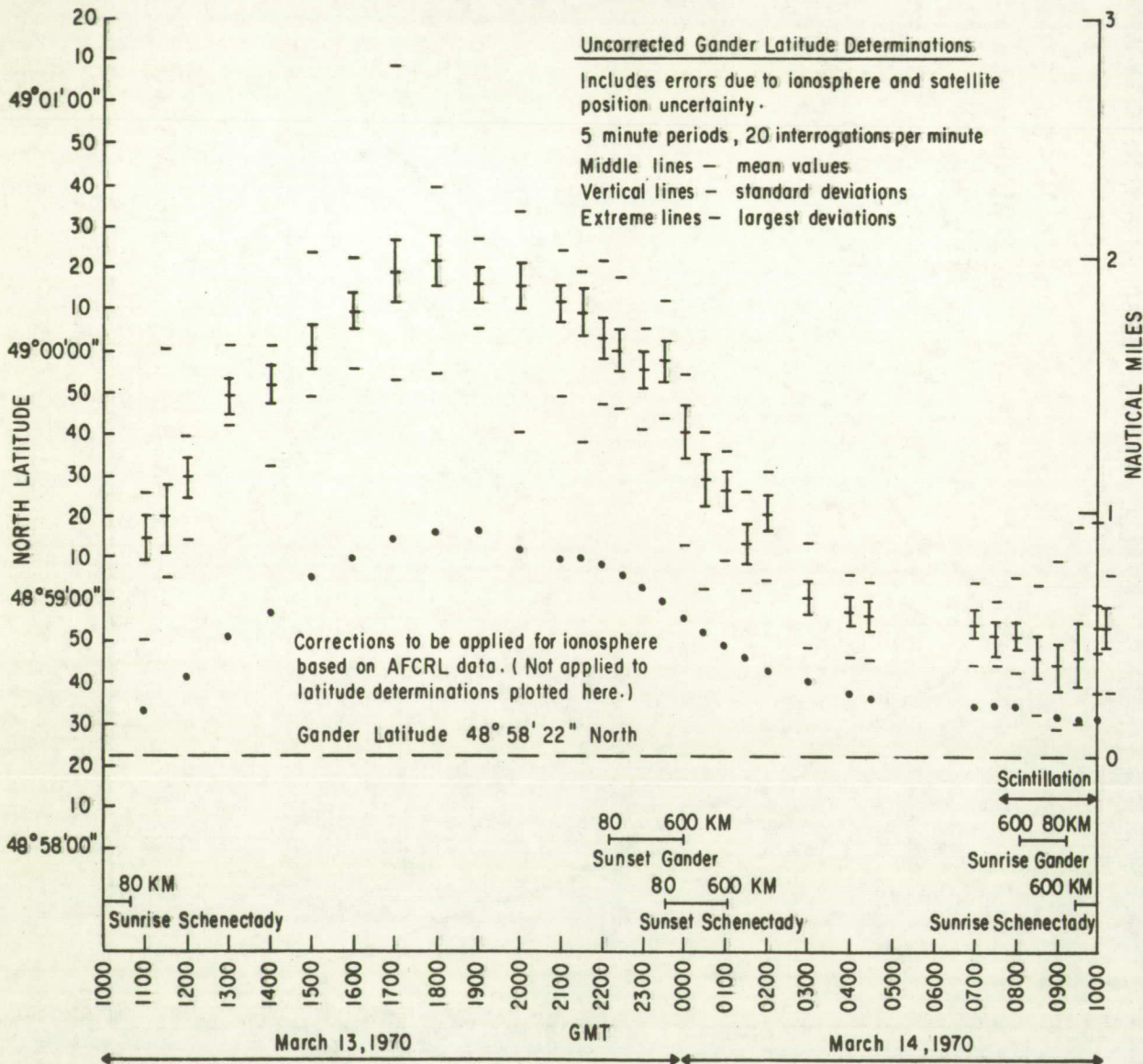


FIGURE 11-13

UNCORRECTED LATITUDE DETERMINATIONS

24 HOUR RANGING TEST
GANDER - ATS-3 - OBSERVATORY



for each five minute period by selecting a range measurement that was on or very close to the best fit curve through the data points. The range measurement was used in a computer program to determine the latitude of Gander. Estimates of the equipment time delay and an estimate of three microseconds for the minimum delay through the ionosphere were included as constants. The resulting plot showing the latitude determinations, their standard deviation, and their extreme values, includes all of the diurnal and bias contributions to error in the latitude determination. Also plotted on Figure 11-13 are the corrections that should be applied based on the ionosphere measurements furnished by AFCRL. It is emphasized that these corrections were not applied in the latitude determinations on Figure 11-13.

Figure 11-14 shows the Gander latitude determinations when the AFCRL ionospheric corrections are applied. There is a cyclic residual error. It is in phase with the satellite variation in range shown in Figure 11-8, suggesting that the predictions of satellite position have an error of approximately the magnitude postulated in the discussion of Figure 11-11. The use of independent ionospheric data can correct for ionospheric variations but not for satellite position uncertainty.

The use of a calibration transponder, such as used at Gander, can take both factors into account.

Figure 11-15 is a plot of the latitude determinations when the corrections for Gander range measurements are taken from the Schenectady range measurements. Each range calibration measurement at Schenectady was a single range measurement taken within five minutes of the Gander data. The calibration measurement was not selected to correspond to the best fit curve. When the Schenectady calibration corrections were applied to the Gander range measurements, the latitude determinations for Gander are as shown in Figure 11-15.

Reference to Figure 11-11 shows that the diurnal variation at Gander was approximately one hour advanced in phase with respect to the Schenectady data because of the earlier sunrise and sunset time. To determine the accuracy that might be achieved by calibration, data taken at one location are shifted in time to correspond to the time at the user location. The Schenectady curve of Figure 11-11 was shifted one hour to bring it more nearly in phase with the Gander data and the new corrections were applied. When the Gander range measurements were corrected by data points taken approximately one hour different in time, but selected to observe the ionosphere at approximately the same sun time, the latitude determinations for Gander are as depicted in Figure 11-16. The limits of the standard deviations fall within approximately one-half mile of the actual latitude of Gander. More than 2500 latitude determinations are represented by the data shown in Figure 11-16. All of them lie within approximately one nautical mile of the true latitude of the Gander transponder.

Except for the two-hour period of amplitude scintillation, the ionosphere appeared to be undisturbed during the test period. It cannot be assumed that the line-of-position accuracy achieved on the day of the test would be achieved every day, or over other regions of the earth. More test data are required, including periods of magnetic disturbance and for other geographical locations.

For a "normal" ionosphere, as typified by March 13-14, 1970, the results of the tests do support the conclusions of the Interim Report (Contract NAS5-11634) that ground reference transponders at spacings of hundreds of nautical miles are useful in improving position fixing accuracy, and that one nautical mile, one sigma accuracy may be achieved when they are employed.

FIGURE 11-14

24 HOUR RANGING TEST
GANDER - ATS-3 - OBSERVATORY

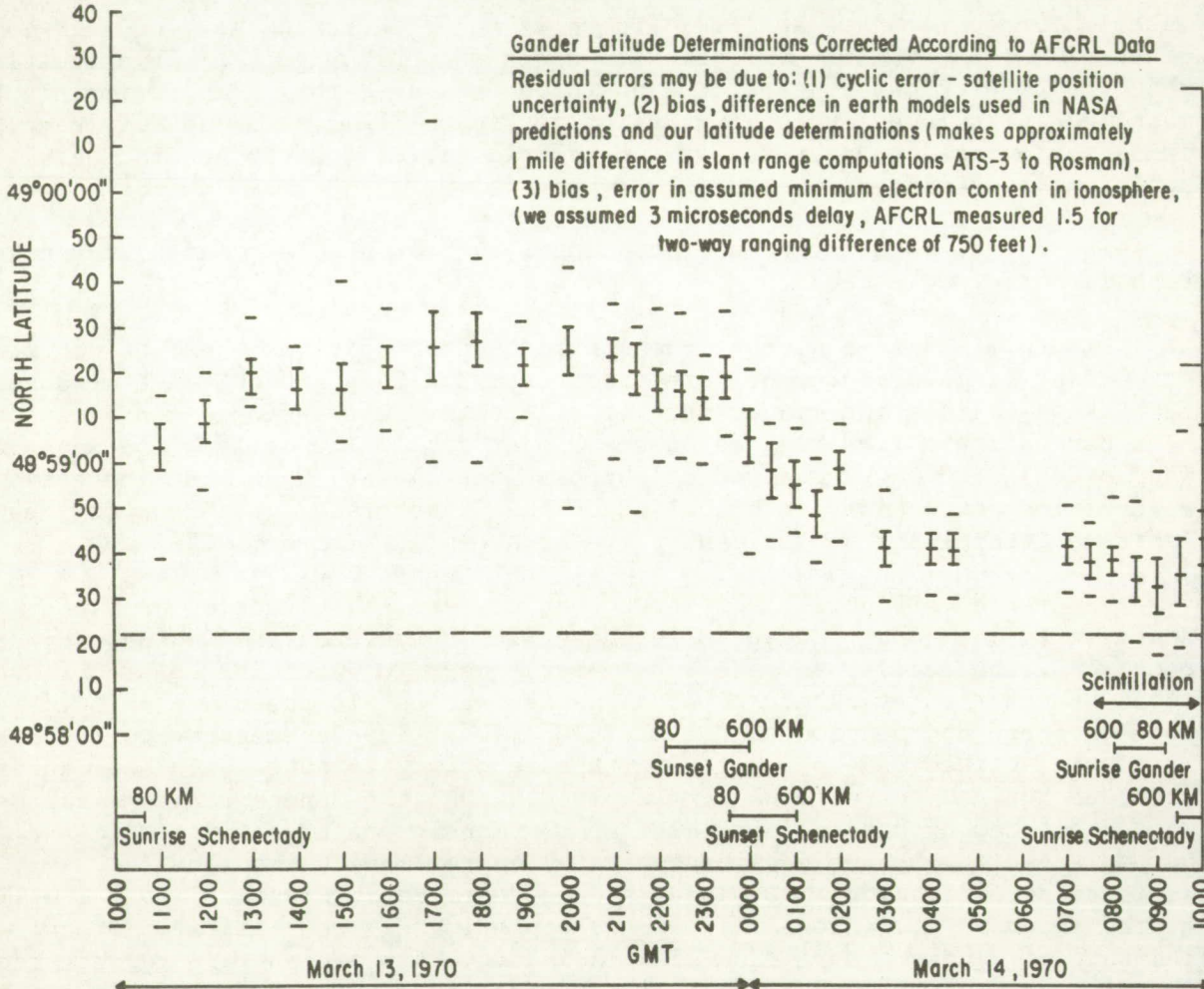


FIGURE 11-15

LATITUDE DETERMINATIONS CORRECTED BY SCHENECTADY RANGE CALIBRATION MEASUREMENTS
Schenectady Measurements Within 5 Minutes of Gander Measurements

24 HOUR RANGING TEST
GANDER - ATS-3 - OBSERVATORY

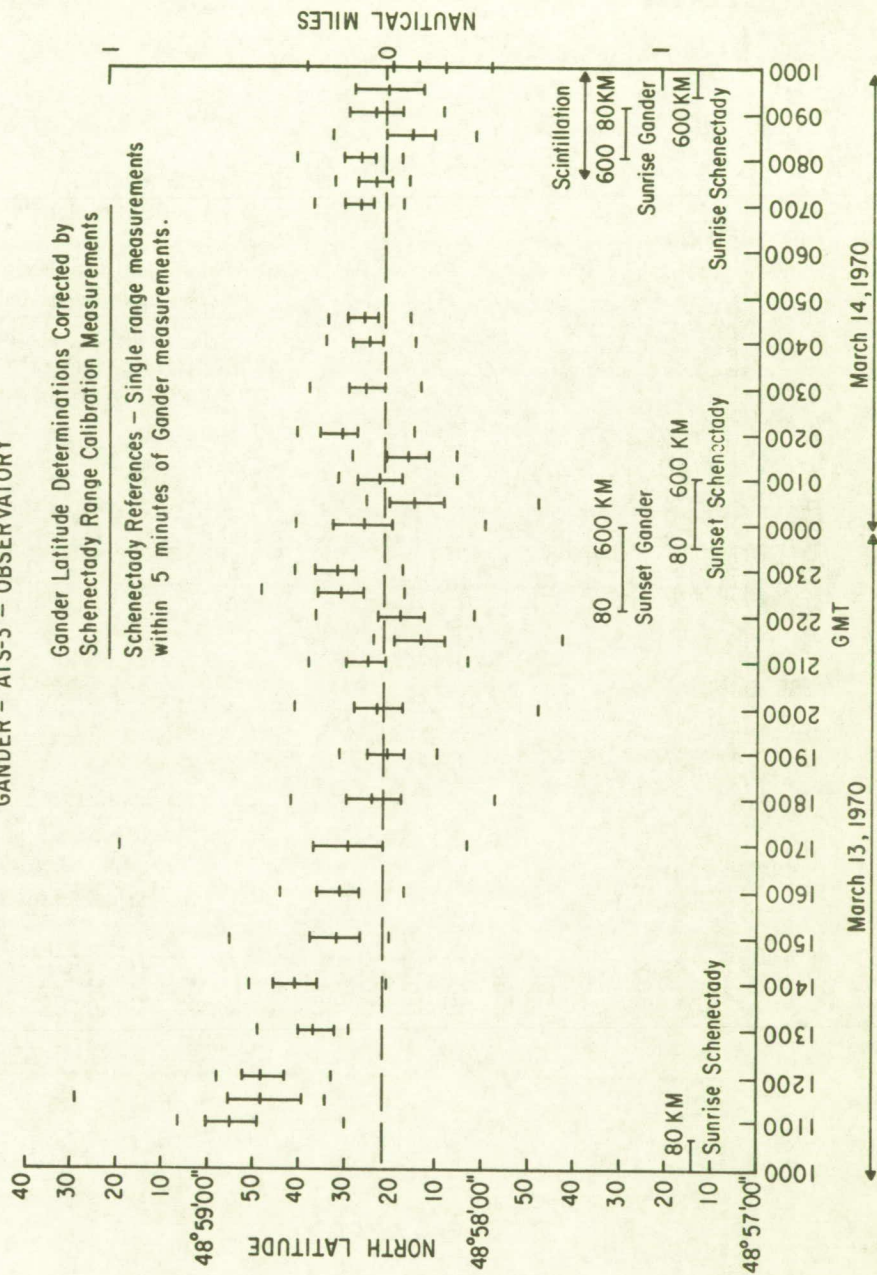
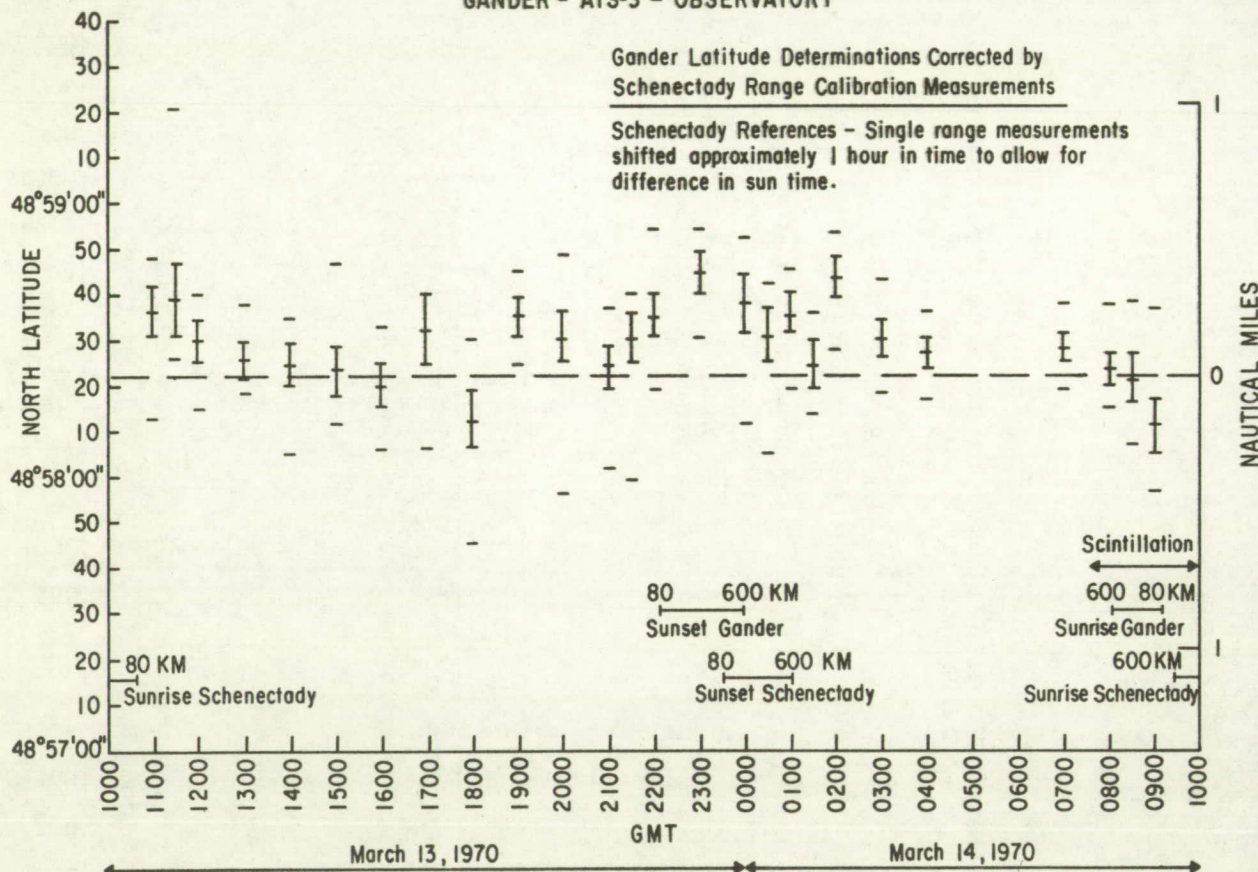


FIGURE 11-16

24 HOUR RANGING TEST
GANDER - ATS-3 - OBSERVATORY



Four-day Synoptic Ionosphere Propagation Measurements - November 1970

A solar flare was reported on October 28, 1970. Starting at 19:05:00 GMT on October 29, ranging measurements were made at intervals on each day through November 2, 1970, from ATS-3 to Shannon, Gander, Schenectady and Seattle. No unusual effects were observed due to the solar flare. The range measurements provided a comparison of the ionosphere over the four ray paths from the satellite to the transponders, and also a day-to-day comparison for each of the four ray paths. There is evidence that the results were affected by errors in predictions of satellite positions.

Range measurements were made during approximately six half hour periods spaced throughout each of the four days. During each half-hour period, approximately 200 range measurements were made to each of the reference transponders and 600 to Schenectady. The number of Schenectady measurements is larger because every interrogation of a distant transponder provides a range from Schenectady to the satellite.

The differences between the measured and computed geometrical slant ranges to the satellite were determined for each range measurement. NASA predictions of satellite position were used in computing the geometrical slant range. A "best fit" quadratic curve was fitted to the differences and the value of the curve at the exact time of a NASA prediction was selected. This process smooths the measured data and minimizes any errors that could result from interpolating between the half-hourly satellite position predictions supplied by NASA.

The differences between the measured and computed geometrical slant ranges are presented in Figures 11-17 through 11-20. The lines connecting the data points are included only as an aid in following the changes; they do not represent data.

The diurnal effect of the ionosphere is clearly evident at each location. The day-to-night change is smallest at Shannon, and increases with the westward position of the station, being largest at Seattle. A check was made to determine if the increased diurnal change with westward location could be due to satellite position prediction errors, but results of the check are not conclusive. The data plotted in Figures 11-17 through 11-20 were based on satellite predictions computed from tracking data with an epoch date of October 23.

Predictions for November 8, based on October 23 and November 8 tracking data were obtained from NASA and are compared in Table 11-6. An error of 0.001 degree in latitude can cause a ranging error larger than 0.5 microsecond for mid-latitude locations. The expected day-to-night ionospheric change is approximately 13-15 microseconds. If the difference between these expected values and the observed values for Shannon and Seattle are due to satellite position errors, the data suggest that the satellite was closer to Seattle than its predicted position by approximately 2500 feet at 1000 GMT each day and farther from Seattle by approximately 4400 feet at 2100 GMT each day. For Shannon, the satellite was closer by approximately 1500 feet than predicted at 1700 GMT.

Figures 11-21 through 11-24 overlay the four days of data for each location to show the day-to-day correlation for each one. The correlations are high, suggesting that a model of the ionosphere could describe the ionosphere for those days within approximately ± 1.5 microseconds. A solar flare sometimes causes the electron content in the ionosphere to increase by as much as 50 percent above the normal value on the day of the event. It drops rapidly at

FIGURE 11-17

DIFFERENCE, MEASURED AND COMPUTED SLANT RANGES
Satellite Prediction Epoch 23 October 1970

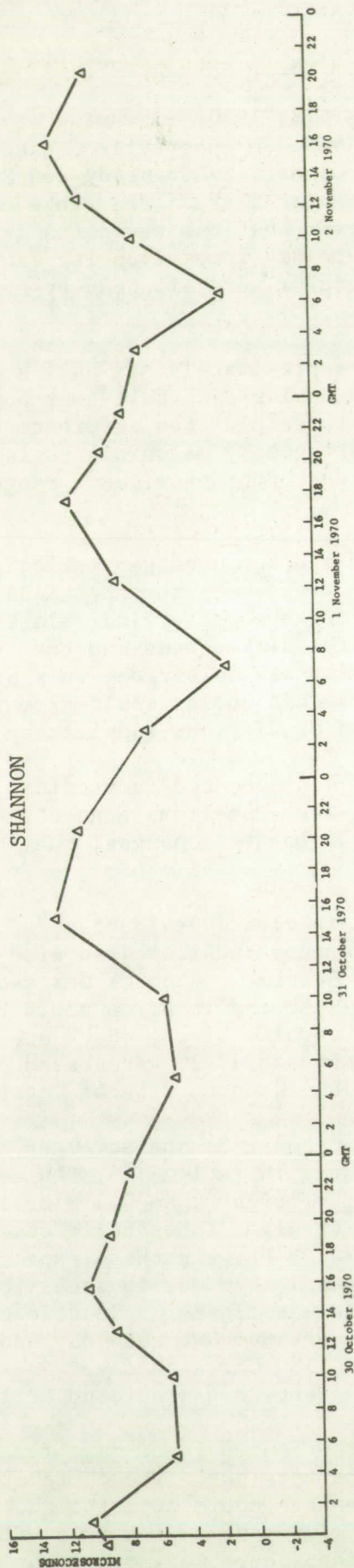


FIGURE 11-18

DIFFERENCE, MEASURED AND COMPUTED SLANT RANGES
Satellite Prediction Epoch 23 October 1970

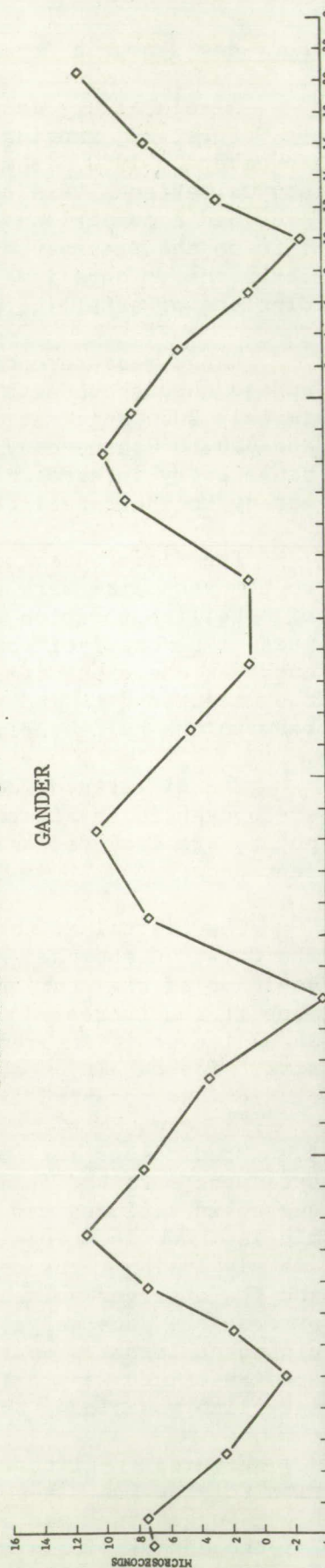


FIGURE 11-19

DIFFERENCE, MEASURED AND COMPUTED SLANT RANGES
Satellite Prediction Epoch 23 October 1970

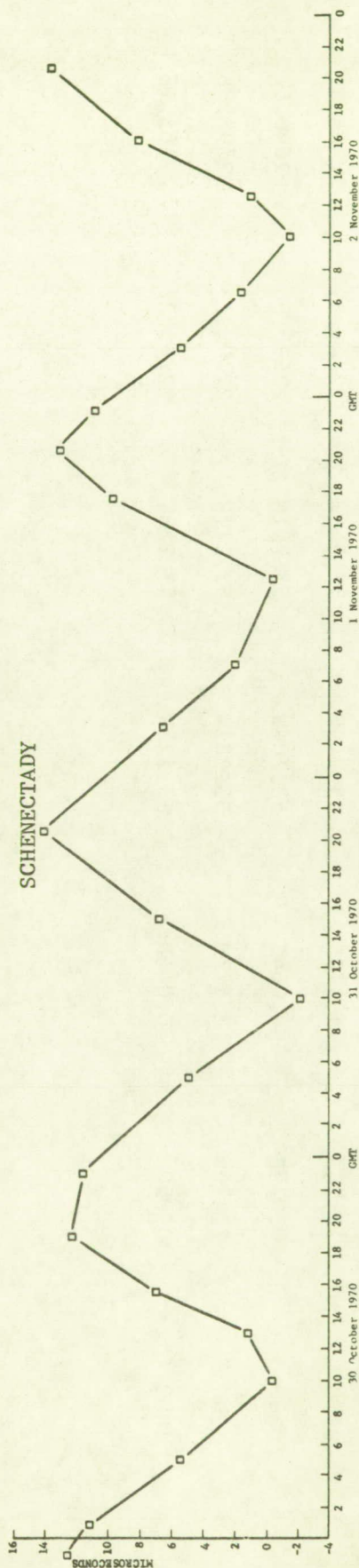


FIGURE 11-20

DIFFERENCE, MEASURED AND COMPUTED SLANT RANGES
Satellite Prediction Epoch 23 October 1970

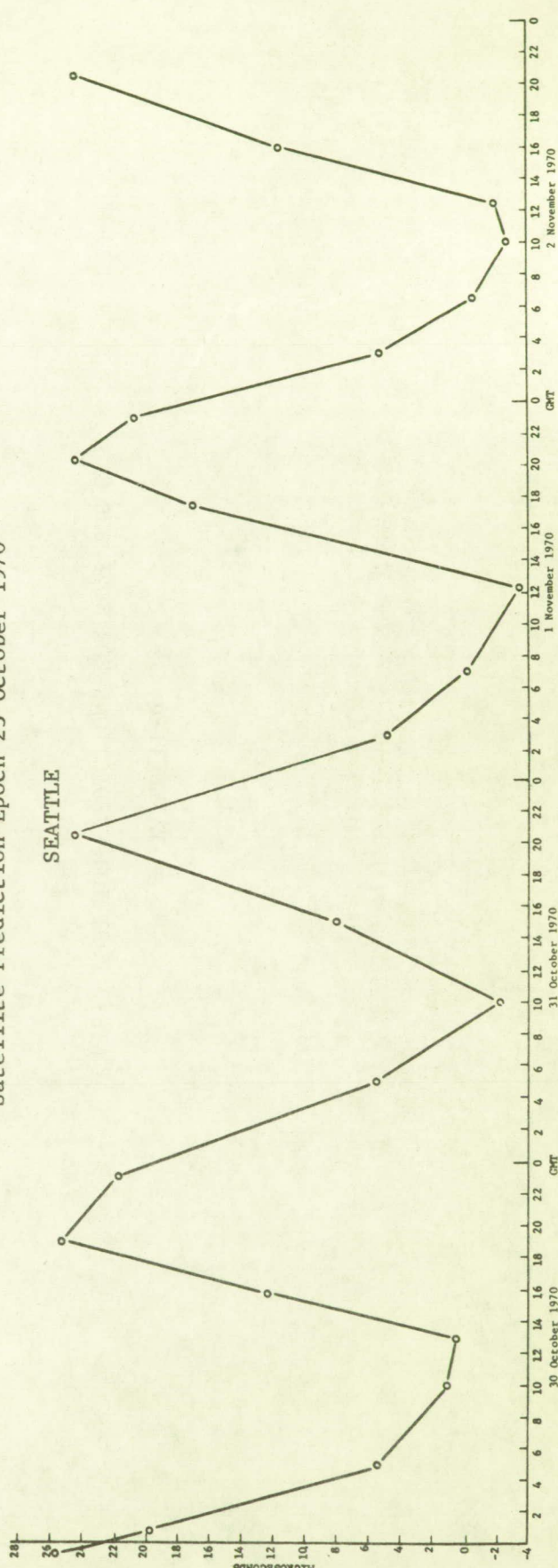


TABLE 11-6
ATS-3 POSITION PREDICTIONS FOR NOVEMBER 8

Time (GMT)	Latitude		Longitude		Earth Center Distance	
	Epoch Date October 23	Epoch Date November 8	Epoch Date October 23	Epoch Date November 8	Epoch Date October 23	Epoch Date November 8
0000	1.174S	1.175S	53.949W	53.946W	22743.99	22744.01
0600	0.070S	0.064S	53.704W	53.701W	22690.56	22690.67
1200	1.176N	1.177N	53.282W	53.279W	22708.73	22708.68
1800	0.050N	0.044N	53.227W	53.223W	22763.27	22763.13

FIGURE 11-21

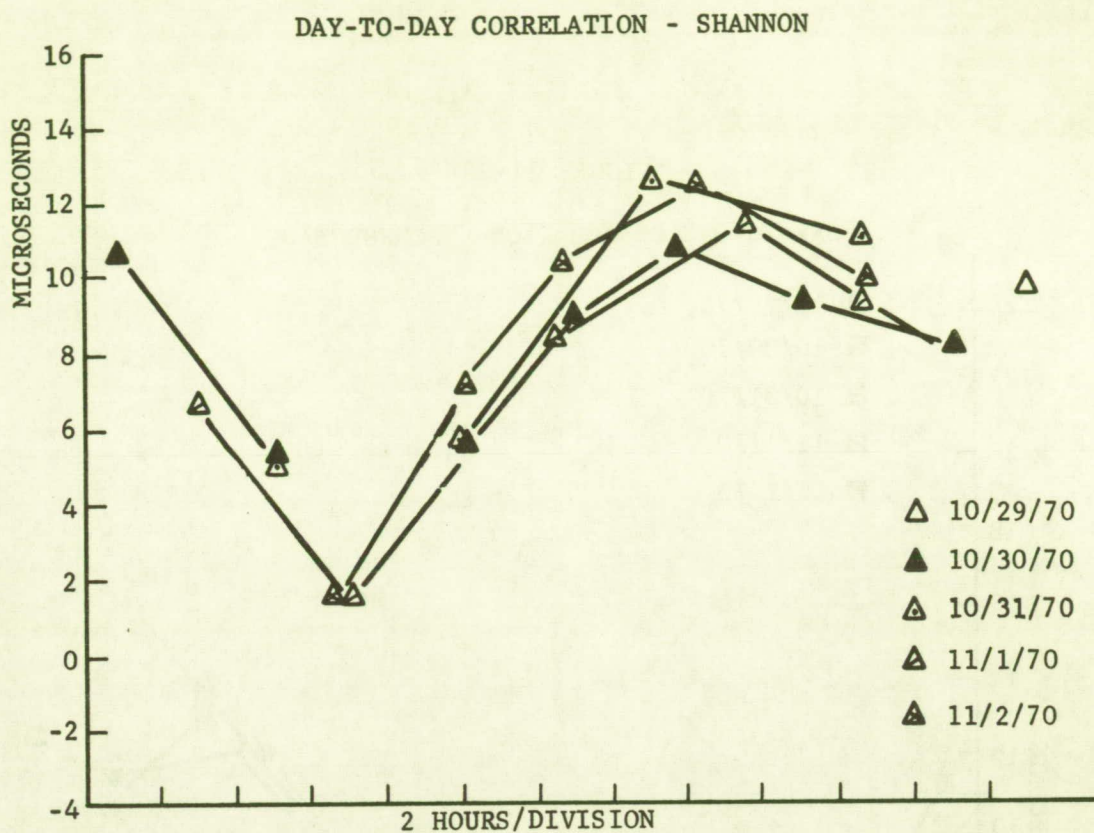


FIGURE 11-22

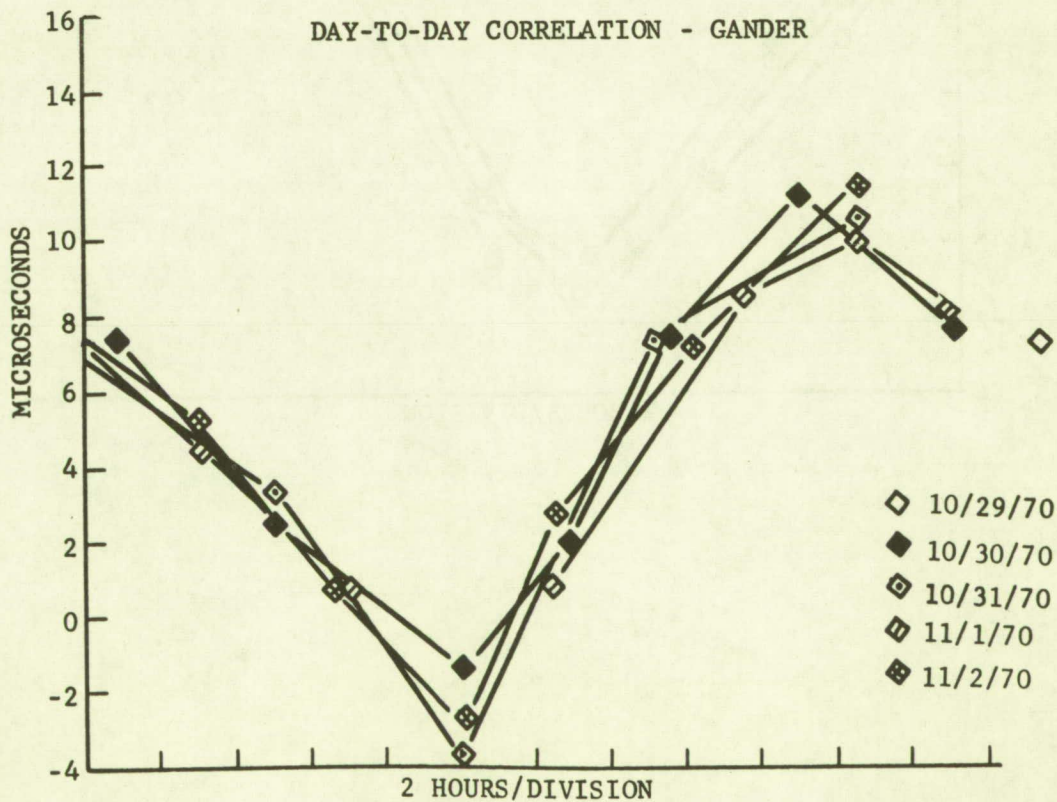


FIGURE 11-23

DAY-TO-DAY CORRELATION - SCHENECTADY

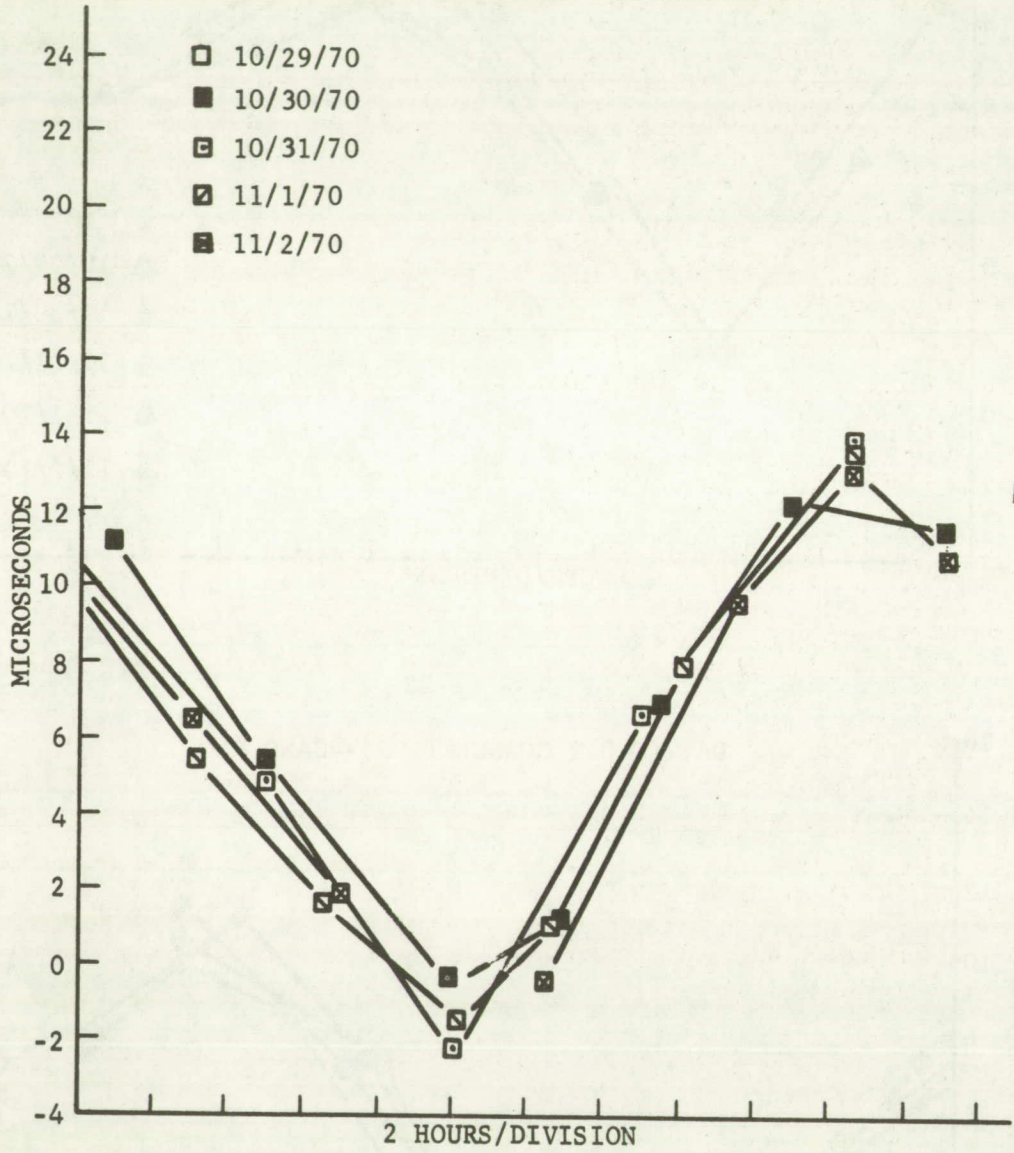
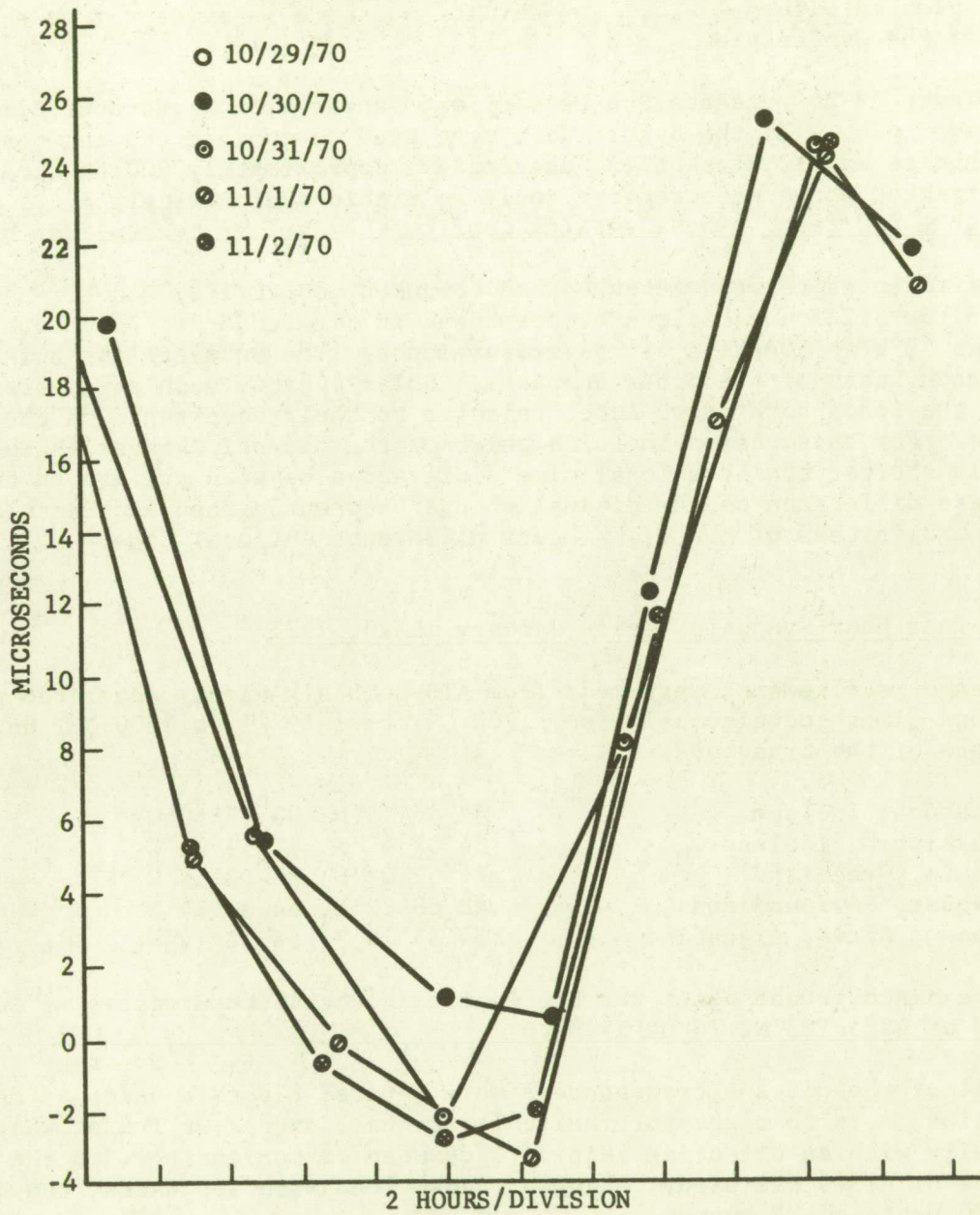


FIGURE 11-24

DAY-TO-DAY CORRELATION - SEATTLE



dusk to a value that is lower than normal. On the following few days the peak content is lower than on a "normal" day, but gradually approaches the normal value. Delay in the ionosphere is directly related to electron content along the ray path. The day-to-day change observed in the experiment shows no effect of the solar flare.

Correlation of the diurnal changes for Schenectady and Gander is indicated by the plot in Figure 11-25. The earlier sun time is evident from the advanced phase of the Gander plot.

Figure 11-26 presents Schenectady and Gander with a one hour time shift in the Gander plot. If the Gander data were used to correct ranging measurements for vehicles as far distant as Schenectady, approximately 900 nautical miles, the corrected range measurements would be within approximately ± 1.5 microseconds, or ± 700 feet. These results confirm the earlier twenty-four hour test.

Differences between measured and computed geometrical slant ranges are plotted for all four stations superimposed in Figure 11-27. The satellite longitude was 57°W at the time of the measurements. The subsatellite point is west of Shannon, east of the other stations. Solar events, such as sunrise and sunset in the ionosphere occur later relative to their occurrence on the ground at Seattle. For this reason the time shift of the diurnal changes in ionospheric delay is shorter than the local time differences between the ground transponders. The phase difference of the diurnal change between Shannon and Seattle is about five hours instead of the eight hours difference in local time.

Twenty-four Hour Synoptic Test - January 19-20, 1971

Range measurements were made from ATS-3 to six widely separated ground locations almost continuously from 1200 GMT on 1/19/71 to 1200 GMT on 1/20/71. Locations of the transponders were:

Shannon, Ireland	$52^{\circ}46'55''\text{N}$, $08^{\circ}55'50''\text{W}$
Reykjavik, Iceland	$64^{\circ}07'47''\text{N}$, $21^{\circ}56'12''\text{W}$
Thule, Greenland	$76^{\circ}32'08''\text{N}$, $68^{\circ}23'58''\text{W}$
Gander, Newfoundland	$48^{\circ}58'22''\text{N}$, $54^{\circ}30'14''\text{W}$
Buenos Aires, Argentina	$34^{\circ}35'10''\text{S}$, $58^{\circ}22'10''\text{W}$

The sixth ground point was the General Electric Observatory at Schenectady, located at $42^{\circ}50'53''\text{N}$, $74^{\circ}04'15''\text{W}$.

All of the distant transponders were General Electric units as described in Section 3, with eight-turn helical antennas, except at Thule, where a four-turn helix with an effective gain of 6 dB when communicating with the linear antennas of ATS-3 was used. Shannon transmitted with 100 Watts, the others with 300 Watts of RF output.

The interrogation rate was matched to the spin rate of ATS-3 to minimize the effects of the signal fade on each revolution. (Section 5). The depth of the fade was approximately 8 dB on the detected signals from the transponders, with a fading characteristic as shown in Figure 5-16. The spin rate of ATS-3 was 100 revolutions per minute, and the interrogation rate was 25 per minute.

The automatic sequence of interrogations was Gander, Shannon, Buenos Aires, Reykjavik, and Thule.

FIGURE 11-25

CORRELATION OF DIURNAL CHANGES FOR SCHENECTADY AND GANDER

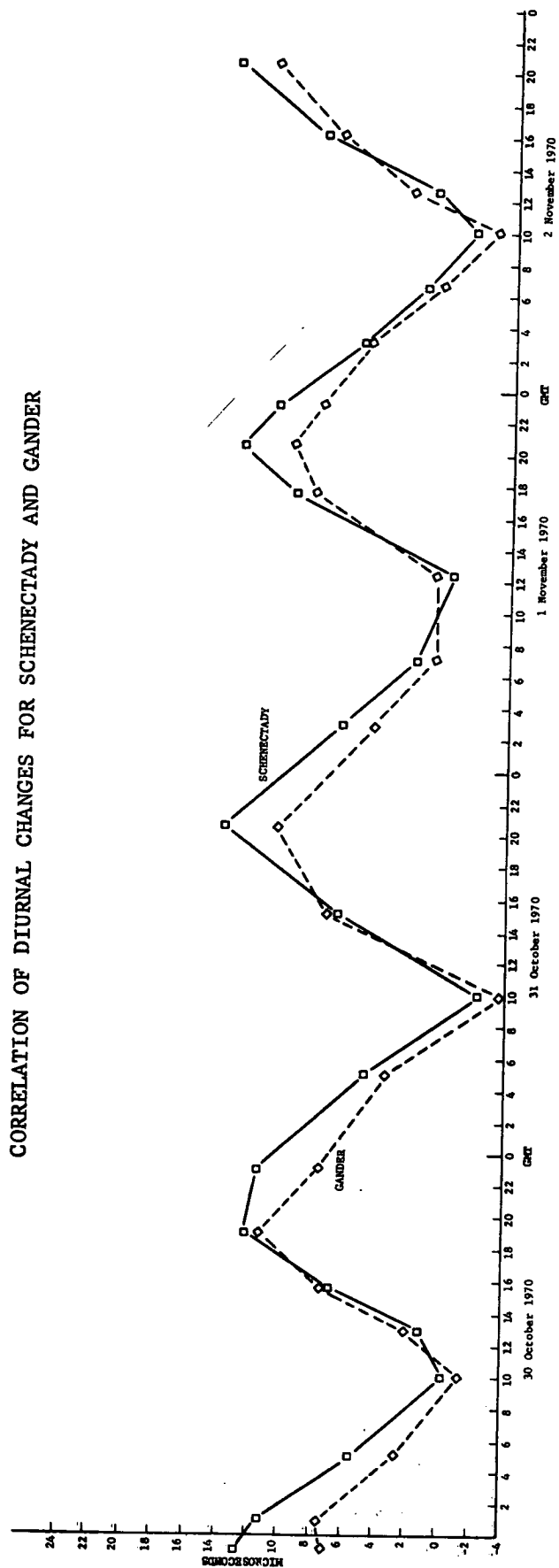


FIGURE 11-26

CORRELATION OF DIURNAL CHANGES FOR SCHENECTADY AND GANDER

The Gander Range Measurements Shifted 1 Hour in Time

To Allow For Difference In Sun Time

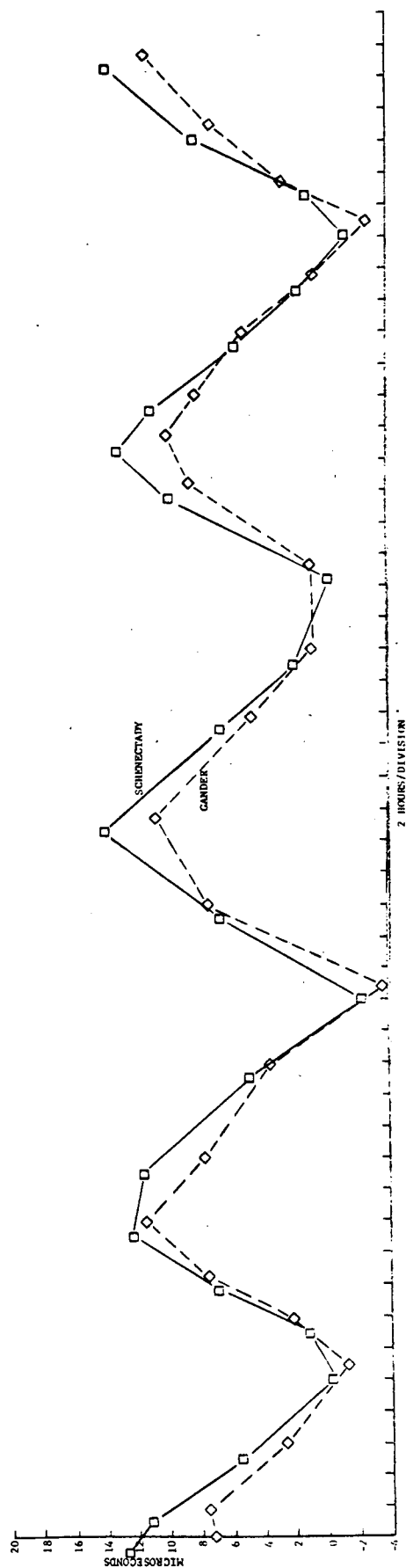
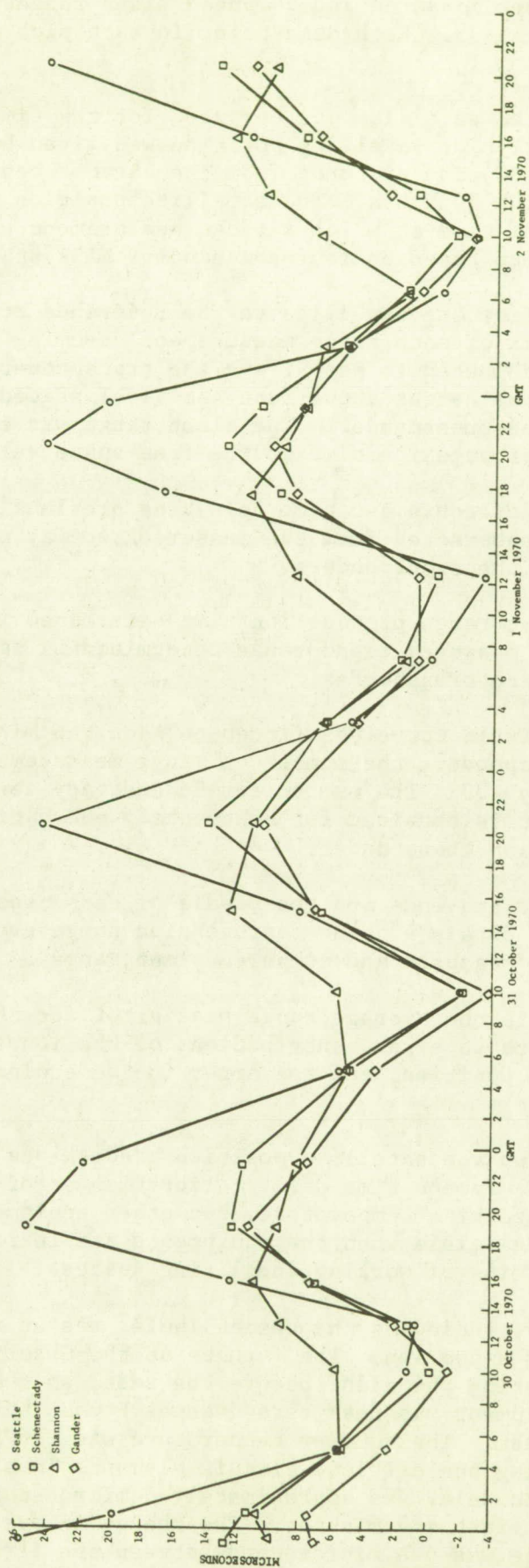


FIGURE 11-27

DIFFERENCE, MEASURED AND COMPUTED SLANT RANGES - FOUR STATIONS



Differences between measured and computed slant ranges are plotted in Figures 11-28 through 11-33. Each data point in each plot was computed as follows:

1. The position of the satellite was computed for the time of each individual range measurement. The satellite position was given by NASA in terms of latitude, longitude, and distance from the earth's center on each half hour throughout the 24 hours. The satellite position was interpolated for each second of time at which a range measurement was made, using a cubic interpolation based on four consecutive NASA statements of position.
2. The slant range from the satellite to the reference transponder was computed for the time of each range measurement assuming the satellite to be at the position computed in step 1 and the transponder to be at the latitude, longitude and height above mean sea level stated by the organization that installed the transponder. The slant range was expressed in micro-seconds two-way propagation time at the free-space velocity of light.
3. The fixed value for equipment time delay, as previously determined for the transponder was subtracted from the measured two-way propagation time from the satellite to the transponder.
4. The computed slant range propagation time determined in step 2 was subtracted from the measured slant range determined by step 3 for each range measurement to each transponder.
5. A "best-fit quadratic curve was fitted to each ten minutes of data. For each remote transponder, the number of range measurements in ten minutes was approximately 200. The number for Schenectady is larger because a range measurement is obtained for Schenectady every time a measurement is made to any distant transponder.
6. The values of the two ends and the middle of each "best-fit" quadratic curve were averaged to obtain a value representing the average value of the differences between measured and computed slant ranges.

Each data point is the average range bias error for the ten minute period. It is the sum of the range error contributions of the ionosphere, the error in the assumed satellite position, and the error in the equipment time delay calibration.

The ionosphere and the satellite position predictions each have a diurnal pattern of change. Equipment time delay calibration error is a fixed value. It is subject to change with temperature, but other equipment tests have shown that the change is negligible when the equipments are in rooms kept within the normal temperature limits of working and living spaces.

Each transponder, including the one at Thule, was at normal room temperatures, with one brief exception. The furnace at the Observatory in Schenectady ceased to function during the night before the test, so that the temperature of the room and the equipment was near zero degrees F when the operators arrived to prepare for the test. The outdoor temperature was -26°F. After starting the furnace and heating the critical circuit elements in the phase-matcher correlator, the change in delay was approximately 5 microseconds in the decreasing direction during the first ten minutes. The change in average range measurements to the satellite was one microsecond between the first and second ten

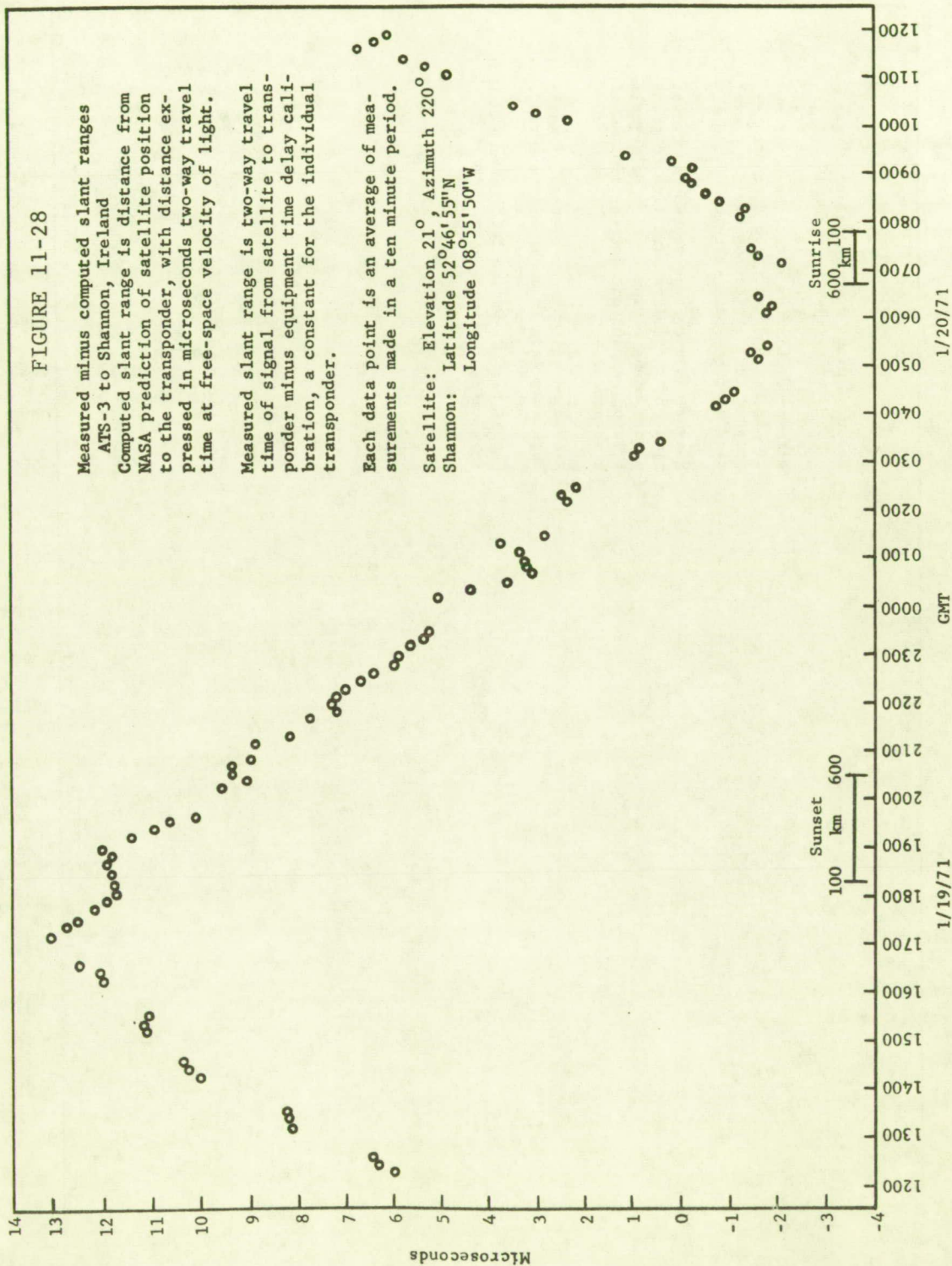
FIGURE 11-28

Measured minus computed slant ranges
ATS-3 to Shannon, Ireland
Computed slant range is distance from
NASA prediction of satellite position
to the transponder, with distance ex-
pressed in microseconds two-way travel
time at free-space velocity of light.

Measured slant range is two-way travel
time of signal from satellite to trans-
ponder minus equipment time delay cali-
bration, a constant for the individual
transponder.

Each data point is an average of mea-
surements made in a ten minute period.

Satellite: Elevation 21° , Azimuth 220°
Shannon: Latitude $52^{\circ}46'55''N$
Longitude $08^{\circ}55'50''W$



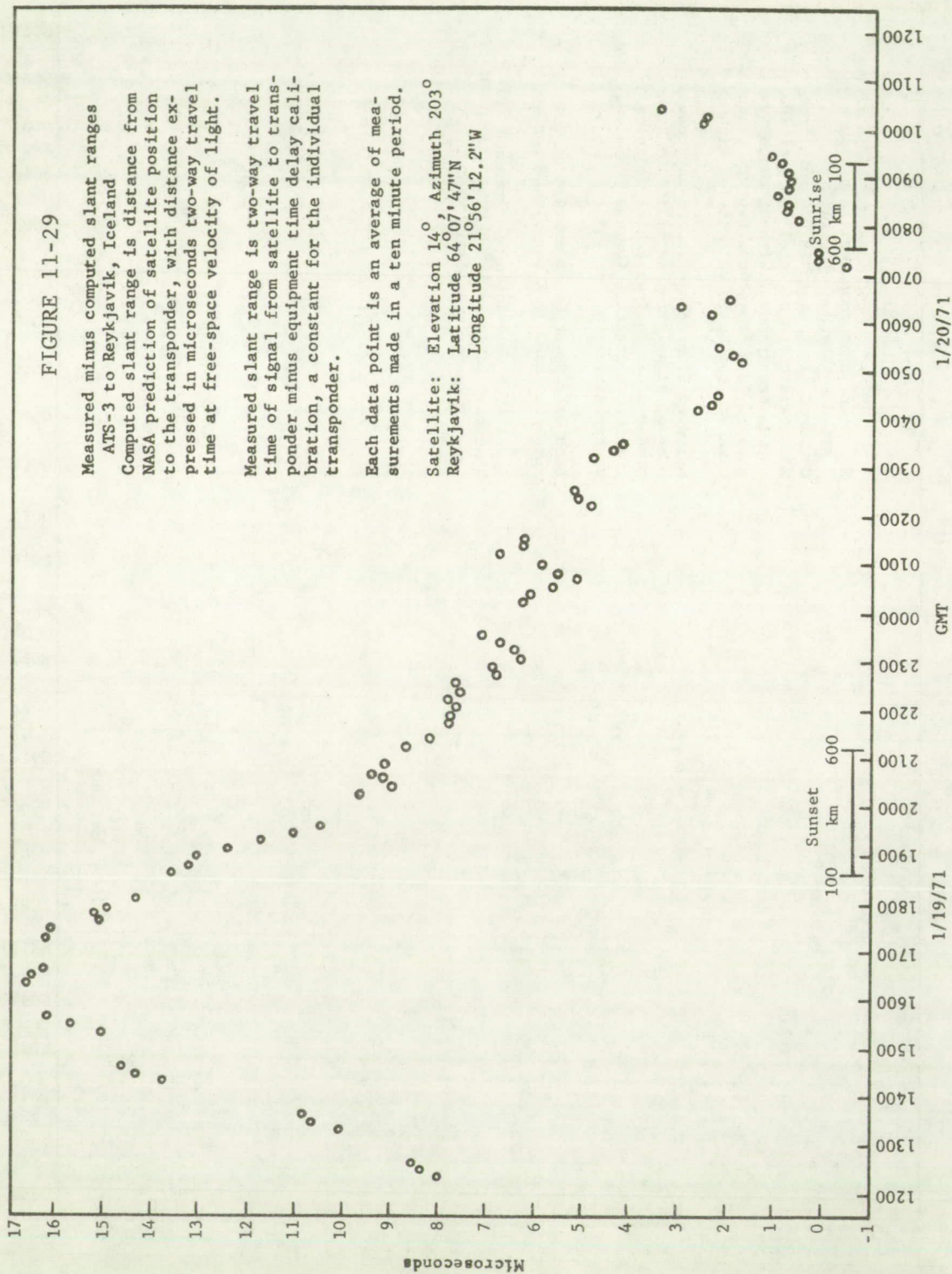


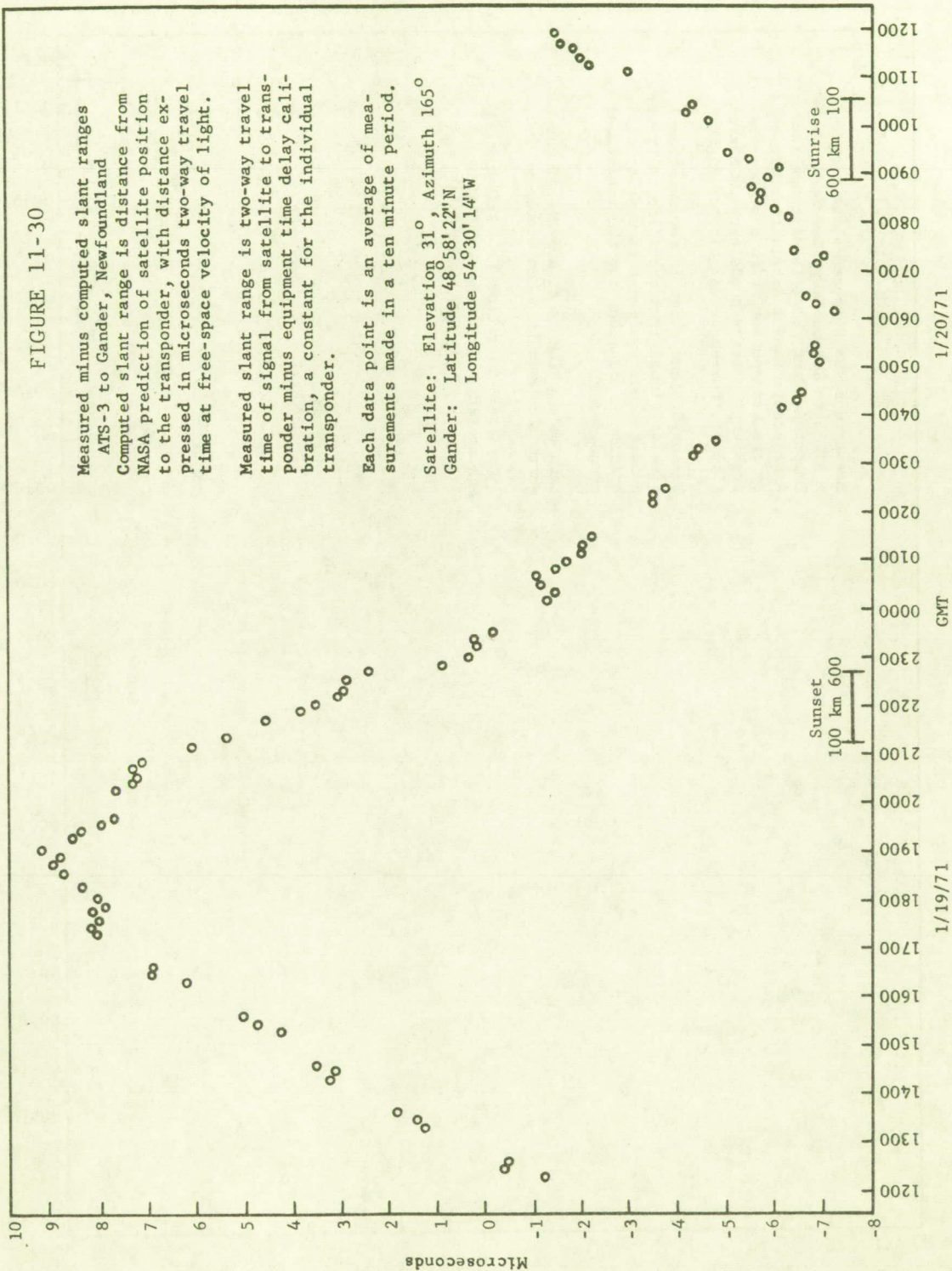
FIGURE 11-30

Measured minus computed slant ranges
 ATS-3 to Gander, Newfoundland
 Computed slant range is distance from
 NASA prediction of satellite position
 to the transponder, with distance ex-
 pressed in microseconds two-way travel
 time at free-space velocity of light.

Measured slant range is two-way travel
 time of signal from satellite to trans-
 ponder minus equipment time delay cali-
 bration, a constant for the individual
 transponder.

Each data point is an average of mea-
 surements made in a ten minute period.

Satellite: Elevation 31° , Azimuth 165°
 Gander: Latitude $48^{\circ}58'22''N$
 Longitude $54^{\circ}30'14''W$



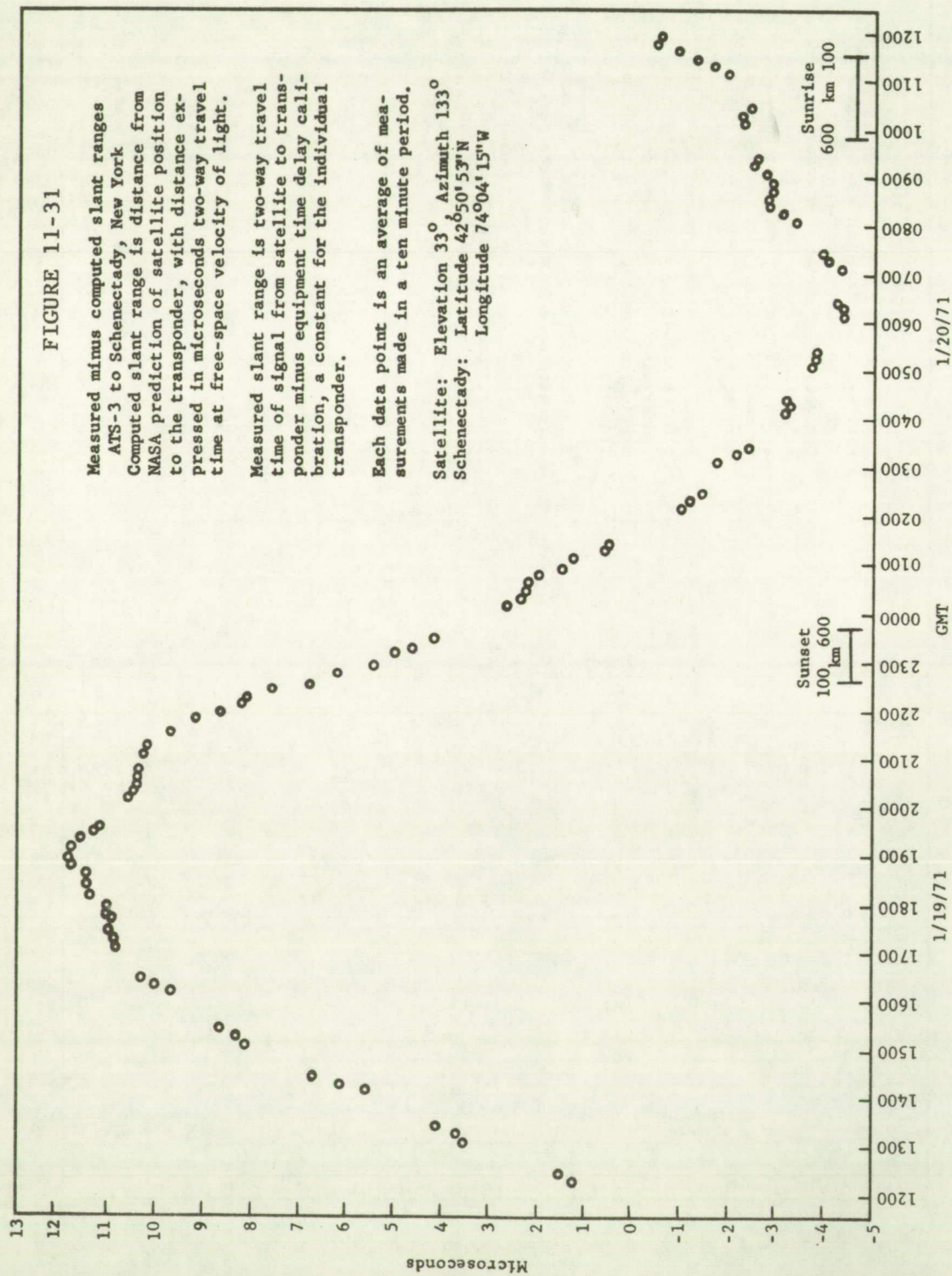


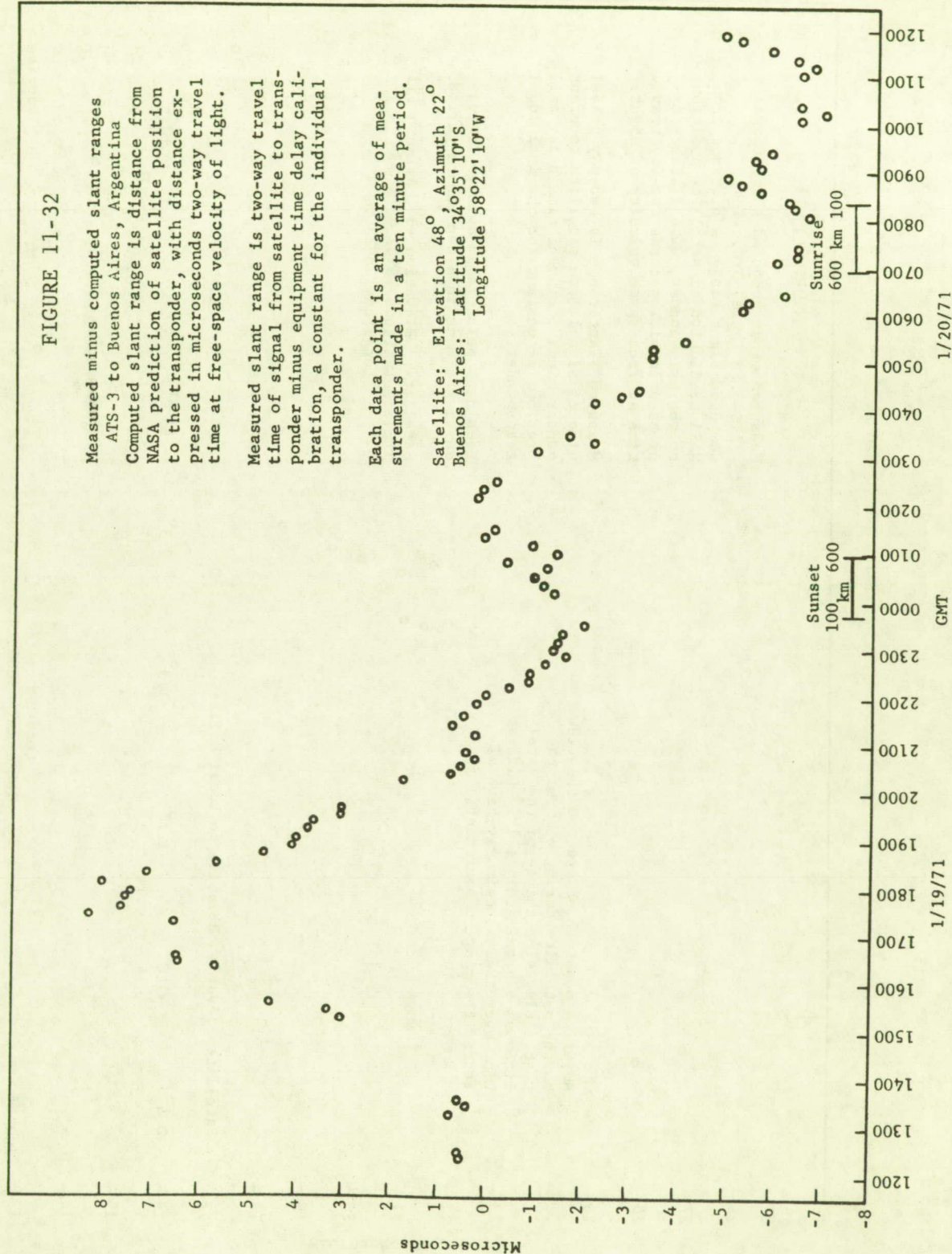
FIGURE 11-32

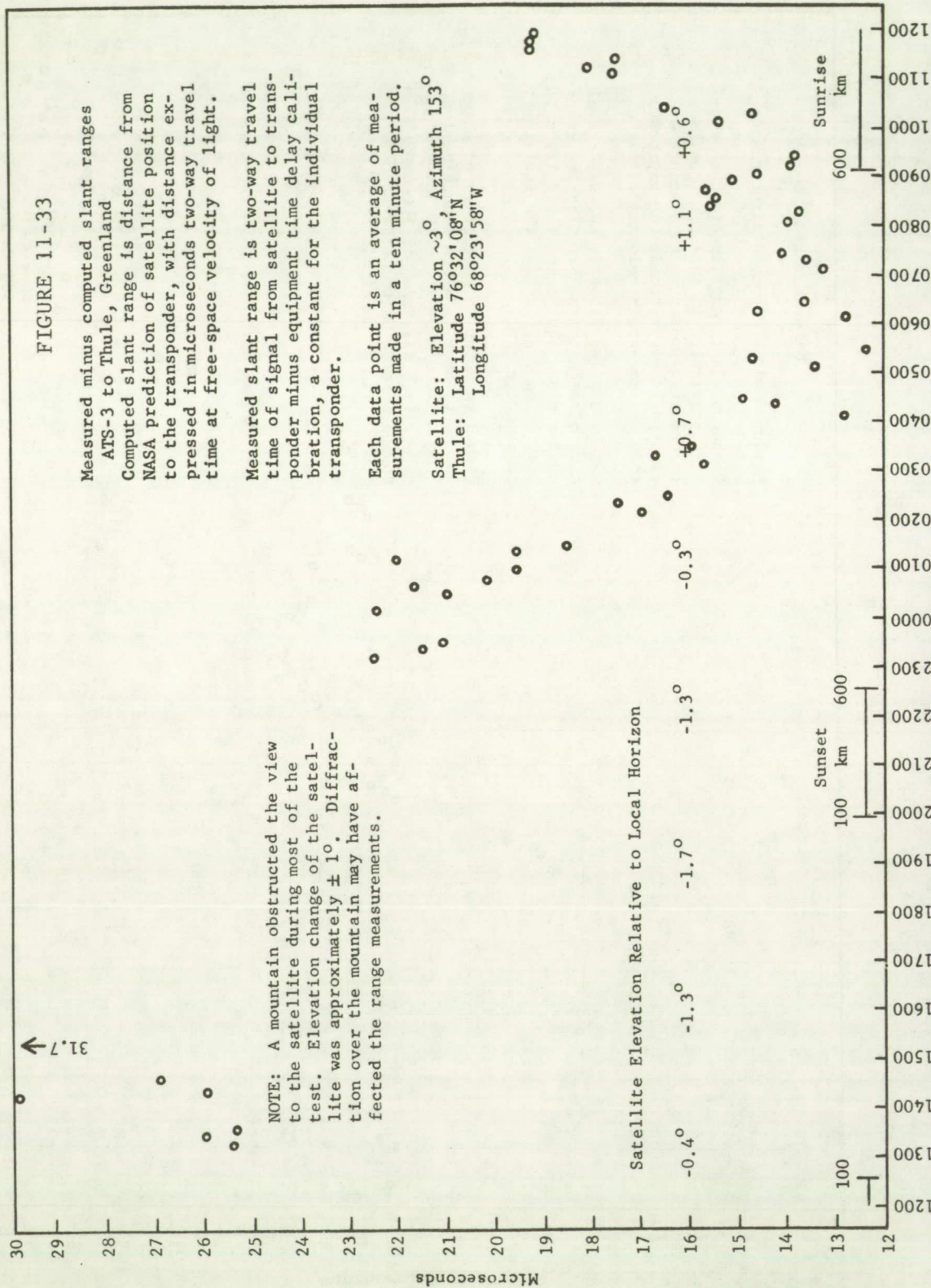
Measured minus computed slant ranges
ATS-3 to Buenos Aires, Argentina
Computed slant range is distance from
NASA prediction of satellite position
to the transponder, with distance ex-
pressed in microseconds two-way travel
time at free-space velocity of light.

Measured slant range is two-way travel
time of signal from satellite to trans-
ponder minus equipment time delay cali-
bration, a constant for the individual
transponder.

Each data point is an average of mea-
surements made in a ten minute period.

Satellite: Elevation 48° , Azimuth 22°
Buenos Aires: Latitude $34^{\circ}35'10''S$
Longitude $58^{\circ}22'10''W$





minute periods. There was no apparent effect due to temperature change in the subsequent averages.

Some of the data points in Figures 11-28 through 11-33 show a "negative" delay; that is, a measured time that is shorter than the computed slant range. A true negative delay is impossible, since the signal cannot propagate faster than the speed of light. The apparent negative delay is due to satellite position prediction errors and/or an assumed equipment time delay that is longer than the actual equipment time delay.

Except for the Thule measurements, the plots are believed to show ionospheric delay changes with high resolution. The standard deviations of the individual measurements relative to "best fit" curves were approximately one microsecond or less, so that the ten minute averages have a precision of a fraction of a microsecond. It is believed that even the small changes from one average data point to the next are truly indicative of changes in ionosphere delay, and are not random measurement variations.

Satellite position prediction errors contribute a smooth, approximately sinusoidal diurnal variation that will add to the ionospheric delay variation to change its apparent amplitude. Except for the amplitude of the diurnal change, and fixed bias error due to error in equipment calibration, the curves present a synoptic measurement of the ionosphere delay for the slant range paths from the satellite to Shannon, Reykjavik, Gander, Schenectady and Buenos Aires.

An unanticipated factor altered the test at Thule. The transponder antenna was located so that the satellite was behind a mountain for most of the 24-hour period. We were unaware of the mountain, and did not anticipate the loss of signal because a previous test with an aircraft at the same location on July 10, 1970 was successful. On July 10, the ATS-3 satellite as seen from Thule was at 175° azimuth, and 5° elevation. On January 19-20, 1971 it was at 153° and at a lower elevation. A check with an aeronautical chart shows that the satellite was in clear view of the transponder on July 10, 1970, but that the elevation of the mountain was 4.1° as viewed from the transponder on January 19-20. Satellite elevation angles above a spherical earth horizon and the local horizon were as follows:

TABLE 11-7

SATELLITE ELEVATION ANGLES

<u>Date</u>	<u>Time, GMT</u>	<u>Satellite Elevation Above Spherical Earth Horizon</u>	<u>Satellite Elevation Relative to Local Horizon</u>
1/19/71	1100	4.39	+0.3
	1300	3.70	-0.4
	1600	2.73	-1.3
	1900	2.36	-1.7
	2200	2.80	-1.3
1/20/71	0100	3.79	+0.3
	0400	4.77	+0.7
	0700	5.13	+1.1
	1000	4.68	+0.6

The transponder responded to interrogations and they were received at Schenectady from the start of the test until approximately 14:30 GMT, when they faded out. The signals were again detectable at approximately 23:00 GMT. Reference to Table 11-7 indicates that the transponder received signals from the satellite, responded, and its returns were received at Schenectady until the satellite was approximately 1.0° below the local horizon. Propagation between the transponder and the satellite depended on diffraction over the mountain during some portion of the test period.

The scatter of the Thule range measurements on January 19-20 was much greater than the scatter of the other transponders, especially just before the satellite signal was fully attenuated and just after it returned. It is probable that diffraction over the mountain resulted in range measurements that were longer than the direct line-of-sight path. Reduced signal level and diffraction effects may have contributed to the scatter. There was a diurnal change in ionospheric delay even though the sun does not rise at Thule on January 19 or 20. It does rise in the ionosphere along the transponder-to-satellite ray path.

Sunrise and sunset within the ionosphere along the ray path from each transponder to the satellite is shown in Figures 11-28 through 11-33. The sunrise times near the top of the ionosphere at 600 kilometers and near the lower limit of the ionosphere at 100 kilometers are plotted with connecting lines; similarly for sunset, which occurs first at 100 kilometers and later reaches 600 kilometers. It is important to note that the sunrise and sunset times are along the ray path, not above the transponder.

Shannon, Reykjavik, Gander and Schenectady all had diurnal changes in ionosphere propagation delay that appear to follow sunlight effects in the ionosphere. Electron content and delay increase rapidly after sunrise, then continue to increase more slowly until after local noon. Content then drops slowly until sunset in the ionosphere along the ray path. It decreases rapidly, during sunset, then more slowly until it reaches a minimum before sunrise.

The duration of the daytime peak for each of the transponders, except Thule and Buenos Aires, corresponds to the length of the day at the latitude of the ray path in the ionosphere. The March 13-14 test for Schenectady and Gander (Figure 11-34) show the same period for the daytime peak with Gander shifted approximately one hour earlier in time. In March, the length of day is nearly equal at Schenectady and Gander. In the January 19 test (Figure 11-35) the daytime peak is shorter at Gander than Schenectady, corresponding to the shorter winter day at the higher northern latitude.

The Buenos Aires pattern of diurnal change did not follow the pattern of the northern hemisphere mid-latitude locations. Electron content did not increase continuously after sunrise, and the diurnal peak was shorter in proportion to the length of the day than was true for the other locations. There was an increase in electron content at sunset, starting at approximately 0000 GMT and peaking at approximately 0200 GMT. The small peak in electron content after sunset may be a frequent occurrence at Buenos Aires. It is apparent in ionospheric sounder measurements of critical frequency of the F-layer at Buenos Aires. For example, plots of average values for each month from February through June 1969 show evidence of a peak between 2000 and 2200 local time.

Figure 11-36 shows the average values for those months as presented in "Ionospheric Data", U.S. Department of Commerce, National Oceanic and Atmospheric

Figure 11-34

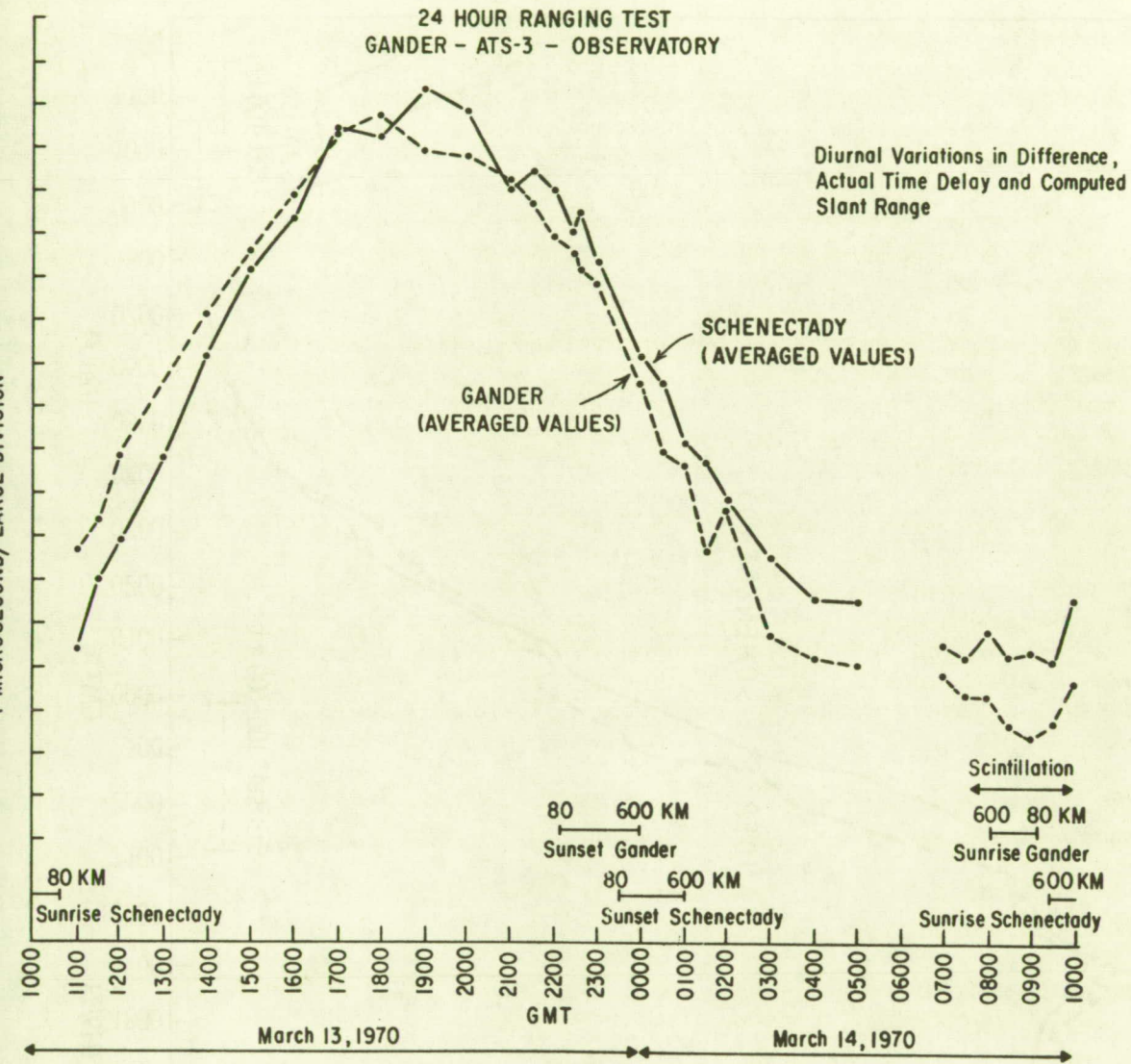
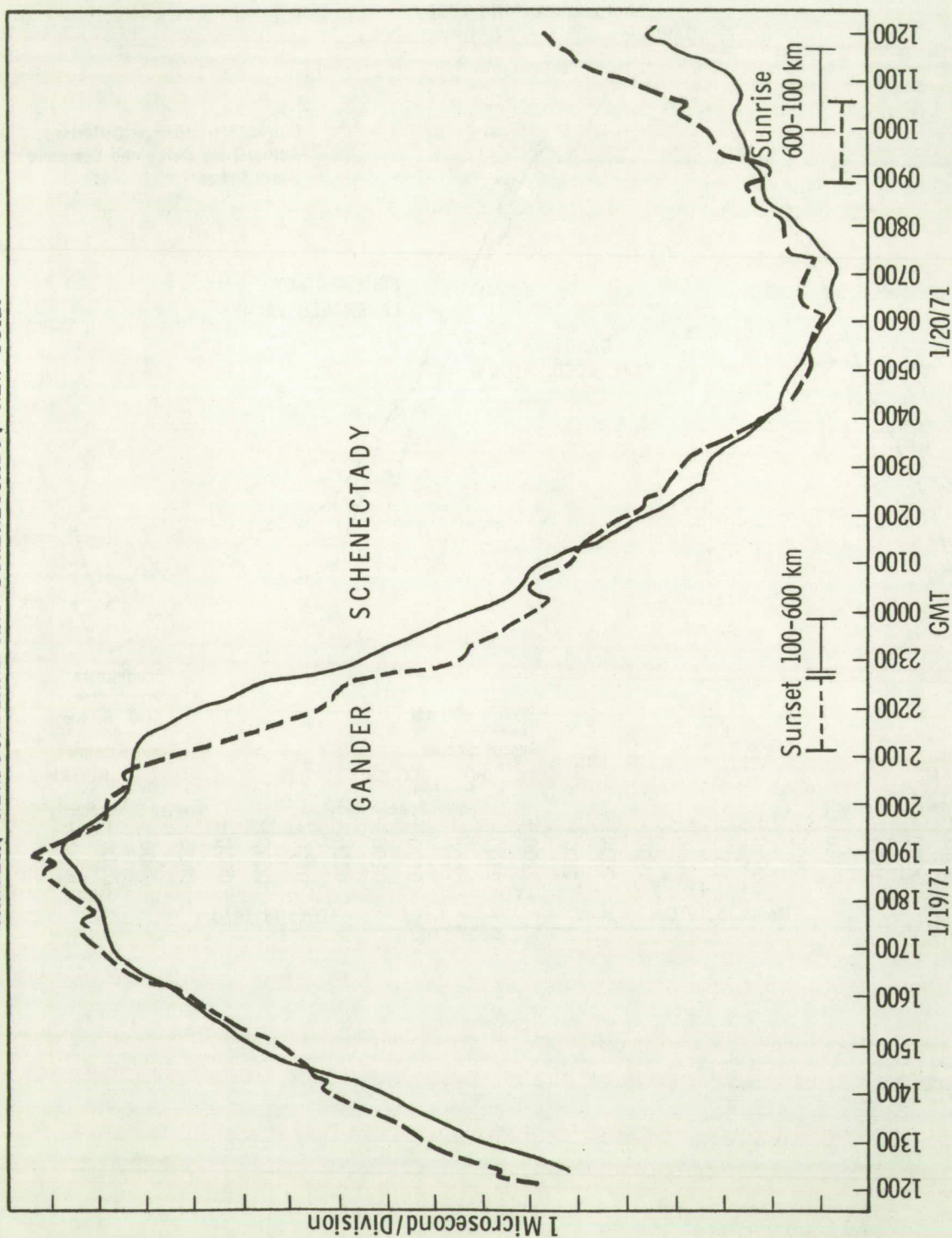


FIGURE 11-35

CORRELATION OF DIFFERENCES BETWEEN COMPUTED AND MEASURED SLANT RANGES
GANDER, NEWFOUNDLAND AND SCHENECTADY, NEW YORK



Administration Bulletin FA-318, February 1971. The critical frequency for the F-layer may be related to electron content by

$$f_o^2 = 80 \times 10^6 N_e$$

where f_o = critical frequency of F-layer in Hz

N_e = electron density (electrons cubic centimeter)

(Dr. G. H. Millman, General Electric Heavy Military Electronic Systems, private correspondence.)

The integrated electron content along the ray path and propagation delay as observed in the satellite range measurements are directly related to the maximum electron density of the F-layer.

Although the January 19 satellite measurements for Buenos Aires appear to be in agreement with the characteristics of other data taken over a period of time, the quantity of our data is not sufficient to estimate the time or geographical correlations of ionospheric characteristics in areas of the earth that share an ionosphere structure similar to the path between Buenos Aires and ATS-3.

Data collected by the Shannon, Reykjavik, Gander and Schenectady transponders are believed sufficient to show that ground reference transponders spaced about one thousand miles apart are useful for correcting range measurements at VHF for aircraft and ships along the principal North Atlantic routes. Under all the conditions of the tests, over various seasons of the year, during several days in succession, and at all hours of the day and night, the correlations of measurements appear adequate to provide range corrections sufficient for one nautical mile, one sigma position fix accuracy. None of the data were taken when a severe magnetic storm was known to have occurred, although the attempt was made to observe the effects, as on the four-day test following the solar flare on October 28, 1970.

Ionospheric Scintillation, October 15, 1970

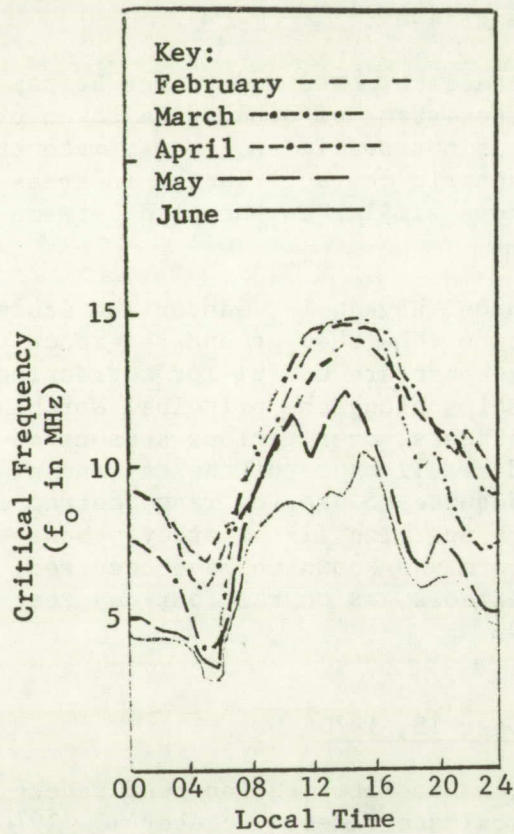
Air Force Cambridge Research Laboratories reported severe scintillation on the following dates and approximate times: October 13, 1970 (0100-0900 GMT); October 14, 1970 (0200-0600 GMT); October 15, 1970 (0315-0600 GMT); October 16, 1970 (0200-0800 GMT). In each case the scintillation started and ended abruptly at the approximate times listed. Figure 11-37 is a reproduction of the AFCRL signal level recording for the October 15, 1970 data.

A communications test with a Pan American 747 aircraft enroute from New York to Paris was conducted between 0300 and 0600 GMT on October 15, 1970. Ground terminals participating in the experiment were Aeronautical Radio, Inc., at Annapolis, Maryland; Pan American Airways, at Miami, Florida; Hughes Aircraft, at Los Angeles, California; Boeing Aircraft, at Seattle, Washington; and the General Electric Radio-Optical Observatory at Schenectady, New York.

Severe scintillation was observed at Schenectady between 0315-0318 GMT and again at 0332 through 0615 GMT, when the satellite was turned off.

FIGURE 11-36

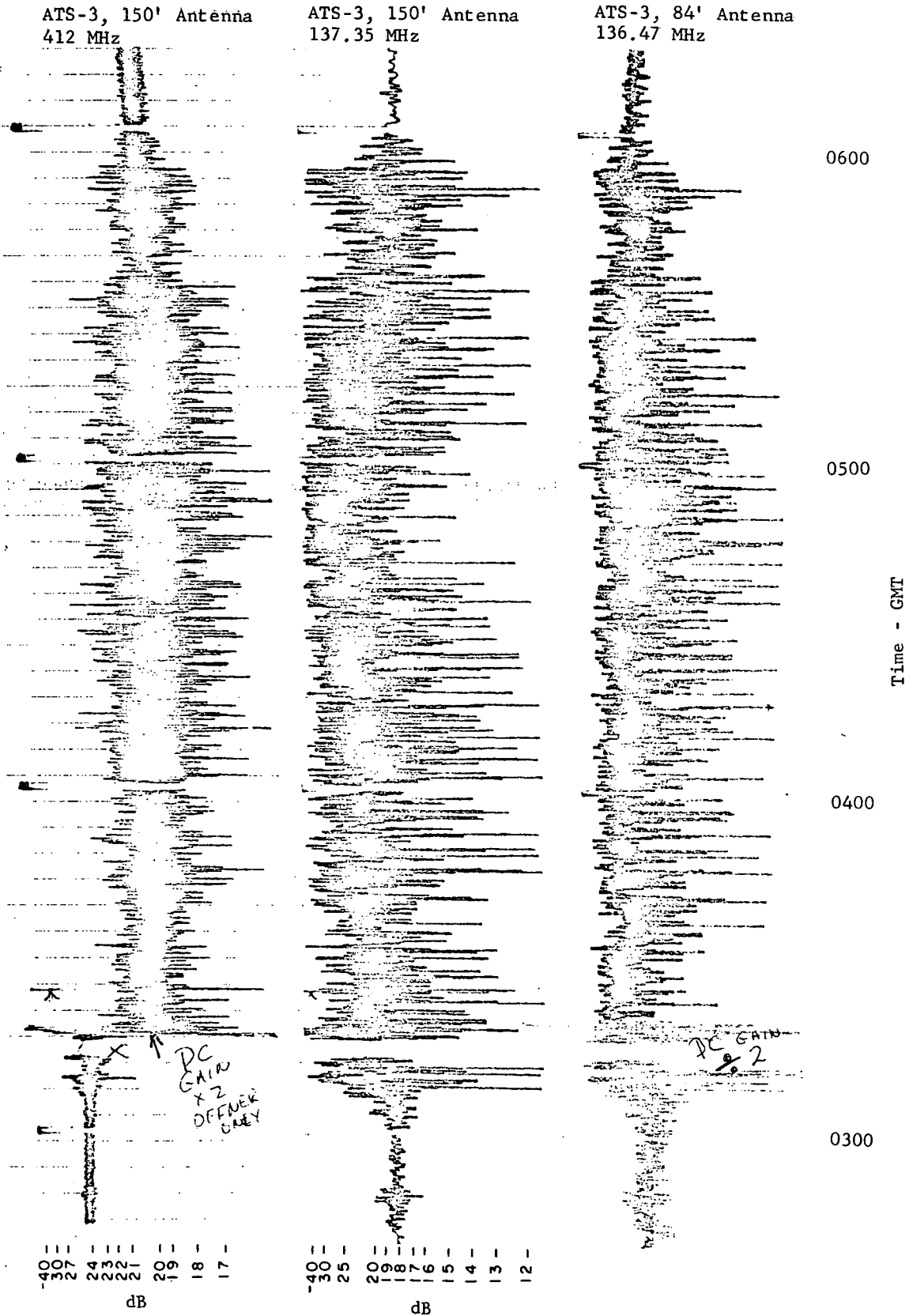
F-LAYER CRITICAL FREQUENCY
BUENOS AIRES MONTHLY AVERAGES
(February - June 1969)



"Ionospheric Data", U.S. Department of Commerce,
National Oceanic and Atmospheric Administration
Bulletin FA-318, February 1971.

FIGURE 11-37

SCINTILLATION OBSERVED AT HAMILTON, MASSACHUSETTS BY
AIR FORCE CAMBRIDGE RESEARCH LABORATORIES (10/15/70)



Neither the airplane nor any of the other ground terminals reported that the scintillation produced noticeable effects on their communications.

Figure 11-38 is a portion of the signal level recording made at the Observatory. The recording on the right hand portion of each chart was made from a receiver attached to the 30 foot diameter antenna which has a net gain of 19 dB. The recording on the left hand portion of each chart was made from a receiver attached to an eight-turn helical antenna, having a net gain of about 8.5 dB for the linearly polarized signals from the ATS-3 satellite, when line losses are taken into account. Increasing signal level is toward the right on the right hand channel and toward the left on the left hand channel. Some portions of the chart recording show what appears to be a fading at a rate more than once per second. It is due to spin modulation of the satellite, not to scintillation.

The signal levels received from the aircraft and the other ground terminals are identified on the chart recording as follows: G2 - Goddard mobile number 2 operated by Pan American at Miami; A/C - 747 aircraft enroute from New York to Paris transmitting with 500 Watts of power through a Boeing crossed slot antenna designed for 125 and 131 MHz, but retuned with a simple modification for the 133 and 149 MHz frequencies of ATS-3; B - Boeing at Seattle; A - Aeronautical Radio at Annapolis, Maryland; LA - Goddard mobile at Los Angeles, operated by Hughes Aircraft.

The voice communications received on the 30 foot antenna from the aircraft and from all of the ground terminals were recorded on magnetic tape at the Observatory. A copy of the recording, on a standard cassette, may be borrowed from the General Electric Company for comparison with the chart recordings as presented in this report.

The signal level without scintillation is approximately -98 dBm, when receiving with the 30 foot diameter antenna. During the scintillation the signal level increased approximately 7 dB above the non-scintillating level, and it dropped occasionally more than 30 dB below the non-scintillating level. The drop-outs were always of very short duration. The 19 dB gain of the 30 foot dish provided a large fading margin so that the severe scintillation had very little effect on the voice communications signals. If the antenna gain had been 0 dB, the drop-outs would have been more frequent. The voice signals were detected when the signal dropped to about 30 dB below the non-scintillating level, suggesting that a 0 dB antenna would have provided approximately 10 dB fading margin. This is consistent with other observations.

It is important to note that speech is highly redundant and that short drop-outs do not have a significant effect on intelligibility. The effect on other forms of communication, such as digital which is less redundant, would have to be considered in evaluating VHF communications performance when scintillation is present.

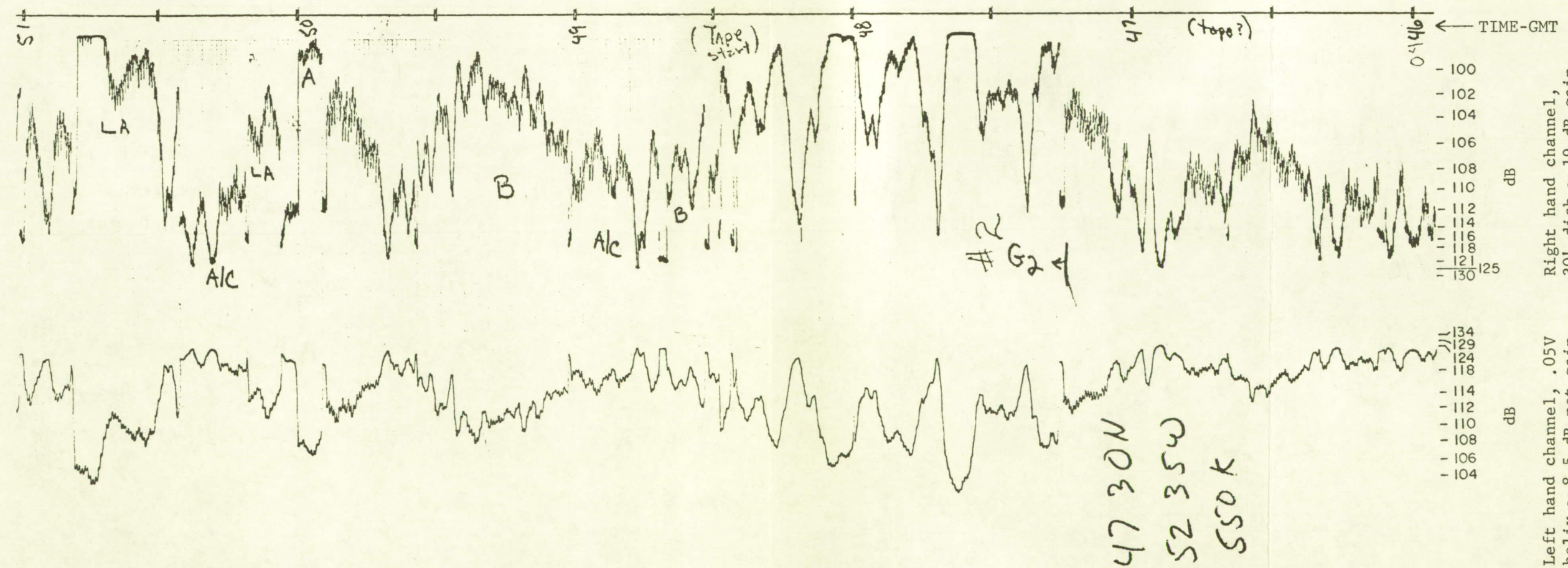
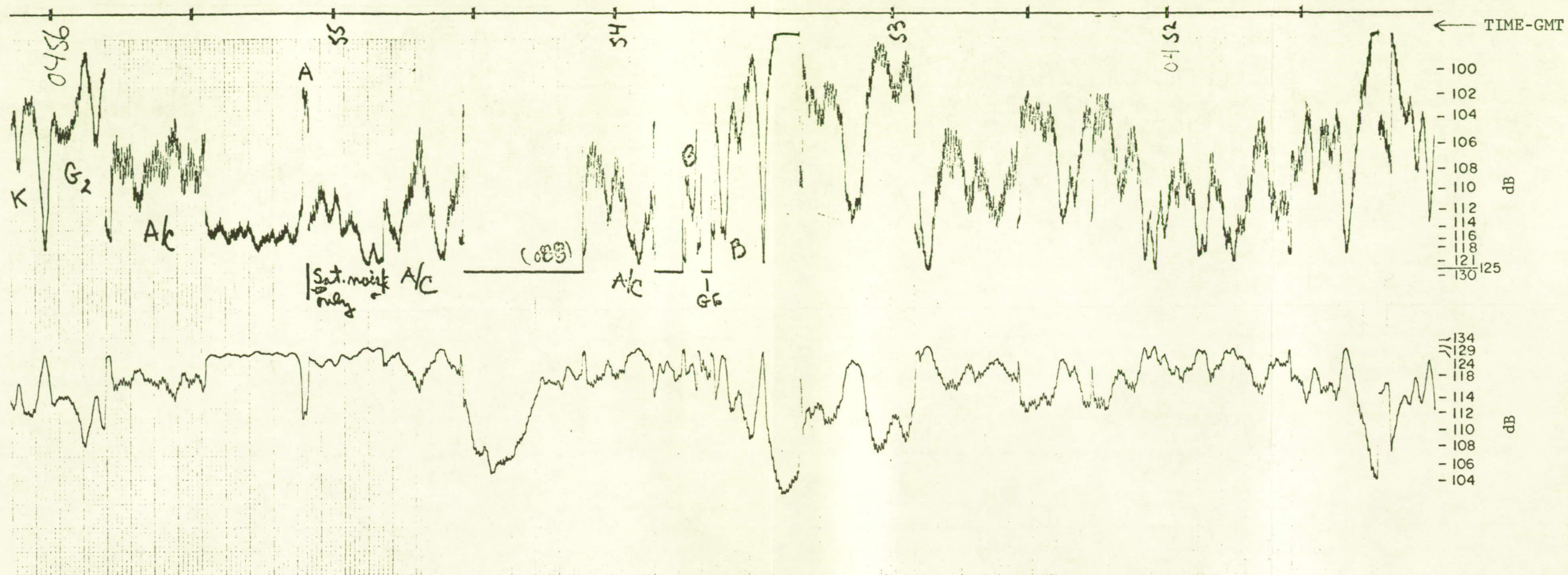


FIGURE 11-38 CONTINUED

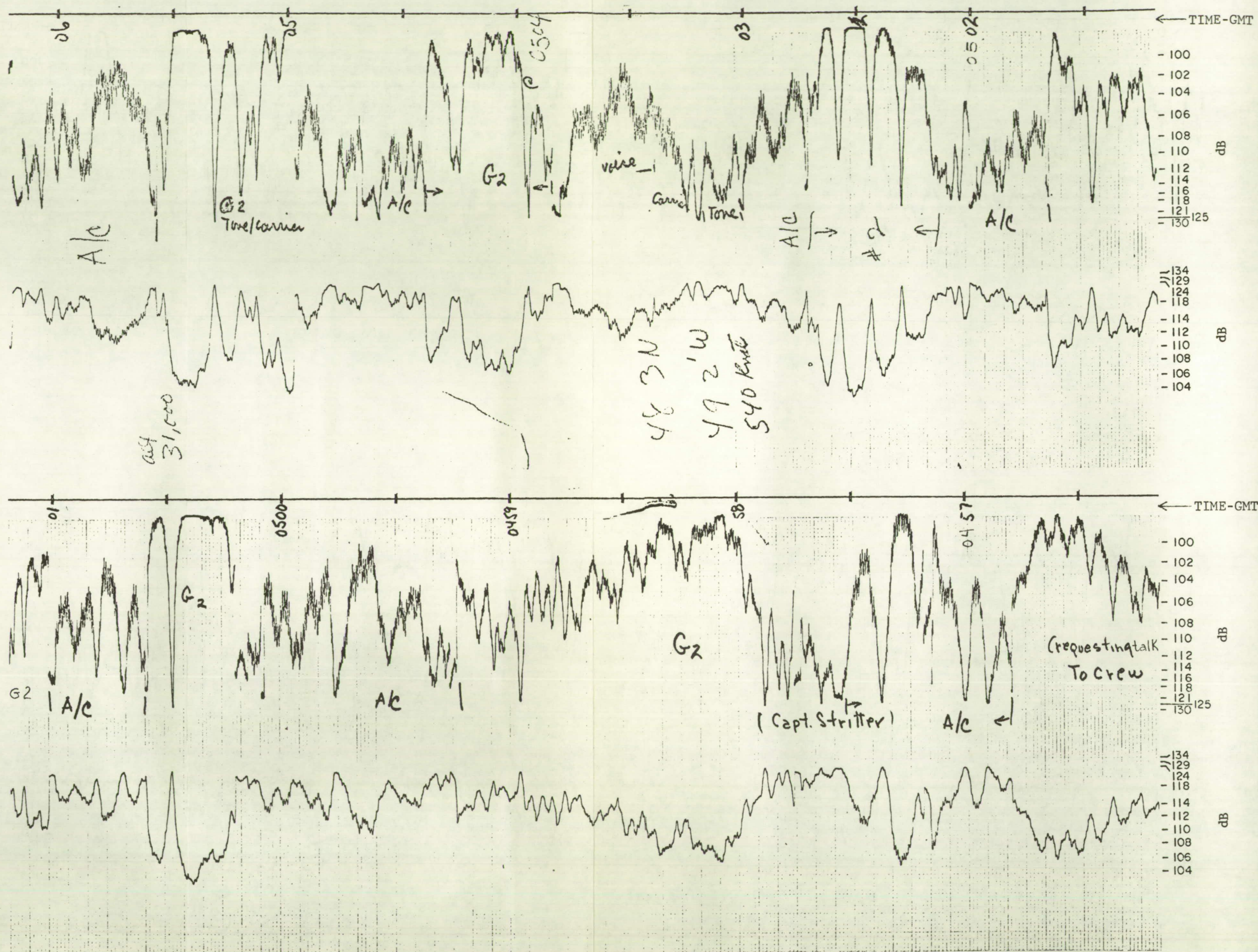


FIGURE 11-38 CONTINUED

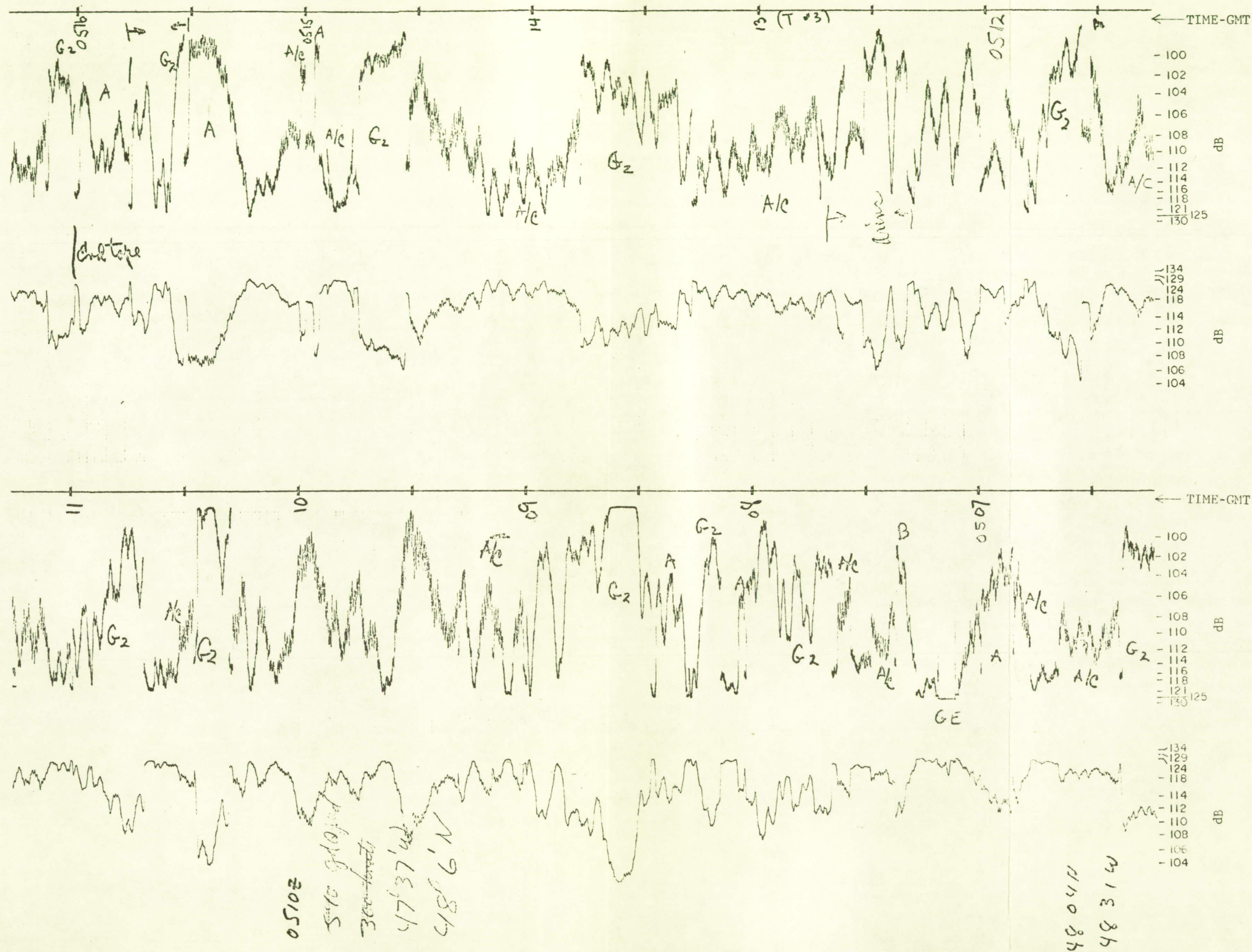
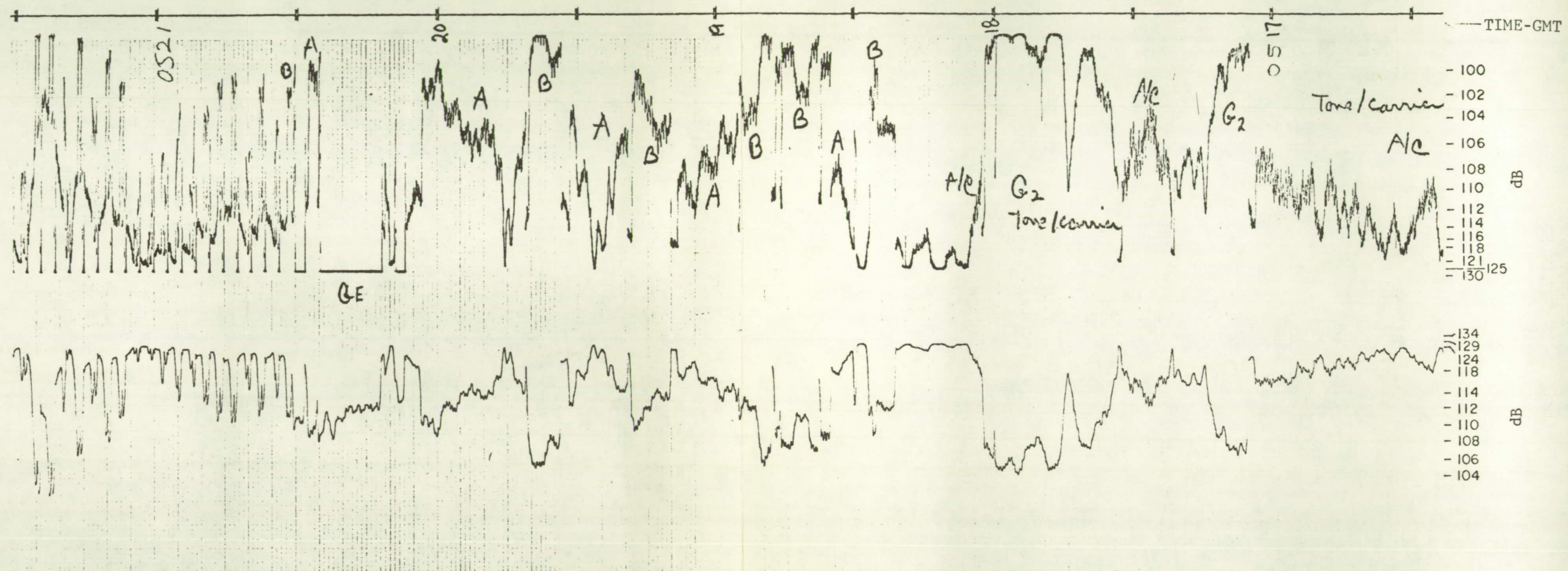


FIGURE 11-38 CONTINUED



NEW TECHNOLOGY

There has been no new technology developed on this contract.

PUBLICATIONS

Papers

The following papers have been presented or co-authored by Roy E. Anderson during the course of contract NAS5-11634 and contain results obtained from the work done on that contract:

"VHF Propagation Effects on Range Measurements from Satellites," Presented at the Symposium on the Application of Atmospheric Studies to Satellite Transmissions, Sponsored by AFCRL, September 1969.

"Ranging and Position Fixing from Satellites at VHF," Presented at the NEREM Symposium, 1969.

"Experimental Evaluation of VHF for Position Fixing by Satellite," Presented at the AIAA Third Communications Satellite Systems Conference, Los Angeles, California, April, 1970.

"Results of Marine Position Fixing Experiments Using ATS Satellites," Presented at the RTCM Assembly Meeting, San Francisco, California, May 1, 1970.

"Progress and Goals for Aeronautical Applications of Space Technology," Presented at the Fall Eurospace Meeting in Venice, Italy, September 1970. (Co-author - D. Fink, General Electric Space Division)

"Satellites for Merchant Marine Management and Ship Operation," America's International Maritime Trade Show, Baltimore, Maryland, April 7, 1971. (Co-authors - Capt. A. Fiore, U.S. Merchant Marine Academy, and J. Chernoff, ITT)

"Results of an Experiment to Locate and Read Data from Unmanned Transponders Using Satellites," 21st National Telemetry Conference, Washington, D. C., April 13, 1971.

Reports

The following internal General Electric Company reports have been prepared by Roy E. Anderson during the course of contract NAS5-11634 and contain results of work done on that contract or related efforts:

"Preliminary Experiments on Multipath Effects on One-way Range Measurements in Rural and Urban Environments," MO-69-0779, July 1969.

"Ranging and Position Fixing Experiments Using Satellites: 24-Hour Ranging Test, March 13-14, 1970," 70-C-198, June 1970.

APPENDIX I

DATA FROM COMSAT CORPORATION

Comsat Laboratories, Clarksburg, Maryland was equipped with a tone-code correlator and participated in some of the ranging experiments. They measured the inter-arrival times between their receptions of the interrogation signal from the distant transponder as it was relayed by the satellite. The inter-arrival time, minus user and satellite equipment delays, is the propagation time from the satellite to the transponder and return to the satellite.

Comsat computed a linear regression fit to the range measurements that they recorded. The linear regression fit, corresponding to the quadratic "best fit" curve of General Electric, is used to remove the effect of the changing range to the satellite as it moves relative to a fixed point on the earth's surface. Comsat computed standard deviations relative to the linear regression fit.

When Comsat and General Electric data were compared, they were found to be in close agreement.

Standard deviations reported by Comsat during the January 19-20, 1971 propagation test on Gander and Buenos Aires were as follows:

<u>Date</u>	<u>Time - GMT</u>	<u>Gander</u>	<u>Buenos Aires</u>
1/19	1806-1816		1.544 μ sec.
	1905-1914		1.148
	2002-2010		1.2
	2103-2111		1.207
	2204-2215		1.198
	2301-2310		1.33
1/20	0000-0009		1.369
	0100-0109		1.142
	1500-1511	1.036 μ s	

"The most significant result is that the standard deviation of the total inter-arrival time about the regression line is 1.2 microseconds on the average. This corresponds to an error (precision) of 600 feet along the line of propagation to the responder.

"It should also be noted that a linear regress fit is all that is needed to correct for the satellite's motion. The variations around the regression line seem to be random dispersals, and the correlation dropouts or misses also appear to be random."

"The interrogation method used in these tests works very well and similar techniques should be seriously considered as a means for transmission of data to and from aircraft, and for the communications management of a multiple access aeronautical satellite voice communications system. Its use in the present tests is of course limited only to the range determination."

(The above excerpts are from Comsat Corporation Technical Memorandum CL-26-71, "Satellite Ranging Experimental Results," R. Costales - currently being published.)

APPENDIX II

MODEL FOR IONOSPHERE CORRECTIONS

The following two references were used to establish a model for the effects of the ionosphere on the ranging error.

G. H. Millman, "A Survey of Tropospheric, Ionospheric, and Extra-terrestrial Effects on Radio Propagation Between the Earth and Space Vehicles", General Electric Company Report TIS R66EMH1, 1966.

R. W. Lawrence, D. J. Posakony, O. Garriott, and S. C. Hall, "The Total Electron Content of the Ionosphere at Middle Latitudes Near the Peak of the Solar Cycle", Journal of Geophysical Research, Volume 68, Number 7, April 1, 1963, page 1889.

The first reference is used to predict the effect of elevation angle and the second reference the diurnal effect on ranging error.

The following notation is used in this appendix.

E Line-of-sight elevation angle to the satellite

R_a Actual slant range

R_m Measured slant range

$$\Delta = R_m - R_a$$

h Representative ionosphere altitude, say mean altitude

t Local time (of day) on the line-of-sight at altitude h

f(t) A function of t such that $0 \leq f(t) \leq 1$

$g_{\max}(E)$ Maximum value of Δ as a function of E

$g_{\min}(E)$ Minimum value of Δ as a function of E

The empirical model developed in this appendix should be considered a provisional "engineering prototype" since no effort has been made to account for the "thickness" of the ionosphere or the fact that two frequencies are used in the transmissions. Assuming an inverse square frequency effect, the effect of frequency can easily be accounted for.

In order to easily incorporate the data contained in the two references cited above, the following model for the range error was adopted:

$$\Delta = ba^{f(t)}$$

where $0 \leq t \leq 24$ hours

$$\max f(t) = 1$$

$$\min f(t) = 0$$

$$a > 1$$

Obviously over the range of $f(t)$

$$\Delta_{\min} = b \qquad \Delta_{\max} = ab$$

The first reference gives the ionosphere range errors $g_{\min}(E)$ at mid-night ($t = 0$) and $g_{\max}(E)$ at noon ($t = 12$) as a function of the elevation angle E . Therefore

$$b = g_{\min}(E) = \Delta_{\min}$$

$$a = g_{\max}(E)/g_{\min}(E) = \Delta_{\max}/\Delta_{\min}$$

As noted above $g_{\min}(E)$ and $g_{\max}(E)$ are inversely proportional to frequency. The functions $g_{\max}(E)$ and $g_{\min}(E)$ are shown in Figure II-1.

The second reference (Figure II-1) contains curves showing six diurnal interval effects over various times of the season. These six curves were normalized* and suitably averaged to give the diurnal effect shown in Figure II-2.

The resulting empirical equation for the ionosphere effect is

$$\Delta = k g_{\min}(E) \left[\frac{g_{\max}(E)}{g_{\min}(E)} \right]^{f(t)}$$

where the proportionality k can be adjusted to account for long-term variations in ionosphere activity/intensity. The procedure for using this equation is to first use the local ground time of day, the line-of-sight elevation angle, E , to the satellite and some mean ionosphere altitude h to compute the local time t at the intersection of the line-of-sight ray and the mean altitude h . Then the range error is computed by the above equation.

It should be noted that the ratio $g_{\max}(E)/g_{\min}(E)$ is frequency invariant so that the above equation could be compensated for frequency by

$$\Delta = k \left(\frac{f_{\text{nom}}}{f} \right)^2 g_{\min}(E) \left[\frac{g_{\max}(E)}{g_{\min}(E)} \right]^{f(t)}$$

where $g_{\min}(E)$ is evaluated for $f = f_{\text{nom}}$.

* by the equation

$$f(t) = \frac{\log(\Delta(t)) - \log(\Delta_{\min})}{\log(\Delta_{\max}) - \log(\Delta_{\min})}$$

FIGURE II-1

RANGE ERROR DUE TO IONOSPHERE,
DAY AND NIGHT, VERSUS ELEVATION ANGLE

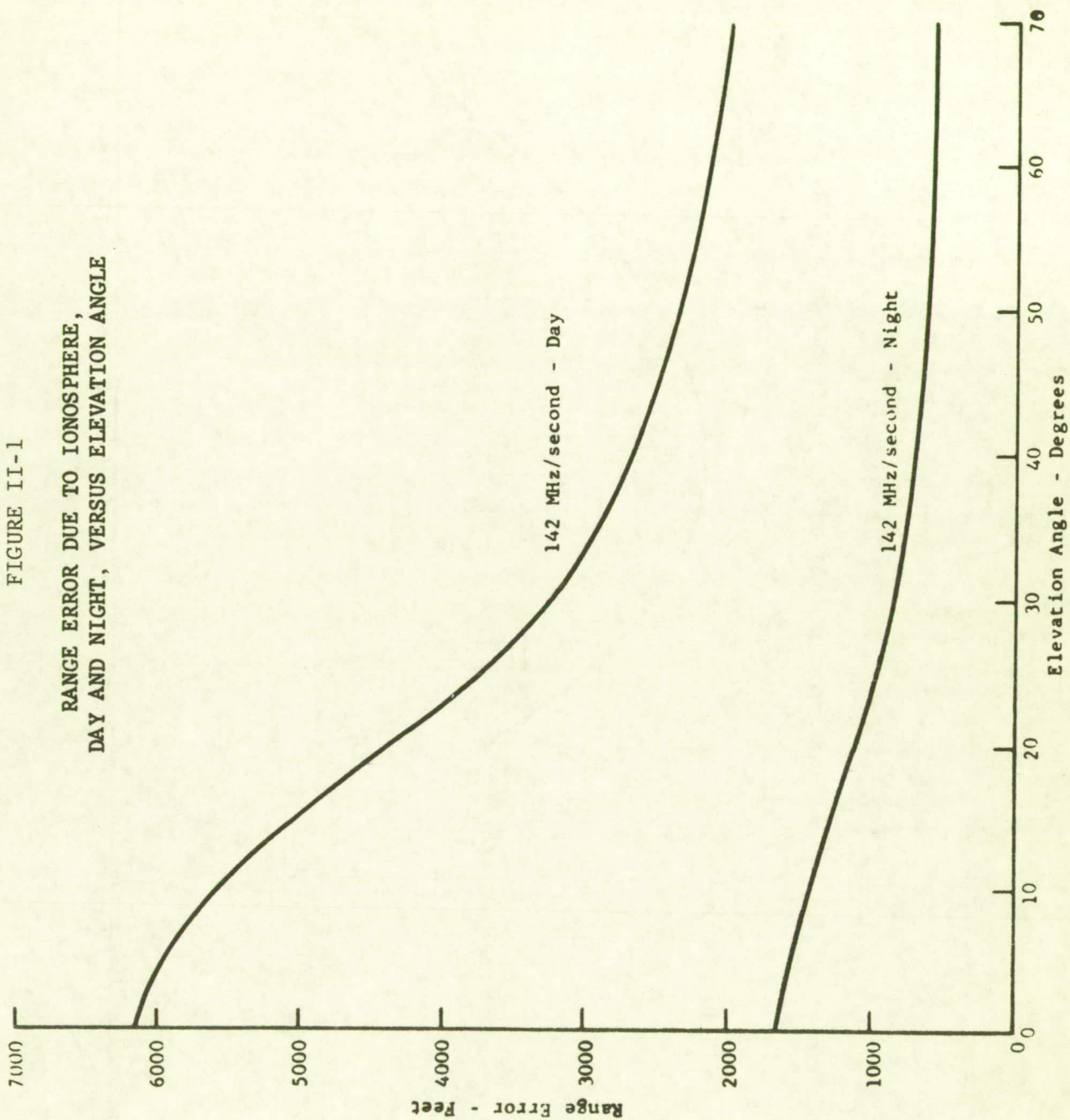
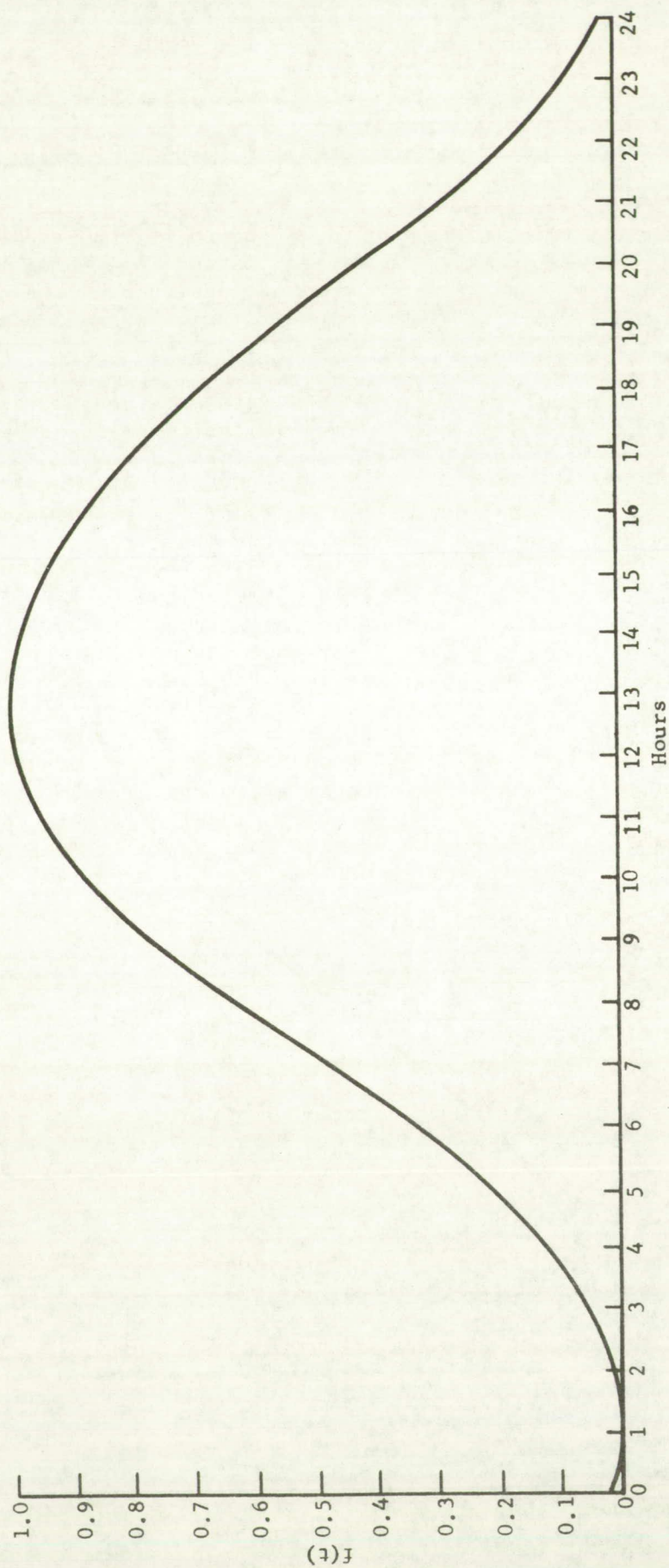


FIGURE II-2
 DIURNAL VARIATION IN RANGE DUE TO IONOSPHERE (NORMALIZED)



APPENDIX III

FLIGHT RECORDS FURNISHED BY THE FEDERAL AVIATION ADMINISTRATION

The excellent flight records supplied by the Federal Aviation Administration (FAA) staff at their National Aviation Facilities Experimental Center (NAFEC) were essential to the detailed analysis of the data obtained during aircraft flight tests. This appendix includes small samples to show the formats of the data that they supplied.

An example of the detailed analysis made possible by the completeness of the FAA flight records was the determination of the reasons for two individual fixes that were in error by unusually large amounts. During the flight test on 12/1/70 (Figure 6-8), a fix obtained at 17:46:49 was in error by approximately 11 miles with respect to the radar fix at the same instant of time. An examination of the data recorded at the Observatory did not show anything unusual in the signal but the FAA recording revealed the presence of local air traffic control interference that affected the tone portion of the tone-code ranging interrogation received in the aircraft. The interference apparently ended coincidentally with the start of the code as received in the aircraft so that phase matching was imperfect but the code was received and correlated so that the aircraft responded. (Figure III-1)

Another fix at 19:02:36 (Figure 6-11) was in error by 7.5 miles. An examination of the FAA flight recording in the aircraft revealed that spin modulation of the satellite caused a drop in signal level received in the aircraft just prior to the reception of the code, again affecting the accuracy of the phase match. (Figure III-2)

In both cases the fixes are displaced along a hyperbolic line of position. The phase of the tone received in the aircraft was affected but the signals returned from the aircraft through the two satellites were not affected.

Similar signal recordings in the aircraft revealed the effects of orthogonal Faraday rotation polarization when using a linearly polarized antenna and the comparisons of the three antenna models used during the experiments with respect to aircraft headings and elevation and azimuth angles to ATS-1 and ATS-3.

Another example of the detailed data furnished by NAFEC is shown in Figure III-3. Together with the chart recordings in the aircraft and chart recordings made on the signals received at the Observatory for the same interrogations, such information proved useful in evaluating the specific propagation effects and antenna pattern variations on signal reliability and ranging accuracy.

FIGURE III-1

EFFECT OF LOCAL RADIO FREQUENCY INTERFERENCE ON TONE-CODE
RANGING SIGNAL RECEIVED IN DC-6 AIRCRAFT

17:46:49 GMT Interference Occurred During Interrogation —

FIGURE III-2

EFFECTS OF ATS-3 SPIN MODULATION ON TONE-CODE RANGING
SIGNAL RECEIVED IN DC-6 AIRCRAFT

1903

19:02:36 GMT

Satellite VHF Position Determination Subsystem Experimentation

From: 1000L To: 1000L

GMT Time	Aircraft Pitch (Degrees)	Aircraft Roll (Degrees)	Aircraft Airspeed (Knots)	Aircraft Altitude (000 Ft.)	Aircraft Heading (Degrees)	Antenna Mode	Signal Level in dBm G E Recvr (Maximum & Minimum)	Number of Interrog.	Number of Replies	Remarks Code
1507	+12.5	—	150	18	82	H	114 125	10	0	
1508	—	—	150	18	92	H	109 118	9	4	
1509	—	—	165	18.5	122	H	110 120	19	15	
1510	—	—	180	18.5	122	H	114 121	10	6	
1511	—	—	182	18.5	122	H	113 122	7	0	
1512	—	—	193	18.5	122	H		0	0	
1513	—	—	190	18.5	122	H	115 118	2	2	
1514	—	—	190	18.5	122	H	110 120	12	12	
1515	—	—	190	18.5	122	H	117 120	14	13	
1516	0	—	190	18.5	122	H	109 120	12	12	
1517	—	—	188	18.5	122	H	124 125	—	3	
1518	0	—	190	18.5	122	H		0	0	
1519	-0.5	—	190	18.5	122	H	123 125	2	0	
1520	0	—	190	18.5	122	H		0	0	
1521	-0.5	—	195	18.5	122	H	114 125	12	0	

NOTES ON REDUCTION OF AIRCRAFT DERIVED DATA FOR JULY 1970
SURVEILLANCE TESTS IN FAA AIRCRAFT N-114

1. Data has been reduced on the basis of one minute samples.
2. Aircraft Pitch data is tagged with a plus sign for "nose up" and minus sign for "nose down".
3. Aircraft Roll data is tagged with a letter "R" to indicate "roll right" and a letter "L" to indicate "roll left".
4. Antenna Mode data is tagged "Z" for Zenith Mode, "H" for Horizon Mode and "B" for Blade Antenna.
5. Signal Level data is presented as the maximum and minimum signal levels that occurred during the one minute data sample coincident with the ground station interrogations.
6. The Number of Interrogations data is a count of the total number of interrogations received during the one minute data sample. This count will include all interrogations, recognized as such from the AGC voltage deviation, that occurred whether addressed to the FAA responders on board N-114 or other responders. In cases where no interrogation was detected from the AGC voltage recording yet a reply was sent from the aircraft the interrogation was not counted since it could not be verified as a valid interrogation.
7. The Number of Replies data is a count of the ~~total~~ number of replies, as determined from a special sensor attached to the transmitter output, that occurred during the one minute data sample. Manual keying of the responder or voice keying indications were not included.
8. The Remarks Code data was limited to three instructions. The delta sign (Δ) indicates that the aircraft is positioned on a Benchmark at the airport listed as "To"; the letters "TTI" indicate that there was a temporary transmission interruption; and the asterisk (*) symbol indicates that the data for that particular one minute data sample is further detailed in other line entries.
9. All data entries that contain a dash (---) symbol indicate that the data for that particular entry was not reducible for any of a number of reasons. Where this symbol appears repeatedly for the aircraft parameters it indicates a malfunction that occurred in the Automated Data Acquisition System for those channels being recorded.

EXPLANATION OF FLIGHT TEST DATA FURNISHED BY FAA AS SHOWN IN FIGURE III-3

APPENDIX IV

USER CODES

Code	USER	1024 Cycles of Tone	Binary Sequence 15-Bit Word Sync	15-Bit Address
1	Sea Robin	1 1-----1	0 0 0 1 1 1 0 0 1 1 0 1 1 1 1	1 0 0 0 0 0 0 1 1 1 1 0 0 0 0
2	CPD	1 1-----1	0 0 0 1 1 1 1 0 0 1 1 0 1 1 1	0 1 0 0 0 0 0 1 0 1 0 1 1 0 0
3	NASA Van	1 1-----1	0 0 0 1 1 1 1 0 0 1 1 0 1 1 1	1 1 0 0 0 0 0 0 1 0 1 1 1 0 0
4	FAA Aircraft	1 1-----1	0 0 0 1 1 1 1 0 0 1 1 0 1 1 1	0 0 1 0 0 0 0 0 1 1 0 1 1 1 0
5	Pan Am 747	1 1-----1	0 0 0 1 1 1 1 0 0 1 1 0 1 1 1	1 0 1 0 0 0 0 1 0 0 1 1 0 1 0
6	Gander	1 1-----1	0 0 0 1 1 1 1 0 0 1 1 0 1 1 1	0 1 1 0 0 0 0 1 1 0 0 0 1 1 0
7	Shannon	1 1-----1	0 0 0 1 1 1 1 0 0 1 1 0 1 1 1	1 1 1 0 0 0 0 0 0 1 1 0 1 1 0
8	Buenos Aires*	1 1-----1	0 0 0 1 1 1 1 0 0 1 1 0 1 1 1	0 0 0 1 0 0 0 1 1 0 1 1 1 1 0
9	Iceland	1 1-----1	0 0 0 1 1 1 1 0 0 1 1 0 1 1 1	1 0 0 1 0 0 0 0 0 1 0 1 1 1 0
10	Seattle, Washington	1 1-----1	0 0 0 1 1 1 1 0 0 1 1 0 1 1 1	0 1 0 1 0 0 0 0 1 1 1 0 0 1 0
11	FAA Mobile	1 1-----1	0 0 0 1 1 1 1 0 0 1 1 0 1 1 1	1 1 0 1 0 0 0 1 0 0 0 0 0 1 0

* Used in earlier tests by Coast Guard Cutters Valiant and Rush.

GOVERNMENT

DEPARTMENT OF COMMERCE

Beery, W. (Inst. of Telecommunications, Boulder)
Fiore, Capt. A. (US Merchant Marine Academy)
*Kurz, C. (Maritime Administration)
McCready, Capt. L. S. (US Merchant Marine Academy)
Travis, Capt. H. O. (US Merchant Marine Academy)
Wheatley, S. (Maritime Administration)

DEPARTMENT OF TRANSPORTATION

Anderson, J. (Transportation Systems Center)
Beam, R. (Office of Telecommunications)
Dorian, C. (Office of Telecommunications)
Gutwein, J. (Transportation Systems Center)
Haroulis, G. (Transportation Systems Center)
Keane, L. (Transportation Systems Center)
Veronda, C. (Transportation Systems Center)

FEDERAL AVIATION ADMINISTRATION

Carr, F. S.
*DeZoute, O.
*Dunmire, C. E.
*Hirshon, S.
Jefferson, F. (NAFEC)
Meier, R. W.
Storrs, E.
Weber, J.

FEDERAL COMMUNICATIONS COMMISSION

Budge, F. O.
Peterson, H.
*Spence, R.

US COAST GUARD

*Felton, W.
Fenton, R.
*Hampton, G. H.

NASA HEADQUARTERS

Burke, J.
Ehrlich, E.
Kramer, M.
Marsten, R.
Fiebelkorn, LTC

NASA LANGLEY

Lawrence, H.
*Morrell, F.

NASA GODDARD

Golden, T.
Gubin, S.
*Horouchi, H.
*Jones, A.
*Laughlin, G.
Maracus, Dr.
Metzger, E.
Orr, G.
Ramasastry, J.
*Schmidd, P.
*Seddon, C.
*Taylor, C.
Baker, J. L.

OTHER GOVERNMENT DISTRIBUTION

*Aarons, J. (ARCRL)
Arendt, P. (US Army Electronics Lab.)
Deem, P. S. (USAF)
*Easton, R. (NRL)
*Haase, R. (USNUSL)
Haughton, T. J. (USN Oceanographic Office)
Haydon, G. (ESSA)
Jansky, D. (Office of Telecom. Policy)
Klobuchar, J. (AFCRL)
Speaker, R. (BUWEPS)
Stoddard, W. J. (NOAA)
**Walsh, J. B. (Office - Secy. of the A.F.)
Raish, L. R. (Office of Telecom. Policy)

Dept. of the Navy, Astronautics Div.
Office of the Secretary of Defense,
Communications & Electronics
US Coast Guard, Aids to Navigation Div.
SAMSO (SMAOO), Los Angeles A.F. Station

* Executive Summary Only
** Both Executive Summary and
Complete Report

AERONAUTICAL RADIO INC.

*Carnes, W.
Pettry, C.
*Slavin, T.

AIR TRANSPORT ASSOCIATION

*Poritzky, S.
White, F.

COMSAT CORPORATION

Campanella, J.
Costales, R.
*Istvan, E.
Klein, P.
*Levatic, J.
Martin, E.

HUGHES AIRCRAFT

*Boucher, R.
*Lutz, S.

MITRE CORPORATION

Noyer, R. O. (Washington)
Downey, E. J. (Bedford, Mass.)
McGinn, J. F. (Bedford, Mass.)

PAN AMERICAN AIRWAYS

Bohannon, R.
*McCloud, B.

WESTINGHOUSE

*Keats, E.
Mueller, E. J.

CONSULTANTS

Chisholm, J. (Sierra Research)
*Rosenberg, P. (Rosenberg Assoc.)
*Weihe, V.

OTHER INDUSTRY DISTRIBUTION

Aerospace Corporation - R. L. Dutcher
Applied Information Industries - J. Bar
Automated Marine Inc. - B. Mendoza
Aviation Week Magazine - P. Klass

*Bell Labs - J. Unger
*Bendix - J. Lumsden

*Communication & Systems Inc. - L. G. F.
*General Motors - E. L. Hughes
*Greyhound Corp. - F. Paternoster

ITT Aerospace/Optical - J. Chernoch
*ITT Federal Labs - S. H. Dodington
*Marine Telephone Co. Inc. - M. Miller
Philco - *H. Goett; D. Middlebrook

*RCA - M. W. Mitchell

*Smithsonian Inst. - G. Weiffenbach
*Sperry-Rand - L. Kapanka

**Stanford Research Inst. - P. A. Portman

*TRW - D. T. Otten

*Western Geophysical Company - A. Moody

American Institute of Navigation
Hughes Aircraft, Guidance & Controls

UNIVERSITIES

*Filkins, L. (Univ. of Michigan)
*Goblick, T. J. (MIT, Lincoln Labs)
*Herrick, S. (Univ. of California)
*Kershner, R. (Johns Hopkins APL)
*Suomi, V. E. (Univ. of Wisconsin)

**Augustana College (Library)
MIT, Lincoln Labs (Library)

*Rensselaer Polytechnic Inst. (Library)
*State Univ. of N.Y. at Albany (Library)
*Union College (Library)

*Executive Summary Only

**Both Executive Summary and Complete Report

EXPERIMENT PARTICIPANTS (OUTSIDE OF USA)

IRELAND (Department of Posts and Telegraphs)

Es, G. (Dublin)
alaigh, D. (Dublin)
eill, D. (Shannon)

IRELAND (Civil Aviation Administration)

oed-Hansen, A. (Reykjavik)
nusson, L. (Reykjavik)

CANADA (Canadian Department of Transport)

ttley, F. (Ottawa, Ontario)
the, S. (Ottawa, Ontario)
ong, J. (Gander, Newfoundland)
ks, E. (Gander, Newfoundland)

ARGENTINA (Argentine Air Force)

sagrande, O. L. (General Electric Company representative)
opies to be forwarded to the Argentine Air Force)

FOREIGN DISTRIBUTION

AUSTRALIA

Davis, E. B. (Australian Department of Supply)

ENGLAND

British Aircraft Corp.
Pugh, B.

Decca Navigator Co. Ltd.
Halliwell, D.
*Powell, C.

Dept. of Trade & Industry
Parker, J. S.
Robinson, J.

Hawker Siddeley Dynamics
Hickman, P. L.

Marconi Company Ltd.
*Beck, G. E.
Wright, D. J.

Ministry of Technology
Neate, R. A.

Royal Aircraft Establishment
Bailey, N.
Hirst, D.

FRANCE

Manualli, B. (Centre National d'Etudes Spatiales)

GERMANY

Freiesleben, H. (Deutsche Gesellschaft fur Raketentechnik und Raumfahrtforschung)
Hartl, P. (Institute fur Satellitenelek)
*Rudolf, J. (Telefunken)

JAPAN

*Shoji, K. (Tokyo University of Mercantile Marine)

NORWAY

Melby, K. (Royal Norwegian Council for Scientific and Industrial Research)
Rambal, A. (Standard Telefon og Kabel Fabrikk)

ORGANIZATIONS (foreign and international)

British Institute of Navigation

French Institute of Navigation

ESRO (Mr. Van Den Kerckhov, ESTEG, Netherlands)

CNES (Mr. A. Lebaut)

ICAO (Mr. C. E. Bellringer)

UNITED NATIONS (V. V. Azarencov, Outer Space Affairs Officer)

EUROSPACE (Yves Demerliac, Secretary General)

GENERAL ELECTRIC COMPANY

AIRCRAFT EQUIPMENT DIVISION

*Grimm, D. (ASPO)
Matt, S. (Avionic Controls)

DEFENSE PROGRAMS DIVISION

Lees, B. (Washington Office)
McClennan, J. (Lexington Office)
*Rogers, D. (Washington Office)
Schorr, S. (TEMPO)

ELECTRONIC SYSTEMS DIVISION

*Brown, B. (HMES)
*Hackette, C. (HMES)
*Jett, B. (ASRO)
Millman, G. (HMES)
*Mullen, E. (E. Lab.)
*Nelson, D. W. (HMES)
*Robb, R. (HMES)

RE-ENTRY & ENVIRONMENTAL SYSTEMS PRODUCTS

Cheney, R. (Ocean Systems)
*McCabe, R. (Ocean Systems)
Sierzenski, R. (Ocean Systems)
Wyeth, H.

SPACE PRODUCTS DIVISION

Braham, H.
*Clemson, D. B.
Davies, D.
*Davis, L. K.
*Gross, W.
*Haviland, R.
*Hesselbacher, R.
Hoffman, H. (Apollo)
Douglas, W. (Tech. & Oper. Services)
Loftus, J.

CANADIAN GENERAL ELECTRIC

deBuda, R.

COMMUNICATION SYSTEMS DIVISION

*Gifford, R. (TPD)
Gordon, R. (MRD)
*Merigo, M. (MRD)
Sisson, R. (MRD)

AEROSPACE BUSINESS GROUP

*Porter, R. W. (Scientific and
Technological Affairs)

CORPORATE RESEARCH & DEVELOPMENT

Garrett, R. W.
Lewis, J. R.
**Nial, W. R.
Orlowski, E. J.
*Rustay, R.
*Schulmann, E.
*Waldron, W. K.
*Whitten, J. R.

GENERAL ELECTRIC ARGENTINA SA

**Casagrande, O. L.

*Executive Summary only

**Both Executive Summary and Complete